

September 2006

Revision 16

NAC-STC

NAC Storage Transport Cask

SAFETY ANALYSIS REPORT

Volume 1 of 2
Docket No. 71-9235



Atlanta Corporate Headquarters: 3950 East Jones Bridge Road, Norcross, Georgia 30092 USA
Phone 770-447-1144, Fax 770-447-1797, www.nacintl.com

List of Effective Pages

Master Table of Contents	1.1-1 Revision 16
i Revision 16	1.1-2 Revision 16
ii Revision 16	1.1-3 Revision 16
iii Revision 16	1.1-4 Revision 16
iv Revision 16	1.1-5 Revision 16
v Revision 16	1.1-6 Revision 16
vi Revision 16	1.1-7 Revision 16
vii Revision 16	1.1-8 Revision 16
viii Revision 16	1.2-1 Revision 16
ix Revision 16	1.2-2 Revision 16
x Revision 16	1.2-3 Revision 16
xi Revision 16	1.2-4 Revision 16
xii Revision 16	1.2-5 Revision 16
xiii Revision 16	1.2-6 Revision 16
xiv Revision 16	1.2-7 Revision 16
xv Revision 16	1.2-8 Revision 16
xvi Revision 16	1.2-9 Revision 16
xvii Revision 16	1.2-10 Revision 16
	1.2-11 Revision 16
	1.2-12 Revision 16
	1.2-13 Revision 16
	1.2-14 Revision 16
	1.2-15 Revision 16
	1.2-16 Revision 16
	1.2-17 Revision 16
	1.2-18 Revision 16
	1.2-19 Revision 16
	1.2-20 Revision 16
	1.2-21 Revision 16
	1.2-22 Revision 16
	1.2-23 Revision 16
	1.2-24 Revision 16
	1.2-25 Revision 16
	1.2-26 Revision 16
	1.2-27 Revision 16
	1.2-28 Revision 16
	1.2-29 Revision 16
	1.2-30 Revision 16
Chapter 1	
1-i Revision 16	
1-ii Revision 16	
1-iii Revision 16	
1-iv Revision 16	
1-v Revision 16	
1-1 Revision 16	
1-2 Revision 16	
1-3 Revision 16	
1-4 Revision 16	
1-5 Revision 16	
1-6 Revision 16	
1-7 Revision 16	
1-8 Revision 16	
1-9 Revision 16	
1-10 Revision 16	
1-11 Revision 16	

List of Effective Pages (continued)

1.2-31	Revision 16
1.2-32	Revision 16
1.2-33	Revision 16
1.2-34	Revision 16
1.2-35	Revision 16
1.2-36	Revision 16
1.2-37	Revision 16
1.2-38	Revision 16
1.2-39	Revision 16
1.2-40	Revision 16
1.2-41	Revision 16
1.2-42	Revision 16
1.2-43	Revision 16
1.2-44	Revision 16
1.3-1	Revision 16

Chapter 2

2-i	Revision 16
2-ii	Revision 16
2-iii	Revision 16
2-iv	Revision 16
2-v	Revision 16
2-vi	Revision 16
2-vii	Revision 16
2-viii	Revision 16
2-ix	Revision 16
2-x	Revision 16
2-xi	Revision 16
2-xii	Revision 16
2-xiii	Revision 16
2-xiv	Revision 16
2-xv	Revision 16
2-xvi	Revision 16
2-xvii	Revision 16
2-xviii	Revision 16
2-xix	Revision 16
2-xx	Revision 16

2-xxi	Revision 16
2-xxii	Revision 16
2-xxiii	Revision 16
2-xxiv	Revision 16
2-xxv	Revision 16
2-xxvi	Revision 16
2-xxvii	Revision 16
2-xxviii	Revision 16
2-xxix	Revision 16
2-xxx	Revision 16
2-xxxi	Revision 16
2-xxxii	Revision 16
2-xxxiii	Revision 16
2-xxxiv	Revision 16
2-xxxv	Revision 16
2-xxxvi	Revision 16
2-xxxvii	Revision 16
2-xxxviii	Revision 16
2-xxxix	Revision 16
2-xl	Revision 16
2-xli	Revision 16
2-xlii	Revision 16
2-xliii	Revision 16
2-xliv	Revision 16
2-xlv	Revision 16
2-xlvi	Revision 16
2-xlvii	Revision 16
2-xlviii	Revision 16
2-xlix	Revision 16
2-l	Revision 16
2-li	Revision 16
2-lii	Revision 16
2-liii	Revision 16
2-liv	Revision 16
2-lv	Revision 16
2-lvi	Revision 16
2-lvii	Revision 16

List of Effective Pages (continued)

2-lviii.....	Revision 16	2.3.2-3	Revision 16
2-1	Revision 16	2.3.2-4	Revision 16
2.1.1-1	Revision 16	2.3.2-5	Revision 16
2.1.1-2	Revision 16	2.3.3-1	Revision 16
2.1.1-3	Revision 16	2.3.3-2	Revision 16
2.1.1-4	Revision 16	2.3.4-1	Revision 16
2.1.2-1	Revision 16	2.3.4-2	Revision 16
2.1.2-2	Revision 16	2.3.4-3	Revision 16
2.1.2-3	Revision 16	2.3.5-1	Revision 16
2.1.2-4	Revision 16	2.3.5-2	Revision 16
2.1.2-5	Revision 16	2.3.6-1	Revision 16
2.1.3-1	Revision 16	2.3.6-2	Revision 16
2.1.3-2	Revision 16	2.3.6-3	Revision 16
2.1.3-3	Revision 16	2.3.6-4	Revision 16
2.1.3-4	Revision 16	2.3.6-5	Revision 16
2.1.3-5	Revision 16	2.3.7-1	Revision 16
2.1.3-6	Revision 16	2.3.8-1	Revision 16
2.1.3-7	Revision 16	2.4-1	Revision 16
2.1.3-8	Revision 16	2.4.1-1	Revision 16
2.1.3-9	Revision 16	2.4.2-1	Revision 16
2.1.3-10	Revision 16	2.4.3-1	Revision 16
2.1.3-11	Revision 16	2.4.4-1	Revision 16
2.1.3-12	Revision 16	2.4.4-2	Revision 16
2.1.3-13	Revision 16	2.4.4-3	Revision 16
2.1.3-14	Revision 16	2.4.4-4	Revision 16
2.1.3-15	Revision 16	2.4.4-5	Revision 16
2.2-1	Revision 16	2.4.4-6	Revision 16
2.2-2	Revision 16	2.4.4-7	Revision 16
2.2-3	Revision 16	2.4.4-8	Revision 16
2.2-4	Revision 16	2.4.4-9	Revision 16
2.2-5	Revision 16	2.4.4-10	Revision 16
2.2-6	Revision 16	2.4.5-1	Revision 16
2.2-7	Revision 16	2.4.6-1	Revision 16
2.3.1-1	Revision 16	2.5.1-1	Revision 16
2.3.1-2	Revision 16	2.5.1-2	Revision 16
2.3.2-1	Revision 16	2.5.1-3	Revision 16
2.3.2-2	Revision 16	2.5.1-4	Revision 16

List of Effective Pages (continued)

2.5.1-5	Revision 16	2.5.2-6	Revision 16
2.5.1-6	Revision 16	2.5.2-7	Revision 16
2.5.1-7	Revision 16	2.5.2-8	Revision 16
2.5.1-8	Revision 16	2.5.2-9	Revision 16
2.5.1-9	Revision 16	2.5.2-10	Revision 16
2.5.1-10	Revision 16	2.5.2-11	Revision 16
2.5.1-11	Revision 16	2.5.2-12	Revision 16
2.5.1-12	Revision 16	2.5.2-13	Revision 16
2.5.1-13	Revision 16	2.5.2-14	Revision 16
2.5.1-14	Revision 16	2.5.2-15	Revision 16
2.5.1-15	Revision 16	2.5.2-16	Revision 16
2.5.1-16	Revision 16	2.5.2-17	Revision 16
2.5.1-17	Revision 16	2.5.2-18	Revision 16
2.5.1-18	Revision 16	2.5.2-19	Revision 16
2.5.1-19	Revision 16	2.5.2-20	Revision 16
2.5.1-20	Revision 16	2.5.2-21	Revision 16
2.5.1-21	Revision 16	2.5.2-22	Revision 16
2.5.1-22	Revision 16	2.5.2-23	Revision 16
2.5.1-23	Revision 16	2.5.2-24	Revision 16
2.5.1-24	Revision 16	2.5.2-25	Revision 16
2.5.1-25	Revision 16	2.5.2-26	Revision 16
2.5.1-26	Revision 16	2.5.2-27	Revision 16
2.5.1-27	Revision 16	2.5.2-28	Revision 16
2.5.1-28	Revision 16	2.5.2-29	Revision 16
2.5.1-29	Revision 16	2.6-1	Revision 16
2.5.1-30	Revision 16	2.6-2	Revision 16
2.5.1-31	Revision 16	2.6.1-1	Revision 16
2.5.1-32	Revision 16	2.6.1-2	Revision 16
2.5.1-33	Revision 16	2.6.1-3	Revision 16
2.5.1-34	Revision 16	2.6.1-4	Revision 16
2.5.1-35	Revision 16	2.6.1-5	Revision 16
2.5.1-36	Revision 16	2.6.1-6	Revision 16
2.5.2-1	Revision 16	2.6.1-7	Revision 16
2.5.2-2	Revision 16	2.6.2-1	Revision 16
2.5.2-3	Revision 16	2.6.2-2	Revision 16
2.5.2-4	Revision 16	2.6.2-3	Revision 16
2.5.2-5	Revision 16	2.6.2-4	Revision 16

List of Effective Pages (continued)

2.6.2-5	Revision 16	2.6.7.2-12	Revision 16
2.6.2-6	Revision 16	2.6.7.2-13	Revision 16
2.6.2-7	Revision 16	2.6.7.2-14	Revision 16
2.6.2-8	Revision 16	2.6.7.2-15	Revision 16
2.6.3-1	Revision 16	2.6.7.2-16	Revision 16
2.6.4-1	Revision 16	2.6.7.2-17	Revision 16
2.6.5-1	Revision 16	2.6.7.2-18	Revision 16
2.6.5-2	Revision 16	2.6.7.3-1	Revision 16
2.6.6-1	Revision 16	2.6.7.3-2	Revision 16
2.6.7-1	Revision 16	2.6.7.3-3	Revision 16
2.6.7.1-1	Revision 16	2.6.7.3-4	Revision 16
2.6.7.1-2	Revision 16	2.6.7.3-5	Revision 16
2.6.7.1-3	Revision 16	2.6.7.3-6	Revision 16
2.6.7.1-4	Revision 16	2.6.7.3-7	Revision 16
2.6.7.1-5	Revision 16	2.6.7.3-8	Revision 16
2.6.7.1-6	Revision 16	2.6.7.3-9	Revision 16
2.6.7.1-7	Revision 16	2.6.7.3-10	Revision 16
2.6.7.1-8	Revision 16	2.6.7.3-11	Revision 16
2.6.7.1-9	Revision 16	2.6.7.4-1	Revision 16
2.6.7.1-10	Revision 16	2.6.7.4-2	Revision 16
2.6.7.1-11	Revision 16	2.6.7.4-3	Revision 16
2.6.7.1-12	Revision 16	2.6.7.4-4	Revision 16
2.6.7.1-13	Revision 16	2.6.7.4-5	Revision 16
2.6.7.1-14	Revision 16	2.6.7.4-6	Revision 16
2.6.7.1-15	Revision 16	2.6.7.4-7	Revision 16
2.6.7.1-16	Revision 16	2.6.7.4-8	Revision 16
2.6.7.2-1	Revision 16	2.6.7.4-9	Revision 16
2.6.7.2-2	Revision 16	2.6.7.4-10	Revision 16
2.6.7.2-3	Revision 16	2.6.7.4-11	Revision 16
2.6.7.2-4	Revision 16	2.6.7.4-12	Revision 16
2.6.7.2-5	Revision 16	2.6.7.4-13	Revision 16
2.6.7.2-6	Revision 16	2.6.7.4-14	Revision 16
2.6.7.2-7	Revision 16	2.6.7.4-15	Revision 16
2.6.7.2-8	Revision 16	2.6.7.4-16	Revision 16
2.6.7.2-9	Revision 16	2.6.7.4-17	Revision 16
2.6.7.2-10	Revision 16	2.6.7.4-18	Revision 16
2.6.7.2-11	Revision 16	2.6.7.4-19	Revision 16

List of Effective Pages (continued)

2.6.7.4-20	Revision 16	2.6.7.4-57	Revision 16
2.6.7.4-21	Revision 16	2.6.7.4-58	Revision 16
2.6.7.4-22	Revision 16	2.6.7.4-59	Revision 16
2.6.7.4-23	Revision 16	2.6.7.5-1	Revision 16
2.6.7.4-24	Revision 16	2.6.7.5-2	Revision 16
2.6.7.4-25	Revision 16	2.6.7.5-3	Revision 16
2.6.7.4-26	Revision 16	2.6.7.5-4	Revision 16
2.6.7.4-27	Revision 16	2.6.7.5-5	Revision 16
2.6.7.4-28	Revision 16	2.6.7.5-6	Revision 16
2.6.7.4-29	Revision 16	2.6.7.5-7	Revision 16
2.6.7.4-30	Revision 16	2.6.7.5-8	Revision 16
2.6.7.4-31	Revision 16	2.6.7.5-9	Revision 16
2.6.7.4-32	Revision 16	2.6.7.5-10	Revision 16
2.6.7.4-33	Revision 16	2.6.7.5-11	Revision 16
2.6.7.4-34	Revision 16	2.6.7.5-12	Revision 16
2.6.7.4-35	Revision 16	2.6.7.5-13	Revision 16
2.6.7.4-36	Revision 16	2.6.7.6-1	Revision 16
2.6.7.4-37	Revision 16	2.6.7.6-2	Revision 16
2.6.7.4-38	Revision 16	2.6.7.6-3	Revision 16
2.6.7.4-39	Revision 16	2.6.7.6-4	Revision 16
2.6.7.4-40	Revision 16	2.6.7.6-5	Revision 16
2.6.7.4-41	Revision 16	2.6.7.6-6	Revision 16
2.6.7.4-42	Revision 16	2.6.7.6-7	Revision 16
2.6.7.4-43	Revision 16	2.6.7.6-8	Revision 16
2.6.7.4-44	Revision 16	2.6.7.6-9	Revision 16
2.6.7.4-45	Revision 16	2.6.7.6-10	Revision 16
2.6.7.4-46	Revision 16	2.6.7.6-11	Revision 16
2.6.7.4-47	Revision 16	2.6.7.6-12	Revision 16
2.6.7.4-48	Revision 16	2.6.7.6-13	Revision 16
2.6.7.4-49	Revision 16	2.6.7.7-1	Revision 16
2.6.7.4-50	Revision 16	2.6.7.7-2	Revision 16
2.6.7.4-51	Revision 16	2.6.7.7-3	Revision 16
2.6.7.4-52	Revision 16	2.6.7.7-4	Revision 16
2.6.7.4-53	Revision 16	2.6.7.7-5	Revision 16
2.6.7.4-54	Revision 16	2.6.8-1	Revision 16
2.6.7.4-55	Revision 16	2.6.9-1	Revision 16
2.6.7.4-56	Revision 16	2.6.10-1	Revision 16

List of Effective Pages (continued)

2.6.10.1-1	Revision 16	2.6.12.2-1	Revision 16
2.6.10.1-2	Revision 16	2.6.12.2-2	Revision 16
2.6.10.2-1	Revision 16	2.6.12.2-3	Revision 16
2.6.10.2-2	Revision 16	2.6.12.2-4	Revision 16
2.6.10.2-3	Revision 16	2.6.12.2-5	Revision 16
2.6.10.2-4	Revision 16	2.6.12.3-1	Revision 16
2.6.10.3-1	Revision 16	2.6.12.3-2	Revision 16
2.6.10.3-2	Revision 16	2.6.12.3-3	Revision 16
2.6.10.3-3	Revision 16	2.6.12.3-4	Revision 16
2.6.10.3-4	Revision 16	2.6.12.3-5	Revision 16
2.6.10.3-5	Revision 16	2.6.12.3-6	Revision 16
2.6.10.3-6	Revision 16	2.6.12.3-7	Revision 16
2.6.10.3-7	Revision 16	2.6.12.4-1	Revision 16
2.6.11-1	Revision 16	2.6.12.4-2	Revision 16
2.6.11-2	Revision 16	2.6.12.4-3	Revision 16
2.6.11.1-1	Revision 16	2.6.12.5-1	Revision 16
2.6.11.1-2	Revision 16	2.6.12.5-2	Revision 16
2.6.11.1-3	Revision 16	2.6.12.5-3	Revision 16
2.6.11.1-4	Revision 16	2.6.12.6-1	Revision 16
2.6.11.2-1	Revision 16	2.6.12.6-2	Revision 16
2.6.11.2-2	Revision 16	2.6.12.7-1	Revision 16
2.6.11.2-3	Revision 16	2.6.12.7-2	Revision 16
2.6.11.2-4	Revision 16	2.6.12.7-3	Revision 16
2.6.11.2-5	Revision 16	2.6.12.7-4	Revision 16
2.6.11.2-6	Revision 16	2.6.12.7-5	Revision 16
2.6.11.2-7	Revision 16	2.6.12.7-6	Revision 16
2.6.11.2-8	Revision 16	2.6.12.7-7	Revision 16
2.6.11.2-9	Revision 16	2.6.12.7-8	Revision 16
2.6.11.2-10	Revision 16	2.6.12.7-9	Revision 16
2.6.11.2-11	Revision 16	2.6.12.7-10	Revision 16
2.6.11.3-1	Revision 16	2.6.12.7-11	Revision 16
2.6.12-1	Revision 16	2.6.12.7-12	Revision 16
2.6.12-2	Revision 16	2.6.12.7-13	Revision 16
2.6.12-3	Revision 16	2.6.12.7-14	Revision 16
2.6.12-4	Revision 16	2.6.12.7-15	Revision 16
2.6.12-5	Revision 16	2.6.12.7-16	Revision 16
2.6.12.1-1	Revision 16	2.6.12.7-17	Revision 16

List of Effective Pages (continued)

2.6.12.7-18	Revision 16	2.6.13.3-1	Revision 16
2.6.12.7-19	Revision 16	2.6.13.3-2	Revision 16
2.6.12.7-20	Revision 16	2.6.13.3-3	Revision 16
2.6.12.7-21	Revision 16	2.6.13.3-4	Revision 16
2.6.12.7-22	Revision 16	2.6.13.4-1	Revision 16
2.6.12.8-1	Revision 16	2.6.13.4-2	Revision 16
2.6.12.8-2	Revision 16	2.6.13.4-3	Revision 16
2.6.12.9-1	Revision 16	2.6.13.4-4	Revision 16
2.6.12.9-2	Revision 16	2.6.13.4-5	Revision 16
2.6.12.9-3	Revision 16	2.6.13.5-1	Revision 16
2.6.12.9-4	Revision 16	2.6.13.5-2	Revision 16
2.6.12.9-5	Revision 16	2.6.13.6-1	Revision 16
2.6.12.9-6	Revision 16	2.6.13.6-2	Revision 16
2.6.12.9-7	Revision 16	2.6.13.7-1	Revision 16
2.6.12.9-8	Revision 16	2.6.13.7-2	Revision 16
2.6.12.9-9	Revision 16	2.6.13.8-1	Revision 16
2.6.12.9-10	Revision 16	2.6.13.9-1	Revision 16
2.6.12.9-11	Revision 16	2.6.13.10-1	Revision 16
2.6.12.10-1	Revision 16	2.6.13.11-1	Revision 16
2.6.12.11-1	Revision 16	2.6.13.11-2	Revision 16
2.6.12.12-1	Revision 16	2.6.13.11-3	Revision 16
2.6.12.13-1	Revision 16	2.6.13.12-1	Revision 16
2.6.12.13-2	Revision 16	2.6.13.12-2	Revision 16
2.6.12.13-3	Revision 16	2.6.14-1	Revision 16
2.6.12.13-4	Revision 16	2.6.14-2	Revision 16
2.6.13-1	Revision 16	2.6.14-3	Revision 16
2.6.13-2	Revision 16	2.6.14-4	Revision 16
2.6.13-3	Revision 16	2.6.14-5	Revision 16
2.6.13.1-1	Revision 16	2.6.14-6	Revision 16
2.6.13.1-2	Revision 16	2.6.14-7	Revision 16
2.6.13.2-1	Revision 16	2.6.14-8	Revision 16
2.6.13.2-2	Revision 16	2.6.14.1-1	Revision 16
2.6.13.2-3	Revision 16	2.6.14.1-2	Revision 16
2.6.13.2-4	Revision 16	2.6.14.2-1	Revision 16
2.6.13.2-5	Revision 16	2.6.14.2-2	Revision 16
2.6.13.2-6	Revision 16	2.6.14.2-3	Revision 16
2.6.13.2-7	Revision 16	2.6.14.2-4	Revision 16

List of Effective Pages (continued)

2.6.14.2-5	Revision 16	2.6.14.8-1	Revision 16
2.6.14.2-6	Revision 16	2.6.14.8-2	Revision 16
2.6.14.2-7	Revision 16	2.6.14.8-3	Revision 16
2.6.14.2-8	Revision 16	2.6.14.8-4	Revision 16
2.6.14.2-9	Revision 16	2.6.14.8-5	Revision 16
2.6.14.2-10	Revision 16	2.6.14.8-6	Revision 16
2.6.14.2-11	Revision 16	2.6.14.9-1	Revision 16
2.6.14.2-12	Revision 16	2.6.14.10-1	Revision 16
2.6.14.2-13	Revision 16	2.6.14.11-1	Revision 16
2.6.14.2-14	Revision 16	2.6.14.11-2	Revision 16
2.6.14.2-15	Revision 16	2.6.14.11-3	Revision 16
2.6.14.2-16	Revision 16	2.6.14.11-4	Revision 16
2.6.14.3-1	Revision 16	2.6.14.11-5	Revision 16
2.6.14.3-2	Revision 16	2.6.14.12-1	Revision 16
2.6.14.3-3	Revision 16	2.6.14.12-2	Revision 16
2.6.14.4-1	Revision 16	2.6.14.12-3	Revision 16
2.6.14.4-2	Revision 16	2.6.14.12-4	Revision 16
2.6.14.4-3	Revision 16	2.6.14.12-5	Revision 16
2.6.14.4-4	Revision 16	2.6.15-1	Revision 16
2.6.14.5-1	Revision 16	2.6.15.1-1	Revision 16
2.6.14.5-2	Revision 16	2.6.15.1-2	Revision 16
2.6.14.5-3	Revision 16	2.6.15.2-1	Revision 16
2.6.14.6-1	Revision 16	2.6.15.2-2	Revision 16
2.6.14.7-1	Revision 16	2.6.15.2-3	Revision 16
2.6.14.7-2	Revision 16	2.6.15.2-4	Revision 16
2.6.14.7-3	Revision 16	2.6.15.2-5	Revision 16
2.6.14.7-4	Revision 16	2.6.15.2-6	Revision 16
2.6.14.7-5	Revision 16	2.6.15.2-7	Revision 16
2.6.14.7-6	Revision 16	2.6.15.3-1	Revision 16
2.6.14.7-7	Revision 16	2.6.15.3-2	Revision 16
2.6.14.7-8	Revision 16	2.6.15.3-3	Revision 16
2.6.14.7-9	Revision 16	2.6.15.3-4	Revision 16
2.6.14.7-10	Revision 16	2.6.15.4-1	Revision 16
2.6.14.7-11	Revision 16	2.6.15.4-2	Revision 16
2.6.14.7-12	Revision 16	2.6.15.4-3	Revision 16
2.6.14.7-13	Revision 16	2.6.15.4-4	Revision 16
2.6.14.7-14	Revision 16	2.6.15.5-1	Revision 16

List of Effective Pages (continued)

2.6.15.6-1	Revision 16	2.6.16.5-1	Revision 16
2.6.15.6-2	Revision 16	2.6.16.5-2	Revision 16
2.6.15.6-3	Revision 16	2.6.16.5-3	Revision 16
2.6.15.7-1	Revision 16	2.6.16.6-1	Revision 16
2.6.15.8-1	Revision 16	2.6.16.6-2	Revision 16
2.6.15.9-1	Revision 16	2.6.16.6-3	Revision 16
2.6.15.10-1	Revision 16	2.6.16.7-1	Revision 16
2.6.15.11-1	Revision 16	2.6.16.7-2	Revision 16
2.6.15.11-2	Revision 16	2.6.16.7-3	Revision 16
2.6.15.11-3	Revision 16	2.6.16.7-4	Revision 16
2.6.15.12-1	Revision 16	2.6.16.7-5	Revision 16
2.6.15.12-2	Revision 16	2.6.16.7-6	Revision 16
2.6.16-1	Revision 16	2.6.16.7-7	Revision 16
2.6.16-2	Revision 16	2.6.16.7-8	Revision 16
2.6.16-3	Revision 16	2.6.16.7-9	Revision 16
2.6.16-4	Revision 16	2.6.16.7-10	Revision 16
2.6.16-5	Revision 16	2.6.16.7-11	Revision 16
2.6.16-6	Revision 16	2.6.16.7-12	Revision 16
2.6.16.1-1	Revision 16	2.6.16.8-1	Revision 16
2.6.16.1-2	Revision 16	2.6.16.8-2	Revision 16
2.6.16.2-1	Revision 16	2.6.16.8-3	Revision 16
2.6.16.2-2	Revision 16	2.6.16.8-4	Revision 16
2.6.16.2-3	Revision 16	2.6.16.8-5	Revision 16
2.6.16.2-4	Revision 16	2.6.16.8-6	Revision 16
2.6.16.2-5	Revision 16	2.6.16.8-7	Revision 16
2.6.16.2-6	Revision 16	2.6.16.9-1	Revision 16
2.6.16.2-7	Revision 16	2.6.16.10-1	Revision 16
2.6.16.2-8	Revision 16	2.6.16.11-1	Revision 16
2.6.16.2-9	Revision 16	2.6.16.11-2	Revision 16
2.6.16.2-10	Revision 16	2.6.16.11-3	Revision 16
2.6.16.2-11	Revision 16	2.6.16.11-4	Revision 16
2.6.16.3-1	Revision 16	2.6.16.12-1	Revision 16
2.6.16.3-2	Revision 16	2.6.16.12-2	Revision 16
2.6.16.3-3	Revision 16	2.6.16.13-1	Revision 16
2.6.16.4-1	Revision 16	2.6.16.13-2	Revision 16
2.6.16.4-2	Revision 16	2.6.16.14-1	Revision 16
2.6.16.4-3	Revision 16	2.6.17-1	Revision 16

List of Effective Pages (continued)

2.6.17-2	Revision 16	2.6.19-20	Revision 16
2.6.17-3	Revision 16	2.6.19-21	Revision 16
2.6.17-4	Revision 16	2.6.19-22	Revision 16
2.6.17-5	Revision 16	2.6.19-23	Revision 16
2.6.17-6	Revision 16	2.6.20-1	Revision 16
2.6.17-7	Revision 16	2.6.20-2	Revision 16
2.6.17-8	Revision 16	2.6.20-3	Revision 16
2.6.17-9	Revision 16	2.6.20-4	Revision 16
2.6.17-10	Revision 16	2.6.20-5	Revision 16
2.6.17-11	Revision 16	2.6.20-6	Revision 16
2.6.17-12	Revision 16	2.6.20-7	Revision 16
2.6.17-13	Revision 16	2.6.20-8	Revision 16
2.6.18-1	Revision 16	2.6.20-9	Revision 16
2.6.18-2	Revision 16	2.6.20-10	Revision 16
2.6.18-3	Revision 16	2.6.20-11	Revision 16
2.6.18-4	Revision 16	2.6.20-12	Revision 16
2.6.18-5	Revision 16	2.6.20-13	Revision 16
2.6.18-6	Revision 16	2.6.20-14	Revision 16
2.6.19-1	Revision 16	2.6.20-15	Revision 16
2.6.19-2	Revision 16	2.6.20-16	Revision 16
2.6.19-3	Revision 16	2.6.20-17	Revision 16
2.6.19-4	Revision 16	2.6.20-18	Revision 16
2.6.19-5	Revision 16	2.6.20-19	Revision 16
2.6.19-6	Revision 16	2.6.20-20	Revision 16
2.6.19-7	Revision 16	2.6.21-1	Revision 16
2.6.19-8	Revision 16	2.6.21-2	Revision 16
2.6.19-9	Revision 16	2.7-1	Revision 16
2.6.19-10	Revision 16	2.7-2	Revision 16
2.6.19-11	Revision 16	2.7.1-1	Revision 16
2.6.19-12	Revision 16	2.7.1-2	Revision 16
2.6.19-13	Revision 16	2.7.1.1-1	Revision 16
2.6.19-14	Revision 16	2.7.1.1-2	Revision 16
2.6.19-15	Revision 16	2.7.1.1-3	Revision 16
2.6.19-16	Revision 16	2.7.1.1-4	Revision 16
2.6.19-17	Revision 16	2.7.1.1-5	Revision 16
2.6.19-18	Revision 16	2.7.1.1-6	Revision 16
2.6.19-19	Revision 16	2.7.1.1-7	Revision 16

List of Effective Pages (continued)

2.7.1.1-8	Revision 16	2.7.1.4-6	Revision 16
2.7.1.1-9	Revision 16	2.7.1.4-7	Revision 16
2.7.1.1-10	Revision 16	2.7.1.4-8	Revision 16
2.7.1.1-11	Revision 16	2.7.1.4-9	Revision 16
2.7.1.1-12	Revision 16	2.7.1.4-10	Revision 16
2.7.1.1-13	Revision 16	2.7.1.4-11	Revision 16
2.7.1.1-14	Revision 16	2.7.1.5-1	Revision 16
2.7.1.1-15	Revision 16	2.7.1.5-2	Revision 16
2.7.1.2-1	Revision 16	2.7.1.5-3	Revision 16
2.7.1.2-2	Revision 16	2.7.1.6-1	Revision 16
2.7.1.2-3	Revision 16	2.7.1.6-2	Revision 16
2.7.1.2-4	Revision 16	2.7.1.6-3	Revision 16
2.7.1.2-5	Revision 16	2.7.1.6-4	Revision 16
2.7.1.2-6	Revision 16	2.7.1.6-5	Revision 16
2.7.1.2-7	Revision 16	2.7.1.6-6	Revision 16
2.7.1.2-8	Revision 16	2.7.1.6-7	Revision 16
2.7.1.2-9	Revision 16	2.7.1.6-8	Revision 16
2.7.1.2-10	Revision 16	2.7.1.6-9	Revision 16
2.7.1.2-11	Revision 16	2.7.1.6-10	Revision 16
2.7.1.2-12	Revision 16	2.7.1.6-11	Revision 16
2.7.1.2-13	Revision 16	2.7.1.6-12	Revision 16
2.7.1.2-14	Revision 16	2.7.1.6-13	Revision 16
2.7.1.2-15	Revision 16	2.7.1.6-14	Revision 16
2.7.1.3-1	Revision 16	2.7.1.6-15	Revision 16
2.7.1.3-2	Revision 16	2.7.1.6-16	Revision 16
2.7.1.3-3	Revision 16	2.7.2-1	Revision 16
2.7.1.3-4	Revision 16	2.7.2.1-1	Revision 16
2.7.1.3-5	Revision 16	2.7.2.1-2	Revision 16
2.7.1.3-6	Revision 16	2.7.2.1-3	Revision 16
2.7.1.3-7	Revision 16	2.7.2.1-4	Revision 16
2.7.1.3-8	Revision 16	2.7.2.1-5	Revision 16
2.7.1.3-9	Revision 16	2.7.2.2-1	Revision 16
2.7.1.4-1	Revision 16	2.7.2.2-2	Revision 16
2.7.1.4-2	Revision 16	2.7.2.2-3	Revision 16
2.7.1.4-3	Revision 16	2.7.2.2-4	Revision 16
2.7.1.4-4	Revision 16	2.7.2.2-5	Revision 16
2.7.1.4-5	Revision 16	2.7.2.2-6	Revision 16

List of Effective Pages (continued)

2.7.2.2-7	Revision 16	2.7.7-4	Revision 16
2.7.2.2-8	Revision 16	2.7.8-1	Revision 16
2.7.2.2-9	Revision 16	2.7.8-2	Revision 16
2.7.2.3-1	Revision 16	2.7.8-3	Revision 16
2.7.2.3-2	Revision 16	2.7.8-4	Revision 16
2.7.2.3-3	Revision 16	2.7.8.1-1	Revision 16
2.7.2.3-4	Revision 16	2.7.8.1-2	Revision 16
2.7.2.3-5	Revision 16	2.7.8.1-3	Revision 16
2.7.2.3-6	Revision 16	2.7.8.1-4	Revision 16
2.7.2.4-1	Revision 16	2.7.8.1-5	Revision 16
2.7.2.4-2	Revision 16	2.7.8.1-6	Revision 16
2.7.2.4-3	Revision 16	2.7.8.1-7	Revision 16
2.7.2.4-4	Revision 16	2.7.8.1-8	Revision 16
2.7.2.4-5	Revision 16	2.7.8.1-9	Revision 16
2.7.2.4-6	Revision 16	2.7.8.1-10	Revision 16
2.7.2.4-7	Revision 16	2.7.8.1-11	Revision 16
2.7.2.5-1	Revision 16	2.7.8.1-12	Revision 16
2.7.2.6-1	Revision 16	2.7.8.1-13	Revision 16
2.7.3.1-1	Revision 16	2.7.8.1-14	Revision 16
2.7.3.2-1	Revision 16	2.7.8.1-15	Revision 16
2.7.3.2-2	Revision 16	2.7.8.1-16	Revision 16
2.7.3.2-3	Revision 16	2.7.8.1-17	Revision 16
2.7.3.2-4	Revision 16	2.7.8.1-18	Revision 16
2.7.3.2-5	Revision 16	2.7.8.1-19	Revision 16
2.7.3.3-1	Revision 16	2.7.8.1-20	Revision 16
2.7.3.3-2	Revision 16	2.7.8.1-21	Revision 16
2.7.3.3-3	Revision 16	2.7.8.1-22	Revision 16
2.7.3.4-1	Revision 16	2.7.8.1-23	Revision 16
2.7.3.4-2	Revision 16	2.7.8.1-24	Revision 16
2.7.3.5-1	Revision 16	2.7.8.1-25	Revision 16
2.7.3.6-1	Revision 16	2.7.8.1-26	Revision 16
2.7.4-1	Revision 16	2.7.8.1-27	Revision 16
2.7.5-1	Revision 16	2.7.8.1-28	Revision 16
2.7.6-1	Revision 16	2.7.8.1-29	Revision 16
2.7.7-1	Revision 16	2.7.8.1-30	Revision 16
2.7.7-2	Revision 16	2.7.8.1-31	Revision 16
2.7.7-3	Revision 16	2.7.8.1-32	Revision 16

List of Effective Pages (continued)

2.7.8.1-33	Revision 16	2.7.9-1	Revision 16
2.7.8.1-34	Revision 16	2.7.9-2	Revision 16
2.7.8.1-35	Revision 16	2.7.9-3	Revision 16
2.7.8.1-36	Revision 16	2.7.9-4	Revision 16
2.7.8.1-37	Revision 16	2.7.9-5	Revision 16
2.7.8.1-38	Revision 16	2.7.9-6	Revision 16
2.7.8.1-39	Revision 16	2.7.9-7	Revision 16
2.7.8.1-40	Revision 16	2.7.9-8	Revision 16
2.7.8.1-41	Revision 16	2.7.9-9	Revision 16
2.7.8.1-42	Revision 16	2.7.9-10	Revision 16
2.7.8.1-43	Revision 16	2.7.9-11	Revision 16
2.7.8.2-1	Revision 16	2.7.9-12	Revision 16
2.7.8.2-2	Revision 16	2.7.9-13	Revision 16
2.7.8.3-1	Revision 16	2.7.9-14	Revision 16
2.7.8.3-2	Revision 16	2.7.9-15	Revision 16
2.7.8.3-3	Revision 16	2.7.9-16	Revision 16
2.7.8.3-4	Revision 16	2.7.9-17	Revision 16
2.7.8.3-5	Revision 16	2.7.9-18	Revision 16
2.7.8.3-6	Revision 16	2.7.9-19	Revision 16
2.7.8.3-7	Revision 16	2.7.9-20	Revision 16
2.7.8.3-8	Revision 16	2.7.9-21	Revision 16
2.7.8.3-9	Revision 16	2.7.9-22	Revision 16
2.7.8.3-10	Revision 16	2.7.9-23	Revision 16
2.7.8.3-11	Revision 16	2.7.9-24	Revision 16
2.7.8.3-12	Revision 16	2.7.9-25	Revision 16
2.7.8.3-13	Revision 16	2.7.9-26	Revision 16
2.7.8.4-1	Revision 16	2.7.9-27	Revision 16
2.7.8.4-2	Revision 16	2.7.9-28	Revision 16
2.7.8.4-3	Revision 16	2.7.9-29	Revision 16
2.7.8.4-4	Revision 16	2.7.9-30	Revision 16
2.7.8.4-5	Revision 16	2.7.9-31	Revision 16
2.7.8.4-6	Revision 16	2.7.9-32	Revision 16
2.7.8.4-7	Revision 16	2.7.9-33	Revision 16
2.7.8.4-8	Revision 16	2.7.9-34	Revision 16
2.7.8.4-9	Revision 16	2.7.9-35	Revision 16
2.7.8.4-10	Revision 16	2.7.9-36	Revision 16
2.7.8.5-1	Revision 16	2.7.9-37	Revision 16

List of Effective Pages (continued)

2.7.9-38	Revision 16	2.7.12-7	Revision 16
2.7.9-39	Revision 16	2.7.12-8	Revision 16
2.7.9-40	Revision 16	2.7.12-9	Revision 16
2.7.10-1	Revision 16	2.7.12-10	Revision 16
2.7.10-2	Revision 16	2.7.13-1	Revision 16
2.7.10-3	Revision 16	2.7.13-2	Revision 16
2.7.10-4	Revision 16	2.7.13-3	Revision 16
2.7.10-5	Revision 16	2.7.13-4	Revision 16
2.7.10-6	Revision 16	2.7.13.1-1	Revision 16
2.7.10-7	Revision 16	2.7.13.1-2	Revision 16
2.7.10-8	Revision 16	2.7.13.1-3	Revision 16
2.7.10-9	Revision 16	2.7.13.1-4	Revision 16
2.7.10-10	Revision 16	2.7.13.1-5	Revision 16
2.7.10-11	Revision 16	2.7.13.1-6	Revision 16
2.7.10-12	Revision 16	2.7.13.1-7	Revision 16
2.7.11-1	Revision 16	2.7.13.1-8	Revision 16
2.7.11-2	Revision 16	2.7.13.1-9	Revision 16
2.7.11-3	Revision 16	2.7.13.1-10	Revision 16
2.7.11-4	Revision 16	2.7.13.1-11	Revision 16
2.7.11-5	Revision 16	2.7.13.1-12	Revision 16
2.7.11-6	Revision 16	2.7.13.1-13	Revision 16
2.7.11-7	Revision 16	2.7.13.1-14	Revision 16
2.7.11-8	Revision 16	2.7.13.1-15	Revision 16
2.7.11-9	Revision 16	2.7.13.1-16	Revision 16
2.7.11-10	Revision 16	2.7.13.1-17	Revision 16
2.7.11-11	Revision 16	2.7.13.1-18	Revision 16
2.7.11-12	Revision 16	2.7.13.2-1	Revision 16
2.7.11-13	Revision 16	2.7.13.2-2	Revision 16
2.7.11-14	Revision 16	2.7.13.3-1	Revision 16
2.7.11-15	Revision 16	2.7.13.3-2	Revision 16
2.7.11-16	Revision 16	2.7.13.3-3	Revision 16
2.7.12-1	Revision 16	2.7.13.3-4	Revision 16
2.7.12-2	Revision 16	2.7.13.4-1	Revision 16
2.7.12-3	Revision 16	2.7.13.4-2	Revision 16
2.7.12-4	Revision 16	2.7.13.4-3	Revision 16
2.7.12-5	Revision 16	2.7.13.4-4	Revision 16
2.7.12-6	Revision 16	2.7.13.4-5	Revision 16

List of Effective Pages (continued)

2.7.13.4-6	Revision 16	2.9-3	Revision 16
2.7.13.4-7	Revision 16	2.9-4	Revision 16
2.7.13.4-8	Revision 16	2.9-5	Revision 16
2.7.13.5-1	Revision 16	2.9-6	Revision 16
2.7.13.5-2	Revision 16	2.9-7	Revision 16
2.7.14-1	Revision 16	2.9-8	Revision 16
2.7.14-2	Revision 16	2.9-9	Revision 16
2.7.14-3	Revision 16	2.9-10	Revision 16
2.7.14-4	Revision 16	2.9-11	Revision 16
2.7.14-5	Revision 16	2.10.1-1	Revision 16
2.7.14-6	Revision 16	2.10.1-2	Revision 16
2.7.14-7	Revision 16	2.10.1-3	Revision 16
2.7.14-8	Revision 16	2.10.1-4	Revision 16
2.7.14-9	Revision 16	2.10.2-1	Revision 16
2.7.14-10	Revision 16	2.10.2-2	Revision 16
2.7.14-11	Revision 16	2.10.2-3	Revision 16
2.7.14-12	Revision 16	2.10.2-4	Revision 16
2.7.14-13	Revision 16	2.10.2-5	Revision 16
2.7.15-1	Revision 16	2.10.2-6	Revision 16
2.7.15-2	Revision 16	2.10.2-7	Revision 16
2.7.15-3	Revision 16	2.10.2-8	Revision 16
2.7.15-4	Revision 16	2.10.2-9	Revision 16
2.7.15-5	Revision 16	2.10.2-10	Revision 16
2.7.15-6	Revision 16	2.10.2-11	Revision 16
2.7.15-7	Revision 16	2.10.2-12	Revision 16
2.7.15-8	Revision 16	2.10.2-13	Revision 16
2.7.15-9	Revision 16	2.10.2-14	Revision 16
2.7.15-10	Revision 16	2.10.2-15	Revision 16
2.7.15-11	Revision 16	2.10.2-16	Revision 16
2.7.15-12	Revision 16	2.10.2-17	Revision 16
2.7.15-13	Revision 16	2.10.2-18	Revision 16
2.7.15-14	Revision 16	2.10.2-19	Revision 16
2.7.15-15	Revision 16	2.10.2-20	Revision 16
2.7.15-16	Revision 16	2.10.2-21	Revision 16
2.8-1	Revision 16	2.10.2-22	Revision 16
2.9-1	Revision 16	2.10.2-23	Revision 16
2.9-2	Revision 16	2.10.2-24	Revision 16

List of Effective Pages (continued)

2.10.2-25	Revision 16	2.10.2-62	Revision 16
2.10.2-26	Revision 16	2.10.2-63	Revision 16
2.10.2-27	Revision 16	2.10.2-64	Revision 16
2.10.2-28	Revision 16	2.10.2-65	Revision 16
2.10.2-29	Revision 16	2.10.2-66	Revision 16
2.10.2-30	Revision 16	2.10.2-67	Revision 16
2.10.2-31	Revision 16	2.10.2-68	Revision 16
2.10.2-32	Revision 16	2.10.2-69	Revision 16
2.10.2-33	Revision 16	2.10.2-70	Revision 16
2.10.2-34	Revision 16	2.10.2-71	Revision 16
2.10.2-35	Revision 16	2.10.2-72	Revision 16
2.10.2-36	Revision 16	2.10.2-73	Revision 16
2.10.2-37	Revision 16	2.10.2-74	Revision 16
2.10.2-38	Revision 16	2.10.2-75	Revision 16
2.10.2-39	Revision 16	2.10.2-76	Revision 16
2.10.2-40	Revision 16	2.10.2-77	Revision 16
2.10.2-41	Revision 16	2.10.2-78	Revision 16
2.10.2-42	Revision 16	2.10.2-79	Revision 16
2.10.2-43	Revision 16	2.10.2-80	Revision 16
2.10.2-44	Revision 16	2.10.2-81	Revision 16
2.10.2-45	Revision 16	2.10.2-82	Revision 16
2.10.2-46	Revision 16	2.10.2-83	Revision 16
2.10.2-47	Revision 16	2.10.2-84	Revision 16
2.10.2-48	Revision 16	2.10.2-85	Revision 16
2.10.2-49	Revision 16	2.10.2-86	Revision 16
2.10.2-50	Revision 16	2.10.2-87	Revision 16
2.10.2-51	Revision 16	2.10.2-88	Revision 16
2.10.2-52	Revision 16	2.10.2-89	Revision 16
2.10.2-53	Revision 16	2.10.2-90	Revision 16
2.10.2-54	Revision 16	2.10.2-91	Revision 16
2.10.2-55	Revision 16	2.10.2-92	Revision 16
2.10.2-56	Revision 16	2.10.2-93	Revision 16
2.10.2-57	Revision 16	2.10.3-1	Revision 16
2.10.2-58	Revision 16	2.10.3-2	Revision 16
2.10.2-59	Revision 16	2.10.3-3	Revision 16
2.10.2-60	Revision 16	2.10.3-4	Revision 16
2.10.2-61	Revision 16	2.10.3-5	Revision 16

List of Effective Pages (continued)

2.10.3-6	Revision 16	2.10.4-36	Revision 16
2.10.3-7	Revision 16	2.10.4-37	Revision 16
2.10.4-1	Revision 16	2.10.4-38	Revision 16
2.10.4-2	Revision 16	2.10.4-39	Revision 16
2.10.4-3	Revision 16	2.10.4-40	Revision 16
2.10.4-4	Revision 16	2.10.4-41	Revision 16
2.10.4-5	Revision 16	2.10.4-42	Revision 16
2.10.4-6	Revision 16	2.10.4-43	Revision 16
2.10.4-7	Revision 16	2.10.4-44	Revision 16
2.10.4-8	Revision 16	2.10.4-45	Revision 16
2.10.4-9	Revision 16	2.10.4-46	Revision 16
2.10.4-10	Revision 16	2.10.4-47	Revision 16
2.10.4-11	Revision 16	2.10.4-48	Revision 16
2.10.4-12	Revision 16	2.10.4-49	Revision 16
2.10.4-13	Revision 16	2.10.4-50	Revision 16
2.10.4-14	Revision 16	2.10.4-51	Revision 16
2.10.4-15	Revision 16	2.10.4-52	Revision 16
2.10.4-16	Revision 16	2.10.4-53	Revision 16
2.10.4-17	Revision 16	2.10.4-54	Revision 16
2.10.4-18	Revision 16	2.10.4-55	Revision 16
2.10.4-19	Revision 16	2.10.4-56	Revision 16
2.10.4-20	Revision 16	2.10.4-57	Revision 16
2.10.4-21	Revision 16	2.10.4-58	Revision 16
2.10.4-22	Revision 16	2.10.4-59	Revision 16
2.10.4-23	Revision 16	2.10.4-60	Revision 16
2.10.4-24	Revision 16	2.10.4-61	Revision 16
2.10.4-25	Revision 16	2.10.4-62	Revision 16
2.10.4-26	Revision 16	2.10.4-63	Revision 16
2.10.4-27	Revision 16	2.10.4-64	Revision 16
2.10.4-28	Revision 16	2.10.4-65	Revision 16
2.10.4-29	Revision 16	2.10.4-66	Revision 16
2.10.4-30	Revision 16	2.10.4-67	Revision 16
2.10.4-31	Revision 16	2.10.4-68	Revision 16
2.10.4-32	Revision 16	2.10.4-69	Revision 16
2.10.4-33	Revision 16	2.10.4-70	Revision 16
2.10.4-34	Revision 16	2.10.4-71	Revision 16
2.10.4-35	Revision 16	2.10.4-72	Revision 16

List of Effective Pages (continued)

2.10.4-73	Revision 16	2.10.4-110	Revision 16
2.10.4-74	Revision 16	2.10.4-111	Revision 16
2.10.4-75	Revision 16	2.10.4-112	Revision 16
2.10.4-76	Revision 16	2.10.4-113	Revision 16
2.10.4-77	Revision 16	2.10.4-114	Revision 16
2.10.4-78	Revision 16	2.10.4-115	Revision 16
2.10.4-79	Revision 16	2.10.4-116	Revision 16
2.10.4-80	Revision 16	2.10.4-117	Revision 16
2.10.4-81	Revision 16	2.10.4-118	Revision 16
2.10.4-82	Revision 16	2.10.4-119	Revision 16
2.10.4-83	Revision 16	2.10.4-120	Revision 16
2.10.4-84	Revision 16	2.10.4-121	Revision 16
2.10.4-85	Revision 16	2.10.4-122	Revision 16
2.10.4-86	Revision 16	2.10.4-123	Revision 16
2.10.4-87	Revision 16	2.10.4-124	Revision 16
2.10.4-88	Revision 16	2.10.4-125	Revision 16
2.10.4-89	Revision 16	2.10.4-126	Revision 16
2.10.4-90	Revision 16	2.10.4-127	Revision 16
2.10.4-91	Revision 16	2.10.4-128	Revision 16
2.10.4-92	Revision 16	2.10.4-129	Revision 16
2.10.4-93	Revision 16	2.10.4-130	Revision 16
2.10.4-94	Revision 16	2.10.4-131	Revision 16
2.10.4-95	Revision 16	2.10.4-132	Revision 16
2.10.4-96	Revision 16	2.10.4-133	Revision 16
2.10.4-97	Revision 16	2.10.4-134	Revision 16
2.10.4-98	Revision 16	2.10.4-135	Revision 16
2.10.4-99	Revision 16	2.10.4-136	Revision 16
2.10.4-100	Revision 16	2.10.4-137	Revision 16
2.10.4-101	Revision 16	2.10.4-138	Revision 16
2.10.4-102	Revision 16	2.10.4-139	Revision 16
2.10.4-103	Revision 16	2.10.4-140	Revision 16
2.10.4-104	Revision 16	2.10.4-141	Revision 16
2.10.4-105	Revision 16	2.10.4-142	Revision 16
2.10.4-106	Revision 16	2.10.4-143	Revision 16
2.10.4-107	Revision 16	2.10.4-144	Revision 16
2.10.4-108	Revision 16	2.10.4-145	Revision 16
2.10.4-109	Revision 16	2.10.4-146	Revision 16

List of Effective Pages (continued)

2.10.4-147	Revision 16	2.10.4-184	Revision 16
2.10.4-148	Revision 16	2.10.4-185	Revision 16
2.10.4-149	Revision 16	2.10.4-186	Revision 16
2.10.4-150	Revision 16	2.10.4-187	Revision 16
2.10.4-151	Revision 16	2.10.4-188	Revision 16
2.10.4-152	Revision 16	2.10.4-189	Revision 16
2.10.4-153	Revision 16	2.10.4-190	Revision 16
2.10.4-154	Revision 16	2.10.4-191	Revision 16
2.10.4-155	Revision 16	2.10.4-192	Revision 16
2.10.4-156	Revision 16	2.10.4-193	Revision 16
2.10.4-157	Revision 16	2.10.4-194	Revision 16
2.10.4-158	Revision 16	2.10.4-195	Revision 16
2.10.4-159	Revision 16	2.10.4-196	Revision 16
2.10.4-160	Revision 16	2.10.4-197	Revision 16
2.10.4-161	Revision 16	2.10.4-198	Revision 16
2.10.4-162	Revision 16	2.10.4-199	Revision 16
2.10.4-163	Revision 16	2.10.4-200	Revision 16
2.10.4-164	Revision 16	2.10.4-201	Revision 16
2.10.4-165	Revision 16	2.10.4-202	Revision 16
2.10.4-166	Revision 16	2.10.4-203	Revision 16
2.10.4-167	Revision 16	2.10.4-204	Revision 16
2.10.4-168	Revision 16	2.10.4-205	Revision 16
2.10.4-169	Revision 16	2.10.4-206	Revision 16
2.10.4-170	Revision 16	2.10.4-207	Revision 16
2.10.4-171	Revision 16	2.10.4-208	Revision 16
2.10.4-172	Revision 16	2.10.4-209	Revision 16
2.10.4-173	Revision 16	2.10.4-210	Revision 16
2.10.4-174	Revision 16	2.10.4-211	Revision 16
2.10.4-175	Revision 16	2.10.4-212	Revision 16
2.10.4-176	Revision 16	2.10.4-213	Revision 16
2.10.4-177	Revision 16	2.10.4-214	Revision 16
2.10.4-178	Revision 16	2.10.4-215	Revision 16
2.10.4-179	Revision 16	2.10.4-216	Revision 16
2.10.4-180	Revision 16	2.10.4-217	Revision 16
2.10.4-181	Revision 16	2.10.4-218	Revision 16
2.10.4-182	Revision 16	2.10.4-219	Revision 16
2.10.4-183	Revision 16	2.10.4-220	Revision 16

List of Effective Pages (continued)

2.10.4-221	Revision 16	2.10.4-258	Revision 16
2.10.4-222	Revision 16	2.10.4-259	Revision 16
2.10.4-223	Revision 16	2.10.4-260	Revision 16
2.10.4-224	Revision 16	2.10.4-261	Revision 16
2.10.4-225	Revision 16	2.10.4-262	Revision 16
2.10.4-226	Revision 16	2.10.4-263	Revision 16
2.10.4-227	Revision 16	2.10.4-264	Revision 16
2.10.4-228	Revision 16	2.10.4-265	Revision 16
2.10.4-229	Revision 16	2.10.4-266	Revision 16
2.10.4-230	Revision 16	2.10.4-267	Revision 16
2.10.4-231	Revision 16	2.10.4-268	Revision 16
2.10.4-232	Revision 16	2.10.4-269	Revision 16
2.10.4-233	Revision 16	2.10.4-270	Revision 16
2.10.4-234	Revision 16	2.10.4-271	Revision 16
2.10.4-235	Revision 16	2.10.4-272	Revision 16
2.10.4-236	Revision 16	2.10.4-273	Revision 16
2.10.4-237	Revision 16	2.10.4-274	Revision 16
2.10.4-238	Revision 16	2.10.4-275	Revision 16
2.10.4-239	Revision 16	2.10.4-276	Revision 16
2.10.4-240	Revision 16	2.10.4-277	Revision 16
2.10.4-241	Revision 16	2.10.4-278	Revision 16
2.10.4-242	Revision 16	2.10.4-279	Revision 16
2.10.4-243	Revision 16	2.10.4-280	Revision 16
2.10.4-244	Revision 16	2.10.4-281	Revision 16
2.10.4-245	Revision 16	2.10.4-282	Revision 16
2.10.4-246	Revision 16	2.10.4-283	Revision 16
2.10.4-247	Revision 16	2.10.4-284	Revision 16
2.10.4-248	Revision 16	2.10.4-285	Revision 16
2.10.4-249	Revision 16	2.10.4-286	Revision 16
2.10.4-250	Revision 16	2.10.4-287	Revision 16
2.10.4-251	Revision 16	2.10.4-288	Revision 16
2.10.4-252	Revision 16	2.10.5-1	Revision 16
2.10.4-253	Revision 16	2.10.5-2	Revision 16
2.10.4-254	Revision 16	2.10.5-3	Revision 16
2.10.4-255	Revision 16	2.10.5-4	Revision 16
2.10.4-256	Revision 16	2.10.5-5	Revision 16
2.10.4-257	Revision 16	2.10.5-6	Revision 16

List of Effective Pages (continued)

2.10.5-7	Revision 16	2.10.6-22	Revision 16
2.10.5-8	Revision 16	2.10.6-23	Revision 16
2.10.5-9	Revision 16	2.10.6-24	Revision 16
2.10.5-10	Revision 16	2.10.6-25	Revision 16
2.10.5-11	Revision 16	2.10.6-26	Revision 16
2.10.5-12	Revision 16	2.10.6-27	Revision 16
2.10.5-13	Revision 16	2.10.6-28	Revision 16
2.10.5-14	Revision 16	2.10.6-29	Revision 16
2.10.5-15	Revision 16	2.10.6-30	Revision 16
2.10.5-16	Revision 16	2.10.6-31	Revision 16
2.10.5-17	Revision 16	2.10.6-32	Revision 16
2.10.5-18	Revision 16	2.10.6-33	Revision 16
2.10.5-19	Revision 16	2.10.6-34	Revision 16
2.10.5-20	Revision 16	2.10.6-35	Revision 16
2.10.5-21	Revision 16	2.10.6-36	Revision 16
2.10.5-22	Revision 16		
2.10.6-1	Revision 16	13 drawings in Sections	
2.10.6-2	Revision 16	2.10.6.6 and 2.10.6.7	
2.10.6-3	Revision 16		
2.10.6-4	Revision 16	2.10.6-37	Revision 16
2.10.6-5	Revision 16	2.10.6-38	Revision 16
2.10.6-6	Revision 16	2.10.6-39	Revision 16
2.10.6-7	Revision 16	2.10.6-40	Revision 16
2.10.6-8	Revision 16	2.10.6-41	Revision 16
2.10.6-9	Revision 16	2.10.6-42	Revision 16
2.10.6-10	Revision 16	2.10.6-43	Revision 16
2.10.6-11	Revision 16	2.10.6-44	Revision 16
2.10.6-12	Revision 16	2.10.6-45	Revision 16
2.10.6-13	Revision 16	2.10.6-46	Revision 16
2.10.6-14	Revision 16	2.10.6-47	Revision 16
2.10.6-15	Revision 16	2.10.6-48	Revision 16
2.10.6-16	Revision 16	2.10.6-49	Revision 16
2.10.6-17	Revision 16	2.10.6-50	Revision 16
2.10.6-18	Revision 16	2.10.6-51	Revision 16
2.10.6-19	Revision 16	2.10.6-52	Revision 16
2.10.6-20	Revision 16	2.10.6-53	Revision 16
2.10.6-21	Revision 16	2.10.6-54	Revision 16

List of Effective Pages (continued)

2.10.6-55	Revision 16	2.10.7-4	Revision 16
2.10.6-56	Revision 16	2.10.7-5	Revision 16
2.10.6-57	Revision 16	2.10.7-6	Revision 16
2.10.6-58	Revision 16	2.10.7-7	Revision 16
2.10.6-59	Revision 16	2.10.7-8	Revision 16
2.10.6-60	Revision 16	2.10.7-9	Revision 16
2.10.6-61	Revision 16	2.10.7-10	Revision 16
2.10.6-62	Revision 16	2.10.7-11	Revision 16
2.10.6-63	Revision 16	2.10.7-12	Revision 16
2.10.6-64	Revision 16	2.10.7-13	Revision 16
2.10.6-65	Revision 16	2.10.7-14	Revision 16
2.10.6-66	Revision 16	2.10.7-15	Revision 16
2.10.6-67	Revision 16	2.10.7-16	Revision 16
2.10.6-68	Revision 16	2.10.7-17	Revision 16
2.10.6-69	Revision 16	2.10.7-18	Revision 16
2.10.6-70	Revision 16	2.10.7-19	Revision 16
2.10.6-71	Revision 16	2.10.7-20	Revision 16
2.10.6-72	Revision 16	2.10.7-21	Revision 16
2.10.6-73	Revision 16	2.10.7-22	Revision 16
2.10.6-74	Revision 16	2.10.7-23	Revision 16
2.10.6-75	Revision 16	2.10.7-24	Revision 16
2.10.6-76	Revision 16	2.10.7-25	Revision 16
2.10.6-77	Revision 16	2.10.7-26	Revision 16
2.10.6-78	Revision 16	2.10.8-1	Revision 16
2.10.6-79	Revision 16	2.10.8-2	Revision 16
2.10.6-80	Revision 16	2.10.8-3	Revision 16
2.10.6-81	Revision 16	2.10.8-4	Revision 16
2.10.6-82	Revision 16	2.10.8-5	Revision 16
2.10.6-83	Revision 16	2.10.8-6	Revision 16
2.10.6-84	Revision 16	2.10.8-7	Revision 16
2.10.6-85	Revision 16	2.10.8-8	Revision 16
2.10.6-86	Revision 16	2.10.8-9	Revision 16
2.10.6-87	Revision 16	2.10.8-10	Revision 16
2.10.6-88	Revision 16	2.10.8-11	Revision 16
2.10.7-1	Revision 16	2.10.8-12	Revision 16
2.10.7-2	Revision 16	2.10.8-13	Revision 16
2.10.7-3	Revision 16	2.10.8-14	Revision 16

List of Effective Pages (continued)

2.10.8-15	Revision 16	2.10.11-6	Revision 16
2.10.8-16	Revision 16	2.10.11-7	Revision 16
2.10.8-17	Revision 16	2.10.11-8	Revision 16
2.10.8-18	Revision 16	2.10.12-1	Revision 16
2.10.8-19	Revision 16	2.10.12-2	Revision 16
2.10.8-20	Revision 16	2.10.12-3	Revision 16
2.10.8-21	Revision 16	2.10.12-4	Revision 16
2.10.8-22	Revision 16	2.10.12-5	Revision 16
2.10.8-23	Revision 16	2.10.12-6	Revision 16
2.10.8-24	Revision 16	2.10.12-7	Revision 16
2.10.9-1	Revision 16	2.10.12-8	Revision 16
2.10.9-2	Revision 16	2.10.12-9	Revision 16
2.10.9-3	Revision 16	2.10.12-10	Revision 16
2.10.9-4	Revision 16	2.10.12-11	Revision 16
2.10.9-5	Revision 16	2.10.12-12	Revision 16
2.10.9-6	Revision 16	2.10.12-13	Revision 16
2.10.9-7	Revision 16	2.10.12-14	Revision 16
2.10.9-8	Revision 16	2.10.12-15	Revision 16
2.10.9-9	Revision 16	2.10.12-16	Revision 16
2.10.9-10	Revision 16	2.10.12-17	Revision 16
2.10.9-11	Revision 16	2.10.12-18	Revision 16
2.10.10-1	Revision 16	2.10.12-19	Revision 16
2.10.10-2	Revision 16	2.10.12-20	Revision 16
2.10.10-3	Revision 16	2.10.12-21	Revision 16
2.10.10-4	Revision 16	2.10.12-22	Revision 16
2.10.10-5	Revision 16	2.10.12-23	Revision 16
2.10.10-6	Revision 16	2.10.12-24	Revision 16
2.10.10-7	Revision 16	2.10.12-25	Revision 16
2.10.10-8	Revision 16	2.10.12-26	Revision 16
2.10.10-9	Revision 16	2.10.12-27	Revision 16
2.10.10-10	Revision 16	2.10.12-28	Revision 16
2.10.10-11	Revision 16	2.10.12-29	Revision 16
2.10.11-1	Revision 16	2.10.12-30	Revision 16
2.10.11-2	Revision 16	2.10.12-31	Revision 16
2.10.11-3	Revision 16		
2.10.11-4	Revision 16		
2.10.11-5	Revision 16		
		4 drawings in Section 2.10.12	

List of Effective Pages (continued)

Chapter 3	
3-i	Revision 16
3-ii	Revision 16
3-iii	Revision 16
3-iv	Revision 16
3-v	Revision 16
3-vi	Revision 16
3.1-1	Revision 16
3.1-2	Revision 16
3.1-3	Revision 16
3.1-4	Revision 16
3.1-5	Revision 16
3.1-6	Revision 16
3.1-7	Revision 16
3.1-8	Revision 16
3.1-9	Revision 16
3.1-10	Revision 16
3.1-11	Revision 16
3.2-1	Revision 16
3.2-2	Revision 16
3.2-3	Revision 16
3.2-4	Revision 16
3.2-5	Revision 16
3.2-6	Revision 16
3.2-7	Revision 16
3.2-8	Revision 16
3.2-9	Revision 16
3.2-10	Revision 16
3.2-11	Revision 16
3.2-12	Revision 16
3.2-13	Revision 16
3.2-14	Revision 16
3.3-1	Revision 16
3.3-2	Revision 16
3.3-3	Revision 16
3.3-4	Revision 16
3.3-5	Revision 16
3.3-6	Revision 16
3.4-1	Revision 16
3.4-2	Revision 16
3.4-3	Revision 16
3.4-4	Revision 16
3.4-5	Revision 16
3.4-6	Revision 16
3.4-7	Revision 16
3.4-8	Revision 16
3.4-9	Revision 16
3.4-10	Revision 16
3.4-11	Revision 16
3.4-12	Revision 16
3.4-13	Revision 16
3.4-14	Revision 16
3.4-15	Revision 16
3.4-16	Revision 16
3.4-17	Revision 16
3.4-18	Revision 16
3.4-19	Revision 16
3.4-20	Revision 16
3.4-21	Revision 16
3.4-22	Revision 16
3.4-23	Revision 16
3.4-24	Revision 16
3.4-25	Revision 16
3.4-26	Revision 16
3.4-27	Revision 16
3.4-28	Revision 16
3.4-29	Revision 16
3.4-30	Revision 16
3.4-31	Revision 16
3.4-32	Revision 16
3.4-33	Revision 16
3.4-34	Revision 16
3.4-35	Revision 16

List of Effective Pages (continued)

3.4-36	Revision 16	3.4-73	Revision 16
3.4-37	Revision 16	3.4-74	Revision 16
3.4-38	Revision 16	3.4-75	Revision 16
3.4-39	Revision 16	3.4-76	Revision 16
3.4-40	Revision 16	3.4-77	Revision 16
3.4-41	Revision 16	3.4-78	Revision 16
3.4-42	Revision 16	3.4-79	Revision 16
3.4-43	Revision 16	3.4-80	Revision 16
3.4-44	Revision 16	3.4-81	Revision 16
3.4-45	Revision 16	3.4-82	Revision 16
3.4-46	Revision 16	3.4-83	Revision 16
3.4-47	Revision 16	3.4-84	Revision 16
3.4-48	Revision 16	3.4-85	Revision 16
3.4-49	Revision 16	3.4-86	Revision 16
3.4-50	Revision 16	3.4-87	Revision 16
3.4-51	Revision 16	3.4-88	Revision 16
3.4-52	Revision 16	3.4-89	Revision 16
3.4-53	Revision 16	3.5-1	Revision 16
3.4-54	Revision 16	3.5-2	Revision 16
3.4-55	Revision 16	3.5-3	Revision 16
3.4-56	Revision 16	3.5-4	Revision 16
3.4-57	Revision 16	3.5-5	Revision 16
3.4-58	Revision 16	3.5-6	Revision 16
3.4-59	Revision 16	3.5-7	Revision 16
3.4-60	Revision 16	3.5-8	Revision 16
3.4-61	Revision 16	3.5-9	Revision 16
3.4-62	Revision 16	3.5-10	Revision 16
3.4-63	Revision 16	3.5-11	Revision 16
3.4-64	Revision 16	3.5-12	Revision 16
3.4-65	Revision 16	3.5-13	Revision 16
3.4-66	Revision 16	3.5-14	Revision 16
3.4-67	Revision 16	3.5-15	Revision 16
3.4-68	Revision 16	3.5-16	Revision 16
3.4-69	Revision 16		
3.4-70	Revision 16		
3.4-71	Revision 16		
3.4-72	Revision 16		

Chapter 4

4-i	Revision 16
-----------	-------------

List of Effective Pages (continued)

4-ii.....	Revision 16	4.5-6.....	Revision 16
4.1-1.....	Revision 16	4.5-7.....	Revision 16
4.1-2.....	Revision 16	4.5-8.....	Revision 16
4.1-3.....	Revision 16	4.5-9.....	Revision 16
4.1-4.....	Revision 16	4.5-10.....	Revision 16
4.1-5.....	Revision 16	4.5-11.....	Revision 16
4.1-6.....	Revision 16	4.5-12.....	Revision 16
4.1-7.....	Revision 16	4.5-13.....	Revision 16
4.1-8.....	Revision 16	4.5-14.....	Revision 16
4.1-9.....	Revision 16	4.5-15.....	Revision 16
4.2-1.....	Revision 16	4.5-16.....	Revision 16
4.2-2.....	Revision 16	4.5-17.....	Revision 16
4.2-3.....	Revision 16	4.5-18.....	Revision 16
4.2-4.....	Revision 16	4.5-19.....	Revision 16
4.2-5.....	Revision 16	4.5-20.....	Revision 16
4.2-6.....	Revision 16	4.5-21.....	Revision 16
4.2-7.....	Revision 16	4.5-22.....	Revision 16
4.2-8.....	Revision 16	4.5-23.....	Revision 16
4.2-9.....	Revision 16	4.5-24.....	Revision 16
4.2-10.....	Revision 16	4.5-25.....	Revision 16
4.2-11.....	Revision 16	4.5-26.....	Revision 16
4.2-12.....	Revision 16	4.5-27.....	Revision 16
4.2-13.....	Revision 16	4.5-28.....	Revision 16
4.2-14.....	Revision 16	4.5-29.....	Revision 16
4.2-15.....	Revision 16	4.5-30.....	Revision 16
4.2-16.....	Revision 16	4.5-31.....	Revision 16
4.2-17.....	Revision 16	4.5-32.....	Revision 16
4.3-1.....	Revision 16	4.5-33.....	Revision 16
4.3-2.....	Revision 16		
4.3-3.....	Revision 16		
4.3-4.....	Revision 16		
4.4-1.....	Revision 16		
4.5-1.....	Revision 16		
4.5-2.....	Revision 16		
4.5-3.....	Revision 16		
4.5-4.....	Revision 16		
4.5-5.....	Revision 16		

Chapter 5

5-i.....	Revision 16
5-ii.....	Revision 16
5-iii.....	Revision 16
5-iv.....	Revision 16
5-v.....	Revision 16
5-vi.....	Revision 16

List of Effective Pages (continued)

5-vii.....	Revision 16	5.2-3	Revision 16
5-viii.....	Revision 16	5.2-4	Revision 16
5-1	Revision 16	5.2-5	Revision 16
5-2	Revision 16	5.2-6	Revision 16
5-3	Revision 16	5.2-7	Revision 16
5.1-1	Revision 16	5.2-8	Revision 16
5.1-2	Revision 16	5.2-9	Revision 16
5.1-3	Revision 16	5.2-10	Revision 16
5.1-4	Revision 16	5.2-11	Revision 16
5.1-5	Revision 16	5.2-12	Revision 16
5.1-6	Revision 16	5.2-13	Revision 16
5.1-7	Revision 16	5.2-14	Revision 16
5.1-8	Revision 16	5.2-15	Revision 16
5.1-9	Revision 16	5.2-16	Revision 16
5.1-10	Revision 16	5.2-17	Revision 16
5.1-11	Revision 16	5.2-18	Revision 16
5.1-12	Revision 16	5.2-19	Revision 16
5.1-13	Revision 16	5.2-20	Revision 16
5.1-14	Revision 16	5.2-21	Revision 16
5.1-15	Revision 16	5.2-22	Revision 16
5.1-16	Revision 16	5.2-23	Revision 16
5.1-17	Revision 16	5.2-24	Revision 16
5.1-18	Revision 16	5.2-25	Revision 16
5.1-19	Revision 16	5.2-26	Revision 16
5.1-20	Revision 16	5.2-27	Revision 16
5.1-21	Revision 16	5.2-28	Revision 16
5.1-22	Revision 16	5.2-29	Revision 16
5.1-23	Revision 16	5.2-30	Revision 16
5.1-24	Revision 16	5.2-31	Revision 16
5.1-25	Revision 16	5.2-32	Revision 16
5.1-26	Revision 16	5.2-33	Revision 16
5.1-27	Revision 16	5.2-34	Revision 16
5.1-28	Revision 16	5.2-35	Revision 16
5.1-29	Revision 16	5.2-36	Revision 16
5.1-30	Revision 16	5.2-37	Revision 16
5.2-1	Revision 16	5.2-38	Revision 16
5.2-2	Revision 16	5.2-39	Revision 16

List of Effective Pages (continued)

5.3-1	Revision 16	5.4-6	Revision 16
5.3-2	Revision 16	5.4-7	Revision 16
5.3-3	Revision 16	5.4-8	Revision 16
5.3-4	Revision 16	5.4-9	Revision 16
5.3-5	Revision 16	5.4-10	Revision 16
5.3-6	Revision 16	5.4-11	Revision 16
5.3-7	Revision 16	5.4-12	Revision 16
5.3-8	Revision 16	5.4-13	Revision 16
5.3-9	Revision 16	5.4-14	Revision 16
5.3-10	Revision 16	5.4-15	Revision 16
5.3-11	Revision 16	5.4-16	Revision 16
5.3-12	Revision 16	5.4-17	Revision 16
5.3-13	Revision 16	5.4-18	Revision 16
5.3-14	Revision 16	5.4-19	Revision 16
5.3-15	Revision 16	5.4-20	Revision 16
5.3-16	Revision 16	5.4-21	Revision 16
5.3-17	Revision 16	5.4-22	Revision 16
5.3-18	Revision 16	5.4-23	Revision 16
5.3-19	Revision 16	5.4-24	Revision 16
5.3-20	Revision 16	5.4-25	Revision 16
5.3-21	Revision 16	5.4-26	Revision 16
5.3-22	Revision 16	5.4-27	Revision 16
5.3-23	Revision 16	5.4-28	Revision 16
5.3-24	Revision 16	5.4-29	Revision 16
5.3-25	Revision 16	5.4-30	Revision 16
5.3-26	Revision 16	5.4-31	Revision 16
5.3-27	Revision 16	5.4-32	Revision 16
5.3-28	Revision 16	5.4-33	Revision 16
5.3-29	Revision 16	5.4-34	Revision 16
5.3-30	Revision 16	5.4-35	Revision 16
5.3-31	Revision 16	5.4-36	Revision 16
5.3-32	Revision 16	5.4-37	Revision 16
5.4-1	Revision 16	5.4-38	Revision 16
5.4-2	Revision 16	5.4-39	Revision 16
5.4-3	Revision 16	5.5-1	Revision 16
5.4-4	Revision 16	5.5-2	Revision 16
5.4-5	Revision 16	5.5-3	Revision 16

List of Effective Pages (continued)

5.5-4	Revision 16	5.5-41	Revision 16
5.5-5	Revision 16	5.5-42	Revision 16
5.5-6	Revision 16	5.5-43	Revision 16
5.5-7	Revision 16	5.5-44	Revision 16
5.5-8	Revision 16	5.5-45	Revision 16
5.5-9	Revision 16	5.5-46	Revision 16
5.5-10	Revision 16	5.5-47	Revision 16
5.5-11	Revision 16	5.5-48	Revision 16
5.5-12	Revision 16	5.5-49	Revision 16
5.5-13	Revision 16	5.5-50	Revision 16
5.5-14	Revision 16	5.5-51	Revision 16
5.5-15	Revision 16	5.5-52	Revision 16
5.5-16	Revision 16	5.5-53	Revision 16
5.5-17	Revision 16	5.5-54	Revision 16
5.5-18	Revision 16	5.5-55	Revision 16
5.5-19	Revision 16	5.5-56	Revision 16
5.5-20	Revision 16	5.5-57	Revision 16
5.5-21	Revision 16	5.5-58	Revision 16
5.5-22	Revision 16	5.5-59	Revision 16
5.5-23	Revision 16	5.5-60	Revision 16
5.5-24	Revision 16	5.5-61	Revision 16
5.5-25	Revision 16		
5.5-26	Revision 16		
5.5-27	Revision 16		
5.5-28	Revision 16		
5.5-29	Revision 16		
5.5-30	Revision 16		
5.5-31	Revision 16		
5.5-32	Revision 16		
5.5-33	Revision 16		
5.5-34	Revision 16		
5.5-35	Revision 16		
5.5-36	Revision 16		
5.5-37	Revision 16		
5.5-38	Revision 16		
5.5-39	Revision 16		
5.5-40	Revision 16		

Chapter 6

6-i	Revision 16
6-ii	Revision 16
6-iii	Revision 16
6-iv	Revision 16
6-v	Revision 16
6-vi	Revision 16
6.1-1	Revision 16
6.1-2	Revision 16
6.1-3	Revision 16
6.1-4	Revision 16
6.1-5	Revision 16
6.1-6	Revision 16
6.2-1	Revision 16

List of Effective Pages (continued)

6.2-2	Revision 16	6.4.3-6	Revision 16
6.2-3	Revision 16	6.4.3-7	Revision 16
6.2-4	Revision 16	6.4.3-8	Revision 16
6.2-5	Revision 16	6.4.3-9	Revision 16
6.2-6	Revision 16	6.4.3-10	Revision 16
6.2-7	Revision 16	6.4.3-11	Revision 16
6.2-8	Revision 16	6.4.3-12	Revision 16
6.2-9	Revision 16	6.4.3-13	Revision 16
6.2-10	Revision 16	6.4.3-14	Revision 16
6.2-11	Revision 16	6.4.3-15	Revision 16
6.3-1	Revision 16	6.4.3-16	Revision 16
6.3-2	Revision 16	6.4.3-17	Revision 16
6.3-3	Revision 16	6.4.3-18	Revision 16
6.3-4	Revision 16	6.4.3-19	Revision 16
6.3-5	Revision 16	6.4.3-20	Revision 16
6.3-6	Revision 16	6.4.3-21	Revision 16
6.3-7	Revision 16	6.4.3-22	Revision 16
6.3-8	Revision 16	6.4.3-23	Revision 16
6.3-9	Revision 16	6.4.3-24	Revision 16
6.3-10	Revision 16	6.4.3-25	Revision 16
6.4-1	Revision 16	6.4.3-26	Revision 16
6.4-2	Revision 16	6.4.3-27	Revision 16
6.4.1-1	Revision 16	6.4.3-28	Revision 16
6.4.2-1	Revision 16	6.4.3-29	Revision 16
6.4.2-2	Revision 16	6.4.4-1	Revision 16
6.4.2-3	Revision 16	6.4.4-2	Revision 16
6.4.2-4	Revision 16	6.4.4-3	Revision 16
6.4.2-5	Revision 16	6.4.4-4	Revision 16
6.4.2-6	Revision 16	6.4.4-5	Revision 16
6.4.2-7	Revision 16	6.4.4-6	Revision 16
6.4.2-8	Revision 16	6.4.4-7	Revision 16
6.4.2-9	Revision 16	6.4.4-8	Revision 16
6.4.3-1	Revision 16	6.4.4-9	Revision 16
6.4.3-2	Revision 16	6.4.4-10	Revision 16
6.4.3-3	Revision 16	6.4.4-11	Revision 16
6.4.3-4	Revision 16	6.4.4-12	Revision 16
6.4.3-5	Revision 16	6.4.4-13	Revision 16

List of Effective Pages (continued)

6.4.4-14	Revision 16	6.5.1-19	Revision 16
6.4.4-15	Revision 16	6.5.1-20	Revision 16
6.4.4-16	Revision 16	6.5.1-21	Revision 16
6.4.4-17	Revision 16	6.5.2-1	Revision 16
6.4.4-18	Revision 16	6.5.2-2	Revision 16
6.4.4-19	Revision 16	6.5.2-3	Revision 16
6.4.4-20	Revision 16	6.5.2-4	Revision 16
6.4.4-21	Revision 16	6.5.2-5	Revision 16
6.4.4-22	Revision 16	6.5.2-6	Revision 16
6.4.4-23	Revision 16	6.5.2-7	Revision 16
6.4.4-24	Revision 16	6.5.2-8	Revision 16
6.4.4-25	Revision 16	6.5.2-9	Revision 16
6.4.4-26	Revision 16	6.5.2-10	Revision 16
6.4.4-27	Revision 16	6.5.2-11	Revision 16
6.4.4-28	Revision 16	6.5.2-12	Revision 16
6.4.4-29	Revision 16	6.5.2-13	Revision 16
6.4.4-30	Revision 16	6.5.2-14	Revision 16
6.5-1	Revision 16	6.5.2-15	Revision 16
6.5-2	Revision 16	6.5.2-16	Revision 16
6.5.1-1	Revision 16	6.5.2-17	Revision 16
6.5.1-2	Revision 16	6.5.2-18	Revision 16
6.5.1-3	Revision 16	6.5.2-19	Revision 16
6.5.1-4	Revision 16	6.5.2-20	Revision 16
6.5.1-5	Revision 16	6.6-1	Revision 16
6.5.1-6	Revision 16	6.6-2	Revision 16
6.5.1-7	Revision 16	6.7-1	Revision 16
6.5.1-8	Revision 16	6.7-2	Revision 16
6.5.1-9	Revision 16	6.7-3	Revision 16
6.5.1-10	Revision 16	6.7-4	Revision 16
6.5.1-11	Revision 16	6.7-5	Revision 16
6.5.1-12	Revision 16	6.7-6	Revision 16
6.5.1-13	Revision 16	6.7-7	Revision 16
6.5.1-14	Revision 16	6.7-8	Revision 16
6.5.1-15	Revision 16	6.7-9	Revision 16
6.5.1-16	Revision 16	6.7-10	Revision 16
6.5.1-17	Revision 16	6.7-11	Revision 16
6.5.1-18	Revision 16	6.7-12	Revision 16

List of Effective Pages (continued)

6.7-13	Revision 16	6.7-50	Revision 16
6.7-14	Revision 16	6.7-51	Revision 16
6.7-15	Revision 16	6.7-52	Revision 16
6.7-16	Revision 16	6.7-53	Revision 16
6.7-17	Revision 16	6.7-54	Revision 16
6.7-18	Revision 16	6.7-55	Revision 16
6.7-19	Revision 16	6.7-56	Revision 16
6.7-20	Revision 16	6.7-57	Revision 16
6.7-21	Revision 16	6.7-58	Revision 16
6.7-22	Revision 16	6.7-59	Revision 16
6.7-23	Revision 16	6.7-60	Revision 16
6.7-24	Revision 16	6.7-61	Revision 16
6.7-25	Revision 16	6.7-62	Revision 16
6.7-26	Revision 16	6.7-63	Revision 16
6.7-27	Revision 16	6.7-64	Revision 16
6.7-28	Revision 16	6.7-65	Revision 16
6.7-29	Revision 16	6.7-66	Revision 16
6.7-30	Revision 16	6.7-67	Revision 16
6.7-31	Revision 16	6.7-68	Revision 16
6.7-32	Revision 16	6.7-69	Revision 16
6.7-33	Revision 16	6.7-70	Revision 16
6.7-34	Revision 16	6.7-71	Revision 16
6.7-35	Revision 16	6.7-72	Revision 16
6.7-36	Revision 16	6.7-73	Revision 16
6.7-37	Revision 16	6.7-74	Revision 16
6.7-38	Revision 16	6.7-75	Revision 16
6.7-39	Revision 16	6.7-76	Revision 16
6.7-40	Revision 16	6.7-77	Revision 16
6.7-41	Revision 16	6.7-78	Revision 16
6.7-42	Revision 16	6.7-79	Revision 16
6.7-43	Revision 16	6.7-80	Revision 16
6.7-44	Revision 16	6.7-81	Revision 16
6.7-45	Revision 16	6.7-82	Revision 16
6.7-46	Revision 16	6.7-83	Revision 16
6.7-47	Revision 16	6.7-84	Revision 16
6.7-48	Revision 16	6.7-85	Revision 16
6.7-49	Revision 16	6.7-86	Revision 16

List of Effective Pages (continued)

6.7-87	Revision 16	6.7-124	Revision 16
6.7-88	Revision 16	6.7-125	Revision 16
6.7-89	Revision 16	6.7-126	Revision 16
6.7-90	Revision 16	6.7-127	Revision 16
6.7-91	Revision 16	6.7-128	Revision 16
6.7-92	Revision 16	6.7-129	Revision 16
6.7-93	Revision 16	6.7-130	Revision 16
6.7-94	Revision 16	6.7-131	Revision 16
6.7-95	Revision 16	6.7-132	Revision 16
6.7-96	Revision 16	6.7-133	Revision 16
6.7-97	Revision 16	6.7-134	Revision 16
6.7-98	Revision 16	6.7-135	Revision 16
6.7-99	Revision 16	6.7-136	Revision 16
6.7-100	Revision 16	6.7-137	Revision 16
6.7-101	Revision 16	6.7-138	Revision 16
6.7-102	Revision 16	6.7-139	Revision 16
6.7-103	Revision 16	6.7-140	Revision 16
6.7-104	Revision 16	6.7-141	Revision 16
6.7-105	Revision 16	6.7-142	Revision 16
6.7-106	Revision 16	6.7-143	Revision 16
6.7-107	Revision 16	6.7-144	Revision 16
6.7-108	Revision 16	6.7-145	Revision 16
6.7-109	Revision 16	6.7-146	Revision 16
6.7-110	Revision 16	6.7-147	Revision 16
6.7-111	Revision 16	6.7-148	Revision 16
6.7-112	Revision 16	6.7-149	Revision 16
6.7-113	Revision 16	6.7-150	Revision 16
6.7-114	Revision 16	6.7-151	Revision 16
6.7-115	Revision 16	6.7-152	Revision 16
6.7-116	Revision 16	6.7-153	Revision 16
6.7-117	Revision 16	6.7-154	Revision 16
6.7-118	Revision 16	6.7-155	Revision 16
6.7-119	Revision 16	6.7-156	Revision 16
6.7-120	Revision 16	6.7-157	Revision 16
6.7-121	Revision 16	6.7-158	Revision 16
6.7-122	Revision 16	6.7-159	Revision 16
6.7-123	Revision 16	6.7-160	Revision 16

List of Effective Pages (continued)

6.7-161	Revision 16	6.7-198	Revision 16
6.7-162	Revision 16	6.7-199	Revision 16
6.7-163	Revision 16	6.7-200	Revision 16
6.7-164	Revision 16	6.7-201	Revision 16
6.7-165	Revision 16	6.7-202	Revision 16
6.7-166	Revision 16	6.7-203	Revision 16
6.7-167	Revision 16	6.7-204	Revision 16
6.7-168	Revision 16	6.7-205	Revision 16
6.7-169	Revision 16	6.7-206	Revision 16
6.7-170	Revision 16	6.7-207	Revision 16
6.7-171	Revision 16	6.7-208	Revision 16
6.7-172	Revision 16	6.7-209	Revision 16
6.7-173	Revision 16	6.7-210	Revision 16
6.7-174	Revision 16	6.7-211	Revision 16
6.7-175	Revision 16	6.7-212	Revision 16
6.7-176	Revision 16	6.7-213	Revision 16
6.7-177	Revision 16	6.7-214	Revision 16
6.7-178	Revision 16	6.7-215	Revision 16
6.7-179	Revision 16	6.7-216	Revision 16
6.7-180	Revision 16	6.7-217	Revision 16
6.7-181	Revision 16	6.7-218	Revision 16
6.7-182	Revision 16	6.7-219	Revision 16
6.7-183	Revision 16	6.7-220	Revision 16
6.7-184	Revision 16	6.7-221	Revision 16
6.7-185	Revision 16	6.7-222	Revision 16
6.7-186	Revision 16	6.7-223	Revision 16
6.7-187	Revision 16	6.7-224	Revision 16
6.7-188	Revision 16	6.7-225	Revision 16
6.7-189	Revision 16	6.7-226	Revision 16
6.7-190	Revision 16	6.7-227	Revision 16
6.7-191	Revision 16	6.7-228	Revision 16
6.7-192	Revision 16	6.7-229	Revision 16
6.7-193	Revision 16	6.7-230	Revision 16
6.7-194	Revision 16	6.7-231	Revision 16
6.7-195	Revision 16	6.7-232	Revision 16
6.7-196	Revision 16	6.7-233	Revision 16
6.7-197	Revision 16	6.7-234	Revision 16

List of Effective Pages (continued)

6.7-235	Revision 16	6.7-272	Revision 16
6.7-236	Revision 16	6.7-273	Revision 16
6.7-237	Revision 16	6.7-274	Revision 16
6.7-238	Revision 16	6.7-275	Revision 16
6.7-239	Revision 16	6.7-276	Revision 16
6.7-240	Revision 16	6.7-277	Revision 16
6.7-241	Revision 16	6.7-278	Revision 16
6.7-242	Revision 16	6.7-279	Revision 16
6.7-243	Revision 16	6.7-280	Revision 16
6.7-244	Revision 16	6.7-281	Revision 16
6.7-245	Revision 16	6.7-282	Revision 16
6.7-246	Revision 16	6.7-283	Revision 16
6.7-247	Revision 16	6.7-284	Revision 16
6.7-248	Revision 16	6.7-285	Revision 16
6.7-249	Revision 16	6.7-286	Revision 16
6.7-250	Revision 16	6.7-287	Revision 16
6.7-251	Revision 16	6.7-288	Revision 16
6.7-252	Revision 16	6.7-289	Revision 16
6.7-253	Revision 16	6.7-290	Revision 16
6.7-254	Revision 16	6.7-291	Revision 16
6.7-255	Revision 16	6.7-292	Revision 16
6.7-256	Revision 16	6.7-293	Revision 16
6.7-257	Revision 16	6.7-294	Revision 16
6.7-258	Revision 16	6.7-295	Revision 16
6.7-259	Revision 16	6.7-296	Revision 16
6.7-260	Revision 16	6.7-297	Revision 16
6.7-261	Revision 16	6.7-298	Revision 16
6.7-262	Revision 16	6.7-299	Revision 16
6.7-263	Revision 16	6.7-300	Revision 16
6.7-264	Revision 16	6.7-301	Revision 16
6.7-265	Revision 16	6.7-302	Revision 16
6.7-266	Revision 16	6.7-303	Revision 16
6.7-267	Revision 16	6.7-304	Revision 16
6.7-268	Revision 16	6.7-305	Revision 16
6.7-269	Revision 16	6.7-306	Revision 16
6.7-270	Revision 16	6.7-307	Revision 16
6.7-271	Revision 16	6.7-308	Revision 16

List of Effective Pages (continued)

6.7-309 Revision 16
6.7-310 Revision 16
6.7-311 Revision 16
6.7-312 Revision 16
6.7-313 Revision 16
6.7-314 Revision 16
6.7-315 Revision 16
6.7-316 Revision 16
6.7-317 Revision 16
6.7-318 Revision 16
6.7-319 Revision 16
6.7-320 Revision 16
6.7-321 Revision 16
6.7-322 Revision 16
6.7-323 Revision 16
6.7-324 Revision 16
6.7-325 Revision 16
6.7-326 Revision 16
6.7-327 Revision 16
6.7-328 Revision 16
6.7-329 Revision 16
6.7-330 Revision 16
6.7-331 Revision 16
6.7-332 Revision 16
6.7-333 Revision 16

Chapter 7

7-i Revision 16
7-ii Revision 16
7-1 Revision 16
7-2 Revision 16
7-3 Revision 16
7.1-1 Revision 16
7.1-2 Revision 16
7.1-3 Revision 16
7.1-4 Revision 16

7.1-5 Revision 16
7.1-6 Revision 16
7.1-7 Revision 16
7.1-8 Revision 16
7.1-9 Revision 16
7.1-10 Revision 16
7.1-11 Revision 16
7.1-12 Revision 16
7.2-1 Revision 16
7.2-2 Revision 16
7.2-3 Revision 16
7.2-4 Revision 16
7.2-5 Revision 16
7.3-1 Revision 16
7.3-2 Revision 16
7.3-3 Revision 16
7.3-4 Revision 16
7.3-5 Revision 16
7.3-6 Revision 16
7.3-7 Revision 16
7.3-8 Revision 16
7.3-9 Revision 16
7.4-1 Revision 16
7.4-2 Revision 16
7.4-3 Revision 16
7.4-4 Revision 16
7.5-1 Revision 16
7.6-1 Revision 16
7.6-2 Revision 16
7.6-3 Revision 16
7.6-4 Revision 16

Chapter 8

8-i Revision 16
8-ii Revision 16
8-1 Revision 16

List of Effective Pages (continued)

8.1-1 Revision 16
8.1-2 Revision 16
8.1-3 Revision 16
8.1-4 Revision 16
8.1-5 Revision 16
8.1-6 Revision 16
8.1-7 Revision 16
8.1-8 Revision 16
8.1-9 Revision 16
8.1-10 Revision 16
8.1-11 Revision 16
8.1-12 Revision 16
8.1-13 Revision 16
8.1-14 Revision 16
8.1-15 Revision 16
8.1-16 Revision 16
8.1-17 Revision 16
8.1-18 Revision 16
8.1-19 Revision 16
8.1-20 Revision 16
8.1-21 Revision 16
8.2-1 Revision 16
8.2-2 Revision 16
8.2-3 Revision 16
8.2-4 Revision 16
8.2-5 Revision 16
8.2-6 Revision 16
8.2-7 Revision 16
8.2-8 Revision 16
8.3-1 Revision 16
8.4-1 Revision 16
8.4-2 Revision 16
8.4-3 Revision 16
8.4-4 Revision 16
8.4-5 Revision 16
8.4-6 Revision 16
8.4-7 Revision 16

8.4-8 Revision 16
8.4-9 Revision 16

Chapter 9

9-i Revision 16
9-1 Revision 16
9-2 Revision 16
9-3 Revision 16
9-4 Revision 16
9-5 Revision 16
9-6 Revision 16
9-7 Revision 16
9-8 Revision 16
9-9 Revision 16
9-10 Revision 16
9-11 Revision 16
9-12 Revision 16
9-13 Revision 16

Master Table of Contents

1.0	GENERAL INFORMATION	1-1
1.1	Introduction.....	1.1-1
1.2	Package Description	1.2-1
1.2.1	Packaging.....	1.2-1
1.2.2	Operational Features	1.2-21
1.2.3	Contents of Packaging	1.2-21
1.3	Appendices.....	1.3-1
1.3.1	Quality Assurance.....	1.3-1
1.3.2	License Drawings	1.3-1
2.0	STRUCTURAL EVALUATION	2-1
2.1	Structural Design	2.1.1-1
2.1.1	Discussion.....	2.1.1-1
2.1.2	Design Criteria.....	2.1.2-1
2.1.2.1	Discussion.....	2.1.2-1
2.1.2.2	Allowable Stress Limits - Ductile Failure	2.1.2-2
2.1.3	Miscellaneous Structural Failure Modes	2.1.3-1
2.1.3.1	Brittle Fracture	2.1.3-1
2.1.3.2	Fatigue - Normal Operation.....	2.1.3-5
2.1.3.3	Extreme Total Stress Intensity Range.....	2.1.3-10
2.1.3.4	Inner Shell Buckling Design Criteria.....	2.1.3-11
2.1.3.5	Creep Considerations at Elevated Temperatures	2.1.3-15
2.1.3.6	Impact Limiter Deformation Limits.....	2.1.3-15
2.2	Weights and Centers of Gravity.....	2.2-1
2.3	Mechanical Properties of Materials	2.3.1-1
2.3.1	Discussion.....	2.3.1-1
2.3.2	Austenitic Stainless Steels	2.3.2-1
2.3.3	Precipitation-Hardened Stainless Steel.....	2.3.3-1
2.3.4	Bolting Materials	2.3.4-1
2.3.5	Aluminum Alloys.....	2.3.5-1

Master Table of Contents (Continued)

2.3.6	Shielding Material.....	2.3.6-1
2.3.6.1	Chemical Copper Grade Lead.....	2.3.6-1
2.3.6.2	NS-4-FR.....	2.3.6-1
2.3.7	Impact Limiter Materials	2.3.7-1
2.3.8	Spacer Materials	2.3.8-1
2.4	General Standards for All Packages	2.4-1
2.4.1	Minimum Package Size	2.4.1-1
2.4.2	Tamperproof Feature	2.4.2-1
2.4.3	Positive Closure	2.4.3-1
2.4.4	Chemical and Galvanic Reactions	2.4.4-1
2.4.4.1	Component Operating Environment.....	2.4.4-1
2.4.4.2	Component Material Categories	2.4.4-2
2.4.4.3	General Effects of Identified Reactions.....	2.4.4-8
2.4.4.4	Adequacy of the Cask Operating Procedures	2.4.4-9
2.4.4.5	Effects of Reaction Products.....	2.4.4-9
2.4.5	Cask Design	2.4.5-1
2.4.6	Continuous Venting	2.4.6-1
2.5	Lifting and Tiedown Standards.....	2.5.1-1
2.5.1	Lifting Devices	2.5.1-1
2.5.1.1	Lifting Trunnion Analysis	2.5.1-1
2.5.1.2	Lid Lifting Device	2.5.1-14
2.5.1.3	Canister Lifting	2.5.1-19
2.5.2	Tiedown Devices	2.5.2-1
2.5.2.1	Discussion and Loads	2.5.2-1
2.5.2.2	Rear Support	2.5.2-11
2.5.2.3	Front Support	2.5.2-23
2.5.2.4	Tiedown Evaluation for the CY-MPC Configuration with Balsa Impact Limiters.....	2.5.2-24
2.6	Normal Conditions of Transport.....	2.6-1
2.6.1	Heat.....	2.6.1-1
2.6.1.1	Heat Condition for the NAC-STC Cask in the Directly Loaded Fuel and Yankee-MPC Configurations.....	2.6.1-1
2.6.1.2	Heat Condition for the NAC-STC Cask in the CY-MPC Configuration	2.6.1-5

Master Table of Contents (Continued)

2.6.2	Cold.....	2.6.2-1
2.6.2.1	Cold Condition for the NAC-STC Cask in the Directly Loaded Fuel and Yankee-MPC Configurations.....	2.6.2-1
2.6.2.2	Cold Condition for the NAC-STC Cask in the CY-MPC Configuration	2.6.2-6
2.6.3	Reduced External Pressure	2.6.3-1
2.6.4	Increased External Pressure	2.6.4-1
2.6.5	Vibration	2.6.5-1
2.6.6	Water Spray	2.6.6-1
2.6.7	Free Drop (1 Foot)	2.6.7-1
2.6.7.1	One-Foot End Drop.....	2.6.7.1-1
2.6.7.2	One-Foot Side Drop.....	2.6.7.2-1
2.6.7.3	One-Foot Corner Drop.....	2.6.7.3-1
2.6.7.4	Impact Limiters.....	2.6.7.4-1
2.6.7.5	Closure Analysis - Normal Conditions of Transport.....	2.6.7.5-1
2.6.7.6	Neutron Shield Analysis	2.6.7.6-1
2.6.7.7	Upper Ring/Outer Shell Intersection Analysis	2.6.7.7-1
2.6.8	Corner Drop (1 Foot)	2.6.8-1
2.6.9	Compression	2.6.9-1
2.6.10	Penetration	2.6.10-1
2.6.10.1	Impact Limiter - Penetration.....	2.6.10.1-1
2.6.10.2	Neutron Shield Shell - Penetration	2.6.10.2-1
2.6.10.3	Port Cover - Penetration	2.6.10.3-1
2.6.11	Fabrication Conditions.....	2.6.11-1
2.6.11.1	Lead Pour	2.6.11.1-1
2.6.11.2	Cooldown.....	2.6.11.2-1
2.6.11.3	Lead Creep	2.6.11.3-1
2.6.12	Fuel Basket Analysis (For Directly Loaded Fuel) - Normal Transport Conditions	2.6.12-1
2.6.12.1	Detailed Analysis - PWR Basket for Directly Loaded Fuel	2.6.12.1-1
2.6.12.2	Finite Element Model Description - Directly Loaded PWR Fuel Basket.....	2.6.12.2-1
2.6.12.3	Thermal Expansion Evaluation of Support Disk - Directly Loaded PWR Fuel Basket.....	2.6.12.3-1

Master Table of Contents (Continued)

2.6.12.4	Stress Evaluation of Support Disk for a 1-Foot End Drop Load Condition (Directly Loaded Fuel Configuration).....	2.6.12.4-1
2.6.12.5	Stress Evaluation of Support Disk (Directly Loaded Fuel Configuration) for Thermal Plus a 1-Foot End Drop Combined Load Condition.....	2.6.12.5-1
2.6.12.6	Stress Evaluation of Threaded Rods and Spacer Nuts for a 1-Foot End Drop Load Condition (Directly Loaded Fuel Configuration).....	2.6.12.6-1
2.6.12.7	Stress Evaluation of Support Disk (Directly Loaded Fuel Configuration) for a 1-Foot Side Drop Impact Load Condition	2.6.12.7-1
2.6.12.8	Stress Evaluation of Support Disk (Directly Loaded Fuel Configuration) for Thermal Plus a 1-Foot Side Drop Combined Load Condition.....	2.6.12.8-1
2.6.12.9	Support Disk Web Stresses for a 1-Foot Side Drop Condition (Directly Loaded Fuel Configuration)	2.6.12.9-1
2.6.12.10	Support Disk Shear Stresses for a 1-Foot Side Drop and a 1-Foot End Drop Conditions (Directly Loaded Fuel Configuration).....	2.6.12.10-1
2.6.12.11	Bearing Stress - Basket Contact with Inner Shell (Directly Loaded Fuel Configuration)	2.6.12.11-1
2.6.12.12	Evaluation of Triaxial Stress for the Fuel Basket Support Disk (Directly Loaded Fuel Configuration)	2.6.12.12-1
2.6.12.13	Fuel Basket (Directly Loaded Fuel Configuration) Weldment Analysis for 1-Foot Drop	2.6.12.13-1
2.6.13	Transportable Storage Canister Analysis - Normal Transport Condition	2.6.13-1
2.6.13.1	Yankee-MPC Canister Description and Analysis.....	2.6.13.1-1
2.6.13.2	Yankee-MPC Canister Finite Element Model	2.6.13.2-1
2.6.13.3	Thermal Expansion Evaluation of Yankee-MPC Canister for Spent Fuel	2.6.13.3-1
2.6.13.4	Stress Evaluation of the Yankee-MPC Canister for 1-Foot End Drop Load Condition	2.6.13.4-1
2.6.13.5	Stress Evaluation of the Yankee-MPC Canister for Thermal Plus a 1-Foot End Drop Load Condition.....	2.6.13.5-1

Master Table of Contents (Continued)

2.6.13.6	Stress Evaluation of the Yankee-MPC Canister for a 1-Foot Side Drop Load Condition	2.6.13.6-1
2.6.13.7	Stress Evaluation of the Yankee-MPC Canister for Thermal Plus a 1-Foot Side Drop Load Condition	2.6.13.7-1
2.6.13.8	Yankee-MPC Canister Shear Stresses for a 1-Foot Side Drop and a 1-Foot End Drop Condition	2.6.13.8-1
2.6.13.9	Yankee-MPC Canister Bearing Stresses for 1-Foot Side Drop	2.6.13.9-1
2.6.13.10	Yankee-MPC Canister Buckling Evaluation for 1-Foot End Drop	2.6.13.10-1
2.6.13.11	Yankee-MPC Canister Lifting Evaluation.....	2.6.13.11-1
2.6.13.12	Yankee-MPC Canister Closure Weld Evaluation – Normal Conditions	2.6.13.12-1
2.6.14	Yankee-MPC Fuel Basket Analysis - Normal Conditions of Transport ..	2.6.14-1
2.6.14.1	Detailed Analysis - Yankee-MPC Fuel Basket.....	2.6.14.1-1
2.6.14.2	Finite Element Model Description - Yankee-MPC Fuel Basket.....	2.6.14.2-1
2.6.14.3	Thermal Expansion Evaluation of Yankee-MPC Fuel Basket Support Disk	2.6.14.3-1
2.6.14.4	Stress Evaluation of Yankee-MPC Fuel Basket Support Disk for a 1-Foot End Drop Condition	2.6.14.4-1
2.6.14.5	Stress Evaluation of Yankee-MPC Fuel Basket Support Disk for Thermal Plus a 1-Foot End Drop Combined Condition	2.6.14.5-1
2.6.14.6	Stress Evaluation of Yankee-MPC Basket Tie Rods and Spacers for a 1-Foot End Drop Load Condition	2.6.14.6-1
2.6.14.7	Stress Evaluation of Yankee-MPC Fuel Basket Support Disk for a 1-Foot Side Drop Load Condition	2.6.14.7-1
2.6.14.8	Stress Evaluation of Yankee-MPC Fuel Basket Support Disk for Thermal Plus a 1-Foot Side Drop Combined Condition	2.6.14.8-1
2.6.14.9	Yankee-MPC Fuel Basket Support Disk Shear Stresses for 1-Foot Drops	2.6.14.9-1
2.6.14.10	Bearing Stress - Basket Contact with Canister Shell.....	2.6.14.10-1
2.6.14.11	Yankee-MPC Fuel Basket Weldment Analysis for 1-Foot End Drop	2.6.14.11-1

Master Table of Contents (Continued)

2.6.14.12	Yankee-MPC Fuel Basket Support Disk - Buckling Evaluation (Normal Conditions of Transport).....	2.6.14.12-1
2.6.15	CY-MPC Transportable Storage Canister Analysis – Normal Conditions of Transport	2.6.15-1
2.6.15.1	Analysis Description – CY-MPC Canister	2.6.15.1-1
2.6.15.2	Finite Element Model Description – CY-MPC Canister	2.6.15.2-1
2.6.15.3	Thermal Expansion of CY-MPC Canister Containing Fuel	2.6.15.3-1
2.6.15.4	Stress Evaluation of the CY-MPC Canister for 1-Foot End Drop Load Condition.....	2.6.15.4-1
2.6.15.5	Stress Evaluation of the Canister for Thermal Plus a 1-Foot End Drop Load Condition	2.6.15.5-1
2.6.15.6	Stress Evaluation of the Canister for a 1-Foot Side Drop Load Condition	2.6.15.6-1
2.6.15.7	Stress Evaluation of the CY-MPC Canister for Thermal Plus a 1-Foot Side Drop Load Condition.....	2.6.15.7-1
2.6.15.8	CY-MPC Canister Shear Stresses for a 1-Foot Side Drop and a 1-Foot End Drop Condition	2.6.15.8-1
2.6.15.9	CY-MPC Canister Bearing Stresses for a 1-Foot Side Drop	2.6.15.9-1
2.6.15.10	CY-MPC Canister Buckling Evaluation for 1-Foot End Drop.....	2.6.15.10-1
2.6.15.11	CY-MPC Canister Lifting Evaluation	2.6.15.11-1
2.6.15.12	CY-MPC Canister Closure Weld Evaluation – Normal Conditions of Transport	2.6.15.12-1
2.6.16	CY-MPC Fuel Basket Analysis – Normal Conditions of Transport	2.6.16-1
2.6.16.1	Detailed Analysis of the CY-MPC Fuel Basket	2.6.16.1-1
2.6.16.2	CY-MPC Fuel Basket Finite Element Model Description ..	2.6.16.2-1
2.6.16.3	Thermal Expansion Evaluation of the CY-MPC Support Disk	2.6.16.3-1
2.6.16.4	Stress Evaluation of the CY-MPC Support Disk for a 1-Foot End Drop	2.6.16.4-1
2.6.16.5	Stress Evaluation of the CY-MPC Support Disk for a Combined Thermal and 1-Foot End Drop Load Condition	2.6.16.5-1
2.6.16.6	Stress Evaluation of CY-MPC Tie Rods and Spacers for 1-Foot End Drop.....	2.6.16.6-1

Master Table of Contents (Continued)

2.6.16.7	Stress Evaluation of CY-MPC Support Disk for a 1-Foot Side Drop	2.6.16.7-1
2.6.16.8	Stress Evaluation of the CY-MPC Support Disk for a Combined Thermal and 1-Foot Side Drop Load Condition	2.6.16.8-1
2.6.16.9	CY-MPC Support Disk Shear Stresses for 1-Foot Drop	2.6.16.9-1
2.6.16.10	Bearing Stress – Basket Contact with Canister Shell – CY-MPC	2.6.16.10-1
2.6.16.11	CY-MPC Fuel Basket Weldment Analysis for 1-Foot End Drop	2.6.16.11-1
2.6.16.12	CY-MPC Fuel Basket Support Disk – Buckling Evaluation	2.6.16.12-1
2.6.16.13	Stress Evaluation of the CY-MPC Support Disk for 1-Foot Oblique Drop.....	2.6.16.13-1
2.6.16.14	Stress Evaluation of the CY-MPC Support Disk for a Combined Thermal and 1-Foot Oblique Drop Load Condition	2.6.16.14-1
2.6.17	CY-MPC Reconfigured Fuel Assembly Analysis and Damaged Fuel Can Analysis – Normal Conditions of Transport	2.6.17-1
2.6.17.1	CY-MPC Reconfigured Fuel Assembly Evaluation	2.6.17-1
2.6.17.2	CY-MPC Damaged Fuel Can Evaluation	2.6.17-8
2.6.18	Spacer Design for Canistered Fuel – Normal Conditions of Transport....	2.6.18-1
2.6.18.1	Spacer Evaluation for Yankee-MPC Canister Fuel and GTCC Waste	2.6.18-1
2.6.18.2	Spacer Evaluation for CY-MPC Canister Fuel and GTCC Waste.....	2.6.18-2
2.6.19	Greater Than Class C (GTCC) Basket Analysis – Normal Conditions of Transport.....	2.6.19-1
2.6.19.1	Yankee-MPC GTCC Basket Analysis.....	2.6.19-1
2.6.19.2	CY-MPC GTCC Basket Analysis.....	2.6.19-6
2.6.20	Yankee-MPC Reconfigured Fuel Assembly and Damaged Fuel Can Analysis – Normal Conditions of Transport.....	2.6.20-1
2.6.20.1	Yankee-MPC Reconfigured Fuel Assembly (RFA) Evaluation	2.6.20-1
2.6.20.2	Yankee-MPC Damaged Fuel Can Evaluation	2.6.20-13
2.6.21	Fuel Rod Retainer	2.6.21-1

Master Table of Contents (Continued)

2.7	Hypothetical Accident Conditions.....	2.7-1
2.7.1	Free Drop (30 Feet).....	2.7.1-1
2.7.1.1	Thirty-Foot End Drop	2.7.1.1-1
2.7.1.2	Thirty-Foot Side Drop	2.7.1.2-1
2.7.1.3	Thirty-Foot Corner Drop	2.7.1.3-1
2.7.1.4	Thirty-Foot Oblique Drop.....	2.7.1.4-1
2.7.1.5	Lead Slump Resulting From a Cask Drop Accident.....	2.7.1.5-1
2.7.1.6	Closure Analysis - Hypothetical Accident Conditions	2.7.1.6-1
2.7.2	Puncture	2.7.2-1
2.7.2.1	Puncture - Cask Side Midpoint.....	2.7.2.1-1
2.7.2.2	Puncture - Center of Outer Lid	2.7.2.2-1
2.7.2.3	Puncture - Center of Cask Bottom	2.7.2.3-1
2.7.2.4	Puncture - Port Cover	2.7.2.4-1
2.7.2.5	Puncture Accident - Shielding Consequences	2.7.2.5-1
2.7.2.6	Puncture - Conclusion.....	2.7.2.6-1
2.7.3	Thermal	2.7.3.1-1
2.7.3.1	Discussion	2.7.3.1-1
2.7.3.2	Pressure Stress Evaluation	2.7.3.2-1
2.7.3.3	Thermal Stress Evaluation	2.7.3.3-1
2.7.3.4	Bolts - Closure Lids (Thermal Accident)	2.7.3.4-1
2.7.3.5	Performance Summary - Thermal Accident	2.7.3.5-1
2.7.3.6	Conclusion	2.7.3.6-1
2.7.4	Crush.....	2.7.4-1
2.7.5	Immersion - Fissile Material.....	2.7.5-1
2.7.6	Immersion - All Packages.....	2.7.6-1
2.7.7	Damage Summary.....	2.7.7-1
2.7.8	Directly Loaded Fuel Basket Analysis - Accident Conditions	2.7.8-1
2.7.8.1	Stress Evaluation of Support Disk - Directly Loaded Fuel Configuration	2.7.8.1-1
2.7.8.2	Stress Evaluation of the Directly Loaded Fuel Basket Threaded Rods and Spacer Nuts - Accident Condition	2.7.8.2-1
2.7.8.3	Assessment of Buckling – Directly Loaded Fuel Basket	2.7.8.3-1
2.7.8.4	Directly Loaded Fuel Basket Fuel Tube Analysis	2.7.8.4-1
2.7.8.5	Directly Loaded Fuel Basket Weldment Analysis for 30-Foot End Drop	2.7.8.5-1
2.7.9	Yankee-MPC Fuel Basket Analysis - Accident Conditions	2.7.9-1
2.7.9.1	Detailed Analysis – Yankee-MPC Fuel Basket.....	2.7.9-5

Master Table of Contents (Continued)

2.7.9.2	Stress Evaluation of the Yankee-MPC Tie Rods and Spacers for a 30-Foot End Drop Load Condition	2.7.9-24
2.7.9.3	Yankee-MPC Basket Support Disk - Buckling Evaluation (Accident Conditions).....	2.7.9-26
2.7.9.4	Yankee-MPC Fuel Tube Analysis	2.7.9-31
2.7.9.5	Yankee-MPC Basket Weldment Analysis for 30-Foot End Drop	2.7.9-34
2.7.10	Greater Than Class C (GTCC) Waste Basket Analysis - Accident Conditions	2.7.10-1
2.7.10.1	Yankee-MPC GTCC Basket Evaluation.....	2.7.10-1
2.7.10.2	CY-MPC GTCC Basket Analysis – Accident Conditions.....	2.7.10-9
2.7.11	Yankee-MPC Transportable Storage Canister Analysis - Accident Conditions	2.7.11-1
2.7.11.1	Canister - Accident Analysis Description.....	2.7.11-2
2.7.11.2	Analysis Results.....	2.7.11-2
2.7.11.3	Canister Buckling Evaluation for the 30-Foot End Drop	2.7.11-9
2.7.11.4	Canister Closure Weld Evaluation – Accident Conditions...	2.7.11-10
2.7.11.5	Dynamic Loading Effect – Structural Lid Weld.....	2.7.11-11
2.7.12	CY-MPC Transportable Storage Canister Analysis – Accident Conditions	2.7.12-1
2.7.12.1	Canister – Accident Analysis Description.....	2.7.12-1
2.7.12.2	Analysis Results.....	2.7.12-2
2.7.12.3	Canister Buckling Evaluation for the 30-Foot End Drop	2.7.12-3
2.7.12.4	CY-MPC Canister Closure Weld Evaluation – Accident Conditions	2.7.12-4
2.7.13	CY-MPC Fuel Basket Analysis – Accident Conditions	2.7.13-1
2.7.13.1	Stress Evaluation of CY-MPC Support Disk.....	2.7.13.1-1
2.7.13.2	Stress Evaluation of Tie Rods and Spacers for 30-Foot End Drop Load Condition for the CY-MPC	2.7.13.2-1
2.7.13.3	CY-MPC Fuel Basket Support Disk – Buckling Evaluation (Accident Condition)	2.7.13.3-1
2.7.13.4	Fuel Tube Analysis – CY-MPC.....	2.7.13.4-1
2.7.13.5	CY-MPC Fuel Basket Weldment Analysis for 30-Foot End Drop	2.7.13.5-1
2.7.14	CY-MPC Reconfigured Fuel Assembly and Damaged Fuel Can Evaluation – Accident Conditions	2.7.14-1

Master Table of Contents (Continued)

2.7.14.1	CY-MPC Reconfigured Fuel Assembly Weldment Evaluation	2.7.14-1
2.7.14.2	CY-MPC Damaged Fuel Can – Accident Conditions	2.7.14-9
2.7.15	Yankee-MPC Reconfigured Fuel Assembly and Damaged Fuel Can Analysis – Hypothetical Accident Conditions	2.7.15-1
2.7.15.1	Yankee-MPC Reconfigured Fuel Assembly (RFA) Evaluation	2.7.15-1
2.7.15.2	Yankee-MPC Damaged Fuel Can Evaluation	2.7.15-13
2.8	Special Form	2.8-1
2.9	Fuel Rod Buckling Assessment	2.9-1
2.9.1	Fuel Rod Buckling Assessment for Directly Loaded 17 x 17 PWR Fuel	2.9-1
2.9.2	Fuel Rod Buckling Assessment for Yankee-Class Canistered Fuel	2.9-7
2.9.3	Fuel Rod Buckling Assessment for CY-MPC Canistered Fuel	2.9-10
2.10	Appendices	2.10.1-1
2.10.1	Computer Program Descriptions	2.10.1-1
2.10.1.1	ANSYS	2.10.1-1
2.10.1.2	RBCUBED - A Program to Calculate Impact Limiter Dynamics	2.10.1-2
2.10.1.3	LS-DYNA	2.10.1-3
2.10.2	Finite Element Analysis	2.10.2-1
2.10.2.1	Model Descriptions	2.10.2-1
2.10.2.2	Loading Conditions	2.10.2-15
2.10.2.3	Finite Element Analysis Procedures	2.10.2-26
2.10.2.4	Finite Element Documentation Procedures	2.10.2-31
2.10.3	LS-DYNA Computer Code	2.10.3-1
2.10.3.1	Predicting Impact Deceleration using Strain Rate Sensitive Properties	2.10.3-1
2.10.3.2	Accounting for Strain Rate Sensitivity by Interpolation	2.10.3-2
2.10.4	Detailed Finite Element Stress Summaries - Directly Loaded Fuel Configuration	2.10.4-1
2.10.5	Inner Shell Buckling Analysis	2.10.5-1
2.10.5.1	Buckling Analysis	2.10.5-1
2.10.5.2	Analysis Results	2.10.5-2

Master Table of Contents (Continued)

2.10.5.3	Verification of the Code Case N-284 Buckling Evaluation of the NAC-STC Inner Shell and Transition Sections.....	2.10.5-3
2.10.5.4	Buckling Evaluation of the Inner Shell for the Yankee-MPC Fuel Configuration	2.10.5-9
2.10.5.5	Buckling Evaluation of the Inner Shell for the CY-MPC Fuel Configuration	2.10.5-14
2.10.6	Scale Model Test Program for the NAC-STC	2.10.6-1
2.10.6.1	Introduction.....	2.10.6-1
2.10.6.2	Purpose.....	2.10.6-2
2.10.6.3	Discussion	2.10.6-2
2.10.6.4	Eighth-Scale Redwood Impact Limiter Compression Tests ...	2.10.6-9
2.10.6.5	Quarter-Scale Model Drop Tests	2.10.6-14
2.10.6.6	NAC-STC Quarter-Scale Model Drawings	2.10.6-36
2.10.6.7	NAC-STC Eighth-Scale Model Drawings.....	2.10.6-36
2.10.7	Redwood Impact Limiter Force-Deflection Curves and Data – Directly Loaded Fuel Configuration.....	2.10.7-1
2.10.7.1	Potential Energy and Cask Drop Impact Motion.....	2.10.7-1
2.10.7.2	Conversion of Potential Energy to Kinetic Energy	2.10.7-9
2.10.7.3	Deceleration Forces and Energy Absorption Calculation.....	2.10.7-10
2.10.7.4	RBCUBED Calculated Force-Deflection Graphs.....	2.10.7-13
2.10.8	Bolts - Closure Lids (Stress Evaluations)	2.10.8-1
2.10.8.1	Analysis Approach.....	2.10.8-1
2.10.8.2	Inner Lid Closure Bolt Analyses	2.10.8-2
2.10.8.3	Outer Lid Closure Bolt Analyses.....	2.10.8-15
2.10.9	Lead Slump Evaluation.....	2.10.9-1
2.10.9.1	Methodology/Finite Element Analysis	2.10.9-2
2.10.9.2	Analysis Result	2.10.9-3
2.10.9.3	Conclusion	2.10.9-4
2.10.10	Assessment of the Effect of the Revised Temperature Distribution on Structural Qualification.....	2.10.10-1
2.10.10.1	Evaluation Methodology.....	2.10.10-1
2.10.10.2	Temperature Dependent Stress Results	2.10.10-3
2.10.10.3	Conclusions - Revised Temperature Distribution Evaluation	2.10.10-7
2.10.11	Sensitivity Studies of the Yankee-MPC Canistered Fuel Basket Analysis	2.10.11-1
2.10.11.1	Yankee-MPC Fuel Basket Drop Orientation	2.10.11-1

Master Table of Contents (Continued)

2.10.11.2	Gap Stiffness	2.10.11-2
2.10.11.3	Finite Element Mesh for the Support Disk Ligaments	2.10.11-3
2.10.12	Confirmatory Testing Program –Balsa Impact Limiters and Attachments	2.10.12-1
2.10.12.1	Confirmatory Testing Program Results Summary	2.10.12-1
2.10.12.2	Acceptance Criteria for Model Performance	2.10.12-3
2.10.12.3	Description of 30-Foot Drop Tests Performed at SNL	2.10.12-4
2.10.12.4	Results/Evaluation for the 30-Foot Side Drop Test.....	2.10.12-8
2.10.12.5	Results/Evaluation for the 30-Foot Top Corner Drop Test.....	2.10.12-10
2.10.12.6	Results/Evaluation for the 30-Foot Top End Drop Test.....	2.10.12-12
2.10.12.7	LS-DYNA Analyses of the NAC-STC Quarter-Scale Model	2.10.12-14
3.0	THERMAL EVALUATION.....	3.1-1
3.1	Discussion.....	3.1-1
3.1.1	Directly Loaded (Uncanistered) Fuel	3.1-2
3.1.2	Canistered Yankee Class Fuel	3.1-4
3.1.3	Canistered Connecticut Yankee Fuel.....	3.1-6
3.1.4	Canistered Greater Than Class C Waste.....	3.1-8
3.2	Summary of Thermal Properties of Materials	3.2-1
3.2.1	Conductive Properties.....	3.2-1
3.2.2	Radiative Properties.....	3.2-1
3.2.3	Convective Properties	3.2-7
3.2.4	Neutron Shield (NS-4-FR) Thermal Conductivity	3.2-8
3.3	Technical Specifications for Components	3.3-1
3.3.1	Radiation Protection Components	3.3-1
3.3.2	Safe Operating Ranges.....	3.3-2
3.4	Thermal Evaluation for Normal Conditions of Transport	3.4-1
3.4.1	Thermal Models.....	3.4-1
3.4.2	Maximum Temperatures.....	3.4-26
3.4.3	Minimum Temperatures.....	3.4-30
3.4.4	Maximum Internal Pressure.....	3.4-30

Master Table of Contents (Continued)

3.4.5	Maximum Thermal Stresses	3.4-44
3.4.6	Summary of NAC-STC Performance for Normal Transport Conditions	3.4-44
3.4.7	Normal Heat-up Transient	3.4-44
3.4.8	Assessment Criteria for the Package Passive Heat Rejection System.....	3.4-45
3.5	Hypothetical Accident Thermal Evaluation	3.5-1
3.5.1	Thermal Model.....	3.5-1
3.5.2	Package Conditions and Environment.....	3.5-4
3.5.3	Package Temperatures	3.5-5
3.5.4	Maximum Internal Pressure.....	3.5-7
3.5.5	Maximum Thermal Stresses	3.5-10
3.5.6	Evaluation of Package Performance for Hypothetical Accident Thermal Conditions	3.5-10
4.0	CONTAINMENT.....	4.1-1
4.1	Containment Boundary	4.1-1
4.1.1	Containment Vessel	4.1-2
4.1.2	Containment Penetrations	4.1-2
4.1.3	Seals and Welds	4.1-2
4.1.4	Closure	4.1-4
4.2	Containment Requirements for Normal Conditions of Transport	4.2-1
4.2.1	Containment of Radioactive Material.....	4.2-2
4.2.2	Pressurization of Containment Vessel	4.2-3
4.2.3	Containment Criterion for Normal Conditions of Transport	4.2-5
4.3	Containment Requirements for Hypothetical Accident Conditions	4.3-1
4.3.1	Fission Gas Products.....	4.3-1
4.3.2	Containment of Radioactive Material.....	4.3-2
4.3.3	Calculation of Allowable Leak Rate for Directly Loaded Fuel With Viton O-Rings.....	4.3-2
4.3.4	Containment Criterion for Accident Conditions.....	4.3-3
4.4	Special Requirements	4.4-1
4.5	Appendix.....	4.5-1
4.5.1	Metallic O-Rings.....	4.5-1

Master Table of Contents (Continued)

4.5.2	Blended Polytetrafluoroethylene (PTFE) O-Rings.....	4.5-14
4.5.3	Expansion Foam.....	4.5-18
4.5.4	Fiberfrax Ceramic Fiber Paper	4.5-21
4.5.5	Viton O-Rings.....	4.5-27
4.5.6	Sample SAS2H Input File.....	4.5-32
5.0	SHIELDING EVALUATION.....	5-1
5.1	Discussion and Results	5.1-1
5.1.1	Design Criteria.....	5.1-1
5.1.2	Design Basis Fuel	5.1-2
5.1.3	Shielding Materials	5.1-6
5.1.4	Results.....	5.1-6
5.2	Source Specification	5.2-1
5.2.1	Directly Loaded Fuel Source Specification.....	5.2-1
5.2.2	Yankee Class Fuel and GTCC Waste Source Specification.....	5.2-4
5.2.3	Connecticut Yankee Fuel and GTCC Waste Source Specification	5.2-7
5.3	Model Specification.....	5.3-1
5.3.1	Directly Loaded Fuel Model.....	5.3-1
5.3.2	Yankee-MPC Fuel and GTCC Waste Model Specifications.....	5.3-4
5.3.3	CY-MPC Fuel and GTCC Waste Model Specifications.....	5.3-6
5.4	Shielding Evaluation.....	5.4-1
5.4.1	Computer Code Descriptions and Results	5.4-1
5.5	Sample Input Files	5.5-1
5.5.1	Sample Input Files for Directly Loaded Fuel	5.5-1
6.0	CRITICALITY EVALUATION.....	6.1-1
6.1	Discussion and Results	6.1-1
6.1.1	Directly Loaded Fuel	6.1-1
6.1.2	Canistered Yankee Class Fuel	6.1-2
6.1.3	Canistered Connecticut Yankee Fuel.....	6.1-4
6.2	Package Fuel Loading	6.2-1

Master Table of Contents (Continued)

6.3	Criticality Model Specification	6.3-1
6.3.1	Calculational Methodology	6.3-1
6.3.2	Description of Calculational Models.....	6.3-1
6.3.3	Package Regional Densities.....	6.3-3
6.3.4	Fuel Region Densities	6.3-3
6.3.5	Water Reflector Densities	6.3-4
6.3.6	Cask Material Densities	6.3-5
6.4	Criticality Calculation.....	6.4-1
6.4.1	Fuel Loading Optimization.....	6.4.1-1
6.4.2	Criticality Results for Directly Loaded, Uncanistered Fuel	6.4.2-1
6.4.3	Criticality Results for Canistered Yankee Class Fuel.....	6.4.3-1
6.4.4	Criticality Results for Canistered Connecticut Yankee Fuel	6.4.4-1
6.5	Critical Benchmark Experiments	6.5-1
6.5.1	Benchmark Experiments and Applicability for CSAS25	6.5.1-1
6.5.2	MONK8a Validation in Accordance with NUREG/CR-6361	6.5.2-1
6.6	References	6.6-1
6.7	Supplemental Data	6.7-1
7.0	OPERATING PROCEDURES	7-1
7.1	Outline of Procedures for Receipt and Loading the Cask	7.1-1
7.1.1	Receiving Inspection.....	7.1-1
7.1.2	Preparation of Cask for Loading.....	7.1-1
7.1.3	Loading the NAC-STC Cask	7.1-5
7.2	Preparation for Transport.....	7.2-1
7.2.1	Preparation for Transport (Immediately After Loading)	7.2-1
7.2.2	Preparation for Transport (After Long-Term Storage).....	7.2-2
7.3	Outline of Procedures for Unloading the Cask.....	7.3-1
7.3.1	Receiving Inspection.....	7.3-1
7.3.2	Preparation of the NAC-STC Cask for Unloading	7.3-1

Master Table of Contents (Continued)

7.3.3	Unloading the NAC-STC Cask.....	7.3-4
7.3.4	Preparation of Empty Cask for Transport.....	7.3-7
7.4	Leak Test Requirements	7.4-1
7.4.1	Containment Verification Leak Test Procedures.....	7.4-1
7.4.2	Leak Testing for Transport After Long-Term Storage	7.4-2
7.4.3	Leak Testing for Transport After Loading without Interim Storage	7.4-3
7.4.4	Corrective Action.....	7.4-4
7.5	Railcar Design and Certification Requirements	7.5-1
7.5.1	Railcar and Tie-Down Design Requirements	7.5-1
7.5.2	Railcar Tie-Down Design Loadings	7.5-1
7.5.3	Railcar and Tie-Down Certification	7.5-1
7.6	Procedures for Loading and Unloading the Transportable Storage Canister	7.6-1
7.6.1	Loading and Closing the Transportable Storage Canister	7.6-1
7.6.2	Opening and Unloading the Transportable Storage Canister	7.6-3
8.0	ACCEPTANCE TESTS AND MAINTENANCE PROGRAM	8-1
8.1	Fabrication Requirements and Acceptance Tests	8.1-1
8.1.1	Weld Procedures, Examination, and Acceptance	8.1-1
8.1.2	Structural and Pressure Tests	8.1-3
8.1.3	Leak Tests	8.1-6
8.1.4	Component Tests	8.1-8
8.1.5	Tests for Shielding Integrity	8.1-11
8.1.6	Thermal Test.....	8.1-13
8.1.7	Neutron Absorber Tests	8.1-16
8.1.8	Transportable Storage Canister.....	8.1-19
8.2	Maintenance Program	8.2-1
8.2.1	Structural and Pressure Tests of the Cask.....	8.2-1
8.2.2	Leak Tests	8.2-2
8.2.3	Subsystems Maintenance	8.2-3
8.2.4	Valves, Rupture Disks and Gaskets on the Containment Vessel.....	8.2-3
8.2.5	Shielding	8.2-3
8.2.6	Periodic Thermal Test.....	8.2-4

Master Table of Contents (Continued)

8.2.7	Miscellaneous	8.2-6
8.2.8	Maintenance Program Schedule	8.2-7
8.3	Quick-Disconnect Valves	8.3-1
8.4	Cask Body Fabrication.....	8.4-1
8.4.1	General Fabrication Procedures.....	8.4-1
8.4.2	Description of Lead Pour Procedures	8.4-5
9.0	REFERENCES.....	9-1

THIS PAGE INTENTIONALLY LEFT BLANK

Table of Contents

1.0	GENERAL INFORMATION	1-1
1.1	Introduction.....	1.1-1
1.2	Package Description	1.2-1
1.2.1	Packaging.....	1.2-1
1.2.2	Operational Features	1.2-21
1.2.3	Contents of Packaging	1.2-21
1.3	Appendices.....	1.3-1
1.3.1	Quality Assurance.....	1.3-1
1.3.2	License Drawings	1.3-1

List of Figures

Figure 1.1-1	Major Cask Dimensions.....	1.1-8
Figure 1.2-1	Operational Schematic for the NAC-STC	1.2-26
Figure 1.2-2	Yankee-MPC Reconfigured Fuel Assembly.....	1.2-27
Figure 1.2-3	Yankee-MPC Damaged Fuel Can.....	1.2-28
Figure 1.2-4	CY-MPC Reconfigured Fuel Assembly	1.2-29
Figure 1.2-5	CY-MPC Damaged Fuel Can	1.2-30
Figure 1.2-6	CY-MPC Failed Rod Storage Canister.....	1.2-31

List of Tables

Table 1-1	Terminology.....	1-2
Table 1.2-1	Design Characteristics of the NAC-STC	1.2-32
Table 1.2-2	NAC-STC Design Basis Directly Loaded Fuel Characteristics	1.2-40
Table 1.2-3	NAC-STC Design Basis Yankee Class Fuel Characteristics.....	1.2-41
Table 1.2-4	NAC-STC Design Basis Connecticut Yankee Fuel Characteristics.....	1.2-42
Table 1.2-5	Isotopic Constituents of Yankee GTCC Waste	1.2-43
Table 1.2-6	Isotopic Constituents of Connecticut Yankee GTCC Waste	1.2-44

List of Drawings

423-800, sheets 1-3	Rev 14	Cask Assembly – NAC-STC Cask
423-802, sheets 1-7	Rev 20	Cask Body – NAC-STC Cask
423-803, sheets 1-2	Rev 8	Lid Assembly – Inner, NAC-STC Cask
423-804, sheets 1-3	Rev 8	Details - Inner Lid, NAC-STC Cask
423-805, sheets 1-2	Rev 6	Lid Assembly – Outer, NAC-STC Cask
423-806	Rev 7	Port Coverplate Assy – Inner Lid, NAC-STC Cask
423-807, sheets 1-3	Rev 3	Assembly, Port Cover, NAC-STC Cask
423-209	Rev 0	Impact Limiter Assy – Upper, NAC-STC Cask
423-210	Rev 0	Impact Limiter Assy – Lower, NAC-STC Cask
423-257	Rev 2	Balsa Impact Limiter, Upper, NAC-STC Cask
423-258	Rev 2	Balsa Impact Limiter, Lower, NAC-STC Cask
423-811, sheets 1-2	Rev 11	Details – NAC-STC Cask
423-812	Rev 6	Nameplates – NAC-STC Cask
423-843	Rev 2	Transport Assembly, Balsa Impact Limiters, NAC-STC
423-859	Rev 0	Attachment Hardware, Balsa Limiters, NAC-STC
423-870	Rev 5	Fuel Basket Assembly, PWR, 26 Element, NAC-STC Cask
423-871	Rev 5	Bottom Weldment, Fuel Basket, PWR, 26 Element, NAC-STC Cask
423-872	Rev 6	Top Weldment, Fuel Basket, PWR, 26 Element, NAC- STC Cask
423-873	Rev 2	Support Disk and Misc. Basket Details, PWR, 26 Element, NAC-STC Cask
423-874	Rev 2	Heat Transfer Disk, Fuel Basket, PWR, 26 Element, NAC-STC Cask
423-875, sheets 1-2	Rev 7	Tube, NAC-STC Cask
423-900	Rev 6	Package Assembly Transportation, NAC-STC Cask
423-901	Rev 2	Transportation Package Concept, NAC-STC Cask
455-800, sheets 1-2	Rev 2	Assembly, Transport Cask, MPC-Yankee
455-801, sheets 1-2	Rev 3	Assembly, Transport Cask, NAC-MPC
455-820, sheets 1-2	Rev 2	Spacers, Transport Cask, MPC-Yankee

List of Drawings (Continued)

455-870	Rev 5	Canister Shell, MPC-Yankee
455-871, sheets 1-2	Rev 8	Details, Canister, MPC-Yankee
455-871, sheets 1-3	Rev 7P2	Details, Canister, MPC-Yankee
455-872, sheets 1-2	Rev 12	Assembly, Transportable Storage Canister (TSC), MPC-Yankee
455-872, sheets 1-2	Rev 11P1	Assembly, Transportable Storage Canister (TSC), MPC-Yankee
455-873	Rev 4	Assembly, Drain Tube, Canister, MPC-Yankee
455-881, sheets 1-3	Rev 8	PWR Fuel Tube, MPC-Yankee
455-887, sheets 1-3	Rev 4	Basket Assembly, 24 GTCC Container, MPC-Yankee
455-888, sheets 1-2	Rev 8	Assembly, Transportable Storage Canister (TSC), 24 GTCC Container, MPC-Yankee
455-891, sheets 1-2	Rev 1	Bottom Weldment, Fuel Basket, MPC-Yankee
455-891, sheets 1-3	Rev 2P0	Bottom Weldment, Fuel Basket, MPC-Yankee
455-892, sheets 1-2	Rev 3	Top Weldment, Fuel Basket, MPC-Yankee
455-892, sheets 1-3	Rev 3P0	Top Weldment, Fuel Basket, MPC-Yankee
455-893	Rev 3	Support Disk and Misc. Basket Details, MPC-Yankee
455-894	Rev 2	Heat Transfer Disk, Fuel Basket, MPC-Yankee
455-895, sheets 1-2	Rev 5	Fuel Basket Assembly, MPC-Yankee
455-895, sheets 1-2	Rev 5P0	Fuel Basket Assembly, MPC-Yankee
455-919	Rev 2	Retainer, United Nuclear Test Assy, MPC-Yankee
414-801, sheets 1-2	Rev 1	Cask Assembly, NAC-STC, CY-MPC
414-820	Rev 0	Canister Spacer CY-MPC
414-870	Rev 3	Canister Shell, CY-MPC
414-871, sheets 1-2	Rev 6	Details, Canister CY-MPC
414-872, sheets 1-3	Rev 6	Assembly, Transportable Storage Canister (TSC), CY-MPC
414-873	Rev 2	Drain Tube Assembly, CY-MPC
414-874	Rev 0	Shim, Canister, CY-MPC
414-875	Rev 0	Spacer Shim, Canister, CY-MPC
414-881, sheets 1-2	Rev 4	Fuel Tube, Transportable Storage Canister (TSC), CY-MPC
414-882, sheets 1-2	Rev 4	Oversize Fuel Tube, Transportable Storage Canister (TSC), CY-MPC
414-887, sheets 1-4	Rev 4	Basket Assembly, GTCC, CY-MPC
414-888, sheets 1-2	Rev 4	Canister Shell, GTCC, CY-MPC

List of Drawings (Continued)

414-889, sheets 1-3	Rev 7	Assembly, Transportable Storage Canister (TSC), GTCC, CY-MPC
414-891	Rev 3	Bottom Weldment, Fuel Basket CY-MPC
414-892, sheets 1-3	Rev 3	Top Weldment Fuel Basket CY-MPC
414-893, sheets 1-2	Rev 2	Support Disk and Misc. Basket Details CY-MPC
414-894	Rev 0	Heat Transfer Disk, Fuel Basket CY-MPC
414-895, sheets 1-2	Rev 4	Fuel Basket Assembly CY-MPC
Yankee-Class Reconfigured Fuel Assembly		
YR-00-060	Rev D3	Yankee-Class Reconfigured Fuel Assembly
YR-00-061	Rev D4	Yankee-Class Reconfigured Fuel Assembly Shell Weldment
YR-00-062, Sheet 1	Rev D4	Yankee-Class Reconfigured Fuel Assembly Top End Fitting Assembly
YR-00-062, Sheet 2	Rev D2	Yankee-Class Reconfigured Fuel Assembly Top End Plate
YR-00-062, Sheet 3	Rev D1	Yankee-Class Reconfigured Fuel Assembly Top End Template
YR-00-063	Rev D4	Yankee-Class Reconfigured Fuel Assembly Bottom End Fitting Assy.
YR-00-064	RevD4	Yankee-Class Reconfigured Fuel Assembly Nozzle Bolt and Alignment Pin
YR-00-065	Rev D2	Yankee-Class Reconfigured Fuel Assembly Fuel Basket Assembly
YR-00-066, Sheet 1	Rev D5	Yankee-Class Reconfigured Fuel Assembly Fuel Tube Assembly
YR-00-066, Sheet 2	Rev D3	Yankee-Class Reconfigured Fuel Assembly Fuel Tube Assembly
Yankee Rowe Damaged Fuel Can		
455-901	Rev 0P0	Can Assembly, Damaged Fuel, MPC-Yankee
455-902, sheets 1-5	Rev 0P4	Can Details, Damaged Fuel, MPC-Yankee
Connecticut Yankee Damaged Fuel Can		
414-901	Rev 1	Assembly, Damaged Fuel Can, CY-MPC
414-902, sheets 1-3	Rev 3	Details, Damaged Fuel Can, CY-MPC
Connecticut Yankee Reconfigured Fuel Assembly		
414-903, sheets 1-2	Rev 1	Reconfigured Fuel Assembly, CY- MPC
414-904, sheets 1-3	Rev 0	Details, Reconfigured Fuel Assembly, CY- MPC

THIS PAGE INTENTIONALLY LEFT BLANK

1.0 GENERAL INFORMATION

NAC International (NAC) has designed a Storable Transport Cask (NAC-STC) for spent nuclear fuel. The United States Nuclear Regulatory Commission (NRC) licenses the NAC-STC for the transport of spent nuclear fuel. This Safety Analysis Report (SAR) addresses the ability of the NAC-STC to satisfy the NRC transportation requirements for spent fuel, either directly loaded in the cask (uncanistered) or in a canister, and Greater Than Class C (GTCC) waste in a Transportable Storage Canister, as prescribed in 10 CFR 71.

The Transportable Storage Canister is a component of the NAC-MPC dry storage system. The NAC-MPC is provided in two configurations. The first is designed to store Yankee Class spent fuel and GTCC waste and is referred to as the Yankee-MPC. The second is designed to store Connecticut Yankee spent fuel and GTCC waste and is referred to as the CY-MPC.

This chapter presents a general introduction to the transport cask and a description of its design features. The terminology used throughout this report is summarized in Table 1-1.

The NAC-STC may be shipped by rail, barge, or heavy-haul vehicle. The NAC-STC is assigned a Transport Index (TI) of 21 based on the shielding evaluation summarized in Section 5.1.4. As shown in Chapter 6, the Criticality Safety Index (CSI) is zero, since an infinite number of packages with optimum moderation remain subcritical.

The NAC-STC has been designed to satisfy the international requirements of the International Atomic Energy Agency (IAEA), in addition to U.S. requirements prescribed in 10 CFR 71.

Table 1-1 Terminology

Balsa Impact Limiter	A device constructed primarily of balsa wood with limited use of redwood. This device is designed to dissipate energy during normal and accident conditions impact events for packages weighing up to 260,000 lb. The balsa impact limiter is 128 inches in diameter with balsa wood providing primary protection during end and corner impact events and redwood for side impact events.
Cask Model	NAC-STC
NAC-STC Cask	This packaging consists of a spent-fuel storable transport cask body with dual closure lids and energy-absorbing impact limiters.
Packaging	The assembly of components necessary to ensure compliance with the packaging requirements of 10 CFR 71. Within this report, the packaging is denoted as the NAC-STC.
Package	The packaging with its radioactive contents (payload), as presented for transport (10 CFR 71.4). Within this report, the package is denoted as the NAC-STC, the NAC-STC cask or, simply, the cask.
Contents (Payload)	Twenty-six (26) pressurized water reactor (PWR) fuel assemblies in the directly loaded fuel (uncanistered) configuration or a sealed Transportable Storage Canister containing Yankee Class or Connecticut Yankee spent fuel or Greater Than Class C waste.
Containment System	The components of the packaging intended to retain the radioactive material during transport.
Cask Body	
- Multiwall Body	Construction of the cask body, which consists of concentric layers of the inner shell, gamma shielding, outer shell and neutron shielding materials.
- Neutron Shield	Consists of the stainless steel shell, gussets, and end plates, copper-stainless steel (Cu/SS) fins, and the solid NS-4-FR neutron shielding material.

Table 1-1 Terminology (continued)

NS-4-FR	A solid, synthetic polymer developed by BISCO Products, Inc. and supplied by the Japan Atomic Power Company and its licensees. NS-4-FR is a borated hydrogenous material, which results in neutron absorption capabilities similar to borated water.
Lifting Trunnions	Four, high-strength stainless steel components welded to the top forging that are used in pairs for lifting and handling the cask.
Top Forging	
- Interlid Port	A penetration in the top forging that is used as (1) a drain for the interlid region and (2) a pressure test port for the outer lid seal.
- Pressure Port	A penetration in the top forging that houses a pressure transducer, which may be used to monitor the pressure in the interlid region during storage.
- Port Cover Assembly	Includes the port cover body, spacer, retainer, bolts and O-rings.
- Pressure Transducer	An instrument for measurement of pressure in a confined space.
- O-ring	An O-ring seals the interfaces between separate cask components.
- PTFE	Blended Polytetrafluoroethylene (PTFE) is an O-ring material used as a sealing component between metallic surfaces.
- Viton	A fluorocarbon rubber O-ring material used as a sealing component between metallic surfaces.
- Interseal	Refers to the region between pairs of O-rings.

Table 1-1 Terminology (continued)

Bottom Inner Forging	The cup-shaped component that forms the bottom of the NAC-STC cavity.
Bottom Outer Forging	The ring-shaped component that forms the bottom outer region of the NAC-STC.
Bottom Plate	The plate welded to the bottom outer forging, which forms the bottom of the cask. The bottom plate encloses the neutron shielding material in the bottom of the cask.
Rotation Trunnion Recesses	Two stainless steel blocks, each provided with a deep machined groove suitable to accept the rear cask support. These recesses are welded onto the outer shell near the bottom of the cask.
Cask Cavity	The volume of space within the containment boundary.
Transportable Storage Canister (Canister)	The stainless steel cylindrical shell, bottom end plate, shield lid, and structural lid that holds the canistered fuel basket or Greater Than Class C Waste.
Canister Spacer	Structures that position the canister in the NAC-STC cavity during transport. The Yankee-MPC uses two spacers constructed of aluminum honeycomb material encased in a shell constructed of 6061-T6 aluminum alloy. The CY-MPC uses a single spacer constructed of concentric rings of stainless steel welded to a stainless steel base plate.

Table 1-1 Terminology (continued)

Fuel Basket	The structure located in the cask cavity or transportable storage canister to support the fuel assemblies.
- Support Disk	A circular stainless steel plate with square holes machined in a symmetrical pattern. The support disk is the primary lateral load-bearing component of the basket. Each square hole in the support disk is a location for a fuel tube.
- Heat Transfer Disk	A circular aluminum plate with square holes machined in a symmetrical pattern. The heat transfer disk enhances heat transfer in the fuel basket. Each square hole in the heat transfer disk is a location for a fuel tube.
- Fuel Tube	A stainless steel tube having a square cross-section. There are two Fuel Tube configurations. The standard Fuel Tube has BORAL or TalBor neutron absorber material on the four exterior surfaces and has different dimensions for the directly loaded and canistered fuel baskets. The enlarged Fuel Tube, used in the canistered fuel basket, has a larger interior cross-section and does not have neutron absorber material on the exterior surfaces.
- Threaded Rod	Aligns and supports the support disks and heat transfer disks in the fuel basket in the cask cavity.
- Spacer Nut	Installed on the threaded rod between the support disks to properly position and provide axial support for the support disks and heat transfer disks in the fuel basket in the cask cavity.
- Tie Rod	Aligns the support disks and heat transfer disks in the fuel basket structure located in the NAC-STC cask cavity or in the transportable storage canister.
- Split Spacer	Installed on the tie rod between the support disks to properly position and provide axial support for the support disks and the heat transfer disks.

Table 1-1 Terminology (continued)

Outer Lid	A secondary containment closure that is bolted to the top forging during transport.
- Outer Lid Bolts	Retain the outer lid.
Inner Lid	The primary containment closure for transport, located directly on top of the cask cavity inside the top forging.
- Drain Port	Located in the inner lid to permit draining of the cask cavity.
- Vent Port	Located in the inner lid to aid in draining and backfilling the cask cavity.
- Port Coverplates	The sealed covers that protect the vent and drain ports.
- Interseal Test Port	The test port between pairs of O-rings that permits testing of the containment seal. The test port is closed by a threaded plug with a metallic O-ring.
- Inner Lid Bolts	Retain the inner lid.
Quick Disconnect	The quick disconnect valved nipple used in the vent, drain, interlid, and inner lid interseal test port to close off the port. The drain port quick disconnect may be valved or unvalved.
Interlid Region	The space between the inner and outer lids.
Transport Impact Limiters (Upper and Lower)	Impact limiters designed for use exclusively during transport of the NAC-STC. They protect the cask by limiting impact loads during the 1-foot free drop (normal conditions of transport) and the 30-foot free drop (hypothetical accident conditions).
Transport Configuration	The transport cask configuration using either metallic or non-metallic O-ring seals in the cask containment boundary.
Storage Configuration	The transport cask configuration using metallic O-ring seals in the cask containment boundary.

Table 1-1 Terminology (continued)

Yankee-MPC Contents	Up to 36 intact Yankee Class pressurized-water reactor (PWR) spent fuel assemblies, Reconfigured Fuel Assemblies, and Recaged Fuel Assemblies. Up to four fuel assemblies may be loaded in Damaged Fuel Cans. The maximum total contents weight in the Transportable Storage Canister is 30,600 pounds, not including the weight of the Damaged Fuel Cans, which are defined to be components of the fuel basket.
CY-MPC Contents	Up to 26 Connecticut Yankee PWR spent fuel assemblies (including fuel inserts), CY-MPC Reconfigured Fuel Assemblies and CY-MPC Damaged Fuel Cans containing Connecticut Yankee intact or damaged fuel to a maximum total contents weight of 35,100 pounds.
Yankee Class Spent Fuel	Fuel that includes United Nuclear Type A and Type B, Combustion Engineering Type A and Type B, Exxon-ANF Type A and Type B, Westinghouse Type A and Type B and failed fuel cages that are bound by the above fuel types.
Connecticut Yankee Spent Fuel	15 x 15 PWR fuel assemblies manufactured by Westinghouse, Gulf Nuclear/Gulf General Atomic, NUMEC and Babcock and Wilcox.
Connecticut Yankee Fuel Inserts	Reactor Control Cluster Assemblies, flow mixers or stainless steel rods that may be inserted in, and stored with, the Connecticut Yankee spent fuel.
Yankee-MPC Recaged Fuel Assembly	A Yankee Class Combustion Engineering fuel assembly lattice (skeleton) holding United Nuclear fuel rods with no empty fuel rod positions.

Table 1-1 Terminology (continued)

Reconfigured Fuel Assembly	A stainless steel container having approximately the same external dimensions as a standard spent fuel assembly that ensures criticality control geometry and permits gaseous and liquid media to escape while preventing dispersal of gross particulates. The reconfigured fuel assembly may contain intact fuel rods, damaged fuel rods and fuel debris from any type of Yankee Class or Connecticut Yankee spent fuel assembly.
CY-MPC Damaged Fuel Can	A stainless steel container that confines a damaged Connecticut Yankee spent fuel assembly, which allows gaseous and liquid media to escape but minimizes the dispersal of gross particulate. Connecticut Yankee damaged fuel assemblies must be loaded in the CY-MPC damaged fuel can. The damaged fuel can may also hold an Intact Fuel Assembly, a Lattice or a Failed Rod Storage Canister.
Yankee-MPC Damaged Fuel Can	A stainless steel container that is similar to an enlarged fuel tube and that confines a Yankee Class Intact Fuel Assembly, Damaged Fuel Assembly, Recaged Fuel Assembly or a Reconfigured Fuel Assembly. A damaged fuel can is closed on its end by screened openings that allow gaseous and liquid media to escape, but minimize the dispersal of gross particulate. Use of the damaged fuel can requires that four cans be used in the canister in conjunction with a special shield lid machined to accept the cans.
Fuel Rod Retainer	A retainer used for the Gulf United Nuclear Fuel (GUNF) lead test assemblies to retain the removable fuel rods within the fuel assembly during normal and accident conditions of transport.

Table 1-1 Terminology (continued)

Intact Fuel Assembly	A fuel assembly without known or suspected cladding defects greater than pinhole leaks or hairline cracks. Connecticut Yankee fuel assemblies with missing fuel rods, or with missing fuel rods replaced with solid filler rods, or with structural damage, are considered intact fuel assemblies, provided that they have no damaged fuel rods. Yankee Class fuel assemblies with missing fuel rods replaced with Zircaloy or stainless steel rods, or with structural damage, are considered intact fuel assemblies provided that they have no damaged fuel rods.
Intact Fuel Rod	A fuel rod without known or suspected cladding defects greater than pinhole leaks or hairline cracks.
Damaged Fuel Assembly	A fuel assembly containing at least one damaged fuel rod with a known or suspected cladding defect greater than a hairline crack or a pinhole leak, or an assembly that cannot be handled by normal means, or both. Yankee Class fuel assemblies containing up to 20 fuel rod positions that are either missing or that are holding individual fuel rods classified as damaged.
Damaged Fuel Rod	A fuel rod with known or suspected cladding defects greater than pinhole leaks or hairline cracks.
Fuel Debris	Fuel in the form of particles, loose pellets and fragmented rods or assemblies.
Greater Than Class C Waste (GTCC)	Irradiated and surface contaminated metal, usually stainless steel, whose disposal is controlled by 10 CFR 61 due to the presence of very long-lived isotopes, including ⁵⁹ Ni, ⁹⁴ Nb and ¹⁴ C. This waste results from reactor decommissioning.

Table 1-1 Terminology (continued)

Personnel Barrier	An expanded metal screen with appropriate support structure that is installed between the impact limiters and covers the cask during transport. The expanded metal screen, and its support structure, are aluminum. The personnel barrier precludes incidental contact with the cask surface, which may be at elevated temperature compared to the rail car.
Lattice	A fuel assembly structure that is used to hold up to 204 Intact Fuel Rods or Damaged Fuel Rods from other fuel assemblies. A Lattice is sometimes called a fuel skeleton, cage or structural cage. It is built from the same components as a standard fuel assembly, but some of those components may be modified slightly, such as relaxed grids, to accommodate the distortion that may be present in a Damaged Fuel Rod. The outside dimensions are identical to a standard fuel assembly.
Failed Rod Storage Canister	A handling container for moving up to 60 individual intact or damaged fuel rods in stainless steel tubes into a CY-MPC Damaged Fuel Can. The steel tubes are held in place by regularly spaced plates welded in an open stainless steel frame. The failed rod storage canister, which is closed at the top end by a bolted closure and at the bottom by a welded plate to capture the fuel rods in the tubes, must be loaded in a CY-MPC Damaged Fuel Can.
Redwood Impact Limiter	A device constructed primarily of redwood with limited use of balsa wood. This device is designed to dissipate energy during normal and accident conditions impact events for packages weighing up to 250,000 lb. The redwood impact limiter is 124 inches in diameter with redwood providing primary protection during end and side impact events and balsa wood for corner impact events.

Table 1-1 Terminology (continued)

Structural Damage

Damage to the fuel assembly that does not prevent handling the fuel assembly by normal means. Structural damage is defined as partially torn, abraded, dented or bent grid straps, end fittings or guide tubes. The damaged grid straps or end fittings must continue to provide support to the fuel rods, as designed, and may not be completely torn or missing. Guide tubes cannot be ruptured and must be continuous between the upper and lower end fittings. Fuel assemblies with structural damage are considered to be intact fuel assemblies provided that they do not have failed or damaged fuel rods.

THIS PAGE INTENTIONALLY LEFT BLANK

1.1 Introduction

The NAC-STC is designed to safely transport spent fuel assemblies in two configurations and Greater Than Class C (GTCC) waste in a canistered configuration. The fuel assemblies may be placed directly into a fuel basket installed in the cask cavity (uncanistered) or sealed in a transportable storage canister (canistered).

The design basis spent fuels for the uncanistered (directly loaded) configuration are the Westinghouse 17×17 or 15×15 PWR fuel assemblies and Framatome-Cogema 17×17 PWR fuel assemblies. These fuels bound smaller array Westinghouse and similar Babcock & Wilcox and Combustion Engineering PWR fuel assemblies.

There are two canistered fuel configurations. The first is designed to store up to 36 intact Yankee Class spent fuel and reconfigured fuel assemblies and is referred to as the Yankee-MPC. The second is designed to store up to 26 Connecticut Yankee fuel assemblies, reconfigured fuel assemblies and damaged fuel in CY-MPC damaged fuel cans, and is referred to as the CY-MPC.

Yankee Class fuel includes United Nuclear, Combustion Engineering, Exxon-ANF, and Westinghouse Type A and Type B fuel designs. The Type A and Type B fuel designs are complementary configurations that accommodate the use of a cruciform control blade in reactor operations.

Connecticut Yankee spent fuel includes 15×15 PWR fuel assemblies having a square cross-section. The fuel specifications that serve as the design basis for the CY-MPC are presented in Section 1.2.3. The Connecticut Yankee fuel consists of fuel assemblies manufactured by Westinghouse, Gulf Nuclear/Gulf General Atomic, NUMEC and Babcock & Wilcox.

The canister configurations also accommodate GTCC waste. The Yankee-MPC and CY-MPC canister and GTCC basket accommodate up to 24 fuel assembly sized containers of GTCC waste. The GTCC canister designs have the same external dimensions as the respective spent fuel canisters, but have different basket designs.

The NAC-STC, when loaded, has a maximum design weight of 260,000 pounds. The NAC-STC provides a radioactive material containment boundary for maximum safety during the handling

and transport operations required for spent-fuel shipment. The general configuration of the NAC-STC and the major cask dimensions are shown in Figure 1.1-1.

The NAC-STC cask may be transported after loading with or without a period of interim storage. The structural components of the transport containment boundary are the:

- (1) Inner shell center section and upper and lower inner shell rings (transition sections);
- (2) Bottom inner forging; and,
- (3) Top forging.

The closure components of the containment boundary for transport without interim storage after loading are the:

- (1) Inner lid and inner lid O-ring;
- (2) Vent port coverplate and the coverplate inner O-ring; and,
- (3) Drain port coverplate and the coverplate inner O-ring.

As described in the following sections, the O-rings may be either metallic or nonmetallic.

The closure components of the containment boundary for transport after an extended period of storage are the:

- (1) Inner lid and inner lid outer metallic O-ring;
- (2) Inner lid interseal test port threaded plug with metallic O-ring;
- (3) Vent port coverplate and the coverplate outer metallic O-ring;
- (4) Vent port coverplate interseal test hole threaded plug with metallic O-ring;
- (5) Drain port coverplate and the coverplate outer metallic O-ring; and,
- (6) Drain port coverplate interseal test hole threaded plug with metallic O-ring.

Metallic O-rings are required for the storage configuration and are qualified for transport prior to shipment in accordance with the operating procedure.

The NAC-STC is designed to meet 10 CFR 71 and IAEA Safety Series No. TS-R-1 licensing requirements for spent fuel transport packages. The transport licensing requirements include providing safe containment during the handling and transport of spent nuclear fuel. Certain design features of the NAC-STC that have been included for the sole purpose of satisfying

storage licensing requirements also provide added safety for transport conditions. The design features of the NAC-STC include: inner and outer lids, redundant seals at each containment boundary penetration, cavity penetrations located in the inner lid, and a puncture-resistant outer shell and outer lid.

This Safety Analysis Report is written for transport cask licensing only. Design features related to storage cask licensing are included for clarity and for ease of review.

The NAC-STC closure design provides dual lids for transport and storage operations, as well as protection of the vent and drain ports that are located in the inner lid. This design permits performance of a periodic verification leak test on the containment seals prior to transport following extended storage. Both the inner and outer lids are installed during transport and storage.

The inner lid and its O-rings are the major removable components in the primary containment boundary. Two concentric O-rings are used to seal the inner lid to the cask cavity flange. An O-ring test port connects to the annulus between the two O-rings to permit leak testing.

The vent and drain port coverplates, which protect the vent and drain ports located in the inner lid, are also part of the primary containment boundary of the cask. Each coverplate is sealed by two concentric O-rings.

As described in Section 4.1, the inner O-rings of the inner lid and two coverplates are the containment boundary for contents (either directly loaded fuel or a loaded transportable storage canister) that is loaded for transport without interim site storage. The outer O-rings of these components are the containment boundary for directly loaded fuel that is to be transported after an extended period of storage.

The inner lid and coverplate O-rings may be either metallic or non-metallic as shown in the License Drawings. However, metallic O-rings must be used when the NAC-STC is directly loaded for long-term storage or for the transport of canistered contents. The metallic O-rings provide long-term sealing capability in an elevated temperature and radiation environment.

The outer lid provides a sealed secondary closure for transport and storage operations using a single O-ring. The O-ring may be either metallic or non-metallic. The outer lid protects the inner lid and the vent and drain ports from external puncture events.

There are two penetrations in the top forging: an interlid port, which serves primarily as a drain for the interlid region, and a pressure port, which may house a transducer that monitors the pressure in the interlid region during storage. During transport, the pressure port is closed by a threaded plug. The pressure port plug is covered by the transport port coverplate. The interlid and pressure port penetrations in the top forging are protected by SA-705, Type 630, 17-4 precipitation-hardened (PH) stainless steel port covers with two piston-type blended polytetrafluoroethylene (PTFE) O-rings.

The body of the NAC-STC is a smooth right-circular cylinder of multiwall construction, consisting of stainless steel inner and outer shells separated by lead gamma radiation shielding, which is poured in place. The center section of the inner shell is fabricated from Type 304 stainless steel. At each end of the inner shell center section, inner shell rings fabricated from Type XM-19 stainless steel provide the transition to the bottom inner forging and the top forging. The outer shell is also fabricated from Type 304 stainless steel. The inner and outer shells are welded to the Type 304 stainless steel top forging, which is a ring that is machined to mate with the inner and outer lids. The inner and outer shells are also welded to the Type 304 stainless steel bottom inner and outer forgings, respectively. The cask bottom consists of the two forgings and a plate with neutron shield material sandwiched between the bottom inner forging and the bottom plate. Neutron shield material is also placed in an annulus that surrounds the cask outer shell along the length of the cask cavity. The neutron shielding material is a solid synthetic polymer (NS-4-FR). The neutron shield annulus is enclosed by a Type 304 stainless steel shell and by end plates that are welded to the outer shell. Two pressure relief valves are provided in the bottom of the neutron shield annulus to relieve pressure in the neutron shield annulus due to a severe thermal accident condition (fire). Neutron shielding is also provided on the top of the cask by a layer of NS-4-FR enclosed in the inner lid.

Redundant lifting capability for the NAC-STC is provided by four lifting trunnions welded to the top forging at 90-degree intervals. Rotation trunnion recesses are located on the outer shell near

the bottom of the cask to permit the NAC-STC to be rotated to the horizontal position and to provide longitudinal tiedown restraint in the aft direction. A Type 304 stainless steel shear ring is provided at the top end of the radial neutron shield to supply longitudinal restraint when the cask is positioned horizontally for transport in the front support structure.

For fuel assemblies loaded directly into the NAC-STC, a stainless steel basket locates and supports the 26 PWR fuel assemblies in the cask cavity. The basket design utilizes a series of high-strength stainless steel support disks to support the fuel assemblies in stainless steel tubes, which include BORAL or TalBor neutron absorber sheets ($0.02 \text{ g/cm}^2 \text{ }^{10}\text{B}$ minimum). Aluminum heat transfer disks are provided to enhance the thermal performance of the package. The heat transfer disks are also supported by the stainless steel basket.

For the Yankee-MPC canistered configuration, two aluminum honeycomb spacers, placed one above the canister and one below, locate the canister in the cask cavity so that the location of the center of gravity of the packaging is the same as it is for the uncanistered fuel packaging. The aluminum honeycomb is enclosed in a 6061-T6 aluminum alloy shell. In the CY-MPC canistered configuration, a single stainless steel spacer, placed below the canister, is used to position the canister so that the location of the center of gravity of the packaging is the same as it is for the uncanistered fuel packaging.

The canister shell, bottom and welded shield and structural lids are fabricated from stainless steel. The basket for the canistered configuration is similar in design to that used for directly loaded fuel. Two basket configurations are used for Connecticut Yankee fuel. A 26-assembly basket is used for all of the fuel types except Westinghouse Vantage 5H. Vantage 5H fuel must be installed in the 24-assembly basket, which may also hold other Connecticut Yankee fuel types. The construction of the two basket configurations is identical except that two fuel loading positions of the 26-assembly basket are blocked to form the 24-assembly basket.

The Yankee-MPC canisters may contain one or more Reconfigured Fuel Assemblies. The Yankee Reconfigured Fuel Assembly is shown in Figure 1.2-2. It is designed to contain up to 64 Yankee Class fuel rods, or portions thereof, which are classified as failed, and to maintain the geometric positions of the rods. The external dimensions and the top end fitting of the Yankee Reconfigured Fuel Assembly are the same as those of a standard Yankee Class fuel assembly, allowing it to be handled in the same way as a standard assembly.

The Yankee-MPC Damaged Fuel Can, shown in Figure 1.2-3, is designed for Yankee fuel classified as intact or damaged. This configuration provides four stainless steel damaged fuel cans located in the four corner positions of the basket. A damaged fuel can is similar to an enlarged fuel tube, except that the can is closed on the bottom end with a screened plate that is welded into place and closed on the top by a screened lid, which is held in place by the damaged fuel shield lid once the canister is closed. The square holes in the four corner positions of the Yankee-MPC basket top and bottom weldments are enlarged to allow the damaged fuel can to be removed or inserted after the basket is assembled. The damaged fuel can is captured between the canister bottom plate and the shield lid to preclude vertical movement and to hold the can lid in place. The shield lid has four machined recesses on the underside to mate with the damaged fuel can lids.

The Yankee-MPC is also designed to hold recaged fuel assemblies. Recaged fuel assemblies consist of a Combustion Engineering fuel assembly lattice holding United Nuclear fuel rods. Fuel rods removed from United Nuclear fuel assemblies for inspection or testing cannot be reinstalled in the United Nuclear fuel assembly lattice. The Combustion Engineering fuel assembly lattice provides the same grid support structure as did the original United Nuclear fuel assembly lattice, but it does not have the shroud fixture used to preclude water impingement on the fuel rods. No empty fuel rod positions are permitted in the recaged Combustion Engineering fuel assembly lattice.

The CY-MPC canister may contain one or more Reconfigured Fuel Assemblies, Damaged Fuel Cans, or Failed Rod Storage Containers. The CY-MPC Reconfigured Fuel Assembly is shown in Figure 1.2-4. It consists of a 10 x 10 array of stainless steel tubes attached to upper and lower end fittings that are similar to those used on standard fuel assemblies. The diameter of the tubes is sized to allow the insertion of individual damaged or bowed fuel rods. The design allows the release of gaseous products and liquids, but minimizes the dispersal of particulates.

The CY-MPC Damaged Fuel Can is shown in Figure 1.2-5. It is designed to hold a complete fuel assembly, which may be intact or damaged, a lattice or a failed rod storage canister. The CY-MPC Damaged Fuel Can has a square cross-section that is slightly larger than a standard Connecticut Yankee fuel assembly. The damaged fuel can is fabricated from stainless steel and has top and bottom closures that allow the release of gaseous products and liquids, but minimizes the dispersal of particulates.

The CY-MPC Failed Rod Storage Canister, shown in Figure 1.2-6, is similar in design to the CY-MPC Reconfigured Fuel Assembly but holds only a maximum of 60 fuel rods classified as failed in stainless steel tubes.

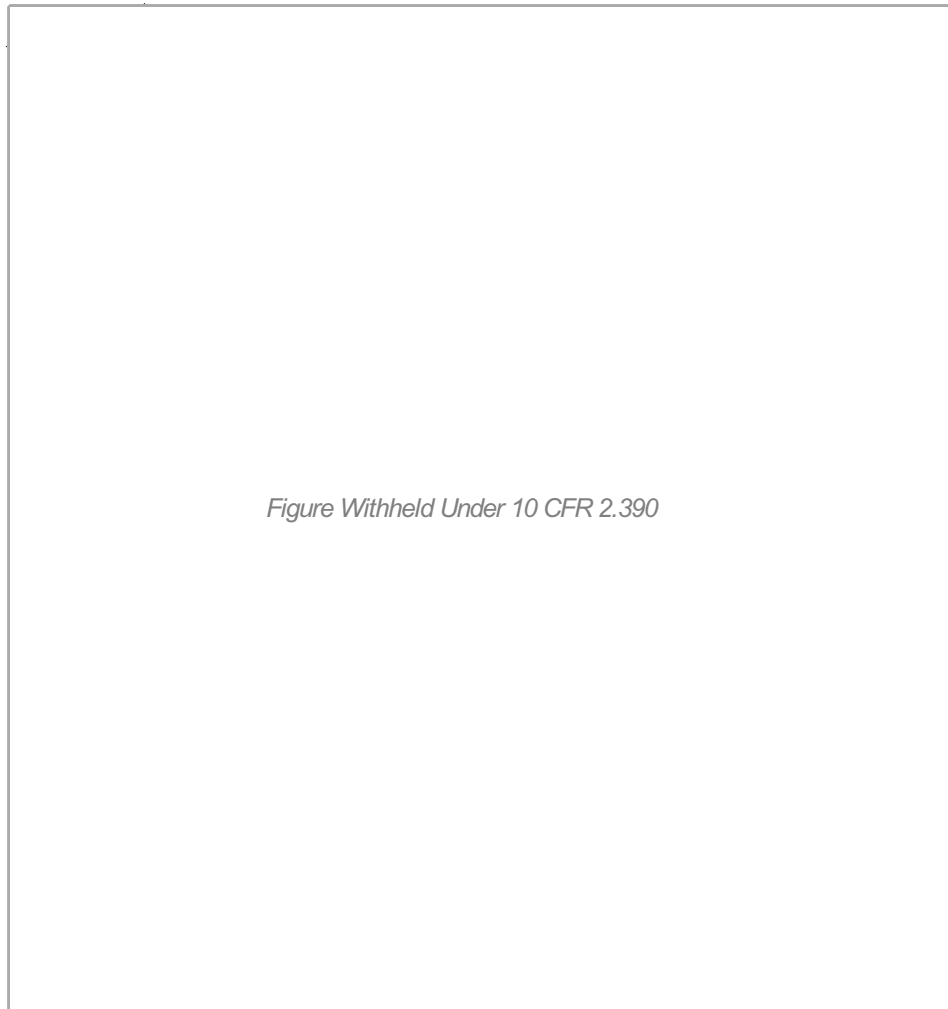
Some of the Connecticut Yankee fuel assemblies will be stored with flow mixers, reactor control cluster assemblies (RCCA) or stainless steel rods installed. Flow mixers are thimble plug assemblies used during reactor operation to maintain equal coolant flow in fuel assemblies that do not contain a reactor control cluster. Reactor control clusters were used to control the reactivity of the Connecticut Yankee reactor during operations and shutdown. Some Connecticut Yankee fuel assemblies may have missing fuel rods and/or may have solid filler rods replacing the missing fuel rods.

A maximum of two assemblies with up to two irradiated stainless steel filler rods per assembly may be loaded in the CY-MPC canister. These assemblies may only be loaded in the two central basket positions.

Two impact limiter designs consisting of a combination of redwood and balsa wood, encased in Type 304 stainless steel, are provided to limit the g-loads acting on the cask during a drop accident load condition. The g-loads are limited by the crush strength of the wood contained in the impact limiters. The predominately balsa wood impact limiter (the balsa impact limiter) is designed for use with all the proposed contents. The predominately redwood impact limiters (the redwood impact limiter) may only be used with directly loaded fuel or the Yankee-MPC configurations.

Any number of NAC-STCs may be shipped at one time, with each cask on its own railcar. The NAC-STC may also be shipped in any number on board ships, barges, or special heavy-haul vehicles.

Figure 1.1-1 Major Cask Dimensions



Dimensions in inches

1.2 Package Description

This section presents a basic description of the NAC-STC and the contents that may be transported. An operational schematic of the cask is presented in Figure 1.2-1. Detailed dimensional drawings are provided in Section 1.3.2. The design characteristics of the NAC-STC are summarized in Table 1.2-1.

1.2.1 Packaging

1.2.1.1 Gross Weight

The maximum gross transport weight of the NAC-STC spent-fuel shipping cask is calculated to be 249,700 pounds for directly loaded fuel with the standard (redwood) impact limiters and is 254,589 pounds for CY-MPC canistered GTCC waste with the lightweight (balsa) impact limiters. When the NAC-STC is loaded on its railcar, the gross weight of the railcar (including cask, impact limiters, supports, and personnel barrier) will satisfy the requirements of the Association of American Railroads. The calculated component weights, detailed in Tables 2.2-1 through 2.2-5, are summarized as:

Component	Directly Loaded Fuel Weight (pounds)	Yankee-MPC Canistered Fuel Weight (pounds)	Yankee-MPC Canistered GTCC Waste Weight (pounds)	CY-MPC Canistered Fuel Weight (pounds)	CY-MPC Canistered GTCC Waste Weight (pounds)
Cask Body	175,970	175,970	175,970	175,970	175,970
Basket	16,820	--	--		
Fuel or GTCC Waste	39,000	30,600	12,340	35,100	20,230
Canister	--	14,600	14,600	16,666	16,666
Canister Basket	--	9,530	26,471	14,055	28,926
Spacers	--	860	860	1,374	1,374
Total (calculated)	231,790	231,560	230,241	243,165	243,166
With Standard (Redwood) Impact Limiters	249,520	249,290	247,971	--	--
With Lightweight (Balsa) Impact Limiters	243,213	242,983	241,664	254,588	254,589
Analysis Weight	250,000	250,000	250,000	260,000	260,000

The weight of the CY-MPC fuel basket is that of the 26-assembly basket. The weight of the 24-assembly basket is 13,451 pounds.

1.2.1.2 Material of Construction, Dimensions and Fabrication

The NAC-STC body is of cylindrical, multiwall construction. The materials of construction of the structural components of the cask body are Type 304, Type XM-19, and Type 17-4 PH stainless steel. The primary structural components of the cask are the inner and outer shells. Poured-in-place chemical copper lead fills the annulus between the inner and outer shells and serves as the primary gamma radiation shield. The top forging, which is a ring that forms the upper end of the cask, is welded to the inner and outer shells. The SA-336 Type 304 stainless steel inner lid is recessed in and bolted to the top forging. The SA-705, Type 630, H1150, 17-4 PH stainless steel outer lid is bolted into the end of the top forging. The vent and drain ports are recessed into the inner lid and are each protected by an SA-240, Type 304 stainless steel port coverplate. The interlid port and the pressure port are recessed in the top forging and are protected by SA-705, Type 630, 17-4 PH stainless steel port covers. At the lower end of the cask, the inner and outer shells are welded to the cask bottom, which consists of two forgings and a plate, a cup-shaped bottom inner forging that is the lower end of the cask cavity, a ring-shaped bottom outer forging that forms the exterior of the cask bottom and connects the outer shell to the bottom inner forging, and a bottom plate that is the bottom end of the cask. Neutron radiation shielding is provided by NS-4-FR, a poured-in-place solid synthetic neutron-absorbing polymer, which surrounds the outer shell along the cavity region and is enclosed by a shell and end plates that are welded to the outer shell. A layer of NS-4-FR is enclosed in the inner lid and in the cask bottom to provide neutron shielding at the ends of the cask during cask loading operations. Twenty-four explosively bonded copper and Type 304 stainless steel fins are located in the radial neutron shield to enhance the heat rejection capability of the NAC-STC and to support the neutron shield shell and end plates. The cask is passively cooled.

In the event of an accident during transport where impact force(s) may be applied to the cask, the NAC-STC is protected by energy-absorbing impact limiters that consist of balsa wood (the balsa impact limiter), or a combination of redwood and balsa wood (the redwood impact limiter), enclosed in a stainless steel shell. The cup-shaped impact limiters fit over each end of the cask and dissipate kinetic energy by crushing the wood at known force values, limiting the g-loads acting on the cask during an impact load condition.

The NAC-STC is provided with four lifting trunnions on the outside of the top forging at 90-degree intervals. The lifting trunnions are fabricated from SA-705, Type 630, 17-4 PH stainless steel. Only two diametrically opposite trunnions are required to lift the NAC-STC.

Two additional lifting trunnions are provided for those facilities that require redundant lifting. Two rotation trunnion recesses are located on the outer shell near the bottom of the cask. The NAC-STC safely transports spent fuel assemblies in two configurations.

The fuel may be placed directly in a fuel basket installed in the cask cavity, or the fuel may be sealed in a transportable storage canister that is installed in the cask.

The NAC-STC directly loaded fuel basket has a capacity of 26 PWR fuel assemblies. The fuel basket design uses Type 17-4 PH stainless steel support disks to support the fuel assemblies in Type 304 stainless steel tubes. The support disks are spaced and retained by Type 17-4 PH stainless steel, square spacer nuts, which are assembled on six 1.625-inch diameter Type 17-4 PH threaded rods. Type 6061-T651 aluminum alloy heat transfer disks are supported by the stainless steel basket assembly to enhance heat rejection of the package.

The transportable storage canister is constructed of Type 304L stainless steel. The canister is closed with a shielding lid and a separate structural lid, both of which are welded in place. The shielding lid is constructed of Type 304 stainless steel, and the structural lid is constructed of Type 304L stainless steel. The canister contains a basket that provides support and geometry control for Yankee Class spent fuel, Connecticut Yankee spent fuel, Yankee Class GTCC waste or Connecticut Yankee GTCC waste. The spent fuel basket used in the canister is similar in design to the directly loaded fuel basket.

The materials of construction and detailed component and assembly dimensions for the NAC-STC are shown in the License Drawings. The major components are described in the following sections.

1.2.1.2.1. Cask Body

The outer shell, the center section of the inner shell, the top and bottom forgings, the bottom plate, and the inner lid of the NAC-STC are manufactured from Type 304 stainless steel. Type 304 stainless steel has well-documented mechanical properties and a long history of use in similar applications. It is a commonly welded material and is readily available throughout the world. Type 304 stainless steel possesses good strength and adequate toughness in the operating temperature range of the NAC-STC. The center section of the inner shell is 1.5 inches thick and has an inner diameter of 71.0 inches. Welded to the top and bottom of the inner shell center section are the inner shell rings. The inner shell rings are manufactured from Type XM-19

high-strength stainless steel. The inner shell rings connect the bottom inner forging and the ring-shaped top forging to the center section of the inner shell. The inner shell rings are 2.0 inches thick at the end that is welded to the forgings and have a 3.0-inch-long taper down to a 1.5-inch thickness at the weld joint to the inner shell center section. The top and bottom inner shell rings reduce the stress concentration at the inner shell interface with the top and bottom forgings. Type XM-19 stainless steel has well-documented mechanical properties and is suitable for welding to the Type 304 stainless steel components.

Two forgings and a plate comprise the bottom of the cask body. The separate forgings are necessary to facilitate the pouring of the lead. These forgings are assembled with full-penetration welds and act as a single structural unit when fabrication is complete. The bottom components are differentiated here for clarity as the bottom inner forging, the bottom outer forging, and the bottom plate. The bottom inner forging is cup-shaped. The bottom of the cup is 6.2 inches thick. The side of the cup, which is welded to the bottom inner shell ring, is 2.0 inches thick.

The outer shell is concentric with the inner shell and is 2.65 inches thick. The outer shell is welded to the bottom outer forging, which is ring-shaped. The bottom outer forging is the outer ring portion of the cask bottom and is 3.9 inches thick in the radial direction at the location of the neutron shield material. The bottom outer forging is also welded to the outside diameters of the bottom inner forging and the bottom plate. The bottom plate is a 5.45-inch thick plate. A 2.0-inch thick, 78.9-inch diameter layer of NS-4-FR neutron shielding material is enclosed between the bottom inner forging and the bottom plate. Two rotation trunnion recesses are located approximately 180 degrees apart and are welded to the exterior of the outer shell just above the bottom of the neutron shield. Sixteen 1 - 8 UNC holes, equally spaced on a 76.0-inch diameter, are tapped into the bottom plate for attachment of the bottom transport impact limiter.

The upper inner shell ring and the upper end of the outer shell are welded to the ring-shaped top forging. On the inner diameter of the top forging is a recessed ledge. The inner lid is completely recessed into the top forging and mates with the ledge. The outer lid is bolted into the end of the top forging. Thirty-six outer lid bolts secure the outer lid to the top forging. The inner lid rests on a ledge in the top forging that is the sealing surface for the two metallic O-rings and the land for the 42 inner lid bolts. Two guide pins are installed in two of the inner lid bolt holes during cask loading and unloading operations and, along with alignment marks, assist in aligning and ensuring proper seating of the inner lid. Similar procedures are used to assist in the proper

alignment of the outer lid. Four lifting trunnions are welded to the top forging to permit cask lifting and handling with either a redundant or a nonredundant lifting yoke.

Radial gamma radiation shielding for the NAC-STC is provided by the inner shell, the outer shell, and the 3.7-inch thickness of American Society of Testing Materials (ASTM) B29 chemical copper lead located in the annulus between the inner and outer shells. The lead also serves as an elastic support for the outer shell during a puncture event and for the inner shell during a side impact event.

Radial neutron shielding for the NAC-STC is provided by NS-4-FR, which is a solid synthetic polymer originally developed by BISCO Products, Inc. and is now supplied by the Japan Atomic Power Company and its licensees. This solid neutron shielding material is selected to eliminate leakage and maintenance problems and to alleviate other concerns attendant with using a liquid neutron shield. NS-4-FR has a high-hydrogen content to provide for neutron attenuation, is doped with boron to minimize the number of secondary gammas generated, is stable at elevated temperature service, and is fire retardant. A 5.5-inch-thick layer of NS-4-FR is installed in the annulus formed by the outer shell, the 0.250-inch-thick neutron shield shell, and the 0.472-inch (12 mm) thick neutron shield end plates.

The inner shell, inner shell rings, top forging, bottom inner forging, and the inner lid establish a cask cavity that is 165.0 inches long and 71.0 inches in diameter.

The calculated weight of the cask body is 175,970 pounds. The overall length of the cask body is 193.0 inches, and the maximum outside diameter is 99.1 inches across the corners of the neutron shield shell.

1.2.1.2.2 Inner Lid and Bolts

The inner lid and its O-rings are the principal installed components of the NAC-STC containment boundary. The O-rings may be either metallic or nonmetallic, depending on cask use. The inner lid is 9.0 inches thick, 79.0 inches in diameter, and is fabricated from Type 304 stainless steel. The top portion of the inner lid is a 2.0-inch-thick, 67.5-inch-diameter layer of NS-4-FR neutron shielding material enclosed by a 1.0-inch-thick, Type 304 stainless steel coverplate that is welded in place. The 42 inner lid bolts are 1 1/2 - 8 UN socket head cap screws fabricated from SB-637, Grade N07718 nickel alloy steel bolt material. This bolt material has a coefficient of thermal expansion that is very similar to that of the Type 304

stainless steel inner lid and top forging and, thus, alleviates differential thermal expansion effects.

The inner lid is recessed to a depth of 11.8 inches into the top forging to provide clearance for the outer lid. The inner lid bolt holes are located on a ledge machined into the inner lid, so that the bolt heads are below the top surface of the lid. The top surface of the inner lid has threaded holes for the attachment of a lid-lifting device. The bottom of the inner lid is sealed to the top forging of the cask body by two O-rings. The O-rings may be either metallic or nonmetallic, depending on the cask use. Metallic O-rings are used for storage and for transport following storage. Either metallic or nonmetallic O-rings may be used for transport of directly loaded fuel without interim storage after loading. The outer metallic O-ring provides the primary containment seal for transport after storage, while the inner O-ring (either metallic or nonmetallic) provides the primary containment seal for transport without interim storage after loading. An interseal test port is provided and is equipped with a 1/4-inch quick-disconnect valved nipple to allow leak testing of the inner lid O-rings. The interseal test port plug is part of the containment boundary for transport after a period of storage. As shown on Drawing 423-804, the O-ring grooves on the underside of the inner lid are either square to accommodate metallic O-rings or have a truncated triangular shape to accommodate nonmetallic O-rings.

Three ports are recessed into the inner lid: the vent port, the drain port, and the interseal test port. These ports are described in Section 1.2.1.2.4.

1.2.1.2.3 Outer Lid and Bolts

The outer lid, bolts and O-ring, when bolted to the top forging, provide a sealed secondary closure. The outer lid is 5.25 inches thick in the central region, 86.7 inches in diameter, and is fabricated from SA-705, Type 630, H1150, 17-4 PH stainless steel. The 36 outer lid bolts are 1-8 UNC socket head cap screws fabricated from SA-564, Type 630, H1150, 17-4 PH stainless steel. The bolt material is identical to that of the outer lid, alleviating any differential thermal expansion effects.

The outer lid is bolted to the top forging of the NAC-STC. The lid bolt holes are countersunk into the lid so that the bolt heads are below the top surface of the lid. The bottom surface of the outer lid is sealed to the top forging by one O-ring, which is replaced prior to transport. The O-ring may be either metallic or nonmetallic. The interlid port, located in the top forging, is used to test the seal of the O-ring in the outer lid. The top surface of the outer lid has threaded

holes for the attachment of a lid-lifting device and for the attachment of the upper transport impact limiter. As shown on Drawing 423-805, the O-ring groove on the underside of the outer lid is either square to accommodate a metallic O-ring or has a truncated triangular shape to accommodate a Viton O-ring.

1.2.1.2.4 Ports and Port Covers

The NAC-STC design includes five ports: three in the inner lid and two in the top forging. The vent, drain and interseal test ports are recessed in the inner lid and provide access to the cask containment. Recessed in the top forging are two noncontainment ports, the interlid port for interlid region drainage and outer lid O-ring leak testing, and the pressure port, which is provided for monitoring of the pressure in the interlid region during storage.

The vent port is a 1.0-inch diameter penetration through the inner lid and is closed by a quick-disconnect valved nipple (quick disconnect). The quick disconnect is not considered to be a containment barrier. The vent port is used to access the cask cavity following the fuel loading to drain, dry, leak test and backfill it with inert gas prior to transport. The vent port coverplate uses a two O-ring design, similar to the inner lid. The O-rings may be either metallic or non-metallic, depending on the cask use. Metallic O-rings are used for storage and for transport following storage. Either metallic or non-metallic O-rings may be used for transport without interim storage after loading. The outer metallic O-ring provides the primary containment seal for transport after storage, while the inner O-ring (either metallic or non-metallic) provides the primary containment seal for transport without interim storage after loading.

The drain port is a 1.0-inch diameter penetration through the inner lid that is used to fill and drain the cask cavity. The drain port is also closed by a quick disconnect, which is not considered to be a containment barrier. Similar to the vent port, the drain port coverplate uses a two O-ring design. The O-rings may be either metallic or non-metallic, depending on the cask use. Metallic O-rings are used for storage and for transport following storage. Either metallic or non-metallic O-rings may be used for transport without interim storage after loading. The outer metallic O-ring provides the primary containment seal for transport after storage, while the inner O-ring (either metallic or non-metallic) provides the primary containment seal for transport without interim storage after loading. Alignment marks on the top surface of the inner lid and the top forging assist in aligning the drain port in the lid and the drain tube in the cask cavity. The interseal test port is also closed by a quick disconnect, which is not considered to be a containment barrier. The interseal test port containment is a threaded plug with a metallic O-ring.

The pressure port, located in the top forging, houses the transducer that monitors the pressure in the interlid region during storage. The pressure transducer is removed during transport. The interlid port penetrates the top forging into the region between the inner and the outer lids and serves as a drain for the interlid region and as a port to pressurize the interlid region for seal testing purposes. The interlid port is closed by a quick disconnect. The basic geometry of the interlid and pressure ports and port covers is identical. Each port has a 4.5-inch diameter opening that is a minimum of 1.1 inches deep. Concentric with the port opening is a 2.93-inch diameter bore. This bore acts as a lead-in to the 2.875-inch diameter bore that serves as the sealing surface for the two piston-type blended polytetrafluoroethylene (PTFE) O-rings in the port cover.

Both of the port covers are fabricated from SA-705, Type 630, H1150, 17-4 PH stainless steel. The port covers resemble a cup-shape and have the geometrical appearance of a thick round end plate with a cylindrical body. The end plate of the port cover is 4.5 inches in diameter and 1.0 inch thick. The three 3/8 - 16 UNC port cover bolts, which are fabricated from SA-193, Grade B6, Type 410 stainless steel, are countersunk flush with the top of the port cover. There are two piston-type PTFE O-rings on the cylindrical body of the port covers with a seal test port between the O-rings. A retainer is bolted to the open end of the cylindrical body of the port cover to retain the O-rings and the spacer between them after assembly. The port cover design permits the thick end plate to absorb an impact, while any deflection of the end plate results in the O-rings sliding in the bore of the port with the seal maintained.

The basic geometry of the vent port and coverplate, and the drain port and coverplate, are identical to each other. Each port has a 6.53-inch diameter opening in the inner lid that is 1.8 inches deep. Concentric with the port opening is a 3.25-inch diameter bore that houses the 1.0-inch diameter quick disconnect. As shown in Drawing 423-806, the 1.0-inch thick vent and drain port coverplates are fabricated from SA-240, Type 304 stainless steel. When installed, the port coverplates are recessed 0.8 inch below the top surface of the inner lid. The vent and drain port coverplates are sealed to the inner lid by the metallic O-rings on the bottom face of each port coverplate. The four 1/2 - 13 UNC port coverplate bolts are fabricated from SA-193, Grade B6, Type 410 stainless steel. The bolt holes are countersunk so that the bolt heads are flush with the top of the port coverplate.

1.2.1.2.5 Lifting Trunnions and Rotation Trunnion Recesses

The NAC-STC has four lifting trunnions that are fabricated from SA-705, Type 630, H1150, 17-4 PH stainless steel and are welded into 2.0-inch deep recesses in the top forging at 90-degree intervals around the cask circumference. Only two diametrically opposite lifting trunnions are required to lift the NAC-STC. The lifting trunnions are 5.5 inches in diameter and have a load-bearing width of 2.5 inches. The trunnions are machined to create a 0.38-inch thick end flange, which acts as a safety stop to ensure proper engagement and to prevent inadvertent disengagement of the lifting yoke.

There are two rotation trunnion recesses located near the bottom end of the NAC-STC. The rotation trunnion recesses are located approximately 18 inches above the bottom of the cask in line with two of the lifting trunnion, but 3.0 inches offset from the cask centerline to ensure that rotation of the cask occurs in the proper direction. Each recess is fabricated from SA-705, Type 630, 17-4 PH stainless steel and is groove-welded to the bottom outer forging. The recess is 6.0 inches square and 4.13 inches deep, with a full radius at the top of the recess that engages with the rotation support. The neutron shield shell is cut out to accommodate the rotation trunnion recesses.

1.2.1.2.6 Transport Impact Limiters

The NAC-STC is equipped with removable, cup-shaped impact limiters that are bolted over each end of the cask to ensure that the design impact loads for the cask are not exceeded for any of the defined normal operation or accident drop conditions. The NAC-STC transport impact limiters are provided in two configurations. The standard configuration is constructed of a combination of redwood and balsa wood and is referred to as the redwood impact limiter. The other configuration is constructed using only balsa wood and is referred to as the balsa impact limiter. Both configurations are completely enclosed in a stainless steel shell. The upper impact limiter has cutouts in its inside diameter for clearance with the lifting trunnions. The impact limiters absorb the energy of a cask drop by crushing the redwood and/or balsa wood. The force required to crush the impact limiter is determined by the amount and location of the wood and its grain direction. The upper and lower impact limiters are bolted over each end of the cask body by 16 equally spaced attachment rods and nuts. The lightweight impact limiters have a lower weight and improved crush characteristics compared to the standard impact limiters, and accommodate a higher cask content weight and higher cask total weight. As shown in Section

1.2.1.1, the lightweight impact limiters must be used in the transport of the CY-MPC canister configurations. Either impact limiter design may be used with the directly loaded fuel or Yankee-MPC configurations. The two impact limiter configurations are similar in size and shape. The redwood impact limiters have a total weight of 17,730 pounds. The total weight of the balsa impact limiters is 11,423 pounds.

1.2.1.2.7 Directly Loaded Fuel Basket

The NAC-STC has one directly loaded fuel basket configuration and three (3) canistered fuel basket configurations. The canistered fuel basket configurations are described in Section 1.2.1.2.8. The directly loaded basket and the canistered baskets are constructed of stainless steel with aluminum heat transfer disks and are of similar design.

The directly loaded fuel basket design is a right-circular cylinder configuration with square fuel tubes laterally supported by a series of support disks, which are retained by square spacer nuts on threaded rods at six locations. The nuts are torqued at installation to provide a solid load path in compression between the support disks. The support disks are 0.5-inch thick, 70.86-inch diameter 17-4 PH stainless steel disks spaced 4.87 inches center-to-center with square holes for the fuel tubes. The top end weldment and the bottom end weldment are fabricated from Type 304 stainless steel, are geometrically similar to the support disks, and are 1.0-inch thick. The threaded rods have a 1-5/8 – 8 UN thread diameter and are fabricated from Type 17-4 PH stainless steel. The nuts are 2.5-inch square bars that are also fabricated from Type 17-4 PH stainless steel. The fuel tubes are fabricated from Type 304 stainless steel and provide support for the encased neutron absorber sheet on each of the four sides. The neutron absorber provides criticality control in the basket. No structural credit is taken for the stainless steel tubes as a contributor to the total structural strength of the basket and support of the fuel assemblies.

The NAC-STC directly loaded fuel basket accommodates 26 PWR fuel assemblies in an aligned configuration in 8.78-inch inside dimension square fuel tubes, which have 0.142-inch thick walls. The fuel tubes are supported in the basket assembly between the top and bottom weldment plates. The hole in the top weldment is 8.75 inches square. The hole in the bottom weldment is 8.65 inch square. The basket design traps the fuel tube between the top and bottom weldment preventing axial movement of the fuel tube. The minimum width of the support disk webs between the fuel tubes is 1.5 inches, but two webs have a width of 3.3 inches.

Twenty Type 6061-T651 aluminum alloy heat transfer disks, 0.625-inches thick, 70.65 inches in diameter, are supported by the threaded rods and spacer nuts, which also support and locate the stainless steel support disks. These aluminum disks are located at the center of the axial spacing between the stainless steel support disks and are sized to eliminate contact with the cask inner shell and basket threaded rods as a result of differential thermal expansion.

The NAC-STC has been designed to facilitate filling with water and subsequent draining. A 1.0-inch rounded notch is located at the bottom of each fuel tube, ensuring that there will be free flow between the inner tube regions and the disk regions. Water will naturally fill and drain between the basket disks and the cask body. Water will also flow between the disks in the gap between each of the tubes and the disk that surrounds it. Each of the disks also has four 1-inch diameter holes to supplement the flow of water between the disks. Also, to facilitate flow to the drain line, the bottom plate is positioned by supports 1.5 inches above the bottom of the cask. These design features have been provided to ensure that there is a free flow of water in the cask basket that results in even filling and draining of the cask.

1.2.1.2.8 Transportable Storage Canister

There are two transportable storage canister configurations. One configuration is used for Yankee Class spent fuel and GTCC waste (Yankee-MPC). The other is used for Connecticut Yankee spent fuel and GTCC waste (CY-MPC). The canisters differ only in overall length and in the thickness of some components. The transportable storage canister consists of four (4) principle components. These are the canister, canister basket, shield lid and structural lid. The canister consists of an annular right-circular shell closed at one end by a bottom plate. The shell is constructed of 5/8-inch rolled Type 304L stainless steel plate. The edges of the rolled plates are joined with full penetration welds. The Type 304L stainless steel bottom plate is attached to the shell by also using a full penetration weld. The canister shell is constructed in accordance with ASME Code Section III, Subsection NB. The inside and outside diameter of the canister are 69.39 inches and 70.64 inches, respectively.

The overall external length of the Yankee-MPC canister is 122.5 inches, the inside depth is 121.5 inches and the bottom plate is 1.0-inch thick. The overall external length of the CY-MPC canister is 151.75 inches, the inside depth is 150.0 inches and the bottom plate is 1.75-inches thick.

After loading, the canister is closed by a shield lid and structural lid, each welded to the canister shell. The design of the shield lid and structural lid provides redundant confinement seals at the top of the canister. Both the shield lid and structural lid welds are examined in accordance with ASME Code Section V.

The shield lid of both canister configurations is a 5-inch thick Type 304 stainless steel plate. It is joined to the canister shell using a partial penetration weld. The shield lid contains the drain and fill penetrations and provides gamma radiation protection to operators for the draining, drying and inerting operations attendant to sealing the canister. After the shield lid is welded in place, the shield lid weld is leak tested in accordance with ANSI N14.5-1997 to ensure that the required leaktightness is achieved.

The structural lid of both canister configurations is a 3-inch-thick Type 304L stainless steel plate. It is attached to the canister shell with a partial penetration weld. Removable lifting fixtures threaded in the structural lid are used to lift the loaded canister.

1.2.1.2.8.1 Canistered Fuel Baskets

There are three (3) canistered fuel basket configurations. The Yankee-MPC basket accommodates 36 spent fuel assemblies. The CY-MPC basket is provided in a 26 assembly and a 24-assembly configuration.

The Yankee-MPC Fuel Basket

The Yankee-MPC fuel basket is used to position up to 36 intact Yankee Class fuel assemblies, Reconfigured Fuel Assemblies and recaged fuel assemblies, including four fuel assemblies or Reconfigured Fuel Assemblies loaded in damaged fuel cans (four are required due to shield lid configuration), within the canister and to maintain geometry control of the fuel during all of the transport (and storage) conditions. These three basket configurations are not interchangeable.

The fuel basket design is a right-circular cylinder with square fuel tubes, laterally supported by a series of support disks, which are retained by split spacers on tie rods at eight locations. The split spacers are installed to provide a solid load path in compression between the support disks. The support disks are 0.5-inch thick, 69.15-inch diameter 17-4 PH stainless steel disks spaced 4.4 inches center-to-center with square holes for the fuel tubes or damaged fuel cans. The top end disk (top weldment) and the bottom end disk (bottom weldment) are fabricated from Type 304 stainless steel. They are geometrically similar to the support disks and are 0.5-inch thick.

The tie rods have a 1-1/8-inch diameter and are fabricated from Type 304 stainless steel. The split spacers are 2.5 inches in diameter by 1.416 inches long with an additional 2.0 inch diameter by 0.539 inch long extension, and they are also fabricated from Type 304 stainless steel.

There are three basket configurations consisting of two fuel tube configurations and a damaged fuel can configuration. Both fuel tube configurations are fabricated from 18 gauge Type 304 stainless steel sheet. The first, the standard configuration, has a square interior cross-section of 7.8 inches and is encased with BORAL sheets on all four outside surfaces of the fuel tube. The second, the enlarged fuel tube configuration, has a square interior cross-section of 8.0 inches, but does not have exterior BORAL sheets on the sides. The enlarged fuel tubes are restricted to the four corner positions of the basket. The neutron absorber provides criticality control in the basket. No structural credit is assumed for the stainless steel tubes as a contributor to the total structural strength of the basket and support of the fuel assemblies.

The canistered fuel basket accommodates fuel assemblies in the fuel tubes. The fuel tubes are supported in the basket assembly between the top and bottom weldment plates. The hole in the top weldment is 7.78 inches square. The hole in the bottom weldment is 6.0 inches square. The top of the fuel tube has a flange surface, which extends to 8.65 inches square. The basket design traps the fuel tube between the top and bottom weldments, preventing axial movement of the fuel tube. The minimum width of the support disk webs between the fuel tubes is 0.75 inch. The support disks used in the three basket configurations are identical.

The damaged fuel can is similar to the enlarged fuel tube in that it does not have exterior neutron absorber sheets on the sides and is restricted to the four corner positions of the basket. The damaged fuel can is closed on its bottom end by a stainless steel bottom plate having screened openings. After loading, the can is closed on its top by a stainless steel lid that also has screened openings. The top plate and can body incorporate lifting fixtures that allow movement of the loaded can, if necessary, and installation and removal of the can lid. The damaged fuel can extends through the bottom and top weldments of the basket, and is captured between the damaged fuel shield lid and canister bottom plate. The damaged fuel can lid is held in place by the damaged fuel shield lid, which is machined on the underside in four places to mate with the damaged fuel can lid. The screened openings allow the filling, draining and vacuum drying of the damaged fuel can, but preclude the release of gross particulate material to the canister interior.

To permit removal, if necessary, of the damaged fuel can, the top and bottom weldment openings in the four corner positions of the damaged fuel basket configurations are sized to allow the can to be inserted or removed with the basket assembled. Consequently, the damaged fuel can is not captured between the weldments.

Fourteen (14) Type 6061-T651 aluminum alloy heat transfer disks, 0.5-inches thick and 68.87 inches in diameter, are supported by the tie rods and split spacers, which also support and locate the stainless steel support disks. These aluminum disks are located at the center of the axial spacing between the stainless steel support disks and are sized to preclude contact with the cask inner shell and basket tie rods as a result of differential thermal expansion. Holes in the heat transfer disks for the fuel tubes, damaged fuel cans and tie rods are sized to accommodate thermal expansion occurring after the fuel is placed into the basket. The heat transfer disks used in the three configurations are identical.

The canistered fuel basket has been designed to facilitate filling with water and subsequent draining. The top lid and bottom plate of the damaged fuel can incorporate screened openings to allow water to fill and drain during loading and canister closure operations. Each of the disks has three (3) 1.25-inch diameter holes to facilitate free water flow between disks. Water will also flow between the disks in the gap between each of the tubes. To facilitate flow to the drain line, the bottom plate is positioned by supports 1.5 inches above the bottom of the cask. These design features have been provided to ensure that there is a free flow of water in the cask basket between the inner tube regions and the disk regions that results in even filling and draining of the cask.

As shown in Table 1.2-2, there are minor weight variations between Yankee Class fuel assembly types. Fuel assembly types may be mixed within the basket, provided that the contents weight limit of 30,600 pounds is not exceeded. Mixing fuel types within the weight limit can result in a basket containing 36 fuel assemblies, whereas loading a basket with only Westinghouse fuel would result in the basket containing 34 assemblies.

The CY-MPC Fuel Baskets

The CY-MPC fuel basket is provided in both a 26 and a 24 assembly configuration. The two configurations are identical except that the top weldment of the 24 assembly configurations has only 24 fuel tube penetrations (See Drawing 414-892). As described in Section 1.2.3.1, the 24 assembly basket is used for loading Zircaloy clad spent fuel with an enrichment above 3.93 wt % ^{235}U or stainless steel clad spent fuel with an enrichment above 4.03 wt % ^{235}U .

The CY-MPC fuel basket design is a right-circular cylinder with square fuel tubes laterally supported by a series of support disks, which are retained by split spacers on tie rods at six locations. The split spacers are installed to provide a solid load path in compression between the support disks. The support disks are 0.5-inch thick, 69.15-inch diameter 17-4 PH stainless steel disks spaced 4.59 inches center-to-center with square holes for the fuel tubes. The top end disk (top weldment) and the bottom end disk (bottom weldment) are fabricated from Type 304 stainless steel. They are geometrically similar to the support disks and are 0.5-inch thick. The tie rods have a 1-5/8-inch diameter and are fabricated from Type 304 stainless steel. The split spacers are 2.88 inches in diameter by 1.485 inches long with an additional 2.5-inch diameter by 0.56-inch long extension, and they are also fabricated from Type 304 stainless steel. The fuel tubes are fabricated from Type 304 stainless steel and provide support for encased neutron absorber sheet welded onto each of the four external sides. The neutron absorber provides criticality control in the basket. No structural credit is assumed for the stainless steel tubes as a contributor to the total structural strength of the basket and support of the fuel assemblies.

Four fuel positions in each basket configuration are 9.1-inches square with the remaining (either 22 or 20 fuel positions) being 8.7-inches square. The larger fuel positions are designated "oversize" fuel positions and are intended to accommodate CY damaged fuel cans and fuel assemblies with dimensions that exceed the fuel design dimensions due to reactor events. The fuel tubes are supported in the basket assembly between the top and bottom weldment plates and have composite 0.14-inch thick walls. The fuel position holes in the bottom weldment are 8.57 inches square. The top of the fuel tube has a flange surface, which extends to 9.6 inches square, except that the flange surface of the oversize fuel tubes is 10.0 inches square. The basket design traps the fuel tube between the top and bottom weldments, preventing axial movement of the fuel tube. The minimum width of the support disk webs between the fuel tubes is 1.0 inches.

Twenty-seven (27) Type 6061-T651 aluminum alloy heat transfer disks, 0.5-inches thick and 68.87 inches in diameter, are supported by the tie rods and split spacers, which also support and locate the twenty-eight (28) stainless steel support disks. These aluminum disks are located at the center of the axial spacing between the stainless steel support disks and are sized to preclude contact with the cask inner shell and basket tie rods as a result of differential thermal expansion.

The canistered fuel basket has been designed to facilitate filling with water and subsequent draining. Each of the disks has three (3) 1.25-inch diameter holes to facilitate water flow between disks. Water will also flow between the disks in the gap between each of the tubes. To

facilitate flow to the drain line, the bottom plate is positioned by supports 1.5 inches above the bottom of the cask. These design features have been provided to ensure that there is a free flow of water in the cask basket that results in even filling and draining of the cask.

As shown in Table 1.2-4, there are enrichment differences between Connecticut Yankee fuel types. The 24 assembly basket is used for loading Zircaloy clad spent fuel with an enrichment above 3.93 wt % ^{235}U or stainless steel clad spent fuel with an enrichment above 4.03 wt % ^{235}U .

1.2.1.2.8.2 Canistered GTCC Basket

There are two canistered GTCC basket configurations. The Yankee-MPC GTCC basket design is similar to the Yankee Class fuel basket in that the basket is a modified tube and disk design that positions and supports up to 24 Yankee Class GTCC waste containers. The CY-MPC GTCC basket design uses a series of curved plates and support ribs to form a canister holding 24 tubes that provide 24 loading positions. The designs accommodate the geometry of the existing GTCC waste.

Yankee-MPC GTCC Basket

The Yankee-MPC GTCC basket is a right-circular cylinder with square tubes laterally supported by a series of eight support disks. The support disks are 1.0-inch thick, 68.98-inches diameter, Type 304 stainless steel disks that are spaced 15.60 inches center-to-center. The support disks are open in the center region to accommodate twenty-four 8.20-inch square tubes. The tubes are supported full length by 2.5-inch thick support walls all around the center region. The support disks are retained in position by welding to the support walls of the basket. The basket accommodates GTCC waste containers in an aligned configuration in 7.82-inch square inside dimension Type 304 stainless steel tubes, which have 0.25-inch-thick walls. The basket is a modified tube and disk design. The maximum loaded weight of a GTCC container is 514 pounds, so the maximum content weight is 12,340 pounds for 24 containers.

CY-MPC GTCC Basket

The CY-MPC GTCC basket is a right-circular cylinder formed by a series of 1.75-inch thick Type 304 stainless steel plates that provide the principal shielding for the GTCC waste. The basket is supported by 12 support ribs that extend the length of the basket. The support ribs are 1.25-inch thick, Type 304 stainless steel, spaced at 30° intervals around the basket circumference. Twenty-four stainless steel tubes form the GTCC waste loading positions in the

interior of the cylinder formed by the plates. The tubes have a 0.375-inch thick wall and an inside dimension of 8.74 inches to accept GTCC waste containers. Formed plates are used to conform the outer square tubes to the circular basket. The maximum loaded weight of GTCC waste is 18,742 pounds for 24 containers. The maximum weight of a loaded container is 1,210 pounds.

1.2.1.2.8.3 Canister Transport Spacers

The Yankee-MPC fuel or GTCC waste canister is located in the NAC-STC cavity by two (2) aluminum honeycomb spacers. One spacer is installed below the canister and one above. The aluminum honeycomb is an engineered material having well-defined load-bearing and crush characteristics established by design and fabrication. The two (2) spacers have different lengths and are not interchangeable. The aluminum honeycomb is encased within a thin 6061-T6 aluminum alloy skin that precludes the entry of incidental water, contamination and foreign materials into the honeycomb structure. The spacers support the canister in all of the normal operations, but may deform during hypothetical accident events.

The bottom spacer is nominally 14 inches high and 69.0 inches in diameter. The top spacer is 28 inches high and 70.6 inches in diameter. Removable lifting lugs are used to install and remove the spacers.

The CY-MPC fuel or GTCC waste canister is located in the NAC-STC cavity by a single stainless steel spacer formed by a series of concentric rings welded to a stainless steel base plate. The spacer is installed below the canister. The spacers support the canister in all of the normal operations, but may deform during hypothetical accident events.

The bottom spacer is nominally 12.7 inches high and 70.6 inches in diameter. Removable lifting lugs are used to install and remove the spacer.

1.2.1.2.8.4 Reconfigured Fuel Assemblies

The reconfigured fuel assemblies are used with both the Yankee-MPC and CY-MPC configurations. The reconfigured fuel assembly is designed to confine fuel rods, or portions thereof, which are classified as damaged fuel, and to maintain the geometric configuration of those fuel rods. The assemblies are designed to allow the draining of free water and the backfilling of the rods and surrounding region with helium. Since there is no significant remaining "gap activity" in the failed rods, pressure retention is not a concern.

The Yankee-MPC Reconfigured Fuel Assembly consists of a shell (square tube with end fittings) and a basket assembly that supports 64 tubes in an 8 x 8 array, which hold the failed rods. The shell, basket assembly and tubes are stainless steel. The spent fuel rods are confined in the fuel tubes, which are closed with end plugs. The shell is closed with top and bottom end fittings. The tube end plugs and the shell end fittings have drilled holes to permit draining, drying and helium backfilling. The Yankee-MPC Reconfigured Fuel Assembly is shown in Figure 1.2-2.

The CY-MPC Reconfigured Fuel Assembly consists of a 10×10 array of stainless steel tubes attached to upper and lower end fittings that are similar to those used on standard fuel assemblies. The tubes are designed to hold individual fuel rods that have been removed from fuel assemblies. The diameter of the tubes is sized to allow the insertion of individual damaged or bowed fuel rods. The cross-section dimension restricts loading to one of the four "oversize fuel" basket positions described in Section 1.2.1.2.8.1. The CY-MPC reconfigured fuel assembly is shown in Figure 1.2-4.

1.2.1.2.8.5 CY-MPC Damaged Fuel Cans

The damaged fuel can is designed to hold a complete fuel assembly, which may be intact or damaged. It may also hold a lattice or failed rod storage canister. Damaged fuel includes fuel assemblies that have one or more individual fuel rods that are classified as failed. The damaged fuel can has a square cross-section that is slightly larger than a standard Connecticut Yankee fuel assembly. Consequently, loading of the damaged fuel can is restricted to one of the four corner "oversize fuel" basket positions. The damaged fuel can is fabricated from stainless steel and has top and bottom closures that allow the release of gaseous products and liquids but minimizes the dispersal of particulates. The CY-MPC damaged fuel can is shown in Figure 1.2-5. The CY-MPC Failed Rod Storage Canister is shown in Figure 1.2-6.

1.2.1.2.8.6 Yankee-MPC Damaged Fuel Cans

The Yankee-MPC damaged fuel can may contain an intact, recaged, reconfigured or damaged spent fuel assembly, but may not contain individual fuel rods not in an assembly array. A canister configured for damaged fuel has a basket design that allows the damaged fuel can to be placed in the basket after the damaged fuel can is loaded, and a canister shield lid design that is machined on its underside to mate with the lid of the damaged fuel can. The shield lid and basket designed for the damaged fuel can cannot be used interchangeably with other canister

configurations. The damaged fuel can is constructed of stainless steel and has a welded closure on its bottom end and a removable lid on the top end. The damaged fuel can lid and bottom closure are screened to allow the filling, draining and vacuum drying of the can, and to preclude the release of gross particulate to the canister during operations or storage events. The damaged fuel can has the same cross-section dimensions as the enlarged fuel tube and does not have attached neutron absorber plates on its exterior. The corner fuel positions of the basket top and bottom weldments are enlarged so that the damaged fuel can may be removed from the basket if necessary. The can is captured between the canister shield lid and bottom plate to limit axial movement. The Yankee-MPC damaged fuel can is shown in Figure 1.2-3.

1.2.1.3 Heat Dissipation

The NAC-STC design basis decay heat dissipation capability is:

Directly Loaded Fuel	22.1 kW
Canistered Yankee Class Fuel	12.5 kW
Canistered Yankee Class GTCC	2.9 kW
Canistered Connecticut Yankee Fuel	17 kW
Canistered Connecticut Yankee GTCC	5 kW

The use of aluminum heat transfer disks in the basket and the use of 24 explosively bonded copper/stainless steel fins extending through the NS-4-FR solid neutron shield aid in the heat transfer capability of the NAC-STC. The heat dissipation features of the NAC-STC are entirely passive. No active or support cooling mechanisms are required during transport. A detailed discussion of the thermal characteristics of the NAC-STC is provided in Chapter 3.

The directly loaded basket accommodates 26 PWR fuel assemblies with a maximum decay heat load of 0.85 kilowatts per assembly.

The Yankee-MPC configuration accommodates up to 36 assemblies, depending on assembly type. The maximum canistered fuel assembly decay heat load is 0.347 kilowatts per assembly for a canister of 36 assemblies and 0.259 kilowatts per assembly for a canister of 34 stainless steel-clad assemblies. The basket may also contain one or more Yankee-MPC Reconfigured Fuel Assemblies with a maximum heat load of 0.102 kW per assembly.

The CY-MPC configuration accommodates up to 26 assemblies, depending on assembly type. The maximum canistered fuel assembly decay heat load is 0.654 kilowatts per assembly for a canister of 26 assemblies. The basket may also contain one or more CY-MPC Reconfigured Fuel Assemblies with a maximum heat load of 0.321 kW per assembly or CY-MPC Damaged Fuel Cans with a maximum heat load of 0.654 kW per can.

1.2.1.4 Coolants

There are no coolants utilized within the NAC-STC. An inert helium gas atmosphere is used to backfill the cask cavity during transport.

1.2.1.5 Shielding

A 3.7-inch thickness of chemical copper lead and a 4.4-inch total thickness of stainless steel are maintained between the cask contents and the exterior radial surface of the NAC-STC for the attenuation of gamma radiation. Additional radial shielding is provided to reduce the gamma radiation contribution above the radial neutron shield by a 0.47-inch stainless steel ring attached to the top weldment. A thickness of 5.5 inches of solid, borated neutron shielding material (NS-4-FR), which extends beyond the full length of the active fuel region, is provided for radial neutron shielding. The inner and outer lids provide a total thickness of 12.25 inches of stainless steel on the top end of the cask to attenuate gamma radiation from the fuel and assembly hardware. A 2.0-inch-thick disk of solid, borated NS-4-FR is provided in the inner lid for neutron shielding on the top end of the cask. When transporting canistered fuel, the canister shield and structural lids provide an additional total thickness of eight inches of steel that provides significant attenuation of gamma radiation at the top end of the cask. The canister shell also provides an additional 0.62 inches of stainless steel shielding in the top radial direction. The cask provides 11.65 inches of stainless steel gamma radiation shielding material and 2.0 inches of solid, borated NS-4-FR neutron shielding material. The bottom of the canister provides an additional one inch of stainless steel shielding at the bottom in the axial direction of the cask. A detailed description of the NAC-STC shielding design, as well as the shielding analysis, is provided in Chapter 5.

1.2.1.6 Protrusions

There are no outer protrusions on the NAC-STC other than the four external lifting trunnions that are welded to the top forging near the upper end of the cask. The lifting trunnions are within the envelope protected by the impact limiters. The inner lid and all of the port covers are recessed into the cask body and do not protrude above the cask surface. The outer lid forms a smooth surface with its recessed bolts.

1.2.2 Operational Features

The NAC-STC is designed for ease of operation. The cask is designed to be easily loaded, unloaded, and handled at a nuclear facility. The configuration and surface finish of the cask exterior surfaces have been designed to facilitate and minimize cask decontamination efforts. The inner lid, the outer lid, and the port covers are all one-piece components designed to reduce handling times and to maintain personnel dose rates as low as reasonably achievable (ALARA). Quick-disconnect fittings are provided in the vent and drain ports, the inner lid interseal test port and in the interlid port for improved handling operations. All operational features are shown on the license drawings provided in Section 1.3.2. An operational schematic for the NAC-STC is shown in Figure 1.2-1. Operating procedures are provided in Chapter 7 for both canistered and directly loaded (uncanistered) fuel operations.

1.2.3 Contents of Packaging

Shipments in the NAC-STC shall not exceed the following limits:

1. The maximum content weight of the NAC-STC shall not exceed 67,200 pounds in the CY-MPC configuration and 56,000 pounds in the Yankee-MPC and directly loaded configurations.
2. The limits specified in Tables 1.2-2 through 1.2-4 for the design basis fuels shall not be exceeded.

3. The total decay heat of the cavity contents shall not exceed 22.1 kilowatts for directly loaded fuel, 12.5 kilowatts for Yankee Class canistered fuel and 17 kilowatts for Connecticut Yankee canistered fuel.
4. The total weight of the Zircaloy and/or stainless steel clad fuel assemblies shall not exceed 30,600 pounds in the Yankee-MPC, 35,100 pounds in the CY-MPC and 39,000 pounds for directly loaded fuel.
5. The total weight of the Yankee-MPC and CY-MPC GTCC canistered waste shall not exceed 12,340 pounds and 18,742 pounds, respectively.
6. Any number of NAC-STC casks may be shipped at one time on a railcar, a ship, a barge, or a heavy-haul vehicle.
7. Radiation levels shall not exceed the requirements of 10 CFR 71.47, 10 CFR 71.51, and IAEA Safety Standard Series No. TS-R-1, Common Provision B3.
8. Surface contamination levels shall not exceed the requirements of 10 CFR 71.87(i) and IAEA Safety Standard Series No. TS-R-1, Common Provision B4.

1.2.3.1 Design Basis Spent Fuel

The NAC-STC is designed to safely transport spent fuel assemblies in two configurations. The fuel assemblies may be directly loaded into a fuel basket installed in the cask cavity (uncanistered) or sealed in a transportable storage canister (canistered). The design basis fuel assemblies for the uncanistered configuration are the Framatome-Cogema 17×17 and Westinghouse 17×17 or 15×15 PWR fuel assemblies. These assemblies bound smaller array Westinghouse, and similar Babcock & Wilcox, and Combustion Engineering PWR fuel assemblies. The NAC-STC can transport 26 directly loaded PWR fuel assemblies.

The key parameters of the design basis directly loaded spent fuel assemblies are provided in Table 1.2-2.

In the Yankee-MPC configuration, the NAC-STC can transport up to 36 Yankee Class fuel assemblies, including Yankee-MPC Reconfigured Fuel Assemblies and recaged fuel assemblies, including four intact or damaged fuel assemblies or Reconfigured Fuel Assemblies loaded in Yankee-MPC damaged fuel cans (four are required due to shield lid configuration). Any intact spent fuel assembly with fuel rods removed shall have each of the empty fuel rod positions filled

with a solid rod fabricated from Zircaloy or stainless steel. Damaged fuel assemblies may contain empty positions provided the combined number of damaged rods and empty positions does not exceed 20 in any single assembly. The key parameters of the design basis Yankee-MPC spent fuel assemblies are provided in Table 1.2-3. The maximum and minimum enrichments shown in Table 1.2-3 are nominal values for the manufacturer and type of fuel assembly shown. Certain fuel assemblies of the same manufacturer and type have enrichment values nominally above or below these values due to the method by which enrichment tolerances were applied during fabrications. The effects of these minor variations are considered in Section 5.4.1.2 and 6.4.3.1 and are shown to be not significant. The NAC-STC can also transport up to 24 containers of Yankee Class GTCC waste.

In the CY-MPC configuration, the NAC-STC can transport up to 26 Connecticut Yankee fuel assemblies, including CY-MPC Reconfigured Fuel Assemblies and CY-MPC Damaged Fuel Cans. CY-MPC Reconfigured Fuel Assemblies and Damaged Fuel Cans must be loaded in one of the four "oversize fuel" loading positions in the CY-MPC fuel basket. The NAC-STC can also transport up to 24 containers of Connecticut Yankee GTCC waste.

Solid stainless steel rods, approximately 21 inches long, may be inserted into Connecticut Yankee intact and damaged fuel assembly RCCA guide tubes not containing a RCCA. The stainless steel rods are intended to displace the water from the lower end of the RCCA guide tubes during draining of the canister. The height of the first drainage hole of the RCCA guide tube is over 21 inches from the bottom of the tube. The 20 RCCA guide tubes per assembly could retain significant amounts of water. This water would be required to be removed by vacuum drying. The small diameter of the RCCA guide tubes, the height of water in the tube, and the minimal decay heat in the location of the tubes would make removal of the water by the vacuum drying process extremely difficult. The rods will be installed in the assemblies prior to loading the assemblies into the canister.

1.2.3.2 Greater Than Class C Waste

Greater Than Class C (GTCC) waste is defined in 10 CFR 61.55(a)(3) and (4) by the concentration of long-lived radionuclides, i.e., ^{14}C , ^{59}Ni , and ^{94}Nb , and/or short-lived radionuclides, i.e., ^3H , ^{60}Co , and ^{63}Ni . The disposal of GTCC waste is controlled by 10 CFR 61.

GTCC waste consists of radiation activated and surface contaminated steel, and/or plasma cutting debris (dross). Stainless steel core baffle structure, which is located adjacent to the reactor vessel in a high neutron flux field, is the major component of GTCC waste.

Yankee Class GTCC Waste

The principal Yankee Class GTCC waste consists of the segmented core baffle structure, but it includes miscellaneous hardware consisting of sectioned source vanes and sectioned fuel assembly cage guide tubes, grid straps and end fittings. The core baffle structure is plasma cut underwater into pieces of a size that are loaded into containers that have the same external dimensions as a "Yankee Class" fuel assembly. Dross (fines and debris) is generated by the underwater plasma cutting of the core baffle structure. The dross is solid particulate debris, varying in size from approximately 8 microns to over 850 microns and having a density approximately 24 percent lower than the parent material. The dross material does not generate, nor release, radioactive gases.

Dross material is collected from the spent fuel pool in buckets, in metallic sock filters, or by vacuuming and is discharged directly into a GTCC container. No credit is taken for the sock filters in retaining the dross material. The GTCC containers have an 80 micron screen held between perforated plates in the top and bottom end fittings. Based on an experimental study of plasma cutting debris particle size, the 80 micron screen in the GTCC containers retains in excess of 95 percent of the dross material. Up to 24 GTCC containers, having a total weight of 12,340 pounds, can be placed in the GTCC basket/canister. The reference volume for the design basis GTCC is 43,147 inches³.

A portion of the GTCC waste consists of three sectioned fuel assembly cage components (guide tubes, grid straps and end fittings) and four sectioned source vanes. This material is primarily stainless steel, inconel and Zircaloy activated by exposure in the reactor core. The fuel assembly cage material and source vanes are inserted directly in to one of the interior loading positions of the GTCC canister. Debris from the fuel assembly sectioning operation is captured in filters that are placed in a GTCC container to preclude dispersal.

The principal isotopic constituents of typical Yankee Class GTCC waste are presented in Table 1.2-5. The radionuclide composition of the waste was determined based on radiochemical assay of samples and dose rate measurements of the waste containers. The isotopes that primarily contribute to the radiological source term are ⁵⁴Mn, ⁵⁵Fe, ⁶⁰Co, and ⁶³Ni. The source terms applied in the evaluation of the GTCC waste are presented in Section 5.2.

Any contents, such as residual water or filter media, that are subject to the production of radiolytically generated combustible gases will be limited so that the quantity of any individual combustible gas will not exceed 4% by volume within any volume of a canister containing GTCC waste. A determination of the combustible gas generation within a sealed canister will be made prior to transport to demonstrate that the 4% limit will not be exceeded from the time the canister is sealed through a period equal to twice the expected shipment duration. Furthermore, the GTCC waste will be evaluated prior to loading to ensure that none of the activated material or filter media contents produce chemical or galvanic corrosion reactions with the stainless steel canister.

Table 1.2-5 provides the inventory of radionuclides in the core baffle and dross material.

Connecticut Yankee GTCC Waste

The Connecticut Yankee GTCC waste consists of sections of the core baffle, core barrel, core support plate and miscellaneous related hardware associated with these components. The major components were hydrolaser cut underwater into pieces of a size that are loaded into containers that have the same external dimensions as a Connecticut Yankee fuel assembly. Any dross material (fines and debris) generated by the cutting operations will be disposed of as low level radioactive waste.

The GTCC containers have 80 micron perforated plates that screen the drain holes in the top and bottom end fittings to allow water draining and vacuum drying. Up to 24 GTCC containers, having a total weight of 18,742 pounds, can be placed in the GTCC basket/canister. The maximum weight of a single loaded GTCC container is 1,210 pounds.

The principal isotopic constituents of the Connecticut Yankee GTCC waste, resulting from activation and surface contamination, are presented in Table 1.2-6. The radionuclide composition of the waste was determined based on radiochemical assay of samples and dose rate measurements of the waste containers. The isotopes that primarily contribute to the radiological source term are ^{54}Mn , ^{55}Fe , ^{60}Co , and ^{63}Ni . The source terms applied in the evaluation of the GTCC waste are presented in Section 5.2.

The GTCC waste is solid and the waste containers have screened openings in the top and bottom that permit water draining and vacuum drying. Consequently, no hydrogen generation as a result of residual water occurs.

Figure 1.2-1 Operational Schematic for the NAC-STC

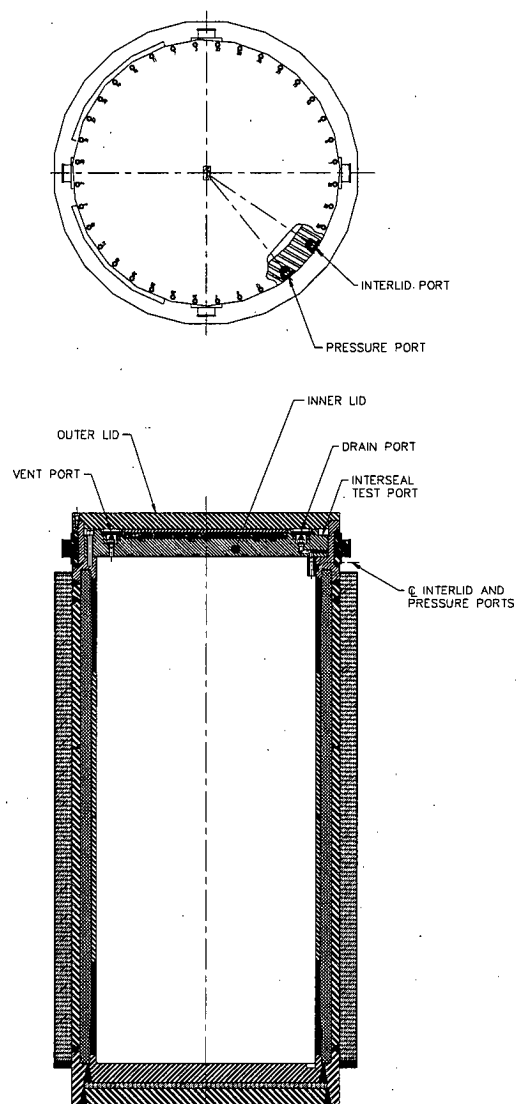


Figure 1.2-2 Yankee-MPC Reconfigured Fuel Assembly



Figure Withheld Under 10 CFR 2.390

Figure 1.2-3 Yankee-MPC Damaged Fuel Can

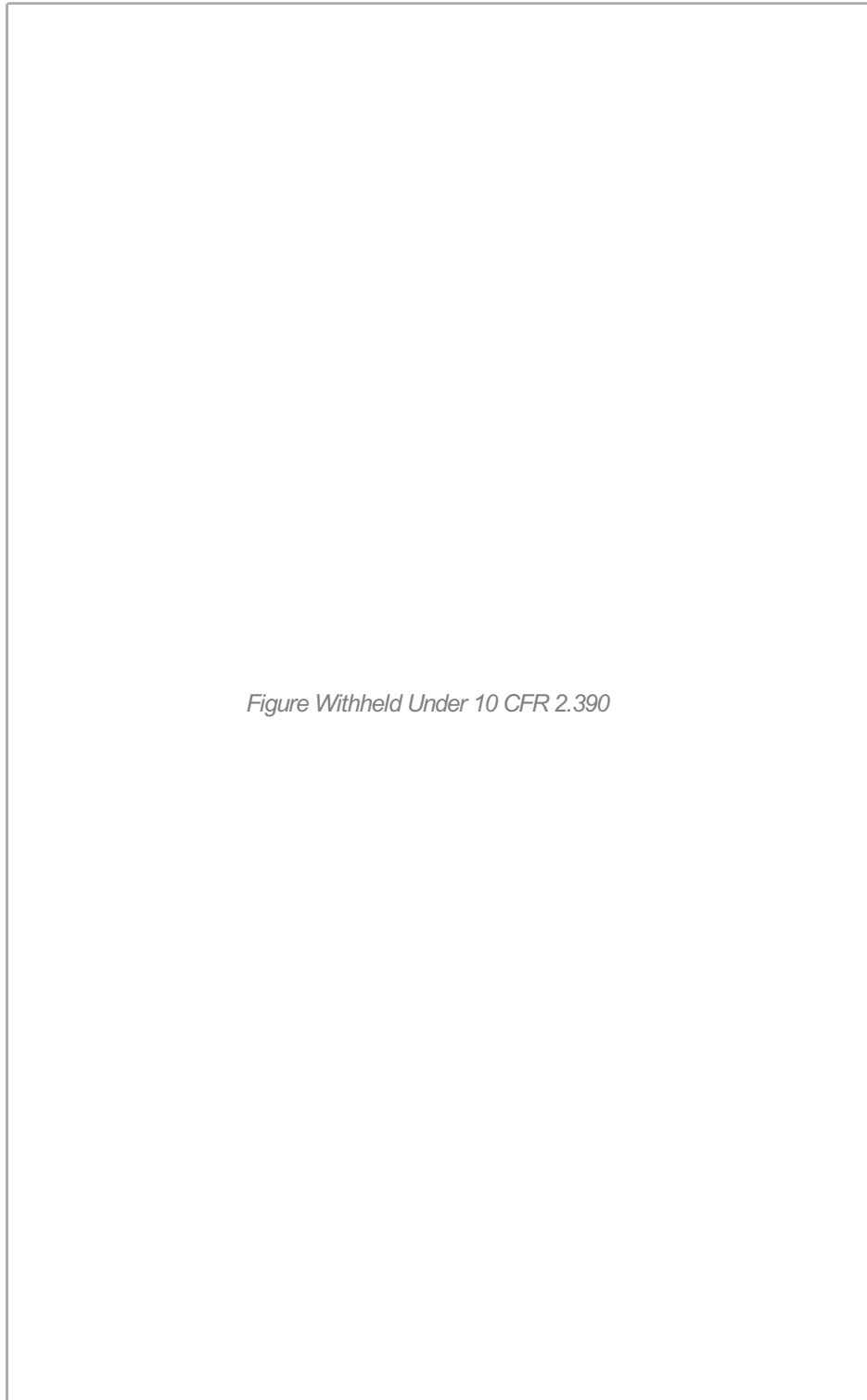


Figure 1.2-4 CY-MPC Reconfigured Fuel Assembly

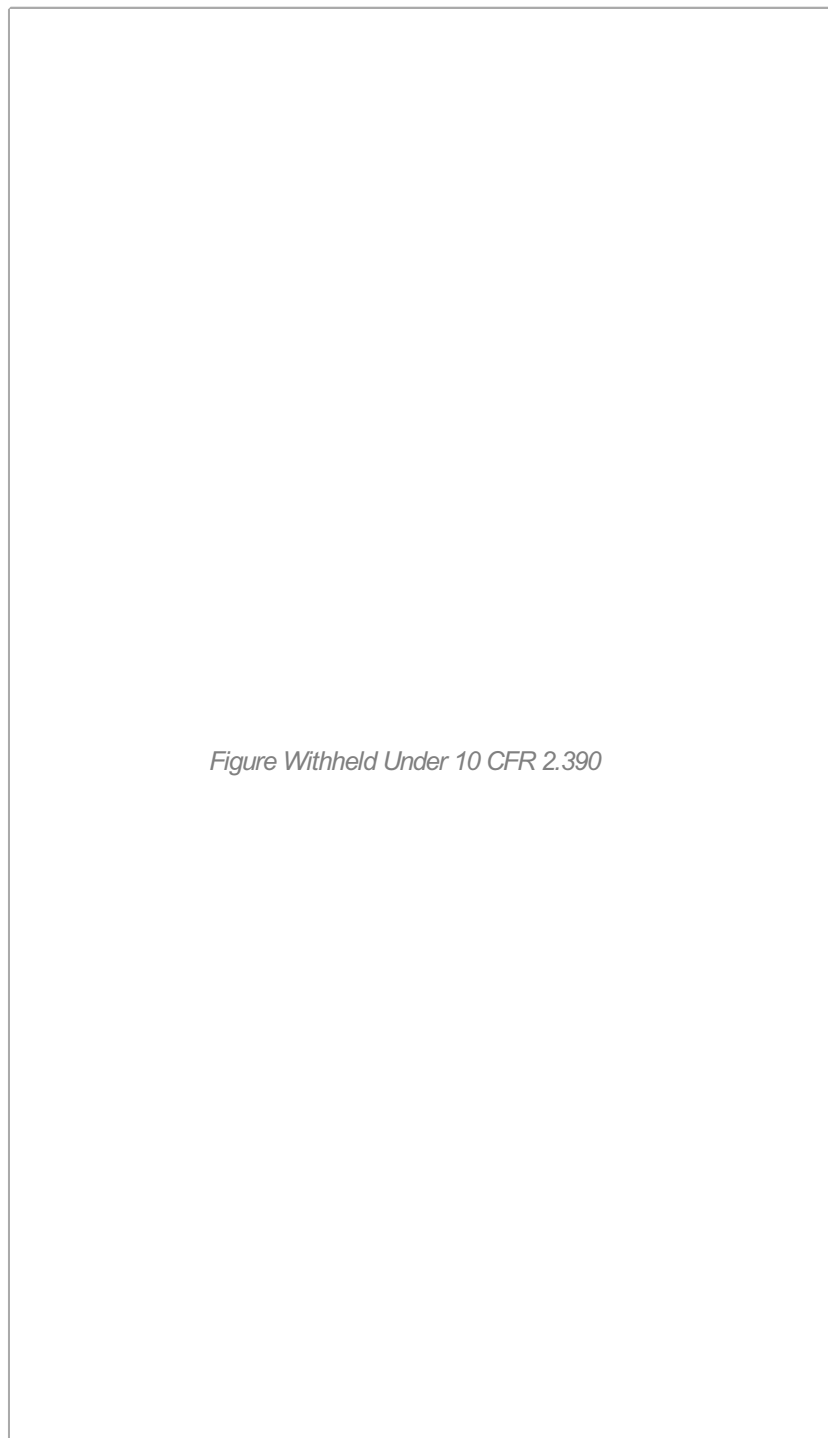


Figure 1.2-5 CY-MPC Damaged Fuel Can

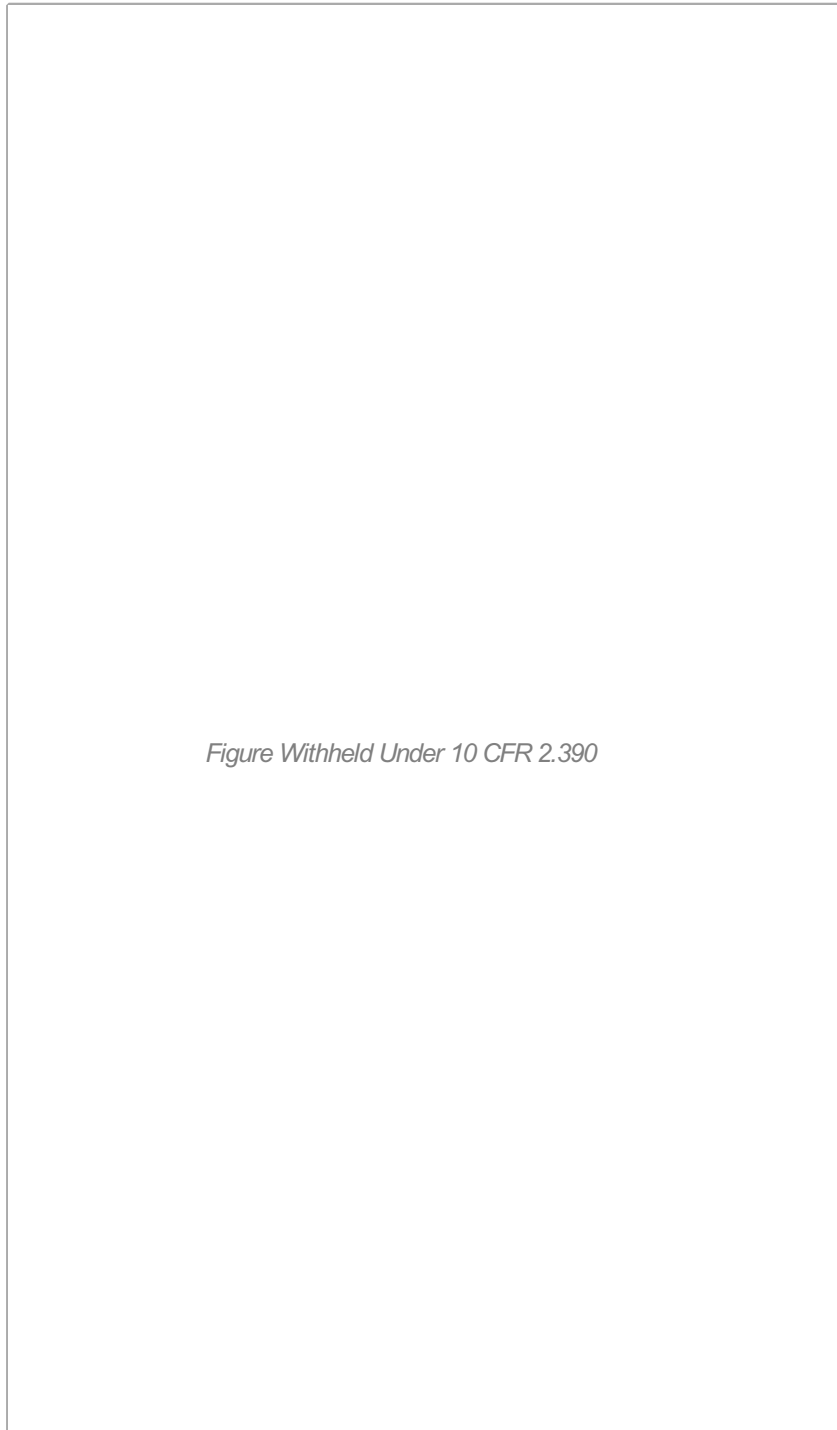


Figure Withheld Under 10 CFR 2.390

Figure 1.2-6 CY-MPC Failed Rod Storage Canister

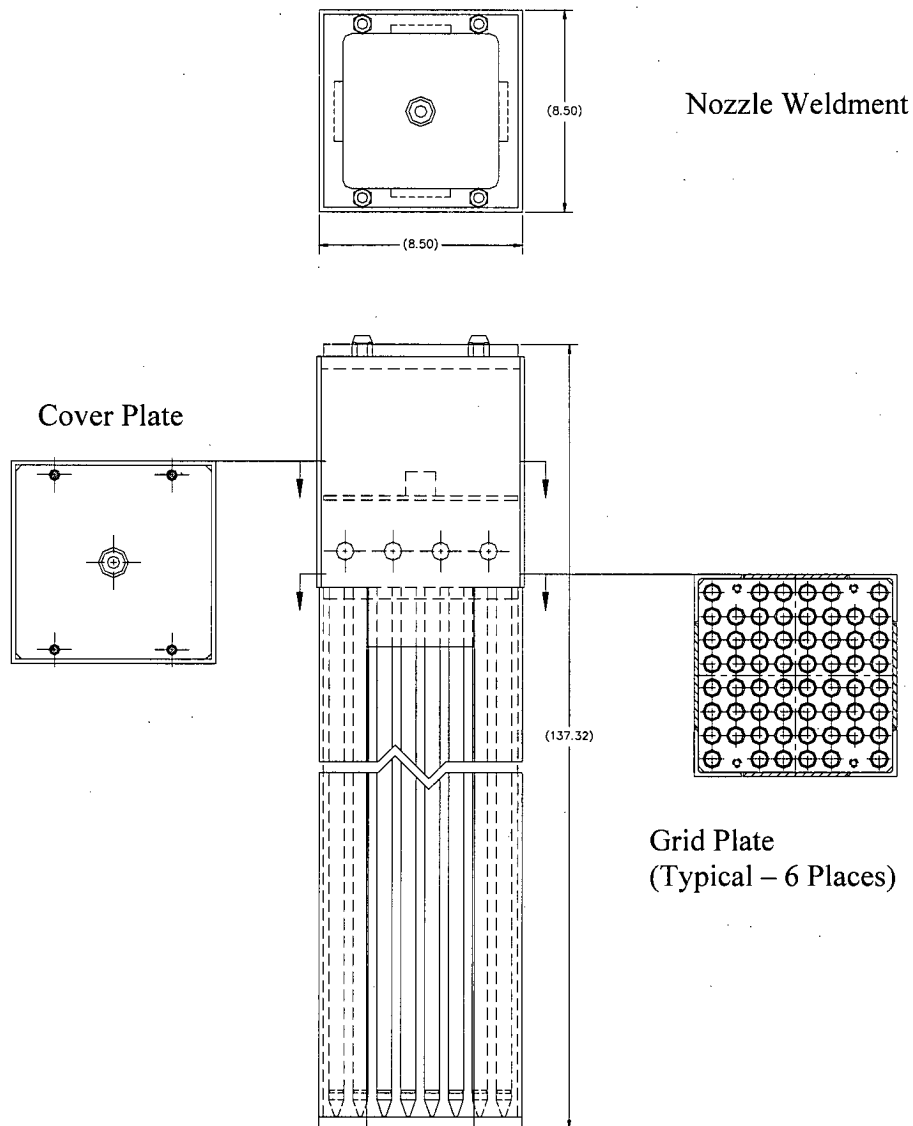


Table 1.2-1 Design Characteristics of the NAC-STC

Design Characteristic		Dimension ¹	Material
Cask	Overall Length (without impact limiters)	193.0	
Cask	Maximum Cross-Section Diameter		
	- Across Corners	99.0	
	- Across Flats	98.20	
Cask	Cavity Length	165.0	
Cask	Cavity Diameter	71.0	
Cask	Capacity		
	- Directly Loaded	26 assemblies	PWR Fuel Assemblies
Yankee Class			
	- Canistered Fuel	36 assemblies	Yankee Class (zircaloy clad)
	- Canistered Fuel	34 assemblies	Yankee Class (stainless clad)
	- Canistered GTCC Waste	24 containers	Yankee GTCC Waste
Connecticut Yankee (CY)			
	- Canistered Fuel	26 assemblies	CY fuel except Vantage 5
	- Canistered Fuel	24 assemblies	CY fuel including Vantage 5 fuel
	- Canistered GTCC Waste	24 containers	CY GTCC Waste
Cask	Cavity Atmosphere		
	- Backfill Gas	---	Helium
	- Backfill Pressure	1.0 atm. abs.	
Cask	Interlid and Interseal Regions		
	- Backfill Gas	---	Helium
	- Backfill Pressure	1.0 atm. abs.	

1. Dimensions in inches unless otherwise noted.

Table 1.2-1 Design Characteristics of the NAC-STC (continued)

Design Characteristic	Dimension ¹	Material
Inner Shell - Thickness	1.5	Type 304 Stainless Steel
Inner Shell Ring		Type XM-19 Stainless Steel
- Shell Region Thickness	1.5	
- Transition Region Thickness	2.0	
Gamma Shield - Thickness		Chemical Copper Lead
- Shell Region Thickness	3.70	
- Transition Region Thickness	3.20 (min)	
Outer Shell - Thickness	2.65	Type 304 Stainless Steel
Top Forging - Radial Thickness at cavity diameter	7.85	Type 304 Stainless Steel
Bottom Thickness (Total)	13.65	
- Bottom Inner Forging	6.20	Type 304 Stainless Steel
- Bottom Outer Forging (Radial at bottom neutron shield)	3.9	Type 304 Stainless Steel
- Bottom Plate	5.45	Type 304 Stainless Steel
- Neutron Shielding Material	2.00	NS-4-FR, Solid Synthetic Polymer

1. Dimensions in inches unless otherwise noted.

Table 1.2-1 Design Characteristics of the NAC-STC (continued)

Design Characteristic	Dimension ¹	Material
Neutron Shield - Thickness		
- Neutron Shielding Material	5.50	NS-4-FR, Solid Synthetic Polymer
- Shell	0.25	Type 304 Stainless Steel
- End Plates	0.472	Type 304 Stainless Steel
Lifting Trunnion - Diameter	5.50	Type 17-4 PH Stainless Steel
Rotation Trunnion Recess - Thickness	5.75	Type 17-4 PH Stainless Steel
Inner Lid - Thickness (Total)	9.0	
- Rim and Central Region	6.0	Type 304 Stainless Steel
- Neutron Shielding Material	2.0	NS-4-FR, Solid Synthetic Polymer
- Coverplate	1.0	Type 304 Stainless Steel
- Bolts (42)	1-1/2 - 8 UN	SB-637, GR N07718, Nickel Alloy

1. Dimensions in inches unless otherwise noted.

Table 1.2-1 Design Characteristics of the NAC-STC (continued)

Design Characteristic	Dimension ¹	Material
Outer Lid		
- Body Thickness	5.25	SA-705, Type 630 Stainless Steel
- Bolts (36)	1 - 8 UNC	SA-564, Type 630 17-4PH Stainless Steel
Inner Lid Port Coverplate		
- Body Thickness	1.0	Type 304 Stainless Steel
- Bolts (4)	1/2 - 13 UNC	SA-193, Grade B6, Type 410, Stainless Steel
Port Cover		
- Body Thickness	1.0	SA 240, Type 304 Stainless Steel
- Bolts (4)	1/2 - 13 UNC-2A	SA-193, GR B6, Type 410 Stainless Steel
Canister Spacers		
- Yankee-MPC Top Spacer	28.0 x 70.6 (dia)	Aluminum Honeycomb with 6061-T6 Aluminum Outer Shell
- Yankee-MPC Bottom Spacer	14.0 x 68.9 (dia)	Aluminum Honeycomb with 6061-T6 Aluminum Outer Shell
- CY-MPC Bottom Spacer	12.7 x 70.6 (dia)	ASTM A240, Type 304 Stainless Steel

1. Dimensions in inches unless otherwise noted.

Table 1.2-1 Design Characteristics of the NAC-STC (continued)

Design Characteristics	Dimension ¹	Material
Fuel Basket (Directly Loaded)		
- End Weldments (Plate)	1.0 x 70.86 dia.	Type 304 Stainless Steel
- Support Disks	0.5 x 70.86 dia.	Type 17-4 PH Stainless Steel
- Heat Transfer Disks	0.625 x 70.65 dia.	Type 6061-T651 aluminum alloy
- Tube	8.78 x 8.78 x 0.048	Type 304 Stainless Steel encasing neutron absorber
- Spacer Nuts	2.5 Square	Type 17-4 PH Stainless Steel
- Threaded Rod (6)	1-5/8 - 8 UN	Type 17-4 PH Stainless Steel
Canister		
- Shell (Plate)	5/8	Type 304L Stainless Steel
- Shield Lid (Plate)	5	Type 304L Stainless Steel
- Structural Lid (Plate)	3	Type 304 Stainless Steel
- Shell Bottom (Plate)		
- Yankee-MPC	1.0	Type 304L Stainless Steel
- CY-MPC	1.75	Type 304L Stainless Steel

1. Dimensions in inches unless otherwise noted.

Table 1.2-1 Design Characteristics of the NAC-STC (continued)

Design Characteristics	Dimension ¹	Material
Yankee-MPC Canister Fuel Basket		
- End Weldments	0.5 x 68.98 dia.	Type 304 Stainless Steel
- Support Disks	0.5 x 69.15 dia.	Type 17-4 PH Stainless Steel
- Heat Transfer Disks	0.5 x 68.87 dia.	Type 6061-T651 Aluminum Alloy
- Tube	7.80 x 7.80 x 0.048	Type 304 Stainless Steel encasing neutron absorber
- Spacers	2.5 dia.	Type 304 Stainless Steel
- Tie Rods (8)	1-1/8 dia.	Type 304 Stainless Steel
Yankee-MPC Canister GTCC Basket		
- Support Walls	2.5 x 111.3	Type 304 Stainless Steel
- Support Disks	1.0 x 68.98 dia.	Type 304 Stainless Steel
- Tube	8.32 x 8.32 x 0.25	Type 304 Stainless Steel
CY-MPC Canister Fuel Basket		
- End Weldments	0.5 x 68.98 dia.	Type 304 Stainless Steel
- Support Disks	0.5 x 69.15 dia.	Type 17-4 PH Stainless Steel
- Heat Transfer Disks	0.5 x 68.87 dia.	Type 6061-T651 Aluminum Alloy
- Tube	8.72 x 8.72 x 0.048	Type 304 Stainless Steel encasing neutron absorber
- Oversized Tube	9.12 x 9.12 x 0.048	Type 304 Stainless Steel encasing neutron absorber
- Spacers	2.88 dia.	Type 304 Stainless Steel
- Tie Rods (6)	1-5/8 dia.	Type 304 Stainless Steel

1. Dimensions in inches unless otherwise noted.

Table 1.2-1 Design Characteristics of the NAC-STC (continued)

Design Characteristics	Dimension ¹	Material
CY-MPC Canister GTCC Basket		
- Support Walls	1.75 x 141.5	Type 304 Stainless Steel
- Support Ribs	1.25 x 141.5	Type 304 Stainless Steel
- Tube (Inside Dimension)	8.74 x 8.74 x 0.375	Type 304 Stainless Steel
Seals (O-rings) for Storage Configuration		
- Inner Lid		
- Inner	0.25 dia. x 72.251 dia.	Type 321 Stainless Steel
- Outer	0.25 dia. x 73.497 dia.	Type 321 Stainless Steel
- Port Coverplates		
- Inner	0.125 dia. x 3.875 dia.	Type 321 Stainless Steel
- Outer	0.125 dia. x 4.500 dia.	Type 321 Stainless Steel
- Outer Lid	0.250 dia. x 82.060 dia.	Type 321 Stainless Steel
- Port Covers		
- Primary	0.103 dia. x 2.675 dia.	PTFE
- Secondary	0.103 dia. x 2.675 dia.	PTFE

1. Dimensions in inches unless otherwise noted.

Table 1.2-1 Design Characteristics of the NAC-STC (continued)

Design Characteristics	Dimension ¹	Material
Seals (O-rings) for Immediate Transport Configuration		
- Inner Lid		
- Inner	0.25 dia. x 72.251 dia.	Viton ²
- Outer	0.25 dia. x 73.497 dia.	Viton ²
- Port Coverplates		
- Inner	0.125 dia. x 3.875 dia.	Viton or Type 321 Stainless Steel
- Outer	0.125 dia. x 4.500 dia.	Viton or Type 321 Stainless Steel
- Outer Lid	0.250 dia. x 82.060 dia.	Viton ²
- Port Covers		
- Primary	0.103 dia. x 2.675 dia.	PTFE
- Secondary	0.103 dia. x 2.675 dia.	PTFE

1. Dimensions in Inches unless otherwise noted.

2. 0.25 diameter, Type 321 stainless steel O-rings (same as storage configuration) may also be used.

Table 1.2-2 NAC-STC Design Basis Directly Loaded Fuel Characteristics

Parameter	Westinghouse PWR Fuel		Framatome-Cogema	
	17 x 17	15 x 15	17 x 17	17 x 17 Ref. ⁴
Maximum Number of Assemblies	26	26	26	26
Maximum Assembly Weight, lbs ¹	1467	1440	1463	1472
Maximum Assembly Length, in	160	160	162	162
Active Fuel Length, in	144	144	144	144.25
Fuel Rod Cladding	Zircaloy-4	Zircaloy-4	Zirconium Alloy	Zirconium Alloy
Maximum Uranium, kgU	464	465	464	464
Maximum Initial ²³⁵ U, wt %	Note 2	Note 2	Note 2	Note 2
Minimum Initial ²³⁵ U, wt %	Note 3	Note 3	Note 3	Note 3
Maximum Burnup, MWD/MTU	45,000	45,000	45,000	45,000
Maximum Assembly Decay Heat, kW	0.85	0.85	0.85	0.85
Maximum Cask Decay Heat, kW	22.1	22.1	22.1	22.1
Minimum Cool Time, yr	Note 3	Note 3	Note 3	Note 3

1. Actual assembly weights are provided for information only. A conservative weight is used for analysis. These assemblies are the design basis fuel assemblies for the structural, thermal and shielding evaluations. The fuel used for the criticality evaluation is the Westinghouse 17x17OFA. Physical properties for the OFA assembly are provided in Table 6.2-1.
2. Based on criticality analysis. Maximum initial enrichment is variable between 4.2 and 4.5 wt % ²³⁵U.
3. Minimum initial enrichment and cool time are based on a fuel loading table, shown in Table 5.4-5.
4. Similar to the Framatome-Cogema 17 x 17, except with expanded fuel characteristics.

Table 1.2-3 NAC-STC Design Basis Yankee Class Fuel Characteristics

Parameter	Yankee Class Fuel ^{1,2}				
	United Nuclear Type A	Combustion ³ Type A	Westinghouse Type B	Exxon Type A	Yankee RFA
Maximum Number of Assemblies	36	36	34	36	36
Maximum Assembly Weight, lbs ⁶	≤950	≤950	≤950	≤950	≤950
Maximum Assembly Length, in	111.25	111.79	111.25	111.56	111.79
Active Fuel Length, in	91	91	92	91	91
Fuel Rod Cladding	Zircaloy	Zircaloy	Stainless Steel	Zircaloy	Zircaloy
Maximum Uranium, kgU	245.6	239.4	286.9	239.4	70.0
Maximum Initial ²³⁵ U, wt % ⁵	4.0	3.9	4.94	4.0	4.0
Minimum Initial ²³⁵ U, wt % ⁵	4.0	3.7 ³	4.94	3.5	3.5
Maximum Burnup, MWD/MTU	32,000	36,000	32,000	36,000	36,000
Maximum Assembly Decay Heat, kW	0.272	0.347	0.259	0.316	0.097
Maximum Cask Decay Heat, kW	9.8	12.5	8.8	11.4 ⁴	3.5
Minimum Cool Time, yr	11.0	8.1	22.0	10 ⁴	8.0

1. The Yankee Class Fuel includes United Nuclear Type A and Type B, Combustion Engineering Type A and Type B, Exxon-ANF Type A and Type B and Westinghouse Type A and Type B. The United Nuclear Type A is the most reactive assembly and is used as the design basis fuel for criticality analyses. The Combustion Type A is the design basis fuel for shielding and thermal evaluations. The Westinghouse Type B fuel is the design basis fuel for structural weight considerations. The Yankee Class design basis fuels bound a Yankee Class Reconfigured Fuel Assembly.
2. The maximum number of mixed Type Yankee Class fuel assemblies is limited to 36 or to 30,600 lbs, total loaded assembly weight.
3. The NAC-STC can also accommodate canistered Combustion Engineering 3.5 wt % enriched fuel having a minimum cool time of 7 years and a burnup of 32,000 MWD/MTU.
4. The limit corresponds to Exxon assemblies with Zircaloy in-core hardware. Exxon assemblies with steel in-core hardware are limited by a minimum cool time of 16 years and a maximum decay heat of 9.7 kW.
5. Nominal enrichment fabrication values.
6. Up to 36 intact fuel assemblies of any type, not exceeding 30,600 pounds total weight, are authorized.

Table 1.2-4 NAC-STC Design Basis Connecticut Yankee Fuel Characteristics

Parameter	Connecticut Yankee Fuel ^{5, 6, 9}				
	PWR ^{1,4} 15x15	PWR ² 15x15	PWR ³ 15x15 Enriched > 3.93 wt% ²³⁵ U	CY-MPC RFA ⁷	CY-MPC DFC ⁸
Maximum Number of Assemblies	26	26	24	4	4
Maximum Assembly Weight, lbs	≤1,500	≤1500	≤1500	≤1600	≤1600
Maximum Assembly Length, in	137.1	137.1	137.1	141.5	141.5
Maximum Active Fuel Length, in	121.8	121.35	120.6	121.8	121.8
Fuel Rod Cladding	SS	Zircaloy	Zircaloy	Zirc/SS	Zirc/SS
Maximum Uranium, kgU	433.7	397.1	390	212	433.7
Maximum Initial ²³⁵ U, wt%	4.03	3.93	4.61	4.61	4.61
Minimum Initial ²³⁵ U, wt%	3.00	2.95	2.95	2.95	2.95
Maximum Burnup, MWD/MTU	38,000	43,000	43,000	43,000	43,000
Maximum Assembly Decay Heat, kW	0.654	0.654	0.654	0.321	0.654
Maximum Cask Decay Heat, kW	17	17	17	17	17
Minimum Cool Time, years	10	10	10	10	10

1. Connecticut Yankee stainless steel clad spent fuel includes assemblies manufactured by Westinghouse Electric Co. (Westinghouse), Babcock & Wilcox (B&W) Fuel Co., Gulf General Atomic (GGA), Gulf Nuclear Fuel Co. (GNFC), and Nuclear Materials and Manufacturing Co. (NUMEC).
2. Connecticut Yankee zircaloy clad spent fuel includes assemblies manufactured by Gulf General Atomic (GGA), Nuclear Materials and Manufacturing Co. (NUMEC), and Babcock & Wilcox (B&W) Fuel Co.
3. The Westinghouse Vantage 5H zircaloy clad spent fuel assemblies have an initial uranium enrichment greater than 3.93% wt ²³⁵U. They are the most reactive and are used as the design basis fuel for criticality analyses.
4. The Westinghouse stainless steel clad spent fuel assemblies are used as the design basis fuel for shielding, thermal, and structural evaluations.
5. Intact fuel assemblies may have a reactor control cluster assembly (RCCA) installed and are not restricted as to loading position in the basket.
6. Intact fuel assemblies may have a flow mixer (FM) installed. Assemblies with flow mixers installed must be loaded into one of the eight interior fuel loading positions in the basket.
7. Reconfigured fuel assemblies (RFA) must be loaded in one of the four oversize fuel loading positions.
8. Damaged Fuel Cans (DFC) must be loaded in one of the four oversize fuel loading positions.
9. Solid stainless steel rods may be inserted into CY fuel assembly RCCA guide tubes for fuel assemblies not containing a RCCA.

Table 1.2-5 Isotopic Constituents of Yankee GTCC Waste

Isotope	Baffle Activity (Ci)		Average Dross Activity (Ci)		Total Activity (Ci)		Total Activity (Ci) ¹	
	Activation	Surface	Activation	Surface	Baffle (15)	Dross (6)	Total (21)	Design Basis (24)
Tritium	4.52E+01	1.68E-04	5.59E+00	2.07E-05	4.52E+01	5.59E+00	5.08E+01	--
Carbon-14	4.90E+01	1.42E-03	6.06E+00	1.76E-04	4.90E+01	6.06E+00	5.50E+01	--
Manganese-54	7.72E+01	1.62E-03	9.57E+00	2.01E-04	7.72E+01	9.57E+00	8.68E+01	1.00E+02
Iron-55	7.07E+04	9.09E-01	8.75E+03	1.13E-01	7.07E+04	8.75E+03	7.94E+04	8.75E+04
Cobalt-60	1.02E+05	2.01E+00	1.26E+04	2.49E-01	1.02E+05	1.26E+04	1.14E+05	1.25E+05
Nickel-63	2.79E+04	6.64E-01	3.45E+03	8.22E-02	2.79E+04	3.45E+03	3.13E+04	3.35E+04
Technetium-99	1.36E-01	1.76E-04	1.68E-02	2.18E-05	1.36E-01	1.69E-02	1.53E-01	--
Cesium-134	0.00	5.32E-03	0.00	6.59E-04	5.32E-03	6.59E-04	5.98E-03	--
Cesium-137	0.00	2.49E-01	0.00	3.09E-02	2.49E-01	3.09E-02	2.80E-01	--
Cerium-144	0.00	1.05E-03	0.00	1.30E-04	1.05E-03	1.30E-04	1.18E-03	--
Plutonium-238	0.00	2.61E-03	0.00	3.23E-04	2.61E-03	3.23E-04	2.93E-03	--
Plutonium-239/240	0.00	6.65E-03	0.00	8.24E-04	6.65E-03	8.24E-04	7.48E-03	--
Plutonium-241	0.00	2.09E-01	0.00	2.59E-02	2.09E-01	2.59E-02	2.35E-01	--
Americium-241	0.00	3.94E-03	0.00	4.88E-04	3.94E-03	4.88E-04	4.43E-03	--
Curium-242	0.00	1.89E-07	0.00	2.35E-08	1.89E-07	2.35E-08	2.13E-07	--
Curium-243/244	0.00	1.48E-03	0.00	1.84E-04	1.48E-03	1.84E-04	1.67E-03	--
Ruthenium-106	0.00	1.82E-03	0.00	2.25E-04	1.82E-03	2.25E-04	2.04E-03	--
Strontium-89	0.00	3.81E-13	0.00	4.72E-14	3.81E-13	4.72E-14	4.29E-13	--
Strontium-90	0.00	2.20E-01	0.00	2.72E-02	2.20E-01	2.72E-02	2.47E-01	--
Iodine-129LLD	0.00	1.12E-04	0.00	1.38E-05	1.12E-04	1.38E-05	1.25E-04	--
Antimony-125	0.00	1.40E-02	0.00	1.73E-03	1.40E-02	1.73E-03	1.57E-02	--
Silver-110m	0.00	1.07E-04	0.00	1.33E-05	1.07E-04	1.33E-05	1.20E-04	--
Cobalt-57	0.00	3.96E-05	0.00	4.90E-06	3.96E-05	4.90E-06	4.45E-05	--
Niobium-94	6.63E-01	0.00	8.21E-02	0.00	6.63E-01	8.21E-02	7.45E-01	--
Nickel-59	1.52E+02	0.00	1.88E+01	0.00	1.52E+02	1.88E+01	1.71E+02	--
Zinc-65	6.78E-01	0.00	8.39E-02	0.00	6.78E-01	8.39E-02	7.62E-01	--

1. Isotopes except Manganese, Iron, Cobalt and Nickel are limited to a total of 500 curies per canister.

Table 1.2-6 Isotopic Constituents of Connecticut Yankee GTCC Waste

Isotope	GTCC Activity ¹	
	Curies/gram	Estimated Curies
Carbon-14	1.17E-05	1.13E+02
Manganese-54	5.10E-06	4.90E+01
Iron-55	1.07E-02	1.03E+05
Cobalt-60	2.04E-02	1.96E+05
Nickel-63	4.39E-05	4.22E+02
Technetium-99	7.46E-03	7.18E+04
Niobium-94	1.65E-07	1.59E+00
Nickel-59	2.96E-08	2.85E-01
Total		3.71E+05

1. The GTCC activity is based on the activity of the core baffle components and a GTCC contents weight of 21,200 lbs that bounds all the GTCC waste and is, therefore, conservative with respect to source strength.

1.3 Appendices

1.3.1 Quality Assurance

The U.S. NRC has assigned Approval Number 18 to the NAC International Quality Assurance program, which satisfies the provisions of Subpart H of 10 CFR 71.

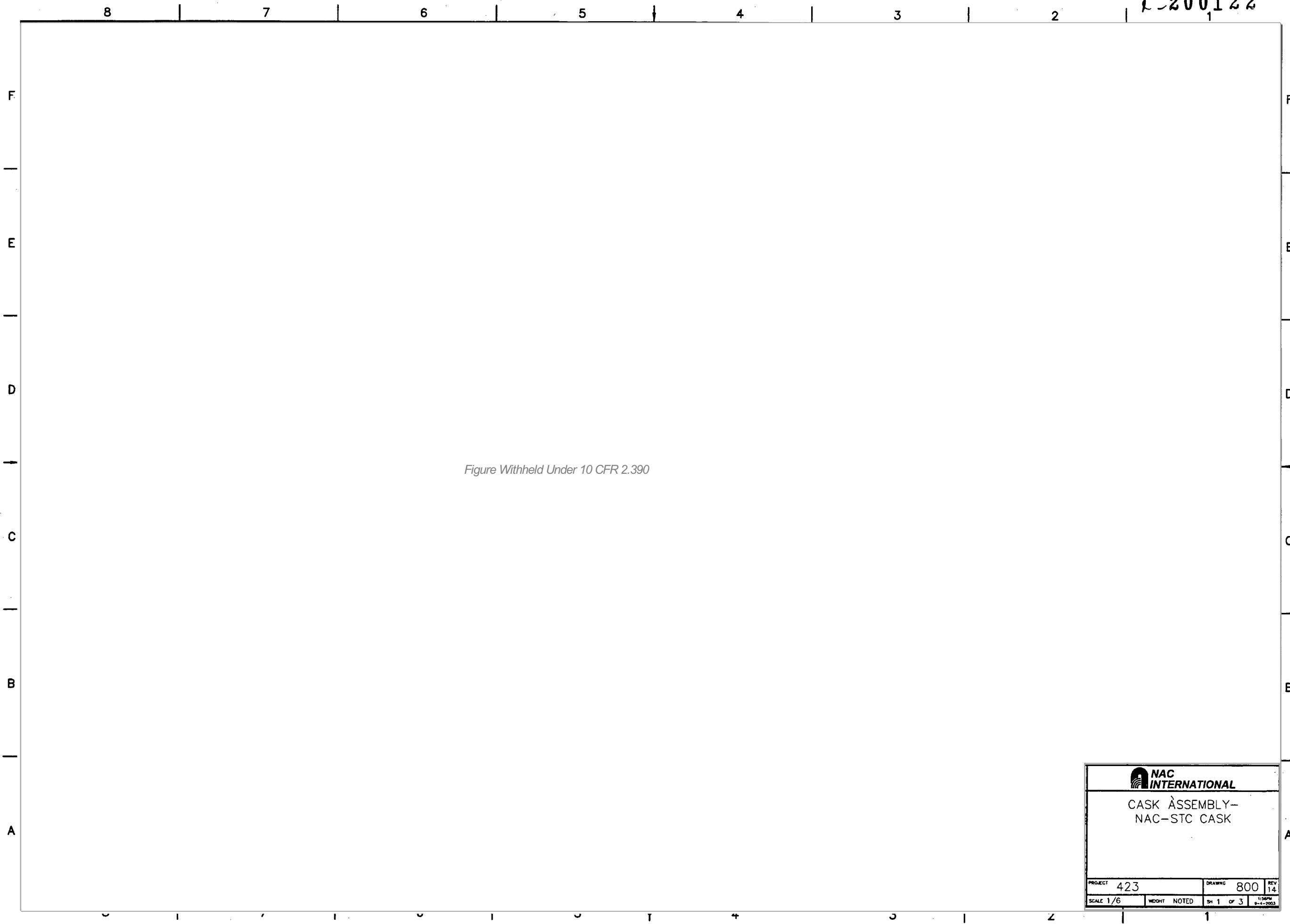
The Quality Assurance program provides control over all activities designated important to safety that are applicable to the design, fabrication, assembly, testing, maintenance, repair, modification and use of the packaging for transportation of radioactive materials. The program applies controls to the various activities in a graded approach, such that the effort expended on an activity is consistent with its importance to safety. The program is consistent in approach and method with Regulatory Guide 7.10.


In accordance with the requirements of 10 CFR 71.37(a), the approved Quality Assurance program has been applied to the design and analysis of the packaging, and will be applied to the packaging fabrication, assembly, testing, maintenance, repair, and modification. An equivalent U.S. NRC-approved program maintained by a Registered User shall be applied to the use of the packaging.

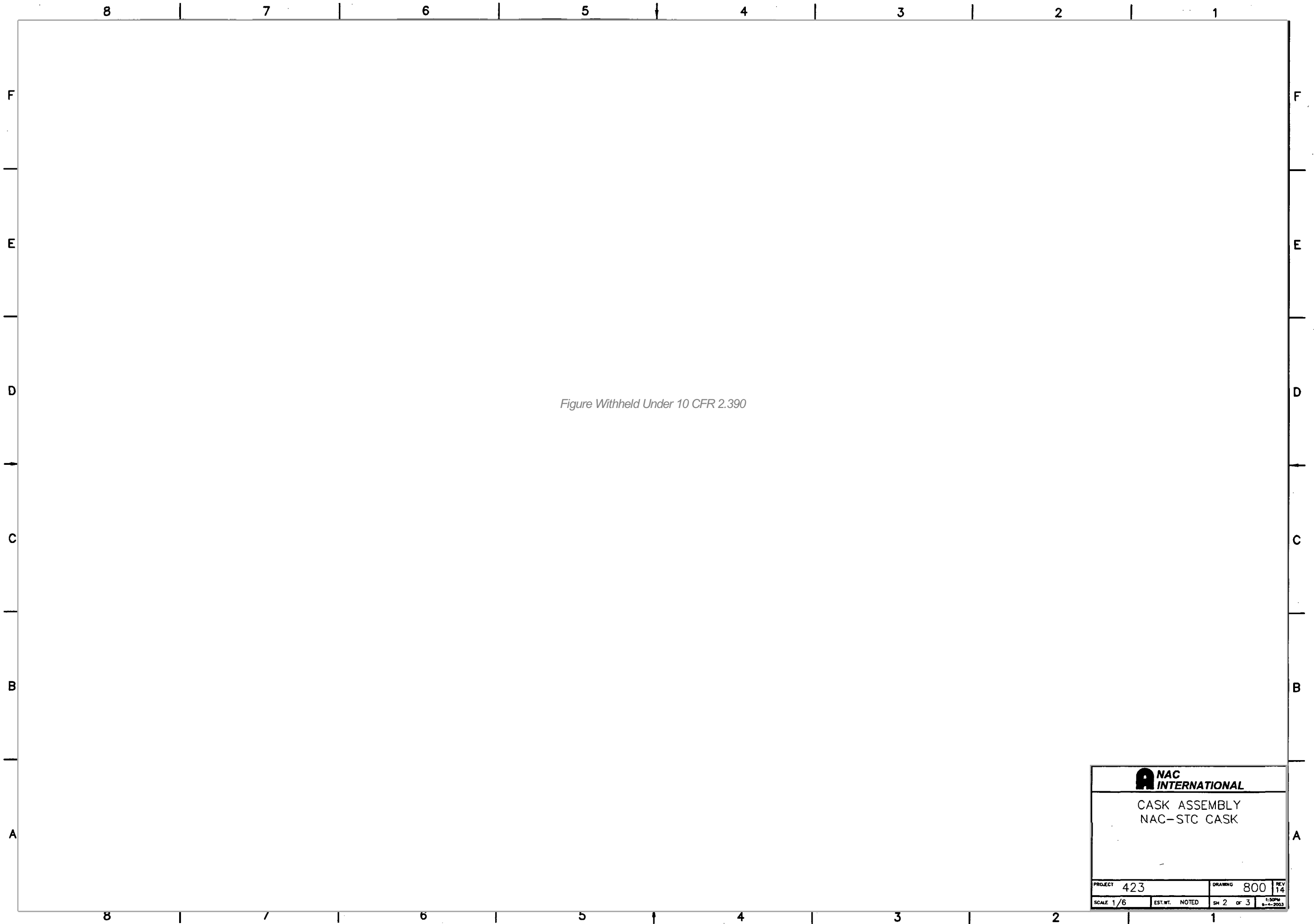
1.3.2 License Drawings


This section contains the license drawings pertinent to the NAC-STC, the Yankee-MPC, the Yankee Class Reconfigured Fuel Assembly, the CY-MPC, the CY-MPC Reconfigured Fuel Assembly and Damaged Fuel Can. The List of Drawings is presented in the Table of Contents for Chapter 1.

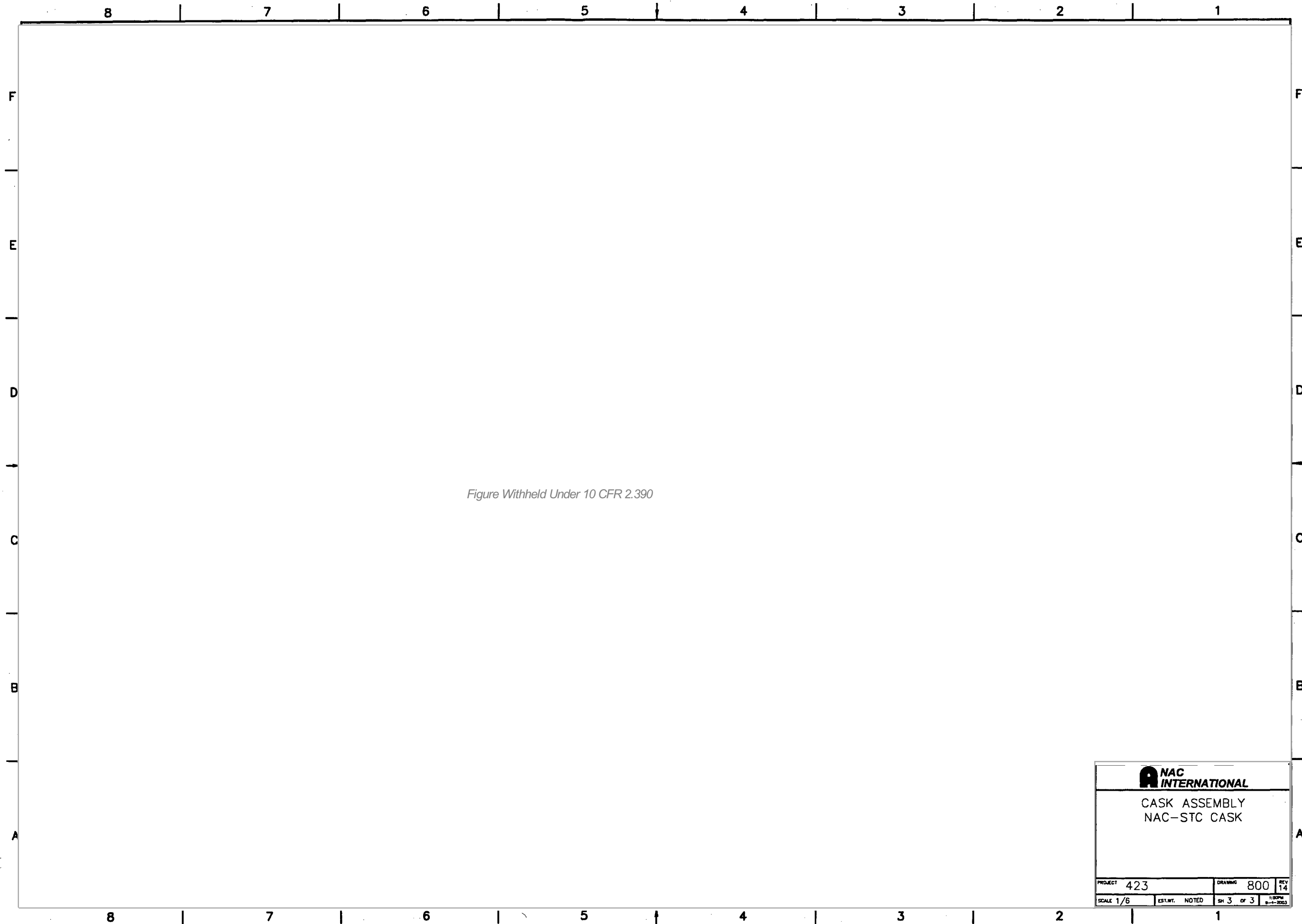
THIS PAGE INTENTIONALLY LEFT BLANK




 NAC INTERNATIONAL			
CASK ASSEMBLY- NAC-STC CASK			
PROJECT	423	DRAWING	800
SCALE 1/6	WEIGHT NOTED	SH 1 OF 3	REV 14

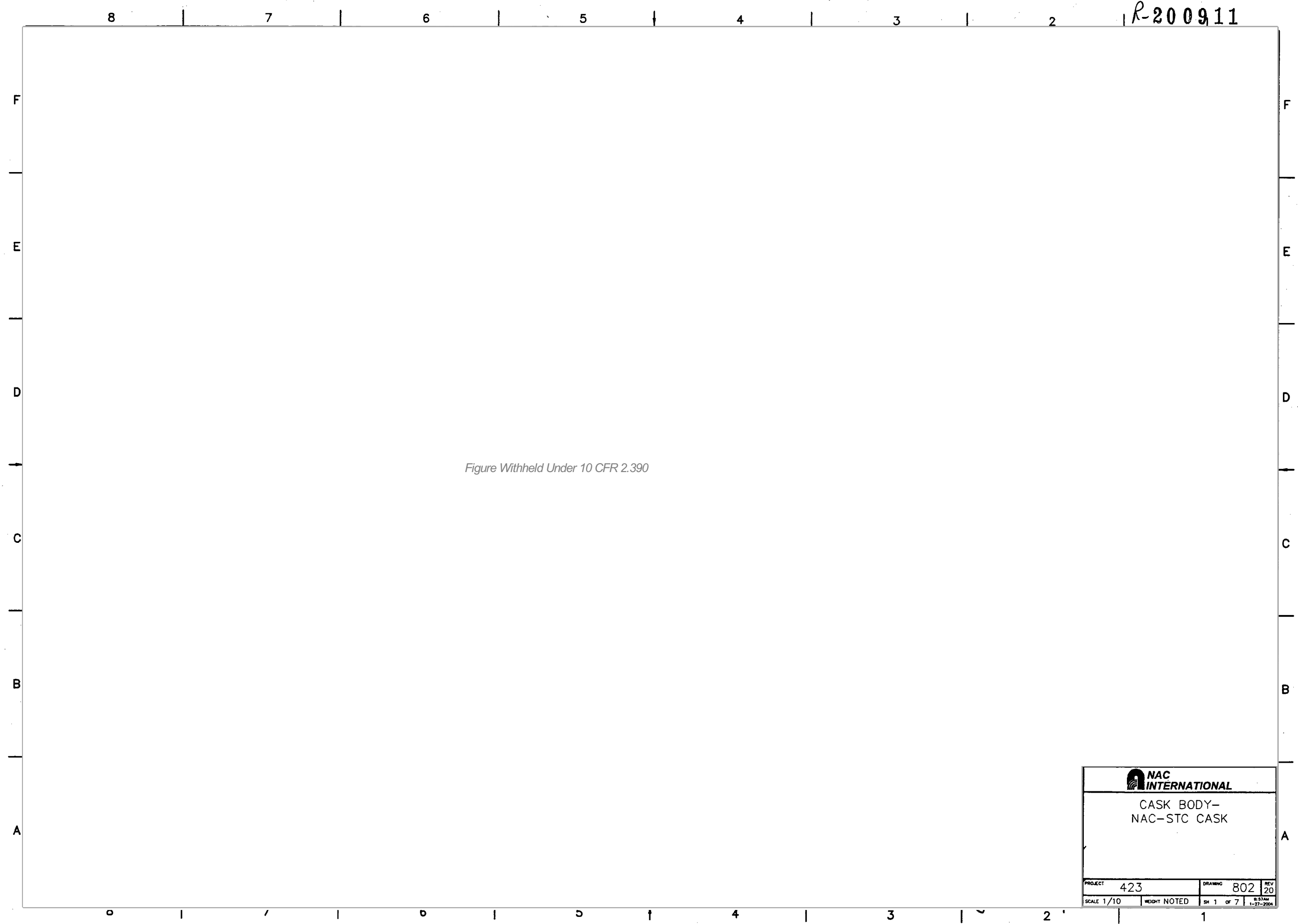



 NAC INTERNATIONAL			
CASK ASSEMBLY NAC-STC CASK			
PROJECT	423	DRAWING	800
SCALE	1/6	EST. WT.	NOTED
SH	2	OF	3
		REV	14
		1:500PM 8-14-2003	

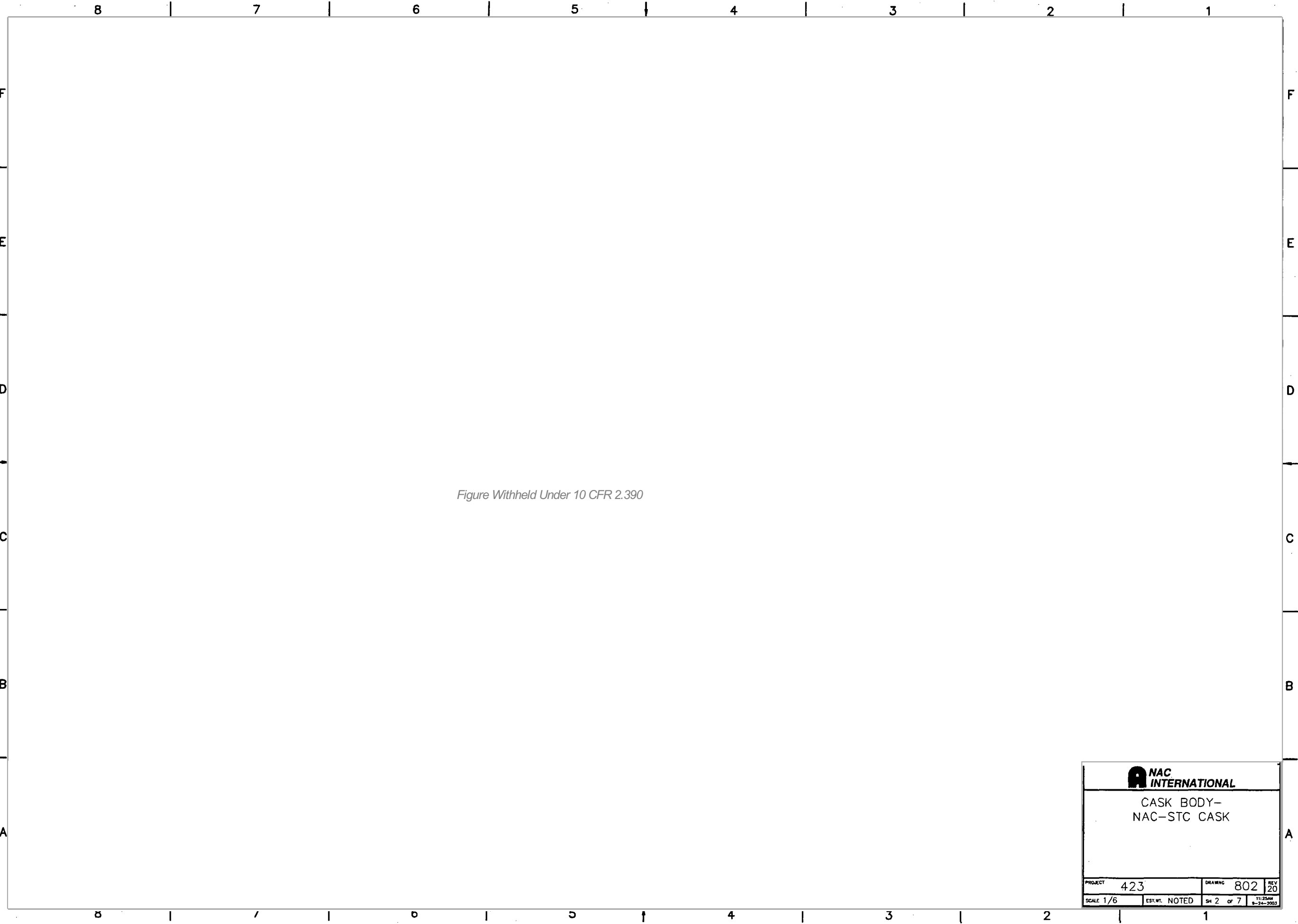



 NAC INTERNATIONAL			
CASK ASSEMBLY NAC-STC CASK			
PROJECT 423		DRAWING 800	
SCALE 1/6		REV 14	
EST. WT. NOTED		SH 3 OF 3	

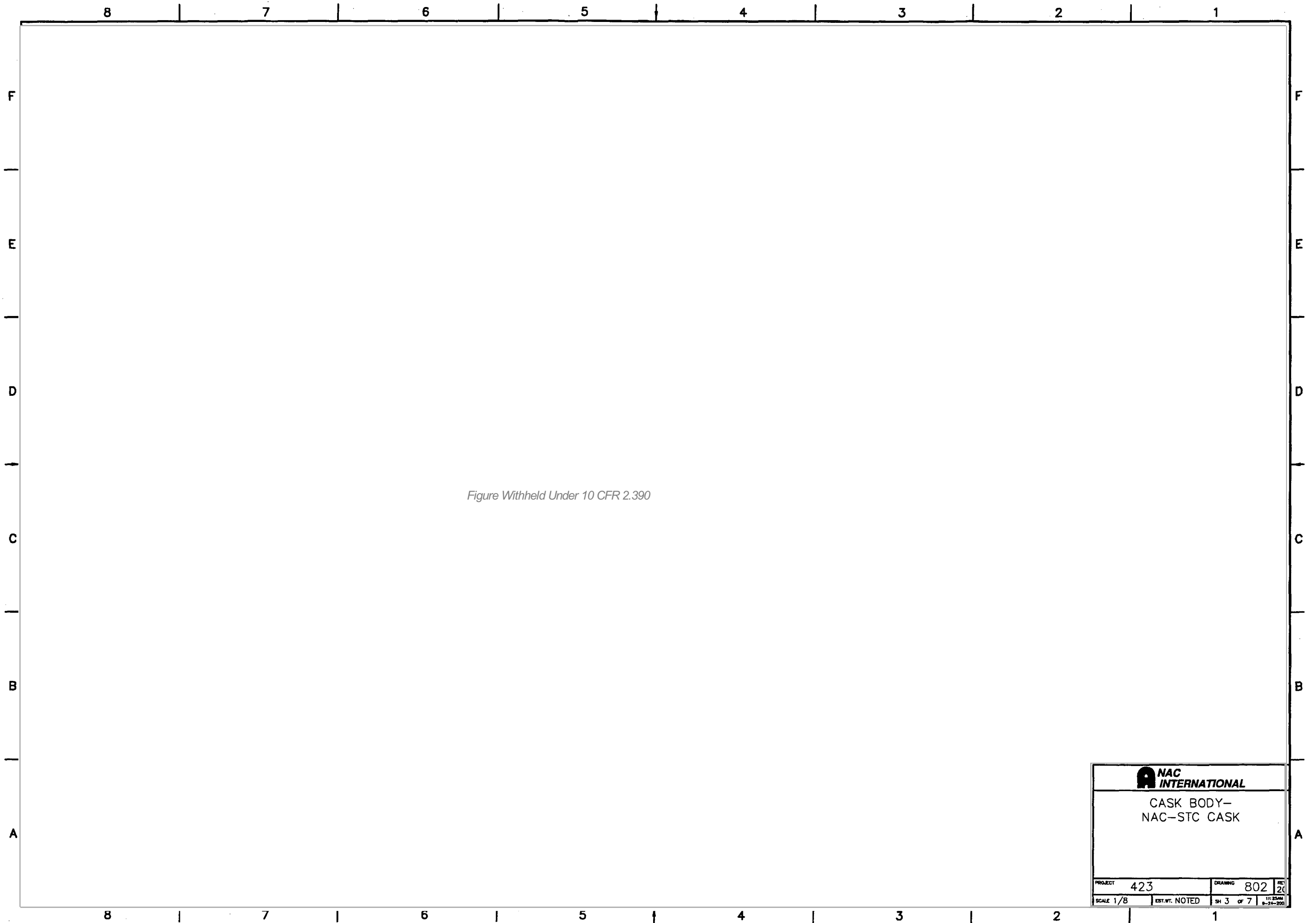
R-200911




 NAC INTERNATIONAL			
CASK BODY- NAC-STC CASK			
PROJECT	423	DRAWING	802
SCALE 1/10	WEIGHT NOTED	SH 1 OF 7	REV 20



 NAC INTERNATIONAL			
CASK BODY- NAC-STC CASK			
PROJECT	423	DRAWING	802
SCALE 1/6	EST. WT. NOTED	SH 2 OF 7	REV 20 11/25/01 9-24-2003



 NAC INTERNATIONAL	
CASK BODY— NAC—STC CASK	
PROJECT 423	DRAWING 802
SCALE 1/8	EST. WT. NOTED
SH 3 OF 7	11/25/84 8-24-200

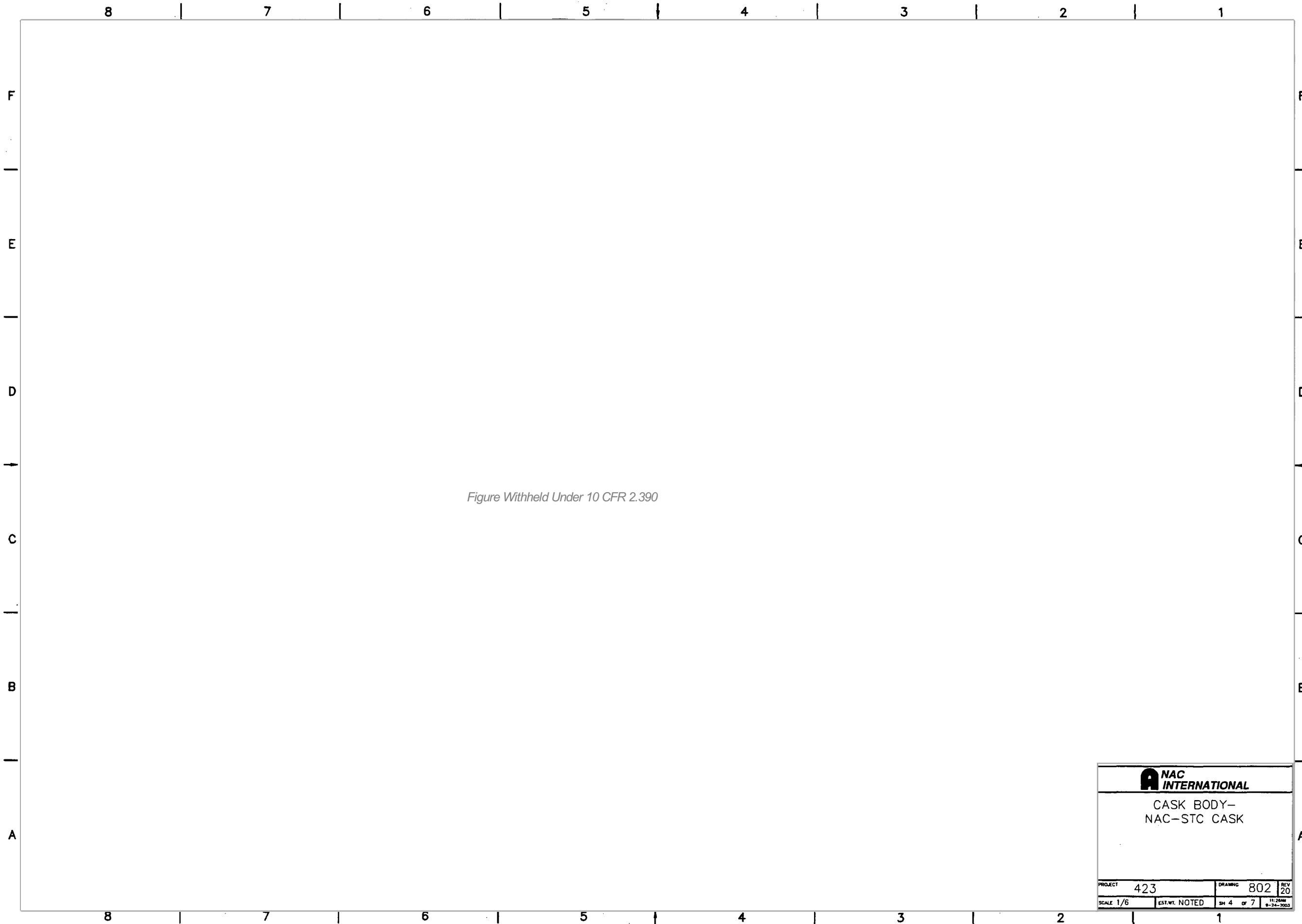
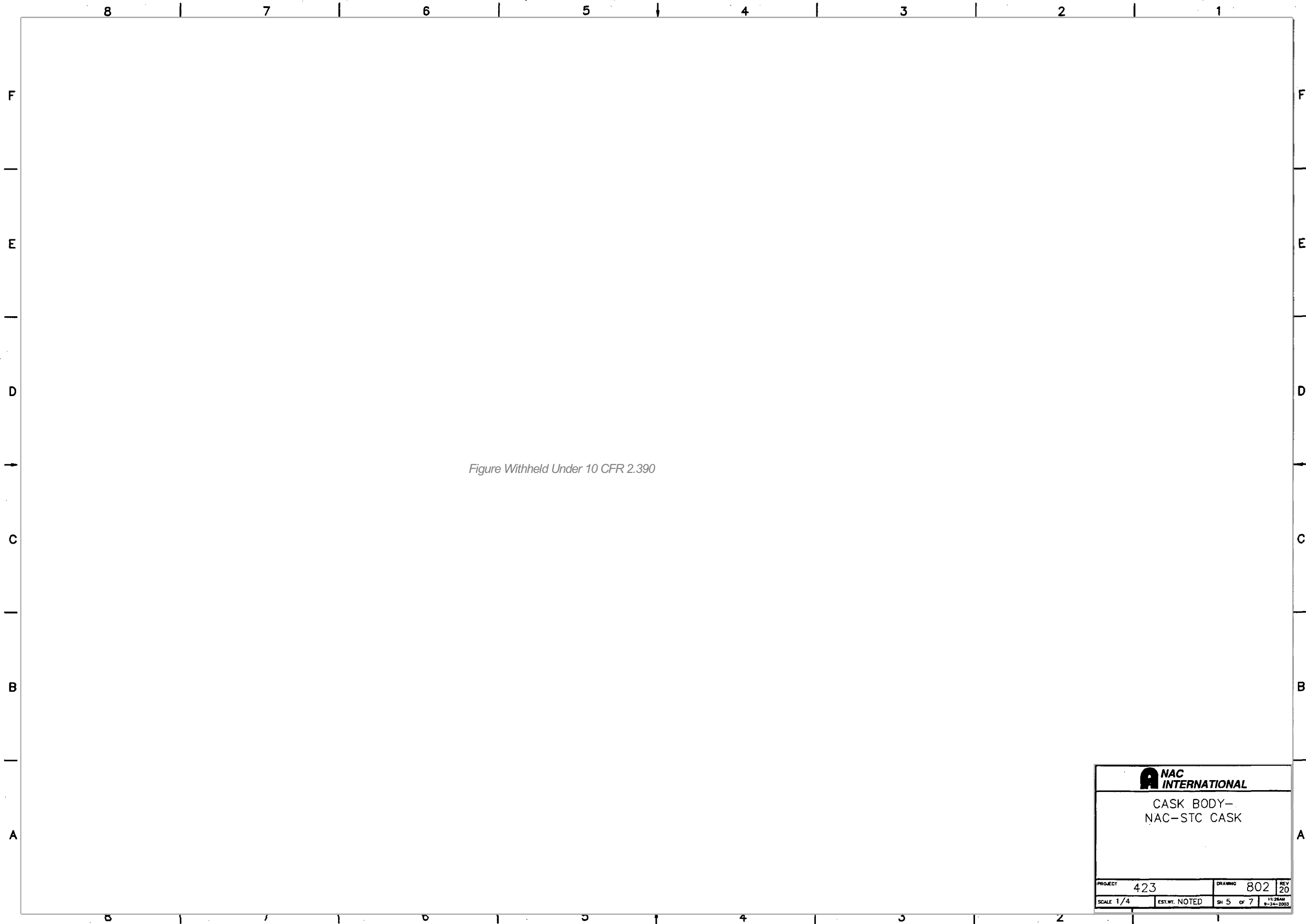
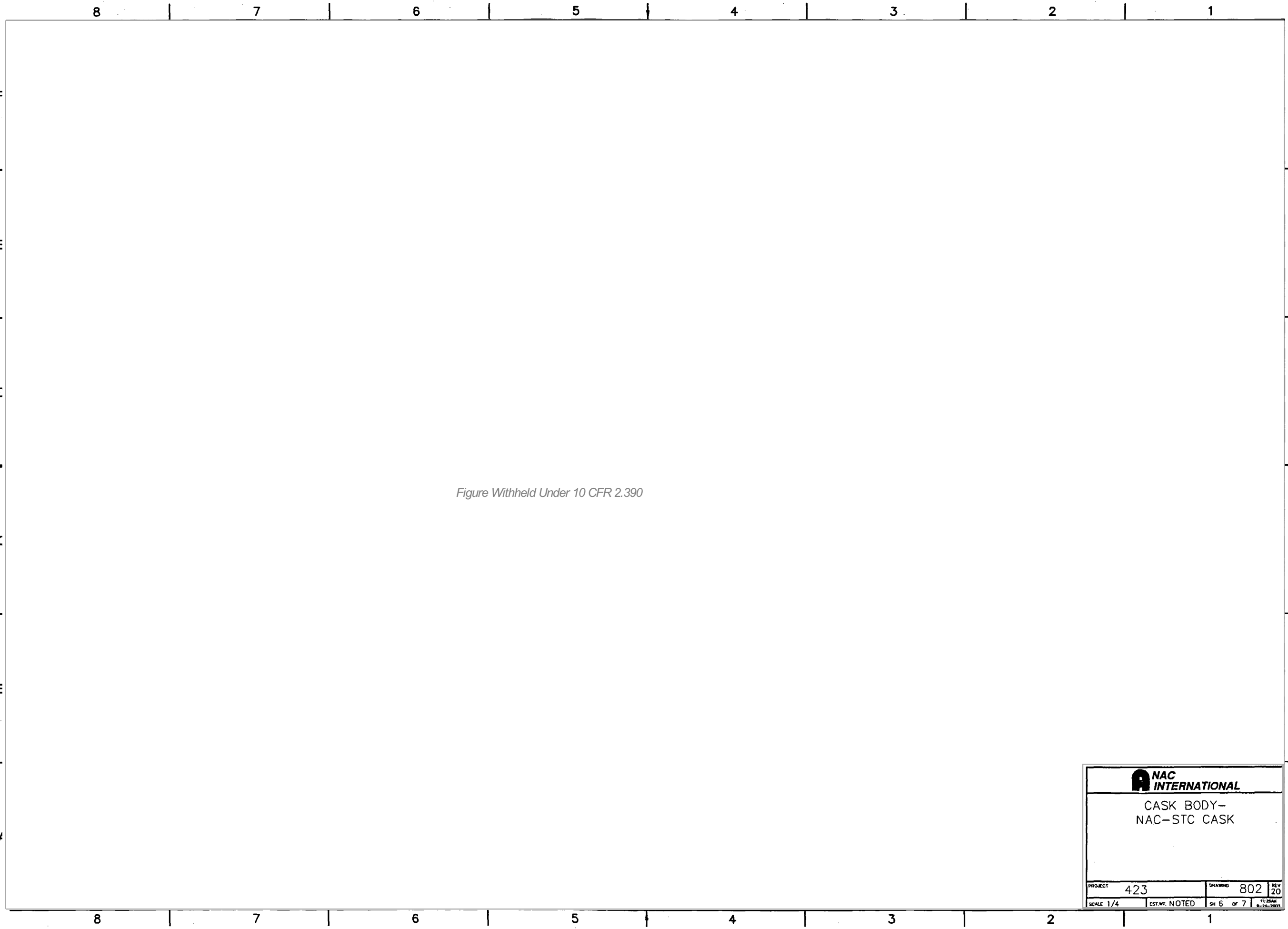



Figure Withheld Under 10 CFR 2.390

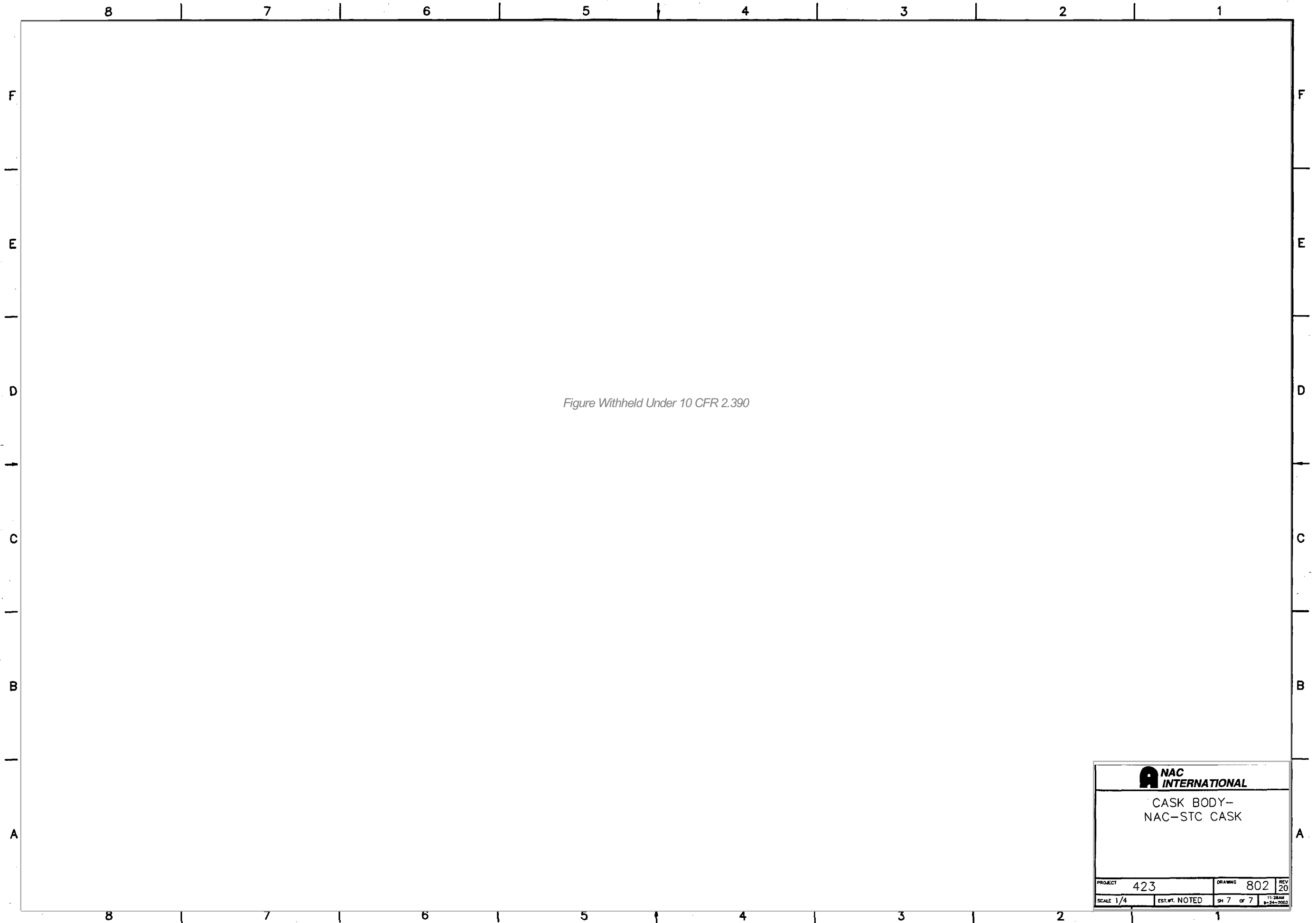
NAC INTERNATIONAL			
CASK BODY- NAC-STC CASK			
PROJECT	423	DRAWING	802
SCALE	1/6	EST. WT. NOTED	SH 4 OF 7
		REV	20




NAC INTERNATIONAL			
CASK BODY- NAC-STC CASK			
PROJECT	423	DRAWING	802
SCALE 1/4	EST. WT. NOTED	SH 5 OF 7	REV 20
11:28AM 8-24-2000			



 NAC INTERNATIONAL			
CASK BODY- NAC-STC CASK			
PROJECT	423	DRAWING	802
		REV	20
SCALE	1/4	EST. WT. NOTED	SH 6 OF 7
11/25/01 8-74-2001			



 NAC INTERNATIONAL			
CASK BODY- NAC-STC CASK			
PROJECT	423	DRAWING	802
SCALE 1/4"	EST. WT. NOTED	SH 7 OF 7	REV 20

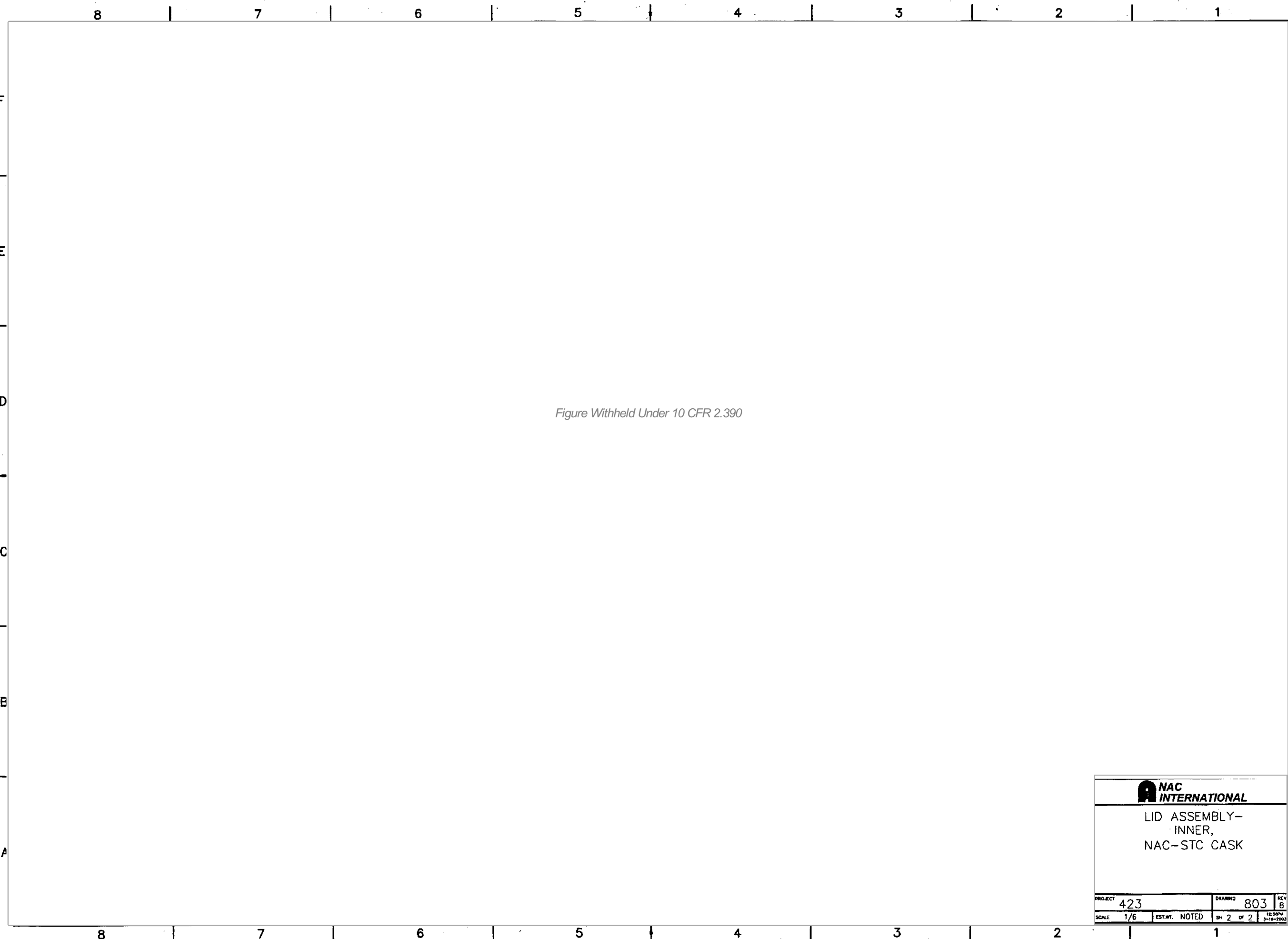
151868

Figure Withheld Under 10 CFR 2.390

 **NAC
INTERNATIONAL**

LID ASSEMBLY-
INNER,
NAC-STC CASK

PROJECT	423	DRAWING	803	REV.	8
SCALE	1/8	EST. BY	NOTED	SH	1 OF 2



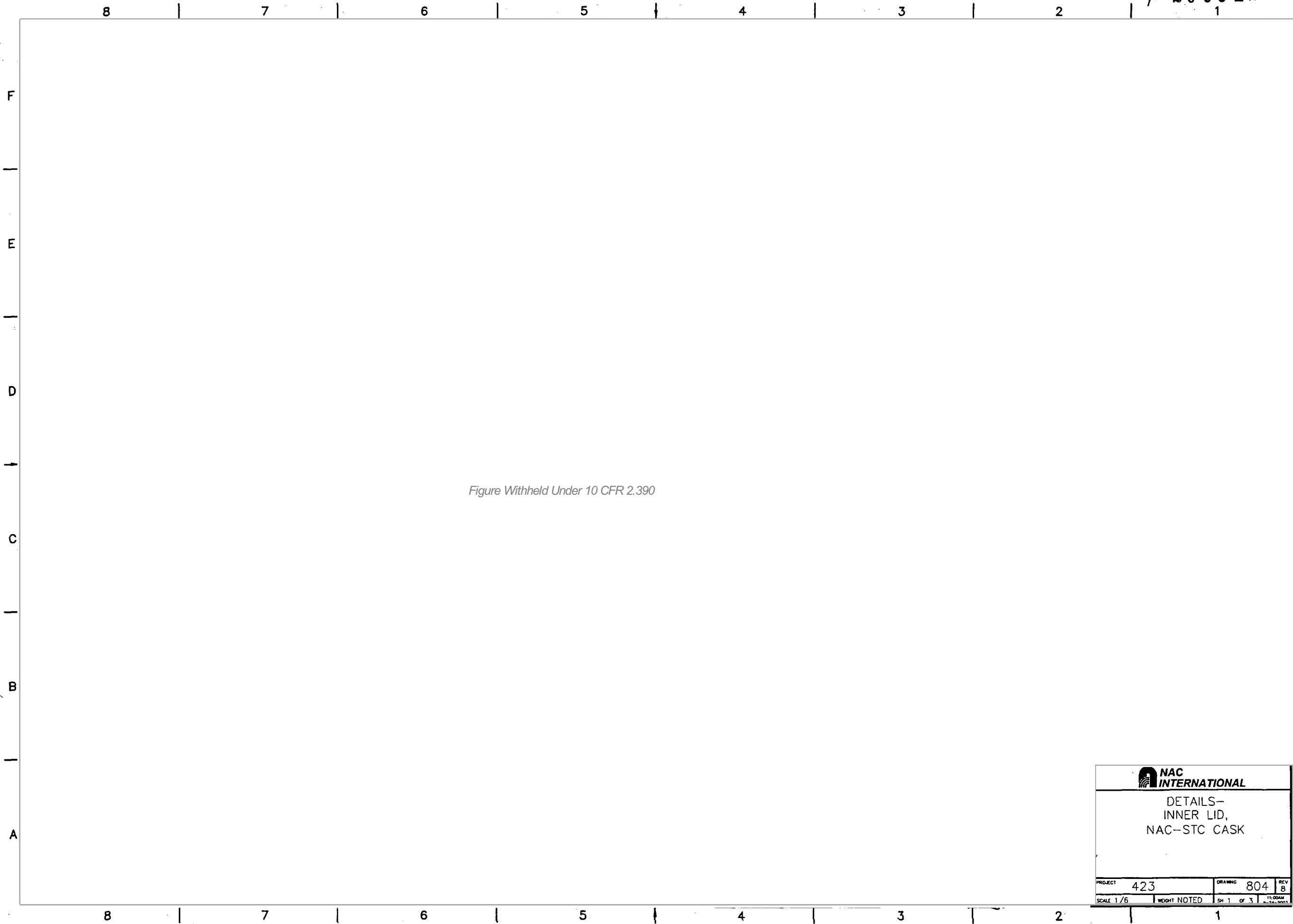
NAC
INTERNATIONAL


LID ASSEMBLY-
INNER,
NAC-STC CASK

PROJECT	423	DRAWING	803	REV	8
SCALE	1/6	EST. BY	NOTED	SH	2 OF 2

12-58PM
3-18-2003

R-200912



 NAC INTERNATIONAL			
DETAILS— INNER LID, NAC—STC CASK			
PROJECT	423	DRAWING	804
SCALE	1/6	WEIGHT NOTED	SH 1 OF 3
		REV	8

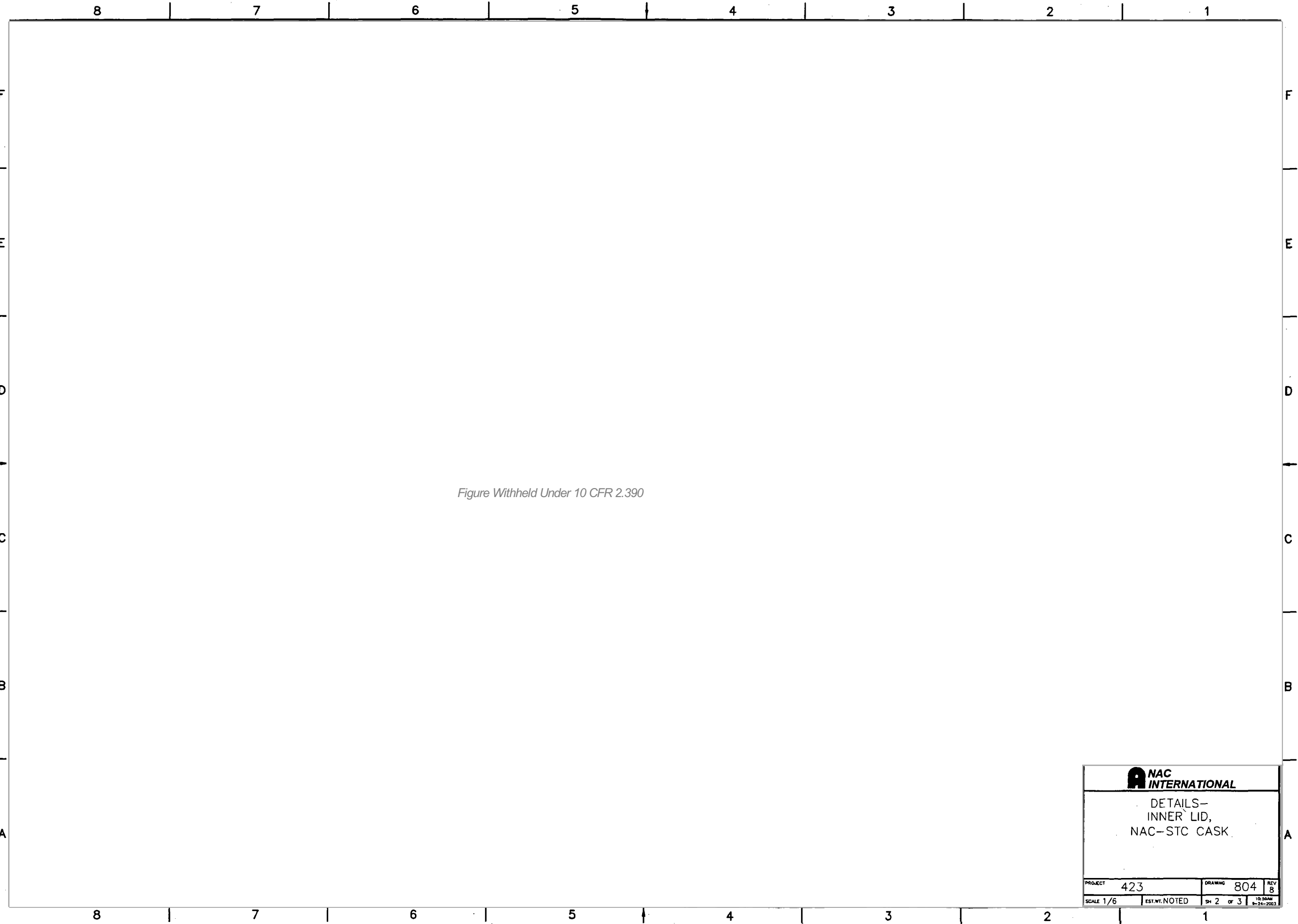

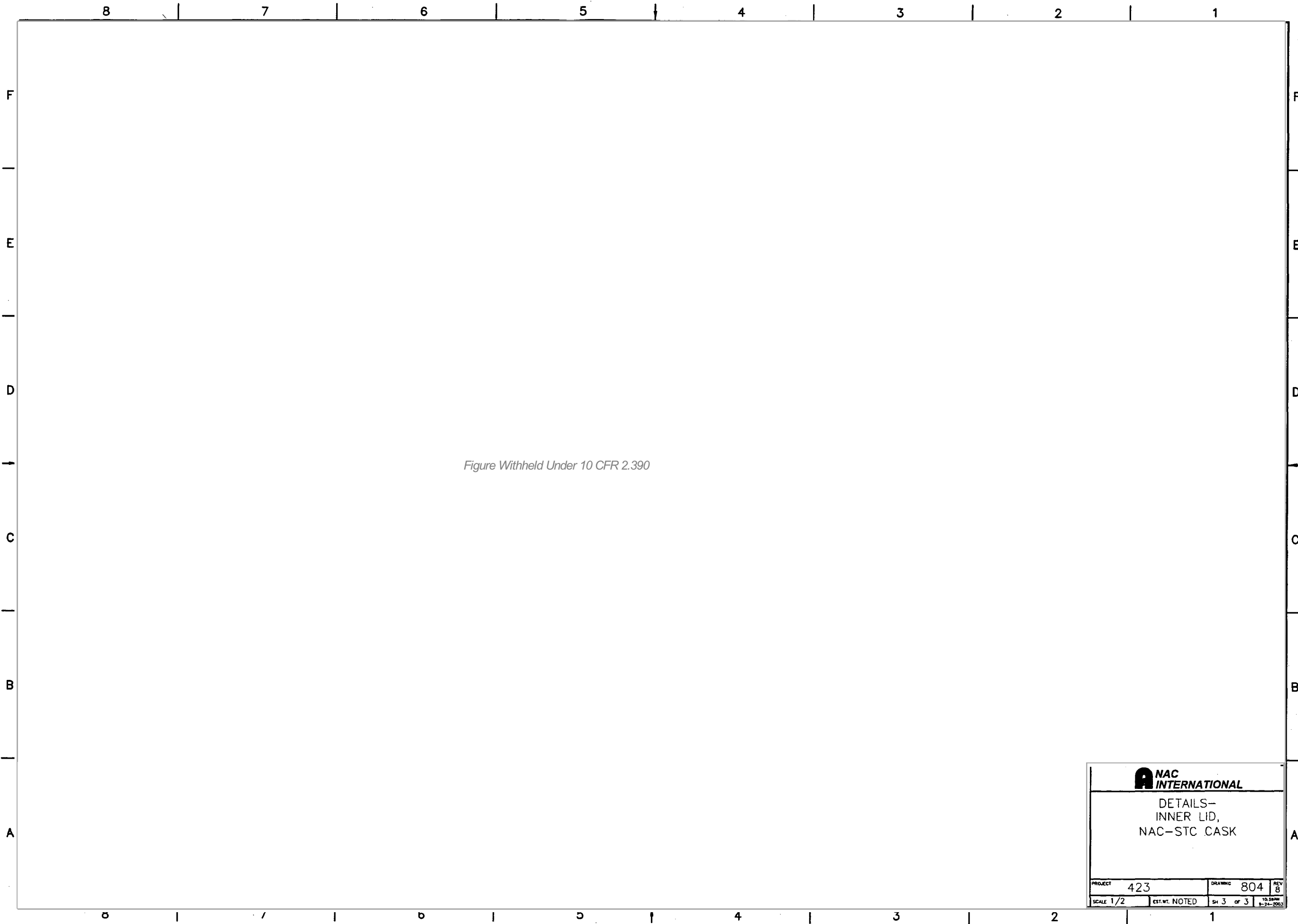



Figure Withheld Under 10 CFR 2.390


 NAC INTERNATIONAL			
DETAILS— INNER LID, NAC-STC CASK			
PROJECT	423	DRAWING	804
SCALE 1/6	EST. WT. NOTED	SH 2 OF 3	REV 8 10:50AM 8-14-2013




 NAC INTERNATIONAL			
DETAILS— INNER LID, NAC-STC CASK			
PROJECT	423	DRAWING	804
SCALE	1/2	EST. BY	NOTED
SH	3	OF	3
		REV	8
		10-24-2003	

15187.0

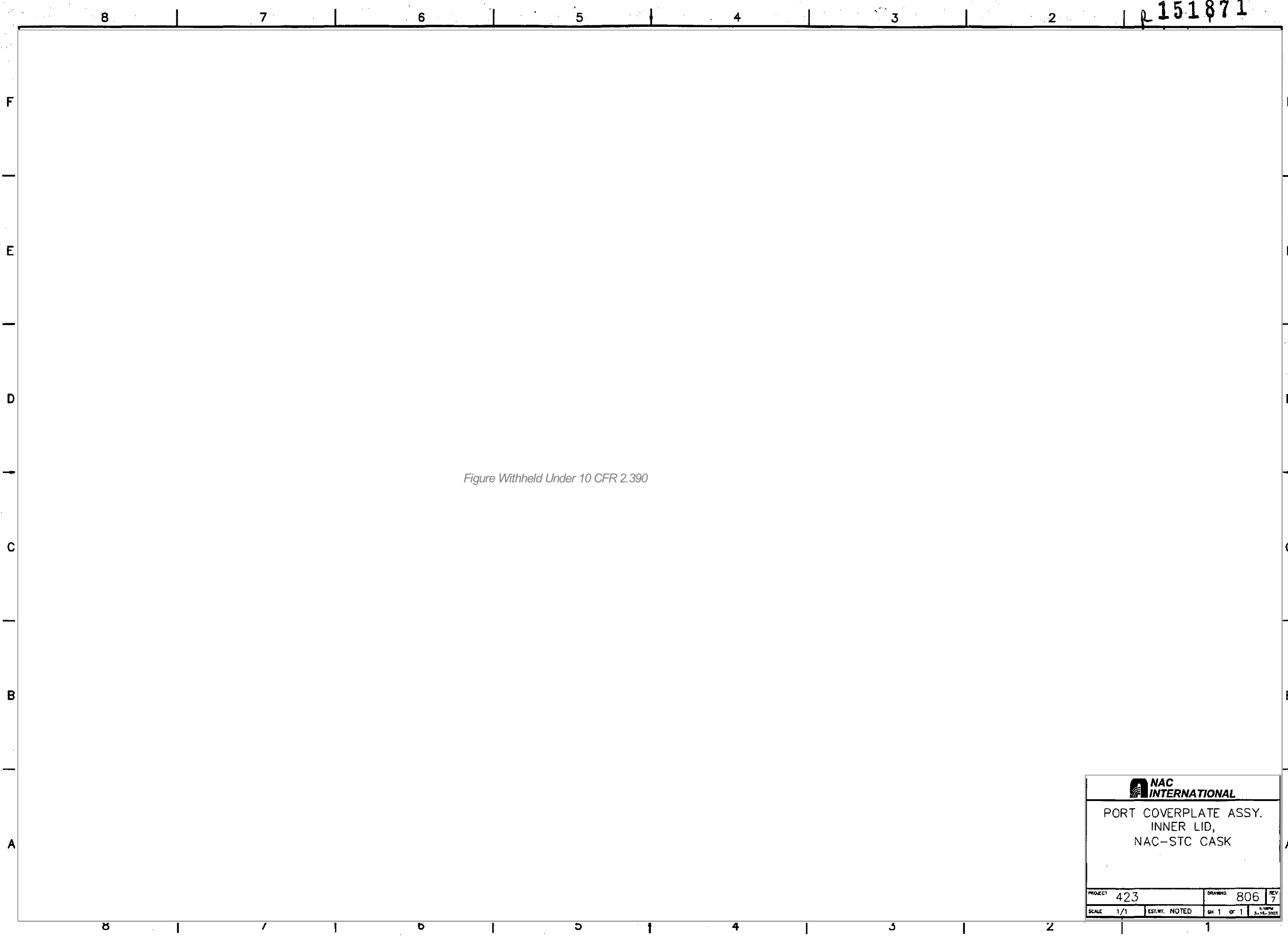
Figure Withheld Under 10 CFR 2.390


 NAC INTERNATIONAL			
LID ASSEMBLY, OUTER, NAC-STC CASK			
PROJECT	423	DRAWING	805
SCALE	1/8	EST. WT. NOTED	SH 1 OF 2
		REV	6



 NAC INTERNATIONAL			
LID ASSEMBLY, OUTER, NAC-STC CASK			
PROJECT	423	DRAWING	805
SCALE	1/6	EST. WT. NOTED	SH 2 OF 2
		REV	6

151871



 NAC INTERNATIONAL			
PORT COVERPLATE ASSY. INNER LID, NAC-STC CASK			
PROJECT	423	DRAWING	806
SCALE	1/1	EST. BY, NOTED	SH 1 OF 1
		REV	7
		3-14-2001	

8

7

6

5

4

3

2

151450₁

F

E

D

C

B

A

F

E

D

C

B

A

Figure Withheld Under 10 CFR 2.390

 **NAC
INTERNATIONAL**

ASSEMBLY,
PORT COVER,
NAC-STC CASK

PROJECT	423	DRAWING	807	REV	3
SCALE	2:1	EST. WT.	10LBS	SH	1 OF 3

2-8-2003

8

7

6

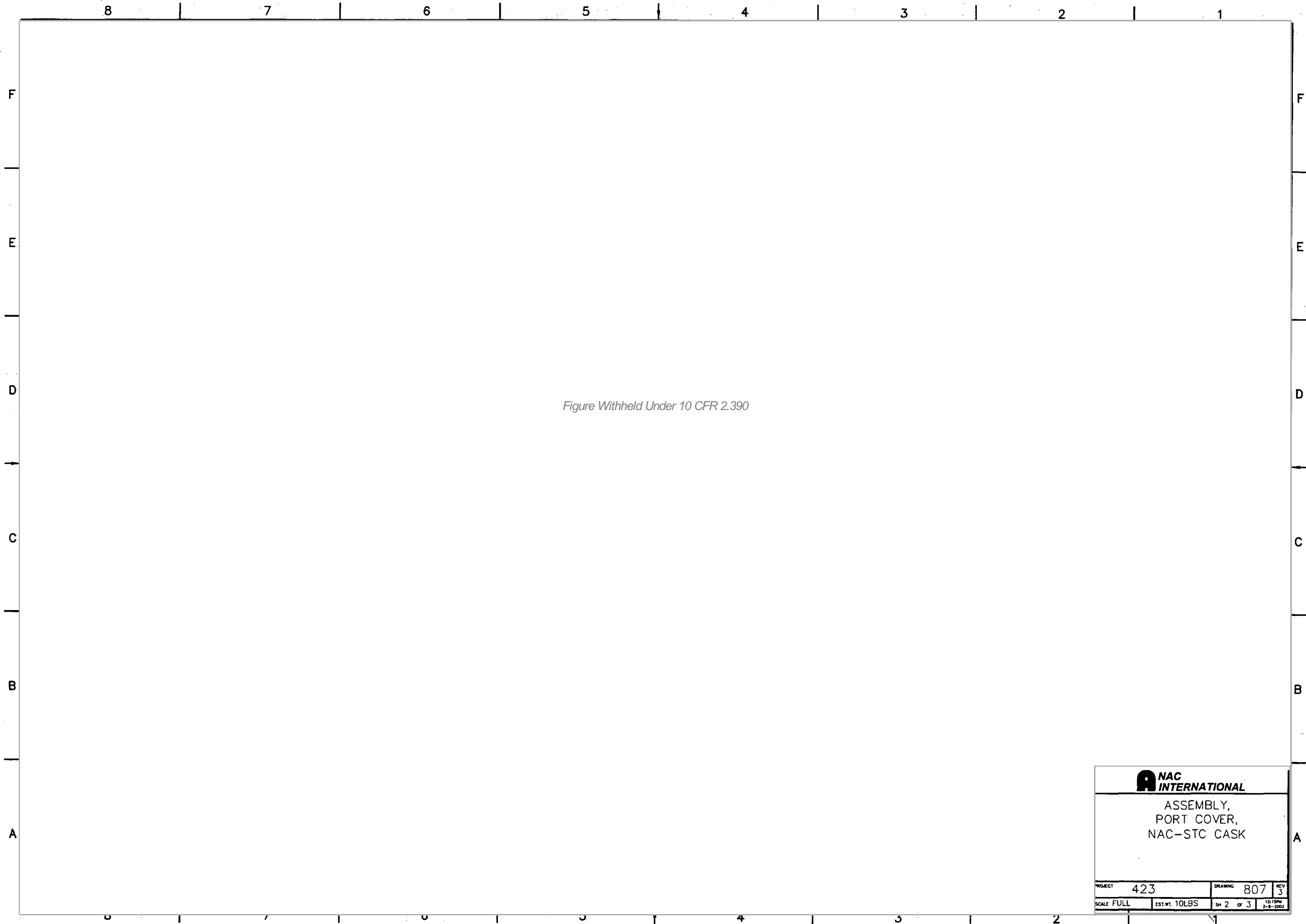
5

4

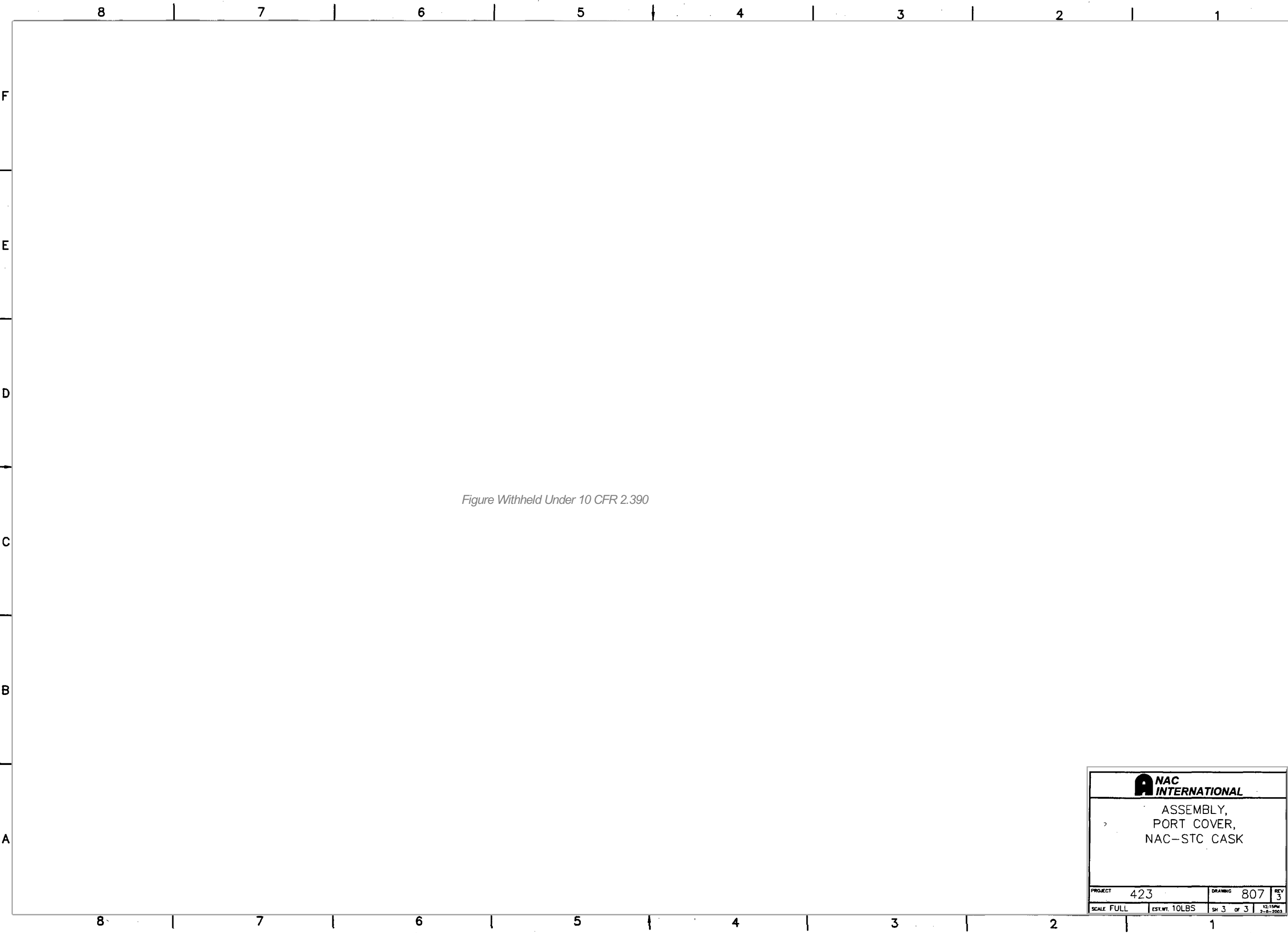
3

2

1



NAC INTERNATIONAL			
ASSEMBLY, PORT COVER, NAC-STC CASK			
PROJECT	423	DRAWING	807
SCALE	FULL	SH 2 OF 3	REV 3
EST. WT. 10LBS		12/15/04 2-8-2003	



NAC INTERNATIONAL			
ASSEMBLY, PORT COVER, NAC-STC CASK			
PROJECT	423	DRAWING	807
SCALE	FULL	EST. WT.	10LBS
SH	3	OF	3
		12:15PM	2-6-2003

Figure Withheld Under 10 CFR 2.390

NUCLEAR ASSURANCE CORPORATION			
MONTICELLO, GEORGIA 30080			
IMPACT LIMITER ASSY- UPPER, NAC-STC CASK			
PROJECT	423	SECTION PACKAGE	209
SCALE	1/8	EXT. WT.	8865 LBS
		SH	1 OF 1
		REV 0	

A

Figure Withheld Under 10 CFR 2.390

NUCLEAR ASSURANCE CORPORATION			
IMPACT LIMITER ASSY- LOWER, NAC-STC CASK			
PROJECT	423	DESIGN PACKAGE	210
SCALE	1/8	EST.WT.140 LBS	BY 1 OF 1

Figure Withheld Under 10 CFR 2.390



 NAC INTERNATIONAL			
BALSA IMPACT LIMITER, UPPER, NAC-STC CASK			
PROJECT	423	DRAWING	257
SCALE	1/10	EST. WT.	6,500#
SH	1	OF	1
10-11-2001		REV 2	

Figure Withheld Under 10 CFR 2.390

 NAL INTERNATIONAL				
BALSA IMPACT LIMITER, LOWER, NAC-STC CASK				
PROJECT	423	DRAWING	258	REV 2
SCALE	1/10	EST. WT.	6,500#	SH 1 OF 1 B. JAM 10-18-2001

A

Figure Withheld Under 10 CFR 2.390



 NAC INTERNATIONAL			
DETAILS, NAC-STC CASK			
PROJECT	423	DRAWING	811
SCALE	1/1	EST. WT.	SH 1 OF 2
		REV 11	

Figure Withheld Under 10 CFR 2.390

 NAC INTERNATIONAL			
DETAILS, NAC-STC CASK			
PROJECT	423	DRAWING	811
		REV	11
SCALE	1/1	EST. WT.	SH 2 OF 2
		12:56PM 2-27-2003	

A

Figure Withheld Under 10 CFR 2.390



 NAC INTERNATIONAL			
NAMEPLATES— NAC—STC CASK			
PROJECT	423	DRAWING	812
		REV	6
SCALE	FULL	WEIGHT	SH 1 OF 1
		10-04MM 8-24-2003	



Figure Withheld Under 10 CFR 2.390

 NAC INTERNATIONAL				
TRANSPORT ASSEMBLY, BALSA IMPACT LIMITERS, NAC-STC				
PROJECT	423	DRAWING	843	REV 2
SCALE	1/12	EST. WT. NOTED	SH 1 OF 1	3:40PM 10-25-2003

1

1

A

Figure Withheld Under 10 CFR 2.390

NAC

INTERNATIONAL


ATTACHMENT HARDWARE,
BALSA LIMITERS,
NAC-STC

PROJECT	423	DRAWING	859	REV	0
SCALE	1/1	EST.WT.	N/A	SH	1 OF 1
				2.73PM	8-16-2000

1

A


Figure Withheld Under 10 CFR 2.390

 NAC INTERNATIONAL			
FUEL BASKET ASSEMBLY, PWR, 26 ELEMENT, NAC-STC CASK			
PROJECT	423	DRAWING	870
			REV 5
SCALE 1/6	WEIGHT NOTED	SH 1 OF 1	10:22AM 8-24-2003

A




Figure Withheld Under 10 CFR 2.390

			
BOTTOM WELDMENT; FUEL BASKET, PWR, 26 ELEMENT, NAC-STC CASK			
PROJECT	423	DRAWING	871
		REV	5
SCALE	1/5	EST. WT.	645#
		SH	1 OF 1
		3-18-2003	


A

Figure Withheld Under 10 CFR 2.390

 NAC INTERNATIONAL			
TOP WELDMENT, FUEL BASKET, PWR, 26 ELEMENT, NAC-STC CASK			
PROJECT	423	DRAWING	872
SCALE	1/5	EST. WT.	SH 1 OF 1
		REV 6 10:56 AM 8-8-2002	

A

Figure Withheld Under 10 CFR 2.390


 NAC INTERNATIONAL			
SUPPORT DISK AND MISC BASKET DETAILS, PWR, 26 ELEMENT, NAC-STC CASK			
PROJECT	423	DRAWING	873
		REV	2
SCALE	1/5	EST. WT.	SH 1 OF 1
		5-8-2002	

A

Figure Withheld Under 10 CFR 2.390


NUCLEAR ASSURANCE CORPORATION			
NORCROSS, GEORGIA 30092			
HEAT TRANSFER DISK, FUEL BASKET, PWR, 26 ELEMENT, NAC-STC CASK			
PROJECT	423	DESIGN PACKAGE	DRAWING 8/4
SCALE 1/5	EST. NO. 105#	SH. 1 OF 1	REV. 2

Figure Withheld Under 10 CFR 2.390

 NAC INTERNATIONAL			
TUBE, NAC-STC CASK			
PROJECT 423		DRAWING 875	REV 7
SCALE 1/1	WEIGHT NOTED	SH 1 OF 2	4-20PM 6-8-2004

A

Figure Withheld Under 10 CFR 2.390

 NAC INTERNATIONAL			
TUBE, NAC-STC CASK			
PROJECT	423	DRAWING	875
SCALE	1/1	WEIGHT NOTED	SH 2 OF 2
		REV 7	

A

Figure Withheld Under 10 CFR 2.390


 NAC INTERNATIONAL			
PACKAGE ASSEMBLY TRANSPORTATION NAC-STC CASK			
PROJECT	423	DRAWING	900
		REV	6
SCALE	1/10	EST. WT.	NOTED
		SH	1 OF 1
		Z. OPPM. 1-15-2003	

Figure Withheld Under 10 CFR 2.390

NUCLEAR ASSURANCE CORPORATION			
TRANSPORTATION PACKAGE CONCEPT NAC-STC CASK			
PROJECT	423	DESIGN PACKAGE	DRAWING 901
SCALE 1/25	EXT. VCL.	SH 1 OF 1	REV 2

Figure Withheld Under 10 CFR 2.390



 NAC INTERNATIONAL			
ASSEMBLY, TRANSPORT CASK, MPC-YANKEE			
PROJECT	455	DRAWING	800
SCALE	1/6	EST. WT.	SH 1 OF 2
		REV 2	
		© 1984 8-10-2000	

Figure Withheld Under 10 CFR 2.390

 NAC INTERNATIONAL			
ASSEMBLY, TRANSPORT CASK, MPC-YANKEE			
PROJECT	455	DRAWING	800
SCALE	1/6	SH	2 OF 2
EST. WT.			
		REV	2

A

Figure Withheld Under 10 CFR 2.390



 NAC INTERNATIONAL			
ASSEMBLY, TRANSPORT CASK, NAC-MPC			
PROJECT	455	DRAWING	801
		REV	3
SCALE	1/6	EST. WT.	SH 1 OF 2
		A11PM 12-10-2001	

Figure Withheld Under 10 CFR 2.390

 NAC INTERNATIONAL			
ASSEMBLY, TRANSPORT CASK, NAC-MPC			
PROJECT	455	DRAWING	801
		REV	3
SCALE	1/6	EST. WT.	SH 2 OF 2
		11:49 AM 12-10-2001	

A

Figure Withheld Under 10 CFR 2.390



 NAC INTERNATIONAL				
SPACERS, TRANSPORT CASK, MPC-YANKEE				
PROJECT	455	DRAWING	820	REV 2
SCALE 1/8	EST. WT. NOTED	SH 1	OF 2	10-16-2003

Figure Withheld Under 10 CFR 2.390

 NAC INTERNATIONAL			
SPACERS, TRANSPORT CASK, MPC-YANKEE			
PROJECT	455	DRAWING	820
			REV 2
SCALE 1/8	EST. WT. NOTED	SH 2 OF 2	1:42PM 8-27-2003

A

Figure Withheld Under 10 CFR 2.390

NAC

INTERNATIONAL


CANISTER SHELL,
MPC-YANKEE

PROJECT	455	DRAWING	870	REV	5
SCALE	1/8	EST. WT.	SH 1 OF 1	4:23PM 12-13-2022	

A


A solid black rectangular redaction bar covering the bottom portion of the drawing area.

Figure Withheld Under 10 CFR 2.390

 NAC INTERNATIONAL			
DETAILS, CANISTER, MPC-YANKEE			
PROJECT	455	DRAWING	871
		REV	8
SCALE 1/8	EST. WT.	SH 1 OF 2	11:42AM 12-28-2002

A

Figure Withheld Under 10 CFR 2.390

 NAC INTERNATIONAL			
DETAILS, CANISTER, MPC—YANKEE			
PROJECT	455	DRAWING	871
		REV	8
SCALE 1/8	EST. WT.	SH 2 OF 2	11:43AM 12-28-2002

A

Figure Withheld Under 10 CFR 2.390


 NAC INTERNATIONAL			
DETAILS, CANISTER, MPC-YANKEE			
PROJECT	455	DRAWING	871
		REV	7P2
SCALE	1/8	EST. BY	SH 1 OF 3
		4-18-2003	

Figure Withheld Under 10 CFR 2.390




 NAC INTERNATIONAL			
DETAILS, CANISTER, MPC-YANKEE			
PROJECT	455	DRAWING	871
SCALE	1/8	SH	2 OF 3
EST. WT.			
			REV 7P2
			2-10PM 4-14-2003

Figure Withheld Under 10 CFR 2.390

 NAC INTERNATIONAL			
DETAILS, CANISTER, MPC-YANKEE			
PROJECT	455	DRAWING	871
		REV	7P2
SCALE	1/8	EST. WT.	SH 3 OF 3
		4-14-2003	


A

Figure Withheld Under 10 CFR 2.390

 NAC INTERNATIONAL			
ASSEMBLY, TRANSPORTABLE STORAGE CANISTER (TSC), MPC-YANKEE			
PROJECT	455	DRAWING	872
		REV	12
SCALE	1/8	EST. WT.	SH 1 OF 2
		9:36AM 12-27-2002	

A

Figure Withheld Under 10 CFR 2.390

			
ASSEMBLY, TRANSPORTABLE STORAGE CANISTER (TSC), MPC-YANKEE			
PROJECT	455	DRAWING	872
SCALE	1/8	SH	2 OF 2
EST. WT.		S. SEAN 12-27-2022	

A

Figure Withheld Under 10 CFR 2.390




 NAC INTERNATIONAL			
ASSEMBLY, TRANSPORTABLE STORAGE CANISTER (TSC), MPC-YANKEE			
PROJECT 455		DRAWING 872	REV 11P1
SCALE 1/8	EST. WT.	SH 1 OF 2	8:27AM 1-14-2003
1			

Figure Withheld Under 10 CFR 2.390

 NAC INTERNATIONAL			
ASSEMBLY, TRANSPORTABLE STORAGE CANISTER (TSC), MPC-YANKEE			
PROJECT	455	DRAWING	872
		REV	11P1
SCALE	1/8	EST. WT.	SH 2 OF 2
		1-8-2003	


A

Figure Withheld Under 10 CFR 2.390

 NAC INTERNATIONAL			
ASSEMBLY, DRAIN TUBE, CANISTER MPC-YANKEE			
PROJECT	455	DRAWING	873
		REV	4
SCALE	FULL	EST. BY	SH 1 OF 1
		E-44AM 12-30-2003	


A

Figure Withheld Under 10 CFR 2.390

 NAC INTERNATIONAL			
PWR FUEL TUBE, MPC-YANKEE			
PROJECT	455	DRAWING	881
		REV	8
SCALE 1/1	EST. BY	NOTED	SH 1 OF 3
		11/07/01 5-13-2002	


A

Figure Withheld Under 10 CFR 2.390

 NAC INTERNATIONAL			
PWR FUEL TUBE, MPC-YANKEE			
PROJECT	455	DRAWING	881
		REV	8
SCALE 1/1	EST.WT. NOTED	SH 2 OF 3	11:14AM 5-15-2002


A

Figure Withheld Under 10 CFR 2.390

 NAC INTERNATIONAL			
PWR FUEL TUBE, MPC-YANKEE			
PROJECT	455	DRAWING	881
		REV	8
SCALE 1/1	EST. WT. NOTED	SH 3 OF 3	12-11PM 5-9-2002


A

Figure Withheld Under 10 CFR 2.390

 NAC INTERNATIONAL				
BASKET ASSEMBLY, 24 GTCC CONTAINER MPC-YANKEE				
PROJECT 455		DRAWING 887		REV 4
SCALE 1/8	EST. WT.	SH 1	OF 3	4:13PM 10-31-2001


A

Figure Withheld Under 10 CFR 2.390

			
BASKET ASSEMBLY, 24 GTCC CONTAINER, MPC-YANKEE			
PROJECT 455		DRAWING 887	
SCALE 1/8		REV 4	
EST. WT.		SH 2 OF 3	
		4:12PM 10-31-2001	

A

Figure Withheld Under 10 CFR 2.390

 NAC INTERNATIONAL			
BASKET ASSEMBLY, 24 GTCC CONTAINER, MPC-YANKEE			
PROJECT	455	DRAWING	887
SCALE 1/8	EST. WT.	SH 3 OF 3	REV 4 12:27PM 10-31-2001

A

Figure Withheld Under 10 CFR 2.390




 NAC INTERNATIONAL			
ASSEMBLY, TRANSPORTABLE STORAGE CANISTER (TSC), 24 GTCC CONTAINER, MPC-YANKEE			
PROJECT	455	DRAWING	888
		REV	8
SCALE	1/8"	EST. WT.	SH 1 OF 2
		B. 27AM 1-13-2003	

Figure Withheld Under 10 CFR 2.390

			
ASSEMBLY, TRANSPORTABLE STORAGE CANISTER (TSC), 24 GTCC CONTAINER, MPC-YANKEE			
PROJECT 455		DRAWING 888	
SCALE 1/8		REV 8	
EST. WT.		SH 2 OF 2	
1		12-30-2002	


A

Figure Withheld Under 10 CFR 2.390

 NAC INTERNATIONAL			
BOTTOM WELDMENT, FUEL BASKET; MPC-YANKEE			
PROJECT	455	DRAWING	891
		REV	1
SCALE	1/5	EST. WT.	SH 1 OF 2
		T:30AM 8-24-2003	


A

Figure Withheld Under 10 CFR 2.390

			
BOTTOM WELDMENT, FUEL BASKET, MPC-YANKEE			
PROJECT	455	DRAWING	891
SCALE 1/5		EST. WT. NOTED	SH 2 OF 2
			7:50AM 8-9-2000


A

Figure Withheld Under 10 CFR 2.390

 NAC INTERNATIONAL			
BOTTOM WELDMENT, FUEL BASKET, MPC-YANKEE			
PROJECT	455	DRAWING	891
SCALE	1/5	SH	1 OF 3
EST. WT.			415PM 5-3-2002


A

Figure Withheld Under 10 CFR 2.390

 NAC INTERNATIONAL			
BOTTOM WELDMENT, FUEL BASKET, MPC-YANKEE			
PROJECT	455	DRAWING	891
		REV	2P0
SCALE 1/5	EST.WT. NOTED	SH 2 OF 3	8:03AM 4-6-2002


A

Figure Withheld Under 10 CFR 2.390

			
BOTTOM WELDMENT, FUEL BASKET, MPC-YANKEE			
PROJECT	455	DRAWING	891
		REV	2P0
SCALE	1/5	EST. WT. NOTED	SH 3 OF 3
		4-11PM 5-3-2002	


A

Figure Withheld Under 10 CFR 2.390

			
TOP WELDMENT, FUEL BASKET, MPC-YANKEE			
PROJECT	455	DRAWING	892
		REV	3
SCALE	1/5	EST. WT. NOTED	SH 1 OF 2
		B: SAAM 4-4-2002	


A

Figure Withheld Under 10 CFR 2.390

 NAC INTERNATIONAL			
TOP WELDMENT, FUEL BASKET, MPC-YANKEE			
PROJECT	455	DRAWING	892
		REV	3
SCALE	1/5	EST. WT. NOTED	SH 2 OF 2
		B:SEAN	4-4-2002


A

Figure Withheld Under 10 CFR 2.390

 NAC INTERNATIONAL			
TOP WELDMENT, FUEL BASKET, MPC-YANKEE			
PROJECT 455		DRAWING 892	
SCALE 1/5		REV. 3P0	
EST. WT. NOTED		SH. 1 OF 3	
		11/10AM 5-7-2003	


A

Figure Withheld Under 10 CFR 2.390

 NAC INTERNATIONAL			
TOP WELDMENT, FUEL BASKET, MPC-YANKEE			
PROJECT	455	DRAWING	892
SCALE	1/5	EST. WT. NOTED	SH 2 OF 3
		1	REV 3P0 5-7-2002


A

Figure Withheld Under 10 CFR 2.390

			
TOP WELDMENT, FUEL BASKET, MPC-YANKEE			
PROJECT	455	DRAWING	892
SCALE 1/5		EST. BY, NOTED	SH 3 OF 3
			REV 3P0
			11/11/00 9-7-2002


A

Figure Withheld Under 10 CFR 2.390

 NAC INTERNATIONAL			
SUPPORT DISK AND MISC. BASKET DETAILS, MPC-YANKEE			
PROJECT	455	DESIGN PACKAGE	DRAWING 893
			REV 3
SCALE 1/5	EST. WT. NOTED	SH 1 OF 1	8:34AM 6-25-08

A

Figure Withheld Under 10 CFR 2.390

 NAC INTERNATIONAL			
HEAT TRANSFER DISK, FUEL BASKET, MPC-YANKEE			
PROJECT	455	DRAWING	894
SCALE	1/5	EST. WT.	57 LBS
		SH	1 OF 1
		10-03AM 3-8-2001	

A

Figure Withheld Under 10 CFR 2.390




 NAC INTERNATIONAL				A		
FUEL BASKET ASSEMBLY, MPC-YANKEE						
PROJECT	455	DRAWING	895		REV	5
SCALE	1/6	EST. WT.	SH 1 OF 2		© 2003 1-2-2003	
		1				

Figure Withheld Under 10 CFR 2.390

 NAC INTERNATIONAL			
FUEL BASKET ASSEMBLY, MPC-YANKEE			
PROJECT 455		DRAWING 895	REV 5
SCALE 1/6	EST. WT.	SH 2 OF 2	BY DMM 1-2-2003


A

Figure Withheld Under 10 CFR 2.390

 NAC INTERNATIONAL			
FUEL BASKET ASSEMBLY, MPC-YANKEE			
PROJECT	455	DRAWING	895
		REV	SP0
SCALE	1/6	EST. WT.	SH 1 OF 2
		11/1/00 8-3-2002	


A

Figure Withheld Under 10 CFR 2.390

 NAC INTERNATIONAL			
FUEL BASKET ASSEMBLY, MPC-YANKEE			
PROJECT	455	DRAWING	895
		REV	5P0
SCALE	1/6	EST. BY	SN 2 OF 2
		11-17-AM 4-4-2002	

A


Figure Withheld Under 10 CFR 2.390

 NAC INTERNATIONAL			
RETAINER, UNITED NUCLEAR TEST ASSEMBLY, MPC-YANKEE			
PROJECT	455	DRAWING	919
		REV	2
SCALE	1/1	EST. BY	NOTED
		SH	1 OF 1
		12-30-2002	

A


1

Figure Withheld Under 10 CFR 2.390

 NAC INTERNATIONAL			
CASK ASSEMBLY, NAC-STC, CY-MPC			
PROJECT	414	DRAWING	801
		REV	1
SCALE	1/6	EST. BY	NOTED
		SH	1 OF 2
		11-43AM 12-10-2001	

A

Figure Withheld Under 10 CFR 2.390

 NAC INTERNATIONAL			
CASK ASSEMBLY, NAC-STC, CY-MPC			
PROJECT	414	DRAWING	801
		REV	1
SCALE	1/6	EST. BY	NOTED
		SH	2 OF 2
		11:43AM 12-10-2001	

A

Figure Withheld Under 10 CFR 2.390




 NAC INTERNATIONAL			
CANISTER SPACER CY-MPC			
PROJECT	414	DRAWING	820
SCALE	1/6	EST. WT.	SH. 1 OF 1
		REV 0	
		11-25-88	

Figure Withheld Under 10 CFR 2.390

 NAC INTERNATIONAL			
CANISTER SHELL, CY-MPC			
PROJECT 414		DRAWING 870	REV 3
SCALE 1/8	EST. WT. NOTED	SH 1 OF 1	10-0000 9-26-2002
1			


A

Figure Withheld Under 10 CFR 2.390

 NAC INTERNATIONAL			
DETAILS, CANISTER CY-MPC			
PROJECT	414	DRAWING	871
		REV	6
SCALE 1/8	EST. WT. NOTED	SH 1 OF 2	6:35AM 4-1-2004


A

Figure Withheld Under 10 CFR 2.390

 NAC INTERNATIONAL			
DETAILS, CANISTER CY-MPC			
PROJECT	414	DRAWING	871
SCALE	1/8	EST. WT. NOTED	SH 2 OF 2
		REV 6	
		S. SEAR 4-1-2004	


1

Figure Withheld Under 10 CFR 2.390

 NAC INTERNATIONAL			
ASSEMBLY, TRANSPORTABLE STORAGE CANISTER (TSC), CY-MPC			
PROJECT 414		DRAWING 872	
SCALE 1/8		REV 6	
WEIGHT NOTED		SH 1 OF 3	
		1-21-2004	


A

Figure Withheld Under 10 CFR 2.390

 NAC INTERNATIONAL			
ASSEMBLY, TRANSPORTABLE STORAGE CANISTER (TSC), CY-MPC			
PROJECT	414	DRAWING	872
		REV	6
SCALE	1/8	EST. WT. NOTED	SH 2 OF 3
		2.57PM 1-15-2004	

A

Figure Withheld Under 10 CFR 2.390

 NAC INTERNATIONAL			
ASSEMBLY, TRANSPORTABLE STORAGE CANISTER (TSC), CY-MPC			
PROJECT	414	DRAWING	872
			REV 6
SCALE 1/8	EST.WT. NOTED	SH 3 OF 3	2:58PM 1-15-2004

A

Figure Withheld Under 10 CFR 2.390



 NAC INTERNATIONAL			
DRAIN TUBE ASSEMBLY, CY-MPC			
PROJECT	414	DRAWING	873
		REV	2
SCALE	1/1	EST. WT. NOTED	SH 1 OF 1
		8.00AM 7-22-2003	

Figure Withheld Under 10 CFR 2.390

 NAC INTERNATIONAL				
SHIM, CANISTER CY-MPC				
PROJECT 414		DRAWING 874		REV 0
SCALE 1/2	WEIGHT	SH 1 OF 1	1:03PM 8-10-2003	

A

Figure Withheld Under 10 CFR 2.390


 NAC INTERNATIONAL			
SPACER SHIM, CANISTER, CY-MPC			
PROJECT	414	DRAWING	875
		REV	0
SCALE	1/3	WEIGHT NOTED	SH 1 OF 1
		E-ZONE 6-3-2003	

Figure Withheld Under 10 CFR 2.390



 NAC INTERNATIONAL			
FUEL TUBE, TRANSPORTABLE STORAGE CANISTER (TSC), CY-MPC			
PROJECT	414	DRAWING	881
SCALE	1/1	EST. WT.	SH 1 OF 2
		REV 4	
		10-2-2002	

Figure Withheld Under 10 CFR 2.390

			
FUEL TUBE, TRANSPORTABLE STORAGE CANISTER (TSC), CY-MPC			
PROJECT	414	DRAWING	881
SCALE	1/1	EST. WTL.	SH 2 OF 2
		10-23AM 5-8-2002	

A

Figure Withheld Under 10 CFR 2.390




 NAC INTERNATIONAL			
OVERSIZE FUEL TUBE, TRANSPORTABLE STORAGE CANISTER (TSC), CY-MPC			
PROJECT	414	DRAWING	882
SCALE	1/1	EST. WT.	SH 1 OF 2
		REV 4 5-8-2002	

Figure Withheld Under 10 CFR 2.390

 NAC INTERNATIONAL			
OVERSIZE FUEL TUBE, TRANSPORTABLE STORAGE CANISTER (TSC), CY-MPC			
PROJECT	414	DRAWING	882
SCALE	1/1	EST. WT.	SH 2 OF 2
		11:05AM 5-9-2002	


A

Figure Withheld Under 10 CFR 2.390

			
BASKET ASSEMBLY, GTCC, CY-MPC			
PROJECT	414	DRAWING	887
SCALE	1/8	EST. WT. NOTED	SH 1 OF 4
		2:05PM 2-11-2003	


A

Figure Withheld Under 10 CFR 2.390

 NAC INTERNATIONAL			
BASKET ASSEMBLY, GTCC, CY-MPC			
PROJECT	414	DRAWING	887
		REV	4
SCALE	1/8	EST. WT. NOTED	SH 2 OF 4
		4-15PM 2-3-2003	


A

Figure Withheld Under 10 CFR 2.390

			
BASKET ASSEMBLY, GTCC, CY-MPC			
PROJECT	414	DRAWING	887
SCALE	1/2	EST. WT. NOTED	SH 3 OF 4
		12:50PM 2-3-2003	

A

Figure Withheld Under 10 CFR 2.390

			
BASKET ASSEMBLY, GTCC, CY-MPC			
PROJECT	414	DRAWING	887
SCALE 1/8		EST. BY, NOTED	SH 4 OF 4
		B. E. SAN 2-6-2003	

A

Figure Withheld Under 10 CFR 2.390




 NAC INTERNATIONAL			
CANISTER SHELL, GTCC, CY-MPC			
PROJECT	414	DRAWING	888
		REV	4
SCALE 1/8	EST.WT. NOTED	SH 1 OF 2	2:30PM 2-4-2003

Figure Withheld Under 10 CFR 2.390

			
CANISTER SHELL, GTCC, CY-MPC			
PROJECT	414	DRAWING	888
		REV	4
SCALE	1/8	EST. WT. NOTED	SH 2 OF 2
		1/20PM 2-3-2003	


A

Figure Withheld Under 10 CFR 2.390

 NAC INTERNATIONAL				
ASSEMBLY, TRANSPORTABLE STORAGE CANISTER (TSC), GTCC CY-MPC				
PROJECT 414		DRAWING 889		REV 7
SCALE 1/8	WEIGHT NOTED	SH 1	OF 3	11:43PM 11-22-2004


A

Figure Withheld Under 10 CFR 2.390

			
ASSEMBLY, TRANSPORTABLE STORAGE CANISTER (TSC), GTCC CY-MPC			
PROJECT	414	DRAWING	889
		REV	7
SCALE	1/8	EST. WT. NOTED	SH 2 OF 3
		1-22-2004	


A

Figure Withheld Under 10 CFR 2.390

 NAC INTERNATIONAL			
ASSEMBLY, TRANSPORTABLE STORAGE CANISTER (TSC), GTCC CY-MPC			
PROJECT	414	DRAWING	889
		SH	3
SCALE	1/8	EST. WT. NOTED	1
		OF	3
		REV	7
		2-11PM 1-20-2004	


A

Figure Withheld Under 10 CFR 2.390

			
BOTTOM WELDMENT, FUEL BASKET CY-MPC			
PROJECT 414		DRAWING 891	REV 3
SCALE 1/5	EST. WT. NOTED	SH 1 OF 1	12.51PM 11-14-2001


A

Figure Withheld Under 10 CFR 2.390

 NAC INTERNATIONAL			
TOP WELDMENT, FUEL BASKET CY-MPC			
PROJECT	414	DRAWING	892
SCALE 1/5		EST. WT. NOTED	SH 1 OF 3
			REV 3


A

Figure Withheld Under 10 CFR 2.390

 NAC INTERNATIONAL			
TOP WELDMENT, FUEL BASKET CY-MPC			
PROJECT	414	DRAWING	892
		REV	3
SCALE	1/5	EST. WT. NOTED	SH 2 OF 3
		11-21AM 11-14-2001	

A

Figure Withheld Under 10 CFR 2.390


 NAC INTERNATIONAL			
TOP WELDMENT, FUEL BASKET CY-MPC			
PROJECT	414	DRAWING	892
		REV	3
SCALE	1/5	EST. BY	NOTED
		SH	3 OF 3
		11-14-2001	

A

Figure Withheld Under 10 CFR 2.390


A INAC INTERNATIONAL			
SUPPORT DISK AND MISC. BASKET DETAILS CY-MPC			
PROJECT	414	DRAWING	893
SCALE	1/5	EST.WT. NOTED	SH 1 OF 2
		12 20PM 11-13-2001	

Figure Withheld Under 10 CFR 2.390

 ANAC INTERNATIONAL			
SUPPORT DISK AND MISC. BASKET DETAILS CY-MPC			
PROJECT	414	DRAWING	893
		REV	2
SCALE	1/5	EST. WT. NOTED	SH 2 OF 2
		12:24PM 11-13-2001	

A

Figure Withheld Under 10 CFR 2.390

				
HEAT TRANSFER DISK, FUEL BASKET CY-MPC				
PROJECT 414		DRAWING 894		REV 0
SCALE 1/5	EST. WT. NOTED	SH 1	OF 1	10.00AM 12-17-89

A

Figure Withheld Under 10 CFR 2.390



 NAC INTERNATIONAL			
FUEL BASKET ASSEMBLY CY-MPC			
PROJECT	414	DRAWING	895
		REV	4
SCALE	1/6	EST. BY	NOTED
		SH	1 OF 2
		11/14/00 5-8-2002	

Figure Withheld Under 10 CFR 2.390

 NAC INTERNATIONAL			
FUEL BASKET ASSEMBLY CY-MPC			
PROJECT	414	DRAWING	895
		REV	4
SCALE 1/6	EST. WT. NOTED	SH 2 OF 2	11/1/AM 5-8-2002

A

Figure Withheld Under 10 CFR 2.390



		YANKEE ATOMIC ELECTRIC COMPANY 580 MAIN STREET BOLTON, MA.	
		NUCLEAR SERVICES DIVISION	
TITLE:		YANKEE-CLASS RECONFIGURED FUEL ASSEMBLY	
DOC. NO.		YR-00-060	
JOB NO.		W.O. FS00	

Figure Withheld Under 10 CFR 2.390

		YANKEE ATOMIC ELECTRIC COMPANY 580 MAIN STREET BOSTON, MA.	
		NUCLEAR SERVICES DIVISION	
TITLE:		YANKEE-CLASS RECONFIGURED FUEL ASSEMBLY SHELL WELDMENT	
DOC. NO.		YR-00-061	
JOB NO.		W. O. FS00	

12/1/88 10:00 AM 10/1/88 10:00 AM 10/1/88 10:00 AM

Figure Withheld Under 10 CFR 2.390


	
YANKEE ATOMIC ELECTRIC COMPANY 580 MAIN STREET BOLTON, MA.	
NUCLEAR SERVICES DIVISION	
TITLE: YANKEE-CLASS RECONFIGURED FUEL ASSEMBLY TOP END FITTING ASSEMBLY	
ORG. NO. YR-00-062 SH.1	
JOB NO.	W.O. FS00

Figure Withheld Under 10 CFR 2.390



 Duke Engineering & Services <small>A Duke Energy Company</small>		<small>400 DONALD LYNCH BOULEVARD MARLBOROUGH, MA</small>	
TITLE:		YANKEE-CLASS RECONFIGURED FUEL ASSEMBLY TOP END PLATE	
DOC. NO.		YR-00-062 SH.2	
JOB NO.	W. O. FS00		


Figure Withheld Under 10 CFR 2.390

 Duke Engineering & Services. <small>A Duke Energy Company</small>		<small>400 DONALD LYNCH BOULEVARD MARLBOROUGH, MA</small>
TITLE:		YANKEE-CLASS RECONFIGURED FUEL ASSEMBLY TOP END TEMPLATE
REV. NO.		YR-00-062 SH. 3
JOB NO.		

g:\yvesse\name\yr sub\fuel mod\year fuel mod

A

Figure Withheld Under 10 CFR 2.390

		YANKEE ATOMIC ELECTRIC COMPANY 580 MAIN STREET BOLTON, MA.	
		NUCLEAR SERVICES DIVISION	
TITLE:		YANKEE-CLASS RECONFIGURED FUEL ASSEMBLY BOTTOM END FITTING ASSY.	
SPEC. NO.		YR-00-063	
JOB NO.		W.O. FS00	

1
A
6/1/00 10:00 AM 10/1/00 10:00 AM

Figure Withheld Under 10 CFR 2.390




		YANKEE ATOMIC ELECTRIC COMPANY 580 MAIN STREET BOLTON, MA.	
		NUCLEAR SERVICES DIVISION	
TITLE:		YANKEE-CLASS RECONFIGURED FUEL ASSEMBLY NOZZLE BOLT AND ALIGNMENT PIN	
Dwg. No.		YR-00-064	
JOB NO.	W. O. FS00		

Figure Withheld Under 10 CFR 2.390

		YANKEE ATOMIC ELECTRIC COMPANY 500 MAIN STREET BOLTON, MA.	
		NUCLEAR SERVICES DIVISION	
TITLE:		YANKEE-CLASS RECONFIGURED FUEL ASSEMBLY FUEL BASKET ASSEMBLY	
P/N:		YR-00-065	
JOB NO.		W.O. F500	


1
A
of figure assembly shall not be used for

Figure Withheld Under 10 CFR 2.390

	YANKEE ATOMIC ELECTRIC COMPANY 580 MAIN STREET BOLTON, MA.
NUCLEAR SERVICES DIVISION	
TITLE:	YANKEE-CLASS RECONFIGURED FUEL ASSEMBLY FUEL TUBE ASSEMBLY
DOC. NO.	YR-00-066 SH.1
REV. NO.	W.O. FS00

Approved for release by NSA on 09-28-2013 pursuant to E.O. 13526

Figure Withheld Under 10 CFR 2.390

 Duke Engineering & Services <small>A Duke Energy Company</small>		<small>400 DONALD LYNCH BOULEVARD MARLBOROUGH, MA</small>	
TITLE:		YANKEE-CLASS RECONFIGURED FUEL ASSEMBLY FUEL TUBE ASSEMBLY	
REV. NO.		YR-00-066 SH. 2	
JOB NO.		1	

10/1/2000 10:00 AM

Figure Withheld Under 10 CFR 2.390




 NAC INTERNATIONAL			
CAN ASSEMBLY, DAMAGED FUEL, MPC—YANKEE			
PROJECT 455		DRAWING 901	
SCALE FULL		EST. NO. 71#	
SH 1 OF 1		2.50PM 8-3-2007	

Figure Withheld Under 10 CFR 2.390

 NAC INTERNATIONAL			
CAN DETAILS, DAMAGED FUEL, MPC-YANKEE			
PROJECT	455	DRAWING	902
SCALE FULL		EST. WT. NOTED	SH 1 OF 5
			REV 0P4 1-31-2003

A

Figure Withheld Under 10 CFR 2.390


 NAC INTERNATIONAL			
CAN DETAILS, DAMAGED FUEL, MPC-YANKEE			
PROJECT	455	DRAWING	902
		REV	0P4
SCALE	FULL	EST. BY	NOTED
		SH	2 OF 5
		11-18-06 1-21-2003	

A

1

1


Figure Withheld Under 10 CFR 2.390

			
CAN DETAILS, DAMAGED FUEL, MPC-YANKÉE			
PROJECT	455	DRAWING	902
		REV	0P4
SCALE	FULL	EST. WT. NOTED	SH 3 OF 5
		E-1746 1-21-2003	

1


A

Figure Withheld Under 10 CFR 2.390

 NAC INTERNATIONAL			
CAN DETAILS, DAMAGED FUEL, MPC-YANKEE			
PROJECT	455	DRAWING	902
		REV	OP4
SCALE	FULL	EST. WT.	NOTED
		SH. 4	OF 5
		1-21-2003	


A

Figure Withheld Under 10 CFR 2.390

 NAC INTERNATIONAL			
CAN DETAILS, DAMAGED FUEL, MPC-YANKEE			
PROJECT	455	DRAWING	902
		REV	0P4
SCALE	FULL	EST. BY	NOTED
		SH	5 OF 5
		1-18PM 1-21-2003	

A

Figure Withheld Under 10 CFR 2.390

 NAC INTERNATIONAL			
ASSEMBLY, DAMAGED FUEL CAN CY-MPC			
PROJECT	414	DRAWING	901
SCALE	FULL	EST. WT.	127#
SH	1	OF	1
		3.21PM 4-26-2002	

1

A

Figure Withheld Under 10 CFR 2.390




 NAC INTERNATIONAL			
DETAILS, DAMAGED FUEL CAN, CY-MPC			
PROJECT	414	DRAWING	902
		REV	3
SCALE	FULL	EST.WT. NOTED	SH 1 OF 3
		11:33AM 2-27-2003	

Figure Withheld Under 10 CFR 2.390

 NAC INTERNATIONAL			
DETAILS, DAMAGED FUEL CAN, CY-MPC			
PROJECT	414	DRAWING	902
		REV	3
SCALE	FULL	EST. WT. NOTED	SH 2 OF 3
		11-53AM 2-27-2003	
1			

A

Figure Withheld Under 10 CFR 2.390

			
DETAILS, DAMAGED FUEL CAN, CY-MPC			
PROJECT	414	DRAWING	902
		REV	3
SCALE	FULL	EST. BY	NOTED
		SH	3 OF 3
		TJ:LSAM 2-27-2003	
		1	

A

Figure Withheld Under 10 CFR 2.390




 NAC INTERNATIONAL				A
RECONFIGURED FUEL ASSEMBLY CY-MPC				
PROJECT 414		DRAWING 903		
SCALE FULL		REV 1		
EST. WT. NOTED		SH 1 OF 2		4/20PM 3-1-2000
1		1		

Figure Withheld Under 10 CFR 2.390

 NAC INTERNATIONAL			
RECONFIGURED FUEL ASSEMBLY CY-MPC			
PROJECT	414	DRAWING	903
		REV	1
SCALE	FULL	EST. WT. NOTED	SH 2 OF 2
		S-13PM 2-31-100	
		1	


A

Figure Withheld Under 10 CFR 2.390

				
DETAILS, RECONFIGURED FUEL ASSEMBLY CY-MPC				
PROJECT	414	DRAWING	904	REV 0
SCALE	FULL	EST. WT. NOTED	SH 1 OF 3	11-02-08 12-17-08
1				


A

Figure Withheld Under 10 CFR 2.390

			
DETAILS, RECONFIGURED FUEL ASSEMBLY CY-MPC			
PROJECT	414	DRAWING	904
		REV	0
SCALE	FULL	EST. WT. NOTED	SH 2 OF 3
		11/01/AM 12-27-98	

A

Figure Withheld Under 10 CFR 2.390

			
DETAILS, RECONFIGURED FUEL ASSEMBLY CY-MPC			
PROJECT	414	DRAWING	904
SCALE	FULL	EST. WT. NOTED	Sh. 3 OF 3
		11:02AM 12-27-98	

A

1

Table of Contents

2.0	STRUCTURAL EVALUATION	2-1
2.1	Structural Design	2.1.1-1
2.1.1	Discussion	2.1.1-1
2.1.2	Design Criteria	2.1.2-1
2.1.2.1	Discussion	2.1.2-1
2.1.2.2	Allowable Stress Limits - Ductile Failure	2.1.2-2
2.1.3	Miscellaneous Structural Failure Modes	2.1.3-1
2.1.3.1	Brittle Fracture	2.1.3-1
2.1.3.2	Fatigue - Normal Operation	2.1.3-5
2.1.3.3	Extreme Total Stress Intensity Range	2.1.3-10
2.1.3.4	Inner Shell Buckling Design Criteria	2.1.3-11
2.1.3.5	Creep Considerations at Elevated Temperatures	2.1.3-15
2.1.3.6	Impact Limiter Deformation Limits	2.1.3-15
2.2	Weights and Centers of Gravity	2.2-1
2.3	Mechanical Properties of Materials	2.3.1-1
2.3.1	Discussion	2.3.1-1
2.3.2	Austenitic Stainless Steels	2.3.2-1
2.3.3	Precipitation-Hardened Stainless Steel	2.3.3-1
2.3.4	Bolting Materials	2.3.4-1
2.3.5	Aluminum Alloys	2.3.5-1
2.3.6	Shielding Material	2.3.6-1
2.3.6.1	Chemical Copper Grade Lead	2.3.6-1
2.3.6.2	NS-4-FR	2.3.6-1
2.3.7	Impact Limiter Materials	2.3.7-1
2.3.8	Spacer Materials	2.3.8-1
2.4	General Standards for All Packages	2.4-1
2.4.1	Minimum Package Size	2.4.1-1
2.4.2	Tamperproof Feature	2.4.2-1
2.4.3	Positive Closure	2.4.3-1
2.4.4	Chemical and Galvanic Reactions	2.4.4-1

Table of Contents

2.4.4.1	Component Operating Environment.....	2.4.4-1
2.4.4.2	Component Material Categories	2.4.4-2
2.4.4.3	General Effects of Identified Reactions	2.4.4-8
2.4.4.4	Adequacy of the Cask Operating Procedures	2.4.4-9
2.4.4.5	Effects of Reaction Products.....	2.4.4-9
2.4.5	Cask Design	2.4.5-1
2.4.6	Continuous Venting	2.4.6-1
2.5	Lifting and Tiedown Standards.....	2.5.1-1
2.5.1	Lifting Devices	2.5.1-1
2.5.1.1	Lifting Trunnion Analysis	2.5.1-1
2.5.1.2	Lid Lifting Device	2.5.1-14
2.5.1.3	Canister Lifting	2.5.1-19
2.5.2	Tiedown Devices	2.5.2-1
2.5.2.1	Discussion and Loads	2.5.2-1
2.5.2.2	Rear Support	2.5.2-11
2.5.2.3	Front Support	2.5.2-23
2.5.2.4	Tiedown Evaluation for the CY-MPC Configuration with Balsa Impact Limiters	2.5.2-24
2.6	Normal Conditions of Transport.....	2.6-1
2.6.1	Heat.....	2.6.1-1
2.6.1.1	Heat Condition for the NAC-STC Cask in the Directly Loaded Fuel and Yankee-MPC Configurations.....	2.6.1-1
2.6.1.2	Heat Condition for the NAC-STC Cask in the CY-MPC Configuration	2.6.1-5
2.6.2	Cold.....	2.6.2-1
2.6.2.1	Cold Condition for the NAC-STC Cask in the Directly Loaded Fuel and Yankee-MPC Configurations.....	2.6.2-1
2.6.2.2	Cold Condition for the NAC-STC Cask in the CY-MPC Configuration	2.6.2-6
2.6.3	Reduced External Pressure	2.6.3-1
2.6.4	Increased External Pressure	2.6.4-1
2.6.5	Vibration	2.6.5-1
2.6.6	Water Spray	2.6.6-1

Table of Contents

2.6.7	Free Drop (1 Foot)	2.6.7-1
2.6.7.1	One-Foot End Drop.....	2.6.7.1-1
2.6.7.2	One-Foot Side Drop.....	2.6.7.2-1
2.6.7.3	One-Foot Corner Drop.....	2.6.7.3-1
2.6.7.4	Impact Limiters.....	2.6.7.4-1
2.6.7.5	Closure Analysis - Normal Conditions of Transport.....	2.6.7.5-1
2.6.7.6	Neutron Shield Analysis	2.6.7.6-1
2.6.7.7	Upper Ring/Outer Shell Intersection Analysis	2.6.7.7-1
2.6.8	Corner Drop (1 Foot)	2.6.8-1
2.6.9	Compression	2.6.9-1
2.6.10	Penetration	2.6.10-1
2.6.10.1	Impact Limiter - Penetration.....	2.6.10.1-1
2.6.10.2	Neutron Shield Shell - Penetration	2.6.10.2-1
2.6.10.3	Port Cover - Penetration	2.6.10.3-1
2.6.11	Fabrication Conditions.....	2.6.11-1
2.6.11.1	Lead Pour	2.6.11.1-1
2.6.11.2	Cooldown.....	2.6.11.2-1
2.6.11.3	Lead Creep.....	2.6.11.3-1
2.6.12	Fuel Basket Analysis (For Directly Loaded Fuel) - Normal Transport Conditions	2.6.12-1
2.6.12.1	Detailed Analysis - PWR Basket for Directly Loaded Fuel	2.6.12.1-1
2.6.12.2	Finite Element Model Description - Directly Loaded PWR Fuel Basket.....	2.6.12.2-1
2.6.12.3	Thermal Expansion Evaluation of Support Disk - Directly Loaded PWR Fuel Basket.....	2.6.12.3-1
2.6.12.4	Stress Evaluation of Support Disk for a 1-Foot End Drop Load Condition (Directly Loaded Fuel Configuration).....	2.6.12.4-1
2.6.12.5	Stress Evaluation of Support Disk (Directly Loaded Fuel Configuration) for Thermal Plus a 1-Foot End Drop Combined Load Condition.....	2.6.12.5-1
2.6.12.6	Stress Evaluation of Threaded Rods and Spacer Nuts for a 1-Foot End Drop Load Condition (Directly Loaded Fuel Configuration).....	2.6.12.6-1

Table of Contents

2.6.12.7	Stress Evaluation of Support Disk (Directly Loaded Fuel Configuration) for a 1-Foot Side Drop Impact Load Condition	2.6.12.7-1
2.6.12.8	Stress Evaluation of Support Disk (Directly Loaded Fuel Configuration) for Thermal Plus a 1-Foot Side Drop Combined Load Condition.....	2.6.12.8-1
2.6.12.9	Support Disk Web Stresses for a 1-Foot Side Drop Condition (Directly Loaded Fuel Configuration)	2.6.12.9-1
2.6.12.10	Support Disk Shear Stresses for a 1-Foot Side Drop and a 1-Foot End Drop Conditions (Directly Loaded Fuel Configuration).....	2.6.12.10-1
2.6.12.11	Bearing Stress - Basket Contact with Inner Shell (Directly Loaded Fuel Configuration)	2.6.12.11-1
2.6.12.12	Evaluation of Triaxial Stress for the Fuel Basket Support Disk (Directly Loaded Fuel Configuration)	2.6.12.12-1
2.6.12.13	Fuel Basket (Directly Loaded Fuel Configuration) Weldment Analysis for 1-Foot Drop	2.6.12.13-1
2.6.13	Yankee-MPC Transportable Storage Canister Analysis - Normal Transport Condition	2.6.13-1
2.6.13.1	Yankee-MPC Canister Description and Analysis.....	2.6.13.1-1
2.6.13.2	Yankee-MPC Canister Finite Element Model	2.6.13.2-1
2.6.13.3	Thermal Expansion Evaluation of Yankee-MPC Canister for Spent Fuel	2.6.13.3-1
2.6.13.4	Stress Evaluation of the Yankee-MPC Canister for 1-Foot End Drop Load Condition	2.6.13.4-1
2.6.13.5	Stress Evaluation of the Yankee-MPC Canister for Thermal Plus a 1-Foot End Drop Load Condition.....	2.6.13.5-1
2.6.13.6	Stress Evaluation of the Yankee-MPC Canister for a 1-Foot Side Drop Load Condition	2.6.13.6-1
2.6.13.7	Stress Evaluation of the Yankee-MPC Canister for Thermal Plus a 1-Foot Side Drop Load Condition	2.6.13.7-1
2.6.13.8	Yankee-MPC Canister Shear Stresses for a 1-Foot Side Drop and a 1-Foot End Drop Condition	2.6.13.8-1
2.6.13.9	Yankee-MPC Canister Bearing Stresses for 1-Foot Side Drop	2.6.13.9-1

Table of Contents

2.6.13.10	Yankee-MPC Canister Buckling Evaluation for 1-Foot End Drop	2.6.13.10-1
2.6.13.11	Yankee-MPC Canister Lifting Evaluation.....	2.6.13.11-1
2.6.13.12	Yankee-MPC Canister Closure Weld Evaluation – Normal Conditions	2.6.13.12-1
2.6.14	Yankee-MPC Fuel Basket Analysis - Normal Conditions of Transport ..	2.6.14-1
2.6.14.1	Detailed Analysis - Yankee-MPC Fuel Basket.....	2.6.14.1-1
2.6.14.2	Finite Element Model Description - Yankee-MPC Fuel Basket.....	2.6.14.2-1
2.6.14.3	Thermal Expansion Evaluation of Yankee-MPC Fuel Basket Support Disk	2.6.14.3-1
2.6.14.4	Stress Evaluation of Yankee-MPC Fuel Basket Support Disk for a 1-Foot End Drop Condition	2.6.14.4-1
2.6.14.5	Stress Evaluation of Yankee-MPC Fuel Basket Support Disk for Thermal Plus a 1-Foot End Drop Combined Condition	2.6.14.5-1
2.6.14.6	Stress Evaluation of Yankee-MPC Basket Tie Rods and Spacers for a 1-Foot End Drop Load Condition	2.6.14.6-1
2.6.14.7	Stress Evaluation of Yankee-MPC Fuel Basket Support Disk for a 1-Foot Side Drop Load Condition	2.6.14.7-1
2.6.14.8	Stress Evaluation of Yankee-MPC Fuel Basket Support Disk for Thermal Plus a 1-Foot Side Drop Combined Condition	2.6.14.8-1
2.6.14.9	Yankee-MPC Fuel Basket Support Disk Shear Stresses for 1-Foot Drops	2.6.14.9-1
2.6.14.10	Bearing Stress - Basket Contact with Canister Shell.....	2.6.14.10-1
2.6.14.11	Yankee-MPC Fuel Basket Weldment Analysis for 1-Foot End Drop	2.6.14.11-1
2.6.14.12	Yankee-MPC Fuel Basket Support Disk - Buckling Evaluation (Normal Conditions of Transport).....	2.6.14.12-1
2.6.15	CY-MPC Transportable Storage Canister Analysis – Normal Conditions of Transport	2.6.15-1
2.6.15.1	Analysis Description – CY-MPC Canister	2.6.15.1-1
2.6.15.2	Finite Element Model Description – CY-MPC Canister	2.6.15.2-1

Table of Contents

2.6.15.3	Thermal Expansion of CY-MPC Canister Containing Fuel	2.6.15.3-1
2.6.15.4	Stress Evaluation of the CY-MPC Canister for 1-Foot End Drop Load Condition.....	2.6.15.4-1
2.6.15.5	Stress Evaluation of the Canister for Thermal Plus a 1-Foot End Drop Load Condition	2.6.15.5-1
2.6.15.6	Stress Evaluation of the Canister for a 1-Foot Side Drop Load Condition	2.6.15.6-1
2.6.15.7	Stress Evaluation of the CY-MPC Canister for Thermal Plus a 1-Foot Side Drop Load Condition.....	2.6.15.7-1
2.6.15.8	CY-MPC Canister Shear Stresses for a 1-Foot Side Drop and a 1-Foot End Drop Condition	2.6.15.8-1
2.6.15.9	CY-MPC Canister Bearing Stresses for a 1-Foot Side Drop	2.6.15.9-1
2.6.15.10	CY-MPC Canister Buckling Evaluation for 1-Foot End Drop.....	2.6.15.10-1
2.6.15.11	CY-MPC Canister Lifting Evaluation	2.6.15.11-1
2.6.15.12	CY-MPC Canister Closure Weld Evaluation – Normal Conditions of Transport	2.6.15.12-1
2.6.16	CY-MPC Fuel Basket Analysis – Normal Conditions of Transport	2.6.16-1
2.6.16.1	Detailed Analysis of the CY-MPC Fuel Basket	2.6.16.1-1
2.6.16.2	CY-MPC Fuel Basket Finite Element Model Description ..	2.6.16.2-1
2.6.16.3	Thermal Expansion Evaluation of the CY-MPC Support Disk	2.6.16.3-1
2.6.16.4	Stress Evaluation of the CY-MPC Support Disk for a 1-Foot End Drop	2.6.16.4-1
2.6.16.5	Stress Evaluation of the CY-MPC Support Disk for a Combined Thermal and 1-Foot End Drop Load Condition	2.6.16.5-1
2.6.16.6	Stress Evaluation of CY-MPC Tie Rods and Spacers for 1-Foot End Drop.....	2.6.16.6-1
2.6.16.7	Stress Evaluation of CY-MPC Support Disk for a 1-Foot Side Drop	2.6.16.7-1
2.6.16.8	Stress Evaluation of the CY-MPC Support Disk for a Combined Thermal and 1-Foot Side Drop Load Condition	2.6.16.8-1
2.6.16.9	CY-MPC Support Disk Shear Stresses for 1-Foot Drop	2.6.16.9-1

Table of Contents

2.6.16.10	Bearing Stress – Basket Contact with Canister Shell – CY-MPC	2.6.16.10-1
2.6.16.11	CY-MPC Fuel Basket Weldment Analysis for 1-Foot End Drop	2.6.16.11-1
2.6.16.12	CY-MPC Fuel Basket Support Disk – Buckling Evaluation	2.6.16.12-1
2.6.16.13	Stress Evaluation of the CY-MPC Support Disk for 1-Foot Oblique Drop	2.6.16.13-1
2.6.16.14	Stress Evaluation of the CY-MPC Support Disk for a Combined Thermal and 1-Foot Oblique Drop Load Condition	2.6.16.14-1
2.6.17	CY-MPC Reconfigured-Fuel Assembly Analysis and Damaged Fuel Can Analysis – Normal Conditions of Transport	2.6.17-1
2.6.17.1	CY-MPC Reconfigured Fuel Assembly Evaluation	2.6.17-1
2.6.17.2	CY-MPC Damaged Fuel Can Evaluation	2.6.17-8
2.6.18	Spacer Design for Canistered Fuel – Normal Conditions of Transport....	2.6.18-1
2.6.18.1	Spacer Evaluation for Yankee-M PC Canister Fuel and GTCC Waste	2.6.18-1
2.6.18.2	Spacer Evaluation for CY-MPC Canister Fuel and GTCC Waste.....	2.6.18-2
2.6.19	Greater Than Class C (GTCC) Basket Analysis – Normal Conditions of Transport.....	2.6.19-1
2.6.19.1	Yankee-MPC GTCC Basket Analysis.....	2.6.19-1
2.6.19.2	CY-MPC GTCC Basket Analysis.....	2.6.19-6
2.6.20	Yankee-MPC Reconfigured Fuel Assembly and Damaged Fuel Can Analysis – Normal Conditions of Transport.....	2.6.20-1
2.6.20.1	Yankee-MPC Reconfigured Fuel Assembly Evaluation	2.6.20-1
2.6.20.2	Yankee-MPC Damaged Fuel Can Evaluation	2.6.20-13
2.6.21	Fuel Rod Retainer	2.6.21-1
2.7	Hypothetical Accident Conditions.....	2.7-1
2.7.1	Free Drop (30 Feet).....	2.7.1-1
2.7.1.1	Thirty-Foot End Drop	2.7.1.1-1
2.7.1.2	Thirty-Foot Side Drop	2.7.1.2-1
2.7.1.3	Thirty-Foot Corner Drop	2.7.1.3-1

Table of Contents

2.7.1.4	Thirty-Foot Oblique Drop.....	2.7.1.4-1
2.7.1.5	Lead Slump Resulting From a Cask Drop Accident.....	2.7.1.5-1
2.7.1.6	Closure Analysis - Hypothetical Accident Conditions	2.7.1.6-1
2.7.2	Puncture	2.7.2-1
2.7.2.1	Puncture - Cask Side Midpoint.....	2.7.2.1-1
2.7.2.2	Puncture - Center of Outer Lid	2.7.2.2-1
2.7.2.3	Puncture - Center of Cask Bottom	2.7.2.3-1
2.7.2.4	Puncture - Port Cover	2.7.2.4-1
2.7.2.5	Puncture Accident - Shielding Consequences	2.7.2.5-1
2.7.2.6	Puncture - Conclusion.....	2.7.2.6-1
2.7.3	Thermal.....	2.7.3.1-1
2.7.3.1	Discussion	2.7.3.1-1
2.7.3.2	Pressure Stress Evaluation	2.7.3.2-1
2.7.3.3	Thermal Stress Evaluation	2.7.3.3-1
2.7.3.4	Bolts - Closure Lids (Thermal Accident)	2.7.3.4-1
2.7.3.5	Performance Summary - Thermal Accident	2.7.3.5-1
2.7.3.6	Conclusion	2.7.3.6-1
2.7.4	Crush	2.7.4-1
2.7.5	Immersion - Fissile Material.....	2.7.5-1
2.7.6	Immersion - All Packages.....	2.7.6-1
2.7.7	Damage Summary.....	2.7.7-1
2.7.8	Directly Loaded Fuel Basket Analysis - Accident Conditions	2.7.8-1
2.7.8.1	Stress Evaluation of Support Disk - Directly Loaded Fuel Configuration	2.7.8.1-1
2.7.8.2	Stress Evaluation of the Directly Loaded Fuel Basket Threaded Rods and Spacer Nuts - Accident Condition	2.7.8.2-1
2.7.8.3	Assessment of Buckling – Directly Loaded Fuel Basket	2.7.8.3-1
2.7.8.4	Directly Loaded Fuel Basket Fuel Tube Analysis	2.7.8.4-1
2.7.8.5	Directly Loaded Fuel Basket Weldment Analysis for 30-Foot End Drop	2.7.8.5-1
2.7.9	Yankee-MPC Fuel Basket Analysis - Accident Conditions	2.7.9-1
2.7.9.1	Detailed Analysis – Yankee-MPC Fuel Basket	2.7.9-5
2.7.9.2	Stress Evaluation of the Yankee-MPC Tie Rods and Spacers for a 30-Foot End Drop Load Condition	2.7.9-24

Table of Contents

2.7.9.3	Yankee-MPC Basket Support Disk - Buckling Evaluation (Accident Conditions).....	2.7.9-26
2.7.9.4	Yankee-MPC Fuel Tube Analysis	2.7.9-31
2.7.9.5	Yankee-MPC Basket Weldment Analysis for 30-Foot End Drop	2.7.9-34
2.7.10	Greater Than Class C (GTCC) Waste Basket Analysis - Accident Conditions	2.7.10-1
2.7.10.1	Yankee-MPC GTCC Basket Evaluation.....	2.7.10-1
2.7.10.2	CY-MPC GTCC Basket Analysis – Accident Conditions.....	2.7.10-9
2.7.11	Yankee-MPC Transportable Storage Canister Analysis - Accident Conditions	2.7.11-1
2.7.11.1	Canister - Accident Analysis Description.....	2.7.11-2
2.7.11.2	Analysis Results.....	2.7.11-2
2.7.11.3	Canister Buckling Evaluation for the 30-Foot End Drop	2.7.11-9
2.7.11.4	Canister Closure Weld Evaluation – Accident Conditions...	2.7.11-10
2.7.11.5	Dynamic Loading Effect – Structural Lid Weld.....	2.7.11-11
2.7.12	CY-MPC Transportable Storage Canister Analysis – Accident Conditions	2.7.12-1
2.7.12.1	Canister – Accident Analysis Description	2.7.12-1
2.7.12.2	Analysis Results.....	2.7.12-2
2.7.12.3	Canister Buckling Evaluation for the 30-Foot End Drop	2.7.12-3
2.7.12.4	CY-MPC Canister Closure Weld Evaluation – Accident Conditions	2.7.12-4
2.7.13	CY-MPC Fuel Basket Analysis – Accident Conditions	2.7.13-1
2.7.13.1	Stress Evaluation of CY-MPC Support Disk.....	2.7.13.1-1
2.7.13.2	Stress Evaluation of Tie Rods and Spacers for 30-Foot End Drop Load Condition for the CY-MPC	2.7.13.2-1
2.7.13.3	CY-MPC Fuel Basket Support Disk – Buckling Evaluation (Accident Condition)	2.7.13.3-1
2.7.13.4	Fuel Tube Analysis – CY-MPC.....	2.7.13.4-1
2.7.13.5	CY-MPC Fuel Basket Weldment Analysis for 30-Foot End Drop	2.7.13.5-1
2.7.14	CY-MPC Reconfigured Fuel Assembly and Damaged Fuel Can Evaluation – Accident Conditions	2.7.14-1
2.7.14.1	CY-MPC Reconfigured Fuel Assembly Weldment Evaluation	2.7.14-1

Table of Contents

2.7.14.2	CY-MPC Damaged Fuel Can – Accident Conditions	2.7.14-9
2.7.15	Yankee-MPC Reconfigured Fuel Assembly and Damaged Fuel Can Analysis – Hypothetical Accident Conditions.....	2.7.15-1
2.7.15.1	Yankee-MPC Reconfigured Fuel Assembly Evaluation	2.7.15-1
2.7.15.2	Yankee-MPC Damaged Fuel Can Evaluation	2.7.15-13
2.8	Special Form	2.8-1
2.9	Fuel Rod Buckling Assessment	2.9-1
2.9.1	Fuel Rod Buckling Assessment for Directly Loaded 17 x 17 PWR Fuel.....	2.9-1
2.9.2	Fuel Rod Buckling Assessment for Yankee-Class Canistered Fuel	2.9-7
2.9.3	Fuel Rod Buckling Assessment for CY-MPC Canistered Fuel	2.9-10
2.10	Appendices.....	2.10.1-1
2.10.1	Computer Program Descriptions.....	2.10.1-1
2.10.1.1	ANSYS	2.10.1-1
2.10.1.2	RBCUBED - A Program to Calculate Impact Limiter Dynamics	2.10.1-2
2.10.1.3	LS-DYNA	2.10.1-3
2.10.2	Finite Element Analysis.....	2.10.2-1
2.10.2.1	Model Descriptions.....	2.10.2-1
2.10.2.2	Loading Conditions.....	2.10.2-15
2.10.2.3	Finite Element Analysis Procedures	2.10.2-26
2.10.2.4	Finite Element Documentation Procedures	2.10.2-31
2.10.3	LS-DYNA Computer Code.....	2.10.3-1
2.10.3.1	Predicting Impact Deceleration using Strain Rate Sensitive Properties.....	2.10.3-1
2.10.3.2	Accounting for Strain Rate Sensitivity by Interpolation	2.10.3-2
2.10.4	Detailed Finite Element Stress Summaries - Directly Loaded Fuel Configuration.....	2.10.4-1
2.10.5	Inner Shell Buckling Analysis	2.10.5-1
2.10.5.1	Buckling Analysis.....	2.10.5-1
2.10.5.2	Analysis Results.....	2.10.5-2
2.10.5.3	Verification of the Code Case N-284 Buckling Evaluation of the NAC-STC Inner Shell and Transition Sections.....	2.10.5-3

Table of Contents

2.10.5.4	Buckling Evaluation of the Inner Shell for the Yankee-MPC Fuel Configuration	2.10.5-9
2.10.5.5	Buckling Evaluation of the Inner Shell for the CY-MPC Fuel Configuration	2.10.5-14
2.10.6	Scale Model Test Program for the NAC-STC	2.10.6-1
2.10.6.1	Introduction.....	2.10.6-1
2.10.6.2	Purpose.....	2.10.6-2
2.10.6.3	Discussion	2.10.6-2
2.10.6.4	Eighth-Scale Redwood Impact Limiter Compression Tests...	2.10.6-9
2.10.6.5	Quarter-Scale Model Drop Tests	2.10.6-14
2.10.6.6	NAC-STC Quarter-Scale Model Drawings	2.10.6-36
2.10.6.7	NAC-STC Eighth-Scale Model Drawings.....	2.10.6-36
2.10.7	Redwood Impact Limiter Force-Deflection Curves and Data – Directly Loaded Fuel Configuration.....	2.10.7-1
2.10.7.1	Potential Energy and Cask Drop Impact Motion.....	2.10.7-1
2.10.7.2	Conversion of Potential Energy to Kinetic Energy	2.10.7-9
2.10.7.3	Deceleration Forces and Energy Absorption Calculation.....	2.10.7-10
2.10.7.4	RBCUBED Calculated Force-Deflection Graphs.....	2.10.7-13
2.10.8	Bolts - Closure Lids (Stress Evaluations).....	2.10.8-1
2.10.8.1	Analysis Approach.....	2.10.8-1
2.10.8.2	Inner Lid Closure Bolt Analyses	2.10.8-2
2.10.8.3	Outer Lid Closure Bolt Analyses.....	2.10.8-15
2.10.9	Lead Slump Evaluation.....	2.10.9-1
2.10.9.1	Methodology/Finite Element Analysis	2.10.9-2
2.10.9.2	Analysis Result	2.10.9-3
2.10.9.3	Conclusion	2.10.9-4
2.10.10	Assessment of the Effect of the Revised Temperature Distribution on Structural Qualification.....	2.10.10-1
2.10.10.1	Evaluation Methodology.....	2.10.10-1
2.10.10.2	Temperature Dependent Stress Results	2.10.10-3
2.10.10.3	Conclusions - Revised Temperature Distribution Evaluation	2.10.10-7
2.10.11	Sensitivity Studies of the Yankee-MPC Canistered Fuel Basket Analysis	2.10.11-1
2.10.11.1	Yankee-MPC Fuel Basket Drop Orientation	2.10.11-1

Table of Contents

2.10.11.2	Gap Stiffness.....	2.10.11-2
2.10.11.3	Finite Element Mesh for the Support Disk Ligaments	2.10.11-3
2.10.12	Confirmatory Testing Program –Balsa Impact Limiters and Attachments	2.10.12-1
2.10.12.1	Confirmatory Testing Program Results Summary.....	2.10.12-1
2.10.12.2	Acceptance Criteria for Model Performance	2.10.12-3
2.10.12.3	Description of 30-Foot Drop Tests Performed at SNL.....	2.10.12-4
2.10.12.4	Results/Evaluation for the 30-Foot Side Drop Test.....	2.10.12-8
2.10.12.5	Results/Evaluation for the 30-Foot Top Corner Drop Test.....	2.10.12-10
2.10.12.6	Results/Evaluation for the 30-Foot Top End Drop Test.....	2.10.12-12
2.10.12.7	LS-DYNA Analyses of the NAC-STC Quarter-Scale Model	2.10.12-14

List of Figures

Figure 2.3.6-1	Quasi-Static True Stress-Strain Curves for Chemical Copper Grade Lead in Compression.....	2.3.6-2
Figure 2.3.6-2	Neutron Shield Thermal Expansion Coefficient.....	2.3.6-3
Figure 2.5.1-1	Lifting Trunnion Geometry.....	2.5.1-30
Figure 2.5.1-2	Trunnion Weld Geometry	2.5.1-31
Figure 2.5.1-3	Sling Inclination Angle for Outer Lid Lifting	2.5.1-32
Figure 2.5.1-4	Sling Inclination Angle for Inner Lid Lifting	2.5.1-33
Figure 2.5.1-5	Canister Lift Finite Element Model	2.5.1-34
Figure 2.5.1-6	Yankee-MPC Canister Lift Model Stress Intensity Contours (psi).....	2.5.1-35
Figure 2.5.1-7	CY-MPC Canister Lift Model Stress Intensity Contours (psi).....	2.5.1-36
Figure 2.5.2-1	Front Support and Tiedown Geometry	2.5.2-26
Figure 2.5.2-2	Free Body Diagram of Cask Subjected to Lateral Load.....	2.5.2-27
Figure 2.6.7.2-1	Section Locations for Stress Evaluation (Canister Configurations)	2.6.7.2-14
Figure 2.6.7.2-2	Yankee-MPC Cask Model with Pressure Distribution Applied (Side Drop Case).....	2.6.7.2-15
Figure 2.6.7.2-3	CY-MPC Model with Pressure Distribution Applied (Side Drop Case).....	2.6.7.2-16
Figure 2.6.7.4.1-1	NAC-STC with Redwood Impact Limiters	2.6.7.4-22
Figure 2.6.7.4.1-2	Cross-Section of Redwood Impact Limiter	2.6.7.4-23
Figure 2.6.7.4.1-3	Crush Stress-Strain Curves for Redwood (Crush Strength Parallel to Grain)	2.6.7.4-24
Figure 2.6.7.4.1-4	Crush Stress-Strain Curves for Redwood (Crush Strength Perpendicular to Grain)	2.6.7.4-25
Figure 2.6.7.4.1-5	Crush Stress-Strain Curves for Balsa Wood (Crush Strength Parallel to Grain).....	2.6.7.4-26
Figure 2.6.7.4.1-6	Variation of Crush Strength of Redwood and Balsa Wood with Impact Angle at 40 Percent Strain	2.6.7.4-27
Figure 2.6.7.4.1-7	Redwood Impact Limiter Attachment Geometry	2.6.7.4-28
Figure 2.6.7.4.1-8	Anchorage Detail of the Retaining Rod at the End of the Impact Limiter	2.6.7.4-29

List of Figures (Continued)

Figure 2.6.7.4.1-9	RBCUBED Output Summary - Center of Gravity Over Top Corner	2.6.7.4-30
Figure 2.6.7.4.1-10	Free Body Diagram - Upper Impact Limiter - Center of Gravity Over Corner	2.6.7.4-31
Figure 2.6.7.4.1-11	Free Body Diagram - Upper Impact Limiter - Cask Wedging Forces	2.6.7.4-32
Figure 2.6.7.4.2-1	Three-Dimensional View of the Balsa Impact Limiter.....	2.6.7.4-48
Figure 2.6.7.4.2-2	Cross-Sectional View of the Balsa Impact Limiter	2.6.7.4-49
Figure 2.6.7.4.2-3	LS-DYNA Model of the Balsa Impact Limiter	2.6.7.4-50
Figure 2.6.7.4.2-4	Balsa Impact Limiter Drop Orientations	2.6.7.4-51
Figure 2.6.7.4.2-5	Acceleration Time-History for 1-ft Side Drop on the Trunnion (Cold Conditions).....	2.6.7.4-52
Figure 2.6.7.4.2-6	Acceleration Time-History for 1-ft End Drop (Cold Conditions).....	2.6.7.4-53
Figure 2.6.7.4.2-7	Acceleration Time-History for 1-ft Drop onto Corner (Cold Conditions).....	2.6.7.4-54
Figure 2.6.7.4.2-8	Acceleration Time-History for 30-ft Side Drop (Hot and Cold Conditions).....	2.6.7.4-55
Figure 2.6.7.4.2-9	Acceleration Time-History for 30-ft End Drop (Hot and Cold Conditions).....	2.6.7.4-56
Figure 2.6.7.4.2-10	Acceleration Time-History for 30-ft Drop onto Corner (Hot and Cold Conditions).....	2.6.7.4-57
Figure 2.6.7.6-1	Neutron Shield Shell Geometry	2.6.7.6-12
Figure 2.6.10.2-1	Flow Diagram of the Plastic Analysis of Neutron Shield Shell ...	2.6.10.2-3
Figure 2.6.10.3-1	Port Cover Geometry and Loading	2.6.10.3-5
Figure 2.6.10.3-2	Finite Element Model of Port Cover.....	2.6.10.3-6
Figure 2.6.10.3-3	Port Cover Response to Penetration Event	2.6.10.3-7
Figure 2.6.12-1	NAC-STC PWR Fuel Assembly Basket for Directly Loaded Fuel	2.6.12-3
Figure 2.6.12-2	Support Disk Cross-Section Configuration for Directly Loaded Fuel	2.6.12-4
Figure 2.6.12-3	Fuel Tube Configuration for Directly Loaded Fuel.....	2.6.12-5

List of Figures (Continued)

Figure 2.6.12.2-1	Finite Element Model - Thermal Stress Analysis (NAC-STC PWR Basket Support Disk for Directly Loaded Fuel)	2.6.12.2-4
Figure 2.6.12.2-2	Finite Element Model - Side Impact Analysis (NAC-STC PWR Basket Support Disk for Directly Loaded Fuel)	2.6.12.2-5
Figure 2.6.12.3-1	Location of the 20 Maximum SI Nodal Stresses in the NAC-STC Fuel Basket Support Disk for Directly Loaded Fuel - Thermal Condition	2.6.12.3-4
Figure 2.6.12.3-2	Basket Maximum Material Condition for the Directly Loaded Fuel Configuration in the Horizontal Orientation (inches).....	2.6.12.3-5
Figure 2.6.12.3-3	Basket Maximum Material Condition for Directly Loaded Fuel Configuration - Cask Vertical	2.6.12.3-6
Figure 2.6.12.4-1	Support Disk for the Directly Loaded Fuel Configuration - 19.6-g End Drop.....	2.6.12.4-2
Figure 2.6.12.5-1	Location of the 20 Maximum SI Nodal Stresses in the NAC-STC Fuel Basket Support Disk (Directly Loaded Fuel Configuration) - Thermal + 19.6-g End Drop	2.6.12.5-2
Figure 2.6.12.7-1	Support Disk Side Drop Orientations (Directly Loaded Fuel Configuration).....	2.6.12.7-3
Figure 2.6.12.7-2	Locations of Maximum Nodal SI Stresses (Directly Loaded Fuel Configuration - Support Disk) - 18.1-g Side Impact Condition (0° Drop Orientation)	2.6.12.7-4
Figure 2.6.12.7-3	Location of Maximum Nodal SI Stresses (Directly Loaded Fuel Configuration - Support Disk) - 18.1-g Side Impact Condition (15° Drop Orientation)	2.6.12.7-5
Figure 2.6.12.7-4	Location of Maximum Nodal SI Stresses (Directly Loaded Fuel Configuration - Support Disk) - 18.1-g Side Impact Condition (30° Drop Orientation)	2.6.12.7-6
Figure 2.6.12.7-5	Location of Maximum Nodal SI Stresses (Directly Loaded Fuel Configuration - Support Disk) - 18.1-g Side Impact Condition (37° Drop Orientation)	2.6.12.7-7
Figure 2.6.12.7-6	Location of Maximum Nodal SI Stresses (Directly Loaded Fuel Configuration - Support Disk) - 18.1-g Side Impact Condition (45° Drop Orientation)	2.6.12.7-8

List of Figures (Continued)

Figure 2.6.12.7-7	Location of Maximum Nodal SI Stresses (Directly Loaded Fuel Configuration - Support Disk) - 18.1-g Side Impact Condition (60° Drop Orientation)	2.6.12.7-9
Figure 2.6.12.7-8	Location of Maximum Nodal SI Stresses (Directly Loaded Fuel Configuration - Support Disk) - 18.1-g Side Impact Condition (64° Drop Orientation)	2.6.12.7-10
Figure 2.6.12.7-9	Location of Maximum Nodal SI Stresses (Directly Loaded Fuel Configuration - Support Disk) - 18.1-g Side Impact Condition (75° Drop Orientation)	2.6.12.7-11
Figure 2.6.12.7-10	Location of Maximum Nodal SI Stresses (Directly Loaded Fuel Configuration - Support Disk) - 18.1-g Side Impact Condition (90° Drop Orientation)	2.6.12.7-12
Figure 2.6.12.9-1	Node Point Locations for Basket Web Stress Summaries (Directly Loaded Fuel Configuration)	2.6.12.9-2
Figure 2.6.12.13-1	Fuel Basket Weldment Model (Directly Loaded Fuel Configuration)	2.6.12.13-2
Figure 2.6.12.13-2	Fuel Basket Top Weldment Boundary Conditions (Directly Loaded Fuel Configuration)	2.6.12.13-3
Figure 2.6.12.13-3	Fuel Basket Bottom Weldment Boundary Conditions (Directly Loaded Fuel Configuration)	2.6.12.13-4
Figure 2.6.13-1	Yankee-MPC Transportable Storage Canister	2.6.13-2
Figure 2.6.13-2	Yankee-MPC Canister for Fuel Basket or GTCC Basket	2.6.13-3
Figure 2.6.13.2-1	Yankee-MPC Canister Finite Element Model	2.6.13.2-3
Figure 2.6.13.2-2	Yankee-MPC Canister Structural and Shield Lid Finite Element Mesh	2.6.13.2-4
Figure 2.6.13.2-3	Yankee-MPC Structural and Shield Lid Weld Regions Finite Element Mesh	2.6.13.2-5
Figure 2.6.13.2-4	Yankee-MPC Canister Bottom Plate Finite Element Mesh	2.6.13.2-6
Figure 2.6.13.3-1	Identification of the Sections for Evaluating the Linearized Stresses in the Yankee-MPC Canister	2.6.13.3-3
Figure 2.6.13.11-1	Finite Element Model for Yankee-MPC Canister Lift Evaluation	2.6.13.11-3
Figure 2.6.14-1	Yankee-MPC Fuel Basket	2.6.14-5

List of Figures (Continued)

Figure 2.6.14-2	Support Disk Cross Section Configuration - Yankee-MPC Fuel Basket	2.6.14-6
Figure 2.6.14-3	Fuel Tube Configuration - Yankee-MPC Fuel Basket	2.6.14-7
Figure 2.6.14-4	Location of Enlarged Fuel Tubes or Damaged Fuel Cans	2.6.14-8
Figure 2.6.14.1-1	Yankee-MPC Fuel Basket Drop Orientations	2.6.14.1-2
Figure 2.6.14.2-1	Yankee-MPC Basket Support Disk End Drop Model	2.6.14.2-3
Figure 2.6.14.2-2	Yankee-MPC Basket Support Disk Side Drop Model - 0° Orientation	2.6.14.2-4
Figure 2.6.14.2-3	Yankee-MPC Basket Support Disk Side Drop Model - 45° Orientation	2.6.14.2-4
Figure 2.6.14.2-4	CONTAC52 Elements in the Yankee-MPC Support Disk Side Drop Model (Interface between Disks and Canister Shell)	2.6.14.2-5
Figure 2.6.14.2-5	CONTAC49 Elements in the Yankee-MPC Support Disk Side Drop Model (Interface between Canister Shell and Cask Inner Shell)	2.6.14.2-5
Figure 2.6.14.2-6	Yankee-MPC Basket Support Disk Side Drop Model - Refined Mesh Disk	2.6.14.2-6
Figure 2.6.14.2-7	Yankee-MPC Basket Support Disk Side Drop Model - Coarse Mesh Disk	2.6.14.2-6
Figure 2.6.14.2-8	Yankee-MPC Support Disk Side Drop Model - Support Disks Side View	2.6.14.2-7
Figure 2.6.14.2-9	Location of the Sections to Obtain Linearized Stresses for 0° Yankee-MPC Basket Orientation	2.6.14.2-8
Figure 2.6.14.2-10	Location of the Sections to Obtain Linearized Stresses for 45° Yankee-MPC Basket Orientation	2.6.14.2-9
Figure 2.6.14.4-1	Locations of Maximum $P_m + P_b$ Stresses in the Yankee-MPC Fuel Basket, 1-Foot End Drop, Thermal Condition 2	2.6.14.4-2
Figure 2.6.14.5-1	Locations of Maximum $P+Q$ Stresses in the Yankee-MPC Fuel Basket Support Disk for the 1-Foot End Drop, Thermal Condition 2	2.6.14.5-2
Figure 2.6.14.7-1	Locations of Maximum P_m Stresses, Yankee-MPC Basket, Disk 1, 1-Foot Side Drop, 0° Orientation, Thermal Condition 2	2.6.14.7-2

List of Figures (Continued)

Figure 2.6.14.7-2	Locations of Maximum $P_m + P_b$ Stresses, Yankee-MPC Basket, Disk 1, 1-Foot Side Drop, 0° Orientation, Thermal Condition 2	2.6.14.7-3
Figure 2.6.14.7-3	Locations of Maximum P_m Stresses, Yankee-MPC Basket, Disk 5, 1-Foot Side Drop, 45° Orientation, Thermal Condition 2	2.6.14.7-4
Figure 2.6.14.7-4	Locations of Maximum $P_m + P_b$ Stresses, Yankee-MPC Basket, Disk 5, 1-Foot Side Drop, 45° Orientation, Thermal Condition 2	2.6.14.7-5
Figure 2.6.14.8-1	Locations of Maximum P+Q Stresses, Yankee-MPC Basket, Disk 1, 1-Foot Side Drop, 0° Orientation, Thermal Condition 2	2.6.14.8-2
Figure 2.6.14.8-2	Locations of Maximum P+Q Stresses, Yankee-MPC Basket, Disk 5, 1-Foot Side Drop, 45° Orientation, Thermal Condition 2	2.6.14.8-3
Figure 2.6.14.11-1	Finite Element Model of the Yankee-MPC Fuel Basket Top Weldment Plate	2.6.14.11-3
Figure 2.6.14.11-2	Finite Element Model of the Yankee-MPC Fuel Basket Bottom Weldment Plate	2.6.14.11-4
Figure 2.6.15.2-1	CY-MPC Canister Assembly Finite Element Model	2.6.15.2-3
Figure 2.6.15.2-2	CY-MPC Canister Structural and Shield Lid Finite Element Mesh	2.6.15.2-4
Figure 2.6.15.2-3	CY-MPC Canister Structural and Shield Lid Weld Region Finite Element Mesh	2.6.15.2-5
Figure 2.6.15.2-4	CY-MPC Canister Bottom Plate Finite Element Mesh	2.6.15.2-6
Figure 2.6.15.3-1	Identification of the Sections for Evaluating the Linearized Stresses in the Canister	2.6.15.3-3
Figure 2.6.15.11-1	Finite Element Model for CY-MPC Canister Lift Evaluation....	2.6.15.11-3
Figure 2.6.16-1	CY-MPC Fuel Assembly Basket	2.6.16-3
Figure 2.6.16-2	CY-MPC Support Disk Configuration – Canistered Fuel Basket ...	2.6.16-4
Figure 2.6.16-3	CY-MPC Basket Standard Fuel Tube	2.6.16-5
Figure 2.6.16-4	CY-MPC Basket Oversize Fuel Tube	2.6.16-6
Figure 2.6.16.1-1	CY-MPC Basket Drop Orientations	2.6.16.1-2
Figure 2.6.16.2-1	CY-MPC Support Disk Side Drop Model	2.6.16.2-3
Figure 2.6.16.2-2	CY-MPC Support Disk End Drop Model	2.6.16.2-4
Figure 2.6.16.2-3	Cask Orientation	2.6.16.2-5

List of Figures (Continued)

Figure 2.6.16.2-4	CONTAC52 Elements in the CY-MPC Support Disk Side Drop Model.....	2.6.16.2-6
Figure 2.6.16.2-5	Location of the Sections to Obtain Linearized Stresses – CY-MPC Basket Support Disk	2.6.16.2-7
Figure 2.6.16.4-1	Locations of CY-MPC Support Disk Maximum $P_m + P_b$ Stresses, 1-Foot End Drop	2.6.16.4-2
Figure 2.6.16.5-1	Locations of Maximum $P_m + P_b + Q$ Stresses for CY-MPC Support Disk for a 1-Foot End Drop, $T_{max} = 550^\circ\text{F}$ and $T_{min} = 325^\circ\text{F}$	2.6.16.5-2
Figure 2.6.16.7-1	Locations of CY-MPC Support Disk Maximum P_m Stresses, 1-Foot Side Drop, 38° Orientation.....	2.6.16.7-2
Figure 2.6.16.7-2	Locations of CY-MPC Support Disk Maximum $P_m + P_b$ Stresses, 1-Foot Side Drop, 38° Orientation.....	2.6.16.7-3
Figure 2.6.16.8-1	Locations of CY-MPC Support Disk Maximum $P + Q$ Stresses, 1-Foot Side Drop, 38° Orientation.....	2.6.16.8-2
Figure 2.6.16.11-1	Finite Element Model of the CY-MPC Top Weldment Plate.....	2.6.16.11-2
Figure 2.6.16.11-2	Finite Element Model of the CY-MPC Bottom Weldment Plate	2.6.16.11-3
Figure 2.6.17-1	CY-MPC Reconfigured Fuel Assembly Tube Support Grid Finite Element Model	2.6.17-13
Figure 2.6.19-1	Yankee-MPC GTCC Basket Assembly	2.6.19-14
Figure 2.6.19-2	CY-MPC GTCC Basket Tube Array Weldment Finite Element Model	2.6.19-15
Figure 2.6.19-3	CY-MPC GTCC Tube Array Weldment Boundary Conditions (45° Impact Orientation)	2.6.19-16
Figure 2.6.19-4	CY-MPC GTCC Tube Array – Section Locations of Top Five $P_m + P_b$ Stresses for the 75° Basket of the 1-Foot Side Drop Orientation	2.6.19-17
Figure 2.6.19-5	CY-MPC GTCC Basket Shield Shell Assembly Finite Element Model	2.6.19-18
Figure 2.6.19-6	CY-MPC GTCC Basket Shield Shell Assembly Loading and Boundary Conditions (75° Impact Orientation Shown) – Side Drop	2.6.19-19
Figure 2.6.19-7	CY-MPC GTCC Shield Shell – Section Locations of Top Four $P_m + P_b$ Stresses	2.6.19-20

List of Figures (Continued)

Figure 2.7.1.1-1	Location of Sections for CY-MPC Configuration Stress Evaluation	2.7.1.1-10
Figure 2.7.1.2-1	Location of Sections for NAC-STC Cask Body Stress Evaluation for CY-MPC	2.7.1.2-12
Figure 2.7.1.6-1	Finite Element Model - Lid Assembly (Loading Condition 1 - 56.1g Top Impact)	2.7.1.6-9
Figure 2.7.1.6-2	Finite Element Model - Lid Assembly (Loading Condition 2 - Pin Puncture)	2.7.1.6-10
Figure 2.7.1.6-3	Finite Element Model - Lid Assembly (Loading Condition 3 - 56.1-g Top Impact of Cavity Contents Plus Internal Pressure)	2.7.1.6-11
Figure 2.7.2.1-1	NAC-STC Midpoint Section	2.7.2.1-5
Figure 2.7.2.2-1	Finite Element Model - Lid Assembly – Yankee-MPC Pin Puncture	2.7.2.2-5
Figure 2.7.2.2-2	Lid Assembly Finite Element Model – CY-MPC Pin Puncture	2.7.2.2-9
Figure 2.7.2.3-1	NAC-STC Bottom Design Configuration.....	2.7.2.3-6
Figure 2.7.2.4-1	Port Cover Geometry	2.7.2.4-6
Figure 2.7.2.4-2	Puncture of Cask at Port Cover Location (Free Body Diagram)	2.7.2.4-7
Figure 2.7.3.4-1	Bolt Stress - Thermal (Fire) Accident.....	2.7.3.4-2
Figure 2.7.8-1	NAC-STC Directly Loaded 26 PWR Fuel Assembly Basket.....	2.7.8-3
Figure 2.7.8-2	Support Disk Cross-Sectional Configuration for Directly Loaded Fuel Configuration	2.7.8-4
Figure 2.7.8.1-1	Support Disk Drop Orientations	2.7.8.1-11
Figure 2.7.8.1-2	Locations of 20 Maximum Nodal SI Stresses - 55-g Side Drop Impact (0° Drop Orientation)	2.7.8.1-12
Figure 2.7.8.1-3	Locations of 20 Maximum Nodal SI Stresses - 55-g Side Drop Impact (15° Drop Orientation)	2.7.8.1-13
Figure 2.7.8.1-4	Locations of 20 Maximum Nodal SI Stresses - 55-g Side Drop Impact (30° Drop Orientation)	2.7.8.1-14
Figure 2.7.8.1-5	Locations of 20 Maximum Nodal SI Stresses - 55-g Side Drop Impact (37° Drop Orientation)	2.7.8.1-15
Figure 2.7.8.1-6	Locations of 20 Maximum Nodal SI Stresses - 55-g Side Drop Impact (45° Drop Orientation)	2.7.8.1-16

List of Figures (Continued)

Figure 2.7.8.1-7	Locations of 20 Maximum Nodal SI Stresses - 55-g Side Drop Impact (60° Drop Orientation)	2.7.8.1-17
Figure 2.7.8.1-8	Locations of 20 Maximum Nodal SI Stresses - 55-g Side Drop Impact (64° Drop Orientation)	2.7.8.1-18
Figure 2.7.8.1-9	Locations of 20 Maximum Nodal SI Stresses - 55-g Side Drop Impact (75° Drop Orientation)	2.7.8.1-19
Figure 2.7.8.1-10	Locations of 20 Maximum Nodal SI Stresses - 55-g Side Drop Impact (90° Drop Orientation)	2.7.8.1-20
Figure 2.7.8.1-11	Finite Element Model for the Basket Support Disk End Drop.....	2.7.8.1-21
Figure 2.7.8.1-12	Locations of the 20 Maximum Nodal SI Stresses - 56.1-g End Drop.....	2.7.8.1-22
Figure 2.7.8.1-13	Node Point Locations for Basket Web Stress Summaries	2.7.8.1-23
Figure 2.7.8.3-1	Finite Element Model of a Support Disk	2.7.8.3-13
Figure 2.7.8.4-1	Fuel Tube Configuration	2.7.8.4-6
Figure 2.7.8.4-2	Fuel Tube Finite Element Model Grid Loading	2.7.8.4-7
Figure 2.7.8.4-3	Fuel Tube Finite Model Distributed Pressure Loading	2.7.8.4-8
Figure 2.7.8.4-4	Elastic-Plastic Stress Distribution	2.7.8.4-9
Figure 2.7.9-1	Yankee-MPC Fuel Basket Assembly.....	2.7.9-4
Figure 2.7.9.1-1	Cask Orientation	2.7.9-7
Figure 2.7.9.4-1	Yankee-MPC Fuel Tube Configuration.....	2.7.9-33
Figure 2.7.9.5-1	Yankee-MPC Top Weldment Finite Element Model with Structural Boundary Conditions	2.7.9-36
Figure 2.7.9.5-2	Yankee-MPC Top Weldment Finite Element Model with Structural Applied Loads	2.7.9-36
Figure 2.7.9.5-3	Yankee-MPC Bottom Weldment Finite Element Model with Structural Boundary Conditions	2.7.9-37
Figure 2.7.9.5-4	Yankee-MPC Bottom Weldment Finite Element Model with Structural Applied Loads	2.7.9-37
Figure 2.7.11-1	Identification of the Sections for Evaluating the Linearized Stresses in the Canister	2.7.11-4
Figure 2.7.11.5-1	Two-Dimensional Axisymmetric Model of the Upper Section of the Yankee-MPC Canister	2.7.11-14
Figure 2.7.11.5-2	Axial Acceleration (g) Time History for a Top End Impact, Yankee-MPC Canister	2.7.11-15

List of Figures (Continued)

Figure 2.7.11.5-3	Time History for the Ratio of the Dynamic Stress to the Static Stress (SDLF) for the Yankee-MPC Canister Structural Lid Weld (Nominal Gap Stiffness Value)	2.7.11-16
Figure 2.7.12-1	Identification of the Sections for Evaluating the Linearized Stresses in the CY-MPC Canister	2.7.12-6
Figure 2.7.13-1	CY-MPC Canistered Fuel Basket	2.7.13-3
Figure 2.7.13-2	CY-MPC Support Disk Configuration	2.7.13-4
Figure 2.7.13.1-1	Basket Drop Orientations.....	2.7.13.1-2
Figure 2.7.13.1-2	Cask Orientation	2.7.13.1-3
Figure 2.7.13.4-1	CY-MPC Fuel Tube Finite Element Model.....	2.7.13.4-6
Figure 2.7.13.4-2	CY-MPC Fuel Tube Analysis Results – Total Equivalent Strain (Uniform Loading)	2.7.13.4-7
Figure 2.7.13.4-3	CY-MPC Fuel Tube Analysis Results – Total Equivalent Strain (Grid Loading).....	2.7.13.4-8
Figure 2.7.13.5-1	Finite Element Model of CY-MPC the Top Weldment.....	2.7.13.5-2
Figure 2.7.13.5-2	Finite Element Model of the CY-MPC Bottom Weldment	2.7.13.5-2
Figure 2.7.14-1	CY-MPC Reconfigured Fuel Assembly Tube Support Grid Finite Element Model	2.7.14-13
Figure 2.9.1-1	Two-Dimensional Beam Finite Element Model of the PWR 17 by 17 Fuel Rod.....	2.9-5
Figure 2.9.1-2	Mode Shape and First Buckling Shape for the PWR 17 by 17 Fuel Rod.....	2.9-6
Figure 2.9.2-1	First Buckling Mode for the Yankee Class Canistered Fuel	2.9-9
Figure 2.10.2-1	ANSYS Two-Dimensional Finite Element Model - NAC-STC....	2.10.2-35
Figure 2.10.2-2	Cask Bottom (Region A) - NAC-STC ANSYS Two-Dimensional Model.....	2.10.2-36
Figure 2.10.2-3	Cask Lower Transition (Region B) - NAC-STC ANSYS Two-Dimensional Model.....	2.10.2-37
Figure 2.10.2-4	Cask Shells (Region C) - NAC-STC ANSYS Two-Dimensional Model.....	2.10.2-38
Figure 2.10.2-5	Cask Upper Transition (Region D) - NAC-STC ANSYS Two-Dimensional Model.....	2.10.2-39
Figure 2.10.2-6	Cask Top Forging (Region E) - NAC-STC ANSYS Two-Dimensional Model.....	2.10.2-40

List of Figures (Continued)

Figure 2.10.2-7	Cask Lids (Region F) - NAC-STC ANSYS Two-Dimensional Model.....	2.10.2-41	
Figure 2.10.2-8	Circumferential Mesh Spacing (End View) - ANSYS Three-Dimensional Top and Bottom Fine Mesh Models	2.10.2-42	
Figure 2.10.2-9	ANSYS Three-Dimensional Bottom Fine Mesh Finite Element Model - NAC-STC	2.10.2-43	
Figure 2.10.2-10	Details - NAC-STC ANSYS Three-Dimensional Bottom Fine Mesh Model	2.10.2-44	
Figure 2.10.2-11	Cask Bottom (Region A) - NAC-STC ANSYS Bottom Fine Mesh Three-Dimensional Model	2.10.2-45	
Figure 2.10.2-12	Cask Bottom (Region B) - NAC-STC ANSYS Bottom Fine Mesh Three-Dimensional Model	2.10.2-46	
Figure 2.10.2-13	Cask Bottom (Region C) - NAC-STC ANSYS Bottom Fine Mesh Three-Dimensional Model	2.10.2-47	
Figure 2.10.2-14	Cask Lower Transition (Region D) - NAC-STC ANSYS Bottom Fine Mesh Three-Dimensional Model	2.10.2-48	
Figure 2.10.2-15	Cask Lower Transition (Region E) - NAC-STC ANSYS Bottom Fine Mesh Three-Dimensional Model	2.10.2-49	
Figure 2.10.2-16	Cask Lower Shell (Region F) - NAC-STC ANSYS Bottom Fine Mesh Three-Dimensional Model	2.10.2-50	
Figure 2.10.2-17	Cask Lower Shell (Region G) - NAC-STC ANSYS Bottom Fine Mesh Three-Dimensional Model	2.10.2-51	
Figure 2.10.2-18	Cask Upper Shell (Region H) - NAC-STC ANSYS Bottom Fine Mesh Three-Dimensional Model	2.10.2-52	
Figure 2.10.2-19	Cask Lids (Region I) - NAC-STC ANSYS Bottom Fine Mesh Three-Dimensional Model	2.10.2-53	
Figure 2.10.2-20	ANSYS Three-Dimensional Top Fine Mesh Finite Element Model - NAC-STC	2.10.2-54	
Figure 2.10.2-21	Upper Half of NAC-STC ANSYS Three-Dimensional Top Fine Mesh Finite Element Model	2.10.2-55	
Figure 2.10.2-22	Details - NAC-STC ANSYS Three-Dimensional Top Fine Mesh Model	2.10.2-56	
Figure 2.10.2-23	Cask Bottom (Region A) - NAC-STC ANSYS Top Fine Mesh Three-Dimensional Model	2.10.2-57	

List of Figures (Continued)

Figure 2.10.2-24	Cask Lower Transition (Region B) - NAC-STC ANSYS Top Fine Mesh Three-Dimensional Model	2.10.2-58
Figure 2.10.2-25	Cask Lower Shell (Region C) - NAC-STC ANSYS Top Fine Mesh Three-Dimensional Model.....	2.10.2-59
Figure 2.10.2-26	Cask Middle Shell (Region D) - NAC-STC ANSYS Top Fine Mesh Three-Dimensional Model.....	2.10.2-60
Figure 2.10.2-27	Cask Upper Shell (Region E) - NAC-STC ANSYS Top Fine Mesh Three-Dimensional Model.....	2.10.2-61
Figure 2.10.2-28	Cask Upper Transition (Region F) - NAC-STC ANSYS Top Fine Mesh Three-Dimensional Model	2.10.2-62
Figure 2.10.2-29	Cask Upper Transition (Region G) - NAC-STC ANSYS Top Fine Mesh Three-Dimensional Model	2.10.2-63
Figure 2.10.2-30	Cask Top Forging (Region H) - NAC-STC ANSYS Top Fine Mesh Three-Dimensional Model.....	2.10.2-64
Figure 2.10.2-31	Cask Lids (Region I) - NAC-STC ANSYS Top Fine Mesh Three-Dimensional Model.....	2.10.2-65
Figure 2.10.2-32	Load Distribution for Cask Side Drop Impact.....	2.10.2-66
Figure 2.10.2-33	ANSYS Finite Element Model - Structural Component Identification	2.10.2-67
Figure 2.10.2-34	ANSYS Finite Element Model - Representative Section Locations.....	2.10.2-68
Figure 2.10.2-35	Circular Nodal Locations - NAC-STC ANSYS Three- Dimensional Model.....	2.10.2-69
Figure 2.10.2-36	Nodal Identification - NAC-STC ANSYS Three- Dimensional Model.....	2.10.2-70
Figure 2.10.3.2-1	LS-DYNA Model used to Verify the Material Model.....	2.10.3-3
Figure 2.10.3.2-2	Stress-Strain Curve used for the Balsa Material.....	2.10.3-4
Figure 2.10.3.2-3	Finite Element Model for Strain-Rate Dependent Crushable Foam/Wood Block Impact.....	2.10.3-5
Figure 2.10.3.2-4	Stress Time History at 20 ϵ /sec.....	2.10.3-6
Figure 2.10.3.2-5	Stress Time History at 40 ϵ /sec.....	2.10.3-7
Figure 2.10.6-1	Quarter-Scale Model Package Assembly - Ready for Cavity Pressure Test	2.10.6-37
Figure 2.10.6-2	Assembly of Cask - Inner Lid Fitted	2.10.6-38
Figure 2.10.6-3	Assembly of Cask - Fuel Pin Assemblies Located in Basket	2.10.6-39

List of Figures (Continued)

Figure 2.10.6-4	Top End Drop - Cask Penetration into Impact Limiter	2.10.6-40
Figure 2.10.6-5	Side Drop - Detail of Shield Block Impact Near Bottom End.....	2.10.6-41
Figure 2.10.6-6	Repairs to Cask - 50 Metric Ton Hydraulic Press	2.10.6-42
Figure 2.10.6-7	Repairs to Cask - Local Over Pressing	2.10.6-43
Figure 2.10.6-8	Detail of Distortion to Basket Disk No. 6 - Side Drop	2.10.6-44
Figure 2.10.6-9	Deformation of Upper Impact Limiter - Top Corner Drop.....	2.10.6-45
Figure 2.10.6-10	Cask Midpoint Pin Puncture - Outer Shell Deformation.....	2.10.6-46
Figure 2.10.6-11	Center of Outer Lid Pin Puncture - Distortion of Punch	2.10.6-47
Figure 2.10.6-12	Quasi-Static Force-Deflection Curve, Eighth-Scale Model Impact Limiter - End (0-Degree) Impact	2.10.6-48
Figure 2.10.6-13	Quasi-Static Force-Deflection Curve, Eighth-Scale Model Impact Limiter - Corner (24-Degree) Impact.....	2.10.6-49
Figure 2.10.6-14	Force-Deformation Curve, Eighth-Scale Model Impact Limiter - Side (90-Degree) Impact	2.10.6-50
Figure 2.10.6-15	Location of Cask Body Metrology Measurements - Quarter-Scale Model.....	2.10.6-51
Figure 2.10.6-16	Location of Basket Support Disk Metrology Measurements - Quarter Scale Model	2.10.6-52
Figure 2.10.6-17	Strain Gauge Locations - Quarter-Scale Model.....	2.10.6-53
Figure 2.10.6-18	Accelerometer Locations - Quarter-Scale Model	2.10.6-54
Figure 2.10.6-19	Top End Drop (Test No. 1 of Phase 1) - Upper Impact Limiter Deformation (Using Impact Limiters With Aluminum Shells)	2.10.6-55
Figure 2.10.6-20	Top End Drop (Test No. 1 of Phase 1) Strain Data - Gauge S9.1 (Axial) (Using Impact Limiters With Aluminum Shells)	2.10.6-56
Figure 2.10.6-21	Top End Drop (Test No. 1 of Phase 1) Strain Data - Gauge S9.2 (Hoop) (Using Impact Limiters With Aluminum Shells)	2.10.6-57
Figure 2.10.6-22	Top End Drop (Test No. 1 of Phase 1) Accelerometer Data - A2 (1 kHz Filter) (Using Impact Limiters With Aluminum Shells)	2.10.6-58
Figure 2.10.6-23	Side Drop Test (Test No. 3 of Phase 1) Accelerometer Data - A2 (Using Impact Limiters With Aluminum Shells).....	2.10.6-59

List of Figures (Continued)

Figure 2.10.6-24	Side Drop Test (Test No. 3 of Phase 1) - Deformation of Support Disk No. 6 (Using Impact Limiters With Aluminum Shells)	2.10.6-60
Figure 2.10.6-25	Top Corner Drop Test (Test No. 3 of Phase 3) - Impact Limiter Deformations	2.10.6-61
Figure 2.10.6-26	Top Corner Drop Test (Test No. 3 of Phase 3) Accelerometer Data - A1	2.10.6-62
Figure 2.10.6-27	Bottom Oblique Drop Test (Test No. 1 of Phase 4) - Distorted Area of Upper Impact Limiter	2.10.6-63
Figure 2.10.6-28	Bottom Oblique Drop Test (Test No. 1 of Phase 4) - Impact Limiter Deformations	2.10.6-64
Figure 2.10.6-29	Bottom Oblique Drop Test (Test No. 1 of Phase 4) - Impact Limiter Attachment Rods Post-Test Condition	2.10.6-65
Figure 2.10.6-30	Bottom Oblique Drop Test (Test No. 1 of Phase 4) Strain Data - Gauge S9.1 (Axial).....	2.10.6-66
Figure 2.10.6-31	Bottom Oblique Drop Test (Test No. 1 of Phase 4) Strain Data - Gauge S9.2 (Hoop).....	2.10.6-67
Figure 2.10.6-32	Bottom Oblique Drop Test (Test No. 1 of Phase 4) Accelerometer Data - A1 (750 Hz Filter)	2.10.6-68
Figure 2.10.6-33	Bottom Oblique Drop Test (Test No. 1 of Phase 4) Accelerometer Data - A2 (750 Hz Filter)	2.10.6-69
Figure 2.10.6-34	Side Drop Test (Test No. 2 of Phase 4) - Package Immediately After the Drop Test.....	2.10.6-70
Figure 2.10.6-35	Side Drop Test (Test No. 2 of Phase 4) - Deformed Base Impact Limiter After Removal.....	2.10.6-71
Figure 2.10.6-36	Side Drop Test (Test No. 2 of Phase 4) - Impact Limiter Deformations	2.10.6-72
Figure 2.10.6-37	Side Drop Test (Test No. 2 of Phase 4) Strain Data - Gauge S9.1 (Axial).....	2.10.6-73
Figure 2.10.6-38	Side Drop Test (Test No. 2 of Phase 4) Strain Data - Gauge S9.2 (Hoop)	2.10.6-74
Figure 2.10.6-39	Side Drop Test (Test No. 2 of Phase 4) Accelerometer Data -A1 (1 kHz Filter).....	2.10.6-75
Figure 2.10.6-40	Side Drop Test (Test No. 2 of Phase 4) Accelerometer Data -A2 (750 Hz Filter).....	2.10.6-76

List of Figures (Continued)

Figure 2.10.7-1	Side Drop	2.10.7-14
Figure 2.10.7-2	End Drop	2.10.7-15
Figure 2.10.7-3	Oblique Drop	2.10.7-16
Figure 2.10.7-4	Cask Slapdown Geometry	2.10.7-17
Figure 2.10.7-5	Force-Deformation Curve - Lower Redwood Impact Limiter (Bottom End Impact, 0 Degrees)	2.10.7-18
Figure 2.10.7-6	Force-Deformation Curve - Lower Redwood Impact Limiter (Bottom Corner Impact, 24 Degrees)	2.10.7-19
Figure 2.10.7-7	Force-Deformation Curve - Lower Redwood Impact Limiter (Bottom Oblique Impact, 75 Degrees)	2.10.7-20
Figure 2.10.7-8	Force-Deformation Curve - Upper Redwood Impact Limiter (Top End Impact, 0 Degrees)	2.10.7-21
Figure 2.10.7-9	Force-Deformation Curve - Upper Redwood Impact Limiter (Top Corner Impact, 24 Degrees)	2.10.7-22
Figure 2.10.7-10	Force-Deformation Curve - Upper Redwood Impact Limiter (Top Oblique Impact, 75 Degrees)	2.10.7-23
Figure 2.10.7-11	Redwood Impact Limiter Force-Deformation Curve - Side Impact (90 Degrees)	2.10.7-24
Figure 2.10.9-1	Lead Slump - Cask 2D Model Element Plot	2.10.9-5
Figure 2.10.9-2	Lead Slump - Gap Element Plot	2.10.9-6
Figure 2.10.9-3	Lead Slump Displacement	2.10.9-7
Figure 2.10.9-4	Location of Node Points Used in Stress Summary	2.10.9-8
Figure 2.10.10-1	Identification Applicable to Temperature Summary	2.10.10-8
Figure 2.10.10-2	Component Wall Gradient Locations	2.10.10-9
Figure 2.10.11-1	Yankee-MPC Fuel Basket Drop Orientation	2.10.11-5
Figure 2.10.11-2	ANSYS Model for the Yankee-MPC Fuel Basket Support Disk ..	2.10.11-6
Figure 2.10.11-3	ANSYS Model for the Yankee-MPC Support Disk (Detail)	2.10.11-7
Figure 2.10.11-4	ANSYS Models for Yankee-MPC Support Disk Ligament Mesh	2.10.11-8
Figure 2.10.12-1	Typical Filtered Acceleration Time History for the Quarter- Scale Model Side Drop, Overlayed with the Unfiltered Data for the Top End of the Model	2.10.12-17
Figure 2.10.12-2	The FFT for the Unfiltered Accelerometer Time History in Figure 2.10.12-1	2.10.12-18

List of Figures (Continued)

Figure 2.10.12-3	Typical Filtered Acceleration Time History for the Quarter-Scale Model Side Drop, Overlaid with the LS-DYNA Filtered Time History for the Top End of the Model 2.10.12-19
Figure 2.10.12-4	Typical Filtered Acceleration Time History for the Quarter-Scale Model Side Drop, Overlaid with the LS-DYNA Filtered Time History for the Bottom End of the Model 2.10.12-20
Figure 2.10.12-5	Force Deflection Curve for the 30-Foot Side Drop Test 2.10.12-21
Figure 2.10.12-6	Typical Unfiltered Acceleration (Top Accelerometer) Time History for the Quarter-Scale Model Top Corner Drop 2.10.12-22
Figure 2.10.12-7	Typical Filtered Acceleration (Top Accelerometer) Time History for the Quarter-Scale Model Top Corner Side Drop 2.10.12-23
Figure 2.10.12-8	Comparison of Quarter-Scale Top Corner Drop (LS-DYNA and Drop Test) Results (Upper Accelerometer) 2.10.12-24
Figure 2.10.12-9	Force Deflection Curve for the Top Corner Drop 2.10.12-25
Figure 2.10.12-10	Typical Unfiltered Acceleration (Top Accelerometer) Time History for the Quarter-Scale Model Top End Drop 2.10.12-26
Figure 2.10.12-11	The FFT for the Unfiltered Accelerometer Time History in Figure 2.10.12-10 2.10.12-27
Figure 2.10.12-12	Typical Filtered Acceleration (Top Accelerometer) Time History for the Quarter-Scale Model Top End Drop 2.10.12-28
Figure 2.10.12-13	Comparison of Quarter-Scale Top End Drop (LS-DYNA and Drop Test) Results (Upper Accelerometer) 2.10.12-29
Figure 2.10.12-14	Force Deflection Curve for the Top End Drop 2.10.12-30
Figure 2.10.12-15	LS-DYNA Quarter-Scale Model 2.10.12-31

List of Tables

Table 2.1.2-1	Allowable Stress Limits for Containment Structures	2.1.2-4
Table 2.1.2-2	Allowable Stress Limits for Noncontainment Structures	2.1.2-5
Table 2.2-1	NAC-STC Calculated Weights and Centers of Gravity for Directly Loaded Fuel	2.2-3
Table 2.2-2	NAC-STC Calculated Weights and Centers of Gravity for Yankee-MPC Canistered Fuel	2.2-4
Table 2.2-3	NAC-STC Calculated Weights and Centers of Gravity for Canistered Yankee-MPC GTCC Waste.....	2.2-5
Table 2.2-4	NAC-STC Calculated Weights and Centers of Gravity for CY-MPC Canistered Fuel	2.2-6
Table 2.2-5	NAC-STC Calculated Weights and Centers of Gravity for Canistered CY-MPC GTCC Waste	2.2-7
Table 2.3.2-1	Mechanical Properties of SA 240, Type 304 Stainless Steel.....	2.3.2-2
Table 2.3.2-2	Mechanical Properties of SA 336, Type 304 Stainless Steel.....	2.3.2-3
Table 2.3.2-3	Mechanical Properties of Type XM-19 Stainless Steel	2.3.2-4
Table 2.3.2-4	Mechanical Properties of SA-240, Type 304L Stainless Steel.....	2.3.2-5
Table 2.3.3-1	Mechanical Properties of SA-705, SA-693 and SA-564, Type 630, H1150, 17-4 PH Stainless Steel	2.3.3-2
Table 2.3.4-1	Mechanical Properties of SB-637, Grade N07718 Nickel Alloy Steel Bolting Material.....	2.3.4-2
Table 2.3.4-2	Mechanical Properties of SA-193, Grade-B6, High Alloy Steel Bolting Material	2.3.4-3
Table 2.3.5-1	Mechanical Properties of 6061-T651 and 6061-T6 Aluminum Alloy	2.3.5-2
Table 2.3.6-1	Static Mechanical Properties of Chemical Copper Grade Lead	2.3.6-4
Table 2.3.6-2	Mechanical Properties of NS-4-FR.....	2.3.6-5
Table 2.4-1	Summary of NAC-STC Materials Categories and Operating Environments	2.4.4-10
Table 2.5.2-1	Reactions Caused By Tiedown Devices From 10 CFR 71.45(b) Loads.....	2.5.2-28
Table 2.5.2-2	Reactions Caused By Tiedown Devices from AAR Field Manual, Rule 88 Loads.....	2.5.2-29
Table 2.6.7.1-1	Section Locations for Stress Evaluation (Maximums)	2.6.7.1-12
Table 2.6.7.1-2	CY-MPC Critical P _m Stress Summary, 1-ft Top End Drop	2.6.7.1-13

List of Tables (Continued)

Table 2.6.7.1-3	CY-MPC Critical $P_m + P_b$ Stress Summary, 1-ft Top End Drop ..	2.6.7.1-14
Table 2.6.7.1-4	CY-MPC Critical P_m Stress Summary, 1-ft Bottom End Drop	2.6.7.1-15
Table 2.6.7.1-5	CY-MPC Critical $P_m + P_b$ Stress Summary, 1-ft Bottom End Drop	2.6.7.1-16
Table 2.6.7.2-1	Yankee-MPC Critical P_m Stress Summary; 1-ft. Side Drop; Drop Orientation = 90° (ksi)	2.6.7.2-17
Table 2.6.7.2-2	Yankee-MPC Critical $P_m + P_b$ Stress Summary; 1-ft. Side Drop; Drop Orientation = 90° (ksi)	2.6.7.2-17
Table 2.6.7.2-3	CY-MPC Critical P_m Stress Summary, 1-ft Side Drop	2.6.7.2-18
Table 2.6.7.2-4	CY-MPC Critical $P_m + P_b$ Stress Summary, 1-ft Side Drop	2.6.7.2-18
Table 2.6.7.4.1-1	Summary of Results - Impact Limiter Analysis for 1-Foot Free Drop	2.6.7.4-33
Table 2.6.7.4.1-2	Summary of Results - Impact Limiter Analysis for 30-Foot Free Drop	2.6.7.4-35
Table 2.6.7.4.1-3	Summary of Cask Drop Equivalent G-Load Factors	2.6.7.4-37
Table 2.6.7.4.1-4	Summary of 30-Foot Cask Drop Deceleration G-Loads for the Redwood Impact Limiter Obtained from RBCUBED, Tests, and Design	2.6.7.4-38
Table 2.6.7.4.2-1	Redwood Stress-Strain Properties	2.6.7.4-58
Table 2.6.7.4.2-2	Balsa Wood Stress-Strain Properties	2.6.7.4-58
Table 2.6.7.4.2-3	Summary of Results for the Balsa Impact Limiter Normal Conditions of Transport Drop Analysis	2.6.7.4-59
Table 2.6.7.4.2-4	Summary of Results for the Balsa Impact Limiter Hypothetical Accident Conditions Drop Analysis	2.6.7.4-59
Table 2.6.7.5-1	NAC-STC "Hot" Inner Lid Bolt Analysis (Normal Conditions of Transport)	2.6.7.5-11
Table 2.6.7.5-2	NAC-STC "Cold" Inner Lid Bolt Analysis (Normal Conditions of Transport)	2.6.7.5-12
Table 2.6.7.5-3	NAC-STC "Hot and Cold" Outer Lid Bolt Analysis (Normal Conditions of Transport)	2.6.7.5-13
Table 2.6.7.6-1	Neutron Shield Expansion Foam - Manufacturer's Force- Deflection Data	2.6.7.6-13
Table 2.6.7.7-1	Resultant Stress Intensity Values in the Equivalent Ring	2.6.7.7-5

List of Tables (Continued)

Table 2.6.10.2-1	Stress Iteration Table for the Penetration Analysis of the Neutron Shield Shell (13-Pound Cylinder Drop From a 40-Inch Height).....	2.6.10.2-4
Table 2.6.12.3-1	Thermal Stresses (NAC-STC PWR Basket - Directly Loaded Fuel Configuration)	2.6.12.3-7
Table 2.6.12.4-1	Stresses for 1-Foot End Drop Impact with a 19.6-g Deceleration (NAC-STC PWR Basket - Directly Loaded Fuel Configuration).....	2.6.12.4-3
Table 2.6.12.5-1	Combined Stresses for Thermal + 19.6-g End Drop Impact (Directly Loaded Fuel Configuration - Support Disk).....	2.6.12.5-3
Table 2.6.12.7-1	18.1-g Side Impact Stresses for 0-Degree Drop Orientation (NAC-STC PWR Basket - Directly Loaded Fuel Configuration).....	2.6.12.7-13
Table 2.6.12.7-2	18.1-g Side Impact Stresses for 15-Degree Drop Orientation (NAC-STC PWR Basket - Directly Loaded Fuel Configuration).....	2.6.12.7-14
Table 2.6.12.7-3	18.1-g Side Impact Stresses for 30-Degree Drop Orientation (NAC-STC PWR Basket - Directly Loaded Fuel Configuration).....	2.6.12.7-15
Table 2.6.12.7-4	18.1-g Side Impact Stresses for 37-Degree Drop Orientation (NAC-STC PWR Basket - Directly Loaded Fuel Configuration).....	2.6.12.7-16
Table 2.6.12.7-5	18.1-g Side Impact Stresses for 45-Degree Drop Orientation (NAC-STC PWR Basket - Directly Loaded Fuel Configuration).....	2.6.12.7-17
Table 2.6.12.7-6	18.1-g Side Impact Stresses for 60-Degree Drop Orientation (NAC-STC PWR Basket - Directly Loaded Fuel Configuration).....	2.6.12.7-18
Table 2.6.12.7-7	18.1-g Side Impact Stresses for 64-Degree Drop Orientation (NAC-STC PWR Basket - Directly Loaded Fuel Configuration).....	2.6.12.7-19
Table 2.6.12.7-8	18.1-g Side Impact Stresses for 75-Degree Drop Orientation (NAC-STC PWR Basket - Directly Loaded Fuel Configuration).....	2.6.12.7-20

List of Tables (Continued)

Table 2.6.12.7-9	18.1-g Side Impact Stresses for 90-Degree Drop Orientation (NAC-STC PWR Basket - Directly Loaded Fuel Configuration).....	2.6.12.7-21
Table 2.6.12.7-10	18.1-g Side Impact Analysis Results (NAC-STC PWR Basket - Directly Loaded Fuel Configuration)	2.6.12.7-22
Table 2.6.12.9-1	18.1-g Side Impact Web Stresses for 0-Degree Drop Orientation (NAC-STC PWR Basket - Directly Loaded Fuel Configuration).....	2.6.12.9-3
Table 2.6.12.9-2	18.1-g Side Impact Web Stresses for 15-Degree Drop Orientation (NAC-STC PWR Basket - Directly Loaded Fuel Configuration)	2.6.12.9-4
Table 2.6.12.9-3	18.1-g Side Impact Web Stresses for 30-Degree Drop Orientation (NAC-STC PWR Basket - Directly Loaded Fuel Configuration).....	2.6.12.9-5
Table 2.6.12.9-4	18.1-g Side Impact Web Stresses for 37-Degree Drop Orientation (NAC-STC PWR Basket - Directly Loaded Fuel Configuration).....	2.6.12.9-6
Table 2.6.12.9-5	18.1-g Side Impact Web Stresses for 45-Degree Drop Orientation (NAC-STC PWR Basket - Directly Loaded Fuel Configuration).....	2.6.12.9-7
Table 2.6.12.9-6	18.1-g Side Impact Web Stresses for 60-Degree Drop Orientation (NAC-STC PWR Basket - Directly Loaded Fuel Configuration).....	2.6.12.9-8
Table 2.6.12.9-7	18.1-g Side Impact Web Stresses for 64-Degree Drop Orientation (NAC-STC PWR Basket - Directly Loaded Fuel Configuration).....	2.6.12.9-9
Table 2.6.12.9-8	18.1-g Side Impact Web Stresses for 75-Degree Drop Orientation (NAC-STC PWR Basket - Directly Loaded Fuel Configuration).....	2.6.12.9-10
Table 2.6.12.9-9	18.1-g Side Impact Web Stresses for 90-Degree Drop Orientation (NAC-STC PWR Basket - Directly Loaded Fuel Configuration).....	2.6.12.9-11
Table 2.6.13.2-1	Real Constant Sets Defined in Yankee-MPC Canister Model	2.6.13.2-7
Table 2.6.13.2-2	Material Sets Defined in Yankee-MPC Canister Model	2.6.13.2-7

List of Tables (Continued)

Table 2.6.13.3-1	Linearized Stresses in the Yankee-MPC Canister - Thermal Only (Condition 2).....	2.6.13.3-4
Table 2.6.13.4-1	Summary of Critical Sections of the Yankee-MPC Canister for the 1-Foot End Drop Condition.....	2.6.13.4-2
Table 2.6.13.4-2	Internal Pressure Only (20 psi) - Yankee-MPC Canister Primary Membrane Stresses (psi).....	2.6.13.4-3
Table 2.6.13.4-3	Internal Pressure Only (20 psi) - Yankee-MPC Canister Primary Membrane Plus Primary Bending Stresses (psi).....	2.6.13.4-3
Table 2.6.13.4-4	Top End Drop: 1-ft. Drop + Internal Pressure (20 psi) - Yankee-MPC Canister Primary Membrane Stresses (psi).....	2.6.13.4-4
Table 2.6.13.4-5	Top End Drop: 1-ft. Drop + Internal Pressure (20 psi) - Yankee-MPC Canister Primary Membrane Plus Primary Bending Stresses (psi).....	2.6.13.4-4
Table 2.6.13.4-6	Bottom End Drop: 1-ft. Drop + Internal Pressure (0 psi) - Yankee-MPC Canister Primary Membrane Stresses (psi).....	2.6.13.4-5
Table 2.6.13.4-7	Bottom End Drop: 1-ft. Drop + Internal Pressure (0 psi) - Yankee-MPC Canister Primary Membrane Plus Primary Bending Stresses (psi).....	2.6.13.4-5
Table 2.6.13.5-1	Yankee-MPC Canister Bottom End Drop: 1-ft. Drop + Internal Pressure (0 psi) + Thermal (cold) (psi)	2.6.13.5-2
Table 2.6.13.5-2	Yankee-MPC Canister Top End Drop: 1-ft. Drop + Internal Pressure (20 psi) + Thermal (cold) (psi).....	2.6.13.5-2
Table 2.6.13.6-1	Yankee-MPC Canister Side Drop: 1-ft. Drop + Internal Pressure (20 psi) - Primary Membrane Stresses (psi).....	2.6.13.6-2
Table 2.6.13.6-2	Yankee-MPC Canister Side Drop: 1-ft. Drop + Internal Pressure (20 psi) - Primary Membrane Plus Primary Bending Stresses (psi)	2.6.13.6-2
Table 2.6.13.7-1	Yankee-MPC Canister Side Drop: 1-ft. Drop + Internal Pressure (20 psi) + Thermal (cold) (psi).....	2.6.13.7-2
Table 2.6.14.2-1	Listing of Cross Sections for Stress Evaluation of Yankee-MPC Basket Support Disk (0° Basket Drop Orientation)	2.6.14.2-10
Table 2.6.14.2-2	Listing of Cross Sections for Stress Evaluation of Yankee-MPC Support Disk (45° Basket Drop Orientation)	2.6.14.2-14

List of Tables (Continued)

Table 2.6.14.4-1	$P_m + P_b$ Stresses for Yankee-MPC Basket Support Disk— 1-Foot End Drop Thermal Condition 2.....	2.6.14.4-3
Table 2.6.14.4-2	$P_m + P_b$ Stresses for Yankee-MPC Basket Support Disk— 1-Foot End Drop Thermal Condition 3.....	2.6.14.4-4
Table 2.6.14.5-1	$P + Q$ Stresses for Yankee-MPC Basket Support Disk— 1-Foot End Drop Thermal Condition 2.....	2.6.14.5-3
Table 2.6.14.7-1	Summary of Maximum Yankee-MPC Basket Support Disk Stresses for 1-Foot Side Drop	2.6.14.7-6
Table 2.6.14.7-2	P_m Stresses for Yankee-MPC Basket Support Disk—1-Foot Side Drop, 0° Basket Orientation, Thermal Condition 2, Disk Number 1	2.6.14.7-7
Table 2.6.14.7-3	$P_m + P_b$ Stresses for Yankee-MPC Basket Support Disk—1-Foot Side Drop, 0° Basket Orientation, Thermal Condition 2, Disk Number 1	2.6.14.7-8
Table 2.6.14.7-4	P_m Stresses for Yankee-MPC Basket Support Disk—1-Foot Side Drop, 0° Basket Orientation, Thermal Condition 3, Disk Number 1	2.6.14.7-9
Table 2.6.14.7-5	$P_m + P_b$ Stresses for Yankee-MPC Basket Support Disk—1-Foot Side Drop, 0° Basket Orientation, Thermal Condition 3, Disk Number 1	2.6.14.7-10
Table 2.6.14.7-6	P_m Stresses for Yankee-MPC Basket Support Disk—1-Foot Side Drop, 45° Basket Orientation, Thermal Condition 2, Disk Number 5	2.6.14.7-11
Table 2.6.14.7-7	$P_m + P_b$ Stresses for Yankee-MPC Basket Support Disk—1-Foot Side Drop, 45° Basket Orientation, Thermal Condition 2, Disk Number 5	2.6.14.7-12
Table 2.6.14.7-8	P_m Stresses for Yankee-MPC Basket Support Disk—1-Foot Side Drop, 45° Basket Orientation, Thermal Condition 3, Disk Number 5	2.6.14.7-13
Table 2.6.14.7-9	$P_m + P_b$ Stresses for Yankee-MPC Basket Support Disk—1-Foot Side Drop, 45° Basket Orientation, Thermal Condition 3, Disk Number 5	2.6.14.7-14
Table 2.6.14.8-1	Summary of Maximum Yankee-MPC Basket Support Disk Stresses for Thermal Plus 1-Foot Side Drop	2.6.14.8-4

List of Tables (Continued)

Table 2.6.14.8-2	P + Q Stresses for Yankee-MPC Basket Support Disk—1-Foot Side Drop, 0° Basket Orientation, Thermal Condition 2, Disk Number 1	2.6.14.8-5
Table 2.6.14.8-3	P + Q Stresses for Yankee-MPC Basket Support Disk—1 Foot Side Drop, 45° Basket Orientation, Thermal Condition 2, Disk Number 5	2.6.14.8-6
Table 2.6.14.11-1	Minimum Margins of Safety for the Yankee-MPC Fuel Basket Top/Bottom Weldments for a 1-Foot End Drop With and Without Thermal Stresses	2.6.14.11-5
Table 2.6.15.2-1	Real Constant Sets Defined in CY-MPC Canister Model	2.6.15.2-7
Table 2.6.15.2-2	Material Sets Defined in CY-MPC Canister Model	2.6.15.2-7
Table 2.6.15.3-1	CY-MPC Linearized Stresses – Thermal Only (Condition 2)	2.6.15.3-4
Table 2.6.15.4-1	Summary of Critical Sections of the Canister for the 1-Foot End Drop Condition	2.6.15.4-2
Table 2.6.15.4-2	Top End Drop: 1-ft Drop + Internal Pressure (0 psi) – Primary Membrane Stresses (ksi)	2.6.15.4-3
Table 2.6.15.4-3	Top End Drop: 1-ft Drop + Internal Pressure (0 psi) – Primary Membrane Plus Primary Bending Stresses (ksi)	2.6.15.4-3
Table 2.6.15.4-4	Bottom End Drop: 1-ft Drop + Internal Pressure (0 psi) – Primary Membrane Stresses (ksi)	2.6.15.4-4
Table 2.6.15.4-5	Bottom End Drop: 1-ft Drop + Internal Pressure (0 psi) – Primary Membrane Plus Primary Bending Stresses (ksi)	2.6.15.4-4
Table 2.6.15.6-1	Side Drop: 1-ft. Drop + Internal Pressure (20 psi) – Primary Membrane Stresses (ksi)	2.6.15.6-3
Table 2.6.15.6-2	Side Drop: 1-ft. Drop + Internal Pressure (20 psi) – Primary Membrane Plus Primary Bending Stresses (ksi)	2.6.15.6-3
Table 2.6.16.2-1	Cross Sections for Stress Evaluation of CY-MPC Support Disk	2.6.16.2-8
Table 2.6.16.4-1	$P_m + P_b$ Stresses for CY-MPC Support Disk, 1-Foot End Drop ...	2.6.16.4-3
Table 2.6.16.5-1	P + Q Stresses for CY-MPC Support Disk – 1-Foot End Drop $T_{max} = 550^{\circ}\text{F}$ and $T_{min} = 325^{\circ}\text{F}$	2.6.16.5-3
Table 2.6.16.7-1	Summary of Maximum CY-MPC Support Disk Stresses for 1-Foot Side Drop	2.6.16.7-4
Table 2.6.16.7-2	P_m Stresses for CY-MPC Support Disk 1-Foot Side Drop, 0° Basket Orientation	2.6.16.7-5

List of Tables (Continued)

Table 2.6.16.7-3	P_m Stresses for CY-MPC Support Disk 1-Foot Side Drop, 38° Basket Orientation 2.6.16.7-6
Table 2.6.16.7-4	P_m Stresses for CY-MPC Support Disk 1-Foot Side Drop, 63° Basket Orientation 2.6.16.7-7
Table 2.6.16.7-5	P_m Stresses for CY-MPC Support Disk 1-Foot Side Drop, 90° Basket Orientation 2.6.16.7-8
Table 2.6.16.7-6	$P_m + P_b$ Stresses for CY-MPC Support Disk 1-Foot Side Drop, 0° Basket Orientation..... 2.6.16.7-9
Table 2.6.16.7-7	$P_m + P_b$ Stresses for CY-MPC Support Disk 1-Foot Side Drop, 38° Basket Orientation..... 2.6.16.7-10
Table 2.6.16.7-8	$P_m + P_b$ Stresses for CY-MPC Support Disk 1-Foot Side Drop, 63° Basket Orientation..... 2.6.16.7-11
Table 2.6.16.7-9	$P_m + P_b$ Stresses for CY-MPC Support Disk 1-Foot Side Drop, 90° Basket Orientation..... 2.6.16.7-12
Table 2.6.16.8-1	Summary of Maximum CY-MPC Support Disk $P + Q$ Stresses for 1-Foot Side Drop..... 2.6.16.8-3
Table 2.6.16.8-2	$P + Q$ Stresses for CY-MPC Support Disk 1-Foot Side Drop, 0° Basket Orientation..... 2.6.16.8-4
Table 2.6.16.8-3	$P + Q$ Stresses for CY-MPC Support Disk 1-Foot Side Drop, 38° Basket Orientation..... 2.6.16.8-5
Table 2.6.16.8-4	$P + Q$ Stresses for CY-MPC Support Disk 1-Foot Side Drop, 63° Basket Orientation..... 2.6.16.8-6
Table 2.6.16.8-5	$P + Q$ Stresses for CY-MPC Support Disk 1-Foot Side Drop, 90° Basket Orientation..... 2.6.16.8-7
Table 2.6.16.11-1	Minimum Margins of Safety for the CY-MPC Top/Bottom Weldments for a 1-Foot End Drop With and Without Thermal Stresses..... 2.6.16.11-4
Table 2.6.16.12-1	NUREG/CR 6322 Buckling Analysis for the CY-MPC Support Disk 1-Foot Side Drop, 38° Basket Orientation 2.6.16.12-2
Table 2.6.19-1	CY-MPC GTCC Tube Array Weldment P_m Stress Summary – 75° Side Drop, Normal Condition 2.6.19-21
Table 2.6.19-2	CY-MPC GTCC Tube Array Weldment $P_m + P_b$ Stress Summary – 75° Side Drop, Normal Condition 2.6.19-21

List of Tables (Continued)

Table 2.6.19-3	CY-MPC GTCC Tube Array Weld Evaluation - 75° Side Drop, Normal Condition	2.6.19-22
Table 2.6.19-4	CY-MPC GTCC Shield Shell Weldment P_m Stress Summary – 75° Side Drop, Normal Condition	2.6.19-23
Table 2.6.19-5	CY-MPC GTCC Shield Shell Weldment $P_m + P_b$ Stress Summary - 75° Side Drop, Normal Condition.....	2.6.19-23
Table 2.7.1.1-1	NAC-STC Section Locations for CY-MPC Stress Evaluation (Maximums).....	2.7.1.1-11
Table 2.7.1.1-2	NAC-STC Critical P_m Stress Summary for CY-MPC: 30-ft Top End Drop	2.7.1.1-12
Table 2.7.1.1-3	NAC-STC Critical $P_m + P_b$ Stress Summary for CY-MPC: 30-ft Top End Drop.....	2.7.1.1-13
Table 2.7.1.1-4	NAC-STC Critical P_m Stress Summary for CY-MPC: 30-ft Bottom End Drop.....	2.7.1.1-14
Table 2.7.1.1-5	NAC-STC Critical $P_m + P_b$ Stress Summary for CY-MPC: 30-ft Bottom End Drop	2.7.1.1-15
Table 2.7.1.2-1	Yankee-MPC Critical P_m Stress Summary; 30-ft Side Drop; Drop Orientation = 90°	2.7.1.2-13
Table 2.7.1.2-2	Yankee-MPC Critical $P_m + P_b$ Stress Summary; 30-ft Side Drop; Drop Orientation = 90°	2.7.1.2-13
Table 2.7.1.2-3	CY-MPC Configuration Section Locations for Stress Evaluation (Maximums)	2.7.1.2-14
Table 2.7.1.2-4	CY-MPC Configuration Critical P_m Stress Summary: 30-ft Side Drop	2.7.1.2-14
Table 2.7.1.2-5	CY-MPC Configuration Critical $P_m + P_b$ Stress Summary: 30-ft Side Drop	2.7.1.2-15
Table 2.7.1.6-1	Stress Summary - Accident Analyses of the NAC-STC Inner and Outer Lids	2.7.1.6-12
Table 2.7.1.6-2	NAC-STC “Hot” Inner Lid Bolt Analysis (Hypothetical Accident Condition).....	2.7.1.6-14
Table 2.7.1.6-3	NAC-STC “Cold” Inner Lid Bolt Analysis (Hypothetical Accident Condition).....	2.7.1.6-15
Table 2.7.1.6-4	NAC-STC “Hot and Cold” Outer Lid Bolt Analysis (Hypothetical Accident Condition).....	2.7.1.6-16

List of Tables (Continued)

Table 2.7.3.2-1	Cask Internal Pressure Stress Summary - Thermal Accident (125 psig)	2.7.3.2-3
Table 2.7.3.2-2	Canister Pressure Stress Summary - Thermal Accident (50 psig) (Primary Membrane Stress)	2.7.3.2-4
Table 2.7.3.2-3	Canister Pressure Stress Summary - Thermal Accident (50 psig) (Primary Membrane Stress + Bending Stress)	2.7.3.2-5
Table 2.7.7-1	Summary of Maximum Calculated Stresses - 30-Foot Free Drop	2.7.7-2
Table 2.7.7-2	Summary of Maximum Calculated Stresses - Puncture	2.7.7-3
Table 2.7.7-3	Summary of Maximum Calculated Stresses - Thermal (Fire) Accident	2.7.7-4
Table 2.7.8.1-1	Basket 55-g Side Impact Stresses for 0-Degree Drop Orientation	2.7.8.1-24
Table 2.7.8.1-2	Basket 55-g Side Impact Stresses for 15-Degree Drop Orientation	2.7.8.1-25
Table 2.7.8.1-3	Basket 55-g Side Impact Stresses for 30-Degree Drop Orientation	2.7.8.1-26
Table 2.7.8.1-4	Basket 55-g Side Impact Stresses for 37-Degree Drop Orientation	2.7.8.1-27
Table 2.7.8.1-5	Basket 55-g Side Impact Stresses for 45-Degree Drop Orientation	2.7.8.1-28
Table 2.7.8.1-6	Basket 55-g Side Impact Stresses for 60-Degree Drop Orientation	2.7.8.1-29
Table 2.7.8.1-7	Basket 55-g Side Impact Stresses for 64-Degree Drop Orientation	2.7.8.1-30
Table 2.7.8.1-8	Basket 55-g Side Impact Stresses for 75-Degree Drop Orientation	2.7.8.1-31
Table 2.7.8.1-9	Basket 55-g Side Impact Stresses for 90-Degree Drop Orientation	2.7.8.1-32
Table 2.7.8.1-10	Summary of Basket 55-g Side Impact Analysis Results	2.7.8.1-33
Table 2.7.8.1-11	End Drop Impact (56.1 g) Basket Stresses	2.7.8.1-34
Table 2.7.8.1-12	Basket Web Stress 55-g Side Impact for 0-Degree Orientation	2.7.8.1-35

List of Tables (Continued)

Table 2.7.8.1-13	Basket Web Stress 55-g Side Impact for 15-Degree Orientation	2.7.8.1-36
Table 2.7.8.1-14	Basket Web Stress 55-g Side Impact for 30-Degree Orientation	2.7.8.1-37
Table 2.7.8.1-15	Basket Web Stress 55-g Side Impact for 37-Degree Orientation	2.7.8.1-38
Table 2.7.8.1-16	Basket Web Stress 55-g Side Impact for 45-Degree Orientation	2.7.8.1-39
Table 2.7.8.1-17	Basket Web Stress 55-g Side Impact for 60-Degree Orientation	2.7.8.1-40
Table 2.7.8.1-18	Basket Web Stress 55-g Side Impact for 64-Degree Orientation	2.7.8.1-41
Table 2.7.8.1-19	Basket Web Stress 55-g Side Impact for 75-Degree Orientation	2.7.8.1-42
Table 2.7.8.1-20	Basket Web Stress 55-g Side Impact for 90-Degree Orientation	2.7.8.1-43
Table 2.7.8.4-1	Ten Highest Strain Points for Total Energy Analysis.....	2.7.8.4-10
Table 2.7.9.1.2-1	$P_m + P_b$ Stresses for the Yankee-MPC Support Disk - 30-Foot End Drop Thermal Condition 2	2.7.9-10
Table 2.7.9.1.2-2	$P_m + P_b$ Stresses for the Yankee-MPC Support Disk - 30-Foot End Drop Thermal Condition 3	2.7.9-11
Table 2.7.9.1.3-1	Summary of Maximum Yankee-MPC Support Disk Stresses for 30-Foot Side Drop.....	2.7.9-13
Table 2.7.9.1.3-2	P_m Stresses for the Yankee-MPC Support Disk - 30-Foot Side Drop, 0° Basket Orientation, Thermal Condition 2, Disk Number 1	2.7.9-14
Table 2.7.9.1.3-3	$P_m + P_b$ Stresses for the Yankee-MPC Support Disk - 30-Foot Side Drop, 0° Basket Orientation, Thermal Condition 2, Disk Number 5	2.7.9-15
Table 2.7.9.1.3-4	P_m Stresses for the Yankee-MPC Support Disk - 30-Foot Side Drop, 0° Basket Orientation, Thermal Condition 3, Disk Number 1	2.7.9-16

List of Tables (Continued)

Table 2.7.9.1.3-5	$P_m + P_b$ Stresses for the Yankee-MPC Support Disk - 30-Foot Side Drop, 0° Basket Orientation, Thermal Condition 3, Disk Number 5	2.7.9-17
Table 2.7.9.1.3-6	P_m Stresses for the Yankee-MPC Support Disk - 30-Foot Side Drop, 45° Basket Orientation, Thermal Condition 2, Disk Number 3	2.7.9-18
Table 2.7.9.1.3-7	$P_m + P_b$ Stresses for the Yankee-MPC Support Disk - 30-Foot Side Drop, 45° Basket Orientation, Thermal Condition 2, Disk Number 2	2.7.9-19
Table 2.7.9.1.3-8	P_m Stresses for the Yankee-MPC Support Disk - 30-Foot Side Drop, 45° Basket Orientation, Thermal Condition 3, Disk Number 3	2.7.9-20
Table 2.7.9.1.3-9	$P_m + P_b$ Stresses for the Yankee-MPC Support Disk - 30-Foot Side Drop, 45° Basket Orientation, Thermal Condition 3, Disk Number 2	2.7.9-21
Table 2.7.9.1.4-1	Yankee-MPC Support Disk Stress Summary for the 30-Foot Off-Angle Drop.....	2.7.9-23
Table 2.7.10.2-1	CY-MPC GTCC Shield Shell Weldment P_m Stress Summary – 75° Side Drop, Accident Condition	2.7.10-12
Table 2.7.11-1	Canister, 30-Foot Side Drop (Primary Membrane Stress) (psi)	2.7.11-5
Table 2.7.11-2	Canister, 30-Foot Side Drop (Primary Membrane Plus Primary Bending Stress) (psi).....	2.7.11-5
Table 2.7.11-3	Canister, 30-Foot Bottom End Drop (Primary Membrane Stress) (psi).....	2.7.11-6
Table 2.7.11-4	Canister, 30-Foot Bottom End Drop (Primary Membrane Plus Primary Bending Stress) (psi)	2.7.11-6
Table 2.7.11-5	Canister, 30-Foot Top End Drop (Primary Membrane Stress) (psi).....	2.7.11-7
Table 2.7.11-6	Canister, 30-Foot Top End Drop (Primary Membrane Plus Primary Bending Stress) (psi)	2.7.11-7
Table 2.7.11-7	Summary of Minimum Margin of Safety for Canister 30-Foot Drops	2.7.11-8
Table 2.7.12-1	CY-MPC Canister, 30-Foot Side Drop (Primary Membrane Stress) (ksi)	2.7.12-7

List of Tables (Continued)

Table 2.7.12-2	CY-MPC Canister, 30-Foot Side Drop (Primary Membrane Plus Primary Bending Stress) (ksi).....	2.7.12-7
Table 2.7.12-3	CY-MPC Canister, 30-Foot Bottom End Drop Without Internal Pressure (Primary Membrane Stress) (ksi)	2.7.12-8
Table 2.7.12-4	CY-MPC Canister, 30-Foot Bottom End Drop (Primary Membrane Plus Primary Bending Stress) (ksi).....	2.7.12-8
Table 2.7.12-5	CY-MPC Canister, 30-Foot Top End Drop (Primary Membrane Stress) (ksi)	2.7.12-9
Table 2.7.12-6	CY-MPC Canister, 30-Foot Top End Drop (Primary Membrane Plus Primary Bending Stress) (ksi).....	2.7.12-9
Table 2.7.12-7	Summary of Minimum Margin of Safety for CY-MPC Canister 30-Foot Drops	2.7.12-10
Table 2.7.13.1.2-1	$P_m + P_b$ Stresses for CY-MPC Support Disk – 30-Foot End Drop	2.7.13.1-6
Table 2.7.13.1.3-1	Summary of CY-MPC Support Disk Stresses for 30-Foot Side Drop	2.7.13.1-8
Table 2.7.13.1.3-2	P_m Stresses for CY-MPC Support Disk 30-Foot Side Drop, 0° Basket Orientation	2.7.13.1-9
Table 2.7.13.1.3-3	P_m Stresses for CY-MPC Support Disk 30-Foot Side Drop, 38° Basket Orientation.....	2.7.13.1-10
Table 2.7.13.1.3-4	P_m Stresses for CY-MPC Support Disk 30-Foot Side Drop, 63° Basket Orientation.....	2.7.13.1-11
Table 2.7.13.1.3-5	P_m Stresses for CY-MPC Support Disk 30-Foot Side Drop, 90° Basket Orientation.....	2.7.13.1-12
Table 2.7.13.1.3-6	$P_m + P_b$ Stresses for CY-MPC Support Disk 30-Foot Side Drop, 0° Basket Orientation.....	2.7.13.1-13
Table 2.7.13.1.3-7	$P_m + P_b$ Stresses for CY-MPC Support Disk 30-Foot Side Drop, 38° Basket Orientation.....	2.7.13.1-14
Table 2.7.13.1.3-8	$P_m + P_b$ Stresses for CY-MPC Support Disk 30-Foot Side Drop, 63° Basket Orientation.....	2.7.13.1-15
Table 2.7.13.1.3-9	$P_m + P_b$ Stresses for CY-MPC Support Disk 30-Foot Side Drop, 90° Basket Orientation.....	2.7.13.1-16
Table 2.7.13.1.4-1	CY-MPC Support Disk Stress Summary for the 30-Foot Oblique Drop	2.7.13.1-18

List of Tables (Continued)

Table 2.7.13.3-1	NUREG/CR 6322 Buckling Analysis for CY-MPC Support Disk 30-Foot Side Drop, 38° Basket Orientation	2.7.13.3-4
Table 2.10.2-1	Tabulation of Circumferential Mesh Spacing - ANSYS Three-Dimensional Top and Bottom Fine Mesh Models	2.10.2-71
Table 2.10.2-2	Circumferential Plane - Percentage of 180° Arc	2.10.2-72
Table 2.10.2-3	Effective Inner Lid Bolt Properties.....	2.10.2-73
Table 2.10.2-4	Outer Lid Effective Bolt Properties.....	2.10.2-74
Table 2.10.2-5	Identification of ANSYS Model Structural Components, Materials and Allowables; Condition 1	2.10.2-75
Table 2.10.2-6	Deleted	2.10.2-76
Table 2.10.2-7	Deleted	2.10.2-77
Table 2.10.2-8	Section Cut Identification - (2-D Model)	2.10.2-78
Table 2.10.2-9	Section Cut Identification - (3-D Bottom Fine Mesh Model).....	2.10.2-79
Table 2.10.2-10	Section Cut Identification - (3-D Top Fine Mesh Model).....	2.10.2-80
Table 2.10.2-11	Stress Point Locations - 2-D Model.....	2.10.2-81
Table 2.10.2-12	Stress Point Locations - 3-D Bottom Fine Mesh Model.....	2.10.2-86
Table 2.10.2-13	Stress Point Locations - 3-D Top Fine Mesh Model	2.10.2-90
Table 2.10.4-1	Stress Components - 50 psig Internal Pressure + Bolt Preload; 2-D Model; Condition 1	2.10.4-7
Table 2.10.4-2	Stress Components - 12 psig Internal Pressure + Bolt Preload; 2-D Model; Condition 4	2.10.4-11
Table 2.10.4-3	Stress Components - Gravity; 1 g; 3-D Top Model; 0-Degree Circumferential Location; Condition 1	2.10.4-15
Table 2.10.4-4	Stress Components - Gravity; 1 g; 3-D Top Model; 0-Degree Circumferential Location; Condition 4.....	2.10.4-18
Table 2.10.4-5	Stress Components - Thermal Heat, 100°F; 2-D Model; Condition 1	2.10.4-21
Table 2.10.4-6	Stress Components - Thermal Cold, -20°F; 2-D Model; Condition 2	2.10.4-25
Table 2.10.4-7	Stress Components - Thermal Cold, -40°F; 2-D Model; Condition 4	2.10.4-29
Table 2.10.4-8	Stress Components - Impact; 1-Foot Top End Drop; Drop Orientation = 0 Degrees; 2-D Model; Condition 1	2.10.4-33

List of Tables (Continued)

Table 2.10.4-9	Stress Components - Impact; 1-Foot Bottom End Drop; Drop Orientation = 0 Degrees; 2-D Model; Condition 1	2.10.4-37
Table 2.10.4-10	Stress Components - Impact; 1-Foot Side Drop; Drop Orientation = 90 Degrees; 3-D Model; 0-Degree Circumferential Location; Condition 1	2.10.4-41
Table 2.10.4-11	Stress Components - Impact; 1-Foot Top Corner Drop; Drop Orientation = 24 Degrees; 3-D Top Model; 0-Degree Circumferential Location; Condition 1	2.10.4-44
Table 2.10.4-12	Stress Components - Impact; 1-Foot Bottom Corner Drop; Drop Orientation = 24 Degrees; 3-D Bottom Model; 0-Degree Circumferential Location; Condition 1	2.10.4-47
Table 2.10.4-13	Stress Components - Impact; 30-Foot Top End Drop; Drop Orientation = 0 Degrees; 2-D Model; Condition 1	2.10.4-50
Table 2.10.4-14	Stress Components - Impact; 30-Foot Bottom End Drop; Drop Orientation = 0 Degrees; 2-D Model; Condition 1	2.10.4-54
Table 2.10.4-15	Stress Components - Impact; 30-Foot Side Drop; Drop Orientation = 90 Degrees; 3-D Model; 0-Degree Circumferential Location; Condition 1	2.10.4-58
Table 2.10.4-16	Stress Components - Impact; 30-Foot Top Corner Drop; Drop Orientation = 24 Degrees; 3-D Top Model; 0-Degree Circumferential Location; Condition 1	2.10.4-61
Table 2.10.4-17	Stress Components - Impact; 30-Foot Bottom Corner Drop; Drop Orientation = 24 Degrees; 3-D Bottom Model; 0-Degree Circumferential Location; Condition 1	2.10.4-64
Table 2.10.4-18	Stress Components - Impact; 30-Foot Bottom Oblique Drop; Drop Orientation = 15 Degrees; 3-D Bottom Model; 0-Degree Circumferential Location; Condition 1	2.10.4-67
Table 2.10.4-19	Stress Components - Impact; 30-Foot Top Oblique Drop; Drop Orientation = 75 Degrees; 3-D Top Model; 0-Degree Circumferential Location; Condition 1	2.10.4-70

List of Tables (Continued)

Table 2.10.4-20	Stress Components - Impact; 30-Foot Bottom Oblique Drop; Drop Orientation = 75 Degrees; 3-D Bottom Model; 0-Degree Circumferential Location; Condition 1	2.10.4-73
Table 2.10.4-21	Primary Stresses; Heat Condition; 3-D Top Model; 0-Degree Circumferential Location; Condition 1	2.10.4-76
Table 2.10.4-22	Primary + Secondary Stresses; Heat Condition; 3-D Top Model; 0-Degree Circumferential Location; Condition 1	2.10.4-79
Table 2.10.4-23	P_m Stresses; Heat Condition; 3-D Top Model; 0-Degree Circumferential Location; Condition 1	2.10.4-82
Table 2.10.4-24	$P_m + P_b$ Stresses; Heat Condition; 3-D Top Model; 0-Degree Circumferential Location; Condition 1	2.10.4-83
Table 2.10.4-25	S_n Stresses; Heat Condition; 3-D Top Model; 0-Degree Circumferential Location; Condition 1	2.10.4-84
Table 2.10.4-26	Critical P_m Stress Summary; Heat Condition; 3-D Top Model; Condition 1	2.10.4-85
Table 2.10.4-27	Critical $P_m + P_b$ Stress Summary; Heat Condition; 3-D Top Model; Condition 1	2.10.4-86
Table 2.10.4-28	Critical S_n Stress Summary; Heat Condition; 3-D Top Model; Condition 1	2.10.4-87
Table 2.10.4-29	Primary Stresses; Cold Condition; 3-D Top Model; 0-Degree Circumferential Location; Condition 4	2.10.4-88
Table 2.10.4-30	Primary + Secondary Stresses; Cold Condition; 3-D Top Model; 0-Degree Circumferential Location; Condition 4	2.10.4-91
Table 2.10.4-31	P_m Stresses; Cold Condition; 3-D Top Model; 0-Degree Circumferential Location; Condition 4	2.10.4-94
Table 2.10.4-32	$P_m + P_b$ Stresses; Cold Condition; 3-D Top Model; 0-Degree Circumferential Location; Condition 4	2.10.4-95
Table 2.10.4-33	S_n Stresses; Cold Condition; 3-D Top Model; 0-Degree Circumferential Location; Condition 4	2.10.4-96
Table 2.10.4-34	Critical P_m Stress Summary; Cold Condition 3-D; Top Model; Condition 4	2.10.4-97
Table 2.10.4-35	Critical $P_m + P_b$ Stress Summary; Cold Condition; 3-D Top Model; Condition 4	2.10.4-98

List of Tables (Continued)

Table 2.10.4-36	Critical S_n Stress Summary; Cold Condition; 3-D Top Model; Condition 4	2.10.4-99
Table 2.10.4-37	Primary Stresses; 1-Foot Top End Drop; Drop Orientation = 0 Degrees; 2-D Model; Condition 1	2.10.4-100
Table 2.10.4-38	Primary + Secondary Stresses; 1-Foot Top End Drop; Drop Orientation = 0 Degrees; 2-D Model; Condition 1	2.10.4-104
Table 2.10.4-39	P_m Stresses; 1-Foot Top End Drop; Drop Orientation = 0 Degrees; 2-D Model; Condition 1	2.10.4-108
Table 2.10.4-40	$P_m + P_b$ Stresses; 1-Foot Top End Drop; Drop Orientation = 0 Degrees; 2-D Model; Condition 1	2.10.4-109
Table 2.10.4-41	S_n Stresses; 1-Foot Top End Drop; Drop Orientation = 0 Degrees; 2-D Model; Condition 1	2.10.4-110
Table 2.10.4-42	Critical P_m Stress Summary; 1-Foot Top End Drop; Drop Orientation = 0 Degrees; 2-D Model; Condition 1	2.10.4-111
Table 2.10.4-43	Critical $P_m + P_b$ Stress Summary; 1-Foot Top End Drop; Drop Orientation = 0 Degrees; 2-D Model; Condition 1	2.10.4-112
Table 2.10.4-44	Critical S_n Stress Summary; 1-Foot Top End Drop; Drop Orientation = 0 Degrees; 2-D Model; Condition 1	2.10.4-113
Table 2.10.4-45	Critical P_m Stress Summary; 1-Foot Top End Drop; Drop Orientation = 0 Degrees; 2-D Model; Condition 2	2.10.4-114
Table 2.10.4-46	Critical $P_m + P_b$ Stress Summary; 1-Foot Top End Drop; Drop Orientation = 0 Degrees; 2-D Model; Condition 2	2.10.4-115
Table 2.10.4-47	Critical S_n Stress Summary; 1-Foot Top End Drop; Drop Orientation = 0 Degrees; 2-D Model; Condition 2	2.10.4-116
Table 2.10.4-48	Critical P_m Stress Summary; 1-Foot Top End Drop; Drop Orientation = 0 Degrees; 2-D Model; Condition 3	2.10.4-117

List of Tables (Continued)

Table 2.10.4-49	Critical $P_m + P_b$ Stress Summary; 1-Foot Top End Drop; Drop Orientation = 0 Degrees; 2-D Model; Condition 3	2.10.4-118
Table 2.10.4-50	Critical S_n Stress Summary; 1-Foot Top End Drop; Drop Orientation = 0 Degrees; 2-D Model; Condition 3	2.10.4-119
Table 2.10.4-51	Primary Stresses; 1-Foot Bottom End Drop; Drop Orientation = 0 Degrees; 2-D Model; Condition 1	2.10.4-120
Table 2.10.4-52	Primary + Secondary Stresses; 1-Foot Bottom End Drop; Drop Orientation = 0 Degrees; 2-D Model; Condition 1	2.10.4-124
Table 2.10.4-53	P_m Stresses; 1-Foot Bottom End Drop; Drop Orientation = 0 Degrees; 2-D Model; Condition 1	2.10.4-128
Table 2.10.4-54	$P_m + P_b$ Stresses; 1-Foot Bottom End Drop; Drop Orientation = 0 Degrees; 2-D Model; Condition 1	2.10.4-129
Table 2.10.4-55	S_n Stresses; 1-Foot Bottom End Drop; Drop Orientation = 0 Degrees; 2-D Model; Condition 1	2.10.4-130
Table 2.10.4-56	Critical P_m Stress Summary; 1-Foot Bottom End Drop; Drop Orientation = 0 Degrees; 2-D Model; Condition 1	2.10.4-131
Table 2.10.4-57	Critical $P_m + P_b$ Stress Summary; 1-Foot Bottom End Drop; Drop Orientation = 0 Degrees; 2-D Model; Condition 1	2.10.4-132
Table 2.10.4-58	Critical S_n Stress Summary; 1-Foot Bottom End Drop; Drop Orientation = 0 Degrees; 2-D Model; Condition 1	2.10.4-133
Table 2.10.4-59	Critical P_m Stress Summary; 1-Foot Bottom End Drop; Drop Orientation = 0 Degrees; 2-D Model; Condition 2	2.10.4-134
Table 2.10.4-60	Critical $P_m + P_b$ Stress Summary; 1-Foot Bottom End Drop; Drop Orientation = 0 Degrees; 2-D Model; Condition 2	2.10.4-135
Table 2.10.4-61	Critical S_n Stress Summary; 1-Foot Bottom End Drop; Drop Orientation = 0 Degrees; 2-D Model; Condition 2	2.10.4-136

List of Tables (Continued)

Table 2.10.4-62	Critical P_m Stress Summary; 1-Foot Bottom End Drop; Drop Orientation = 0 Degrees; 2-D Model; Condition 3	2.10.4-137
Table 2.10.4-63	Critical $P_m + P_b$ Stress Summary; 1-Foot Bottom End Drop; Drop Orientation = 0 Degrees; 2-D Model; Condition 3	2.10.4-138
Table 2.10.4-64	Critical S_n Stress Summary; 1-Foot Bottom End Drop; Drop Orientation = 0 Degrees; 2-D Model; Condition 3	2.10.4-139
Table 2.10.4-65	Primary Stresses; 1-Foot Side Drop; Drop Orientation = 90 Degrees; 3-D Model; 0-Degree Circumferential Location; Condition 1	2.10.4-140
Table 2.10.4-66	Primary Plus Secondary Stresses; 1-Foot Side Drop; Drop Orientation = 90 Degrees; 3-D Model; 0-Degree Circumferential Location; Condition 1	2.10.4-143
Table 2.10.4-67	P_m Stresses; 1-Foot Side Drop; Drop Orientation = 90 Degrees; 3-D Model; 0-Degree Circumferential Location; Condition 1	2.10.4-146
Table 2.10.4-68	$P_m + P_b$ Stresses; 1-Foot Side Drop; Drop Orientation = 90 Degrees; 3-D Model; 0-Degree Circumferential Location; Condition 1	2.10.4-147
Table 2.10.4-69	S_n Stresses; 1-Foot Side Drop; Drop Orientation = 90 Degrees; 3-D Model; 0-Degree Circumferential Location; Condition 1	2.10.4-148
Table 2.10.4-70	Critical P_m Stress Summary; 1-Foot Side Drop; Drop Orientation = 90 Degrees; 3-D Model; Condition 1	2.10.4-149
Table 2.10.4-71	Critical $P_m + P_b$ Stress Summary; 1-Foot Side Drop; Drop Orientation = 90 Degrees; 3-D Model; Condition 1	2.10.4-150
Table 2.10.4-72	Critical S_n Stress Summary; 1-Foot Side Drop; Drop Orientation = 90 Degrees; 3-D Model; Condition 1	2.10.4-151
Table 2.10.4-73	P_m Stresses; 1-Foot Side Drop; Drop Orientation = 90 Degrees; 3-D Model; 45.9-Degree Circumferential Location; Condition 1	2.10.4-152

List of Tables (Continued)

Table 2.10.4-74	$P_m + P_b$ Stresses; 1-Foot Side Drop; Drop Orientation = 90 Degrees; 3-D Model; 45.9-Degree Circumferential Location; Condition 1	2.10.4-153
Table 2.10.4-75	S_n Stresses; 1-Foot Side Drop; Drop Orientation = 90 Degrees; 3-D Model; 45.9-Degree Circumferential Location; Condition 1	2.10.4-154
Table 2.10.4-76	P_m Stresses; 1-Foot Side Drop; Drop Orientation = 90 Degrees; 3-D Model; 91.7-Degree Circumferential Location; Condition 1	2.10.4-155
Table 2.10.4-77	$P_m + P_b$ Stresses; 1-Foot Side Drop; Drop Orientation = 90 Degrees; 3-D Model; 91.7-Degree Circumferential Location; Condition 1	2.10.4-156
Table 2.10.4-78	S_n Stresses; 1-Foot Side Drop; Drop Orientation = 90 Degrees; 3-D Model; 91.7-Degree Circumferential Location; Condition 1	2.10.4-157
Table 2.10.4-79	P_m Stresses; 1-Foot Side Drop; Drop Orientation = 90 Degrees; 3-D Model; 180-Degree Circumferential Location; Condition 1	2.10.4-158
Table 2.10.4-80	$P_m + P_b$ Stresses; 1-Foot Side Drop; Drop Orientation = 90 Degrees; 3-D Model; 180-Degree Circumferential Location; Condition 1	2.10.4-159
Table 2.10.4-81	S_n Stresses; 1-Foot Side Drop; Drop Orientation = 90 Degrees; 3-D Model; 180-Degree Circumferential Location; Condition 1	2.10.4-160
Table 2.10.4-82	P_m Stresses; 1-Foot Side Drop; Drop Orientation = 90 Degrees; 3-D Model; 67.7-Degree Circumferential Location; Condition 1	2.10.4-161
Table 2.10.4-83	$P_m + P_b$ Stresses; 1-Foot Side Drop; Drop Orientation = 90 Degrees; 3-D Model; 67.7-Degree Circumferential Location; Condition 1	2.10.4-162
Table 2.10.4-84	Primary Stresses; 1-Foot Top Corner Drop; Drop Orientation = 24 Degrees; 3-D Top Model; 0-Degree Circumferential Location; Condition 1	2.10.4-163

List of Tables (Continued)

Table 2.10.4-85	Primary + Secondary Stresses; 1-Foot Top Corner Drop; Drop Orientation = 24 Degrees; 3-D Top Model; 0-Degree Circumferential Location; Condition 1	2.10.4-166
Table 2.10.4-86	P_m Stresses; 1-Foot Top Corner Drop; Drop Orientation = 24 Degrees 3-D Top Model; 0-Degree Circumferential Location; Condition 1	2.10.4-169
Table 2.10.4-87	$P_m + P_b$ Stresses; 1-Foot Top Corner Drop; Drop Orientation = 24 Degrees; 3-D Top Model; 0-Degree Circumferential Location; Condition 1	2.10.4-170
Table 2.10.4-88	S_n Stresses; 1-Foot Top Corner Drop; Drop Orientation = 24 Degrees; 3-D Top Model; 0-Degree Circumferential Location; Condition 1	2.10.4-171
Table 2.10.4-89	Critical P_m Stress Summary; 1-Foot Top Corner Drop; Drop Orientation = 24 Degrees; 3-D Top Model; Condition 1	2.10.4-172
Table 2.10.4-90	Critical $P_m + P_b$ Stress Summary; 1-Foot Top Corner Drop; Drop Orientation = 24 Degrees; 3-D Top Model; Condition 1	2.10.4-173
Table 2.10.4-91	Critical S_n Stress Summary; 1-Foot Top Corner Drop; Drop Orientation = 24 Degrees; 3-D Top Model; Condition 1	2.10.4-174
Table 2.10.4-92	P_m Stresses; 1-Foot Top Corner Drop; Drop Orientation = 24 Degrees; 3-D Top Model; 45.9-Degree Circumferential Location; Condition 1	2.10.4-175
Table 2.10.4-93	$P_m + P_b$ Stresses; 1-Foot Top Corner Drop; Drop Orientation = 24 Degrees; 3-D Top Model; 45.9-Degree Circumferential Location; Condition 1	2.10.4-176
Table 2.10.4-94	P_m Stresses; 1-Foot Top Corner Drop; Drop Orientation = 24 Degrees; 3-D Top Model; 91.7-Degree Circumferential Location; Condition 1	2.10.4-177
Table 2.10.4-95	$P_m + P_b$ Stresses; 1-Foot Top Corner Drop; Drop Orientation = 24 Degrees; 3-D Top Model; 91.7-Degree Circumferential Location; Condition 1	2.10.4-178

List of Tables (Continued)

Table 2.10.4-96	P_m Stresses; 1-Foot Top Corner Drop; Drop Orientation = 24 Degrees; 3-D Top Model; 180-Degree Circumferential Location; Condition 1	2.10.4-179
Table 2.10.4-97	$P_m + P_b$ Stresses; 1-Foot Top Corner Drop; Drop Orientation = 24 Degrees; 3-D Top Model; 180-Degree Circumferential Location; Condition 1	2.10.4-180
Table 2.10.4-98	Primary Stresses; 1-Foot Bottom Corner Drop; Drop Orientation = 24 Degrees; 3-D Bottom Model; 0-Degree Circumferential Location; Condition 1	2.10.4-181
Table 2.10.4-99	Primary + Secondary Stresses; 1-Foot Bottom Corner Drop; Drop Orientation = 24 Degrees; 3-D Bottom Model; 0-Degree Circumferential Location; Condition 1	2.10.4-184
Table 2.10.4-100	P_m Stresses; 1-Foot Bottom Corner Drop; Drop Orientation = 24 Degrees; 3-D Bottom Model; 0-Degree Circumferential Location; Condition 1	2.10.4-187
Table 2.10.4-101	$P_m + P_b$ Stresses; 1-Foot Bottom Corner Drop; Drop Orientation = 24 Degrees; 3-D Bottom Model; 0-Degree Circumferential Location; Condition 1	2.10.4-188
Table 2.10.4-102	S_n Stresses; 1-Foot Bottom Corner Drop; Drop Orientation = 24 Degrees; 3-D Bottom Model; 0-Degree Circumferential Location; Condition 1	2.10.4-189
Table 2.10.4-103	Critical P_m Stress Summary; 1-Foot Bottom Corner Drop; Drop Orientation = 24 Degrees; 3-D Bottom Model; Condition 1	2.10.4-190
Table 2.10.4-104	Critical $P_m + P_b$ Stress Summary; 1-Foot Bottom Corner Drop; Drop Orientation = 24 Degrees; 3-D Bottom Model; Condition 1	2.10.4-191
Table 2.10.4-105	Critical S_n Stress Summary; 1-Foot Bottom Corner Drop; Drop Orientation = 24 Degrees; 3-D Bottom Model; Condition 1	2.10.4-192
Table 2.10.4-106	P_m Stresses; 1-Foot Bottom Corner Drop; Drop Orientation = 24 Degrees; 3-D Bottom Model; 45.9-Degree Circumferential Location; Condition 1	2.10.4-193

List of Tables (Continued)

Table 2.10.4-107	P_m Stresses; 1-Foot Bottom Corner Drop; Drop Orientation = 24 Degrees; 3-D Bottom Model; 45.9-Degree Circumferential Location; Condition 1	2.10.4-194
Table 2.10.4-108	P_m Stresses; 1-Foot Bottom Corner Drop; Drop Orientation = 24 Degrees; 3-D Bottom Model; 91.7-Degree Circumferential Location; Condition 1	2.10.4-195
Table 2.10.4-109	$P_m + P_b$ Stresses; 1-Foot Bottom Corner Drop; Drop Orientation = 24 Degrees; 3-D Bottom Model; 91.7-Degree Circumferential Location; Condition 1	2.10.4-196
Table 2.10.4-110	P_m Stresses; 1-Foot Bottom Corner Drop; Drop Orientation = 24 Degrees; 3-D Bottom Model; 180-Degree Circumferential Location; Condition 1	2.10.4-197
Table 2.10.4-111	$P_m + P_b$ Stresses; 1-Foot Bottom Corner Drop; Drop Orientation = 24 Degrees; 3-D Bottom Model; 180-Degree Circumferential Location; Condition 1	2.10.4-198
Table 2.10.4-112	Primary Stresses; 30-Foot Top End Drop; Drop Orientation = 0 Degrees; 2-D Model; Condition 1	2.10.4-199
Table 2.10.4-113	P_m Stresses; 30-Foot Top End Drop; Drop Orientation = 0 Degrees; 2-D Model; Condition 1	2.10.4-203
Table 2.10.4-114	$P_m + P_b$ Stresses; 30-Foot Top End Drop; Drop Orientation = 0 Degrees; 2-D Model; Condition 1	2.10.4-204
Table 2.10.4-115	Critical P_m Stress Summary; 30-Foot Top End Drop; Drop Orientation = 0 Degrees; 2-D Model; Condition 1	2.10.4-205
Table 2.10.4-116	Critical $P_m + P_b$ Stress Summary; 30-Foot Top End Drop; Drop Orientation = 0 Degrees; 2-D Model; Condition 1	2.10.4-206
Table 2.10.4-117	Critical P_m Stress Summary; 30-Foot Top End Drop; Drop Orientation = 0 Degrees; 2-D Model; Condition 2	2.10.4-207
Table 2.10.4-118	Critical $P_m + P_b$ Stress Summary; 30-Foot Top End Drop; Drop Orientation = 0 Degrees; 2-D Model; Condition 2	2.10.4-208
Table 2.10.4-119	Critical P_m Stress Summary; 30-Foot Top End Drop; Drop Orientation = 0 Degrees; 2-D Model; Condition 3	2.10.4-209

List of Tables (Continued)

Table 2.10.4-120	Critical $P_m + P_b$ Stress Summary; 30-Foot Top End Drop; Drop Orientation = 0 Degrees; 2-D Model; Condition 3	2.10.4-210
Table 2.10.4-121	Primary Stresses; 30-Foot Bottom End Drop; Drop Orientation = 0 Degrees; 2-D Model; Condition 1	2.10.4-211
Table 2.10.4-122	P_m Stresses; 30-Foot Bottom End Drop; Drop Orientation = 0 Degrees; 2-D Model; Condition 1	2.10.4-215
Table 2.10.4-123	$P_m + P_b$ Stresses; 30-Foot Bottom End Drop; Drop Orientation = 0 Degrees; 2-D Model; Condition 1	2.10.4-216
Table 2.10.4-124	Critical P_m Stress Summary; 30-Foot Bottom End Drop; Drop Orientation = 0 Degrees; 2-D Model; Condition 1	2.10.4-217
Table 2.10.4-125	Critical $P_m + P_b$ Stress Summary; 30-Foot Bottom End Drop; Drop Orientation = 0 Degrees; 2-D Model; Condition 1	2.10.4-218
Table 2.10.4-126	Critical P_m Stress Summary; 30-Foot Bottom End Drop; Drop Orientation = 0 Degrees; 2-D Model; Condition 2.....	2.10.4-219
Table 2.10.4-127	Critical $P_m + P_b$ Stress Summary; 30-Foot Bottom End Drop; Drop Orientation = 0 Degrees; 2-D Model; Condition 2	2.10.4-220
Table 2.10.4-128	Critical P_m Stress Summary; 30-Foot Bottom End Drop; Drop Orientation = 0 Degrees; 2-D Model; Condition 3	2.10.4-221
Table 2.10.4-129	Critical $P_m + P_b$ Stress Summary; 30-Foot Bottom End Drop; Drop Orientation = 0 Degrees; 2-D Model; Condition 3	2.10.4-222
Table 2.10.4-130	Primary Stresses; 30-Foot Side Drop; Drop Orientation = 90 Degrees; 3-D Model; 0-Degree Circumferential Location; Condition 1	2.10.4-223
Table 2.10.4-131	P_m Stresses; 30-Foot Side Drop; Drop Orientation = 90 Degrees; 3-D Model; 0-Degree Circumferential Location; Condition 1	2.10.4-226
Table 2.10.4-132	$P_m + P_b$ Stresses; 30-Foot Side Drop; Drop Orientation = 90-Degrees; 3-D Model; 0-Degree Circumferential Location; Condition 1	2.10.4-227

List of Tables (Continued)

Table 2.10.4-133	Critical P_m Stress Summary; 30-Foot Side Drop; Drop Orientation = 90 Degrees; 3-D Model; Condition 1	2.10.4-228
Table 2.10.4-134	Critical $P_m + P_b$ Stress Summary; 30-Foot Side Drop; Drop Orientation = 90 Degrees; 3-D Model; Condition 1	2.10.4-229
Table 2.10.4-135	P_m Stresses; 30-Foot Side Drop; Drop Orientation = 90 Degrees; 3-D Model; 45.9-Degree Circumferential Location; Condition 1	2.10.4-230
Table 2.10.4-136	$P_m + P_b$ Stresses; 30-Foot Side Drop; Drop Orientation = 90 Degrees; 3-D Model; 45.9-Degree Circumferential Location; Condition 1	2.10.4-231
Table 2.10.4-137	P_m Stresses; 30-Foot Side Drop; Drop Orientation = 90 Degrees; 3-D Model; 91.7-Degree Circumferential Location; Condition 1	2.10.4-232
Table 2.10.4-138	$P_m + P_b$ Stresses; 30-Foot Side Drop; Drop Orientation = 90 Degrees; 3-D Model; 91.7-Degree Circumferential Location; Condition 1	2.10.4-233
Table 2.10.4-139	P_m Stresses; 30-Foot Side Drop; Drop Orientation = 90 Degrees; 3-D Model; 180-Degree Circumferential Location; Condition 1	2.10.4-234
Table 2.10.4-140	$P_m + P_b$ Stresses; 30-Foot Side Drop; Drop Orientation = 90 Degrees; 3-D Model; 180-Degree Circumferential Location; Condition 1	2.10.4-235
Table 2.10.4-141	Primary Stresses; 30-Foot Top Corner Drop; Drop Orientation = 24 Degrees; 3-D Top Model; 0-Degree Circumferential Location; Condition 1	2.10.4-236
Table 2.10.4-142	P_m Stresses; 30-Foot Top Corner Drop; Drop Orientation = 24 Degrees; 3-D Top Model; 0-Degree Circumferential Location; Condition 1	2.10.4-239
Table 2.10.4-143	$P_m + P_b$ Stresses; 30-Foot Top Corner Drop; Drop Orientation = 24 Degrees; 3-D Top Model; 0-Degree Circumferential Location; Condition 1	2.10.4-240
Table 2.10.4-144	Critical P_m Stress Summary; 30-Foot Top Corner Drop; Drop Orientation = 24 Degrees; 3-D Top Model; Condition 1	2.10.4-241

List of Tables (Continued)

Table 2.10.4-145	Critical $P_m + P_b$ Stress Summary; 30-Foot Top Corner Drop; Drop Orientation = 24 Degrees; 3-D Top Model; Condition 1	2.10.4-242
Table 2.10.4-146	P_m Stresses; 30-Foot Top Corner Drop; Drop Orientation = 24 Degrees; 3-D Top Model; 45.9-Degree Circumferential Location; Condition 1	2.10.4-243
Table 2.10.4-147	$P_m + P_b$ Stresses; 30-Foot Top Corner Drop; Drop Orientation = 24 Degrees; 3-D Top Model; 45.9-Degree Circumferential Location; Condition 1	2.10.4-244
Table 2.10.4-148	P_m Stresses; 30-Foot Top Corner Drop; Drop Orientation = 24 Degrees; 3-D Top Model; 91.7-Degree Circumferential Location; Condition 1	2.10.4-245
Table 2.10.4-149	$P_m + P_b$ Stresses; 30-Foot Top Corner Drop; Drop Orientation = 24 Degrees; 3-D Top Model; 91.7-Degree Circumferential Location; Condition 1	2.10.4-246
Table 2.10.4-150	P_m Stresses; 30-Foot Top Corner Drop; Drop Orientation = 24 Degrees; 3-D Top Model; 180-Degree Circumferential Location; Condition 1	2.10.4-247
Table 2.10.4-151	$P_m + P_b$ Stresses; 30-Foot Top Corner Drop; Drop Orientation = 24 Degrees; 3-D Top Model; 180-Degree Circumferential Location; Condition 1	2.10.4-248
Table 2.10.4-152	Primary Stresses; 30-Foot Bottom Corner Drop; Drop Orientation = 24 Degrees; 3-D Bottom Model; 0-Degree Circumferential Location; Condition 1	2.10.4-249
Table 2.10.4-153	P_m Stresses; 30-Foot Bottom Corner Drop; Drop Orientation = 24 Degrees; 3-D Bottom Model; 0-Degree Circumferential Location; Condition 1	2.10.4-252
Table 2.10.4-154	$P_m + P_b$ Stresses; 30-Foot Bottom Corner Drop; Drop Orientation = 24 Degrees; 3-D Bottom Model; 0-Degree Circumferential Location; Condition 1	2.10.4-253
Table 2.10.4-155	Critical P_m Stress Summary; 30-Foot Bottom Corner Drop; Drop Orientation = 24 Degrees; 3-D Bottom Model; Condition 1	2.10.4-254

List of Tables (Continued)

Table 2.10.4-156	Critical $P_m + P_b$ Stress Summary; 30-Foot Bottom Corner Drop; Drop Orientation = 24 Degrees; 3-D Bottom Model; Condition 1	2.10.4-255
Table 2.10.4-157	P_m Stresses; 30-Foot Bottom Corner Drop; Drop Orientation = 24 Degrees; 3-D Bottom Model; 45.9-Degree Circumferential Location; Condition 1	2.10.4-256
Table 2.10.4-158	$P_m + P_b$ Stresses; 30-Foot Bottom Corner Drop Orientation = 24 Degrees; 3-D Bottom Model; 45.9-Degree Circumferential Location; Condition 1	2.10.4-257
Table 2.10.4-159	P_m Stresses; 30-Foot Bottom Corner Drop; Drop Orientation = 24 Degrees; 3-D Bottom Model; 91.7-Degree Circumferential Location; Condition	2.10.4-258
Table 2.10.4-160	$P_m + P_b$ Stresses; 30-Foot Bottom Corner Drop; Drop Orientation = 24 Degrees; 3-D Bottom Model; 91.7-Degree Circumferential Location; Condition 1	2.10.4-259
Table 2.10.4-161	P_m Stresses; 30-Foot Bottom Corner Drop; Drop Orientation = 24 Degrees; 3-D Bottom Model; 180-Degree Circumferential Location; Condition 1	2.10.4-260
Table 2.10.4-162	$P_m + P_b$ Stresses; 30-Foot Bottom Corner Drop; Drop Orientation = 24 Degrees; 3-D Bottom Model; 180-Degree Circumferential Location; Condition 1	2.10.4-261
Table 2.10.4-163	Primary Stress; 30-Foot Bottom Oblique Drop; Drop Orientation = 15 Degrees; 3-D Bottom Model; 0-Degree Circumferential Location; Condition 1	2.10.4-262
Table 2.10.4-164	P_m Stresses; 30-Foot Bottom Oblique Drop; Drop Orientation = 15 Degrees; 3-D Bottom Model; 0-Degree Circumferential Location; Condition 1	2.10.4-265
Table 2.10.4-165	$P_m + P_b$ Stresses; 30-Foot Bottom Oblique Drop; Drop Orientation = 15 Degrees; 3-D Bottom Model; 0-Degree Circumferential Location; Condition 1	2.10.4-266
Table 2.10.4-166	Critical P_m Stress Summary; 30-Foot Bottom Oblique Drop; Drop Orientation = 15 Degrees; 3-D Bottom Model; Condition 1	2.10.4-267

List of Tables (Continued)

Table 2.10.4-167	Critical $P_m + P_b$ Stress Summary; 30-Foot Bottom Oblique Drop; Drop Orientation = 15 Degrees; 3-D Bottom Model; Condition 1	2.10.4-268
Table 2.10.4-168	Primary Stresses; 30-Foot Top Oblique Drop; Drop Orientation = 75 Degrees; 3-D Top Model; 0-Degree Circumferential Location; Condition 1	2.10.4-269
Table 2.10.4-169	P_m Stresses; 30-Foot Top Oblique Drop; Drop Orientation = 75 Degrees; 3-D Top Model; 0-Degree Circumferential Location; Condition 1	2.10.4-272
Table 2.10.4-170	$P_m + P_b$ Stresses; 30-Foot Top Oblique Drop; Drop Orientation = 75 Degrees; 3-D Top Model; 0-Degree Circumferential Location; Condition 1	2.10.4-273
Table 2.10.4-171	Critical P_m Stress Summary; 30-Foot Top Oblique Drop; Drop Orientation = 75 Degrees; 3-D Top Model; Condition 1	2.10.4-274
Table 2.10.4-172	Critical $P_m + P_b$ Stress Summary; 30-Foot Top Oblique Drop; Drop Orientation = 75 Degrees; 3-D Top Model; Condition 1	2.10.4-275
Table 2.10.4-173	Primary Stresses; 30-Foot Bottom Oblique Drop; Drop Orientation = 75 Degrees; 3-D Bottom Model; 0-Degree Circumferential Location; Condition 1	2.10.4-276
Table 2.10.4-174	P_m Stresses; 30-Foot Bottom Oblique Drop; Drop Orientation = 75 Degrees; 3-D Bottom Model; 0-Degree Circumferential Location; Condition 1	2.10.4-279
Table 2.10.4-175	$P_m + P_b$ Stresses; 30-Foot Bottom Oblique Drop; Drop Orientation = 75 Degrees; 3-D Bottom Model; 0-Degree Circumferential Location; Condition 1	2.10.4-280
Table 2.10.4-176	Critical P_m Stress Summary; 30-Foot Bottom Oblique Drop; Drop Orientation = 75 Degrees; 3-D Bottom Model; Condition 1	2.10.4-281
Table 2.10.4-177	Critical $P_m + P_b$ Stress Summary; 30-Foot Bottom Oblique Drop; Drop Orientation = 75 Degrees; 3-D Bottom Model; Condition 1	2.10.4-282
Table 2.10.4-178	Primary + Secondary Stresses; Thermal (Fire) Transient; Time = 30 Minutes; With Contents; 2-D Model.....	2.10.4-283

List of Tables (Continued)

Table 2.10.4-179	S _n Stresses; Thermal (Fire) Transient; Time = 30 Minutes; With Contents; 2-D Model	2.10.4-287
Table 2.10.4-180	Critical S _n Stress Summary; Thermal (Fire) Transient; Time = 30 Minutes; With Contents; 2-D Model.....	2.10.4-288
Table 2.10.5-1	Buckling Evaluation Results NAC-STC Inner Shell	2.10.5-15
Table 2.10.5-2	Geometry Parameters for the NAC-STC Inner Shell and Transition Sections	2.10.5-17
Table 2.10.5-3	Capacity Reduction Factors for the NAC-STC Inner Shell And Transition Sections.....	2.10.5-18
Table 2.10.5-4	Fabrication Tolerances for the NAC-STC Inner Shell	2.10.5-19
Table 2.10.5-5	Material Properties for Buckling Analysis Input.....	2.10.5-20
Table 2.10.5-6	Upper Bound Buckling Stresses	2.10.5-21
Table 2.10.5-7	Theoretical Elastic Buckling Stress Values (Temperature Independent Form).....	2.10.5-22
Table 2.10.5-8	Theoretical Elastic Buckling Stresses for Selected Temperatures (SA-240, Type 304 and SA-240, Type XM-19 Stainless Steel).....	2.10.5-22
Table 2.10.6-1	Comparison of Full-Scale Deceleration Values for 30-Foot Drop Impacts	2.10.6-77
Table 2.10.6-2	Top End Drop - Test Data (Test No. 1 of Phase 1)	2.10.6-78
Table 2.10.6-3	Permanent Strains Side Drop Test Using Impact Limiters With Aluminum Shells (Test No. 3 of Phase 1)	2.10.6-79
Table 2.10.6-4	Cask Body and Outer Lid Pretest/Post-Test Metrology Data for Phase 1 Testing	2.10.6-80
Table 2.10.6-5	Fuel Basket Support Disk No. 12 Pretest Metrology Data for Phase 1 Testing	2.10.6-81
Table 2.10.6-6	Fuel Basket Support Disk No. 6 Post-Test Metrology Data for Phase 1 Test 3	2.10.6-82
Table 2.10.6-7	Fuel Basket Support Disk No. 12 Post-Test Metrology Data for Phase 1 Test 3	2.10.6-83
Table 2.10.6-8	Top Corner Drop - Test Data (Test No. 3 of Phase 3).....	2.10.6-84
Table 2.10.6-9	Pin Puncture Drop Tests (Test Nos. 5 and 6 of Phase 3).....	2.10.6-85
Table 2.10.6-10	Bottom Oblique Drop - Test Data (Test No. 1 of Phase 4)	2.10.6-86
Table 2.10.6-11	Cask Body and Outer Lid Pretest/Post-test Metrology Data for Phase 4 Testing	2.10.6-87
Table 2.10.6-12	Side Drop - Test Data (Test No. 2 of Phase 4)	2.10.6-88

List of Tables (Continued)

Table 2.10.7-1	Determination of Maximum Energy Remaining for Secondary Impact – Full-Scale Redwood Impact Limiter.....	2.10.7-25
Table 2.10.7-2	Comparison of Full-Scale Deceleration Values for 30-Foot Drop Impacts	2.10.7-26
Table 2.10.9-1	Summary of 30-Foot End Drop Stress Results on the Outer Shell of the NAC-STC (ANSYS)	2.10.9-9
Table 2.10.9-2	Summary of 30-Foot End Drop Stress Results on the Inner Shell of the NAC-STC (ANSYS).....	2.10.9-10
Table 2.10.9-3	Comparison of Outer Shell Stresses for 30-Foot End Drop	2.10.9-11
Table 2.10.10-1	Comparison of Cask Component Temperatures (Directly Loaded Fuel Configuration)	2.10.10-10
Table 2.10.10-2	Comparison of Cask Component Average Temperature Difference (Directly Loaded Fuel Configuration)	2.10.10-11

2.0 STRUCTURAL EVALUATION

The structural analyses of the NAC-STC spent fuel transportation and storage cask demonstrate that the package satisfies the requirements of Part 71 of Title 10, Chapter 1 of the Code of Federal Regulations—specifically, Subpart E, “Package Approval Standards,” and Subpart F, “Package and Special Form Tests.” It is also designed to satisfy the requirements of IAEA TS-R-1. It is shown that containment is not breached under any of the normal conditions of transport or the hypothetical accident conditions.

The structural analyses presented herein utilize current state-of-the-art methods for calculating stresses in large structures subject to steady state and transient loadings. The evaluation of the structural characteristics of the containment boundary will be based on a conservative interpretation of the requirements of Section III of the “ASME Boiler and Pressure Vessel Code, Nuclear Power Plant Components.” The “ASME Boiler and Pressure Vessel Code” is the recognized standard for pressure vessel analysis, mechanical properties of materials, and allowable stress values.

This section of the Safety Analysis Report demonstrates that the NAC-STC design is capable of meeting the rigors of transport, while carrying spent nuclear fuel in the directly loaded or canistered configurations or Greater Than Class C waste in the canistered configuration. It documents the results of the analyses, which were performed to provide assurance that the NAC-STC design also satisfies the statutory requirements for licensing.

THIS PAGE INTENTIONALLY LEFT BLANK

2.1 Structural Design

2.1.1 Discussion

The NAC-STC is a cylindrical, multiwall cask designed to safely transport directly loaded or canistered spent nuclear fuel or canistered Greater Than Class C (GTCC) waste. The cask accommodates up to 26 directly loaded design basis PWR fuel assemblies. In the canistered fuel or waste configurations, the NAC-STC transports the Multi-Purpose Canister (MPC) of the NAC-MPC system, which is designed for the long-term storage and transport of spent fuel. The NAC-MPC is provided in several configurations to provide efficient storage and transport of spent fuel, damaged fuel and GTCC waste. The NAC-MPC canister system designed for Yankee Class fuel is designated the Yankee-MPC and holds up to 36 Yankee Class fuel assemblies, Reconfigured Fuel Assemblies and Recaged Fuel Assemblies, including up to four fuel assemblies loaded in Damaged Fuel Cans. Using a modified internal basket, the same size canister has 24 loading positions for Yankee GTCC waste. The NAC-MPC canister system designed for Connecticut Yankee is designated the CY-MPC and holds up to 26 Connecticut Yankee fuel assemblies or, using a modified internal basket, up to 24 containers of Connecticut Yankee GTCC waste. The Yankee-MPC and CY-MPC canisters have the same external diameter, but have different overall lengths. The CY-MPC canister system has a higher allowable contents weight than the directly loaded or Yankee-MPC system. To accommodate the higher contents weight, a balsa wood impact limiter is used with the CY-MPC configuration. The balsa wood impact limiter is referred to as the "balsa impact limiter." The balsa impact limiter has performance characteristics comparable to the redwood and balsa wood impact limiters ("redwood impact limiter"), but weighs significantly less. As noted in Section 2.2, the balsa impact limiters can be used with any NAC-STC configuration. However, the redwood impact limiters are used only with the directly loaded and Yankee-MPC configurations.

The primary components of the NAC-STC are: (1) the cask body—inner shell, outer shell, lead shell, and bottom; (2) the inner lid, bolts, and metallic O-rings; (3) the outer lid, bolts, and metallic O-ring; (4) the port covers, port coverplates, bolts, and O-rings; (5) the neutron shield; (6) the trunnions; (7) the transport impact limiters—upper and lower; and (8) the fuel basket. The NAC-STC primary containment boundary for storage and transport after storage consists of: (1) inner shell center section and upper and lower inner shell rings (transition sections); (2) bottom inner forging; (3) top forging; (4) inner lid and inner lid outer metallic O-ring; (5) inner lid interseal test port and its threaded plug with metallic O-ring; (6) vent port coverplate and vent

port coverplate outer metallic O-ring; (7) vent port coverplate interseal test threaded plug with metallic O-ring; (8) drain port coverplate and drain port coverplate outer metallic O-ring; and (9) drain port coverplate interseal test threaded plug with metallic O-ring. The NAC-STC primary containment boundary for transport immediately after loading consists of: (1) inner shell center section and upper and lower inner shell rings (transition sections); (2) bottom inner forging; (3) top forging; (4) inner lid and inner O-ring; (5) vent port coverplate and vent port coverplate inner O-ring; and (6) drain port coverplate and drain port coverplate inner O-ring. For transport without interim storage after loading, either metallic or non-metallic (EPDM or Viton) O-rings may be used in the containment boundary. A detailed discussion of the containment boundary is presented in Chapter 4. As described in Section 7.1.3, for loading of the NAC-STC for immediate shipment, the containment boundary for the inner lid and drain port coverplate are the inner metallic O-rings, rather than the outer O-rings and interseal test plugs. The geometry and the materials of fabrication of the cask components are described in Section 1.2.1 and are shown on the license drawings presented in Section 1.3.2.

The NAC-STC is designed to satisfy the requirements of 10 CFR 71 for the transport of radioactive materials (and the requirements of 10 CFR 72 for the storage of radioactive materials) and the requirements of IAEA TS-R-1. The cask body holds and protects the cask cavity contents for the normal conditions of transport, as well as for the hypothetical accident conditions. The lead located between the inner and outer shells provides the primary gamma radiation shielding for the cask in the radial direction. The cask bottom connects the inner and outer shells, providing for the bottom end closure, as well as both gamma and neutron radiation shielding in the axial direction.

The inner lid, bolts, and O-rings are the primary closure components of the NAC-STC for transport conditions. The outer lid and O-ring provide a secondary closure boundary.

The vent port and the drain port are located in the inner lid and are each protected by a port coverplate. The primary containment boundary at the vent port and at the drain port is the port coverplate and its O-rings. The O-ring is located in the bottom surface of the port coverplate. A second O-ring is also located in the bottom surface of the port coverplate, inside of, and concentric with, the first O-ring.

The forty-two 1 1/2 - 8 UN inner lid bolts are preloaded by an installation torque to restrain rotation of the edge of the inner lid and to maintain a containment seal for the critical load

condition. This condition is a uniformly distributed pressure resulting from the impact of the basket and cavity contents on the inner surface during a top end or top corner impact. The critical design load condition for the inner lid bolts, as listed in Table 2.7.1.6-2, Section 2.7.1.6, is a 54.7 g top corner impact (10 CFR 71 Hypothetical Accident Condition). The critical design load condition for the inner lid is the top end impact, Section 2.7.1.6.

The outer lid is bolted to the top forging by the thirty-six 1 - 8 UNC outer lid bolts, which are installed to a specified torque. The torque provides a total bolt preload that exceeds the maximum applied bolt load for the critical load condition, preventing any lid and O-ring movement that might result in a loss of secondary seal integrity. The critical design load condition for the outer lid bolts, as listed in Table 2.7.1.6-4, Section 2.7.1.6, is a 51.3g side impact (10 CFR 71 Hypothetical Accident Condition). The critical design load condition for the outer lid is the pin puncture accident condition. The NAC-STC outer lid bolts are loaded by the interlid region pressure, the O-ring compression force, and by either the impact limiter crush force during a top end or top corner impact, or by a concentrated center load during a pin puncture impact. The outer lid seal is provided by an O-ring, which is tested by pressurizing the interlid region.

In addition to the main closure, the secondary closure boundary of the NAC-STC also includes the two ports located in the top forging—the interlid port and the pressure port. Each of these ports is protected and sealed by a recessed, bolted port cover with two piston-type (bore seal) PTFE O-rings. The port covers are installed with new O-rings just prior to transport (a slightly different port cover is installed during storage operation). The seal at each port cover is verified by pressure-testing the annulus between the two PTFE O-rings.

The neutron shielding material, NS-4-FR, is a solid synthetic polymer that absorbs the neutron radiation emitted by the cask contents. In addition to the radial neutron shielding along the cask length, neutron shielding is provided in the axial direction at each end of the cask by circular layers of NS-4-FR enclosed in the inner lid and in the cask bottom.

Four external trunnions are welded to the top forging of the NAC-STC at 90-degree intervals around the circumference of the cask. These trunnions are provided for lifting and handling the cask. Either a redundant (four trunnions) or a nonredundant (two trunnions) lifting system may be used. However, each pair of opposing trunnions are conservatively designed to satisfy the heavy lifting requirements of NUREG-0612 for a nonredundant lift, as well as the requirements

of 10 CFR 71.45(a) and paragraph 607 of IAEA TS-R-1. Two rotation trunnion recesses are welded to the bottom outer forging near the bottom of the cask. The neutron shield is cut out to accommodate the placement of the rotation trunnion recesses, which are used to attach the bottom of the cask to the transport vehicle and to rotate the cask from the vertical lifting position to the horizontal position and vice-versa.

As discussed above, two transport impact limiter configurations are used with the NAC-STC cask to limit the impact loads that may act on the cask. The impact limiters absorb the energy of a cask drop impact through the crushing of the wood in the limiters. A balsa impact limiter design must be used when the NAC-STC is transporting spent fuel or GTCC waste in the CY-MPC canister configuration. When transporting directly loaded fuel or the Yankee-MPC canister, either the redwood or balsa impact limiter configuration may be used.

The NAC-STC fuel basket is constructed of stainless steel and has a capacity of 26 PWR fuel assemblies. The fuel basket has a cylindrical shape with a series of support disks that provide lateral support for the square, stainless steel fuel tubes, which encase neutron absorber sheets or plates on each of the four sides. The support disks are separated and supported at 4.87-inch intervals by a threaded rod and spacer nuts at six locations. Aluminum heat transfer disks are located in the central region of the fuel basket and are supported by the six threaded rods and spacer nuts. The stainless steel support disks have adequate strength at the basket temperatures that occur during the transport and/or storage of 26 design-basis PWR fuel assemblies.

For the Yankee Class fuel and GTCC waste, the Yankee-MPC transportable storage canister (canister) serves as the enclosure of the spent fuel assemblies, damaged fuel cans and GTCC waste. The Yankee-MPC canister has a capacity of up to 36 Yankee Class spent fuel elements, or 32 Yankee Class fuel elements and four damaged fuel cans in the four basket corners, or up to 24 loading positions for GTCC waste. Similarly, the CY-MPC canister serves as the enclosure for the Connecticut Yankee spent fuel, damaged fuel cans and GTCC waste. The CY-MPC canister has a capacity of up to 26 Connecticut Yankee spent fuel assemblies or up to 24 containers of GTCC waste. The canister consists of a cylindrical shell with a welded bottom plate, a fuel or GTCC basket, a shield lid and a structural lid. The canister provides leak tight containment of the spent fuel or waste that it holds. This leak tight level of containment is maintained in all of the design basis normal conditions of transport and hypothetical accident conditions. Consequently, it qualifies as the separate inner container required by 10 CFR 71.63(b) for failed or damaged fuel that may be in the canister. The canister is evaluated for normal conditions of transport in Sections 2.6.13 and for hypothetical accident conditions in Section 2.7.11 in the transport configuration.

2.1.2 Design Criteria

2.1.2.1 Discussion

The load conditions that must be considered for the design of a spent-fuel transport cask are defined in 10 CFR 71 and in Regulatory Guide 7.8. Additionally, the NAC-STC is designed for the load conditions defined in 10 CFR 72 for dry storage casks. The stresses in the containment vessel, the noncontainment structure, and the closure bolts of the NAC-STC satisfy the stress limits defined in "Design Criteria for the Structural Analysis of Shipping Cask Containment Vessels," Regulatory Guide 7.6. These limits are essentially the same as those in the "ASME Boiler and Pressure Vessel Code," Section III, Division 1, Subsection NB for Class 1 Components.

The NAC-STC is analyzed as a pressure vessel whose containment boundary is not breached during any loading condition. The cask design provides well-defined load paths that are analyzed using straight-forward, proven structural analysis methods. The structural analysis of the NAC-STC is a linear elastic analysis. In those cases where loadings are open to analytical interpretation, bounding load condition analyses are performed to bracket the actual load condition.

Each normal condition of transport and each hypothetical accident condition will have a combination of various loading types. These load type combinations will define the total load criteria for each condition. The loading types that must be considered will include thermal, external and/or internal pressure, bolt preload, inertia, and cask drop impacts. The NAC-STC is analyzed for normal conditions of transport in Section 2.6 and for hypothetical accident conditions in Section 2.7.

The total stresses in the cask components are calculated as the combination of stresses that result from each of the various load types (thermal, pressure, mechanical) that are part of a given load condition. For those load conditions and components that are analyzed using classical hand-calculational methods, the total stress components are obtained by summation of the individual stress components for each type of load that is a part of the load condition. This summation is appropriate because the individual and total stress components are linear, elastic stresses.

2.1.2.2 Allowable Stress Limits - Ductile Failure

2.1.2.2.1 Containment Structures

Regulatory Guide 7.6 and "ASME Boiler and Pressure Vessel Code," Section III, Subsection NB are used to establish the allowable stress limits for the NAC-STC primary containment boundary for both normal conditions of transport and hypothetical accident conditions. Material property data used in calculating the allowable stress limits corresponds to the design stress intensities (S_m), yield strengths (S_y), and ultimate strengths (S_u), presented in Section 2.3. The NAC-STC primary containment boundary for storage and transport after storage includes: 1) the 6.2-inch thick cup-shaped bottom inner forging (Type 304 stainless steel); 2) the 71.0-inch inside diameter, 1.50-inch thick inner shell (Type XM-19 and Type 304 stainless steel), to which the bottom inner forging is welded; 3) the top forging (Type 304 stainless steel), to which the upper end of the inner shell is welded; 4) the 9.0-inch thick inner lid (Type 304 stainless steel) and its outer metallic O-ring (as well as its interseal test port, threaded plug and metallic O-ring), and 5) the vent and drain port coverplates, outer metallic O-rings and the port coverplate interseal test threaded plugs and metallic O-rings. When loaded for immediate shipment, the containment boundary includes the inner O-rings of the inner lid and drain port cover plate, rather than the outer O-ring and interseal test port. The inner lid is installed and retained using 42 bolts (SB-637, Grade N07718 nickel alloy steel).

A summary of the allowable stress criteria used for containment structures and bolting materials is presented in Table 2.1.2-1. These criteria are consistent with Regulatory Guide 7.6 and applicable parts of Subsection NB-3000 and Appendix F of the "ASME Boiler and Pressure Vessel Code." Analysis section locations on the cask are identified in Section 2.10.2.4.2 to aid in the evaluations of the various load conditions.

For the canistered fuel configuration, the NAC-STC primary containment boundary is unchanged. However, the TSC is designed as a confinement/containment boundary to satisfy 10 CFR 72 spent fuel storage requirements and provides a second containment boundary for the transport of Reconfigured Fuel Assemblies in accordance with the requirements of 10 CFR 71.63. A summary of the allowable stress criteria used for containment structures and bolting materials, including the Yankee-MPC and CY-MPC canisters, is presented in Table 2.1.2-1.

2.1.2.2.2 Noncontainment Structures

Noncontainment structures include all structural members other than the primary containment boundary components, but exclude the lifting trunnions, the rotation trunnion recesses, the lead and the impact limiters. Noncontainment structural members are shown to satisfy essentially the same structural criteria as the containment structure, even though Regulatory Guide 7.6 applies only to containment structures. Allowable stresses for the noncontainment structures and noncontainment bolting materials are presented in Table 2.1.2-2.

The allowable stresses for the lifting and handling components of the NAC-STC are based on the requirements of 10 CFR 71.45(a): material yield strength with a load factor of 3.0. The lifting and handling components of the NAC-STC also satisfy the structural requirements of NUREG-0612: the allowable stress is the material yield strength with a load factor of 6.0 or the material ultimate strength with a load factor of 10.0, depending on which load condition is more critical.

The lead (gamma shielding material) is not stress-limited because its deformation is considered, where appropriate, in the various cask analyses.

The impact limiters are not stress- or deformation-limited. While performing their intended function during a free drop impact, the impact limiter(s) crushes, and thus, absorbs the energy of the impact. Crushing of the impact limiter(s) limits the impact forces that are applied to the cask.

In the canistered configuration, the Transportable Storage Canister provides containment of the spent fuel with a double welded closure. The canister contains a structurally sound, criticality safe, and thermally efficient basket that is a noncontainment structure. The basket provides the structural support to the fuel and maintains the spent fuel in a subcritical configuration during all of the normal conditions of transport and hypothetical accident conditions.

The allowable stresses for noncontainment structures, noncontainment bolting materials, and fuel/waste basket structures are presented in Table 2.1.2-2.

Table 2.1.2-1 Allowable Stress Limits for Containment Structures

Stress Intensity Category	ALLOWABLE STRESS INTENSITY		BOLT MATERIAL ALLOWABLE STRESS INTENSITY*	
	Normal Conditions	Accident Conditions	Normal Conditions	Accident Conditions
Primary Membrane	$1.0 S_m$	Lesser of: $2.4 S_m$ and $0.7 S_u$	$2.0(S_m)_{BM}$	Lesser of: $1.0 S_y$ and $0.7 S_u$
Primary Membrane + Primary Bending	$1.5 S_m$	Lesser of: $3.6 S_m$ and $1.0 S_u$	$3.0(S_m)_{BM}$	$1.0 S_y$
Range of Primary + Secondary	$3.0 S_m$	N/A		
Pure Shear	$0.6 S_m$	$0.42 S_u$		
Bearing	$1.0 S_y$ or $1.5 S_y^{**}$	$1.0 S_u$		
Peak		Per Section 2.1.3.2		
Buckling		Per Section 2.1.3.4		

* Neglecting stress concentrations.

** Distance to edge > distance over which the bearing load is applied.

S_u = Material Ultimate Strength.

S_y = Material Yield Strength.

S_m = Material Design Stress Intensity.

= Lesser of: $S_u/3$ and $2S_y/3$.

$(S_m)_{BM}$ = $S_y/3$ for Bolt Material.

Table 2.1.2-2 Allowable Stress Limits for Noncontainment Structures

Stress Intensity Category	ALLOWABLE STRESS INTENSITY		BOLT MATERIAL ALLOWABLE STRESS INTENSITY*		BASKET MATERIAL ALLOWABLE STRESS**	
	Normal Conditions	Accident Conditions	Normal Conditions	Accident Conditions	Normal Conditions	Accident Conditions
Primary Membrane	$1.0 S_m$	$0.7 S_u$	$2.0(S_m)_{BM}$	S_u	$1.0 S_m$	$0.7 S_u$
Primary Membrane + Primary Bending	$1.5 S_m$	$1.0 S_u$	$3.0(S_m)_{BM}$	$1.0 S_y$	$1.5 S_m$	$1.0 S_u$
Range of Primary + Secondary	$3.0 S_m$	N/A			$3.0 S_m$	N/A
Pure Shear	$0.6 S_m$	$0.42 S_u$			$0.6 S_m$	$0.42 S_u$
Bearing	$1.0 S_y$ or $1.5 S_y^{***}$	$1.0 S_u$			$1.0 S_y$	$1.0 S_u$
Peak	Per Section 2.1.3.2				Per Section 2.6.12.8	
Buckling					Per Section 2.7.8.3	

* Neglecting stress concentrations.

** ASME Code, Section III, Subsection NG.

*** Distance to edge > distance over which the bearing load is applied.

S_u = Material Ultimate Strength.

S_y = Material Yield Strength.

S_m = Material Design Stress Intensity.

= Lesser of: $S_u/3$ and $2S_y/3$.

$(S_m)_{BM}$ = $S_y/3$ for Bolt Material.

THIS PAGE INTENTIONALLY LEFT BLANK

2.1.3 Miscellaneous Structural Failure Modes

2.1.3.1 Brittle Fracture

The primary structural material of the NAC-STC is Type 304 stainless steel. The outer shell, the inner shell, the top forging, the bottom forgings, the inner lid, and the vent and drain port coverplates are fabricated from Type 304 stainless steel. The inner shell rings at each end of the inner shell are fabricated from Type XM-19 stainless steel. For the canistered fuel or GTCC waste configurations: the canister and the structural lid are Type 304L stainless steel; the fuel and GTCC waste tubes, the tie rods, and the top and bottom weldments are Type 304 stainless steel; and the support disks are Type 17-4 PH precipitation—hardened stainless steel. Because Type 304, Type 304L, and Type XM-19 stainless steel are austenitic stainless steel, they do not undergo a ductile-to-brittle transition in the temperature range of interest for a spent-fuel transport and/or storage cask. Therefore, brittle fracture is not a concern.

Regulatory Guide 7.11, "Fracture Toughness Criteria of Base Material for Ferritic Steel Shipping Cask Containment Vessels with a Maximum Wall Thickness of Four Inches (0.1 m)," which identifies fracture toughness criteria, references the criteria contained in NUREG/CR-1815, "Recommendations for Protecting Against Failure by Brittle Fracture in Ferritic Steel Shipping Containers Up to Four Inches Thick." The inner lid bolts are SB-637, Grade N07718 nickel alloy steel bolting material. According to Section 5 of NUREG/CR-1815, bolts are generally not considered fracture-critical components because multiple load paths exist and because bolted systems are designed to be redundant. Therefore, brittle fracture evaluation of the bolts is not required. Conservatively, for purposes of comparison, the nil-ductility transition temperature (NDTT) of the inner lid bolts will be calculated and compared with the requirements of NUREG/CR-1815. Although this method of analysis is not applicable to bolts, it is presented to demonstrate that the bolt material possesses a level of resistance to brittle fracture that is comparable to the other cask component materials. Using the most restrictive requirements of Section 6.2.1.1 of ASTM A-320, the minimum impact energy absorption for high alloy steel bolting material is 20 foot-pounds at -150°F. The Charpy impact measurement may be transformed into a fracture toughness value by using the empirical relation developed in Section 4.2 of NUREG/CR-1815, as follows:

$$K_{ID} = [5E(C_v)]^{0.5}$$
$$= 56,214 \text{ psi-(in)}^{0.5}$$

where:

$$K_{ID} = \text{Dynamic Fracture Toughness, psi-(in)}^{0.5}$$
$$E = \text{Modulus of Elasticity, psi}$$
$$= 31.6 \times 10^6 \text{ psi at } -150^\circ\text{F}$$
$$C_v = \text{Charpy impact measurement, ft-lbs}$$
$$= 20 \text{ ft-lbs}$$

The dynamic fracture toughness is translated to an equivalent NDTT by using the Pellini reference curve given as Figure 2 in NUREG/CR-1815. By interpolation, the temperature relative to NDTT is found as:

$$(T - \text{NDTT}) = 32^\circ\text{F}$$

Accordingly, the nil-ductility transition temperature is:

$$\text{NDTT} = -150 - (+32)$$
$$= -182^\circ\text{F}$$

For Category I fracture critical components and in section thickness at 1.5 inches (bolt diameter), Figure 3 of NUREG/CR-1815 gives the minimum offset, "A," as approximately 60°F. Thus, the required NDTT value is:

$$T_{\text{NDT}} = \text{LST} - A$$
$$= -40 - 60$$
$$= -100^\circ\text{F}$$

where:

$$T_{\text{NDT}} = \text{required maximum NDTT per NUREG/CR-1815}$$
$$\text{LST} = \text{Lowest Service Temperature}$$
$$= -40^\circ\text{F (Regulatory Guide 7.8)}$$
$$A = 60^\circ\text{F (Figure 3, NUREG/CR-1815)}$$

The SB-637, Grade N07718 nickel alloy steel, inner lid bolts can be expected to experience a ductile-to-brittle transition at a temperature of -182°F , whereas the criterion of NUREG/CR-1815 prescribes an NDTT of -100°F . The 82°F margin between criteria requirements and material capability provides conservative assurance that brittle fracture failures will not occur in the nickel alloy steel inner lid bolts.

The outer lid, the outer lid bolts, the port covers, the lifting trunnions, the rotation trunnion recesses, and the fuel basket support disks, threaded rods and spacer nuts are SA-705, SA-693 or SA-564, Type 630, H1150, 17-4 PH stainless steel.

The Transportable Storage Canister (TSC) is fabricated from Type 304L stainless steel. The TSC fuel basket tubes, axial tie rods, and top and bottom weldments, are Type 304 stainless steel. The TSC fuel basket support plate is Type 17-4 PH stainless steel. All of the components of the GTCC basket assembly are Type 304 stainless steel.

Conservatively, for purposes of demonstrating its comparable brittle fracture resistance, the NDTT of the material will be calculated and compared with the requirements of NUREG/CR-1815.

The typical minimum impact energy absorption requirement for Type 17-4 PH, precipitation-hardened stainless steel is 48 foot-pounds at -110°F . This value is obtained from Table 14, Product Data Bulletin No. S-22, "ARMCO 17-4 PH PRECIPITATION-HARDENING STAINLESS STEEL," ARMCO, Inc. The Charpy impact measurement may be transformed into a fracture toughness value by using the empirical relation developed in Section 4.2 of NUREG/CR-1815, as follows:

$$\begin{aligned} K_{ID} &= [5E(C_v)]^{0.5} \\ &= 82,994 \text{ psi-(in)}^{0.5} \end{aligned}$$

where:

$$\begin{aligned} K_{ID} &= \text{Dynamic Fracture Toughness, psi-(in)}^{0.5} \\ E &= \text{Modulus of Elasticity, psi} \\ &= 28.7 \times 10^6 \text{ psi at } -110^{\circ}\text{F} \\ C_v &= \text{Charpy Impact Measurement, ft-lbs} \\ &= 48 \text{ ft-lbs} \end{aligned}$$

The dynamic fracture toughness is translated to an equivalent NDTT by using the Pellini reference curve given as Figure 2 in NUREG/CR-1815. By interpolation, the temperature relative to NDTT is found as:

$$(T - \text{NDTT}) = 65^{\circ}\text{F}$$

Accordingly, the nil-ductility transition temperature is:

$$\begin{aligned}\text{NDTT} &= -110 - (+65) \\ &= -175^{\circ}\text{F}\end{aligned}$$

For Category I fracture critical components and in section thickness of 4.0 inches, Figure 3 of NUREG/CR-1815 gives the minimum offset, "A," as approximately 100°F. Thus, the required NDTT value is:

$$\begin{aligned}T_{\text{NDT}} &= \text{LST} - A \\ &= -40 - 100 \\ &= -140^{\circ}\text{F}\end{aligned}$$

where:

$$\begin{aligned}T_{\text{NDT}} &= \text{Required Maximum NDTT per NUREG/CR-1815} \\ \text{LST} &= \text{Lowest Service Temperature} \\ &= -40^{\circ}\text{F (Regulatory Guide 7.8)} \\ A &= 100^{\circ}\text{F (Figure 3, NUREG/CR-1815)}\end{aligned}$$

The Type 17-4 PH stainless steel components can be expected to experience a ductile-to-brittle transition at a temperature of -175°F, whereas the criterion of NUREG/CR-1815 requires a maximum NDTT of -140°F. The calculated margin of 35°F between criteria requirements and material capability provides conservative assurance that brittle fracture failures will not occur in these high-strength stainless steel components.

2.1.3.2 Fatigue - Normal Operation

The fatigue stress limitations of Regulatory Guide 7.6 are used for the analysis of those components that are, by definition, a part of the primary containment vessel. Paragraph C.3 of Regulatory Guide 7.6 defines the "high cycle" fatigue stress limit for any point in the containment vessel under normal conditions of transport as a limit on the maximum stress intensity range. That limit is equal to twice the allowable alternating stress at 10^6 cycles (S_a) as tabulated in the mechanical properties of materials, Section 2.3, as adjusted by the ratio of the modulus of elasticity used in the development of the material fatigue curve divided by the material's modulus of elasticity at the applicable temperature for the load combination being evaluated. At analysis locations where a structural discontinuity exists, the calculated peak stress intensity range includes appropriate stress concentration effects.

Paragraph C.7 of Regulatory Guide 7.6 defines the "low cycle" fatigue stress limit for any point in the containment vessel for the cask's entire life--initial state, fabrication state, normal conditions of transport, and hypothetical accident--as a limit on the maximum stress intensity range. That limit is equal to twice the allowable alternating stress at 10 cycles (S_a) as tabulated in the mechanical properties of materials, Section 2.3. S_a has been adjusted by the ratio of the material's modulus of elasticity (at the applicable temperature for the load combination being evaluated) to the modulus of elasticity used in the development of the material fatigue curve. At analysis locations where a structural discontinuity exists, the calculated peak stress intensity range includes appropriate stress concentration effects.

A normal operating cycle for transport consists of: 1) loading an empty cask at ambient temperature with contents of maximum heat load, 2) transporting the contents to a destination, and 3) unloading the contents and letting the cask return to ambient temperature. The anticipated number of normal operating cycles is not expected to exceed 240 cycles (12 cycles per year x 20 years).

The fatigue criteria is always satisfied as long as the allowable alternating stress intensity range is greater than the allowable primary plus secondary stress intensity range multiplied by the appropriate stress concentration factor. Subsection NB-3222.2 of the "ASME Boiler and Pressure Vessel Code" defines the allowable primary plus secondary stress intensity range as $3.0 (S_m)$, where S_m is the design stress intensity.

2.1.3.2.1 Cask Body and Inner Lid

For the Type 304 stainless steel cask body at 360°F, conservatively high for stress concentration areas, $S_m = 19.4$ ksi (Section 0) and $3.0 S_m = 58.2$ ksi. The maximum stress concentration in the cask body occurs at two different locations: (1) the intersection of the outer shell and the bottom of the cask; and (2) the holes for the inner lid bolts. At the outer shell/cask bottom intersection, radius $r = 0.5$ inch, thickness $t = 2.65$ inches, so $d = 5.30$ inches (2×2.65), effective width of cask bottom $D = 10.40$ inches $[(2)(2.65 + 2.55)]$, bottom thickness $m = 13.65$ inches; then, $D/d = 1.96$, $m/d = 2.58$, and the stress concentration factor is $K_t = 3.35$ (Peterson, Figure 192). At an inner lid bolt hole, hole radius $r = 0.75$ inch, edge distance $c = 2.155$ inches; then, $r/c = 0.35$ and the stress concentration factor is $K_t = 3.33$ (Peterson, Figure 87). Using a stress concentration factor of 3.35, the maximum allowable peak stress intensity range is $(SI)_{pr} = (3.35)(58.2) = 195.0$ ksi and the peak stress intensity amplitude is $(SI)_{pa} = (SI)_{pr}/2 = 97.5$ ksi. From the "ASME Boiler and Pressure Code," Appendix I, Figure I-9.2.1, the peak stress intensity amplitude is ratioed to incorporate the modulus of elasticity at 360°F, alternating stress intensity $(SI)_a = (97.5)(28.3/26.7) = 103.3$ ksi. The allowable number of cycles associated with an $(SI)_a = 103.3$ ksi is 1400 cycles. This number of allowable cycles considerably exceeds the number of normal operating cycles that the NAC-STC will incur during its lifetime.

For the Type XM-19 stainless steel inner shell rings at each end of the inner shell at 360°F, conservatively high for stress concentration areas, $S_m = 31.0$ ksi (Section 3.3) and $3.0 S_m = 93.0$ ksi. The maximum stress concentration in the inner shell rings (Type XM-19 stainless steel) occurs at the location of the transitions in the outer diameter. The larger inner shell thickness $H = 2.00$ inches, smaller inner shell thickness $h = 1.50$, radius to taper $r = 0.50$ inch, length of taper = 3.00 inches; then $H/h = 1.33$, $r/h = 0.33$, and the stress concentration factor is $K_t = 1.87$ (Peterson, Figure 72a). Conservatively, using a stress concentration factor of 2.0, the maximum allowable peak stress intensity range is $(SI)_{pr} = (2.0)(93.0) = 186.0$ ksi and the peak stress intensity amplitude is $(SI)_{pa} = (SI)_{pr}/2 = 93.0$ ksi. From the "ASME Boiler and Pressure Vessel Code," Appendix I, Figure I-9.2.1, the peak stress intensity amplitude is ratioed to incorporate the modulus of elasticity at 300°F, alternating stress intensity $(SI)_a = (93.0)(28.3/26.8) = 98.2$ ksi.

The allowable number of cycles associated with an $(SI)_a = 98.2$ ksi is 2000 cycles. This number of allowable cycles considerably exceeds the number of normal operating cycles that the NAC-STC will incur during its lifetime.

2.1.3.2.2 Outer Lid

Using a similar method of evaluation for the outer lid (SA-705, Type 630, H1150, 17-4 PH stainless steel) at 200°F, conservatively high for stress concentration areas, $S_m = 45.0$ ksi (Table 2.3.3-1) and $3.0 S_m = 135.0$ ksi. The maximum stress concentration in the outer lid occurs at the bolt hole locations. At the outer lid bolt hole locations, the bolt hole diameter is $d = 1.0$ inch and the bolt hole pitch is $w = 7.30$ inches (36 holes on a 83.70-inch bolt circle). Then, $d/w = 0.137$ and the stress concentration factor is $k_t = 3.07$ (Peterson, Figure 86). Using a stress concentration factor of 3.07, the maximum allowable peak stress intensity range is $(SI)_{pr} = (3.07)(135.0) = 414.5$ ksi and the peak stress intensity amplitude is $(SI)_{pa} = (SI)_{pr}/2 = 207.2$ ksi. From the "ASME Boiler and Pressure Vessel Code," Section III, Appendix I, Figure I-9.2.1, the peak stress intensity amplitude is ratioed to incorporate the modulus of elasticity at 200°F, $(SI)_a = (207.2)(28.3/27.8) = 211.0$ ksi. The allowable number of cycles associated with an $(SI)_a = 211.0$ ksi is 190 cycles. Since this allowable number of cycles is excessively restrictive for the lifetime of a spent fuel transport cask, the grossly conservative evaluation methodology will be revised to use the maximum calculated stress in the outer lid. Since the maximum calculated stress in the outer lid is 19,647 psi (Table 2.7.1.6-1) for a 56.1 g, 30-foot drop top end impact accident load condition, it is very conservative to use this stress value in a normal operating condition fatigue analysis of the outer lid. The maximum peak stress intensity range for the outer lid is $(SI)_{pr} = (3.07)(19.6) = 60.2$ ksi and the peak stress intensity amplitude is $(SI)_{pa} = (SI)_{pr}/2 = 30.1$ ksi. From the "ASME Boiler and Pressure Vessel Code," Section III, Appendix I, Figure I-9.2.1, the peak stress intensity amplitude is ratioed to incorporate the modulus of elasticity at 200°F, $(SI)_a = (30.1)(28.3/27.8) = 30.6$ ksi. The allowable number of cycles associated with an $(SI)_a = 30.6$ ksi is 90,000 cycles. This number of allowable cycles far exceeds the number of Normal Conditions of Transport loading cycles that the NAC-STC will incur during its lifetime of spent fuel transport.

2.1.3.2.3 Bolts

Stress concentration occurs in the inner lid bolts, the outer lid bolts, the port cover bolts, and the port coverplate bolts. The maximum cyclic stress in these bolts is due to the installation preload and thermally induced loads. From Shigley, the preload torque is calculated as:

$$T = \left[\left(\frac{d_m}{2d} \right) \left(\frac{\tan \lambda + \mu \sec \alpha}{1 - \mu \tan \lambda \sec \alpha} \right) + 0.625 \mu \right] (F)(d)$$

where:

F = preload force

d = bolt diameter

d_m = mean diameter of threads

α = one-half the thread angle

μ = coefficient of friction

$$\tan \lambda = \frac{1}{\pi d_m N}$$

N = number of threads per inch

2.1.3.2.3.1 Inner Lid Bolts

The maximum installation torque for each SB-637, Grade N07718 nickel alloy inner lid bolt is 2,740 foot-pounds ($2,540 \pm 200$), or 32,880 inch-pounds; thus, $T = 32,880$ inch-pounds. The nominal inner lid bolt thread diameter is 1.5 inches; thus, $d = 1.5$ inches. Based on the evaluation in Section 2.6.7.5.4.1, the maximum normal tensile stress (preload + thermal) in each inner lid bolt is calculated as 86.3 ksi.

From the "ASME Boiler and Pressure Vessel Code," Section III, NB-3232.3(c), the fatigue strength reduction factor is assumed to be 4.0. In addition, the modulus of elasticity at 200°F is 28.3×10^6 psi (SB-637, Grade N07718 nickel alloy steel). Since the "ASME Boiler and Pressure Vessel Code," Section III, Figure I-9.4 is based on a modulus of elasticity of 30.0×10^6 psi, the equivalent stress range is:

$$\begin{aligned} S_{\text{range}} &= (86,306)(4.0)(30.0 \times 10^6 / 28.3 \times 10^6) \\ &= 365,962 \text{ psi} \end{aligned}$$

The alternating stress is one-half of the stress range, or $S_a = 183,817$ psi. Using Figure I-9.4, Section III, "ASME Boiler and Pressure Vessel Code," the allowable number of normal operating cycles is 301 cycles (one cycle consists of one application and removal of preload). Assuming a maximum of 12 cycles per year for the bolts, a 25.1-year life is projected. Operational procedures will specify replacement of an entire set of these bolts every 240 cycles (20 years), ensuring a fatigue failure margin of safety of + 0.26.

2.1.3.2.3.2 Outer Lid Bolts

The allowable number of normal operating cycles for the outer lid bolts is calculated similarly to that for the inner lid bolts.

The maximum installation torque (T) for an outer lid bolt is 600 foot-pounds, or 7,200 inch-pounds; thus, $T = 7,200$ inch-pounds. The nominal thread diameter of an outer lid bolt is 1.0 inch; thus, $d = 1.0$ inch. Based on the evaluation in Section 2.6.7.5.4.2, the maximum tensile stress in each outer lid bolt is calculated to be 60,743 psi.

Again, assuming a fatigue strength reduction factor of 4.0 and ratioing for the modulus of elasticity at 200°F, 27.6×10^6 psi (SA-564, Type 630, H1150, 17-4 PH stainless steel), the equivalent stress range is $S_{\text{range}} = 264,100$ psi. Then, the alternating stress is $S_a = 132,050$ psi and the allowable number of normal operating cycles is 573 cycles (Figure I-9.1, Appendix I, "ASME Boiler and Pressure Vessel Code"), which is significantly greater than the 240 cycles of normal transport loads that the NAC-STC is expected to incur during its lifetime.

2.1.3.2.3.3 Port Cover Bolts

The allowable number of normal operating cycles for the port cover bolts is calculated similarly to that for the inner lid bolts. The installation torque for a bolt for the port cover is 140 inch-pounds; thus, $T = 140$ inch-pounds. The nominal thread diameter of a bolt for the port cover is 0.375 inch; thus, $d = 0.375$ inch. The calculated tensile force and stress in the port cover bolts are 1,875 pounds and 30,242 psi, respectively. Assuming a fatigue strength reduction factor of

4.0 and ratioing for the modulus of elasticity at 200°F, 28.5×10^6 psi (SA-193, Grade B6 High Alloy Steel Bolting Material), the equivalent stress range is $S_{\text{range}} = 127,335$ psi. Then, the alternating stress is $S_a = 63,667$ psi and the allowable number of normal operating cycles for the bolts for the port cover is 1650 cycles (Figure I-9.4, Appendix I, "ASME Boiler and Pressure Vessel Code"), which is greater than the 240 cycles of normal transport loads that the NAC-STC is expected to incur during its lifetime.

2.1.3.2.3.4 Port Coverplate Bolts

The allowable number of normal operating cycles for the port coverplate bolts is calculated similarly to that for the inner lid bolts. The installation torque for a port coverplate bolt is 300 inch-pounds; thus, $T = 300$ inch-pounds. The nominal thread diameter of a bolt for the port coverplate is 0.5 inch; thus, $D = 0.50$ inch. The calculated tensile force and stress in the port coverplate bolts are 4,110 pounds and 28,964 psi, respectively. Again, assuming a fatigue strength reduction factor of 4.0 and ratioing for the modulus of elasticity at 200°F, 28.5×10^6 psi (SA-193, Grade B6 High Alloy Steel Bolting Material), the equivalent stress range is $S_{\text{range}} = 121,954$ psi. Then, the alternating stress is $S_a = 60,977$ psi and the allowable number of normal operating cycles for the bolts for the port coverplate is 1,700 cycles (Figure I-9.4, Appendix I, "ASME Boiler and Pressure Vessel Code"), which is greater than the 240 cycles of normal transport loads that the NAC-STC is expected to incur during its lifetime.

2.1.3.2.4 Normal Over-the-Rail Vibration

Fatigue concerns associated with normal over-the-rail vibration are addressed in Section 2.6.5.

2.1.3.3 Extreme Total Stress Intensity Range

Paragraph C.7 of Regulatory Guide 7.6 defines the "low cycle" fatigue stress limit for any point in the containment vessel for the cask's entire life—initial state, fabrication state, normal transport conditions and hypothetical accident—as a limit on the maximum stress intensity range. That limit is equal to twice the allowable alternating stress at 10 cycles (S_a) as tabulated in the mechanical properties of materials, Section 2.3. S_a has been adjusted by the ratio of the material's modulus of elasticity (at the applicable temperature for the load combination being evaluated) to the modulus of elasticity used in the development of the material fatigue curve. At analysis locations where a structural discontinuity exists, the calculated peak stress intensity range includes appropriate stress concentration effects.

To conservatively evaluate the stress state in relation to the requirements of Paragraph C.7 of Regulatory Guide 7.6, the worst-case thermal/secondary stress intensity is used. The detailed evaluation of the extreme total stress intensity range for the NAC-STC is performed in Section 2.7.3.3.

2.1.3.4 Inner Shell Buckling Design Criteria

Code Case N-284 (Metal Containment Shell Buckling Design Methods) of the "ASME Boiler and Pressure Vessel Code" is used to analyze the NAC-STC inner shell for structural stability. Structural stability ensures that the inner shell does not buckle during cask fabrication, normal operations, or hypothetical accident conditions. The buckling evaluation requirements of Regulatory Guide 7.6, Paragraph C.5, are shown to be satisfied by the results of the interaction equation calculations of Code Case N-284.

2.1.3.4.1 Code Case N-284

The "ASME Boiler and Pressure Vessel Code" sets forth service limits that are analogous to load conditions found in 10 CFR 71. As stated in Regulatory Guide 7.6, the normal transport conditions correspond to Level A Service Limits, and the hypothetical accident conditions correspond to Level D Service Limits. Service conditions A and D allowable stresses are used in performing the buckling assessment of the inner shell. Level A (normal transport) conditions use a buckling safety factor of 2.0, and Level D (accident) conditions use a buckling safety factor of 1.34. Code Case N-284 addresses both elastic and inelastic buckling.

Interaction equations are used to combine hoop compressive, axial compressive, and in-plane shear loadings. Also, Appendix F of the "ASME Boiler and Pressure Vessel Code," (for Level D Service Loadings) specifically identifies the use of "A Code Case for Metal Containment Shell Buckling" as an acceptable means of addressing buckling issues (paragraph F-1331.5(c)).

Buckling of the inner shell, which is the primary component of containment, is evaluated in the following manner:

1. Determine the theoretical elastic buckling stresses using classical theory.

2. Apply the appropriate factors of safety and interaction equations to elastic and inelastic buckling cases and establish the worst-case compressive and in-plane shear stresses.
3. Calculate and apply capacity reduction factors, which account for differences between classical theory and predicted instability stress for fabricated shells.
4. Calculate plasticity reduction factors and apply them in cases where elastically determined buckling stresses are above the proportional limit.

2.1.3.4.2 Theoretical Elastic Buckling Stresses

Inner shell geometric parameters and material properties are used to follow the elastic buckling evaluation. The theoretical elastic buckling stresses for the inner shell are calculated using the equations of Code Case N-284, the inner shell geometric parameters, and the material yield strength and elastic modulus.

The equations from Code Case N-284 are:

$$S_{\phi eL} = C_{\phi} \frac{Et}{R}$$

$$S_{\theta eL} = S_{reL} = C_{\theta} \frac{Et}{R}$$

$$S_{heL} = C_{\theta h} \frac{Et}{R}$$

$$S_{\phi \theta eL} = C_{\phi \theta} \frac{Et}{R}$$

These elastic buckling stress formulas are for cylindrical shells that are unstiffened.

2.1.3.4.3 Capacity Reduction Factors

Capacity reduction factors, as stated earlier, compensate for differences between classically determined and predicted instability stresses for fabricated shells. The capacity reduction factors were determined using methods described in Section-1500 of Code Case N-284. For the NAC-STC inner shell geometry, the capacity reduction factors are determined by the following expressions:

1. Axial Compression: $\alpha_{\phi L} = [1.0 \times 10^{-5}(S_y)] - 0.033$

2. Hoop Compression: $\alpha_{\theta L} = 0.8$

3. Shear: $\alpha_{\phi \theta L} = 0.8$

In order to directly use the capacity reduction factors, the tolerance requirements of NE-4220 of the "ASME Boiler and Pressure Vessel Code," Subsection NE, must be satisfied. NE-4221.1 and NE-4221.2 set forth the "maximum difference in cross-sectional diameters" and "maximum deviation from true theoretical form for external pressure."

2.1.3.4.4 Plasticity Reduction Factors

Plasticity reduction factors account for nonlinear material behavior, occurring when buckling stresses exceed the proportional limit of the material. Plasticity reduction factors chosen are dependent upon the magnitude of the applied compressive or in-plane shear stress, S_i . Because values for S_i are not directly calculated, the equations used to determine the reduction factors (Section-1600 of Code Case N-284) are presented:

1. Axial Compression

$$\eta_{\phi} = 1.0; \text{ if } [(S_{\phi})(FS)/(S_y)] < 0.55$$

$$\eta_{\phi} = 0.18 / (1 - [0.45 S_y / (S_{\phi})(FS)]);$$

$$\text{if } 0.55 < [(S_{\phi})(FS)/S_y] \leq 0.738$$

$$\eta_{\phi} = 1.31 - [1.15 (S_{\phi})(FS)/S_y]; \text{ if } 0.738 < [(S_{\phi})(FS)/S_y] < 1.0$$

2. Hoop Compression

$$\eta_{\theta} = 1.0; \text{ if } [(S_{\theta})(FS)/S_y] < 0.67$$

$$\eta_{\theta} = 2.53 - 2.29[(S_{\theta})(FS)/S_y]; \text{ if } 0.67 < [(S_{\theta})(FS)/S_y] < 1.0$$

3. Shear

$$\eta_{\phi\theta} = 1.0; \text{ if } [(S_{\phi\theta})(FS)/S_y] \leq 0.48$$

$$\eta_{\phi\theta} = 0.1/(1 - [0.43S_y/(S_{\phi\theta})(FS)]);$$
$$\text{if } 0.48 < [(S_{\phi\theta})(FS)/S_y] \leq 0.6$$

2.1.3.4.5 Upper Bound Magnitudes for Compressive Stresses and In-Plane Shear Stresses

From Section-1600 of Code Case N-284, as an upper limit, the compressive stresses, S_i ($i = \phi$ or θ), must be less than the yield strength, S_y , divided by the appropriate factor of safety ($S_i < S_y/FS$). Similarly, for shear, $S_{\phi\theta}$ must be less than, or equal to, $0.6 S_y$ divided by the appropriate factor of safety ($S_{\phi\theta} < 0.6 S_y/FS$). As stated in Section 2.1.3.4.1, there is a factor of safety of 2.0 for normal transport and a factor of safety of 1.34 for hypothetical accident conditions. Under no circumstances can the values for the upper bound magnitudes of compressive stresses and in-plane shear stresses be exceeded. However, satisfying these limits alone is not sufficient to demonstrate that buckling will not occur. As stated in Section 2.1.3.4.1, the interaction equations must also be satisfied.

2.1.3.4.6 Interaction Equations

Elastic and inelastic interaction equations must be satisfied for all states of compressive and in-plane shear stress. The interaction equations for cylindrical shells are directly available from paragraph 1713.1.1 and paragraph 1713.2.1 of Code Case N-284. Once a stress state is established for a specific shell, plasticity reduction factors can be determined and all appropriate interaction equations checked. Elastic interaction equations must be satisfied and, if any of the uniaxial critical stress values exceed the proportional limit of the fabricated material, the inelastic interaction equations must also be satisfied.

2.1.3.5 Creep Considerations at Elevated Temperatures

Structural components of the NAC-STC cask and fuel basket are fabricated from stainless steel, which does not experience creep below temperatures of 700°F. The fuel basket is the package structural component exposed to the highest temperatures, which remain below 700°F. Therefore, the potential of creep is eliminated from the package, satisfying design considerations relative to the creep failure mode.

2.1.3.6 Impact Limiter Deformation Limits

The NAC-STC impact limiter(s) is intended to crush and thus absorb energy during a free drop accident condition impact. The geometry of the impact limiter and the crush characteristics of the energy-absorbing material are designed to limit the impact forces that are applied to the cask.

The NAC-STC impact limiter(s) limit the deceleration experienced by the cask body to approximately 55.0 g for all impact conditions. The impact force is a function of the crush strength of the energy-absorbing material in the impact limiter and the area of crush. The impact limiter must provide a sufficient depth of energy-absorbing material so that all of the impact energy is absorbed (cask is stopped) before the limiter is crushed to solid "stacked" height (approximately 30 percent of the initial depth).

THIS PAGE INTENTIONALLY LEFT BLANK

2.2 Weights and Centers of Gravity

This section provides the weights and centers of gravity for five transport configurations and two impact limiter configurations. The transport configurations are directly loaded fuel, canistered fuel and GTCC waste using the Yankee-MPC configuration and canistered fuel and GTCC waste using the CY-MPC configuration. There are two impact limiter designs. The redwood design shown in Drawings 423-209 and 423-210 may be used for the directly loaded fuel and the Yankee-MPC configurations. The balsa wood design shown in Drawings 423-257 and 423-258 may be used for the directly loaded fuel and Yankee-MPC configurations, but must be used for the CY-MPC configurations.

The calculated weights of the major components of the NAC-STC directly loaded fuel configuration are tabulated in Table 2.2-1. The table also presents a summary of the weights and center of gravity locations of the NAC-STC for the three cask configurations most likely to occur - empty, under-the-hook loaded with fuel, and loaded with fuel/ready for transport. In Table 2.2-1, the "empty" weight includes the cask basket, but excludes any fuel or water in the cask cavity. The term "loaded with fuel" refers to the directly loaded cask with 26 design basis fuel assemblies in the basket. "Under-the-hook loaded with fuel" describes the directly loaded NAC-STC with water in the cavity, without the outer lid in place, and with the yoke. "Loaded with fuel/ready for transport" describes the directly loaded NAC-STC with helium in the cavity and the upper and lower impact limiters installed on the cask. The axial locations of the centers of gravity are measured from the bottom outer surface of the cask body. The centers of gravity are on the axial centerline of the cask because it is essentially symmetric about that axis.

The design weight of the NAC-STC directly loaded fuel configuration "loaded with fuel/ready for transport" is 250,000 pounds. This design weight is used in all normal transport, hypothetical accident, and lifting/handling analyses for the directly loaded fuel configuration.

The calculated weights of the major components of the Yankee-MPC canistered fuel and GTCC waste configurations of the NAC-STC are tabulated in Tables 2.2-2 and 2.2-3, respectively. The tables also present a summary of the weights and center of gravity locations of the NAC-STC for the three Yankee-MPC cask configurations most likely to occur - empty, under the hook loaded with fuel, and loaded with fuel/ready for transport. In Tables 2.2-2 and 2.2-3, the "empty" weight excludes the transportable storage canister but includes the canister spacer weight. The term "loaded with fuel" refers to the loaded Yankee-MPC canister in the cask, with the noted number of design basis fuel assemblies in the basket. "Under-the-hook loaded with fuel"

describes the loaded NAC-STC without the outer lid in place, and with the yoke. "Loaded with fuel/ready for transport" describes the loaded NAC-STC with helium in the cavity and the upper and lower impact limiters installed on the cask. The axial locations of the centers of gravity are measured from the bottom outer surface of the cask body. The centers of gravity are on the axial centerline of the cask because it is essentially symmetric about that axis. Table 2.2-3 provides similar information for the Yankee-MPC GTCC waste configuration. The design weight of the NAC-STC "loaded with fuel/ready for transport" in the Yankee-MPC configuration is also 250,000 pounds. This design weight is used in all normal transport, hypothetical accident, and lifting/handling analyses.

Similarly, The calculated weights of the major components of the CY-MPC canistered fuel and GTCC waste configurations of the NAC-STC are tabulated in Tables 2.2-4 and 2.2-5, respectively. The tables also present a summary of the weights and center of gravity locations of the NAC-STC for the three CY-MPC cask configurations most likely to occur – empty, under the hook loaded with fuel, and loaded with fuel/ready for transport. The "empty" weight excludes the transportable storage canister but includes the canister spacer weight. The term "loaded with fuel" refers to the loaded CY-MPC canister in the cask, with the noted number of design basis fuel assemblies in the basket. "Under-the-hook loaded with fuel" describes the loaded NAC-STC without the outer lid in place, and with the yoke. "Loaded with fuel/ready for transport" describes the loaded NAC-STC with helium in the cavity and the upper and lower impact limiters installed on the cask. The axial locations of the centers of gravity are measured from the bottom outer surface of the cask body. The centers of gravity are on the axial centerline of the cask because it is essentially symmetric about that axis. Table 2.2-5 provides similar information for the CY-MPC GTCC waste configuration. The design weight of the NAC-STC "loaded with fuel/ready for transport" in the CY-MPC configuration is 260,000 pounds. This design weight is used in all normal transport, hypothetical accident, and lifting/handling analyses.

Table 2.2-1 NAC-STC Calculated Weights and Centers of Gravity for Directly Loaded Fuel

Component	Calculated Weight (lbs)	Center of Gravity* (in)	Calculated Weight (lbs)	Center of Gravity* (in)
Impact Limiter Configuration	Redwood		Balsa	
Body Assembly	157,160		157,160	
Outer Lid	8,120		8,120	
Inner Lid	10,690		10,690	
TOTAL	175,970	96.8	175,970	96.8
Fuel (26 PWR Assemblies @ 1,500 lbs)	39,000		39,000	
Fuel Basket	16,820		16,820	
Water In Cavity	16,430		16,430	
Yoke	2,150		2,150	
Transport Impact Limiters				
Top	8,865	203.6	5,787	203.6
Bottom	8,865	-10.5	5,636	-10.5
TOTAL WEIGHT				
Empty	192,790	96.8	192,790	96.8
Under-the-Hook Loaded with Fuel	242,250	96.0	242,250	96.0
Loaded with Fuel/Ready for Transport	249,520	96.0	243,213	96.0
Design - Loaded with Fuel/Ready for Transport	250,000	96.0	250,000	96.0

* Measured from bottom outer surface of cask body.

Table 2.2-2 NAC-STC Calculated Weights and Centers of Gravity for Yankee-MPC Canistered Fuel

Component	Calculated Weight (lbs)	Center of Gravity* (in)	Calculated Weight (lbs)	Center of Gravity* (in)
Impact Limiter Configuration	Redwood		Balsa	
Body Assembly	157,160		157,160	
Outer Lid	8,120		8,120	
Inner Lid	10,690		10,690	
TOTAL	175,970	96.8	175,970	96.8
Fuel **	30,600	N/A	30,600	N/A
Fuel Basket	9,530	N/A	9,530	N/A
Canister w/Lids	14,600	N/A	14,600	N/A
Spacers				
Top	510	N/A	510	N/A
Bottom	350	N/A	350	N/A
TOTAL WEIGHT OF CONTENTS (Canistered Fuel Basket Configuration)	55,590	N/A	55,590	N/A
Yoke	2,150	N/A	2,150	N/A
Transport Impact Limiters				
Top	8,865	203.6	5,787	203.6
Bottom	8,865	-10.5	5,636	-10.5
TOTAL WEIGHT OF NAC-STC				
Empty	176,830	N/A	176,830	N/A
Under-the-Hook Loaded with Fuel	233,710	N/A	233,710	N/A
Loaded with Fuel/Ready for Transport	249,290	96.0	242,983	96.0
Design - Loaded with Fuel/Ready for Transport	250,000	96.0	250,000	96.0

* Measured from bottom outer surface of cask body.

** Maximum fuel assembly weight is 950 lbs.

Table 2.2-3 NAC-STC Calculated Weights and Centers of Gravity for Canistered
Yankee-MPC GTCC Waste

Component	Calculated Weight (lbs)	Center of Gravity* (in)	Calculated Weight (lbs)	Center of Gravity* (in)
Impact Limiter Configuration	Redwood		Balsa	
Body Assembly	157,160		157,160	
Outer Lid	8,120		8,120	
Inner Lid	10,690		10,690	
TOTAL	175,970	96.8	175,970	96.8
GTCC Waste (24 Tubes Full @ 514 lbs)	12,340	N/A	12,340	N/A
Basket - GTCC Waste	26,471		26,471	
Canister w/Lids	14,600	N/A	14,600	N/A
Spacers				
Top	510	N/A	510	N/A
Bottom	350	N/A	350	N/A
Yoke	2,150	N/A	2,150	N/A
Transport Impact Limiters				
Top	8,865	203.6	5,787	203.6
Bottom	8,865	-10.5	5,636	-10.5
TOTAL WEIGHT				
STC Empty with spacers	176,830	N/A	176,830	N/A
Under-the-Hook Loaded with GTCC Waste	232,391	N/A	232,391	N/A
Loaded with GTCC Waste, Ready for Transport	247,971	N/A	241,664	N/A
Design - Loaded with Fuel or GTCC Waste, Ready for Transport	250,000	96.0	250,000	96.0

* Measured from bottom outer surface of cask body.

Table 2.2-4 NAC-STC Calculated Weights and Centers of Gravity for CY-MPC Canistered Fuel

Component	Calculated Weight 24 Fuel Assemblies (lbs)	Calculated Weight 26 Fuel Assemblies (lbs)	Center of Gravity ¹ (in)
Transport cask body assembly	157,160	157,160	-
Outer lid	8,120	8,120	-
Inner lid	10,690	10,690	-
TOTAL	175,970	175,970	96.8
Fuel	32,400	35,100	N/A
Fuel basket	13,843	14,055	-
Canister with lids	16,666	16,666	N/A
Spacer	1,374	1,374	-
TOTAL WEIGHT OF CONTENTS	64,283	67,195	N/A
Yoke	2,150	2,150	N/A
Transport impact limiters ²	-	-	-
Top	5,787	5,787	205.6
Bottom	5,636	5,636	-15.1
TOTAL WEIGHT of the NAC-STC with the CY-MPC			
Under-the-hook loaded with fuel	242,403	245,315	N/A
Loaded with fuel/ready for transport	251,676	254,588	98.9
Design - Loaded with Fuel - Ready for Transport	260,000	260,000	98.9

1. Measured from bottom outer surface of cask body.

2. Redwood impact limiters cannot be used for the transport of the CY-MPC canister.

Table 2.2-5 NAC-STC Calculated Weights and Centers of Gravity for Canistered CY-MPC GTCC Waste

Component	Calculated weight (lb)	Center of gravity¹ (in.)
Transport cask body assembly	157,160	-
Outer lid	8,120	-
Inner lid	10,690	-
TOTAL	175,970	96.8
24 GTCC Containers	18,742	-
GTCC basket	30,413	-
Canister with lids	16,666	-
Spacer	1,374	-
TOTAL WEIGHT OF CONTENTS	67,196	N/A
Yoke	2,150	N/A
Transport impact limiters ²	-	-
Top	5,787	205.6
Bottom	5,636	-15.1
TOTAL WEIGHT of the NAC-STC with the CY-MPC	-	-
Under-the-hook loaded with waste	245,316	96.4
Loaded with waste/ready for transport	254,589	99.0
Design - Loaded with waste - Ready for Transport	260,000	99.0

1. Measured from bottom outer surface of cask body.

2. Redwood impact limiters cannot be used for the transport of the CY-MPC canister.

THIS PAGE INTENTIONALLY LEFT BLANK

2.3 Mechanical Properties of Materials

2.3.1 Discussion

The structural analyses of the NAC-STC for the normal conditions of transport and the hypothetical accident load conditions use the mechanical properties of the component materials at the appropriate temperature. The mechanical properties at the applicable temperature are also used in calculating the allowable stresses in each component analysis.

The NAC-STC is fabricated from several different materials. Most of the cask body—the center section of the inner shell, the outer shell, the cask bottom, the top forging, and the neutron shield shell—is Type 304 stainless steel. The 31-inch long inner shell rings at each end of the inner shell are Type XM-19 high-strength stainless steel. The remainder of the cask body consists of chemical lead gamma radiation shielding and borated NS-4-FR solid neutron radiation shielding (The radial neutron shield region also contains explosively-bonded copper/Type 304 stainless steel heat transfer “fins.”). The inner lid is Type 304 stainless steel. The outer lid, the outer lid bolts, the port covers, the lifting trunnions, and the rotation trunnion recesses are SA-705 or SA-564, Type 630, H1150 17-4 PH stainless steel. The inner lid bolts are SB-637, Grade N07718 nickel alloy bolting material. The bolts for the port covers and port coverplates are SA-193, Grade B6 (Type 410) stainless steel. The fuel basket is an assembly of SA-693 or SA-564, Type 630, H1150 17-4 PH stainless steel support disks, threaded rods and spacer nuts, Type 304 stainless steel top and bottom end plates, and fuel tubes. Fuel basket heat transfer disks are Type 6061-T651 aluminum alloy. The impact limiters are redwood and balsa or are all balsa encased in thin stainless steel shells. For the canistered configuration of the NAC-STC, the canister and its structural lid are Type 304L stainless steel. The remaining components of the canister and baskets (fuel and GTCC waste) are Type 304 stainless steel with the exception of the support disks, which are 17-4 PH stainless steel, and the heat transfer disks, which are 6061-T651 aluminum alloy. The top and bottom cavity spacers are 5056 aluminum honeycomb encased in thin 6061-T6 aluminum alloy shells for the Yankee-MPC configuration. A single Type 304 stainless steel bottom spacer is used for the CY-MPC configuration.

The “ASME Boiler and Pressure Vessel Code,” Section III, Appendix I, and Standard Handbook for Mechanical Engineers (Baumeister) are the sources of the mechanical properties of Type 304 stainless steel; Type XM-19 stainless steel; SA-705 and SA-564, Type 630, H1150 17-4 PH stainless steel; SB-637, Grade N07718 nickel alloy steel bolting material; SA-193, Grade B6 (Type 410) stainless steel, Type 6061-T6 aluminum alloy, and Type 6061-T651 aluminum alloy.

The effects of temperature variations on the mechanical properties are included. The coefficients of thermal expansion presented in this section represent the mean value for the temperature range from 70°F to the indicated temperature.

2.3.2 Austenitic Stainless Steels

The primary structural components of the NAC-STC body, excluding: (1) the inner shell rings (transition sections of the inner shell); (2) the outer lid; (3) the lifting trunnions; and (4) the rotation trunnion recesses, are fabricated from Type 304 stainless steel. In addition to the cask body components fabricated from Type 304 stainless steel, the fuel tubes and fuel basket top and bottom weldment plates are fabricated from the same material. This material is selected because it is strong, ductile, and highly resistant to corrosion and brittle fracture. Type XM-19 stainless steel is selected for the inner shell rings at the ends of the inner shell because the high strength of Type XM-19 stainless steel provides additional resistance to shear buckling in those sections of the inner shell.

The mechanical properties of SA-240 (plate), Type 304 stainless steel are tabulated in Table 2.3.2-1. The mechanical properties of SA-336 (forging), Type 304 stainless steel are tabulated in Table 2.3.2-2. The mechanical properties of SA-240 (plate), Type XM-19 stainless steel are tabulated in Table 2.3.2-3.

The primary structural components of the Yankee-MPC and CY-MPC canisters and baskets, excluding the support disks and heat transfer disks, are fabricated from Type 304 and Type 304L stainless steels. This material is selected because it is strong, ductile, and highly resistant to corrosion and brittle fractures. The associated mechanical properties of the Type 304 and 304L stainless steels are tabulated in Tables 2.3.2-1, 2.3.2-2 and 2.3.2-4.

Table 2.3.2-1 Mechanical Properties of SA 240, Type 304 Stainless Steel

Property (units)	Temperature (°F)							
	-40	-20	+70	+200	+300	+400	+500	+750
Ultimate Strength ¹ (ksi)	75.0	75.0	75.0	71.0	66.0	64.4	63.5	63.1
Yield Strength ² (ksi)	30.0	30.0	30.0	25.0	22.5	20.7	19.4	17.3
Design Stress Intensity ³ (ksi)	20.0	20.0	20.0	20.0	20.0	18.7	17.5	15.6
Modulus of Elasticity ⁴ (ksi)	28.7E+3	28.7E+3	28.3E+3	27.6E+3	27.0E+3	26.5E+3	25.8E+3	24.4E+3
Alternating Stress ⁵ @ 10 cycles (ksi)	718.0	718.0	708.0	690.5	675.5	663.0	645.5	610.4
Alternating Stress ⁵ @ 10 ⁶ cycles (ksi)	28.7	28.7	28.3	27.6	27.0	26.5	25.8	24.4
Coefficient of Thermal Expansion ⁶ (in/in/°F)	8.13E-6	8.19E-6	8.46E-6	8.79E-6	9.00E-6	9.19E-6	9.37E-6	9.76E-6
Poisson's Ratio ⁷	0.31							
Density (lbm/in ³)	497 lbm/ft ³ (0.288 lbm/in ³)							

¹ "ASME Boiler and Pressure Vessel Code," Section III, Division 1, Appendix I, Table I-3.2.

² "ASME Boiler and Pressure Vessel Code," Section III, Division 1, Appendix I, Table I-2.2.

³ "ASME Boiler and Pressure Vessel Code," Section III, Division 1, Appendix I, Table I-1.2.

⁴ "ASME Boiler and Pressure Vessel Code," Section III, Division 1, Appendix I, Table I-6.0.

⁵ "ASME Boiler and Pressure Vessel Code," Section III, Division 1, Appendix I, Table I-9.1.

⁶ "ASME Boiler and Pressure Vessel Code," Section III, Division 1, Appendix I, Table I-5.0.

⁷ "ASME Boiler and Pressure Vessel Code," Section II, Part D, Table NF-1.

Table 2.3.2-2 Mechanical Properties of SA 336, Type 304 Stainless Steel

Property (units)	Temperature (°F)							
	-40	-20	+70	+200	+300	+400	+500	+750
Ultimate Strength ¹ (ksi)	70.0	70.0	70.0	66.2.0	61.5	60.0	59.3	58.9
Yield Strength ² (ksi)	30.0	30.0	30.0	25.0	22.5	20.7	19.4	17.3
Design Stress Intensity ³ (ksi)	20.0	20.0	20.0	20.0	20.0	18.7	17.5	15.6
Modulus of Elasticity ⁴ (ksi)	28.7E+3	28.7E+3	28.3E+3	27.6E+3	27.0E+3	26.5E+3	25.8E+3	24.4E+3
Alternating Stress ⁵ @ 10 cycles (ksi)	718.0	718.0	708.0	690.5	675.5	663.0	645.5	610.4
Alternating Stress ⁵ @ 10 ⁶ cycles (ksi)	28.7	28.7	28.3	27.6	27.0	26.5	25.8	24.4
Coefficient of Thermal Expansion ⁶ (in/in/°F)	8.13E-6	8.19E-6	8.46E-6	8.79E-6	9.00E-6	9.19E-6	9.37E-6	9.76E-6
Poisson's Ratio ⁷	0.31							
Density ⁸ (lbm/in ³)	497 lbm/ft ³ (0.288 lbm/in ³)							

¹ "ASME Boiler and Pressure Vessel Code," Section III, Division 1, Appendix I, Table I-3.2.

² "ASME Boiler and Pressure Vessel Code," Section III, Division 1, Appendix I, Table I-2.2.

³ "ASME Boiler and Pressure Vessel Code," Section III, Division 1, Appendix I, Table I-1.2.

⁴ "ASME Boiler and Pressure Vessel Code," Section III, Division 1, Appendix I, Table I-6.0.

⁵ "ASME Boiler and Pressure Vessel Code," Section III, Division 1, Appendix I, Table I-9.1.

⁶ "ASME Boiler and Pressure Vessel Code," Section III, Division 1, Appendix I, Table I-5.0.

⁷ "ASME Boiler and Pressure Vessel Code," Section II, Part D, Table NF-1.

⁸ "Nuclear Materials Handbook," Volume 1, Design Data, Property Code 3304.

Table 2.3.2-3 Mechanical Properties of Type XM-19 Stainless Steel

Property (units) ⁹	Temperature (°F)							
	-40	-20	+70	+200	+300	+400	+500	+750
Ultimate Strength ¹ (ksi)	100.0	100.0	100.0	99.5	94.3	90.7	89.1	85.7
Yield Strength ² (ksi)	55.0	55.0	55.0	47.0	43.4	40.8	38.8	35.8
Design Stress Intensity ³ (ksi)	33.3	33.3	33.3	33.2	31.4	30.2	29.7	28.5
Modulus of Elasticity ⁴ (ksi)	28.3E+3	28.3E+3	28.3E+3	27.0E+3	27.0E+3	26.5E+3	25.8E+3	24.4E+3
Alternating Stress ⁵ @ 10 cycles (ksi)	708.0	708.0	708.0	690.5	675.5	663.0	645.5	610.4
Alternating Stress ⁵ @ 10 ⁶ cycles (ksi)	28.3	28.3	28.3	27.6	27.0	26.5	25.8	24.4
Coefficient of Thermal Expansion ⁶ (in/in/°F)	8.13E-6	8.19E-6	8.46E-6	8.79E-6	9.00E-6	9.19E-6	9.37E-6	9.76E-6
Poisson's Ratio ⁷	0.31							
Density ⁸ (lbm/in ³)	497 lbm/ft ³ (0.288 lbm/in ³)							

1 "ASME Boiler and Pressure Vessel Code," Section III, Division 1, Appendix I, Table I-3.1.

2 "ASME Boiler and Pressure Vessel Code," Section III, Division 1, Appendix I, Table I-2.1.

3 "ASME Boiler and Pressure Vessel Code," Section III, Division 1, Appendix I, Table I-1.1.

4 "ASME Boiler and Pressure Vessel Code," Section III, Division 1, Appendix I, Table I-6.0.

5 "ASME Boiler and Pressure Vessel Code," Section III, Division 1, Appendix I, Table I-9.1.

6 "ASME Boiler and Pressure Vessel Code," Section III, Division 1, Appendix I, Table I-5.0.

7 "ASME Boiler and Pressure Vessel Code," Section II, Part D, Table NF-1.

8 "Nuclear Materials Handbook," Volume 1, Design Data, Property Code 3304.

9 SA-182, FXM-19 stainless steel may be substituted for SA-240 XM-19 stainless steel provided that the SA-182 material yield and ultimate strengths are equal to or greater than those of the SA-240 material. The SA-182 forging material and the SA-240 plate material are both XM-19 austenitic stainless steels. Austenitic stainless steels do not experience a ductile-to-brittle transition for the range of temperatures considered in this Safety Analysis Report. Therefore, fracture toughness is not a concern.

Table 2.3.2-4 Mechanical Properties of SA-240, Type 304L Stainless Steel

Property (units)	Temperature (°F)							
	-40	-20	+70	+200	+300	+400	+500	+750
Ultimate Strength ¹ (ksi)	70.0	70.0	70.0	66.2	60.9	58.5	57.8	55.9
Yield Strength ² (ksi)	25.0	25.0	25.0	21.4	19.2	17.5	16.4	14.7
Design Stress Intensity ³ (ksi)	16.7	16.7	16.7	16.7	16.7	15.8	14.8	13.3
Modulus of Elasticity ⁴ (ksi)	28.7E+3	28.7E+3	28.3E+3	27.6E+3	27.0E+3	26.5E+3	25.8E+3	24.4E+3
Alternating Stress ⁵ @ 10 cycles (ksi)	718.0	718.0	708.0	690.5	675.5	663.0	645.5	610.4
Alternating Stress ⁵ @ 10 ⁶ cycles (ksi)	28.7	28.7	28.3	27.6	27.0	26.5	25.8	24.4
Coefficient of Thermal Expansion ⁶ (in/in/°F)	8.13E-6	8.19E-6	8.46E-6	8.79E-6	9.00E-6	9.19E-6	9.37E-6	9.76E-6
Poisson's Ratio ⁷	0.31							
Density ⁸ (lbm/in ³)	503 lbm/ft ³ (0.291 lbm/in ³)							

¹ "ASME Boiler and Pressure Vessel Code," Section II, Part D, Table U.

² "ASME Boiler and Pressure Vessel Code," Section II, Part D, Table Y-1.

³ "ASME Boiler and Pressure Vessel Code," Section II, Part D, Table 2A.

⁴ "ASME Boiler and Pressure Vessel Code," Section II, Part D, Table TM-1.

⁵ "ASME Boiler and Pressure Vessel Code," Section III, Appendix I, Table I-9.1.

⁶ "ASME Boiler and Pressure Vessel Code," Section II, Part D, Table TE-1.

⁷ "ASME Boiler and Pressure Vessel Code," Section II, Part D, Table NF-1.

⁸ "ASME Boiler and Pressure Vessel Code," Section II, Part D, Table NF-2.

THIS PAGE INTENTIONALLY LEFT BLANK

2.3.3 Precipitation-Hardened Stainless Steel

SA-705, SA-693 or SA-564, Type 630, H1150 17-4 PH stainless steel is selected for the NAC-STC outer lid, outer lid bolts, port covers, lifting trunnions, rotation trunnion recesses, and fuel basket structural components because of its high strength combined with good corrosion and brittle fracture resistance. The 17-4 PH or the Type 630, as it is identified in the ASME Code, is a ferritic steel with 17 percent chromium and four percent nickel as compared to Type 304 austenitic steel, which has 18 percent chromium and eight percent nickel. Both materials are referred to as stainless steel by the metals industry and throughout this document. The mechanical properties of this precipitation-hardened stainless steel are tabulated in Table 2.3.3-1.

Table 2.3.3-1 Mechanical Properties of SA-705, SA-693 and SA-564, Type 630,
H1150, 17-4 PH Stainless Steel

Property (units)	Temperature (°F)							
	-40	-20	+70	+200	+300	+400	+500	+650
Ultimate Strength ¹ (ksi)	135.0	135.0	135.0	135.0	135.0	131.4	128.5	125.7 ²
Yield Strength ³ (ksi)	105.0	105.0	105.0	97.1	93.0	89.5	87.0	83.6
Design Stress Intensity ⁴ (ksi)	45.0	45.0	45.0	45.0	45.0	43.8	42.8	41.9
Modulus of Elasticity ⁵ (ksi)	28.7E+3	28.7E+3	28.3E+3	27.6E+3	27.0E+3	26.5E+3	25.8E+3	25.1E+3
Alternating Stress ⁶ @ 10 cycles (ksi)	401.8	401.8	396.2	386.4	378.0	371.0	361.2	341.6
Alternating Stress ⁶ @ 10 ⁶ cycles (ksi)	19.1	19.1	18.9	18.4	18.0	17.7	17.2	16.3
Coefficient of Thermal Expansion ⁷ (in/in/°F)	5.88E-6	5.88E-6	5.89E-6	5.90E-6	5.90E-6	5.91E-6	5.91E-6	5.93E-6
Poisson's Ratio	0.287							
Density (lbm/in ³)	487 lbm/ft ³ (0.282 lbm/in ³)							

1. "ASME Boiler and Pressure Vessel Code," Section III, Division 1, Appendix I, Table I-3.1.
2. Obtained by ratioing from the Design Stress Intensity values.
3. "ASME Boiler and Pressure Vessel Code," Section III, Division 1, Appendix I, Table I-2.1.
4. "ASME Boiler and Pressure Vessel Code," Section III, Division 1, Appendix I, Table I-1.1.
5. "ASME Boiler and Pressure Vessel Code," Section III, Division 1, Appendix I, Table I-6.0.
6. "ASME Boiler and Pressure Vessel Code," Section III, Division 1, Appendix I, Table I-9.1.
7. "ASME Boiler and Pressure Vessel Code," Section III, Division 1, Appendix I, Table I-5.0.

2.3.4 Bolting Materials

The bolting materials for the NAC-STC are selected to provide high strength, good resistance to corrosion and brittle fracture, and coefficients of thermal expansion that are similar to those of the components being joined.

The outer lid bolts are SA-564, Type 630, H1150, 17-4 PH stainless steel with mechanical properties as tabulated in Table 2.3.3-1. The mechanical properties for the inner lid bolt material--SB-637, Grade N07718 nickel alloy bolting material—are tabulated in Table 2.3.4-1. The mechanical properties for the port cover bolts, port coverplate bolts, and fuel/basket spacer bolts material—SA-193, Grade B6 (Type 410) stainless steel--are tabulated in Table 2.3.4-2.

Table 2.3.4-1 Mechanical Properties of SB-637, Grade N07718 Nickel Alloy Steel
Bolting Material

Property (units)	Temperature (°F)							
	-40	-20	+70	+200	+300	+400	+500	+750
Ultimate Strength (ksi)	185.0 ¹	185.0 ¹	185.0 ¹	177.6 ⁵	173.5 ⁵	170.6 ⁵	168.7 ⁵	165.0 ⁵
Yield Strength (ksi)	150.0 ¹	150.0 ¹	150.0 ¹	144.0 ⁵	140.7 ⁵	138.3 ⁵	136.8 ⁵	133.8 ⁵
Design Stress Intensity ¹ (ksi)	50.0	50.0	50.0	48.0	46.9	46.1	45.6	44.6
Modulus of Elasticity ² (ksi)	29.6E+3	29.5E+3	29.0E+3	28.3E+3	27.8E+3	27.6E+3	27.1E+3	26.1E+3
Coefficient of Thermal Expansion ³ (in/in/°F)	6.87E-6	6.90E-6	7.15E-6	7.22E-6	7.33E-6	7.45E-6	7.57E-6	7.82E-6
Alternating Stress ⁴ @ 10 ⁶ cycles (ksi)	13.3	13.7	13.1	12.7	12.5	12.4	12.2	11.7
Poisson's Ratio	0.32							
Density (lbm/in ³)	489 lbm/ft ³ (0.283 lbm/in ³)							

¹ "ASME Boiler and Pressure Vessel Code," Section III, Division 1, Appendix I, Table I-1.3.

² "ASME Boiler and Pressure Vessel Code," Section III, Division 1, Appendix I, Table I-6.0.

³ "ASME Boiler and Pressure Vessel Code," Section III, Division 1, Appendix I, Table I-5.0.

⁴ "ASME Boiler and Pressure Vessel Code," Section III, Division 1, Appendix I, Table I-9.1, Figure I-9.4.

⁵ Obtained by ratioing from the design stress intensity values.

Table 2.3.4-2 Mechanical Properties of SA-193, Grade B6, High Alloy Steel Bolting Material

Property (units)	Temperature (°F)							
	-40	-20	+70	+200	+300	+400	+500	+750
Ultimate Strength (ksi)	110.0 ¹	110.0 ¹	110.0 ¹	104.9 ²	101.5 ²	98.3 ²	95.6 ²	89.4 ²
Yield Strength (ksi)	85.0 ¹	85.0 ¹	85.0 ¹	81.2 ²	78.4 ²	76.0 ²	73.9 ²	69.1 ²
Design Stress Intensity ¹ (ksi)	28.3	28.3	28.3	27.0	26.1	25.3	24.6	23.0
Modulus of Elasticity ⁵ (ksi)	28.8E+3	28.7E+3	28.3E+3	27.6E+3	27.0E+3	26.5E+3	25.8E+3	24.4E+3
Coefficient of Thermal Expansion ⁴ (in/in/°F)	5.73E-6	5.76E-6	5.92E-6	6.15E-6	6.30E-6	6.40E-6	6.48E-6	6.64E-6
Alternating Stress ⁵ @ 10 cycles (ksi)	1104.4	1100.0	1085.0	1058.0	1035.0	1015.0	989.0	935.3
Alternating Stress ⁵ @ 10 ⁶ cycles (ksi)	13.0	12.9	12.7	12.4	12.2	11.9	11.6	11.0
Poisson's Ratio	0.32							
Density (lbm/in ³)	489 lbm/ft ³ (0.283 lbm/in ³)							

¹ "ASME Boiler and Pressure Vessel Code," Section III, Division 1, Appendix I, Table I-1.3.

² Tabulated value is calculated by ratioing from the Design Stress Intensity.

³ "ASME Boiler and Pressure Vessel Code," Section III, Division 1, Appendix I, Table I-6.0.

⁴ "ASME Boiler and Pressure Vessel Code," Section III, Division 1, Appendix I, Table I-5.0.

⁵ "ASME Boiler and Pressure Vessel Code," Section III, Division 1, Appendix I, Table I-9.1, Figure I-9.4.

THIS PAGE INTENTIONALLY LEFT BLANK

2.3.5 Aluminum Alloys

SB-209, Type 6061-T651, aluminum alloy is selected to fabricate the fuel basket heat transfer disks. These disks are not safety related structural load path components and are attached to the fuel basket solely to enhance heat transfer performance of the fuel support structures. The Type 6061-T651 material is selected for high thermal conductivity relative to material weight in addition to being an ASME approved material.

The mechanical properties of SB-209, Type 6061-T651 and Type 6061-T6 aluminum alloy are tabulated in Table 2.3.5-1. These material properties are provided for information and are not intended as documentation for the structural performance of the NAC-STC package. Influence of time and temperature on these properties not identified in the ASME material information is from MIL-HDBK-5F.

The mechanical properties of Type 6061-T651 aluminum alloy for the heat transfer disk in the canistered fuel basket are tabulated in Table 2.3.5-1. There are no heat transfer disks in the canistered GTCC waste basket.

Table 2.3.5-1 Mechanical Properties of 6061-T651 and 6061-T6 Aluminum Alloy

Property (units)	Temperature (°F)						
	+70	+100	+200	+300	+400	+500	+600
Ultimate Strength ^{1,2} (ksi)	42.0	40.7	38.2	31.5	17.2	6.7	3.4
Yield Strength ^{1,2} (ksi)	35.0	33.9	32.2	26.9	14.0	5.3	2.5
Design Stress ¹ Intensity ¹ (ksi)	10.5	10.5	10.5	8.4	4.4	N/A	N/A
Modulus of Elasticity ³ (ksi)	10.0E+3	9.9E+3	9.6E+3	9.2E+3	8.7E+3	8.13E+3 ₅	7.0E+3 ⁵
Coefficient of Thermal Expansion ⁴ (in/in/°F)	—	12.6E-6	12.9E-6	13.22E-6	13.52E-6	13.7E-6 ⁶	14.3E-6 ⁶
Poisson's Ratio	0.33						
Density (lbm/in ³)	0.102						

¹ "ASME Boiler and Pressure Vessel Code," Section III Division 1, Appendix I, Table I-8.4.

² Strength at elevated temperatures calculated using the following relationships from MIL-HDBK-5F, Figures 3.6.2.2.1(a) and 3.6.2.2.1(b);
 $S_{uTemp} = (\%) (S_{u70})$, $S_{yTemp} = (\%) (S_{y70})$

Temp°F	% Value @ Room Temperature					
	100	200	300	400	500	600
S_u	97	91	75	41	16	8
S_y	97	92	77	40	15	7

³ "ASME Boiler and Pressure Vessel Code," Section III, Division 1, Appendix I, Table I-6.0.

⁴ "ASME Boiler and Pressure Vessel Code," Section III, Division 1, Appendix I, Table I-5.0.

⁵ MIL-HDBK-5F, Figure 3.6.2.2.4.

⁶ MIL-HDBK-5F, Figure 3.6.2.0.

2.3.6 Shielding Material

Gamma radiation shielding for the NAC-STC is provided by the steel cask body and lids and by lead in the cask wall. The primary radial gamma radiation shielding for the cask is provided by a cylinder of chemical copper grade lead, which fills the annulus between the inner shell and the outer shell. There is no concern that the lead will experience large deformation or volume change, since it is completely enclosed and is essentially incompressible.

Neutron radiation shielding for the NAC-STC is provided by a solid synthetic polymer, NS-4-FR, located in each end of the cask and around the outside of the outer shell. The solid neutron shield material eliminates leakage and maintenance concerns associated with liquid neutron shields. The NS-4-FR neutron shielding function requires no strength and none is assumed for the structural evaluations.

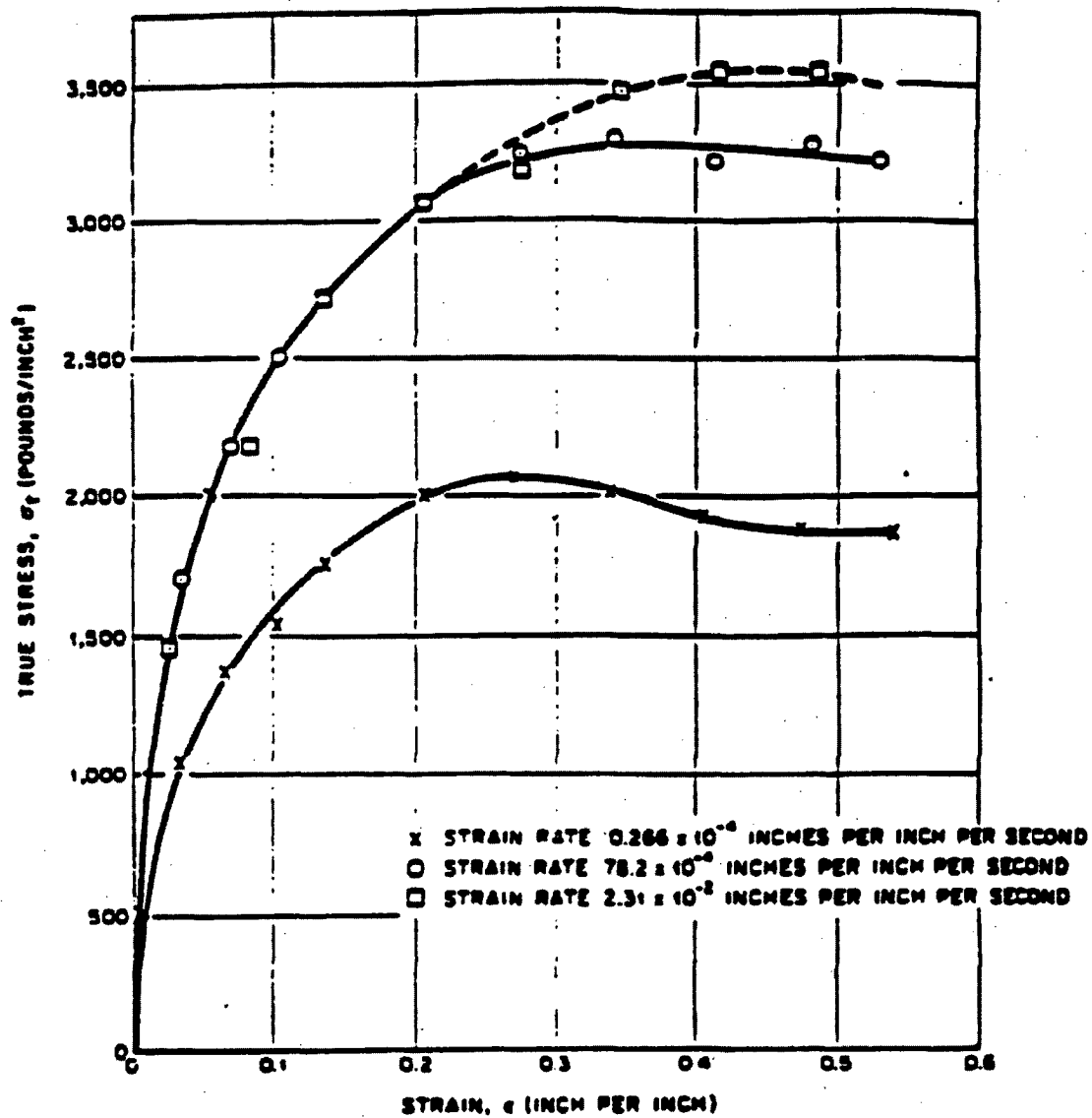
2.3.6.1 Chemical Copper Grade Lead

The coefficient of thermal expansion for lead is of particular significance because it is approximately twice that of stainless steel. The static mechanical properties of Chemical Copper Grade Lead are tabulated in Table 2.3.6-1, and the stress-strain curve for Chemical Copper Grade Lead is presented in Figure 2.3.6-1.

2.3.6.2 NS-4-FR

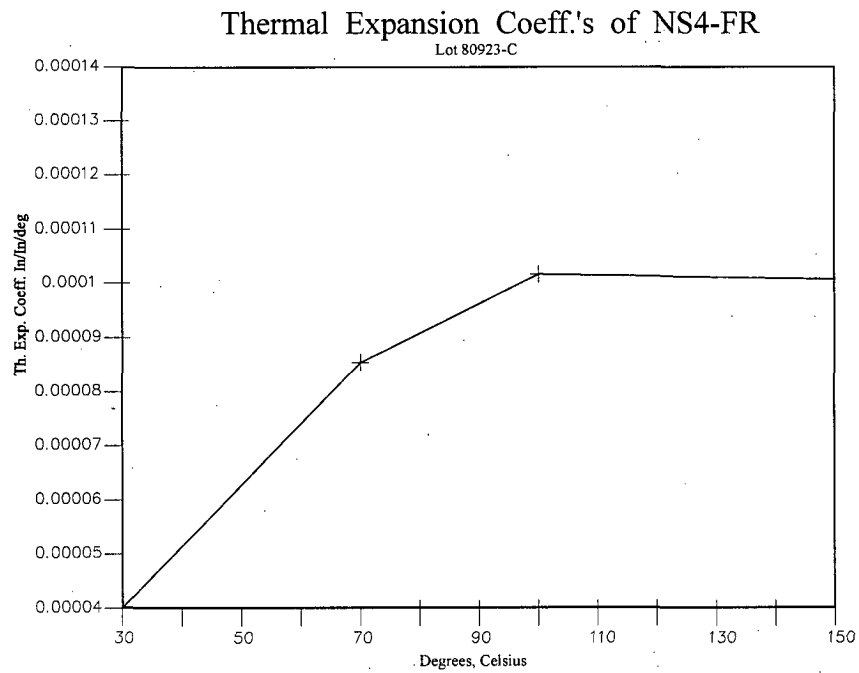
The NS-4-FR neutron shielding material was developed by BISCO Products, Inc. and is now supplied by the Japan Atomic Power Company (JAPC). The mechanical properties of NS-4-FR are tabulated in Table 2.3.6-2. The thermal expansion coefficient is shown in Figure 2.3.6-2.

Figure 2.3.6-1 Quasi-Static True Stress-Strain Curves for Chemical Copper Grade Lead in Compression



Reference: Evans

Figure 2.3.6-2 Neutron Shield Thermal Expansion Coefficient



Note: BISCO Products Data

Table 2.3.6-1 Static Mechanical Properties of Chemical Copper Grade Lead

Property (units)	Temperature (°F)					
	-40	-20	+70	+200	+300	+600
Ultimate Strength ^{1,2} (ksi)	700	680	640	490	380	20
Modulus of Elasticity ³ (ksi)	2.45E+3	2.42E+3	2.28E+3	2.06E+3	1.94E+3	1.5E+3
Coefficient of Thermal Expansion ³ (in/in/°F)	15.6E-6	15.7E-6	16.1E-6	16.6E-6	17.2E-6	20.2E-6
Poisson's Ratio	0.40					
Density (lbm/in ³)	708 lbm/ft ³ (0.41 lbm/in ³)					

- ¹ Tietz.
² Gallagher.
³ NUREG/CR-0481, pages 42, 56 and 66.
⁴ Baumeister, page 6-10.

Table 2.3.6-2 Mechanical Properties of NS-4-FR

Property ¹ (units)	Value
Compressive Modulus (ksi)	561
Coefficient of Thermal Expansion (in/in/°F)	Refer to Figure 2.3.6-2
Density (lbm/in ³)	0.0607

¹ BISCO Products Data.

THIS PAGE INTENTIONALLY LEFT BLANK

2.3.7 Impact Limiter Materials

The transport impact limiters for the NAC-STC are fabricated in two configurations. The first configuration is the "redwood impact limiter," which is described in Section 2.6.7.4.1. The second configuration is the "balsa impact limiter," described in Section 2.6.7.4.2. The balsa impact limiter weighs significantly less than the redwood impact limiter. Both impact limiter configurations absorb the energy of a cask drop impact by crushing the redwood and/or balsa wood in the impact limiter.

The evaluation of the redwood impact limiter design employs the properties for redwood and balsa wood contained in Figures 2.6.7.4.1-3 through 2.6.7.4.1-5. These figures present the crush stress-strain curves for redwood and balsa wood materials.

The evaluation of the balsa impact limiter design employs the properties for redwood and balsa contained in Tables 2.6.7.4.2-1 and 2.6.7.4.2-2. These tables present the crush stress-strain data for redwood and balsa wood materials, respectively.

THIS PAGE INTENTIONALLY LEFT BLANK

2.3.8 Spacer Materials

Spacers are installed in the NAC-STC cask cavity for the transport of the Yankee-MPC and CY-MPC canisters containing either spent fuel or GTCC waste. The spacers are designed to locate the canister axially in the cavity so that the package center of gravity is located approximately in the same position as that of the directly loaded fuel configuration of the cask. Removable lifting lugs are used to install and remove the spacer.

Two spacers (top and bottom) are used in the transport of the Yankee-MPC. Both spacers are fabricated from aluminum honeycomb encased in aluminum alloy shells.

The required aluminum honeycomb material properties are:

- nominal density = 4.5 pcf;
- crush strength = 320 psi;
- compressive strength = 700 psi (typical) and 500 psi (minimum).

The CY-MPC canister is longer than the Yankee-MPC canister and a single stainless steel spacer, installed below the canister, is used. The CY-MPC spacer is formed by a series of concentric rings welded to a stainless steel base plate and is nominally 12.7 inches high and 70.6 inches in diameter.

THIS PAGE INTENTIONALLY LEFT BLANK

2.4 General Standards for All Packages

This section demonstrates that the general requirements found in 10 CFR 71.43 are addressed in the design and analysis of the NAC-STC, a spent-fuel transport and storage packaging. A packaging is defined as the assembly of components necessary to ensure compliance with 10 CFR 71 for the transportation of radioactive contents. The package consists of the packaging with its radioactive contents.

THIS PAGE INTENTIONALLY LEFT BLANK

2.4.1 Minimum Package Size

The minimum transverse dimension of the NAC-STC package is 98.2 inches (249.4 cm), and the minimum longitudinal dimension is 192.96 inches (490.1 cm). Both dimensions are greater than 10 centimeters; therefore, the requirements of 10 CFR 71.43(a) are satisfied.

THIS PAGE INTENTIONALLY LEFT BLANK

2.4.2 Tamperproof Feature

One numbered, crimped wire seal is looped through a hole in the end flange of the lifting trunnion and through a similar hole in an adjacent corner of the upper impact limiter as a tamper indicator. It is necessary to remove the upper impact limiter in order to attain access to the NAC-STC closure assembly (outer lid with bolts and inner lid with bolts); thus, a severed seal will indicate purposeful tampering. This satisfies the Tamperproof Feature requirement of 10 CFR 71.43(b).

The vent port and drain port are protected by bolted coverplates and are located in the inner lid, where access can only be attained by removal of the outer lid. The interlid and pressure ports, which are located in the top forging, are protected by bolted port covers. The port cover bolts are drilled for the installation of lockwire and are crimp sealed with a numbered wireseal device. This satisfies the requirements of 10 CFR 71.43(b). Additionally, a special tool is required to remove these port covers.

THIS PAGE INTENTIONALLY LEFT BLANK

2.4.3 Positive Closure

Inadvertent opening of the inner lid, outer lid, port coverplates, or port covers from the combined effects of shock, vibration, thermal expansion, internal loads and/or external loads cannot occur because of the large preload applied to the lid bolts. Loosening of these bolts is resisted by friction from the large clamping forces produced by the applied bolt preload torque. A cask operations procedure is followed, ensuring that each bolt is torqued. The operating procedure states that bolt torquing is a quality assurance "hold point," requiring verification and witnessing signatures. It is necessary to deliberately loosen the bolts with a wrench to facilitate inadvertent opening. Evidence of attempted unauthorized operation of the cask closure is provided by tamper-indicating features (Section 2.4.2). Therefore, the NAC-STC containment system cannot be opened unintentionally and evidence of attempted unauthorized operation is provided; the requirements of 10 CFR 71.43(c) and (e) are satisfied.

THIS PAGE INTENTIONALLY LEFT BLANK

2.4.4 Chemical and Galvanic Reactions

The materials used in the fabrication and operation of the NAC-STC cask—including coatings, lubricants, and cleaning agents—have been evaluated to determine whether chemical, galvanic, or other reactions among the materials, contents, and environments can occur. All phases of operation—loading, unloading, handling, storage, and transportation—have been considered, in conjunction with the procedures described in Chapter 7, for the environments that may be encountered under normal, off-normal, or accident conditions. Based on the evaluation, there are no potential reactions that could adversely affect the overall integrity of the cask, the fuel basket, the transportable storage canister (when used), or the structural integrity and retrievability of the fuel from the cask. The evaluation conforms to the guidelines of NRC Bulletin 96-04, “Chemical, Galvanic, or Other Reactions in spent Fuel Storage and Transportation Casks,” dated July 5, 1996, and demonstrates that the NAC-STC cask meets the requirements of 10 CFR 71.43(d).

This section and Section 7.6 of the Operating Procedures describe the loading and closing of the transportable storage canisters. At the time of transport of the Yankee-MPC or CY-MPC canisters, the canisters will have been previously loaded and closed in accordance with the requirements of the NAC-MPC Safety Analysis Report for the NAC Multi-Purpose Canister System, Docket Number 72-1025. Since loading of the canisters in the NAC-STC is expected to be performed in a dry environment, there are no chemical, galvanic or corrosion reactions that occur between the stainless steel components of the NAC-STC and the stainless steel NAC-MPC canister. Once the canister is installed in the NAC-STC, the cask cavity atmosphere is inerted with dry helium, further reducing the potential for adverse reactions to occur within the cavity.

2.4.4.1 Component Operating Environment

Most of the component materials of the NAC-STC are exposed to one, or more, of three typical operating environments for casks: 1) a sealed internal cavity containing air, steam, helium, and spent fuel or other radioactive material; 2) an open internal cavity containing pool water (demineralized water - BWR, or borated water with a pH of 4.5 - PWR) and spent fuel or other radioactive material; 3) a sealed internal cavity containing helium, but with the cask in external surroundings, including air, rain water/snow/ice, and marine (salty) water/air. The spent fuel assemblies consist of Zircaloy or stainless steel clad fuel and other fuel assembly components of stainless steel.

Some of the cask components are completely enclosed and are exposed to an unchanging environment that is permanently sealed. These components include shielding materials and the energy-absorbing materials (impact limiters) that are only exposed to the temperature effects of the operating environments. The sealed shielding material regions are typically evacuated and backfilled with helium, while the impact limiter shells are leak tested following fabrication.

Each of the categories of cask component materials is evaluated for potential reactions in each of the operating environments to which those materials are exposed. These environments may occur during fuel loading or unloading, handling, storage or transport, including normal, off-normal, and accident conditions. Two of the operating environments to which the cask component materials are exposed do not provide the conditions necessary for a reaction (corrosion), since both moisture and oxygen must be present for corrosion to occur. The first of these environments is the sealed cavity, backfilled with helium. Helium displaces the oxygen in the cavity effectively precluding corrosion. Galvanic corrosion (i.e., between dissimilar metals that are in contact) could occur, but only if there is water present at the point of contact and the metals are in electrical contact with each other (i.e., mechanically held together). NAC's cask operating procedures provide two helium backfill cycles in series separated by a vacuum-drying cycle for the cask cavity during the preparation of the cask for storage or transport. Therefore, the cask cavity is effectively dry and galvanic corrosion is precluded. The second of these environments are those materials that are completely enclosed (permanently sealed) within another material, e.g., the primary shield materials—lead, NS-4-FR, or the criticality control material—borated aluminum, or the energy-absorbing materials - wood. For the metals, any oxygen that is trapped in the sealed region will be oxidized by the metals until thermodynamic equilibrium is reached, i.e., a thin oxide layer would develop on the lead or aluminum. In a similar manner for the NS-4-FR and the elastomers O-rings, any oxygen that is present will be captured by the hydrogen in the organic material until thermodynamic equilibrium is reached. Since the quantity of oxygen present, if any, is very small, equilibrium is reached very quickly and active corrosion in sealed regions does not occur.

2.4.4.2 Component Material Categories

The component materials evaluated are categorized based on similarity of physical and chemical properties and/or on similarity of component functions. The categories of materials that are considered are: 1) stainless/nickel alloy steels; 2) nonferrous metals; 3) shielding materials; 4) criticality control materials; 5) energy absorbing materials; 6) cellular foams and insulation's; 7) lubricants and greases; and 8) seals. These categories are evaluated based on the environment

to which they could be exposed during operation or use of the cask. The material categories and exposure environments are summarized in Table 2.4-1.

The cask component materials are not reactive among themselves, with the cask's contents, nor with the cask's operating environments during any phase of normal, off-normal, or accident condition loading, unloading, handling, storage or transportation operations. Therefore, since no reactions will occur, no gases or other corrosion byproducts will be generated.

2.4.4.2.1 Stainless/Nickel Alloy Steels

No reaction of the cask component steels (stainless or nickel alloy) is expected in any environment, except for the marine environment, where chloride-containing salt spray might initiate pitting of the steels if the chlorides are allowed to concentrate and stay wet for extended periods of time (weeks). Only the external cask surface could be so exposed. The corrosion rate will, however, be so low that no detectable corrosion products or gases will be generated. Additionally, the NAC-STC has smooth external surfaces, and ridges and crevices have been limited to minimize the collection of such materials as salts.

Galvanic corrosion between the stainless steels, Inconel, and the nickel alloy steels will not occur because there is no effective electrochemical potential difference between these metals. No coatings are applied to the stainless, or nickel alloy steels.

There is a significant electrochemical potential difference between austenitic (300 series) stainless steel and aluminum, copper, and lead. If they are in electrical contact with the austenitic stainless steel, these nonferrous materials could be expected to exhibit corrosion driven by electrochemical EMF when immersed in water. Boiling Water Reactor (BWR) pool water is demineralized water and is not sufficiently conductive to promote detectable corrosion for these metal couples, but Pressurized Water Reactor (PWR) pool water does provide a conductive potential. Because the copper and lead are not directly exposed to water, a reactive environment is not present and no reaction occurs. The only aluminum components that will be in contact with stainless steel and exposed to the pool water are in the fuel baskets. Generally poor electrical contact exists between the stainless steel and the aluminum and then only for the relatively short time that the fuel basket is submersed in water. Galvanic corrosion stops when the electrolyte (water) is removed. Therefore, significant galvanically-driven corrosion does not occur. Copper and lead are in contact with stainless steel, but only in the completely enclosed

(permanently sealed) gamma or neutron shield regions, where no water is present, so no reaction with stainless steel occurs.

There is no potential for a reaction between stainless steel and any silicone products, fluorocarbon elastomers, dry film lubricants, blended polytetrafluoroethylene (PTFE), or ethylene glycol.

Based on the foregoing discussion, there are no significant potential reactions associated with the stainless steel cask components.

2.4.4.2.2 Nonferrous Metals

The nonferrous metals used in the NAC-STC are copper, aluminum, and aluminum bronze. As discussed in the previous section, these nonferrous metals do not produce any significant reaction in contact with stainless steel. Copper fins embedded in the neutron shield (NS-4-FR) region do not react with the NS-4-FR because there is no electrochemical driving potential between the materials.

The only aluminum components exposed to pool water are the heat transfer disks in the fuel baskets. Designer and Nuclear Regulatory Commission safety evaluations and tests of operating dry spent fuel storage systems have concluded that combustible gases, primarily hydrogen, may be produced by a chemical reaction and/or radiolysis when aluminum or aluminum flame-sprayed components are submersed in spent fuel pool water. The evaluations further concluded that it is possible, at higher temperatures (above 150°F - 160°F), for the aluminum/water reaction to produce a hydrogen concentration in the cask or canister that approaches or exceeds the Lower Flammability Limit (LFL) for hydrogen of four percent. NRC Inspection Reports No. 50-266/96005 and 50-301/96005 dated July 01, 1996, for the Point Beach Nuclear Plant concluded that hydrogen generation by radiolysis was insignificant relative to other sources.

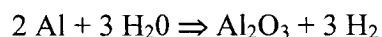
Thus, it is reasonable to conclude that combustible gases, primarily hydrogen, may be produced during loading or unloading operations of the NAC-STC as a result of a chemical reaction between the 6061-T651 aluminum heat transfer disks in the fuel basket and the spent fuel pool water. The generation of combustible gases stops when the water is removed from the cask or canister and the aluminum surfaces are dry. Also, a galvanic reaction may occur at the contact

surfaces between the aluminum disks and the stainless steel tie rods and spacers in the presence of an electrolyte, like the pool water. The galvanic reaction ceases when the electrolyte is removed. The effects of radiolysis are considered insignificant.

The accumulation of combustible gases is only a concern during canistered fuel loading. For direct loading of fuel into the NAC-STC with the bolted closure, there is no ignition source for any combustible gases and the cask is vented to a radioactive waste handling system in operations prior to removal of the water from the cask cavity.

During canister closure operations, a cavity is created inside the canister beneath the shield lid by the drain-down of 50 gallons of water so that the shield lid to canister shell weld can be performed. The cavity beneath the shield lid is approximately 70 inches in diameter and 3 inches deep. Although there is some clearance between the inside diameter of the canister shell and the outside diameter of the shield lid, it is possible that gases released from a chemical reaction inside the canister could accumulate beneath the shield lid. A bare aluminum surface will oxidize when exposed to air, will react chemically in an aqueous solution, and may react galvanically when in contact with stainless steel in the presence of an aqueous solution.

The natural reaction of aluminum in water proceeds as shown below and results in hydrogen being generated:



Aluminum oxide (Al_2O_3) is the dull light gray film that develops on the surface of bare aluminum when it reacts with the oxygen in air or water. The formation of the film is a self limiting reaction as the aluminum metal is isolated from the oxygen source and, thus, acts as a barrier to further oxidation. The oxide film is stable in pH neutral (passive) solutions, but is soluble in borated PWR spent fuel pool water. The oxide film dissolves at a rate dependent upon the pH of the water, the exposure time of the aluminum in the water, and the temperatures of the aluminum and water.

PWR spent fuel pool water is a boric acid and demineralized water solution. The pH, water chemistry and water temperature vary from spent fuel pool to spent fuel pool. Since the reaction rate is largely dependent upon these variables, it may vary considerably from pool to pool. Thus,

an accurate calculation of a combustible gas (hydrogen) generation rate that could be considered representative of spent fuel pools, in general, is very difficult.

For directly loaded fuel, there is no ignition source for any hydrogen gas that might be generated, as the NAC-STC cask is a bolted closure. For the canistered configurations, which are closed by welding the loading and unloading procedures (Section 7.6) incorporate continuous monitoring to preclude welding operations if a concentration of hydrogen gas above 2.4% is detected. If a hydrogen gas concentration exceeding 2.4% is detected, the vacuum system is connected to the vent port and operated for a sufficient period of time to remove at least five times the air volume of the space beneath the shield lid. The system draws ambient air through the gap between the shield lid and the canister shell, thus, drawing out/diluting the hydrogen gas concentration. During welding, the hydrogen gas concentration is continuously monitored using a detector moving ahead of the weld head. The welding operation is stopped if a concentration above 2.4% is detected. Once the root pass weld is completed, there is no further likelihood of a combustible gas burn because the ignition source is isolated from the hydrogen gas source. Once welding has been completed, the cask or canister is drained, vacuum dried and back-filled with helium. These steps ensure safe loading and/or unloading of the NAC-MPC transportable storage canister configurations.

Galvanic corrosion may result when two dissimilar metals are in direct contact with each other in the presence of an electrolytic solution. Each metal has some tendency to ionize, or release electrons. A voltage, or electromotive force (emf), associated with this release of electrons is generated between two dissimilar metals in an electrolytic solution. The emf between aluminum and stainless steel is small and the amount of corrosion is directly proportional to the emf. Loading operations generally take less than 24 hours, after which the electrolyte (water) is drained and the cask or canister is dried and back-filled with helium, effectively halting any galvanic reaction.

Neither the potential chemical or galvanic reactions will have a significant detrimental effect on the ability of the aluminum heat transfer disks to perform their function for all normal and accident conditions associated with transport and dry storage.

2.4.4.2.3 Shielding Materials

The primary shielding materials used in the NAC-STC—lead and NS-4-FR—are completely enclosed and sealed in stainless steel. As previously described, there are no potential reactions of these materials with the stainless steel or with the copper fins.

Therefore, there are no potential reactions associated with the cask shielding materials.

2.4.4.2.4 Criticality Control Material

The criticality control material is a sheet consisting of boron carbide mixed in an aluminum alloy. This material is effectively a sheet of aluminum that is in contact with the aluminum alloy fuel tubes and is exposed to the cask cavity environment. This material is protected by an oxide layer that formed shortly after fabrication. The existing oxide layer effectively precludes further oxidation of the aluminum. Consequently, there are no potential reactions associated with the aluminum-based criticality control material.

2.4.4.2.5 Energy Absorbing Material

The NAC-STC utilizes redwood and balsa wood for energy absorption in the impact limiters. The wood is completely enclosed (sealed) in stainless steel and there are no potential reactions between the wood and the stainless steel shells. The wood is coated with a preservative prior to installation in the impact limiter shell and blocks of wood may be glued together with an epoxy adhesive. These are standard applications of preservatives and adhesives, so no post-application reactions will occur.

There are no potential reactions associated with the energy absorbing material.

2.4.4.2.6 Cellular Foam and Insulation

The NAC-STC utilizes layers of expansion foam and strips of insulation in the solid neutron shield regions. The expansion foam permits thermal expansion of the solid neutron shield material during normal operation, and the insulation protects the expansion foam during final closure welding of the neutron shield shell to the end plate. The foam and the insulation are

nonflammable, nontoxic and noncorrosive silicone products that are used in the casks in a standard design application.

There are no potential reactions associated with the silicone expansion foam or insulation.

2.4.4.2.7 Lubricant and Grease

The dry film lubricants used with the NAC-STC meet the performance and general compositional requirements of the nuclear power industry. NEVER-SEEZ[®] lubricant is used primarily on rotating bearing surfaces. Neolube[®] is used primarily on threaded/mechanical connection surfaces. In addition, Dow Corning High Vacuum Grease is used as an adherent/lubricant to lubricate and retain the O-ring seals in their grooves. None of these lubricants contain elements or compounds prohibited by the NRC. NEVER-SEEZ[®] is a superior, high temperature, anti-seize and extreme pressure lubricant that contains flake particles of pure nickel, graphite and other additives in a special grease carrier. It is used on the trunnion surfaces of the NAC casks. Neolube[®] is 99% pure furnace graphite particles in isopropanol. It has excellent radiation resistance and high chemical purity. It dries as a thin, non-corrosive film with excellent adhesion, does not migrate, and is non-freezable. Dow Corning High Vacuum Grease is a stiff, nonmelting, nonoxidizing, non gumming silicone lubricating material that is insoluble in most solutions. There are no potential reactions associated with these lubricants or grease.

2.4.4.2.8 Seals

The NAC-STC utilizes seals formed from silicone rubber, blended polytetrafluoroethylene (PTFE), and Viton. Viton is a silicon elastomer. Elastomer O-rings are used for transport cask applications because of their excellent short-term sealing capabilities, ease of handling, and more economical cost. All of the seal and gasket materials have stable, non-reactive compositions. There are no potential reactions associated with the NAC-STC seal materials.

2.4.4.3 General Effects of Identified Reactions

No significant potential galvanic or other reactions have been identified for the NAC-STC. The only potential chemical reaction identified for the NAC-STC is that of aluminum with the spent fuel pool water. As discussed in Section 2.4.4.2.2, it is possible at higher temperatures (above 150-160°F) that a flammable concentration of hydrogen might be generated by the

aluminum/water reaction and accumulate beneath the canister shield lid during the canister closure operations. The danger of potential ignition of the hydrogen is precluded by the operating controls and procedures presented in Chapter 7. Therefore, no adverse conditions can result during any phase of cask operations for normal, off-normal, or accident conditions.

2.4.4.4 Adequacy of the Cask Operating Procedures

Based on the results of this evaluation which resulted in only one identified reaction, aluminum in pool water, it is concluded that the NAC-STC operating controls and procedures presented in Chapter 7 are adequate to minimize the occurrence of hazardous conditions.

2.4.4.5 Effects of Reaction Products

No significant potential chemical, galvanic, or other reactions have been identified for the NAC-STC. Therefore, the overall integrity of the cask and the structural integrity and retrievability of the spent fuel is not adversely affected for any cask operations throughout the design basis life of the cask. Based on the evaluation, there will be no change in the cask or fuel cladding thermal properties, and there will be no binding of mechanical surfaces, no change in basket clearances, and no degradation of any safety components either directly or indirectly, since there are no significant reactions identified.

Table 2.4-1 Summary of NAC-STC Materials Categories and Operating Environments

ITEM	MATERIAL	ENVIRONMENT
Stainless Steels/Alloys	304, 304L, XM-19, 17-4PH, Ni Alloy, 410	Sealed Internal Open Internal/ External
Nonferrous Metals	ASTM B152 Cu, 6061-T651 Aluminum Alloy	Sealed Internal Open Internal/External
Shielding Materials	NS-4-FR, Chemical Copper Grade Lead	Enclosed
Criticality Control Materials	Boroncarbide Aluminum 1100	Enclosed
Energy Absorbing Materials	Balsa Wood, Redwood	Enclosed
Cellular Foam/Insulation	Silicone (HT-810 & 800), Silicone Caulk (Dow Corning)	Enclosed
Lubricants & Greases	Never-Seeze® Neolube® High Vacuum Grease® by Dow Corning	Sealed Internal Open Internal
Seals & Gaskets	Silicone Rubber, PTFE, Viton	Sealed Internal Open Internal/ External

2.4.5 Cask Design

The NAC-STC is designed to meet the applicable sections of 10 CFR 71. Criticality, shielding, thermal, radiological and structural requirements of 10 CFR 71 are analytically shown to be satisfied. Conclusions drawn from the structural analyses are supported by quarter-scale model drop tests. The NAC-STC is an exclusive use package designed for transport in a 100°F environment such that personnel barrier temperatures do not exceed 180°F; thus, meeting the requirements of 10 CFR 71.43(g).

THIS PAGE INTENTIONALLY LEFT BLANK

2.4.6 Continuous Venting

The neutron shield is the only vented component of the NAC-STC. It contains a solid synthetic polymer (NS-4-FR), which has been shown by manufacturers' testing to give off small amounts of water vapor at the temperatures that occur during the thermal (fire) accident. To prevent a pressure build up in the neutron shield (under hypothetical fire accident conditions), two relief valves are provided in the bottom end plate. These relief valves are provided to minimize recovery from an over pressure condition. The relief valves do not provide a safety function. No venting of the neutron shield occurs during normal operations conditions; thus, the requirements of 10 CFR 71.43(h) are met.

THIS PAGE INTENTIONALLY LEFT BLANK

2.5 Lifting and Tiedown Standards

2.5.1 Lifting Devices

The NAC-STC has three types of lifting devices: (1) four lifting trunnions; (2) outer lid hoist-eyes; and (3) inner lid hoist-eyes. These lifting devices are designed to satisfy the requirements of 10 CFR 71.45(a). These lifting devices are also designed to meet the requirements of NUREG-0612, "Control of Heavy Loads at Nuclear Power Plants." NUREG-0612 defines specific design criteria to ensure the safe handling of heavy loads in critical regions of nuclear power plants. The design criteria in NUREG-0612 equals, or exceeds, that of 10 CFR 71.

The NAC-STC is equipped with four lifting trunnions located on the top forging near the top of the cask, and spaced at 90-degree intervals. A single two-arm yoke (nonredundant), or a combination of two yokes (redundant) may be used to lift and handle the cask. Each lifting yoke is attached to two diametrically opposite lifting trunnions. An overhead crane lifts the cask by these yokes. No transport impact limiter is attached to the cask during lifting and handling. The lower impact limiter could be attached for protection during handling, but the upper impact limiter cannot be used while the lifting yoke is in place. The inner and outer lid hoist-eyes are used for lifting the lids during installation or removal. The cask is rotated from the horizontal to the vertical position and vice-versa on the two rotation trunnion recesses. The rotation trunnion recesses also support the cask in the rear cask support during transport.

2.5.1.1 Lifting Trunnion Analysis

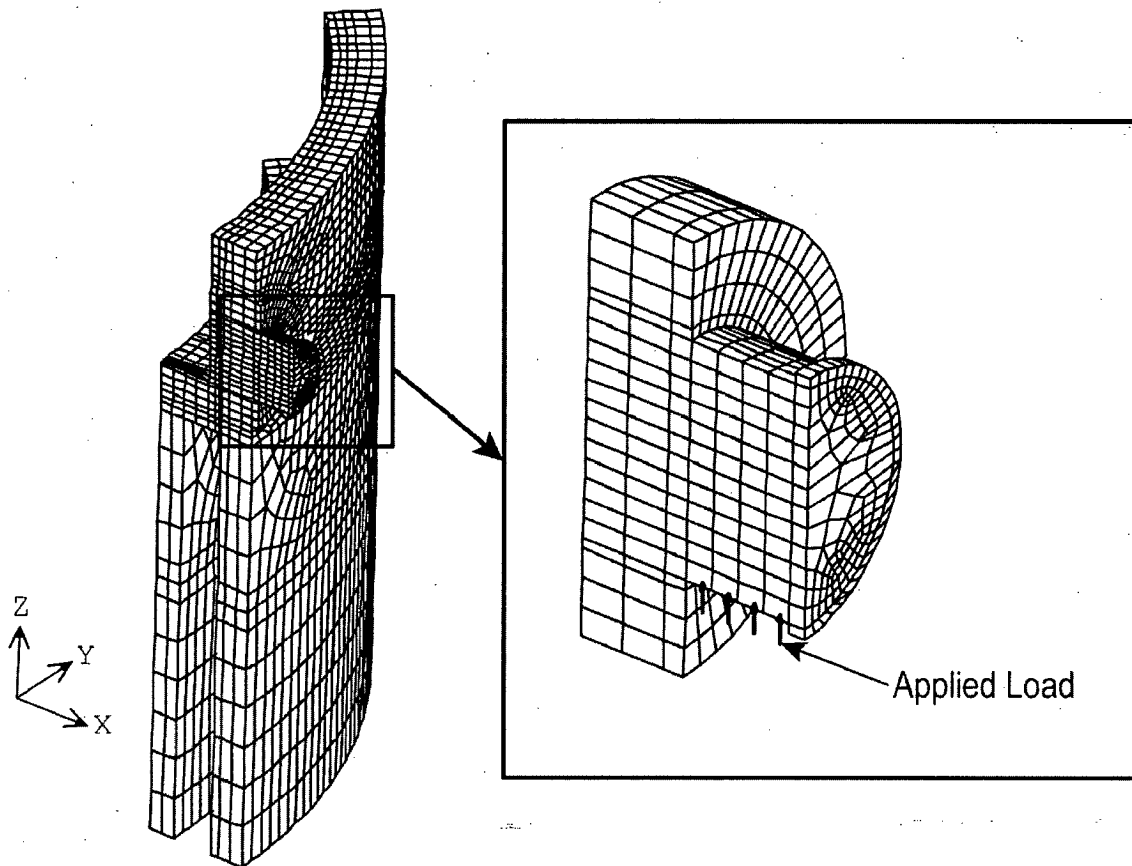
The NAC-STC has four lifting trunnions spaced at 90-degree intervals and located on the top forging near the top of the cask, which allow either a nonredundant, two-arm yoke or a redundant, four-arm yoke to lift and handle the cask. The NAC-STC lifting trunnions are designed to meet the requirements of NUREG-0612 for a nonredundant lifting system; that is, a two-trunnion lift. A redundant four-trunnion lift is less critical. Two lifting trunnions are capable of supporting a maximum load, which is defined as six times the design loaded lift weight of the cask without producing stresses anywhere in the cask in excess of the material yield strength. Any dynamic load effects are negligible when considered in combination with the large applied load factors. Additionally, the lifting trunnions are designed so that failure will not impair the ability of the cask to meet its other safety requirements.

The weight of the NAC-STC is conservatively assumed to be 260,000 pounds for the lifting analysis.

The properties of the materials used in the lifting trunnion analysis are as follows at the conservatively high temperature of 250°F:

- | | | |
|----|-----------------|---|
| 1. | Trunnions | SA-705, Type 630
$S_y = 95.0$ ksi
$S_u = 135.0$ ksi |
| 2. | Top Forging | SA-336, Type 304
$S_y = 23.75$ ksi
$S_u = 63.8$ ksi |
| 3. | Filler Material | AWS E309
$S_y = 30$ ksi
$S_u = 80$ ksi |

A quarter symmetry finite element model (ANSYS 5.5) of the trunnion, weld, and upper forging is used to determine the bending moment and shear stress at the trunnion during lift conditions.



ANSYS SOLID45 elements are used to model all components. A uniform pressure load corresponding to a load of 65,000 lb. (260,000/4) is applied to simulate the loading on the trunnion. A portion of the cask is modeled to assure that the end constraints used for boundary conditions are sufficiently away from the area of interest. Note that the trunnion is only connected to the cask body upper forging at the weld location. For a given cross-section of the trunnion, the bending moment can be determined by the following formula using the finite element analysis results.

$$M = \sum S_i A_i y_i$$

Where:

S_i is the element axial stress (along length of trunnion),
 A_i is the cross-sectional area of the element (perpendicular to axis of trunnion), and
 y_i is the distance from element centroid to the centerline of the trunnion.

The average shear stress on a cross-section is calculated by the volume-weighted average of $\frac{1}{2}$ of the stress intensity from the finite element analysis results. The shear stress is calculated as:

$$S = \sum \frac{SI_i V_i}{2V_{tot}}$$

Where

SI_i is the element stress intensity,
 V_i is the element volume, and
 V_{tot} is the total volume of the selected elements.

2.5.1.1.1 Lifting Trunnion Shank

The diameter of the lifting trunnion shank is 5.5 inches. Figure 2.5.1-1 shows the lifting trunnion geometry. The average shear and the bending moment at the trunnion shank are calculated to be 5,765 psi and 126,055 in-lbs, respectively. The shear and bending stresses at the base of the shank (through Point E in Figure 2.5.1-1) are calculated as:

Yield Strength Criteria (Factor of Safety = 6)

Shear Stress: $S_{sy} = 5,765 \times 6 = 34,590$ psi

$$\begin{aligned}\text{Bending Stress: } S_{by} &= \frac{M_y}{S} \\ &= 46,315 \text{ psi}\end{aligned}$$

where:

$$M_y = 126,055 \times 6 = 756,330 \text{ in-lbs}$$

$$\begin{aligned}S &= \frac{\pi R^3}{4} \text{ in}^3 \text{ (Section Modulus)} \\ &= \frac{\pi (2.75)^3}{4} = 16.33 \text{ in}^3\end{aligned}$$

The combined stress is calculated as:

$$\begin{aligned}S_{ey} &= \left((S_{by})^2 + 3(S_{sy})^2 \right)^{0.5} \\ &= 75,726 \text{ psi}\end{aligned}$$

The margin of safety is:

$$(MS)_y = \frac{95.0}{75.7} - 1 = +0.26$$

Ultimate Strength Criteria (Factor of Safety = 10)

$$\text{Shear Stress: } S_{su} = 5,765 \times 10 = 57,650 \text{ psi}$$

$$\text{Bending Stress: } S_{bu} = \frac{M_u}{S} = 77,192 \text{ psi}$$

where:

$$M_u = 126,055 \times 10 = 1,260,550 \text{ in-lb}$$

$$S = 16.33 \text{ in}^3$$

The combined stress is calculated as:

$$S_{eu} = \left((S_{bu})^2 + 3(S_{su})^2 \right)^{0.5}$$

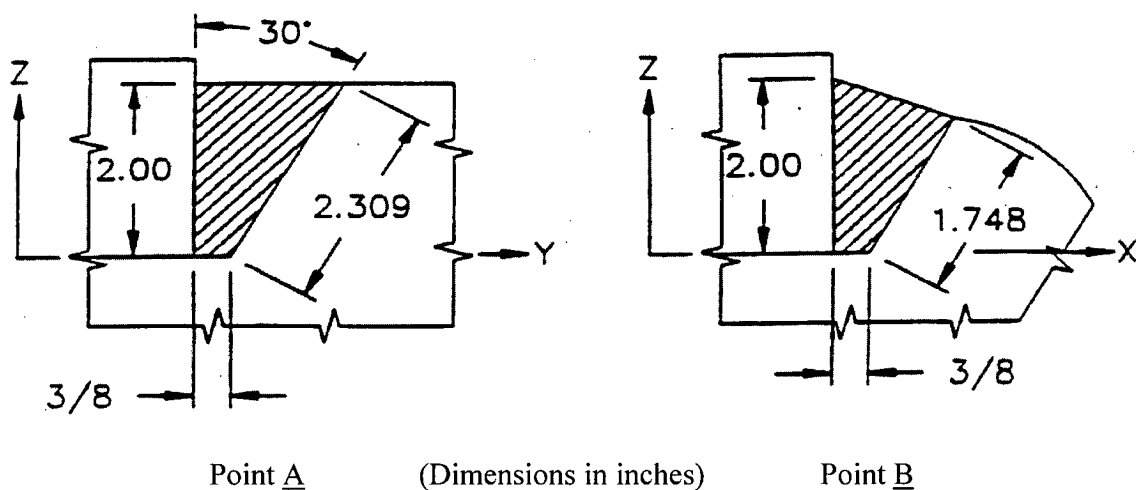
$$= 126,088 \text{ psi}$$

The margin of safety is:

$$(MS)_u = \frac{135.0}{126.1} - 1 = +0.07$$

2.5.1.1.2 Trunnion Base Weld

The lifting trunnions are welded to the top forging of the cask body, as shown in Figures 2.5.1-1 and 2.5.1-2. The trunnions are evaluated at 4 points, A, B, C and D. The weld geometries at points A and B (Figure 2.5.1-1 and Figure 2.5.1-2, respectively) are shown below. Two postulated failures in the analysis of the welded connection are: (1) at the trunnion/weld interface; and (2) at the weld/forging interface. They are evaluated in Section 2.5.1.1.2.1 and Section 2.5.1.1.2.2, respectively. The sections through the trunnion weld are:



2.5.1.1.2.1 Trunnion/Weld Interface

The depth of the weld at the trunnion/weld interface is 2.0 inches, as shown in the weld geometries above. Using the finite element model, the bending moment and average shear at the weld are calculated to be 201,264 in-lbs and 1,669 psi, respectively. The weld analyses using the yield stress and ultimate yield criteria are as follows:

Yield Criteria Analyses (Factor of Safety = 6)

The moment on the weld is:

$$M_{wy} = 201,264 \times 6 = 1,207,584 \text{ in-lbs}$$

The stresses in the weld at point A or C are calculated as follows:

Bending stress, S_{by} , is:

$$\begin{aligned} S_{by} &= \frac{1,207,584}{(\pi)(5.0)^2(2.0)} \\ &= 7,688 \text{ psi} \end{aligned}$$

The Shear stress, S_{sy} , is:

$$S_{sy} = 1,669 \times 6 = 10,014 \text{ psi}$$

The Von Mises stress is:

$$\begin{aligned} S_{ey} &= \left((S_{by})^2 + 3(S_{sy})^2 \right)^{0.5} \\ &= 18,972 \text{ psi} \end{aligned}$$

Conservatively taking the weld as the critical component, the margin of safety is:

$$(MS)_y = \frac{30.0}{19.0} - 1 = +0.58 \text{ (Point A or C)}$$

The stresses in the weld at points B or D are calculated as:

$$S_{sy} = 1,669 \times 6 = 10,014 \text{ psi}$$

Taking the weld as the critical component, the yield shear strength is $0.6 S_m = 0.6(20) = 12 \text{ ksi}$.

The margin of safety is:

$$(MS)_y = \frac{12}{10.0} - 1 = +0.20 \quad (\text{Point B or D})$$

Ultimate Criteria Analyses (Factor of Safety = 10)

The stresses in the weld at points A or C are calculated as follows:

The bending moment on the weld is:

$$M_{ny} = 201,264 \times 10 = 2,012,640 \text{ in-lbs}$$

The bending stress, S_{by} , is:

$$S_{by} = \frac{2,012,640}{\pi (5.0)^2 (2.0)}$$
$$= 12,813 \text{ psi}$$

The average shear stress, S_{su} , is $1,669 \times 10 = 16,690 \text{ psi}$

The Von Mises stress is:

$$S_{eu} = \left((S_{by})^2 + 3(S_{su})^2 \right)^{0.5}$$
$$= 31,620 \text{ psi}$$

Conservatively taking the weld as the critical component, the margin of safety is:

$$(MS)_u = \frac{80.0}{31.6} - 1 = +1.53 \quad (\text{Points A or C})$$

The stresses, S_{su} , at points B or D are calculated as:

$$S_{su} = 1,669 \times 10 = 16,690 \text{ psi}$$

Taking the weld as the critical component and taking the ultimate shear strength as $0.42(80) = 33.6$ ksi, the margin of safety is:

$$(MS)_u = \frac{33.6}{16.7} - 1 = +1.01 \quad (\text{Points B or D})$$

2.5.1.1.2.2 Weld/Forging Interface

The weld/forging interface consists of the 3/8-inch root around the trunnion and surface on the 60-degree truncated cone. The weld/forging interface varies from a maximum at point A to a minimum at point B (see weld sections shown in Section 2.5.1.1.2). It is conservatively assumed that the minimum weld section at point B exists uniformly around the trunnion. In order to simplify the weld-to-forging analysis another conservative assumption is used, taking the critical section as the surface of the cylinder concentric with the trunnion and its surface passing through the intersection of the weld/forging interface and the cask surface (see the weld section at point B shown in Section 2.5.1.1.2). The weld/forging interface at the root of the weld is also neglected.

The radius of the assumed critical section of the weld/forging interface is $5 + 0.375 + (1.748)(\sin 30^\circ) = 6.249$ inches, and the height is $(1.748)(\cos 30^\circ) = 1.514$ inches.

Yield Strength Criteria (Factor of Safety = 6)

The stresses between the weld and forging at points A and C are calculated as follows:

The average shear stress is:

$$S_{sy} = 1,669 \times 6 = 10,014 \text{ psi}$$

The bending stress is:

$$\begin{aligned} S_{by} &= \frac{(201,264)(6)}{(\pi)(6.249)^2(1.514)} \\ &= 6,502 \text{ psi} \end{aligned}$$

The Von Mises stress is:

$$S_{ey} = \left((S_{by})^2 + 3(S_{sy})^2 \right)^{0.5}$$
$$= 18,523 \text{ psi}$$

The yield strength of the forging of 23.75 ksi at a conservatively high temperature of 250°F governs. The margin of safety is calculated as:

$$(MS)_y = \frac{23.75}{18.5} - 1 = +0.28$$

Taking the forging as the critical component, the yield shear strength is $0.6 S_m = 0.6(20) = 12$ ksi.

The Margin of Safety is:

$$(MS)_s = 12.0/10.0 - 1 = +0.20 \quad (\text{Points B or D})$$

Ultimate Strength Criteria (Factor of Safety = 10)

The stresses between the weld and forging at points A and C are calculated as follows:

The average stress is:

$$S_y = 1,669 \times 10 = 16,690 \text{ psi}$$

The bending stress is:

$$S_{by} = \frac{(201,264)(10)}{(\pi)(6.249)^2(1.514)}$$
$$= 10,836 \text{ psi}$$

The Von Mises stress is:

$$S_{ey} = \left((S_{by})^2 + 3(S_{sy})^2 \right)^{0.5}$$

$$= 30,872 \text{ psi}$$

The margin of safety for the forging is:

$$(MS)_u = \frac{63.8}{30.9} - 1 = +1.06$$

Taking the forging as the critical component, the ultimate shear strength is $0.42 S_u = 0.42(63.8) = 26.8 \text{ ksi}$.

The Margin of Safety is:

$$(MS)_s = 26.8/16.7 - 1 = +0.61 \quad (\text{Points B or D})$$

2.5.1.1.3 Trunnion Base

The trunnion base plate is analyzed as a flat circular plate with a fixed outer edge and a trunnion fixed at its center using the equations provided in Young, page 435, Case 21b. The trunnion moment at the midpoint of the embedded thickness of the trunnion base plate for the design lifting load is:

$$M_{tbp} = 2.75 F_{DL}$$

Yield Strength Criteria (Factor of Safety = 6)

The trunnion moment for the Yield Strength Criteria evaluation is:

$$\begin{aligned} (M_{tbp})_y &= 2.75 F_y \\ &= 2.145 \times 10^6 \text{ in-lb} \end{aligned}$$

where:

$$F_y = (260,000/2) \times 6 = 780,000 \text{ lb}$$

The maximum bending stress in the trunnion base plate is:

$$S_r = \frac{\beta(M_{tbp})_y}{at^2}$$

$$= 65,036 \text{ psi}$$

where:

$$a = 5.00 \text{ in}$$

$$b = 2.75 \text{ in}$$

$$b/a = 0.55$$

$$\beta = 0.9475$$

$$t = 2.50 \text{ in}$$

Then, the margin of safety is:

$$(M.S.)_y = \frac{S_y}{S_r} - 1 = +0.46$$

where:

$$S_y = 95.0 \text{ ksi at } 250^\circ\text{F}$$

Ultimate Strength Criteria (Factor of Safety = 10)

The trunnion moment for the Ultimate Strength Criteria evaluation is:

$$\begin{aligned}(M_{tbp})_u &= 2.75 F_u \\ &= 3.575 \times 10^6 \text{ in-lb}\end{aligned}$$

where:

$$F_u = (260,000/2) \times 10 = 1,300,000 \text{ lb}$$

The maximum bending stress in the trunnion base plate is:

$$S_r = \frac{\beta(M_{tbp})_y}{at^2}$$

$$= 108,394 \text{ psi}$$

where:

$$a = 5.00 \text{ in}$$

$$b = 2.75 \text{ in}$$

$$b/a = 0.55$$

$$\beta = 0.9475$$

$$t = 2.50 \text{ in}$$

Then, the margin of safety is:

$$(M.S.)_u = \frac{S_u}{S_r} - 1 = + 0.25$$

where:

$$S_u = 135.0 \text{ ksi at } 250^\circ\text{F}$$

Therefore, the trunnion base plate is structurally adequate for the trunnion design loading conditions.

2.5.1.1.4 Overload in the Lifting Trunnions

According to 10 CFR 71.45(a), any lifting attachment that is a structural part of a cask must be designed so that failure of any lifting device under excessive load would not impair the ability of the cask to meet other requirements of 10 CFR 71. The ultimate shear capacities of the different parts of the lifting trunnion are calculated and compared. To show that the cask will meet the other requirements of 10 CFR 71, the failure should not occur in the shell of the cask before failure of the other parts.

2.5.1.1.4.1 Shank Failure

Lifting trunnion shank (Ultimate Shear Strength):

$$\begin{aligned} F_{tr} &= (\pi)(d^2/4)(0.42S_u) \\ &= 1,347,095 \text{ lb} \end{aligned}$$

where:

$$d = 5.5 \text{ in}$$

$$S_u = 135,000 \text{ psi}$$

2.5.1.1.4.2 Weld/Trunnion Interface Failure

The ultimate shear strength of the weld/trunnion interface is governed by the shear strength of the weld and is calculated as:

$$\begin{aligned} F_u &= (\pi)(10.00)(2.0)(0.42S_u) \\ &= 2,111,150 \text{ lb} \end{aligned}$$

where:

$$\begin{aligned} S_u &= \text{ultimate tensile strength of the weld} \\ &= 80,000 \text{ psi} \end{aligned}$$

2.5.1.1.4.3 Weld/Forging Interface Failure

The width of the weld/forging interface is taken as the mean of the interface widths at points A and B; that is, $(2.309 + 1.748)/2 = 2.028$ inches. The mean radii to the center of the interfaces at points A and B are calculated as:

$$\begin{aligned} R_A &= 5.0 + 0.375 + (0.5)(2.0 \tan 30^\circ) \\ &= 5.95 \\ R_B &= 5.0 + 0.375 + (0.5)(1.748 \sin 30^\circ) \\ &= 5.812 \\ R_{ave} &= 5.881 \text{ inches} \end{aligned}$$

The ultimate shear strength of the weld/forging interface is:

$$\begin{aligned} F_u &= (A_w)(0.42S_u) \\ &= 2,335,539 \text{ lb} \end{aligned}$$

where:

$$\begin{aligned} S_u &= \text{ultimate strength of the forging} \\ &= 63,800 \text{ psi} \\ A_w &= (2\pi)(5.881)(2.028) + (\pi)(5.375^2 - 5.0^2) \\ &= 87.16 \text{ in}^2 \end{aligned}$$

The maximum ultimate shear capacities are:

	<u>Capacity</u>
Lifting Trunnion Shaft	1,347,095 lb
Weld/trunnion interface	2,111,150 lb
Weld/forging interface	2,335,539 lb

Thus, the lifting trunnion shank will fail in shear before the weld or the forging, ensuring that failure caused by excessive overload on the lifting trunnions will not impair the ability of the cask to meet the other requirements of 10 CFR 71.

2.5.1.2 Lid Lifting Device

The inner lid and the outer lid of the NAC-STC will each be lifted using a wire-rope sling that is load-rated for not less than the weight of each individual lid. The sling will be attached to each of the lids using hoist-eyes that are threaded into four equidistant holes on the lids. These holes will be clearly marked by engraved black painted letters on the top surface of each lid. The four slings will attach to a strongback at two points, centered 22.5 inches apart, two slings at each point.

The hoist eyes used in lifting the inner and outer lids are American Drill Bushing Company, Part 23106, or equivalent, with the following specifications:

Thread: 1-8 UNC-2A x 1.54 long
Material: SA-540, Grade B22 Low Alloy Steel
 $S_y = 3S_m = 100.2 \text{ ksi at } 200^\circ\text{F}$
 $A_t = 0.606 \text{ in}^2$
 $I = 0.0252 \text{ in}^4$
 $c = 0.4233 \text{ in}$

2.5.1.2.1 Outer Lid Lifting

The outer lid lifting system uses four 1-8 UNC threaded holes located on a 76.00 inch bolt circle. The four holes are equally spaced. Helical thread inserts are used to increase the wear endurance. The outer lid material is SA-705, Type 630, H1150, 17-4 PH stainless steel.

The outer lid weight (W_o) is 8,120 pounds as shown in Table 2.2-1.

From the requirements of 10 CFR 71.45(a), a load factor of 3 is used in the stress qualification of a lifting device:

$$\begin{aligned} P_y &= (3.0)(W_o) \\ &= 24,360 \text{ lb} \end{aligned}$$

The inclined angle (θ) of the sling for an outer lid lifting condition is illustrated in Figure 2.5.1-3. The sling length is 68.0 inches. The vertical distance from the hoist eye to the strongback is 60.48 inches, for the outer lid.

$$\begin{aligned}\sin \theta &= 60.48/68.00 \\ \theta &= 62.80 \text{ degrees}\end{aligned}$$

The lifting force F_n , and its components F_x and F_y , on each sling, are calculated as:

$$\begin{aligned}F_y &= P_y/4 = 6,090 \text{ lb} \\ F_n &= F_y/\sin \theta = 6,847 \text{ lb} \\ F_x &= (F_n)(\cos \theta) = 3,130 \text{ lb}\end{aligned}$$

Hoist Eye Stress Evaluation for Outer Lid Lifting

The tensile and bending stresses on the critical section of the hoist eye are determined:

$$\begin{aligned}d &= \text{moment arm} = 0.74 \text{ inch} \\ M_z &= (F_x)(d) = 2316 \text{ in-lb} \\ S_a &= F_y/A_t + (M_z)(c)/I = 48,956 \text{ psi}\end{aligned}$$

The shear stress is:

$$S_s = F_x/A_t = 5165 \text{ psi}$$

The principal stresses are:

$$\begin{aligned}s_1, s_2 &= S_a/2 \pm [(S_a/2)^2 + S_s^2]^{0.5} \\ &= +49,495 \text{ and } -539 \text{ psi}\end{aligned}$$

The stress intensity is:

$$S.I. = 50,034 \text{ psi}$$

The resulting margin of safety is:

$$M.S. = (S_y/S.I.) - 1 = \underline{+0.99}$$

Outer Lid Hoist Eye Thread Engagement Evaluation

The outer lid hoist eye is evaluated for the length of thread engagement with the helical insert.

$$\text{Allowable shear stress} = 0.577 S_y = 57.8 \text{ ksi at } 200^\circ\text{F}$$

The shear area for a 1-8 UNC-2A external thread for use with a 1-8 UNC helical coil insert is determined as [Screw Thread Standards for Federal Services (FED-STD-H28/2A), page 5]:

$$A_s = 3.1416 N L_e K_{nmax} [1/(2N) + 0.57735(E_{smin} - K_{nmax})] \\ = 2.07 \text{ in}^2$$

where

$$\begin{aligned} N &= 8 \text{ threads per inch} \\ L_e &= \text{length of engagement} = 1.25 \text{ inch (conservative)} \\ K_{nmax} &= 0.890 \text{ in (max. minor diameter of internal thread)} \\ E_{smin} &= 0.9100 \text{ in (min. pitch diameter of external thread)} \end{aligned}$$

The actual thread length is 1.54 inches, but the effective thread engagement length is conservatively taken to be 1.25 inches. Therefore, the resultant shear stress and margin of safety for the outer lid hoist eye is:

$$\begin{aligned} P_y &= 24,360 \text{ lb} \\ F_y &= P_y/4 = 6090 \text{ lb} \\ T &= F_y/A_s = 2942 \text{ psi} \\ \text{M.S.} &= (0.577 S_y/t) - 1 = \underline{+Large} \end{aligned}$$

Outer Lid Thread Engagement Evaluation

The outer lid material is SA-705 Type 630 forging material. Allowable shear stress = $0.577 S_y = 56.0$ ksi at 200°F, (Table 2.3.3-1). Shear area per length of engagement for a 1 1/8 - 8 UNC internal thread for use with a 1-8 UNC helical coil insert is determined as (FED-STD-H28/2A, page 5):

$$A_s = 3.1416 N D_{smin} [1/(2N) + 0.57735(D_{smin} - E_{nmax})] \\ = 2.67 \text{ in}^2$$

where

$$\begin{aligned} N &= 8 \text{ threads per inch} \\ D_{smin} &= 1.1014 \text{ in (min. major diameter of external thread)} \\ E_{nmax} &= 1.0421 \text{ in (max. pitch diameter of internal thread)} \end{aligned}$$

The actual thread length is 1.54 inches, but the effective thread engagement length is conservatively taken to be 1.25 inches. Therefore, the resultant shear stress and margin of safety for the outer lid is:

$$\tau = F_y / (A_s)(\text{Effective Length}) = 6090 / (2.67)(1.25) = 1825 \text{ psi}$$
$$\text{M.S.} = (0.577 S_y / t) - 1 = (56,000 / 1825) - 1 = \underline{+Large}$$

2.5.1.2.2 Inner Lid Lifting

The inner lid lifting system uses the same approach as the outer lid lifting system. The analysis considers four 1-8 UNC threaded holes located on a 70.41 inch bolt circle. The four holes are equally spaced. Helical thread inserts are used to increase the wear endurance. The inner lid material is Type 304 stainless steel ASME SA-336.

The inner lid weight (W_i) is 10,690 pounds, as documented in Table 2.2-1.

From the requirements of 10 CFR 71.45(a), a load factor of 3 is used in the stress qualification of a lifting device:

$$P_y = (3.0)(W_i)$$
$$= 32,070 \text{ lb}$$

The inclined angle (θ) of the sling for an inner lid lifting condition is illustrated in Figure 2.5.1-4. The sling length is 68.0 inches. The vertical distance from the hoist eye to the strongback is 61.79 inches, for the inner lid.

$$\sin \theta = 61.79 / 68.00$$
$$\theta = 65.3 \text{ degrees}$$

The lifting force F_n , and its components F_x and F_y , on each sling, are calculated as:

$$F_y = P_y / 4 = 8017.5 \text{ lb}$$
$$F_n = F_y / \sin a_i = 8823.5 \text{ lb}$$
$$F_x = (F_n)(\cos a_i) = 3685 \text{ lb}$$

Inner Lid Hoist Eye Stress Evaluation

The tensile and bending stresses on the critical section of the hoist eye are determined:

$$d = \text{moments is} = 0.74 \text{ inch}$$
$$M_z = (F_x)(d) = 2,727 \text{ inch-lb}$$
$$S_a = F_y / A_t + (M_z)(c) / I = 59,035 \text{ psi}$$

The shear stress is:

$$S_s = F_x/A_t = 6,081 \text{ psi}$$

The principal stresses are:

$$\begin{aligned} s_1, s_2 &= S_a/2 \pm [(S_a/2)^2 + S_s^2]^{0.5} \\ &= +59,655 \text{ and } -620 \text{ psi} \end{aligned}$$

The stress intensity is:

$$S.I. = 60,275 \text{ psi}$$

The resulting margin of safety is:

$$MS = (S_y/S.I.) - 1 = +0.66$$

Inner Lid Hoist Eye Thread Engagement Evaluation

The hoist eyes used for the outer and inner lids are identical, therefore the evaluation of the inner lid hoist eye length of thread engagement follows the same approach presented earlier for the outer lid hoist eye.

$$P_y = 32,070 \text{ lb}$$

$$F_y = P_y/4 = 8017.5 \text{ lb}$$

$$t = F_y/A_s = 3873 \text{ psi, where } A_s = 2.07 \text{ in}^2 \text{ as calculated in Section 2.5.1.2.1}$$

$$MS = (0.577 S_y/t) - 1 = + \text{ Large}$$

Inner Lid Thread Engagement Evaluation

The inner lid material is SA-336, Type 304 stainless steel. Allowable shear stress = $0.577 S_y = 14.43 \text{ ksi}$ at 200°F (Table 2.3.2-2). The evaluation of the inner lid thread engagement follows the same approach presented earlier for the outer lid, since both inner and outer lids have 1 1/8 - 8 UNC internal threads for use with a 1-8 UNC helical coil insert. Therefore, the resultant shear stress and margin of safety for the inner lid is:

$$t = F_y/(A_s)(\text{Length}) = 8017.5/(2.67)(1.25) = 2396 \text{ psi}$$

$$MS = (0.577 S_y/t) - 1 = (14,425/2396) - 1 = + \text{ Large}$$

2.5.1.3 Canister Lifting

This section presents the canister lift evaluation for the Yankee-MPC (Section 2.5.1.3.1) and the CY-MPC (Section 2.5.1.3.2).

2.5.1.3.1 Yankee-MPC Canister Lifting

The adequacy of the canister lifting devices is demonstrated by considering each of the hoist rings, the canister structural lid, and the weld that joins the structural lid to the canister shell. Lifting of the canister employs redundant 3-legged lifting slings for single failure proof lifting in accordance with NUREG-0612.

When considering a three-point lifting configuration, the load-bearing members of the canister maintain a factor of safety greater than three based on material yield strength. Additionally, the load-bearing members of the canister maintain a factor of safety greater than five based on material ultimate strength. The hoist rings are designed with a 5 to 1 safety factor based on ultimate. Therefore, the lifting requirements are satisfied. Each lifting device in a three-point lift would experience the following load, F, when lifting the canister (the total load is based on the dead weight of the loaded canister with a dynamic load factor of 10%):

$$F = \frac{54,730 \times 1.1}{3} = 20,068 \text{ lb}$$

The hoist rings used to lift the canister have a rated load capacity of 24,000 pounds with a 5 to 1 safety factor based on material ultimate strength (American Drill Bushing Co.). The length of the hoist ring bolt thread length is 2.23 inches. The following calculation (using formula from Machinery's Handbook) demonstrates that the bolt length is adequate to develop the full strength of the hoist ring.

Definition of Terms:

- D = basic major diameter of bolt threads = 1.5 inches
- n = number of threads per inch = 6
- A_t = tensile area of the bolt thread (in²)

- L_e = minimum thread engagement length for mating materials with equal tensile strengths (in.)
- $K_n \text{max}$ = maximum minor diameter of lid (internal) thread = 1.35 inches
- $E_s \text{min}$ = minimum pitch diameter of bolt (external) threads = 1.3812 inches
- A_s = shear area of bolt threads (in²)
- A_n = shear area of lid threads (in²)
- $D_s \text{min}$ = minimum major diameter of bolt (external) threads = 1.4794 inches
- $E_n \text{max}$ = maximum pitch diameter of lid (internal) threads = 1.4022 inches
- Q = length of thread engagement required to prevent shearing when the mating thread materials are different tensile strengths (in.)
- J = scale factor for calculation of Q
- H = height of sharp "V" thread = 0.1443 inches
- Hoist ring material = 4140 High strength alloy steel
- Tensile strength of 4140 = 180,000 psi
- Hoist ring thread = 1-1/2 - 6 UNC
- Structural lid material = Type 304 L stainless steel
- Temperature of structural lid = 250°F (Maximum calculated temperature = 209°F, Table 3.4-1)
- Tapped hole in structural lid = 1-1/2 - 6 UNC

For steels up to 100,000 psi tensile strength, the tensile area of the bolt thread is given by:

$$A_t = 0.7854 \left(D - \frac{0.9743}{n} \right)^2$$
$$A_t = 0.7854 \left(1.5 - \frac{0.9743}{6} \right)^2 = 1.4053 \text{ in}^2$$

For mating materials having equal tensile strengths, the minimum length of thread engagement is given by:

$$L_e = \frac{2A_t}{3.1416K_n \text{max} \left[\frac{1}{2} + 0.57735n(E_s \text{min} - K_n \text{max}) \right]}$$

$$L_e = 1.0898 \text{ inches}$$

For mating materials of differing tensile strengths:

$$J = \frac{A_s \times \text{tensile strength of bolt thread material}}{A_n \times \text{tensile strength of lid thread material}}$$

The shear areas are calculated as follows:

$$A_s = 3.1416nL_e K_n \max \left[\frac{1}{2n} + 0.57735(E_s \min - K_n \max) \right]$$

$$A_s = 2.8106 \text{ in}^2$$

$$A_n = 3.1416nL_e D_s \min \left[\frac{1}{2n} + 0.57735(D_s \min - E_n \max) \right]$$

$$A_n = 3.887 \text{ in}^2$$

At a temperature of 250°F, the ultimate strength of Type 304L stainless steel is 63,550 psi.

$$J = \frac{A_s \times (S_u)_{\text{bolt}}}{A_n \times (S_u)_{\text{lid}}} \\ = 2.048$$

The length of thread engagement necessary to prevent shearing is:

$$Q = JL_e$$

$$Q = (2.048)(1.0898) = 2.23 \text{ in.}$$

The following calculation determines the minimum required thread engagement length to meet the minimum Factors of Safety based on the actual load that the threads must support.

Minimum thread engagement ($L_{th, \min}$) based on yield shear strength of lid material (304 L):

$$F = 20.08 \text{ kips}$$

$$S_m = 16.7 \text{ ksi}$$

$$\tau_{\text{allow. yield}} = 10 \text{ ksi} \quad (0.6 \times 16.7)$$

$$F.S._{\text{yield, min}} = 3$$

$$\tau_{\text{max}} = \tau_{\text{allow. yield}} / F.S._{\text{yield, min}} = 10 / 3 = 3.33 \text{ ksi}$$

$$A_{\min} = F / \tau_{\max} = 20.08 / 3.33 = 6.03 \text{ in}^2$$

$$L_{\text{th}, \min} = \frac{A_n}{\pi n D_{s, \min} \left[\frac{1}{2n} + 0.57735 \left(D_{s, \min} - E_{n, \max} \right) \right]} = \frac{6.03}{3.57}$$

$$L_{\text{th}, \min} = 1.69 \text{ inches based on Yield Factor of Safety requirement}$$

Minimum thread engagement ($L_{\text{th}, \min}$) based on ultimate shear strength of lid material (304 L):

$$F = 20.08 \text{ kip}$$

$$S_u = 63.55 \text{ ksi}$$

$$\tau_{\text{allow, ultimate}} = 26.7 \text{ ksi } (0.42 S_u)$$

$$F.S._{\text{ultimate, min}} = 5$$

$$\tau_{\max} = \tau_{\text{allow, ultimate}} / F.S._{\text{ultimate, min}} = 26.7 / 5 = 5.34 \text{ ksi}$$

$$A_{\min} = F / \tau_{\max} = 20.08 / 5.34 = 3.76 \text{ in}^2$$

$$L_{\text{th}, \min} = \frac{A_n}{\pi n D_{s, \min} \left[\frac{1}{2n} + 0.57735 \left(D_{s, \min} - E_{n, \max} \right) \right]} = \frac{3.76}{3.57}$$

$$L_{\text{th}, \min} = 1.05 \text{ inches based on Ultimate Factor of Safety requirement}$$

The yield strength factor of safety dictates that the minimum thread engagement length required to meet ANSI N14.6 requirements is 1.69 inches; therefore, the hoist ring bolt thread length of 2.23 inches is adequate.

The structural adequacy of the canister structural lid and weld was evaluated using a finite element representation of the upper portion of the canister using the ANSYS program. As shown in Figure 2.5.1-5, the model represents one-half (180° section) of the upper 50-inches of the canister (including the structural and shield lids). The lids and shell in the model are comprised of SOLID45 elements. CONTAC52 elements are used to model the interaction between the structural lid and the canister shell and between the shield lid and the canister shell, just below the respective lid weld joints. The size of the CONTAC52 gaps was determined from nominal dimensions of contacting components. COMBIN40 elements are used between the structural and shield lids in the axial direction and between the shield lid and the backing ring. These gaps are assigned small gap sizes of 1E-8 inches. All gap/spring elements are assigned a stiffness of 1E8 lb/inch.

To enforce symmetry at the boundary of the model (in the x-y plane), all nodes on the x-y symmetry plane were restrained perpendicular to the symmetry plane (UZ). In addition, the nodes in the x-z plane at the bottom of the model were restrained in the axial direction.

Load-bearing members of a lifting device must be capable of lifting three (3) times the combined weight of the shipping container with which it will be used, plus the weight of intervening components of the lifting device without exceeding the tensile yield strength of their materials of construction. In addition, the lifting components must be capable of lifting five (5) times that combined weight without exceeding the ultimate tensile strength of the materials. NUREG-0612 also requires that the lifting loads must be based on the combined maximum static and dynamic loads that could be imparted on the handling device based on characteristics of the crane that will be used. A dynamic load factor of 10% has been applied.

To simulate the lifting of the canister by a three-point lifting device (the lifting configuration is actually two independent 3-point lifting devices), point loads equal to one-third of the total canister and contents weight plus a dynamic loading factor of 10% were applied to the model.

Because the model represents a half section of the canister, only two point loads were applied 120° apart as shown in Figure 2.5.1-5. Because of the symmetry conditions of the model, the force applied to the node on the symmetry plane was one-half of the value applied at the other location.

The maximum stress intensity generated in the canister model from the applied lifting forces was 3,753 psi, which occurs in the structural lid where the lifting loads were applied (see Figure 2.5.1-6).

As stated previously, the maximum stress intensity in the canister lifting model occurs in the structural lid that is constructed of Type 304L stainless steel. The yield strength (S_y) of Type 304L stainless steel at 250°F is 20,300 psi. The ultimate strength (S_u) of Type 304L stainless steel at 250°F is 63,550 psi.

The factor of safety (FS) for the canister lift based on yield strength is:

$$FS = \frac{S_y}{S_{INT}} = \frac{20,300 \text{ psi}}{3,753 \text{ psi}} = 5.40 > 3$$

The factor of safety for the canister lift based on ultimate strength is:

$$FS = \frac{S_u}{S_{INT}} = \frac{63,550 \text{ psi}}{3,753 \text{ psi}} = 16.93 > 5$$

2.5.1.3.2 CY-MPC Canister Lifting

The adequacy of the CY-MPC canister lifting devices is demonstrated by considering each of the hoist rings, the canister structural lid and the weld that joins the structural lid to the canister shell. Lifting of the canister employs redundant three-legged lifting slings for single failure proof lifting in accordance with NUREG-0612.

When considering a three-point lifting configuration, the load-bearing members of the canister maintain a factor of safety greater than three based on material yield strength. Additionally, the load-bearing members of the canister maintain a factor of safety greater than five based on material ultimate strength. The hoist rings are designed with a 5 to 1 safety factor based on material ultimate strength. Therefore, the lifting requirements are satisfied.

Each lifting device in a three-point lift would experience the following load, F, when lifting the canister (the total load is based on the dead weight of the loaded canister with a dynamic load factor of 10%):

$$F = \frac{66,000 \text{ lb} \times 1.1}{3} = 24,200 \text{ lb}$$

The hoist rings used to lift the canister have a rated load capacity of 30,000 pounds with a 5 to 1 safety factor based on material ultimate strength. The length of the hoist ring bolt is 2.0 inches. From Machinery's Handbook, 25th Edition, the shear area of the structural lid bolt hole threads (A_n) is calculated as:

$$\begin{aligned} A_n &= 3.1416nL_e D_s \min \left[\frac{1}{2n} + 0.57735(D_s \min - E_n \max) \right] \\ &= 3.1416(4.5)(2.0)(1.9751) \left[\frac{1}{2(4.5)} + 0.57735(1.9751 - 1.8681) \right] = 9.654 \text{ in}^2 \end{aligned}$$

where:

- n = 4.5, threads per inch
- L_e = 2.0 in., bolt thread engagement length
- $D_s \min$ = 1.9751 in., minimum major diameter-external thread
- $E_n \max$ = 1.8681 in., maximum pitch diameter-internal thread

The shear stress, τ , in the structural lid bolt hole threads is calculated as:

$$\tau = \frac{F_x}{A_n} = \frac{24,200 \text{ lb}}{9.654 \text{ in}^2} = 2,507 \text{ psi}$$

The canister structural lid is constructed of SA240, Type 304L stainless steel. At a temperature of 300°F (conservative), the Type 304L stainless steel yield strength is 19,200 psi and the ultimate strength is 60,900 psi. Thus, when the thread shear stress of 2,507 psi is compared to the structural lid yield and ultimate strengths, the lifting load factors of safety are:

$$(F.S.)_{\text{yield}} = \frac{0.6S_y}{\text{shear stress}} = \frac{11,520 \text{ psi}}{2,507 \text{ psi}} = 4.6 (> 3)$$

$$(F.S.)_{\text{ultimate}} = \frac{0.5S_u}{\text{shear stress}} = \frac{30,450 \text{ psi}}{2,507 \text{ psi}} = 12.1 (> 5)$$

These factors of safety meet the NUREG-0612 criteria for a redundant lifting system.

The minimum thread engagement (L_{minth}), based on the yield shear strength of the Type 304L lid material is:

$$F_x = 24.20 \text{ kip}$$

$$0.6S_y = 11.52 \text{ ksi}$$

$$F.S._{\text{yield, min}} = 3$$

$$(\tau_{\text{max}})_{\text{allow}} = 0.6S_y / F.S._{\text{yield, min}} = 11.52 \text{ ksi} / 3 = 3.84 \text{ ksi}$$

$$A_{\text{min}} = F / (\tau_{\text{max}})_{\text{allow}} = 24.20 \text{ kip} / 3.84 \text{ ksi} = 6.30 \text{ in}^2$$

$$L_{\text{minth}} = \frac{A_{\text{min}}}{\pi n D_{s \text{ min}} \left[\frac{1}{2n} + 0.57735(D_{s \text{ min}} - E_{n \text{ max}}) \right]} = \frac{6.30}{4.83}$$

$$L_{\text{minth}} = 1.30 \text{ inches, based on the material yield Factor of Safety (F.S.) requirement of 3.}$$

The minimum thread engagement (L_{minth}), based on the ultimate shear strength of the Type 304L lid material is:

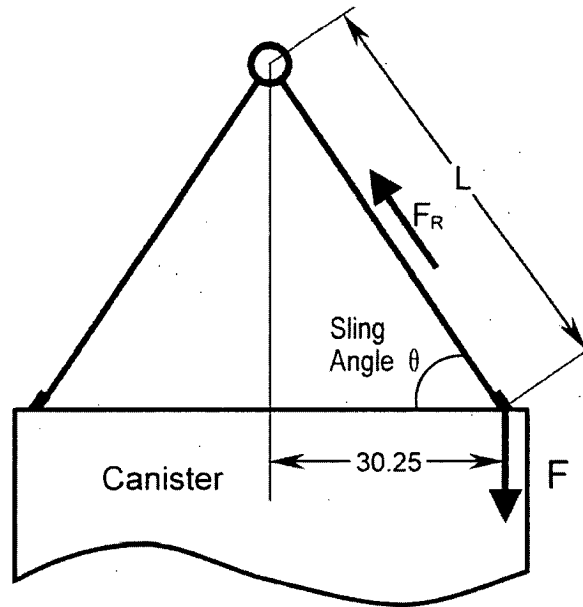
$$F_x = 4.20 \text{ kip}$$

$$\begin{aligned}
 0.5S_u &= 30.45 \text{ ksi} \\
 F.S._{\text{ultimate, min}} &= 5 \\
 (\tau_{\text{max}})_{\text{allow}} &= 0.5S_u / F.S._{\text{ultimate, min}} = 30.45 \text{ ksi} / 5 = 6.09 \text{ ksi} \\
 A_{\text{min}} &= F / (\tau_{\text{max}})_{\text{allow}} = 24.20 \text{ kip} / 6.09 \text{ ksi} = 3.97 \text{ in}^2
 \end{aligned}$$

$$L_{\text{minth}} = \frac{A_{\text{min}}}{\pi n D_{s\text{min}} \left[\frac{1}{2n} + 0.57735(D_{s\text{min}} - E_{n\text{max}}) \right]} = \frac{3.97}{4.83}$$

$L_{\text{minth}} = 0.82$ inch, based on the ultimate Factor of Safety requirement of 5.

Based on the calculated thread engagement lengths, the minimum required engagement length is 1.3 inches based on the yield strength Factor of Safety. This minimum required thread engagement length is bounded by the actual total length of the hoist ring bolt thread engagement, 2.0 inches. The hoist rings are rated at 30,000 lbs with a safety factor of 5.



The relation between the tension in the sling and thus the load on the swivel hoist ring (F_R) is:

$$F_R = \frac{F}{\sin \theta}$$

where:

- F_R = the load on the swivel hoist ring
- F = the handling load on the hoist ring ($66,000 \text{ lb} \times 1.1/3$)

F_R is limited to 30,000 lb, the load rating (with a 5:1 safety factor) of the swivel hoist ring. The minimum sling angle (θ_{\min}) is then determined as:

$$\theta_{\min} = \sin^{-1} \frac{F}{F_R} = \sin^{-1} \frac{24,200}{30,000} = 53.8^\circ$$

For a slight additional margin, the minimum sling angle is set at 60° , requiring a minimum sling length (L) of:

$$L = \frac{30.25}{\cos \theta} = 60.5 \text{ in}$$

Therefore, the minimum allowable distance from the master link of the sling to the top of the canister is $60.5 \sin 60^\circ = 52.4$ inches.

The structural adequacy of the canister structural lid and weld is evaluated using a finite element representation of the upper portion of the canister using the ANSYS program. As shown in Figure 2.5.1-5, the model represents one-half (180° section) of the upper 50-in. of the canister (including the structural and shield lids). The lids and shell are modeled using SOLID45 elements. CONTAC52 elements are used to model the interaction between the structural lid and the canister shell and between the shield lid and the canister shell, just below the respective lid weld joints. The size of the CONTAC52 gaps is determined from nominal dimensions of contacting components. COMBIN40 elements are used between the structural and shield lids in the axial direction and between the shield lid and the backing ring. These gaps are assigned small gap sizes of $1\text{E-}8$ inches. All gap/spring elements are assigned a stiffness of $1\text{E}8$ lbs/in.

To enforce symmetry at the boundary of the model (in the x-y plane), all nodes on the x-y symmetry plane are restrained perpendicular to the symmetry plane (UZ). In addition, the nodes in the x-z plane at the bottom of the model are restrained in the axial direction.

Load-bearing members of a lifting device must be capable of lifting three (3) times the combined weight of the shipping container with which it will be used, plus the weight of intervening components of the lifting device without exceeding the tensile yield strength of their materials of construction. In addition, the lifting components must be capable of lifting five (5) times that combined weight without exceeding the ultimate tensile strength of the materials. NUREG-0612 also requires that the lifting loads must be based on the combined maximum static and dynamic

loads that could be imparted on the handling device based on characteristics of the crane that will be used. A dynamic load factor of 10% has been applied.

To simulate the lifting of the canister by a three-point lifting device (the lifting configuration is actually two independent three-point lifting devices), point loads equal to one-third of the total canister and contents weight plus a dynamic loading factor of 10% are applied to the model. The load is applied in the axial direction of the canister since the horizontal load component due to the angled hoist rings has an insignificant effect on the stresses in the structural lid weld and canister shell. Because the model represents a half section of the canister, only two point loads are applied 120° apart as shown in Figure 2.5.1-5. Because of the symmetry conditions of the model, the force applied to the node on the symmetry plane is one-half of the value applied at the other location. A temperature of 250°F is conservatively used to determine allowable stresses.

The maximum stress intensity generated in the canister model from the applied lifting forces is 4,482 psi, which occurs in the structural lid where the lifting loads are applied (Figure 2.5.1-7).

The maximum stress intensity in the canister lifting model occurs in the structural lid that is constructed of Type 304L stainless steel. The yield strength (S_y) of Type 304L stainless steel at 250°F is 20,300 psi. The ultimate strength (S_u) of Type 304L stainless steel at 250°F is 63,550 psi.

The factor of safety (FS) for the canister lift based on yield strength is:

$$FS = \frac{S_y}{S_{INT}} = \frac{20,300 \text{ psi}}{4,482 \text{ psi}} = 4.53 > 3$$

The factor of safety for the canister lift based on ultimate strength is:

$$FS = \frac{S_u}{S_{INT}} = \frac{63,550}{4,482} = 14.18 > 5$$

2.5.1.3.3 Shield Lid

The shield lid lifting system uses three 1 1/4 -7 UNC-2B threaded holes located on a 60.5 inch bolt circle. The three holes are equally spaced. The shield lid material is Type 304 stainless steel. The weight of the shield lid is 5,390 pounds.

The shield lid is lifted using a wire-rope sling that is load-rated for not less than the weight of the shield lid. The sling is attached to the lid using hoist-eyes that are threaded into the shield lid.

2.5.1.3.4 Structural Lid

The structural lid lifting system uses six 1 1/4 -7 UNC-2B threaded holes located on a 60.5 inch bolt circle. The six holes are equally spaced. The structural lid material is Type 304L stainless steel. The weight of the structural lid is 3,230 pounds.

The structural lid is lifted using a wire-rope sling that is load-rated for not less than the weight of the structural lid. The sling is attached to the lid using three equally spaced hoist-eyes that are threaded into the structural lid.

2.5.1.3.5 Empty Canister and Basket

The empty canister and basket lifting system uses eight hoist eyes threaded into holes located in the top nuts as part of the basket assembly. The holes are on a 62.5-inch bolt circle. The top nut material is Type 304 stainless steel. The weight of the empty canister and basket is 15,510 pounds.

The empty canister and basket are lifted using two wire-rope slings that are each load-rated for not less than the weight of the empty canister and basket assembly. The primary sling is attached to the basket using four equally spaced hoist-eyes that are threaded into the top nuts. The secondary (redundant) sling uses four equally spaced hoist eyes that are threaded into the remaining four top nuts.

Figure 2.5.1-1 Lifting Trunnion Geometry

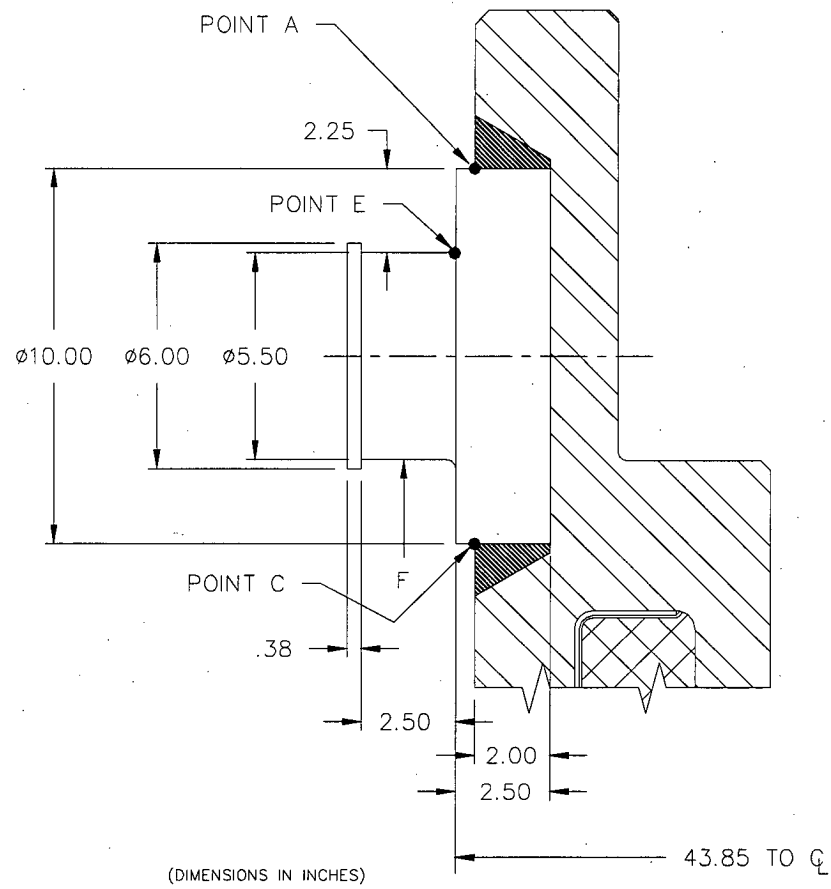


Figure 2.5.1-2 Trunnion Weld Geometry

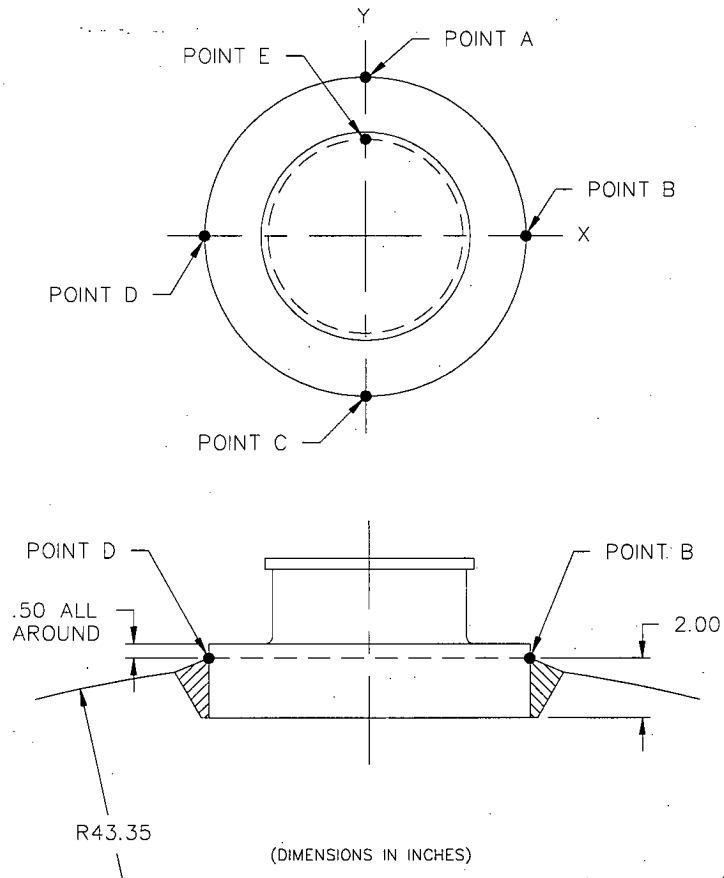


Figure 2.5.1-3 Sling Inclusion Angle for Outer Lid Lifting

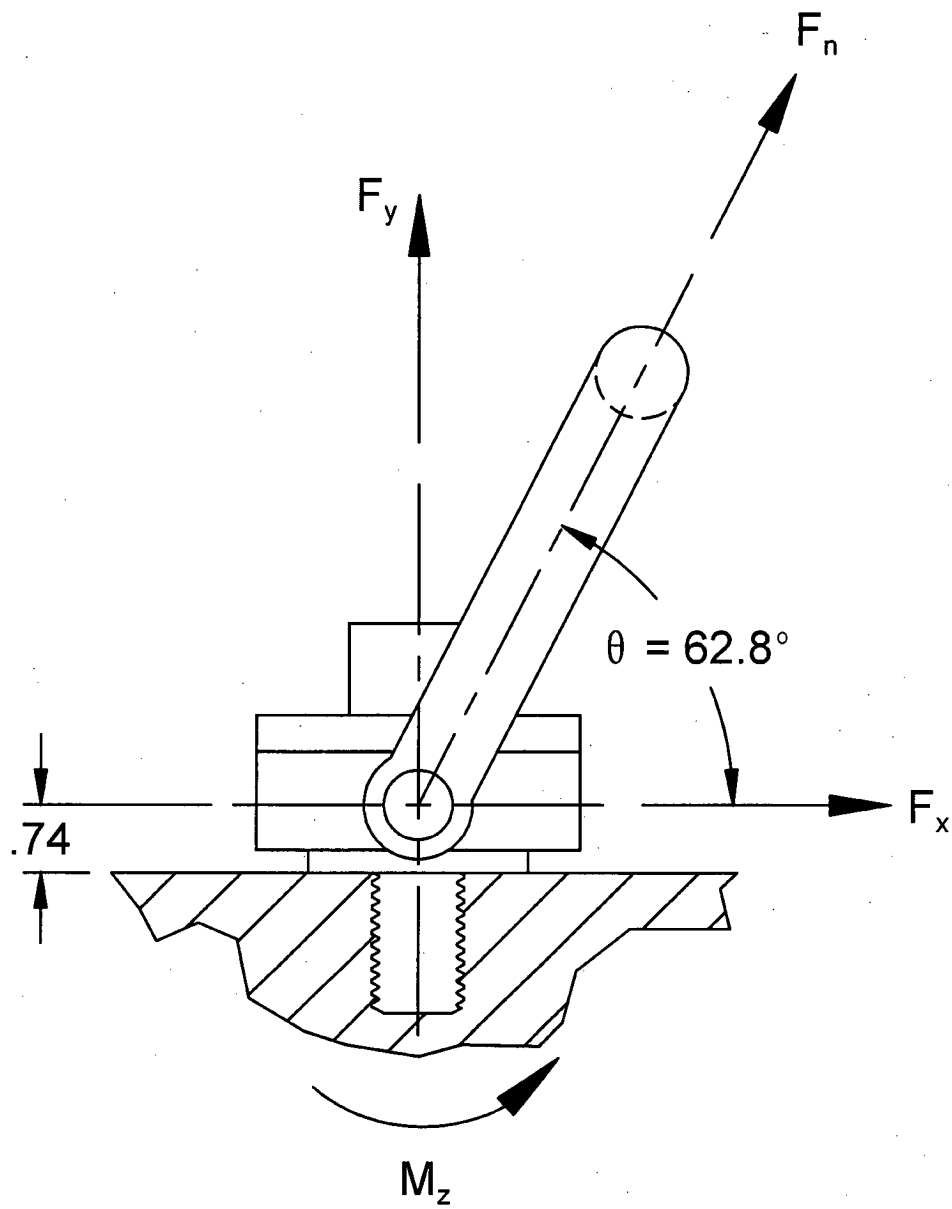


Figure 2.5.1-4 Sling Inclination Angle for Inner Lid Lifting

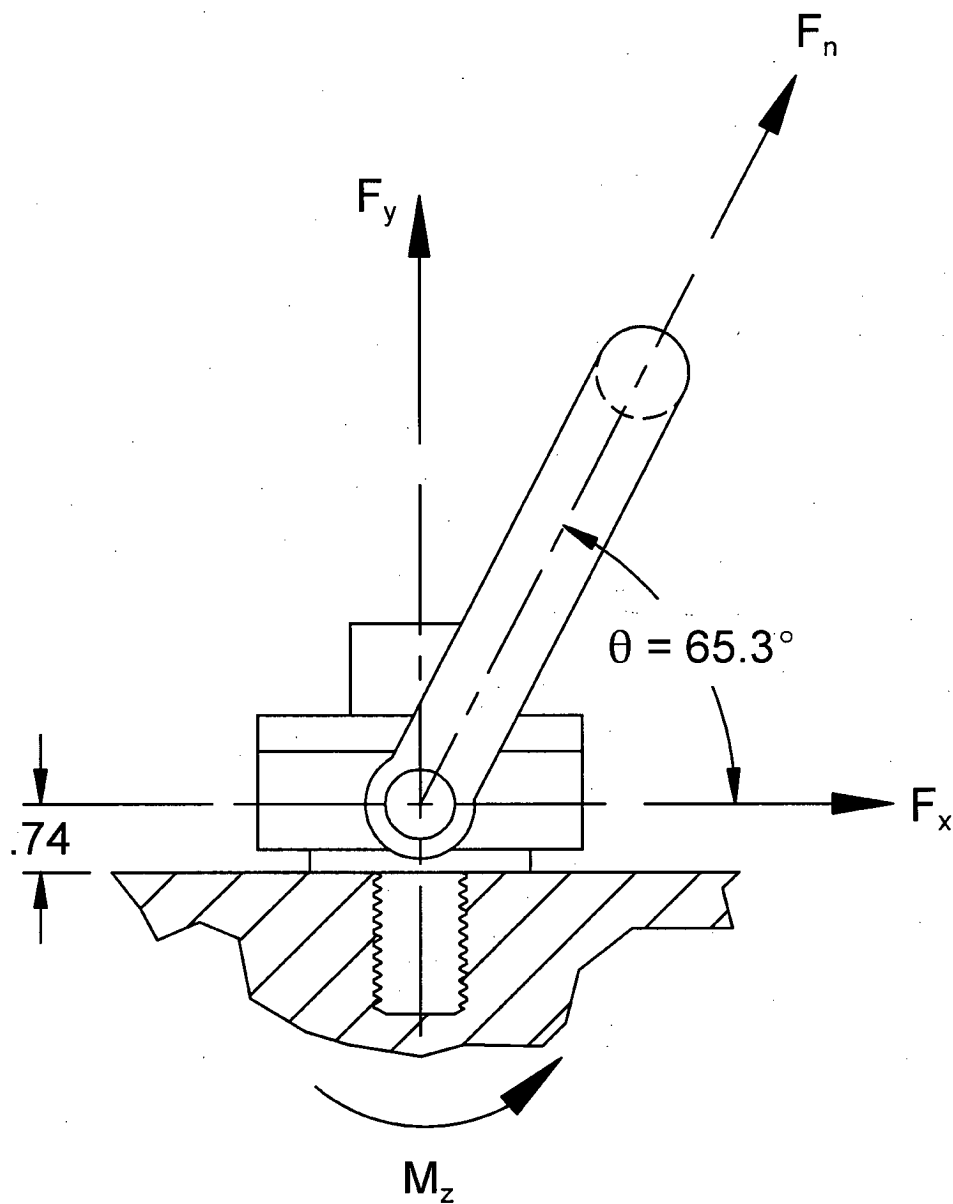


Figure 2.5.1-5 Canister Lift Finite Element Model

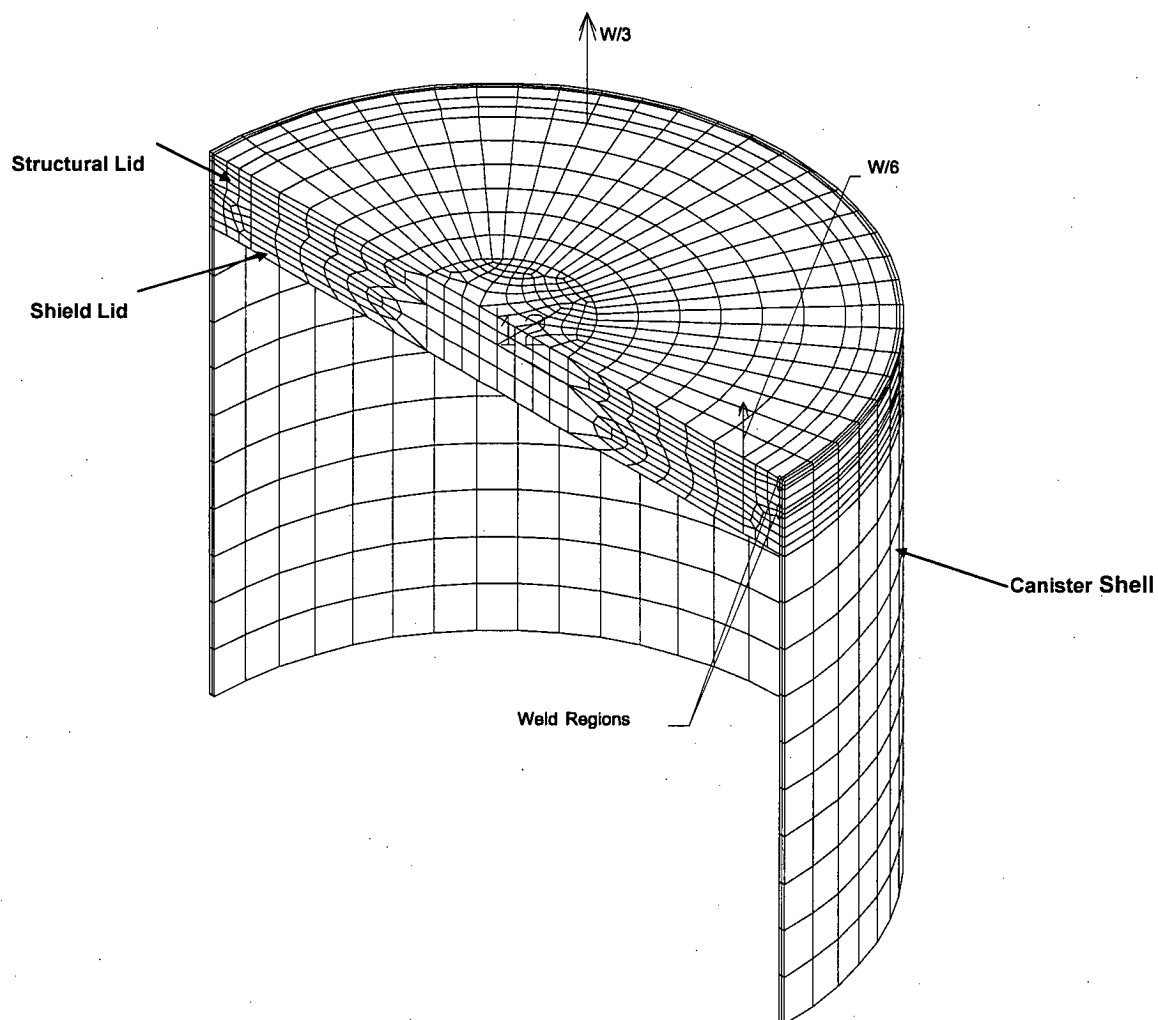


Figure 2.5.1-6 Yankee-MPC Canister Lift Model Stress Intensity Contours (psi)

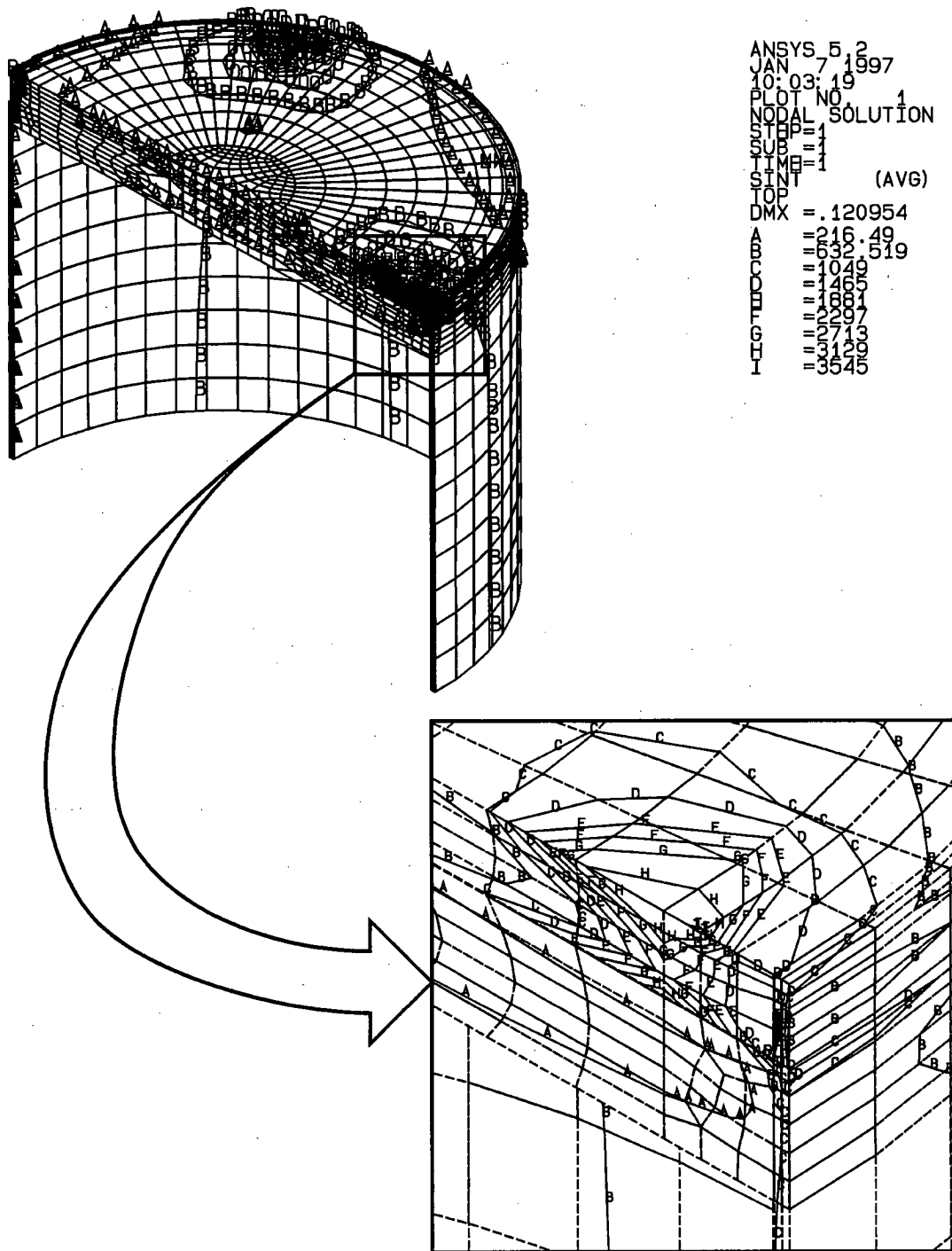
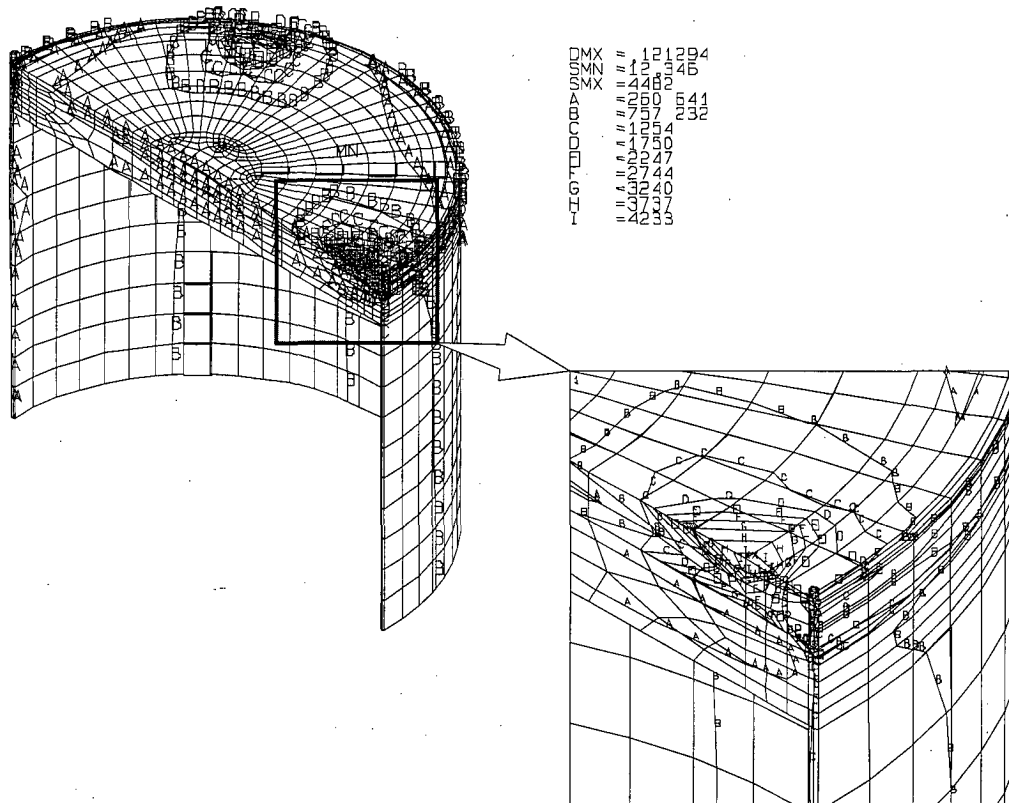


Figure 2.5.1-7 CY-MPC Canister Lift Model Stress Intensity Contours (psi)



2.5.2 Tiedown Devices

The NAC-STC is tied down to the transport vehicle using the following: (a) rotation trunnion recesses near the bottom at point j (Figure 2.5.2-1); and (b) two 46-degree saddle supports, hold-down straps and a shear ring near the top end at point j (Figure 2.5.2-1). Longitudinal force towards the bottom of the cask is resisted by the supports at the rotation trunnion recesses. A shear ring welded to the outer shell resists the longitudinal force towards the top end of the cask. A 0.50-inch gap is provided between the shear ring and the saddle support to accommodate any thermal expansion of the cask.

The tiedown components of the NAC-STC are designed to satisfy the requirements of 10 CFR 71.45(b) and the AAR Field Manual, Rule 88, since rail is the most likely mode of transport. In accordance with 10 CFR 71.45(b), the structural components of the cask that are used for tiedown must be capable of withstanding certain specified forces, without generating stress in any material of the package in excess of its yield strength. These forces are comprised of a static force applied to the center of gravity of the package having a vertical component of 2 times the weight of the package with its contents, a horizontal component along the direction in which the vehicle travels of 10 times the weight of the package with its contents, and a transverse horizontal component of 5 times the weight of the package with its contents. In accordance with Rule 88 of the AAR Field Manual, the tiedowns for rail shipment of radioactive material containers must be capable of withstanding, without generating stress in any material of the tiedown in excess of its yield strength, a static force applied to the package center of gravity having components of 4.0 vertical, 7.5 longitudinal, and 1.8 transverse, times the weight of the package with its contents. The weight of the NAC-STC, loaded and ready for shipment, is 250,000 pounds in the directly loaded and Yankee-MPC configurations, and is 260,000 pounds in the CY-MPC configuration. The CY-MPC configuration weight is bounding. The calculational methodology and results for the cask tiedown evaluation using the 250,000 weight are presented in Sections 2.5.2.1, 2.5.2.2 and 2.5.2.3. The revised stress margins for the 260,000 pound weight are shown in Section 2.5.2.4.

2.5.2.1 Discussion and Loads

The resultant force on the shear ring is assumed to act at the centroid of the contact area between the shear ring and the saddle support. Referring to Figure 2.5.2-1, the distance of the centroid from the center of the cask is determined. Calculate the centroid for $\theta = 60^\circ$ and subtract the contribution of the 14 degree arc.

For $\theta = 60^\circ$:

$$\bar{y} = (A_{\bar{y}_o} - A_{\bar{y}_i}) / (A_o - A_i)$$

$$\bar{y} = [\sin \theta (R_o^3 - R_i^3)] / [3\theta (R_o^2 - R_i^2)]$$

$$\bar{y}_{60} = 36.505 \text{ in (for } \theta = 60^\circ)$$

where:

$$A_o = \theta R_o^2$$

$$A_i = \theta R_i^2$$

$$\bar{y}_o = (2R_o \sin \theta) / 3 \theta$$

$$\bar{y}_i = (2R_i \sin \theta) / 3 \theta$$

$$\theta_{60} = 60^\circ = \pi/3 \text{ radians}$$

$$R_o = 44.925 \text{ in}$$

$$R_i = 43.35 \text{ in}$$

Next, the centroid of the 14-degree arc is determined:

$$\bar{y}_{14} = [2 \sin \theta_1 (R_o^3 - R_i^3)] / [3\theta_1 (R_o^2 - R_i^2)]$$

$$= 43.704 \text{ in (for } \theta_1 = 14^\circ)$$

where:

$$\theta_{14} = 14^\circ = 14\pi/180 \text{ radians}$$

The distance of the centroid from the center of the cask of the actual bearing area between $\theta = 14^\circ$ and $\theta = 60^\circ$ is calculated as:

$$\begin{aligned}\bar{y}_{act} &= \frac{\bar{y}_{60} A_{60} - \bar{y}_{14} A_{14}}{A_{60} - A_{14}} \\&= \frac{\bar{y}_{60} [\theta_{60} (R_o^2 - R_i^2)] - \bar{y}_{14} [\theta_{14} (R_o^2 - R_i^2)]}{\theta_{60} (R_o^2 - R_i^2) - \theta_{14} (R_o^2 - R_i^2)} \\&= 34.31 \text{ in (for } \theta \text{ between } 14^\circ \text{ and } 60^\circ)\end{aligned}$$

where:

$$\begin{aligned}A_{60} &= \theta_{60} (R_o^2 - R_i^2), \text{ area of 60 degree bearing area} \\A_{14} &= \theta_{14} (R_o^2 - R_i^2), \text{ area of 14 degree non-bearing area} \\\bar{y}_{60} &= \text{centroid of 60 degree bearing area from cask axis} \\\bar{y}_{14} &= \text{centroid of 14 degree non-bearing area from cask axis}\end{aligned}$$

There are three loading cases for the tiedown components--vertical, longitudinal, and lateral loads. The reaction forces for each loading case are determined by the equations of equilibrium.

2.5.2.1.1 Vertical Load Per 10 CFR 71.45(b)

Downward Direction

$$F_y = -2W = (-2)(250,000) = -500,000 \text{ lb}$$

Summing moments M_z about point j:

$$SM_z = (-500,000)(80.90) + (2R_{iy})(159.55) = 0$$

$$R_{iy} = +126,763 \text{ lb}$$

Summing vertical forces:

$$2R_{iy} + R_{jy} - 500,000 = 0$$

$$R_{jy} = +246,474 \text{ lb}$$

Note: $R_{ix} = R_{jx} = 0$ because of the gap provided at the shear ring.

Upward Direction

$$F_y = +2W = (+2)(250,000) = +500,000 \text{ lb}$$

Similarly, summing moments M_z about point j:

$$R_{iy} = -126,763 \text{ lb}$$

$$R_{jy} = -246,474 \text{ lb}$$

Note that the support saddle cannot carry any upward load. Hence, the negative R_{jy} is resisted by a tiedown strap.

2.5.2.1.2 Longitudinal Load Per 10 CFR 71.45(b)

Forward Direction

$$F_x = +10W = (+10)(250,000) = +2,500,000 \text{ lb}$$

Summing horizontal forces:

$$2,500,000 + R_{jx} = 0$$

$$R_{jx} = -2,500,000 \text{ lb}$$

Summing moments about j:

$$(+2,500,000)(34.31) + (2R_{iy})(159.55) = 0$$

$$R_{iy} = -268,803 \text{ lb}$$

Summing vertical forces:

$$R_{jy} - (2)(268,803) = 0$$

$$R_{jy} = 537,606 \text{ lb}$$

Aft Direction

$$F_x = -10W = (-10)(250,000) = -2,500,000 \text{ lb}$$

Summing horizontal forces:

$$-2,500,000 + 2R_{ix} = 0$$

$$R_{ix} = +1,250,000 \text{ lb}$$

Summing moments about j:

$$(-2,500,000)(34.31) + (2)(1,250,000)(34.31 + 3) + (2R_{iy})(159.55) = 0$$

$$R_{iy} = -23,504 \text{ lb}$$

Summing vertical forces:

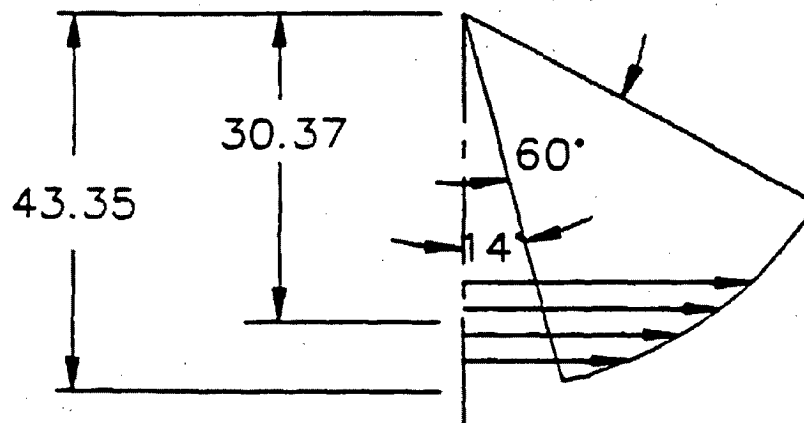
$$R_{jy} - (2)(23,504) = 0$$

$$R_{jy} = 47,008 \text{ lb}$$

2.5.2.1.3 Lateral Load Per 10 CFR 71.45(b)

$$F_z = 5W = (5)(250,000) = 1,250,000 \text{ lb}$$

To find the reactions resisting the above load, it is necessary to find the location of the bearing pressure between the support saddle and the cask surface. The contact surface is one-half of the saddle, as shown below. Assume that the horizontal bearing pressure at any point is proportional to the sine function of the angular distance of the point from the lowest point in the saddle. The distance from the center of the cask to the resultant of the bearing force between the cask and the saddle is calculated as:



Bearing Distribution of Cask in Saddle

For the 60 degree arc:

$$\bar{y} = \frac{A_1 \bar{y}_1 - A_2 \bar{y}_2}{A_1 - A_2}$$

$$= 30.562 \text{ in (for } \theta = 60^\circ)$$

where:

$$A_1 = (\theta_1/2)(43.35)^2 = 983.959 \text{ in}^2$$

$$A_2 = (43.35)^2(\sin \theta_1)(\cos \theta_1)/2 = 406.864 \text{ in}^2$$

$$\bar{y}_1 = (2)(43.35)(\sin 60^\circ)/(3)(\pi/3) = 23.90 \text{ in}$$

$$\bar{y}_2 = (2/3)(43.35 \cos 60^\circ) = 14.45 \text{ in}$$

$$\theta_1 = 60^\circ = \pi/3 \text{ radians}$$

For the 14 degree arc:

$$\bar{y} = \frac{A_1 \bar{y}_1 - A_2 \bar{y}_2}{A_1 - A_2}$$

= 42.56 in, centroidal location of the 14° arc from cask axis

where:

$$A_1 = (\theta_2/2)(43.35)^2 = 229.59 \text{ in}^2$$

$$A_2 = (43.35)^2(\sin \theta_2)(\cos \theta_2)/2 = 220.56 \text{ in}^2$$

$$\theta_2 = 14^\circ = (14/180)(\pi) \text{ radians}$$

$$\bar{y}_1 = \frac{(2)(43.35)(\sin \theta_2)}{3\theta_2} = 28.613 \text{ in}$$

$$\bar{y}_2 = (2/3)(43.35)(\cos \theta_2) = 28.042 \text{ in}$$

The centroidal location of the resultant force acting laterally on the support saddle between the 14 degree and 60 degree angular distance from the vertical is:

$$\bar{y}_{act} = \frac{(30.562)(983.959 - 406.864) - (42.56)(229.59 - 220.56)}{(983.959 - 406.864) - (229.59 - 220.56)}$$

$$= 30.37 \text{ in}$$

Call the location of this centroid: point k.

The horizontal distance from the center of the cask to the support point is 47.01 inches (Figure 2.5.2-2).

Summing moments about the vertical line through k (Figure 2.5.2-2):

$$(1,250,000)(80.90) + R_{iz}(159.55) = 0$$

$$R_{iz} = -633,814 \text{ lb}$$

Summing forces along the Z-axis:

$$1,250,000 - 633,814 + R_{iz} = 0$$

$$R_{jz} = -616,186 \text{ lb}$$

Summing forces along the Y-axis:

$$R_{iy} = -R'_{iy}$$

Summing moments about the longitudinal axis of the cask:

$$(616,186)(30.37) - (633,814)(3) - (-R'_{iy})(47.01 + 47.01) = 0$$

$$-R'_{iy} = 178,814 \text{ lb}$$

$$R_{iy} = -178,814 \text{ lb}$$

Opposite Lateral Load

$$F_z = -5W = (-5)(250,000) = -1,250,000 \text{ lb}$$

The reactions for this case are opposite to the previous case.

2.5.2.1.4 Vertical Load Per AAR Field Manual, Rule 88

Downward Direction

$$F_y = (-4W) = (-4)(250,000) = -1,000,000 \text{ lb}$$

Summing moments M_z about point j:

$$\Sigma M_z = (-1,000,000)(80.90) + (2R_{iy})(159.55) = 0$$

$$R_{iy} = +253,525 \text{ lb}$$

Summing vertical forces:

$$2R_{iy} + R_{jy} - 1,000,000 = 0$$

$$R_{jy} = 492,950 \text{ lb}$$

Note: $R_{ix} = R_{jx} = 0$ because of the gap provided at the shear ring.

Upward Direction

$$F_y = +4W = (+4)(250,000) = +1,000,000 \text{ lb}$$

Similarly, summing moments M_z about point j:

$$R_{iy} = -253,525 \text{ lb}$$

$$R_{jy} = -492,950 \text{ lb}$$

Note that the support saddle cannot carry any upward load. Hence, the negative R_{jy} is resisted by a tiedown strap.

2.5.2.1.5 Longitudinal Load Per AAR Field Manual, Rule 88

Forward Direction

$$F_x = +7.5W = (+7.5)(250,000) = +1,875,000 \text{ lb}$$

Summing horizontal forces:

$$1,875,000 + R_{jx} = 0$$

$$R_{jx} = -1,875,000 \text{ lb}$$

Summing moments about j:

$$(1,875,000)(34.31) + 2R_{iy}(159.55) = 0$$

$$R_{iy} = -201,602 \text{ lb}$$

Summing vertical forces:

$$R_{jy} - (-2)(201,602) = 0$$

$$R_{jy} = 403,204 \text{ lb}$$

Aft Direction

$$F_x = -7.5W = (-7.5)(250,000) = -1,875,000 \text{ lb}$$

Summing horizontal forces:

$$-1,875,000 + 2R_{ix} = 0$$

$$R_{ix} = +937,500 \text{ lb}$$

Summing moments about j:

$$(-1,875,000)(34.31) + (2)(937,500)(34.31 + 3) + (2R_{iy})(159.55) = 0$$

$$R_{iy} = -17,628 \text{ lb}$$

Summing vertical forces:

$$R_{jy} - (2)(17,628) = 0$$

$$R_{jy} = 35,256 \text{ lb}$$

2.5.2.1.6 Lateral Load Per AAR Field Manual, Rule 88

$$F_z = 1.8W = (1.8)(250,000) = 450,000 \text{ lb}$$

Summing moments about the vertical line through k (Figure 2.5.2-2):

$$(450,000)(80.90) + (R_{iz})(159.55) = 0$$

$$R_{iz} = -228,173 \text{ lb}$$

Summing forces along the Z-axis:

$$450,000 - 228,173 + R_{jz} = 0$$

$$R_{jz} = -221,827 \text{ lb}$$

Summing forces along the Y-axis:

$$R_{iy} = -R_{iy}$$

Summing moments about the longitudinal axis of the cask:

$$(221,827)(30.37) - (228,173)(3) - (R_{iy})(47.01 + 47.01) = 0$$

$$R_{iy} = 64,373 \text{ lb}$$

$$R_{iy} = -64,373 \text{ lb}$$

Opposite Lateral Load

$$F_z = -1.8W = (-1.8)(250,000) = -450,000 \text{ lb}$$

The reactions for this case are opposite to the previous case.

2.5.2.1.7 Loads Summary

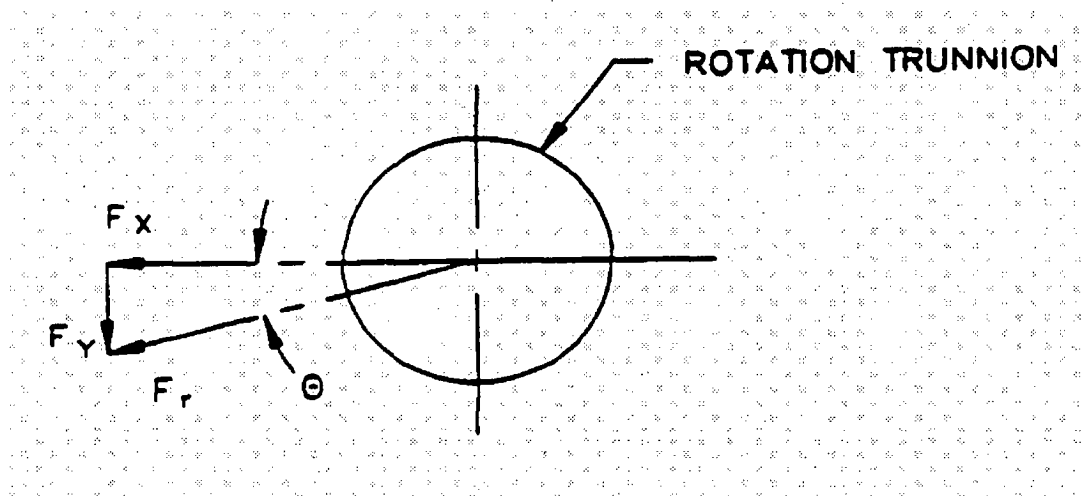
The results of all the loading cases are summarized in Tables 2.5.2-1 and 2.5.2-2.

2.5.2.2 Rear Support

The NAC-STC rear tiedown attachment is at the rotation trunnion recesses. There are two rotation trunnion recesses, which are slots located 18.15 inches above the bottom of the cask, and spaced at approximately 180-degree positions in line with two of the lifting trunnions. Each slot is a machined part, which is welded all around to the cask outer shell. The neutron shield tank shell is cut out to provide access to the slots. The geometry details of the shield tank cut-outs and the rotation trunnion slots are shown in the detailed drawings in Section 1.3.2.

2.5.2.2.1 Loads

The rotation trunnion recesses are analyzed for the cask tiedown load condition defined in 10 CFR 71.45(b) and Rule 88 of the Field Manual of the AAR. The condition used for this analysis assumes that the cask is supported horizontally on a railcar and is subjected to the more limiting of either (1) a 10g longitudinal shock load simultaneously with a 2g vertical shock load and a 5g lateral shock load or (2) a 7.5g longitudinal shock load, a 4g vertical shock load, and a 1.8g lateral shock load. The direct lateral load is transferred to the cask through bearing on the large trunnion slot base. Any dynamic load effects are negligible when considered in combination with the large applied load factors. The critical loads on the rotation trunnions are derived in Section 2.5.2.1 and are summarized in Tables 2.5.2-1 and 2.5.2-2. From these tables, it is apparent that the load conditions specified in 10 CFR 71.45(b) produce the more critical loads on the rotation trunnion.



Resultant Load Determination

$$F_r = \sqrt{(F_x)^2 + (F_y)^2}$$

$$= 1,292,592 \text{ lb}$$

where:

$$F_x = 1,250,000 \text{ lb}$$

$$F_y = -329,081 \text{ lb (Table 2.5.2-1)}$$

then

$$q = \arctan (329,081/1,250,000)$$

$$= 14.75^\circ$$

2.5.2.2.2 Material Properties at 300°F

The yield strength of each material at 300°F, a conservatively high normal conditions temperature, is the allowable stress:

Type 304 stainless steel forging:

$$S_y = 22.5 \text{ ksi}$$

$$S_u = 61.5 \text{ ksi}$$

SA-705, Type 630, 17-4 PH Stainless Steel

$$S_y = 93.0 \text{ ksi}$$

$$S_u = 135.0 \text{ ksi}$$

AWS E309 filler material:

$$S_y = 61.0 \text{ ksi}$$

$$S_u = 80.0 \text{ ksi}$$

The bearing stress ratio is taken from MIL-HDBK-5C where the bearing yield stress for the 17-4 PH, H1150 stainless steels at ambient temperature is specified as 152 ksi. It is assumed that the ratio of bearing stress to yield stress remains constant up to 300°F:

$$S_{bry} = (93.0/105)(152) = 135 \text{ ksi}$$

The shear strength (yield strength criteria) for the different materials are:

Forging: $S_{sy} = 0.6S_y = 13,500 \text{ psi}$

Trunnion: $S_{sy} = 0.6S_y = 55,800 \text{ psi}$

Filler Material: $S_{sy} = 0.65y = 36,600 \text{ psi}$

2.5.2.2.3 Stress Analysis

(Bearing Stress in Trunnion Slot)

$$F_r = 1,292,592 \text{ lb}$$

Length of engagement for 6.00-in diameter pin = 3.88 inches

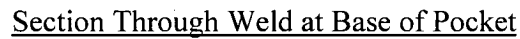
$$A_{br} = (6.00)(3.88) = 23.28 \text{ in}^2$$

$$\begin{aligned} S_{br} &= \frac{F_r}{A_{br}} \\ &= 55,524 \text{ psi} \end{aligned}$$

$$MS = \frac{S_{bry}}{S_{br}} - 1 = + 1.43$$

(Stress in Weld at Interface with Rotation Trunnion Recess)

Assume the entire load transferred to the cask outer shell through the weld at the base of the trunnion.


$$t_e = [(1.50)^2 + (1.375)^2]^{0.5} = 2.035 \text{ inches (Section B-B, 3 Sides)}$$
$$\begin{aligned}\text{Area (A}_w\text{)} &= (19.035)(11.07) - (15.50)(7.00) \\ &= 102.22 \text{ in}^2\end{aligned}$$

$$= 9.801 \text{ in}$$

2.5.2-15

$$\begin{aligned} I_y &= \frac{(11.07)(19.035)^3}{12} + (11.07)(19.035) \left(\frac{19.035}{2} - 9.801 \right)^2 \\ &\quad - \frac{(7.00)(15.50)^3}{12} - (7.00)(15.50)(9.25 - 9.801)^2 \\ &= 4174 \text{ in}^4 \end{aligned}$$

$$b = 17.27 \text{ in}$$

$$h = 9.035 \text{ in}$$

$$t_a = 1.50 \text{ in}$$

$$t_b = 2.035 \text{ in}$$

From Table 2.5.2-1, the loads for Case II are the highest combination loads on the weld group:

$$F_x = 1,250,000 \text{ lb}$$

$$F_y = 329,081 \text{ lb}$$

$$F_r = (F_x^2 + F_y^2)^{0.5} = 1,292,592 \text{ lb}$$

$$e_x = 9.801 - 6.0 = 3.801 \text{ in}$$

$$e_z = 5.8 - 4.13/2 = 3.735 \text{ in}$$

$$M_x = F_y (e_z) = 1,229,118 \text{ in-lb}$$

$$M_y = F_x (e_z) = 4,668,750 \text{ in-lb}$$

$$M_z = F_y (e_x) = 1,250,837 \text{ in-lb}$$

Component stresses on the effective thickness weld group are:

$$S_{AC} = \frac{M_y c_x}{I_y} = \frac{(4,668,750)(9.801)}{(4174)}$$

= 10,963 psi (Bending Stress at Points A and C)

$$S_{BC} = \frac{M_x c_y}{I_x} = \frac{(1,229,118)(5.535)}{1709}$$

= 3981 psi (Bending Stress at Points B and C)

$$S_s = \frac{F_R}{A_w} = \frac{1,292,592}{102.22}$$

= 12,645 psi (Resultant Direct Shear Stress)

$$(S_{ST})_A = \frac{M_z^*}{2 b h t_A} = \frac{1,250,837}{(2)(17.27)(9.035)(1.50)}$$

= 2672 psi (Torsional Shear Stress at Point A)

$$(S_{ST})_B = \frac{M_z^*}{2 b h t_B} = \frac{1,250,837}{(2)(17.27)(9.035)(2.035)}$$

= 1970 psi (Torsional Shear Stress at Point B)

* Seely, Table 14.

The von Mises equivalent stresses at Points A, B, and C are:

$$S_{EA} = \left[S_{AC}^2 + 3(S_S + (S_{ST})_A)^2 \right]^{0.5} = 28,706 \text{ psi}$$

$$S_{EB} = \left[S_{BC}^2 + 3(S_S + (S_{ST})_B)^2 \right]^{0.5} = 25,625 \text{ psi}$$

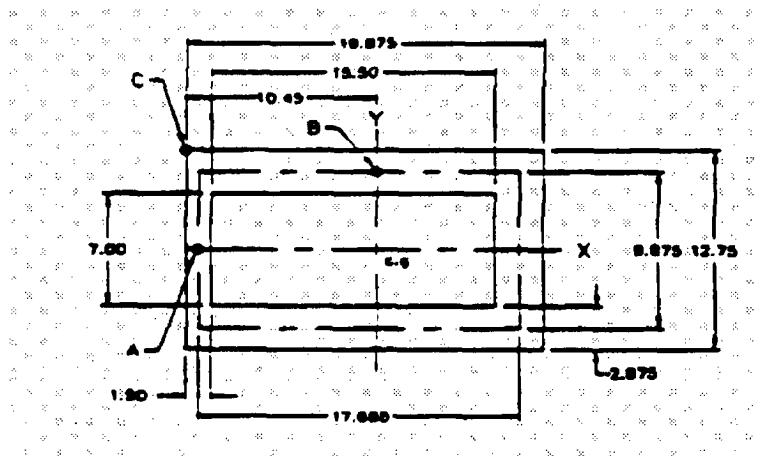
$$S_{EC} = \left[(S_{AC} + S_{BC})^2 + 3S_S^2 \right]^{0.5} = 26,432 \text{ psi}$$

The minimum margin of safety in the weld material at the rotation trunnion recess/weld interface is based on the lower yield strength of the E309 weld filler metal, $S_y = 61.0$ ksi:

$$MS = \frac{61,000}{28,706} - 1 = +1.125$$

(Stress at Cask Body/Rotation Trunnion Recess Weld Interface)

The rotation trunnion recess is welded to the cask body, which is made of Type 304 stainless steel. The strength of Type 304 stainless steel is less than the AWS E309 filler material. The stress at the weld/cask interface is analyzed below. The weld/cask interface is shown.



Section Through Weld/Cask Interface

Section properties of Weld/Cask Interface:

$$\begin{aligned}\text{Area (A}_w) &= (19.875)(12.75) - (15.50)(7.00) \\ &= 144.91 \text{ in}^2\end{aligned}$$

$$b = 17.688 \text{ in}$$

$$h = 9.875 \text{ in}$$

$$t_A = 1.50 \text{ in}$$

$$t_B = 2.875 \text{ in}$$

$$\begin{aligned}\bar{x} &= \frac{(12.75)(19.875)^2/2 - (7.00)(15.50)(1.50 + 15.50/2)}{144.91} \\ &= 10.45 \text{ in}\end{aligned}$$

$$\begin{aligned}I_x &= \frac{(19.875)(12.75)^3}{12} - \frac{(15.50)(7.00)^3}{12} \\ &= 2990 \text{ in}^4\end{aligned}$$

$$\begin{aligned}I_y &= I_y = \frac{(12.75)(19.875)^3}{12} + (12.75)(19.875)(10.45)^2 \\ &\quad - \frac{(7.00)(15.50)^3}{12} - (7.00)(15.50)(10.45 - 9.25)^2 \\ &= 6080 \text{ in}^4\end{aligned}$$

Loads on weld/cask interface:

From Table 2.5.2-1, inspection of the load combinations indicates that Case II is most critical for the rotation trunnion recess:

$$F_x = 1,250,000 \text{ lb}$$

$$F_y = -329,081 \text{ lb}$$

$$F_R = (F_x^2 + F_y^2)^{0.5} = 1,292,592 \text{ lb}$$

$$e_x = 10.45 - 6.0 = 4.45 \text{ in}$$

$$e_z = 5.8 - 4.13/2 = 3.735 \text{ in}$$

$$M_x = F_y (e_z) = 1,229,118 \text{ in-lb}$$

$$M_y = F_x (e_z) = 4,668,750 \text{ in-lb}$$

$$M_z = F_y (e_x) = 1,464,410 \text{ in-lb}$$

Component stresses in the weld/cask interface are:

$$S_{AC} = \frac{M_y c_x}{I_y} = \frac{(4,668,750)(10.45)}{6080}$$

= 8024 psi (Bending Stress at Points A and C)

$$S_{BC} = \frac{M_x c_y}{I_x} = \frac{(1,229,118)(6.375)}{2990}$$

= 2621 psi (Bending Stress at Points B and C)

$$S_s = \frac{F_R}{A_w} = \frac{1,292,592}{144.91}$$

= 8920 psi (Resultant Direct Shear Stress)

$$(S_{ST})_A = \frac{M_z^*}{2 b h t_A} = \frac{1,464,410}{(2)(17.688)(9.875)(1.50)}$$
$$= 2,795 \text{ psi (Torsional Shear Stress at Point A)}$$

$$(S_{ST})_B = \frac{M_z^*}{2 b h t_B} = \frac{1,464,410}{(2)(17.688)(9.875)(2.875)}$$
$$= 1,458 \text{ psi (Torsional Shear Stress at Point B)}$$

The von Mises equivalent stresses at Points A, B, and C are:

$$S_{EA} = \left[S_{AC}^2 + 3(S_S + (S_{ST})_A)^2 \right]^{0.5} = 21,819 \text{ psi}$$

$$S_{EB} = \left[S_{BC}^2 + 3(S_S + (S_{ST})_B)^2 \right]^{0.5} = 18,165 \text{ psi}$$

$$S_{EC} = \left[(S_{AC} + S_{BC})^2 + 3S_S^2 \right]^{0.5} = 18,762 \text{ psi}$$

The minimum margin of safety at the weld/cask interface is based on the lower yield strength material, the Type 304 stainless steel cask body forgings with $S_y = 22.5$ ksi:

$$MS = \frac{22,500}{21,819} - 1 = +0.03$$

The positive margins of safety show that the rotation trunnion recesses satisfy the requirements of 10 CFR 71.45(b).

* Seely, Table 14.

2.5.2.2.4 Overload - Tiedowns

According to 10 CFR 71.45(b)(3), each tiedown device that is a structural part of a package must be designed so that failure of the device under excessive load would not impair the ability of the package to meet the other requirements of 10 CFR 71. For this reason, the shear capacity of the rotation trunnion recesses, welds, and the outer shell are compared.

The weld attaching the rotation trunnion to the outer shell and the lower forging is shown in Section 2.5.2.2.3. The shear capacities of the rotation trunnions, welds, and the outer shell are calculated below.

Weld

The effective shear area of the weld is 98.25 square inches, as previously calculated. The filler material used to weld the rotation trunnion to the cask body is AWS E309 with an ultimate tensile strength of 80.0 ksi. The ultimate shear capacity of the weld is:

$$\begin{aligned} F_w &= (98.25)(0.42)(80,000) \\ &= 3,301,200 \text{ lb} \end{aligned}$$

Cask Body

The area of the interface between the weld and the cask body is 139.22 square inches. The cask body has a tensile strength of 61.5 ksi, which is lower than the tensile strength of 80.0 ksi for the filler material. The cask body, therefore, is the critical part at the interface region. The ultimate shear capacity of the cask body at the interfacing area with the weld is:

$$\begin{aligned} F_{cb} &= (139.22)(0.42)(61,500) \\ &= 3,596,052 \text{ lb} \end{aligned}$$

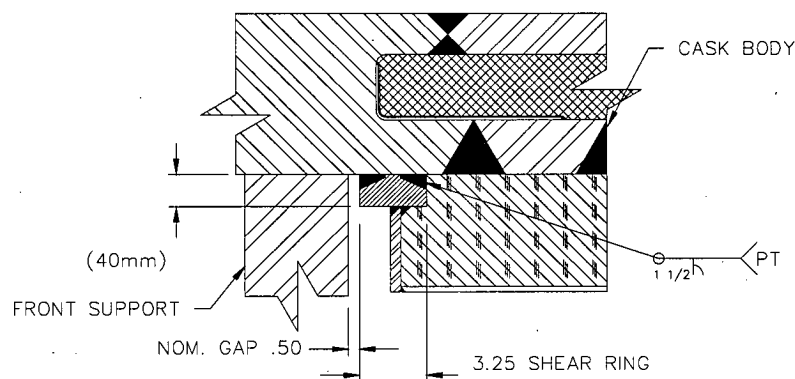
The maximum shear capacities of the weld and the cask body at the interface are summarized as follows:

$$\begin{aligned} \text{Weld} &= 3,301,200 \text{ lb} \\ \text{Cask Body} &= 3,596,052 \text{ lb} \end{aligned}$$

2.5.2.3 Front Support

2.5.2.3.1 Discussion

2.5.2.3.2 Shear Ring



Shear Ring Geometry

The shear ring geometry bears on the shipping frame along two 58-degree arcs (Figure 2.5.2-1). The load on the shear ring is:

$$R_{jx} = 2,500,000 \text{ lb (Section 2.5.2.1.2)}$$

Assuming that 1.575 inches (40 mm) of the ring thickness is in direct bearing against the side of the support frame, the bearing pressure is:

$$S_{brg} = 2,500,000 / (0.64)(\pi)(43.35)(1.575) \\ = 18,211 \text{ psi}$$

The allowable bearing on the surface of Type 304 stainless steel is:

$$(S_{brg})_{Allow} = 23,750 \text{ psi at the conservatively high temperature of } 260^{\circ}\text{F}$$

The margin of safety for bearing is:

$$MS = \frac{23,750}{18,211} - 1 = +0.30$$

The shear stress across the weld is:

$$S_s = R_{jx} / A_w = 2,500,000 / 267.8 = 9,335 \text{ psi}$$

where:

$$A_w = (\pi)(86.7)(116/360)(1.5)(2) + (0.75)(1.5)(4) = 267.8 \text{ in}^2$$

The margin of safety at the conservatively high temperature of 250°F is:

$$MS = \frac{(0.6)(20,000)}{9,335} - 1 = +0.29$$

where:

$$S_m = 20,000 \text{ psi at the conservatively high temperature of } 250^{\circ}\text{F.} \\ \text{(Actual calculated temperature is } 211^{\circ}\text{F)}$$

2.5.2.4 Tiedown Evaluation for the CY-MPC Configuration with Balsa Impact Limiters.

The shipping weight for the CY-MPC fuel configuration is 260,000 pounds, which is a 4% increase in shipping weight over the directly loaded and Yankee-MPC configurations. The methodology of Section 2.5.2.1 is used, applying an increase in the calculated stresses by 4% to determine the margins of safety for the higher CY-MPC weight. This evaluation uses the stress results and figures of Sections 2.5.2.2.3 and 2.5.2.2.4.

From Section 2.5.2.2.3, the stress in the weld at interface with the rotation trunnion recess is evaluated. The corresponding margin for the 260,000-pound shipping weight is:

$$M.S.=135/(1.04 \times 55.52)-1 = + 1.34$$

From Section 2.5.2.2.3, the minimum margin of safety in the weld material at the rotation trunnion recess/weld interface is calculated based on the lower yield strength of the E309 weld material. The corresponding margin of safety for the 260,000 pound shipping weight is:

$$M.S.=61/(1.04 \times 28.7)-1 = + 1.04$$

The margin of safety for the weld/cask interface (Cask Body/Rotation Trunnion Recess Weld Interface) is evaluated using the allowable stress at 250°F, which is higher than the calculated outer cask radial surface temperature at the trunnion recess location (~220°F). The bounding stress is the von Mises equivalent stress at Point A of 21,819 psi. The margin of safety is:

$$M.S.= 23.75/(1.04 \times 21.8)-1 = + 0.05$$

As shown in Section 2.5.2.2.4, the weld fails in shear before the cask body, thereby ensuring that the cask body retains integrity. Since this result is based on material properties, the increase in the weight will not alter the conclusion of 2.5.2.2.4.

From Section 2.5.2.3.2, the shear ring for the front support is evaluated. The margin of safety for the bearing stress for the 260,000-pound weight is:

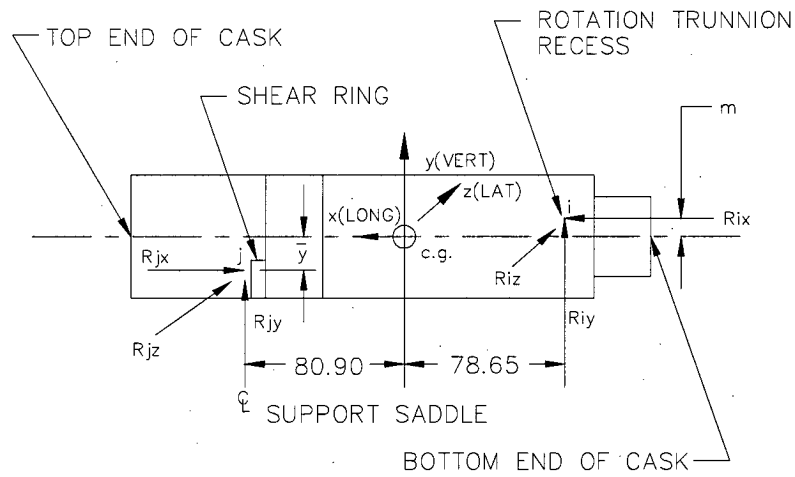
$$M.S.=23.75/(1.04 \times 18.21)-1 = + 0.25$$

Similarly, the margin of safety for the shear stress across the weld is:

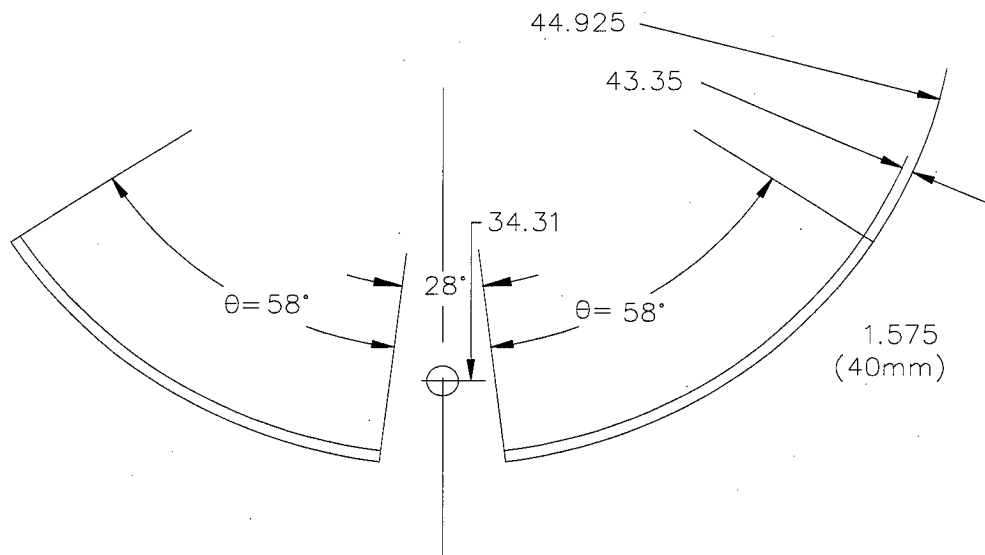
$$M.S.=.6(20)/(1.04 \times 9.34)-1 = + 0.24$$

Based on these results, the NAC STC tie down system for the CY-MPC 260,000 pound transport weight satisfies the requirements of 10 CFR 71.45(b) and the AAR Field Manual, Rule 88.

Figure 2.5.2-1 Front Support and Tiedown Geometry



Free Body Diagram



Shear Ring Geometry

Figure 2.5.2-2 Free Body Diagram of Cask Subjected to Lateral Load

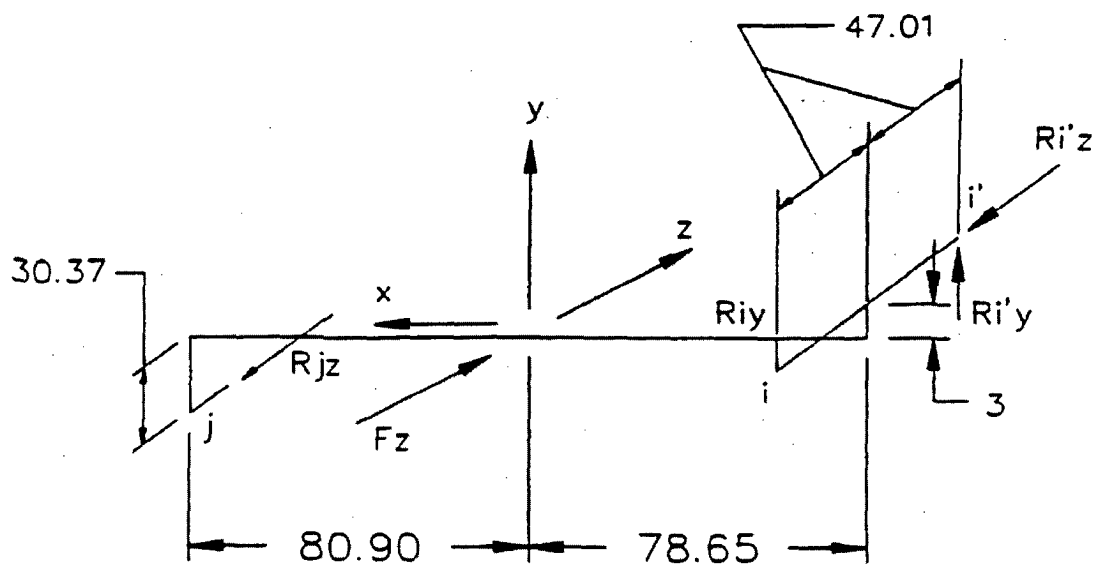


Table 2.5.2-1 Reactions Caused By Tiedown Devices From 10 CFR 71.45(b) Loads

Load Case	Load (lb)	Reactions (lb)					
		R_{jx}	R_{jy}	R_{jz}	R_{ix}	R_{iy}	R_{iz}
A1	$F_y = -500,000$	0	246,474	0	0	126,763	0
A2	$F_y = 500,000$	0	-246,474	0	0	-126,763	0
B1	$F_x = 2,500,000$	-2,500,000	537,606	0	0	-268,803	0
B2	$F_x = -2,500,000$	0	47,008	0	1,250,000	-23,504	0
C1	$F_z = 1,250,000$	0	0	-616,186	0	-178,814	0
C2	$F_z = -1,250,000$	0	0	616,186	0	178,814	633,814
Combined reactions:							
Case I. $A_1 + B_1 + C_1$		-2,500,000	784,080	-616,186	0	-320,854	0
Case II. $A_2 + B_2 + C_1$		0	-199,466	-616,186	1,250,000	-329,081	0
Case III. $A_2 + B_1 + C_1$		-2,500,000	291,132	-616,186	0	-574,380	0
Case IV. $A_2 + B_2 + C_2$		0	-199,466	616,186	1,250,000	28,547	633,814

Table 2.5.2-2 Reactions Caused By Tiedown Devices from AAR Field Manual,
Rule 88 Loads

Load Case	Load (lb)	Reactions (lb)					
		R _{jx}	R _{jy}	R _{jz}	R _{ix}	R _{iy}	R _{iz}
A1	F _y = -1,000,000	0	492,950	0	0	253,525	0
A2	F _y = 1,000,000	0	-492,950	0	0	-253,525	0
B1	F _x = 1,875,000	1,875,000	403,204	0	0	-201,602	0
B2	F _x = -1,875,000	0	35,256	0	937,500	-17,628	0
C1	F _z = 450,000	0	0	-221,827	0	-64,373	0
C2	F _z = -450,000	0	0	221,827	0	64,373	228,173
Combined reactions:							
Case I. A ₁ + B ₁ + C ₁		1,875,000	896,154	-221,827	0	-12,450	0
Case II. A ₂ + B ₂ + C ₁		0	-457,694	-221,827	937,500	-335,526	0
Case III. A ₂ + B ₁ + C ₁		1,875,000	-89,746	-221,827	0	-519,500	0
Case IV. A ₂ + B ₂ + C ₂		0	-457,694	221,827	937,500	-206,780	228,173

THIS PAGE INTENTIONALLY LEFT BLANK

2.6 Normal Conditions of Transport

The 10 CFR 71.71 requires that the NAC-STC be structurally adequate for the following normal conditions of transport: (1) heat, (2) cold, (3) reduced external pressure, (4) increased external pressure, (5) vibration, (6) water spray, (7) free drop, (8) corner drop, (9) compression, and (10) penetration. In the free drop analyses, the cask impact orientation evaluated is the orientation that inflicts the maximum damage to the cask. The 10 CFR 71.71 requires that the evaluation of the cask for the normal conditions of transport be at the most unfavorable ambient temperature in the range from -20°F to +100°F. In this section, the NAC-STC is evaluated for structural integrity for the normal conditions of transport in three configurations - with directly loaded fuel, with the Yankee-MPC and with the CY-MPC. The Yankee-MPC and CY-MPC configurations include spent fuel (intact or damaged) and Greater Than Class C (GTCC) waste.

NAC-STC

Two- and three-dimensional structural analyses of the cask discussed in this section and summarized in the tables presented in Section 2.10.4 are not influenced by the localized changes to the closure system, fuel basket or revised heat transfer analysis. Therefore, cask structural analyses have not been revised. The SAR has been revised to include evaluations of alternate configurations of the cask contents, i.e., (1) fuel assemblies contained in a canister; and (2) GTCC waste contained in a canister.

Revised heat transfer analyses are presented in Chapter 3. Section 2.10.10 presents a comparison of temperature gradients obtained from the different heat transfer analyses and evaluation of conservative margins of safety identified using original temperature distributions in the cask structural qualification. It is concluded from this evaluation that the detailed finite element analyses performed for normal and accident condition loads using the original temperature distributions are conservative; therefore, the original analyses have not been revised.

Temperature distributions for both normal and accident conditions are revised as a result of improvements in the modeling of the boundary conditions used in the heat transfer analyses. These boundary condition improvements better reflect actual conditions than those originally modeled in the cask thermal analyses. The most significant revisions to the boundary conditions included modeling the gap between the basket and inner shell, and consideration of an adiabatic surface for the area of the cask covered by the impact limiter. Additional enhancements are made to the heat transfer analysis resulting from revising the basket to an all-stainless steel structural design. Additional discussion of these enhancements is presented in Chapter 3.

These enhancements resulted in reduced thermal gradients and the associated secondary stresses applicable to the normal condition structural qualification throughout the cask and increased the maximum component temperature in the regions of the cask influenced by the insulating effect of the impact limiter (Section 2.10.10). Based on the fact that these changes in temperature do not create higher stresses in the cask and that the resulting influence to the stress qualification is limited to reducing the temperature dependent material allowable stress, revisions to the structural qualification of the cask for normal conditions are limited to changes in the material allowable stresses and the margins of safety in the stress summary tables in Section 2.10.4.

Yankee-MPC

The Yankee-MPC configuration has the same design weight of 250,000 pounds as the NAC-STC directly loaded configuration. Due to the reduced length of the Yankee Class spent fuel and the load concentration of the canister lids, a separate three-dimensional finite element model is used to evaluate the stresses in the cask body for the normal conditions of transport.

CY-MPC

The CY-MPC configuration has a design weight of 260,000 pounds versus the 250,000 pound design weight of the NAC-STC directly loaded and Yankee-MPC configurations. In conjunction with the higher design weight, the CY-MPC configuration employs a balsa impact limiter design. The balsa impact limiters are significantly lighter than the standard redwood/balsa impact limiter design. A single three-dimensional model is employed to evaluate the stresses in the cask body for normal conditions of transport.

2.6.1 Heat

The NAC-STC body and closure lids are analyzed for structural adequacy in accordance with the requirements of 10 CFR 71.71(c)(1) Heat (normal condition of transport). The cask is loaded, ready for shipment and supported in the horizontal position with an ambient temperature environment of 100°F, an assumed internal pressure of 50 psig, maximum decay heat load, maximum solar insolation, and still air.

2.6.1.1 Heat Condition for the NAC-STC Cask in the Directly Loaded Fuel and Yankee-MPC Configurations

The stress analysis of the cask is performed using both the two-dimensional and the three-dimensional finite element models and the ANSYS computer program. For the two-dimensional analysis, the cask is modeled as an axisymmetric structure using ANSYS STIF42 isoparametric elements. The individual loading conditions of thermal heat, internal pressure, and bolt preload are analyzed using a two-dimensional axisymmetric model, because both the cask structure and the loads are axisymmetric. By contrast, the individual gravity loading condition, and the combined loading conditions must be analyzed using the three-dimensional finite element model, since the gravity loading condition is not axisymmetric. The ANSYS computer program is described in Section 2.10.1.1. The finite element model descriptions are provided in Section 2.10.2.1. The temperature-dependent material properties considered in the analysis are documented in Section 2.3.

For the heat condition, the cask is structurally loaded due to closure lid bolt preload, internal pressure, thermal heat, and gravity. The following four categories of load are considered on the cask:

1. Closure lid bolt preload – For the NAC-STC directly loaded and the Yankee-MPC configurations, the required total bolt preloads on the inner lid bolts and the outer lid bolts are 4.51×10^6 pounds and 6.02×10^5 pounds, respectively. Bolt preload is applied to the model by imposing initial strains to the bolt shafts, as explained in Section 2.10.2.2.3. The bolts are modeled as beam (ANSYS STIF3) elements.

2. Internal pressure - The cask internal pressure is temperature dependent and is evaluated in Section 3.4.4. For analysis purposes, a conservatively assumed internal pressure of 50 psig is applied on the interior surfaces of the cask cavity in the outward normal direction. The 50 psig is conservative, based on the calculated maximum normal operating cavity pressure (MNOP) of 1.8 atmospheres absolute (12 psig) for fuel loaded directly into the cask cavity. The calculated MNOP in the cask cavity for canistered fuel is 1.77 atmospheres absolute (11.31 psig). The cavity pressure is even less for the canistered GTCC waste because no fuel rod fill-gas is present. The pressure loading region includes the lid and upper body forging mating surfaces outward to the inner lid seal centerline.
3. Thermal - The heat transfer analyses performed for maximum normal operating conditions determine the cask temperature distribution for the heat condition. The heat condition considers the cask to be subjected to an ambient temperature of 100°F, with maximum decay heat load (for directly loaded fuel) and maximum solar insolation, in still air. The maximum decay heat load for Yankee Class canistered fuel is 12.5 kW and is 2.9 kW for Yankee GTCC waste. The directly loaded fuel configuration is considered to bound the temperatures associated with the Yankee-MPC configurations. For The cask temperature distribution, obtained for this heat condition, is used as an input to the ANSYS analysis to determine the stresses in the cask. The ANSYS analysis determines the stresses resulting from the thermal expansion of the cask from its initial, 70°F, condition to its normal transport temperature condition. These stresses include the effects of the differential thermal growth within the components, which result from the temperature difference across the walls of the cask. The cask temperature distribution is also used in the ANSYS structural analysis to determine the values of the temperature-dependent material properties.
4. Gravity - The mechanical loads consist of gravity acting on the cask structure and its contents. The cask is assumed to be loaded and resting in the horizontal position on the front and rear cask supports. Mechanical loads resulting from a 1 g application of the total weight (250,000 lbs for the NAC-STC directly loaded and Yankee-MPC configurations) of the cask structure and contents are imposed on the model. The design weight of the empty cask (194,000 lbs) is imposed on the mass of the cask model.

The weight of the cavity contents (56,000 lbs) for directly loaded fuel is imposed on the model as a contents pressure on the contact surface of the cask cavity (Section 2.10.2.2.1 for the contents pressure calculation). The weight of the cavity contents for the

Yankee-MPC canistered fuel configuration is 55,590 pounds, including the top and bottom cask cavity spacers. For the Yankee GTCC waste configuration, the weight of the cavity contents is 54,271 pounds, including the cask cavity spacers. Fabrication stresses are considered to be negligible as demonstrated in Section 2.6.11.

For the two-dimensional NAC-STC directly loaded contents analyses, axisymmetric boundary conditions are applied to the two-dimensional finite element model because axisymmetry exists in the cask geometry and in the loading conditions considered. In addition, a longitudinal support is imposed on an outside corner node at one end of the cask to prevent rigid body motion. If the cask system is in equilibrium, then the reaction force at this support will be zero for the two-dimensional model.

For the three-dimensional finite element models, symmetric boundary conditions are applied to the model by restraining the nodes on the symmetry plane to prevent translations in the direction normal to the symmetry plane. Additional restraints are applied to simulate the orientation and method of support of the cask. The cask is considered to be loaded and resting in the horizontal position on a front saddle and a rear tiedown support. Therefore, nodes at the centerline of the front saddle on the cask outer radius are radially restrained, and one node at the rear tiedown is laterally and longitudinally restrained. When the cask system is in equilibrium, then the sum of the reaction forces at the restraints will be equal to the half-cask weight in the lateral direction and zero in the longitudinal direction. An examination of the magnitude of the reaction forces provides a check of the validity of the finite element evaluation for the heat condition.

The allowable stress limit criteria, for containment and noncontainment structures, are provided in Section 2.1.2. These criteria are used to determine the allowable stresses for each cask component, conservatively using the maximum transport temperature within a given component to determine the allowable stress throughout that component. Note that higher component temperatures result in lower allowable stresses. Table 2.10.2-5 documents the allowable stress values determined for each component, for the temperature distribution (Condition 1) corresponding to the heat condition.

The stresses throughout the cask body are calculated for the individual and combined loading conditions for directly loaded fuel, which envelope the canistered fuel and the canistered waste configurations. The individual loading conditions are: (1) 50 psig internal pressure (including bolt preload), (2) gravity, and (3) thermal heat (100°F) loads. Stress results for the individual loading case of 50 psig internal pressure (including bolt preload) are documented in Table

2.10.4-1. Stress results for the individual gravity cases are documented in Table 2.10.4-3. Stress results for the individual thermal loading cases are documented in Table 2.10.4-5. These are the nodal stress summaries obtained from the finite element analysis results. As described in Section 2.10.2.4.2 and Section 2.10.4, the nodal stresses are documented on the representative section cuts.

The combined loading conditions are: (1) gravity, with bolt preload and 50 psig internal pressure and (2) gravity, with bolt preload, 50 psig internal pressure, and thermal loading. Stress results for the combined loading conditions discussed above are documented in Tables 2.10.4-21 through 2.10.4-28.

These tables document the primary, primary plus secondary, primary membrane (P_m), primary membrane plus primary bending ($P_m + P_b$), primary plus secondary membrane and bending (S_n), and critical P_m , $P_m + P_b$, and S_n stresses in accordance with the criteria presented in Regulatory Guide 7.6. As described in Sections 2.10.2.3 and 2.10.2.4, procedures have been implemented to document the nodal and sectional stresses, as well as to determine the critical stress summary for all cask components.

For the individual loading condition of internal pressure, the maximum calculated membrane stress intensity is 1.1 ksi and the maximum calculated membrane plus bending stress intensity is 1.1 ksi, except that in areas affected by bolt preload, the maximum calculated membrane stress intensity is 7.5 ksi and the maximum calculated membrane plus bending stress intensity is 14.7 ksi. For the individual gravity loading condition, the maximum calculated primary membrane stress intensity is 8.9 ksi, the maximum calculated primary membrane plus primary bending stress intensity is 9.8 ksi, and the maximum calculated primary plus secondary membrane plus bending stress is 24.3 ksi.

As shown in Tables 2.10.4-26 and 2.10.4-27, the margins of safety for primary stresses are all positive for the heat condition. The most critically stressed component in the system is the inner lid. The minimum margin of safety in the inner lid for primary stresses for the heat condition is found to be +1.2, as documented in Table 2.10.4-26. The locations of the most critical sections for each cask component are provided in the critical stress summary tables.

Regulatory Guide 7.6 requires that the range of primary plus secondary stress intensities between any two normal conditions of transport be less than $3.0 S_m$. Therefore, it is necessary to evaluate the range of primary plus secondary stresses between all of the recognized normal conditions of

transport: including the heat, cold, 1-foot end drop, 1-foot side drop, and 1-foot corner drop conditions. A simple, straightforward, and very conservative method of showing compliance with the 3.0 S_m criteria is to establish an allowable stress limit criteria of 1.5 S_m for the range of primary plus secondary stress intensities between each normal condition and the ambient condition. If each normal condition meets the 1.5 S_m allowable stress intensity range criteria at all locations within the cask when paired with the ambient condition, then all pairs of normal conditions will meet the 3.0 S_m stress intensity range criteria.

Table 2.10.4-28 documents the range of primary plus secondary stress intensity between the heat condition and the unloaded, ambient condition. The maximum calculated primary plus secondary stress intensity is shown to be 24.3 ksi, which is less than 1.5 S_m . In conjunction with the 1.5 S_m criteria for the stress intensity range between the ambient condition and each of the other normal conditions, it is therefore concluded that the NAC-STC meets the 3.0 S_m criteria for the primary plus secondary stress intensity range for the heat condition. For the fatigue evaluation of the NAC-STC, Section 2.1.3.2 documents that the requirements of Regulatory Guide 7.6 are satisfied by the 3.0 S_m criteria for the extreme total stress intensity range limit.

The documentation of the adequacy of the NAC-STC in satisfying the buckling criteria for the stresses of the heat condition is presented in Section 2.10.5.

Since the margins of safety are all positive, the NAC-STC, therefore, satisfies the requirements of 10 CFR 71.71(c)(1) for the heat (normal transport) condition for the directly loaded fuel, the canistered fuel configuration and the canistered GTCC waste configuration.

2.6.1.2 Heat Condition for the NAC-STC Cask in the CY-MPC Configuration

The three-dimensional model and analyses used in the 1-foot side drop evaluation for the CY-MPC configuration are also used for the evaluation of the heat condition. The NAC-STC cask with the CY-MPC canistered configuration is modeled as a three-dimensional structure using ANSYS STIF45 isoparametric elements. A detailed description of the three-dimensional finite element model of the NAC-STC cask body for the canistered configurations is provided in Section 2.10.2.1.3. Since some of the loading contributions for the heat condition are axisymmetric, and the NAC-STC cask body is the same geometry for all fuel configurations, results of the two-dimensional model and analyses are combined with the results of the three-dimensional model of the CY-MPC fuel configuration.

Four categories of loads are considered in this evaluation: closure lid bolt preload, internal pressure, thermal expansion, and gravity loading:

1. Closure lid bolt preload – The required bolt preloads on the inner and outer lid bolts are 115,066 pounds per bolt and 36,810 pounds per bolt, respectively. Bolt preload is applied to the model by imposing initial strains to the bolt shafts. The stresses corresponding to the bolt preload with a 50 psig internal pressure for the directly load configuration are reported in Table 2.10.4-1 (for the two dimensional axisymmetric model), and the maximum stress intensity is 1.9 ksi (Location U). To account for the preload and internal pressure for the CY-MPC configuration, the 1.9 ksi is added to the stress intensity due to the 1g lateral load.
2. Internal pressure - The cask internal pressure is temperature dependent and is evaluated in Section 3.4.4. A pressure of 50 psig, which envelops the calculated pressure of 38.1 psig for this configuration, is effectively used by adding the 1.9 ksi (reported above for the bolt preload) to the stress intensity due to the 1 g lateral load.
3. Thermal - The ANSYS analysis determines the stresses arising from the thermal expansion of the cask from its initial 70°F condition, including the effects of the differential thermal growth within the components, which is a result of the temperature difference across the walls of the cask. The cask temperature distributions are also used in the ANSYS structural analyses to determine the values of the temperature-dependent material properties. The heat transfer analysis performed for maximum normal operating conditions determine the cask temperature distribution for the heat condition. The heat condition corresponds to a 100°F ambient temperature, a maximum decay heat load (17 kW), and full solar insolation.

To bound the stresses arising from thermal expansion, the maximum gradient is used in the heat condition evaluation. The maximum temperature gradient is actually associated with the cold condition of -40°F with maximum decay heat and no solar insolation. To ensure that the minimum stress allowable is used, the allowables are taken at the maximum temperature of the inner shell (331°F) for the heat condition described above. The temperature distribution for the canistered GTCC waste is considered to be enveloped by the 17 kW design basis heat load. Individual thermal cases are not evaluated, since the design basis heat load of 22.1 kW for the directly loaded fuel envelops the 17 kW basis heat load for the CY-MPC configuration.

4. Gravity loads - The mechanical loads consist of gravity acting on the cask structure and its contents. The cask is assumed to be loaded and resting in the horizontal position on the front and rear cask supports. Mechanical loads resulting from a 1g application of the total weight (260,000 lbs) of the cask structure and contents are imposed on the model.

These loading conditions are identical to the 1-foot side drop evaluated in 2.6.7.2.2 for the CY-MPC configuration except the 1-foot drop condition employed 20g instead of 1g for the gravity load. To determine the maximum primary stress intensity for the heat condition, the stress intensity due to the 20g loading (in Tables 2.6.7.1-3 and 2.6.7.1-4) can be factored by 1/20 and then added to the stress intensity associated with the 50 psig pressure + bolt preload (1.9 ksi).

The maximum primary stress intensities reported for the P_m and $P_m + P_b$ for the 1-foot side drop are 11.5 ksi and 20.9 ksi, respectively. Factoring these by 1/20 and adding the result to 1.9 ksi for the pressure + bolt preload, result in maximum stress intensities of 2.5 ksi and 2.9 ksi, respectively, for P_m and $P_m + P_b$. Using the minimum allowables of 19.6 ksi for P_m and 29.4 ksi for $P_m + P_b$, reported in Tables 2.6.7.1-3 and Table 2.6.7.1-4, the minimum margin for the cask body for the primary stress intensity P_m and $P_m + P_b$ are +6.8 and +9.1, respectively. It is concluded that the CY-MPC configuration satisfies the primary stress limits for the heat condition.

Using the methodology to evaluate the range of primary plus secondary stress intensities described in 2.6.1.1, the allowable stress intensity of $1.5 S_m$ of 29.4 ksi should be compared to bounding primary plus secondary stress intensity. This value is obtained by adding the maximum thermal stress intensity of 8.1 ksi to 2.9 ksi to obtain 11.0 ksi. Since $11.0 < 29.4$ ksi, it is concluded that the CY-MPC configuration meets the $3.0 S_m$ criteria for the primary plus secondary stress intensity range for the heat condition.

THIS PAGE INTENTIONALLY LEFT BLANK

2.6.2 Cold

The NAC-STC body and closure lids are analyzed for structural adequacy in accordance with the requirements of 10 CFR 71.71(c)(2) Cold (normal condition of transport). The cask is loaded and ready for shipment in the horizontal position, with an ambient temperature environment of -40°F, an assumed internal pressure of 12 psig, no decay heat load, no solar insolation, and in still air and shade.

2.6.2.1 Cold Condition for the NAC-STC Cask in the Directly Loaded Fuel and Yankee-MPC Configurations

The stress analysis of the cask is performed using both the two-dimensional and the three-dimensional finite element models and the ANSYS computer program. For the NAC-STC directly loaded configuration two-dimensional analysis, the cask is modeled as an axisymmetric structure using ANSYS STIF42 isoparametric elements. The individual loading conditions of thermal cold, internal pressure, and bolt preload are analyzed using a two-dimensional axisymmetric model because both the cask structure and the load are axisymmetric. By contrast, the individual gravity loading condition and the combined loading conditions must be analyzed using three-dimensional finite element models, since the gravity loading condition is not axisymmetric. The ANSYS computer program is described in Section 2.10.1.1. The finite element model descriptions are provided in Section 2.10.2.1. The temperature-dependent material properties considered in the analysis are documented in Section 2.3.

For the cold condition, the cask is structurally loaded due to closure lid bolt preload, internal pressure, thermal cold, and gravity. The following four categories of load are considered on the cask:

1. Closure lid bolt preload – For the NAC-STC directly loaded and the Yankee-MPC configurations, the required total bolt preloads on the inner lid bolts and the outer lid bolts are 4.51×10^6 pounds and 6.02×10^5 pounds, respectively. Bolt preload is applied to the model by imposing initial strains to the bolt shafts, as explained in Section 2.10.2.2.3. The bolts are modeled as beam (ANSYS STIF3) elements.
2. Internal pressure - The cask internal pressure is temperature dependent and its maximum value is evaluated in Section 3.4.4. For analysis purposes for the cold condition, an internal pressure of 12 psig is applied on the interior surfaces of the cask cavity in the

outward normal direction. The calculated cavity pressure is -0.8 psia at -40°F for directly loaded fuel. Since the cask cavity is backfilled with helium to 1 atmosphere absolute (0 psig) at an ambient temperature, the cavity pressure at -40°F will be less than 12 psig for both the canistered fuel and the canistered GTCC waste configurations. The pressure loading region includes the lid and upper body forging mating surfaces outward to the inner lid seal centerline.

3. Thermal - The cold condition considers the cask to be subjected to an ambient temperature of -40°F, with no decay heat load and no solar insolation, in still air and shade. This cask temperature distribution calculated for the cold condition is used as an input to the ANSYS analysis to determine the stresses. The ANSYS analysis determines the stresses resulting from the thermal expansion or contraction of the cask from its initial 70°F condition to its normal transport temperature condition. These stresses include the effects of the differential thermal growth within the components, which result from the temperature difference across the walls of the cask. The cask temperature distribution is also used in the ANSYS structural analysis to determine the values of the temperature dependent material properties such as modulus of elasticity, density, and Poisson's ratio.
4. Gravity - The mechanical loads consist of gravity acting on the cask structure and its contents. The cask is assumed to be loaded and resting in the horizontal position on the front and rear cask supports. Mechanical loads resulting from a 1g application of the total weight (250,000 lbs for the directly loaded and Yankee-MPC configurations) of the cask structure and contents are imposed on the model. The weight of the empty cask (194,000 lbs) is imposed on the model as a deceleration on the mass of the cask model. The weight of the cavity contents (56,000 lbs) for directly loaded fuel is imposed on the model as a contents pressure on the contact surface of the cask cavity (see Section 2.10.2.2.1 for the contents pressure calculation). The weight of the cavity contents for the Yankee-MPC canistered fuel configuration is 55,590 pounds, including the top and bottom cask cavity spacers. For the canistered GTCC waste configuration, the weight of the cavity contents is 54,271 pounds. These weights include the cask cavity spacers.

Fabrication stresses are considered to be negligible as demonstrated in Section 2.6.11.

For the two-dimensional analyses, axisymmetric boundary conditions are applied to the two-dimensional finite element model because axisymmetry exists in the cask geometry and in the

loading conditions considered. In addition, a longitudinal support is imposed on an outside corner node at one end of the cask to prevent rigid body motion. If the cask system is in equilibrium, then the reaction force at this support will be zero for the two-dimensional model.

For the three-dimensional finite element models, symmetric boundary conditions are applied to the model by restraining the nodes on the symmetry plane to prevent translations in the direction normal to the symmetry plane. Additional restraints are applied to simulate the orientation and method of support of the cask. The cask is considered to be loaded and resting in the horizontal position on a front saddle and a rear tiedown support. Therefore, nodes at the centerline of the front saddle on the cask outer radius are radially restrained, and one node at the rear tiedown is laterally and longitudinally restrained. When the cask system is in equilibrium, then the sum of the reaction forces at the restraints will be equal to the half-cask weight (125,000 lbs) in the lateral direction and zero in the longitudinal direction. An examination of the magnitude of the reaction forces provides a check of the validity of the finite element evaluation for the cold condition.

For the NAC-STC directly loaded two-dimensional finite element analyses, all of the reaction forces are essentially zero. For the three-dimensional analysis, the reaction resultant in the cask lateral direction is 124,200 pounds. Compared to the half-cask design weight of 125,000 pounds, the unbalanced force of 800 pounds is negligible.

The allowable stress limit criteria for containment and noncontainment structures are provided in Section 2.1.2. These criteria are used to determine the allowable stresses for each cask component, conservatively using the maximum transport temperature within a given component to determine the allowable stress throughout that component. Note that higher component temperatures result in lower allowable stresses.

The stresses throughout the cask body have been calculated for the individual and combined loading conditions for directly loaded fuel, which envelope the canistered fuel and canistered GTCC waste configurations. The individual loading conditions are: (1) 12 psig internal pressure (including bolt preload); (2) gravity; and (3) thermal cold (-40°F) loads. Stress results for the individual loading case of 12 psig internal pressure (including bolt preload) are documented in Table 2.10.4-2.

Stress results for the individual gravity cases are documented in Table 2.10.4-4. Stress results for the individual thermal loading cases are documented in Table 2.10.4-7. These are the nodal

stress summaries obtained from the finite element analysis results. As described in Section 2.10.2.4.2 and Section 2.10.4, the nodal stresses are documented on the representative section cuts.

The combined loading conditions are: (1) gravity, bolt preload, and 12 psig internal pressure and (2) gravity, bolt preload, 12 psig internal pressure, and thermal loading. Stress results for the combined loading conditions discussed above are documented in Tables 2.10.4-29 through 2.10.4-36.

These tables document the primary, primary plus secondary, primary membrane (P_m), primary membrane plus primary bending ($P_m + P_b$), primary plus secondary membrane and bending (S_n), and critical P_m , $P_m + P_b$, and S_n stresses in accordance with the criteria presented in Regulatory Guide 7.6. As described in Section 2.10.2.3 and 2.10.2.4, procedures have been implemented to document the nodal and sectional stresses, as well as to determine the critical stress summary for all cask components.

For the individual loading condition of internal pressure plus bolt preload, the maximum calculated membrane stress intensity is 0.3 ksi and the maximum calculated membrane plus bending stress intensity is 0.4 ksi in areas affected by bolt preload, the maximum calculated membrane stress intensity is 7.8 ksi, and the maximum calculated membrane plus bending stress intensity is 14.9 ksi. For the individual gravity loading condition, the maximum calculated membrane stress intensity is 3.9 ksi and the maximum membrane plus bending stress intensity is 4.2 ksi. For the individual thermal loading condition, the maximum calculated membrane stress intensity is 3.8 ksi and the maximum calculated membrane plus bending stress intensity is 4.0 ksi. For the combined loading condition, the maximum calculated primary membrane stress intensity is 9.2 ksi, the maximum calculated primary membrane plus primary bending stress intensity is 9.8 ksi, and the maximum calculated primary plus secondary membrane plus bending stress intensity is 15.4 ksi.

In order to determine the effect of cask temperature on stress levels, several studies were made, which compared the stress results between the heat and cold condition analyses for the directly loaded fuel configuration. The comparison of gravity stresses between the heat and cold conditions shows that there is only a minimal difference, indicating that cask stresses are essentially independent of the temperature conditions considered in these analyses. The maximum membrane plus bending stress intensity due to gravity for the heat condition, is 4.3 ksi, and the maximum membrane plus bending stress intensity due to gravity for the cold

condition is 4.2 ksi. The difference in gravity stresses between the heat and the cold cases is, therefore, less than 2.3 percent.

A comparison of primary stress intensities, which consider internal pressure, bolt preload, and gravity loadings for the heat and the cold cases for the directly loaded fuel configuration shows that a negligible difference in stress exists. The maximum primary membrane plus primary bending stress intensity for the heat condition is 9.8 ksi; the maximum primary membrane plus primary bending stress intensity for the cold condition is 9.8 ksi. Therefore, the maximum primary membrane plus primary bending stress intensities are essentially the same for the heat and the cold conditions.

A final comparison of primary plus secondary stress intensities, which consider internal pressure, bolt preload, gravity, and thermal loadings for the heat and the cold cases for the directly loaded fuel configuration, shows that a difference in the stress intensities does exist as a result of the thermal expansion or contraction of the cask and the effect of temperature dependent material properties. The maximum primary plus secondary stress intensity for the heat condition is 24.3 ksi, and the maximum primary plus secondary stress intensity for the cold condition is 15.4 ksi. The difference in primary plus secondary stress intensities between the heat and the cold cases is, therefore, 36.6 percent. Based on these comparisons, it is concluded that for loadings, which do not include thermal stress effects, cask stresses are essentially independent of the temperature condition. Furthermore, note that the primary and the primary plus secondary stress intensities are greater for the heat condition than for the cold condition; also, note that allowable stress is a function of temperature, with higher component temperatures resulting in lower allowables.

Therefore, it is concluded that temperature condition 1 (corresponding to the heat condition, i.e., 100°F ambient temperature with maximum decay heat load and maximum solar insolation) is the most critical temperature condition. For this reason, the side, corner, and oblique drop analyses are performed for temperature condition 1. Additional parametric studies are performed for some drop cases in order to verify this conclusion.

As shown in Tables 2.10.4-34 and 2.10.4-35, the margins of safety are all positive for the cold condition. The most critically stressed component in the cask for the cold condition is the top forging. The minimum margin of safety for the cold condition is found to be +1.2, as documented in Table 2.10.4-34. The locations of the most critical sections for each cask component are provided in the critical stress summary tables.

Regulatory Guide 7.6 requires that the range of primary plus secondary stresses between any two normal conditions of transport be less than $3.0 S_m$. Therefore, it is necessary to evaluate the range of primary plus secondary stress intensities between all of the normal conditions of transport: heat, cold, 1-foot end drop, 1-foot side drop, and 1-foot corner drop. A simple, straightforward, and very conservative method of showing compliance with the $3.0 S_m$ criteria is to establish an allowable stress limit criteria of $1.5 S_m$ for the range of primary plus secondary stress intensities between each normal condition and the ambient condition. If each normal condition meets the $1.5 S_m$ allowable stress intensity range criteria at all locations within the cask, when paired with the ambient condition, then all pairs of normal conditions will meet the $3.0 S_m$ stress intensity range criteria.

Table 2.10.4-36 documents the range of primary plus secondary stress intensity between the cold condition and the unloaded, ambient condition. Although the allowable stress is $3.0 S_m$, as documented in this table, the maximum stress intensity range is shown to be 15.4 ksi, which is less than $1.5 S_m$. In conjunction with the $1.5 S_m$ criteria for the stress intensity range between the ambient condition and each of the other normal conditions, it is, therefore, concluded that the NAC-STC meets the $3.0 S_m$ criteria for the stress intensity range.

For the fatigue evaluation of the NAC-STC, Section 2.1.3.2 documents that the requirements of Regulatory Guide 7.6 are satisfied by the $3.0 S_m$ criteria for the extreme total stress intensity range limit.

The documentation of the NAC-STC adequacy in satisfying the buckling criteria for the stresses of the cold condition is presented in Section 2.10.5.

Since the margins of safety are all positive, the NAC-STC, therefore, satisfies the requirements of 10 CFR 71.71(c)(2) for the cold (normal transport) condition for the directly loaded fuel, the canistered fuel configuration, and the canistered GTCC waste configuration.

2.6.2.2 Cold Condition for the NAC-STC Cask in the CY-MPC Configuration

The three-dimensional model and analyses used in the 1-foot side drop evaluation are also used for the evaluation of the cold condition. The NAC-STC cask with the CY-MPC canistered configuration is modeled as a three-dimensional structure using ANSYS STIF45 isoparametric elements. A detailed description of the three-dimensional finite element model of the NAC-STC cask body for the canistered configurations is provided in Section 2.10.2.1.3. Since some of the

loading contributions for the cold condition are axisymmetric, and the NAC-STC cask body is the same geometry for all fuel configurations, results of the two-dimensional model and analyses are combined with the results of the three-dimensional model of the CY-MPC fuel configuration.

Four categories of loads are considered in this evaluation: closure lid bolt preload, internal pressure, thermal expansion, gravity loading:

1. Closure lid bolt preload – The required bolt preloads on the inner lid and outer lid bolts are 115,066 pounds per bolt and 36,810 pounds per bolt, respectively. Bolt preload is applied to the model by imposing initial strains to the bolt shafts. The stresses corresponding to the bolt preload with a 12 psig internal pressure for the directly load configuration are reported in Table 2.10.4-2 (for the two-dimensional axisymmetric model), and the maximum stress intensity is 2.2 ksi (Location U). To account for the preload and internal pressure for the CY-MPC configuration, the 2.2 ksi is added to the stress intensity due to the 1g lateral load.
2. Internal pressure - The cask internal pressure is temperature dependent and is evaluated in Section 3.4.4. For analysis purpose for the cold condition, an internal pressure of 12 psig is used, which envelop a backfill pressure of 0 psig. The 12 psig is effectively used by adding the 2.2 ksi (reported above for the bolt preload) to the stress intensity due to the 1g lateral load.
3. Thermal - The cold transfer analysis performed for maximum normal operating conditions determines the cask temperature distribution for the cold condition. The bounding cold load for the NAC-STC is for the directly loaded fuel of 22.1 kW, which is larger than the CY-MPC configuration 17 kW design cold load. The cold condition corresponds to a - 40°F ambient temperature, no decay heat and no solar insolation.

To bound the stresses arising from thermal expansion, the maximum stress intensity of 7 ksi for the directly loaded fuel (Table 2.10.4-6, location R1) is added to maximum stress intensity of the other loading conditions for the cold condition of the CY-MPC configuration. This stress intensity bounds the actual cold condition described above. To ensure that the minimum stress allowable is used, the allowables are taken at the maximum temperature of the inner shell (331°F) for the cold condition described above. The temperature distribution for the canistered GTCC waste is considered to be enveloped by the 17 kW design basis cold load.

4. Gravity loads - The mechanical loads consist of gravity acting on the cask structure and its contents. The cask is assumed to be loaded and resting in the horizontal position on the front and rear cask supports. Mechanical loads resulting from a 1g application of the total weight (260,000 lbs) of the cask structure and contents are imposed on the model.

These loading conditions are identical to the 1 foot side drop evaluated in 2.6.7.2.2 for the CY-MPC configuration except the 1 foot drop condition employed 20g instead of 1g for the gravity load. Descriptions of the three-dimensional finite element model are contained in 2.6.7.2.2 and 2.10.2.1.3. To determine the maximum primary stress intensity for the cold condition, the stress intensity due to the 20g loading (in Tables 2.6.7.1-2 and 2.6.7.1-3) can be factored by 1/20 and then added to the stress intensity associated with the 50 psig pressure + bolt preload (2.2 ksi). The maximum primary stress intensity reported for P_m and $P_m + P_b$ for the 1-foot side drop are 11.5 ksi and 20.9 ksi, respectively. Factoring these by 1/20 and adding the result to 2.2 ksi for the pressure + bolt preload, results in 2.8 ksi and 3.2 ksi, respectively, for P_m and $P_m + P_b$. Using the minimum allowables of 19.6 ksi for P_m and 29.4 ksi for $P_m + P_b$, reported in Tables 2.6.7.1-4 and 2.6.7.1-5, the minimum margins of safeties for the cask body for the primary stress intensity P_m and $P_m + P_b$ are +6.0 and +8.2, respectively. It is concluded that the CY-MPC configuration satisfies the primary stress limits for the cold condition.

Using the methodology to evaluate the range of $P_m + P_b$ stress intensities described in 2.6.1.1, the allowable stress intensity of $1.5 S_m$ of 29.4 ksi should be compared to the bounding $P_m + P_b$ stress intensity. This value is obtained by adding the maximum thermal stress intensity of 7 ksi to 3.2 ksi to obtain 10.2 ksi. Since $10.2 < 29.4$ ksi, it is concluded that the CY-MPC configuration meets the $3.0 S_m$ criteria for the $P_m + P_b$ stress intensity range for the cold condition.

2.6.3 Reduced External Pressure

The drop in atmospheric pressure to 3.5 psia, as specified in 10 CFR 71.71(c)(3), effectively results in an additional internal pressure in the cask of 11.2 psig. This additional pressure has a negligible effect on the NAC-STC because, in Section 2.6.1, the cask is analyzed for a normal transport conditions internal pressure of 50.0 psig. Since the maximum normal operating pressure, considering 3 percent fuel failure, is 12 psig for directly loaded fuel, 11.3 psig, which is bounding for the canistered fuel configurations, and near 0 psig for the canistered GTCC waste configuration (Section 3.4.4), the total effective internal pressure considering the drop in atmospheric pressure becomes 15.5 psig maximum. The maximum stress in the cask for the 50.0 psig internal pressure is 1,200 psi, Table 2.10.4-1. Thus, the requirements of 10 CFR 71.71(c)(3) are satisfied.

THIS PAGE INTENTIONALLY LEFT BLANK

2.6.4 Increased External Pressure

An increased external pressure of 20 psia (5.3 psig external pressure), as specified in 10 CFR 71.71(c)(4), has a negligible effect on the NAC-STC because of the thick outer shell and end closures of the cask. Conservatively, applying a 20-psi external pressure to the neutron shield shell produces hoop stresses of only 4,151 psi. This stress is negligible. Additionally, Section 2.6.7 addresses many different loading cases, which exceed these prescribed external pressure requirements. Therefore, the requirements of 10 CFR 71.71(c)(4) are satisfied.

THIS PAGE INTENTIONALLY LEFT BLANK

2.6.5 Vibration

The effect of vibrations normally incident to transportation is considered to be negligible for the NAC-STC. This conclusion is based on the fact that the calculated stresses due to vibrations normally incident to transport are much smaller than the calculated stresses for the normal transport 1-foot drop event.

The normal transport 1-foot side drop, discussed in Section 2.6.7.2, results in an impact deceleration equal to 18.12g. This impact force produces a 4,797 psi maximum stress intensity in the inner shell and a 5,620 psi maximum stress intensity in the outer shell of the NAC-STC for the directly loaded fuel configuration. For the canistered fuel configuration, the maximum inner shell and outer shell stress intensities are 22.9 ksi and 18.2 ksi, respectively, for an impact deceleration of 20g (Table 2.6.7.2-2).

As a conservative worst case, it is assumed that the normal transport vibration acceleration is equal to the acceleration equivalent to that which will produce the normal vertical loading imposed on the tiedown devices by 10 CFR 71.45(b)(1). This regulation specifies a load factor of 2.0 to be applied to the package weight; therefore, it is assumed that the tiedown devices and the cask must resist an imposed 2.0g vibration acceleration.

The maximum stress intensity range for normal transport vibration is obtained by multiplying the stress from the 1-foot side drop impact by the ratio of acceleration values from vibration to those for the drop impact. Thus the stress intensities in the outer shell (the critical component) are $S_{\max} = (2/18.12)(5620) = 620$ psi and $S_{\min} = - (2/18.12)(5620) = - 620$ psi, and the maximum stress intensity range is $S_n = 1240$ psi for the directly loaded fuel configuration. For both of the canistered fuel configurations, the inner shell (the critical component) stress intensity for normal transport vibration is estimated by ratioing from the 1-foot drop analysis as $S_{\max} = (2/20)(22.9) = 2.29$ ksi psi. The allowable alternating stress intensity for austenitic stainless steel is determined as the 10^{11} cycle value from the "ASME Boiler and Pressure Vessel Code," Table I-9.2.2, ratioed for the effect of the 300°F temperature. This value is $S_e = 12,975$ psi; therefore, the margin of safety for the critical component of the NAC-STC in the directly loaded fuel configuration for normal transport vibration is:

$$MS = (S_e/S_{alt}) - 1 = (12,975/620) - 1 = +\text{Large}$$

where:

$$S_{alt} = 0.5 S_n$$

The margin of safety for the inner shell for the canistered fuel configurations of the NAC-STC is:

$$MS = (12,975/2,290) - 1 = +\text{Large}$$

During normal transport, the rotation trunnions serve as the rear tiedown for the NAC-STC. The rotation trunnion is the critical tiedown component for all three load axes; the front of the cask is supported in a cradle and restrained vertically by a band attached to the cradle. From Section 2.5.3, the critical component on the rotation trunnion is the attachment weld between the trunnion and the cask outer shell, which has an applied shear stress of 22.7 ksi. This applied shear stress is produced by the 10.2 g resultant from the combined longitudinal and vertical shock (10.0 g longitudinal and 2 g vertical) tiedown load components.

The same method is used to determine the maximum stress intensity range as is used for the cask, except that the ratio of the normal transport vibration acceleration to the resultant acceleration for the combined longitudinal and vertical shock was used. The allowable alternating stress for the weld is the same as that for the cask. The alternating shear stresses are $S_{\max} = (2/10.2)(22,700) = 4,451$ psi and $S_{\min} = - (2/10.2)(22,700) = - 4,451$ psi, and the maximum stress intensity range is $S_n = 8,902$ psi. The margin of safety for the rotation trunnion as a rear tiedown device for normal transport vibration is:

$$M.S. = (S_e/S_{alt}) - 1 = (12,975/4,451) - 1 = + 1.92$$

where:

$$S_{alt} = 0.5 S_n$$

The stability of the tubes comprising the CY-GTCC basket is maintained by the 0.25 inch fillet welds connecting angles and plates to the sides of the 3/8 inch thick tubes. From Table 2.6.19-3, the maximum force computed is 1,223 pounds. For the 0.25 inch thick weld, this corresponds to a stress of $1,223/(0.25 \times 0.707)$ or 6.9 ksi for an acceleration of 20g. To envelope any stresses developed during transport, this S_n is computed by doubling the maximum stress to account for a reversal of the stresses due to vibration. Since the S_{alt} is $0.5 S_n$, and since 6,900 psi is less than 12,975 psi (for 10^{11} cycles), the Margin of Safety is:

$$M.S. = 12,975/6,900 - 1 = + 0.88$$

The NAC-STC satisfies the requirements for normal vibration incident to transportation as required by 10 CFR 71.71(c)(5).

2.6.6 Water Spray

Water causes negligible corrosion of the stainless steel materials used to fabricate the NAC-STC; the cask contents are protected in the sealed cavity. A water spray as specified in 10 CFR 71.71(c)(6) has no adverse effect on this package. The cask surface temperature during the water spray is between 100°F and -40°F. Consequently, the induced thermal stress in the cask components is less than the thermal stresses that occur during the extreme ambient temperature conditions for normal operation. Therefore, the requirements of 10 CFR 71.71(c)(6) are satisfied.

THIS PAGE INTENTIONALLY LEFT BLANK

2.6.7 Free Drop (1 Foot)

The free drop scenario outlined by 10 CFR 71.71(c)(7) requires the NAC-STC to be structurally adequate for a 1-foot drop (normal transport conditions) onto a flat, essentially unyielding horizontal surface in the orientation that inflicts the maximum damage to the cask. The following subsections evaluate the cask body, the impact limiters, the closure lid and bolts, the neutron shield shell, and the upper ring components; for the end, side, and corner drop orientations.

THIS PAGE INTENTIONALLY LEFT BLANK

2.6.7.1 One-Foot End Drop

The NAC-STC is structurally evaluated for the normal condition of transport 1-foot end drop in accordance with the requirements of 10 CFR 71.71. In this event, the NAC-STC (equipped with an impact limiter over each end) falls through a distance of one foot onto a flat, unyielding, horizontal surface. The cask strikes the surface in a vertical position; consequently, an end impact on the bottom end or top end of the cask occurs. The types of loading involved in an end drop event are closure lid bolt preload, internal pressure, thermal, impact load, and inertial body load. There are six credible end impact conditions to be considered, according to Regulatory Guide 7.8:

1. Top end drop with 100°F ambient temperature, maximum decay heat load, and maximum solar insolation.
2. Top end drop with -20°F ambient temperature, maximum decay heat load, and no solar insolation.
3. Top end drop with -20°F ambient temperature, no decay heat load, and no solar insolation.
4. Bottom end drop with 100°F ambient temperature, maximum decay heat load, and maximum solar insolation.
5. Bottom end drop with -20°F ambient temperature, maximum decay heat load, and no solar insolation.
6. Bottom end drop with -20°F ambient temperature, no decay heat load, and no solar insolation.

During an impact event, the cask body will experience a vertical deceleration. Considering the cask as a free body, the impact limiter will apply the load to the cask end to produce the deceleration. Since the deceleration represents an amplification factor for the inertial loading of the cask, the equivalent static method is adopted to perform the impact evaluations. The analyses consider the behavior of the cask to be linearly elastic. Additionally, the fabrication stresses are considered to be negligible (Section 2.6.11).

2.6.7.1.1 One-Foot End Drop Evaluation of the NAC-STC Cask in the Directly Loaded and Yankee-MPC Canistered Fuel Configurations

The NAC-STC cask is modeled as an axisymmetric structure using ANSYS STIF42 isoparametric elements. A detailed description of the two-dimensional finite element model of the NAC-STC is provided in Section 2.10.2.1.1.

Five categories of load—closure lid bolt preload, internal pressure, thermal, impact, and inertial body loads—are considered on the cask:

1. Closure lid bolt preload - The required total bolt preloads on the inner lid bolts and the outer lid bolts are 4.51×10^6 pounds and 6.02×10^5 pounds, respectively, as calculated in Section 2.6.7.5. Bolt preload is applied to the model by imposing initial strains to the bolt shafts, as explained in Section 2.6.7.5. The bolts are modeled as beam (ANSYS STIF3) elements.
2. Internal pressure - The cask internal pressure is temperature dependent and is evaluated in Section 3.4.4. Pressures of 50 psig and 12 psig are applied on the interior surfaces of the cask cavity for the hot ambient and cold ambient cases, respectively. These pressures envelope the calculated pressures for cask configurations—directly loaded fuel (12 psig), canistered fuel (11.3 psig), and canistered GTCC waste (< 11.3 psig).
3. Thermal - The thermal conditions described in Sections 3.4.2 and 3.4.3 determine the cask temperature distributions for the following three combinations of ambient temperature, heat load, and solar insolation for directly loaded fuel:

Condition 1. 100°F ambient temperature, with maximum decay heat load, and maximum solar insolation.

Condition 2. -20°F ambient temperature, with maximum decay heat load, and no insolation.

Condition 3. -40°F ambient temperature, with no decay heat load, and no insolation.

The cask temperature distributions calculated for each of the three temperature conditions discussed above are used as inputs to the ANSYS analyses for the directly loaded fuel

configuration. The ANSYS analysis determines the stresses arising from the thermal expansion of the cask from its initial 70°F condition, including the effects of the differential thermal growth within the components, which is a result of the temperature difference across the walls of the cask. The cask temperature distributions are also used in the ANSYS structural analyses to determine the values of the temperature-dependent material properties.

Additional heat transfer analyses performed in Sections 3.4.2 and 3.4.3 determine the cask temperature distributions for the following two conditions for the canistered fuel configuration:

Condition 4. 100°F ambient temperature, maximum decay heat load (12.5 kW).

Condition 5. -40°F ambient temperature, maximum decay heat load (12.5 kW), and no solar insolation.

Due to the lower heat load (lower decay heat per inch of length), the temperature distribution for canistered fuel is enveloped by that for the directly loaded fuel configuration. The temperature distribution for the canistered GTCC waste (maximum decay heat = 2.9 kW) is also similarly enveloped.

4. Impact loads - The impact loads are induced by the impact limiter acting on the cask end during an end drop condition. The impact loads are determined from the energy absorbing characteristics of the impact limiters, as described in Section 2.6.7.4. The impact load is expressed in terms of the design cask weight (loaded or empty), multiplied by appropriate deceleration factors (g), for details see Section 2.6.7.4.

The impact limiter load is considered to be uniformly applied over the end surface of the finite element model of the cask. The calculation of impact pressure loads is documented in Section 2.10.2.2.2. The following is a summary of the impact pressures applied to the exterior surface of the impacting end, for the different loading scenarios, with the corresponding design deceleration (g) values for the directly loaded fuel configuration.

LOADING CONDITION	IMPACT PRESSURE	DECELERATION
	FOR 1 g	(g)
Top end impact with basket and fuel	42.35 psi	20.0
Top end impact with basket, no fuel	35.86 psi	20.0
Bottom end impact with basket and fuel	42.35 psi	20.0
Bottom end impact with basket, no fuel	35.74 psi	20.0

For the end impact, with directly loaded fuel and basket, a uniform pressure of 847 psi (42.35 psi x [20 g/1 g]) is applied on the exterior surface of the end of the finite element model of the cask. This pressure value is calculated by dividing the total impact load ([20 g/1 g][250,000 lbs] = 5.0×10^6 lbs) by the impact area ($[\pi][43.35]^2 = 5903.8 \text{ in}^2$), which is the surface area of the end of the cask.

It should be noted that the design weight of the cask is 250,000 pounds, which includes the weight of the empty cask (194,000 lbs), plus the weight of the cavity contents (56,000 lbs) for the directly loaded fuel configuration. For those load conditions for which the cask contains no fuel, the basket (design weight 17,000 lbs) is still considered to be in the cask, resulting in a weight of 211,000 pounds for the empty cask with basket. The weights of the cavity contents for the canistered fuel and the canistered GTCC waste configurations are 55,590 pounds and 54,271 pounds, respectively, with the empty cask weight being 194,000 pounds; thus, the weights of the alternate configurations are enveloped by those of the directly loaded fuel configuration.

5. Inertial body load - The inertial effects, which occur during the end impact, are represented by equivalent static forces, in accordance with D'Alembert's principle. Inertial body load includes the weight of the empty cask (194,000 lbs) and the weight of the cavity contents (56,000 lbs) for the directly loaded fuel configuration, which envelopes that of the canistered fuel or the canistered GTCC waste.

Inertial loads resulting from the weight of the empty cask are imposed by applying an appropriate deceleration factor to the cask mass. The applied decelerations are determined by considering the crush strength and the geometry of the impact limiter, as explained in Section 2.6.7.4.

The inertial load resulting from the 56,000-pound contents design weight is represented as an equivalent static pressure load uniformly applied on the interior surface of the

impacting end of the cask. For the load case with no fuel in the cavity, the design weight of the basket (17,000 lbs) is considered to be in the cask; the weight of the basket is represented in the ANSYS finite element model in the same manner as that of the contents.

The following is a summary of the inertial body load for a 1-g deceleration and the design decelerations for the different loading scenarios. The calculations of content pressures are documented in Section 2.10.2.2.1.

<u>LOADING CONDITION</u>	IMPACT PRESSURE	DECELERATION
	<u>FOR 1 g</u>	<u>(g)</u>
Top end impact with basket and fuel	14.14 psi	20.0
Top end impact with basket, no fuel	4.29 psi	20.0
Bottom end impact with basket and fuel	14.14 psi	20.0
Bottom end impact with basket, no fuel	4.29 psi	20.0

In the ANSYS analyses, the inertial body loads are considered together with the impact loads. The results of the two simultaneous loadings are documented as "impact loads."

For an end drop (either top or bottom end) load condition, the NAC-STC cask body is loaded by the weight of the cavity contents on the interior of the inner bottom forging or on the interior of the inner lid and by the impact limiter crushing force on the exterior of the bottom plate or on the exterior of the outer lid. The calculated weight of the cavity contents for the directly loaded fuel configuration of the NAC-STC has been shown to be greater than that of the canistered fuel or GTCC waste configurations. Therefore, the cavity contents loads and the impact limiter loads on the cask for the directly loaded fuel configuration envelope those of the canistered configurations. Then, the detailed finite element stress analysis of the directly loaded fuel configuration for the end drop load conditions bounds similar analyses for the canistered configurations. No additional evaluation of the canistered configurations is required for the end drop load conditions.

The stresses throughout the cask body are calculated for individual and combined loading conditions for the directly loaded fuel configuration, which is the critical configuration. The individual primary loading conditions are: (1) internal pressure (50 psig or 12 psig); (2) thermal heat (100°F); (3) thermal cold (-20°F); (4) top end impact (impact load only); and (5) bottom end impact (impact load only). The combined loading conditions are: (1) the 1-foot top end impact

with bolt preload and 50 psig internal pressure; (2) 1-foot top end impact with bolt preload and 12 psig internal pressure; (3) 1-foot top end impact (without contents) with bolt preload and 12 psig internal pressure; (4) 1-foot bottom end impact with bolt preload and 50 psig internal pressure; (5) 1-foot bottom end impact with bolt preload and 12 psig internal pressure; and (6) 1-foot bottom end impact (without contents) with bolt preload and 12 psig internal pressure.

Because axisymmetry exists in the cask geometry and in the end-drop loading conditions, axisymmetric boundary conditions are represented in the formulation of the isoparametric elements. A longitudinal support is imposed on the corner node located in the non-impacting end of the cask, to prevent rigid body motion. When the cask system is in equilibrium (i.e., the inertial body loads match the impact loads exactly), then the reaction force at this support will be zero. An examination of the magnitude of the reaction forces provides a check of the validity of the finite element evaluation for the 1-foot end drop condition. The reaction at the longitudinal support is 920 pounds/radian for the 20 g 1-foot end drop load condition. This means that the unbalanced force of the cask model system is only $(920)(2\pi)/20 = 289$ pounds. Compared to the cask design weight of 250,000 pounds, the unbalanced force is negligible, amounting to only 0.12 percent of the design weight of the cask.

The allowable stress limit criteria, for containment and noncontainment structures, are provided in Section 2.1.2. These criteria are used to determine the allowable stresses for each cask component, conservatively using the maximum operating temperature within a given component to determine the allowable stress throughout that component. Note that higher temperatures result in lower allowable stresses. A different set of cask component allowable stresses is determined for each of the temperature conditions. Table 2.10.2-5 documents the allowable stress values determined for each component, for the 100°F ambient temperature condition.

The stress results for the 1-foot top end drop loading cases for the NAC-STC with the directly loaded fuel configuration of the cavity contents are presented as follows. Stress results for the individual loading cases of internal pressure are documented in Tables 2.10.4-1 and 2.10.4-2. Stress results for the two thermal cases are provided in Tables 2.10.4-5 and 2.10.4-6. Stress results for the individual 1-foot top and bottom end drop impact loading cases are documented in Table 2.10.4-8 and 2.10.4-9. These are nodal stress summaries obtained from the finite element analysis results. As described in Section 2.10.4, the nodal stresses are documented on the representative section cuts. Stress results for the 1-foot top and bottom end drop combined loading conditions discussed above are documented in Tables 2.10.4-37 through 2.10.4-64. These tables document the primary, primary plus secondary, primary membrane (P_m), primary

membrane plus primary bending ($P_m + P_b$), primary plus secondary membrane plus bending (S_n), and critical P_m , $P_m + P_b$, and S_n stresses in accordance with the criteria presented in Regulatory Guide 7.6. As described in Sections 2.10.2.3 and 2.10.2.4, procedures have been implemented to document the nodal and sectional stresses, as well as to determine the critical (maximum) stress summary for all cask components.

For the 1-foot top end drop impact loading case, the maximum calculated membrane plus bending stress intensity is 19.3 ksi. By comparison, for the combined loading case, including impact, bolt preload, and internal pressure, the maximum calculated primary membrane plus bending stress intensity is 20.7 ksi. The maximum stress intensities due to impact alone are equal to 93 percent of the maximum primary stress intensities due to the combined loading. Therefore, it is concluded that the impact stresses are the governing factor for the 1-foot end drop condition.

For the 1-foot top end drop scenario, ANSYS analyses were performed at the three different temperature conditions outlined above for the directly loaded fuel configuration of the cask. The results from these three analyses show that the maximum $P_m + P_b$ stress intensities are 20.7 ksi, 20.0 ksi, and 18.0 ksi. These three stress results are essentially identical, with the difference between them being less than 13 percent. Since the allowable stress for a component is a function of the component temperature, with higher temperatures resulting in lower allowable stresses, the allowable stress will be lowest for temperature condition 1 because the highest component temperatures occur for that condition. As a result, the margins of safety are smallest for the analysis for temperature condition 1. The minimum margins of safety for the three temperature conditions are + 0.4, + 0.5, + 0.7, respectively. Therefore, it is concluded that the stress results from temperature condition 1 are the most critical for the top end drop accident conditions.

A similar set of ANSYS analyses was performed for the 1-foot bottom end drop case. The maximum $P_m + P_b$ stress intensities for the 1-foot bottom end drop are 13.8 ksi, 14.0 ksi, and 14.1 ksi. The maximum $P_m + P_b$ stress intensities for the bottom end drop are all lower than those for the top end drop. Hence, the top end drop condition is the most critical of the two.

As shown in Tables 2.10.4-37 through 2.10.4-64, the margins of safety for the primary stress intensity category are positive for all of the 1-foot end drop conditions. The most critically stressed component in the system is the inner lid for the top end drop. The minimum margin of safety for $P_m + P_b$ stress intensity for the top end drop condition is found to be +0.4, as

documented in Table 2.10.4-43. The minimum margin of safety for $P_m + P_b$ stress intensity for the bottom end drop condition is found to be +1.1, as documented in Table 2.10.4-60. The locations of the most critical sections for each cask component are provided in the critical stress summary tables.

Regulatory Guide 7.6 requires that the range of primary plus secondary stress intensities between any two normal conditions of transport be less than $3.0 S_m$. Therefore, it is necessary to evaluate the range of primary plus secondary stress intensities between all of the normal conditions of transport including: heat, cold, 1-foot end drop, 1-foot side drop, and 1-foot corner drop conditions. A simple, straightforward, and very conservative method of showing compliance with the $3.0 S_m$ criterion is to establish an allowable stress limit criterion of $1.5 S_m$ for the range of primary plus secondary stress intensities between each normal condition and the ambient condition. If the $1.5 S_m$ allowable stress limit criterion is satisfied at all locations within the cask, then all pairs of normal conditions will satisfy the $3.0 S_m$ stress range criterion.

Tables 2.10.4-44 and 2.10.4-64 document the range of primary plus secondary stress intensities between the 1-foot end drop condition and the unloaded, ambient condition for the top and bottom end drops, respectively. The maximum primary plus secondary stress intensity range (S_n) for the top end drop is 21.6 ksi, which is less than $1.5 S_m$. The maximum primary plus secondary stress intensity range (S_n) for the bottom end drop is 15.9 ksi, which is also less than $1.5 S_m$. In conjunction with the $1.5 S_m$ criterion for the stress range between the ambient condition and each of the other normal conditions, it is, therefore, concluded that the NAC-STC satisfies the $3.0 S_m$ criterion for the primary plus secondary stress intensity range for the 1-foot end drop load conditions.

The fatigue evaluation of the NAC-STC in Section 2.1.3.2 documents that the requirements of Regulatory Guide 7.6 are satisfied, since the $3.0 S_m$ criterion for the primary plus secondary stress intensity range is satisfied for the 1-foot end drop condition.

The documentation of the adequacy of the NAC-STC to satisfy the buckling criteria for the stresses of the 1-foot end drop condition is presented in Section 2.10.5.

Since all of the margins of safety for the 1-foot end drop condition are positive, the NAC-STC with the directly loaded fuel configuration satisfies the requirements of 10 CFR 71.71 for the normal condition of transport 1-foot end drop condition.

The weight of the directly loaded fuel configuration of the NAC-STC envelopes the weight of the Yankee-MPC canistered fuel and canistered GTCC waste configurations for the 1-foot end drop condition. Consequently, the requirements of 10 CFR 71.71 are also met for the Yankee-MPC configuration.

2.6.7.1.2 One-Foot End Drop Evaluation of NAC-STC in the CY-MPC Configuration

The NAC-STC cask with the CY-MPC canistered configuration is modeled as a three dimensional structure using ANSYS STIF45 isoparametric elements. A detailed description of the three-dimensional finite element model of the NAC-STC cask body for the canistered configurations is provided in Section 2.10.2.1.3. While the loading is axisymmetric, the three-dimensional model employed in this evaluation is also used for the 1-foot side drop orientation.

Five categories of loads are considered in this evaluation: closure lid bolt preload, internal pressure, thermal expansion, impact and inertial loading:

1. Closure lid bolt preload - The required bolt preloads on the inner lid bolts and the outer lid bolts are 115,066 pounds per bolt and 36,810 pounds per bolt, respectively. The stresses corresponding to the bolt preload with a 50 psig internal pressure for the directly loaded configuration are reported in Table 2.10.4-1, and the maximum stress intensity is 1.9 ksi (Location U). To account for the preload and internal pressure for the CY-MPC configuration, the 1.9 ksi is added to the stresses due to the 1-foot end drop.
2. Internal pressure - The cask internal pressure is temperature dependent and is evaluated in Section 3.4.4. A pressure of 50 psig, which envelopes the calculated pressure of 38.1 psig for this configuration, is effectively used by adding the 1.9 ksi (reported above for the bolt preload) to the stresses due to the 1-foot end drop.
3. Thermal - The ANSYS analysis determines the stresses arising from the thermal expansion of the cask from its initial 70°F condition, including the effects of the differential thermal growth within the components, which is a result of the temperature difference across the walls of the cask. The cask temperature distributions are also used in the ANSYS structural analyses to determine the values of the temperature-dependent material properties. Heat transfer analyses performed in Sections 3.4.2 and 3.4.3

determine the cask temperature distributions for the following two conditions for the canistered fuel configuration (an analysis for the third condition is not required):

1. 100°F ambient temperature, maximum decay heat load (17 kW).
2. -40°F ambient temperature, maximum decay heat load (17 kW), and no solar insolation.
3. -40°F ambient temperature, no decay heat load, and no solar insolation.

To bound the stresses arising from thermal expansion, the maximum stress intensity (8.1 ksi, Location G5) from Table 2.10.4-5 is added to the maximum stress intensity in the end drop evaluation. The maximum thermal stress intensity is associated with Thermal Condition 1. To ensure that the minimum stress allowable is used, the allowables are taken at the maximum temperature of the inner shell (331°F) for Thermal Condition 1. The temperature distribution for the canistered GTCC waste is considered to be enveloped by the 17 kW design basis heat load. Individual thermal cases are not evaluated since the design basis heat load of 22.1 kW for the directly loaded fuel envelops the 17 kW basis heat load for the CY-MPC configuration.

4. Impact loads - The impact loads are induced by the impact limiter acting on the cask end during an end drop condition. The impact loads are determined from the energy absorbing characteristics of the impact limiters, and the impact load is expressed in terms of the design cask weight (loaded or empty), multiplied by appropriate deceleration factors (g).

Instead of representing the impact load as a pressure applied to the ends of the cask body, the impact limiter load is actually represented by the contact force generated by the gap elements connected at the ends of the cask. (Figure 2.6.7.2-3). It should be noted that the design weight of the cask is 260,000 pounds, which bounds the weight of the empty cask (187,400 lbs), plus the weight of the cavity contents (67,196 lbs) for the CY-MPC fuel configuration. The weight of the cavity contents for the canistered fuel configuration equals that of the canistered GTCC waste configuration.

5. Inertial body load - The inertial effects, which occur during the end impact, are represented by equivalent static forces, in accordance with D'Alembert's principle. Inertial body load includes the weight of the empty cask (194,000 lbs). Inertial loads resulting from the weight of the empty cask are imposed by applying a 20g deceleration

factor to the cask mass. The applied decelerations are determined by considering the crush strength and the geometry of the impact limiter, as explained in Section 2.6.7.4.

The inertial load resulting from the contents design weight is represented as an equivalent static pressure load uniformly applied on the interior surface of the impacting end of the cask. The pressure corresponds to 20 times the contents weight. For the bottom end drop, the pressures are applied to the bottom of the cask cavity, and for the top end drop, the pressures are applied to the inner surface of the inner lid.

Maximum stress values are obtained for the sections shown in Figure 2.6.7.2-1 by linearizing the stresses along the indicated sections. Components and nodes associated with these sections are shown in Table 2.6.7.1-1. A maximum stress intensity for the load case of "Bolt Preload + 50 psi Internal Pressure" obtained from Table 2.10.4-1 is added to the stress intensity for impact load to obtain a stress intensity associated with the combined loading of bolt preload, pressure, thermal expansion, impact and inertial loadings.

The summary of the maximum membrane stresses (P_m) and membrane plus bending ($P_m + P_b$) are presented in Tables 2.6.7.1-2 through 2.6.7.1-5 for the top end drop and the bottom end drop. All margins of safety for the 1-foot end drop condition are positive. Therefore, the NAC-STC cask with the CY-MPC fuel configuration satisfies the requirements of 10 CFR 71.71 for the normal condition of transport 1-foot end drop condition.

Using the methodology to evaluate the range of primary plus secondary stress intensities described in 2.6.1.1, the allowable stress intensity of $1.5 S_m$ of 29.4 ksi should be compared to the bounding primary plus secondary stress intensity. The maximum stress intensity in Table 2.6.7.1-5 (6.1 ksi) corresponds to Section 10, which includes the 1.9 ksi stress for pressure + bolt preload. The largest thermal stress intensity occurs at Section 9, for the corresponding location in Table 2.10.4-5 is 1.8 ksi (Section B5). This results in a primary plus secondary stress intensity of $(1.8 + 5.3)$ 7.1 ksi. At Section 10, adding 6.1 ksi to the maximum thermal stress intensity of 8.1 ksi results in a primary plus secondary stress intensity of 14.2 ksi. These two combinations of stresses bound all other possible primary plus secondary stresses for the end drop condition. Since $14.2 < 29.4$ ksi, it is concluded that the CY-MPC configuration meets the $3.0 S_m$ criteria for the primary plus secondary stress intensity range for the heat condition.

Table 2.6.7.1-1 Section Locations for Stress Evaluation (Maximums)

Section No. ¹	Component Name and Material	Inside Node	Section Location (in.)						
			X	Y	Z	Outside Node	X	Y	Z
1	Transition Shell – XM-19	197	35.5	146.1	0.0	165	37	146.1	0.0
2 ²	Inner Shell – 304	196	35.5	142.0	0.0	164	37	142.0	0.0
3	Inner Shell – 304	189	35.5	94.2	0.0	157	37	94.2	0.0
4	Bottom Forging – 304	130	35.5	14.5	0.0	123	38	14.5	0.0
5	Outer Shell – 304	280	40.7	14.5	0.0	328	43	14.5	0.0
6	Outer Shell – 304	300	40.7	103.2	0.0	358	43	103.2	0.0
7	Top Forging – 304	271	35.5	173.2	0.0	265	37.5	173.2	0.0
8	Top Forging – 304	317	40.7	173.2	0.0	435	43.4	173.2	0.0
9	Bottom Plate – 304	23	3.16	0.0	0.0	34	3.16	5.45	0.0
10	Bottom Forging – 304	53	3.16	7.45	0.0	65	3.16	13.65	0.0
11	Bottom Plate – 304	22	35.5	0.0	0.0	32	35.5	5.45	0.0
12	Bottom Forging – 304	52	35.5	7.45	0.0	62	35.5	13.65	0.0
13	Inner Lid – 304	486	3.52	178.68	0.0	787	3.52	187.65	0.0
14	Outer Lid – 17-4	514	3.52	187.68	0.0	500	3.52	192.96	0.0
15	Inner Lid – 304	485	35.5	178.68	0.0	796	35.5	187.65	0.0
16	Outer Lid – 17-4	497	35.5	187.68	0.0	495	35.5	192.96	0.0

1. Sections are shown in Figure 2.6.7.2-1.
2. This section is at the boundary of transition shell and inner shell. Allowables for 304 Stainless Steel are used for evaluation.

Table 2.6.7.1-2 CY-MPC Critical P_m Stress Summary; 1-ft Top End Drop

Section No.	P _m Stresses (ksi)						Principal Stresses (ksi)			S.I. Impact (ksi)	S.I. Bolt Preload + Pressure** (ksi)	S.I. Total (ksi)	Allowable Stress* (ksi) S _m	Margin of Safety
	S _x	S _y	S _z	S _{xy}	S _{yz}	S _{xz}	S1	S2	S3					
1	0.0	-1.6	0.0	0.0	0.0	0.0	0.0	0.0	-1.6	1.6	1.9	3.5	31.0	7.9
2	0.0	-1.5	0.0	0.0	0.0	0.0	0.0	0.0	-1.5	1.6	1.9	3.5	19.6	4.6
3	0.0	-1.2	0.0	0.0	0.0	0.0	0.0	0.0	-1.2	1.2	1.9	3.1	19.6	5.3
4	0.0	-0.5	0.2	-0.1	0.0	0.0	0.2	0.0	-0.5	0.7	1.9	2.6	19.6	6.5
5	0.0	-0.2	0.2	0.0	0.0	0.0	0.2	0.0	-0.2	0.4	1.9	2.3	19.6	7.5
6	0.0	-1.3	0.3	0.0	0.0	0.0	0.3	0.0	-1.3	1.5	1.9	3.4	19.6	4.8
7	-0.2	-1.3	-0.2	0.0	0.0	0.0	-0.1	-0.2	-1.3	1.2	1.9	3.1	19.6	5.3
8	-0.1	-2.0	-0.1	-0.2	0.0	0.0	0.0	-0.1	-2.1	2.0	1.9	3.9	19.6	4.0
9	-0.2	0.0	-0.2	0.0	0.0	0.0	0.0	-0.2	-0.2	0.2	1.9	2.1	19.6	8.3
10	0.1	0.0	0.2	0.0	0.0	0.0	0.2	0.1	0.0	0.2	1.9	2.1	19.6	8.3
11	-0.2	0.0	-0.2	-0.1	0.0	0.0	0.0	-0.2	-0.2	0.2	1.9	2.1	19.6	8.3
12	0.2	-0.3	0.1	-0.1	0.0	0.0	0.2	0.1	-0.3	0.5	1.9	2.4	19.6	7.2
13	-0.1	-1.0	0.0	0.4	0.0	0.0	0.0	0.0	-1.1	1.2	1.9	3.1	19.6	5.3
14	-0.4	-1.6	0.2	0.2	0.0	0.0	0.2	-0.3	-1.6	-1.8	1.9	3.7	19.6	4.3
15	0.0	-1.1	-0.1	0.0	-0.1	0.0	0.0	-0.1	-1.1	1.1	1.9	3.0	19.6	5.5
16	0.0	-1.4	0.0	-0.2	-0.1	0.0	0.0	0.0	-1.4	1.5	1.9	3.4	19.6	4.8

* Allowable at 331°F (maximum temperature for inner shell).

** Based on internal pressure of 50 psi.

Table 2.6.7.1-3 CY-MPC Critical $P_m + P_b$ Stress Summary; 1-ft Top End Drop

Section No.	$P_m + P_b$ Stresses (ksi)						Principal Stresses (ksi)			S.I. Impact (ksi)	S.I. Bolt Preload + Pressure** (ksi)	S.I. Total (ksi)	Allowable Stress* (ksi) $1.5S_m$	Margin of Safety
	S_x	S_y	S_z	S_{xy}	S_{yz}	S_{xz}	S_1	S_2	S_3					
1	0.0	-1.6	0.0	0.0	0.0	0.0	0.0	0.0	-1.6	1.6	1.9	3.5	46.5	11.3
2	0.0	-1.6	0.0	0.0	0.0	0.0	0.0	0.0	-1.6	1.6	1.9	3.6	29.4	7.2
3	0.0	-1.2	0.0	0.0	0.0	0.0	0.0	0.0	-1.2	1.2	1.9	3.1	29.4	8.5
4	0.0	-1.3	0.0	0.0	0.0	0.0	0.0	0.0	-1.3	1.3	1.9	3.2	29.4	8.2
5	0.0	-0.8	0.0	-0.1	0.0	0.0	0.0	0.0	-0.8	0.8	1.9	2.7	29.4	9.9
6	0.0	-1.3	0.3	0.0	0.0	0.0	0.3	0.0	-1.3	1.6	1.9	3.5	29.4	7.4
7	-0.3	-2.2	-0.5	0.0	0.0	-0.1	-0.3	-0.5	-2.2	1.9	1.9	3.8	29.4	6.7
8	0.0	-3.4	-0.4	-0.1	0.0	0.0	0.0	-0.4	-3.4	3.4	1.9	5.3	29.4	4.6
9	-0.9	0.0	-1.0	0.0	0.0	0.0	0.0	-0.9	-1.0	1.0	1.9	2.9	29.4	9.1
10	1.1	0.0	1.2	0.0	0.0	0.0	1.2	1.1	0.0	1.2	1.9	3.1	29.4	8.5
11	-0.6	0.0	-0.1	-0.1	0.0	0.0	0.0	-0.1	-0.6	0.6	1.9	2.5	29.4	10.8
12	0.9	0.1	0.2	0.0	0.0	0.1	0.9	0.2	0.1	0.8	1.9	2.7	29.4	9.9
13	2.9	-0.2	3.1	0.1	0.0	0.0	3.1	2.9	-0.2	3.3	1.9	5.2	29.4	4.7
14	0.5	-1.4	1.2	-0.4	0.2	0.0	1.1	0.5	-1.5	2.7	1.9	4.6	29.4	5.4
15	-0.1	-1.0	0.7	0.2	0.0	0.0	0.7	0.0	-1.1	1.8	1.9	3.7	29.4	7.0
16	2.0	-1.3	1.6	0.0	-0.1	-0.1	2.0	1.6	-1.3	3.3	1.9	5.2	29.4	4.7

* Allowable at 331°F (maximum temperature for inner shell).

** Based on internal pressure of 50 psi.

Table 2.6.7.1-4 CY-MPC Critical P_m Stress Summary; 1-ft Bottom End Drop

Section No.	P _m Stresses (ksi)						Principal Stresses (ksi)			S.I. Impact (ksi)	S.I. Bolt Preload + Pressure** (ksi)	S.I. Total (ksi)	Allowable Stress* (ksi) S _m	Margin of Safety
	S _x	S _y	S _z	S _{xy}	S _{yz}	S _{xz}	S1	S2	S3					
1	0.0	-1.2	0.0	0.0	0.0	0.0	0.0	0.0	-1.2	1.2	1.9	3.1	31.0	9.0
2	0.0	-1.2	0.0	0.0	0.0	0.0	0.0	0.0	-1.2	1.2	1.9	3.1	19.6	5.3
3	0.0	-1.5	0.0	0.0	0.0	0.0	0.0	0.0	-1.5	1.5	1.9	3.4	19.6	4.8
4	-0.2	-1.6	-0.4	-0.1	0.0	0.0	-0.2	-0.4	-1.6	1.4	1.9	3.3	19.6	4.9
5	0.0	-2.5	-0.3	0.3	0.0	0.0	0.0	-0.3	-2.5	2.6	1.9	4.5	19.6	3.4
6	0.0	-1.4	0.3	0.0	0.0	0.0	0.2	0.0	-1.4	1.6	1.9	3.5	19.6	4.6
7	0.0	-0.8	0.4	0.1	0.0	0.0	0.4	0.0	-0.8	1.1	1.9	3.0	19.6	5.5
8	0.0	-0.6	0.4	-0.2	0.0	0.0	0.4	0.0	-0.6	1.0	1.9	2.9	19.6	5.8
9	-0.5	-2.0	-0.2	-0.6	0.1	0.0	-0.2	-0.3	-2.2	2.1	1.9	4.0	19.6	3.9
10	0.3	-1.0	0.3	-0.3	0.0	0.0	0.3	0.3	-1.1	1.4	1.9	3.3	19.6	4.9
11	-0.3	-1.9	-0.4	0.0	0.3	0.0	-0.3	-0.3	-1.29	1.6	1.9	3.5	19.6	4.6
12	0.4	-0.7	0.4	0.1	0.0	0.0	0.4	0.4	-0.7	1.1	1.9	3.0	19.6	5.5
13	-0.1	-0.1	-0.1	0.1	0.0	0.0	0.0	-0.1	-0.1	0.1	1.9	2.0	19.6	8.8
14	-0.1	-0.1	0.0	0.0	0.0	0.0	0.0	-0.1	-0.2	0.1	1.9	2.0	19.6	8.8
15	-0.1	-0.3	-0.1	0.2	0.0	0.0	0.0	-0.1	-0.4	0.4	1.9	2.3	19.6	7.5
16	0.0	-0.1	0.0	0.1	0.0	0.0	0.0	0.0	-0.1	0.1	1.9	2.0	19.6	8.8

* Allowable at 331°F (maximum temperature for inner shell).

** Based on internal pressure of 50 psi.

Table 2.6.7.1-5 CY-MPC Critical $P_m + P_b$ Stress Summary; 1-ft Bottom End Drop

Section No.	$P_m + P_b$ Stresses (ksi)						Principal Stresses (ksi)			S.I. Impact (ksi)	S.I. Bolt Preload + Pressure** (ksi)	S.I. Total (ksi)	Allowable Stress* (ksi)	Margin of Safety
	S_x	S_y	S_z	S_{xy}	S_{yz}	S_{xz}	S1	S2	S3					
1	0.0	-1.2	0.0	0.0	0.0	0.0	0.0	0.0	-1.2	1.2	1.9	3.1	46.5	14.0
2	0.0	-1.2	0.0	0.0	0.0	0.0	0.0	0.0	-1.2	1.2	1.9	3.1	29.4	8.5
3	0.0	-1.5	0.0	0.0	0.0	0.0	0.0	0.0	-1.5	1.5	1.9	3.4	29.4	7.6
4	-0.4	-2.6	-0.8	-0.1	0.0	-0.1	-0.4	-0.8	-2.6	2.2	1.9	3.1	29.4	8.5
5	0.1	-4.6	-0.8	0.1	0.0	0.0	0.1	-0.8	-4.6	0.8	1.9	2.7	29.4	9.9
6	0.0	-1.4	0.2	0.0	0.0	0.0	0.2	0.0	-1.4	1.6	1.9	3.5	29.4	7.4
7	0.0	-1.0	0.3	0.0	0.0	0.0	0.3	0.0	-1.0	1.3	1.9	3.2	29.4	8.2
8	0.0	-1.2	0.2	0.1	0.0	0.0	0.2	0.0	-1.3	1.5	1.9	3.4	29.4	7.7
9	1.3	-1.3	2.1	-0.4	0.0	0.0	2.1	1.4	-1.3	3.4	1.9	5.3	29.4	4.5
10	3.3	-0.4	3.8	-0.2	0.0	0.0	3.8	3.3	-0.4	4.2	1.9	6.1	29.4	3.8
11	1.5	-1.3	1.4	-0.3	0.2	-0.1	1.6	1.3	-1.3	2.9	1.9	4.8	29.4	5.1
12	1.3	-0.6	0.9	0.2	0.0	0.0	1.3	0.9	-0.6	1.9	1.9	3.8	29.4	6.7
13	1.7	0.1	1.8	0.0	0.0	0.0	1.8	1.7	0.1	1.7	1.9	3.6	29.4	7.2
14	1.0	-0.1	1.1	0.0	0.0	0.0	1.1	0.1	-1.1	1.1	1.9	3.0	29.4	8.8
15	-0.2	-0.4	0.5	0.2	0.0	0.0	0.5	0.0	-0.5	1.1	1.9	3.0	29.4	8.8
16	-0.1	-0.1	0.4	0.1	0.0	0.0	0.4	0.0	-0.2	0.5	1.9	2.4	29.4	11.3

* Allowable at 331°F (maximum temperature for inner shell).

** Based on internal pressure of 50 psi.

2.6.7.2 One-Foot Side Drop

The NAC-STC is structurally evaluated for the normal conditions of transport 1-foot side drop in accordance with the requirements of 10 CFR 71.71. In this event, the NAC-STC (equipped with an impact limiter over each end) falls through a distance of 1 foot onto a flat, unyielding, horizontal surface. The cask strikes the surface in a horizontal position; consequently, a side impact on the cask occurs. The types of loading involved in a side drop accident are closure lid bolt preload, internal pressure, thermal, impact load, and inertial body load. There are three credible side impact conditions to be considered, according to Regulatory Guide 7.8:

1. Side drop with 100°F ambient temperature, maximum decay heat load, and maximum solar insolation.
2. Side drop with -20°F ambient temperature, maximum decay heat load, and no solar insolation.
3. Side drop with -20°F ambient temperature, no decay heat load, and no solar insolation.

During a side drop impact event, the cask body experiences a lateral deceleration. Considering the cask as a free body, the impact limiters apply the load to the side of the cask (in the impact limiter contact area) to produce the deceleration. Since the deceleration represents an amplification factor for the inertial loading of the cask, the equivalent static method is adopted to perform the impact evaluations. The analyses consider the behavior of the cask to be linearly elastic. Additionally, fabrication stresses are considered to be negligible (Section 2.6.11).

2.6.7.2.1 One-Foot Side Drop Evaluation of the NAC-STC Cask in the Directly Loaded and Yankee-MPC Canistered Fuel Configurations

The finite element analysis method is utilized to perform the side drop stress evaluations for the NAC-STC. The 1-foot side drop condition is analyzed using a three-dimensional structural model to accurately represent the non-axisymmetric loads involved in the side drop case. One-half of the cask is modeled as a three-dimensional structure with one plane of symmetry. The ANSYS STIF45 three-dimensional solid element is the primary element type used in the model.

In order to reduce the overall problem of size to satisfy the limitations of the ANSYS program and the computer hardware, two three-dimensional models have been constructed for the directly loaded fuel configuration—the top fine mesh model and the bottom fine mesh model. A single

three-dimensional finite element model is constructed and used for the Yankee-MPC canistered fuel configuration of the NAC-STC. A detailed description of the three-dimensional finite element models of the NAC-STC is presented in Section 2.10.2.1.2 for each of the fuel configurations. The top fine mesh model contains a fine mesh region at the upper half of the cask with a relatively coarse mesh at the bottom end; the bottom fine mesh model contains a fine mesh region at the bottom end of the cask with relatively coarse mesh at the top end. Nevertheless, both models are complete representations of the cask, since the entire cask is modeled. Both models are used in the side drop analyses to obtain the detailed stresses at each end of the cask. The stress results from the fine mesh portion of each model are then combined to provide a final stress summary for the NAC-STC for the 1-foot side drop condition for the directly loaded fuel configuration. For the canistered fuel configuration, the stress results are obtained from the single finite element model of the NAC-STC for the Yankee-MPC configuration.

Five categories of load—closure lid bolt preload, internal pressure, thermal, impact, and body inertia—are considered on the cask:

1. Closure lid bolt preload - The required total bolt preloads on the inner lid and outer lid are 4.51×10^6 pounds and 6.02×10^5 pounds, respectively. Bolt preload is applied to the model by imposing initial strains to the bolt shafts, as explained in Section 2.10.2.2.3. The bolts are modeled as beam (ANSYS STIF4) elements.
2. Internal pressure - The cask internal pressure is temperature dependent and is evaluated in Section 3.4.4. Pressures of 50 psig and 12 psig are applied on the interior surfaces of the cask cavity for the hot ambient and cold ambient cases, respectively. These pressures envelope the calculated pressures for all cask configurations—directly loaded fuel (12 psig), canistered fuel (11.3 psig), and canistered GTCC waste (< 11.3 psig).
3. Thermal - The heat transfer analyses performed in Sections 3.4.2 and 3.4.3 determine the cask temperature distributions for the following three combinations of ambient temperature, heat load, and solar insolation for directly loaded fuel:

Condition 1. 100°F ambient temperature, with maximum decay heat load and maximum solar insolation.

Condition 2. -20°F ambient temperature, with maximum decay heat load, and no solar insolation.

Condition 3. -20°F ambient temperature, with no decay heat load, and no solar insolation.

The cask temperature distributions calculated for each of the three thermal conditions are used as inputs to the ANSYS structural analyses. The ANSYS analyses determine the stresses induced by the thermal expansion of the cask from its initial 70°F condition. The cask temperature distributions are also used in the ANSYS structural analyses to determine the values of the temperature-dependent material properties, such as modulus of elasticity, density, and Poisson's ratio.

Additional heat transfer analyses performed in Sections 3.4.2 and 3.4.3 determine the cask temperature distributions for the following two conditions for the canistered fuel configuration:

Condition 4. 100°F ambient temperature, maximum decay heat load (12.5 kW) and maximum solar insolation.

Condition 5. -40°F ambient temperature, maximum decay heat load (12.5 kW), and no solar insolation.

Due to the lower heat load (lower decay heat per inch of length), the temperature distribution for canistered fuel is enveloped by that for the directly loaded fuel configuration. The temperature distribution for the canistered GTCC waste (maximum decay heat = 2.9 kW) is also similarly enveloped.

4. Impact loads - The impact loads are induced by the impact limiters acting on the cask during a side drop condition. The impact loads are determined from the energy absorbing characteristics of the impact limiters, as described in Section 2.6.7.4. The impact load is expressed in terms of the design cask weight (loaded or empty), multiplied by appropriate deceleration factors (g). The 1-foot side drop evaluations conservatively consider a deceleration factor of 20 g based on the calculated deceleration value of 18.12 g, as documented in Section 2.6.7.4, Table 2.6.7.4.1-3.

The impact limiter load is applied to the finite element model as a distributed pressure over the contact areas between the impact limiters and the cask. The contact area is defined based on the "crush" geometry of the impact limiter. The distribution of impact

pressure is considered to be uniform in the longitudinal direction and is considered to vary in the circumferential direction. A cosine-shaped impact pressure distribution is selected for application in the circumferential direction. The cosine-shaped impact pressure distribution is peaked at the cask cross-section centerline and spread over a 79.4-degree arc on either side of that centerline in the circumferential direction, as shown in Figure 2.10.2-32. The 79.4-degree arc is based on the impact limiter geometry following a side drop crush test. The assumption of a "peaked" pressure distribution is a conservative, classical, stress analysis procedure. Since the center of gravity of the loaded cask is located within 1 inch of the longitudinal middle plane of the cask, the impact load is considered to be evenly divided between the two impact limiters. The impact contact area for a side drop accident consists of the 12.03-inch overlapping region between the impact limiter and the cask at each end of the cask.

The calculation to determine the impact pressure applied to the finite element model is documented in Section 2.10.2.2.2. That calculation is based on a 1-g deceleration condition. The following is a summary of the lateral impact pressures for the eight circumferential sectors for the directly loaded fuel configuration:

ARC (deg)	LATERAL IMPACT PRESSURE FOR 1 g (psi)	DECELERATION (g)
0 - 8.3	163.22	20
8.3 - 17.0	158.67	20
17.0 - 26.2	149.06	20
26.2 - 35.8	133.98	20
35.8 - 45.9	113.17	20
45.9 - 56.5	86.69	20
56.5 - 67.7	54.99	20
67.7 - 79.4	18.96	20

The impact pressures used in the 1-foot side drop analyses are determined by multiplying the pressure values summarized previously by the 1-foot side drop deceleration factor (20 g).

It should be noted that the design weight of the cask is 250,000 pounds, which includes the weight of the empty cask (194,000 lbs), plus the weight of the cavity contents (56,000 lbs) for the directly loaded fuel configuration. For those load conditions in which the cask contains no fuel, the basket (design weight = 17,000 lbs) is still considered to be in the cask, resulting in a weight of 211,000 pounds for the empty cask with basket. The weights of the cavity contents for the canistered fuel and the canistered GTCC waste configurations are 55,590 pounds and 54,271 pounds, respectively, with the empty cask weight being 194,000 pounds; thus, the weights of the alternate configurations are less than those of the directly loaded fuel configuration. Since the package weight for design analysis is the same, 250,000 pounds, for the NAC-STC directly loaded and Yankee-MPC configurations, the calculated lateral impact limited pressure distribution for the directly loaded fuel configuration is also applied to the ANSYS model for the Yankee-MPC configuration.

The inertial body load effects, which occur during the side impact, are represented by equivalent static forces in accordance with D'Alembert's principle. Inertial body load includes the weight of the empty cask (194,000 lbs) and the weight of the cavity contents (56,000 lbs) for the directly loaded fuel configuration, which envelopes that of the canistered fuel or the canistered GTCC waste (refer to previous paragraph).

5. Inertial body load - Inertia loads resulting from the weight of the empty cask are imposed by applying an appropriate deceleration factor to the cask mass. The applied deceleration is 20 g and is applied as explained in the discussion of impact loads.

The inertial load resulting from the 56,000-pound contents design weight is represented as an equivalent static pressure applied on the interior surface of the cask for the directly loaded fuel configuration. Specifically, the equivalent static pressure is applied with a uniform distribution along the cavity length, and with a cosine-shaped distribution in the circumferential direction. The calculation of the contents pressure, as documented in Section 2.10.2.2.1 uses the identical method as that used in the determination of the impact pressures. The following is a summary of the contents pressures for a 1-g deceleration for the eight circumferential sectors for the directly loaded fuel configuration:

ARC	LATERAL IMPACT	
	PRESSURE FOR 1 g	DECELERATION
(deg)	(psi)	(g)
0 - 8.3	6.51	20
8.3 - 17.0	6.33	20
17.0 - 26.2	5.95	20
26.2 - 35.8	5.34	20
35.8 - 45.9	4.51	20
45.9 - 56.5	3.46	20
56.5 - 67.7	2.19	20
67.7 - 79.4	0.76	20

Similarly, inertial load pressures are calculated for the Yankee-MPC canistered fuel configuration. As shown in Figure 2.6.7.2-2, a portion of the inertial load resulting from the 56,000 pound contents design weight is applied on the interior surface of the cask as a uniform distribution along a length of the cavity equal to the length of the canister below the shield and structural lids. The portion of the contents' inertial loading representing the shield and structural lids is distributed along a length of the cavity equal to the thickness of the two lids (8 inches). The axial location of the inertial pressures on the cask cavity represents the actual location of the canister and the lids in the cask. In the circumferential direction, the inertial pressure is applied as a cosine-shaped distribution representing the canister contact region with the cask inner shell over a 60° arc for the 1-foot side drop case (a 90° arc is used for the 30-foot side drop case). Due to the use of an identical canister and the reduced weight of the basket structure plus contents, the canistered Yankee GTCC waste configuration is enveloped by the canistered fuel configuration.

The contents pressures considered in the 1-foot side drop analyses are determined by multiplying the pressure values above by the deceleration factor of 20 g.

In the ANSYS analyses, the inertial body loads are considered together with the impact loads. The results of the two simultaneous loadings are documented as "impact loads."

The stresses throughout the cask body are calculated for individual and combined loading conditions for the directly loaded fuel configuration. The individual loading conditions are: (1) internal pressure (50 psig or 12 psig) plus bolt preload; (2) thermal heat (100°F); (3) thermal cold (-20°F); and (4) 1-foot side impact (impact load only). The combined loading condition is

the 1-foot side impact with bolt preload and 50 psig internal pressure. This is the most critical combined loading condition for the directly loaded fuel configuration based on the discussion in Section 2.7.1.2. Several parametric studies were performed to compare the stress results at the various temperature conditions. The stresses throughout the cask body are calculated for the combined loading condition: 1-foot side impact with bolt preload, 50 psig internal pressure, and 100°F ambient temperature.

The finite element model has one plane of symmetry in the cask geometry and in the side drop loading conditions. Symmetric boundary conditions are applied to the cask finite element model by restraining the nodes on the symmetry plane to prevent translations in the direction normal to the symmetry plane. In addition, two nodes at the outer cask radius on the top and bottom ends of the cask, opposite the points of impact, are restrained laterally (in the drop direction) and the node at the top is restrained in the longitudinal direction to prevent rigid body motion. When the cask system is in equilibrium (i.e., the inertial body loads match the impact loads exactly), then the reaction forces at these supports will be zero. An examination of the magnitude of the reaction forces provides a check of the validity of the finite element evaluation for the 1-foot side drop condition. The sum of reactions in the cask lateral direction for the bottom model is 3,442 pounds for the application of a 20-g load. This means that the unbalanced force of the cask model system is only $3,442/20 = 172.1$ pounds. Compared to one-half of the design weight of the cask, 125,000 pounds, the unbalanced force is negligible, amounting to only 0.1 percent of the design weight of the cask. A similar check done for the top model indicates that the unbalanced force is 0.5 percent of the design weight, which is also negligible.

The allowable stress limit criteria for containment and noncontainment structures are provided in Section 2.1.2. These criteria are used to determine the allowable stresses for each cask component, conservatively using the maximum operating temperature within a given component to determine the allowable stress throughout that component. Note that higher temperatures result in lower allowable stresses. A different set of component allowable stresses is determined for each temperature condition. Table 2.10.2-5 documents the allowable stress values determined for each component for temperature condition 1 (100°F ambient).

The stress results for the 1-foot side drop loading cases for the NAC-STC with the directly loaded fuel configuration of the cavity contents are presented as follows. Stress results for the individual internal pressure loading conditions are documented in Tables 2.10.4-1 and 2.10.4-2. Stress results for the two thermal loading conditions are documented in Tables 2.10.4-5 and 2.10.4-6. Stress results for the individual 1-foot side impact loading condition are documented

in Table 2.10.4-10. These are the nodal stress summaries obtained from the finite element analysis results. As described in Section 2.10.2.4.2, the nodal stresses are documented on the representative section cuts. Stress results for the combined loading condition are documented in Tables 2.10.4-65 through 2.10.4-83. These tables document: (1) the primary stresses for the 0-degree circumferential location; (2) the primary plus secondary stresses for the 0-degree circumferential location; (3) the primary membrane (P_m) stresses for the 0-, 45.9-, 91.7- and 180-degree circumferential locations; (4) the primary membrane plus primary bending ($P_m + P_b$) stresses for the 0-, 45.9-, 91.7- and 180-degree circumferential locations; (5) the primary plus secondary membrane plus bending (S_n) stresses on the 0-, 45.9-, 91.7-, and 180-degree circumferential locations; and (6) the critical P_m , $P_m + P_b$, and S_n stresses. The stress results on the 0-, 45.9-, 91.7- and 180-degree circumferential locations document the stress variation in the circumferential direction. The circumferential locations are illustrated in Figure 2.10.2-8. As described in Sections 2.10.2.3 and 2.10.2.4, procedures have been implemented to document the nodal and sectional stresses, as well as to determine the critical stress summary for all cask components.

Each of the stress summary tables for the directly loaded fuel configuration are prepared by considering the stress results of two analysis runs, the first run using the top fine mesh model and the second run using the bottom fine mesh model. The stress results from the fine mesh portion of each model are used to form the nodal and sectional stress summaries. For the critical stress summaries, stresses for the top forging, inner lid and outer lid are determined from the top fine mesh model results; stresses for the bottom plate and bottom forging are calculated from the bottom fine mesh model results; stresses for the inner shell, the transition sections, and the outer shell are determined as the larger of the stress results from the two models. In order to justify the use of stress results from both models for the side drop evaluation, comparisons are made on the combined loading (impact plus internal pressure) stress results from the two models at the middle section of the cask (Sections L and M in Figure 2.10.2-34, axial location of 96.15 inches from cask bottom). On the 0-degree and 45-degree circumferential locations, the stress results from both models show good agreement, with less than a 9 percent difference. On the 90-degree and 180-degree circumferential locations, where stresses are lower, the stress results from both models are still reasonably comparable, with less than a 13 percent difference. An additional check is performed for sections J and K (axial location of 54.90 inches) and sections N and O (axial location of 137.40 inches), which are about 40 inches away from the center of the cask (Figure 2.10.2-34). The stress results from both models also show good agreement, with less than 10 percent difference for the 0-, 45.9- and 90-degree circumferential locations. Therefore, it

is concluded that the combined stress results from the top fine mesh model and the bottom fine mesh model for the 1-foot side drop condition are valid and conservative.

It is worthwhile to mention that the most critical stress for the impact loading condition and that for the primary loading condition are essentially identical for the directly loaded fuel configuration, with a maximum difference of 5 percent. Therefore, it is concluded that the impact stresses are the governing factor for the 1-foot side drop condition.

As shown in the critical P_m and $P_m + P_b$ stress summaries (Tables 2.10.4-70 and 2.10.4-71) for the directly loaded fuel configuration, the critical stresses for most of the cask components occur on the 0-degree circumferential location, which contains the line of impact. It is also observed that for the cask inner shell, the maximum calculated stresses are located on the circumferential locations in the 67.7-degree region. This is because the maximum shearing stresses are located near the 67.7-degree circumferential location.

Similarly, the stress results for the canistered fuel configuration of the NAC-STC for the 100°F ambient temperature combined load condition are presented in Figure 2.6.7.2-1 and Tables 2.6.7.2-1 and 2.6.7.2-2. Only the inner and outer shells and their attachment regions to the top and bottom forgings are evaluated for the canistered fuel configuration because the canistered contents loading on the cask cavity does not significantly change the stresses in the end components of the cask from those for the directly loaded fuel configuration.

As shown in Tables 2.10.4-70 and 2.10.4-71, the margins of safety for the primary stress intensity category are positive for the 1-foot side drop condition. The most critically stressed component in the system is the top forging. The minimum margin of safety is found to be +0.6, as documented in Table 2.10.4-70, for the directly loaded fuel configuration. The locations of the most critical sections for each cask component are provided in the critical stress summary tables. For the canistered fuel configuration, Tables 2.6.7.2-1 and 2.6.7.2-2 show that margins of safety are positive with the minimum margin of safety, +0.3, located on the inner shell near the bottom.

Regulatory Guide 7.6 requires that the range of primary plus secondary stresses between any two normal conditions of transport be less than $3.0 S_m$. Therefore, it is necessary to evaluate the range of primary plus secondary stress intensities between all of the normal conditions of transport, including the heat, cold, 1-foot end, 1-foot side, and 1-foot corner drop conditions. A simple, straightforward, and very conservative method of showing compliance with the $3.0 S_m$

criterion is to establish an allowable stress limit criterion of $1.5 S_m$ for the range of primary plus secondary stresses between each normal condition and the ambient condition. If each normal condition meets the $1.5 S_m$ allowable stress limit criterion at all locations within the cask when compared to the ambient condition, then all pairs of normal conditions will meet the $3.0 S_m$ stress range criterion.

Table 2.10.4-72 documents the range of primary plus secondary stress intensities between the 1-foot side drop condition and the unloaded, ambient condition for the directly loaded fuel configuration. The maximum S_n stress intensity range for the directly loaded fuel configuration 1-foot side drop is shown to be 26.9 ksi, which is less than $1.5 S_m$. In conjunction with the $1.5 S_m$ criterion for the stress range between the ambient condition and each of the other normal condition, it is, therefore, concluded that the NAC-STC satisfies the $3.0 S_m$ criterion for the S_n stress range for the 1-foot side drop load condition. The maximum S_n stress intensity range for the canistered fuel configuration 1-foot side drop occurs at Section No. 4 (Figure 2.6.7.2-1) and is estimated by adding the principal stresses in Table 2.6.7.2-2 to those at Point F1 in Table 2.10.4-5, thermal heat condition for directly loaded fuel. The calculated value is $S_n = 23.2$ ksi, which is less than $1.5 S_m$ and satisfies the $3.0 S_m$ criterion.

For the fatigue evaluation of the NAC-STC, Section 2.1.3.2 documents that the requirements of Regulatory Guide 7.6 are satisfied by the $3.0 S_m$ criteria for the extreme total stress intensity range limit. The documentation of the NAC-STC adequacy in satisfying the buckling criteria for the stresses of the 1-foot side drop condition is presented in Section 2.10.5. The NAC-STC maintains its containment capability and, therefore, satisfies the requirements of 10 CFR 71.71 for the normal conditions of transport 1-foot side drop.

During the side drop, the bearing load on the cask cavity wall created by the fuel basket support plates in the directly loaded fuel configuration is a maximum for the normal condition loads. Considering the total cavity design weight of 56,000 pounds being supported by the 31 stainless steel support disks and the contact area being limited to a 90-degree arch length, the bearing stress is:

$$\begin{aligned} S_{br-1g} &= 56,000 / (0.5 \times 31 \times 3.14 \times 71.0 \times 0.25) \\ &= 64.8 \text{ psi} \end{aligned}$$

For the 18.1 g 1-foot drop the maximum bearing stress in the cavity wall is:

$$S_{br-18.1g} = (18.1)(64.8) = 1,170 \text{ psi}$$

Using an allowable based on the maximum inner shell temperature, $1.5 S_y = 32.94 \text{ ksi}$ at 331°F , the margin of safety is:

$$MS = 32.94/1.17 - 1 = +\text{Large}$$

The bearing stress on the cask cavity wall for the Yankee-MPC fuel configuration is lower than that for the directly loaded fuel configuration because the support disk loads bear directly on the canister shell, which increases the bearing region on the cask cavity wall and reduces the bearing stresses. This condition is also true for the Yankee-MPC GTCC waste configuration.

2.6.7.2.2 One-Foot Side Drop Evaluation for the CY-MPC Configuration

The NAC-STC cask with the CY-MPC canistered configuration is modeled as a three-dimensional structure using ANSYS STIF45 isoparametric elements. A detailed description of the three-dimensional finite element model of the NAC-STC cask body for the canistered configurations is provided in Section 2.10.2.1.3. The model used in this evaluation is also used for the 1-foot end drop evaluation.

Five categories of loads are considered in this evaluation: closure lid bolt preload, internal pressure, thermal expansion, impact and inertial loading:

1. Closure lid bolt preload - The required bolt preloads on the inner lid bolts and the outer lid bolts are 115,066 pounds per bolt and 36,810 pounds per bolt, respectively. The principal stresses corresponding to the bolt preload with a 50 psig internal pressure for the directly loaded configuration are reported in Table 2.10.4-1 and the maximum stress intensity is 1.9 ksi (Location U3). To account for the preload and internal pressure for the CY configuration, the 1.9 ksi is added to the stresses due to the 1-foot end drop.
2. Internal pressure - The cask internal pressure is temperature dependent and is evaluated in Section 3.4.4. A pressure of 50 psig, which enveloped the calculated pressure of 38.1 psig for this configuration, is effectively used by adding the 1.9 ksi (reported above for the bolt preload) to the stresses due to the 1-foot end drop.

3. Thermal - The ANSYS analysis determines the stresses arising from the thermal expansion of the cask from its initial 70°F condition, including the effects of the differential thermal growth within the components, which is a result of the temperature difference across the walls of the cask. The cask temperature distributions are also used in the ANSYS structural analyses to determine the values of the temperature-dependent material properties. Heat transfer analyses performed in Sections 3.4.2 and 3.4.3 determine the cask temperature distributions for the following two conditions for the canistered fuel configuration (an analysis for the third condition is not required):
 1. 100°F ambient temperature, maximum decay heat load (17 kW).
 2. -40°F ambient temperature, maximum decay heat load (17 kW), and no solar insolation.
 3. -40°F ambient temperature, no decay heat load, and no solar insolation.

To bound the stresses arising from thermal expansion, the maximum stress intensity (8.1 ksi, location G5) from Table 2.10.4-5, is added to the maximum stress intensity in the side drop evaluation. The maximum thermal stress intensity is associated with Thermal Condition 1. To ensure that the minimum stress allowable is used, the allowables are taken at the maximum temperature of the inner shell (331°F) for Thermal Condition 1. The temperature distribution for the canistered CY GTCC waste is considered to be enveloped by the 17 kW design basis heat load. Individual thermal cases are not evaluated since the design basis heat load of 22.1 kW for the directly loaded fuel envelops the 17 kW basis heat load for the CY-MPC configuration.

4. Impact loads - The impact loads are induced by the impact limiter acting on the sides of the cask top end forging and bottom end forging during a side drop condition. The impact loads are determined from the energy absorbing characteristics of the impact limiters, and the impact load is expressed in terms of the design cask weight (loaded or empty), multiplied by appropriate deceleration factors (g).

Instead of representing the impact load as a pressure applied to the sides of the cask body, the impact limiter load is represented by the contact force generated by the gap elements connected at the sides for the top end forging and the bottom end forging (Similar to that shown for the side drop case shown in Figure 2.6.7.2-3). Details of the gap elements used to represent the impact limiter are also presented in Section 2.10.2.1.3. It should be noted that the design weight of the cask is 260,000 pounds, which bounds

the weight of the empty cask (187,400 lbs), plus the weight of the cavity contents (67,196 lbs) for the directly loaded fuel configuration. The weight of the cavity contents for the canistered fuel equals that of the canistered GTCC waste configuration.

5. Inertial body load - The inertial effects, which occur during the end impact, are represented by equivalent static forces, in accordance with D'Alembert's principle. Inertial loads resulting from the weight of the empty cask are imposed by applying a 20g deceleration factor to the cask mass. The weight of the CY-MPC fuel, basket and canister factored by a 20g acceleration is represented by a surface pressure load. The pressure load for the canister lid and canister body with fuel is applied to the cask body using a cosine-shaped pressure distribution of a half angle of 30°. The total pressure applied to the cask is equal to the total impact load of the contents (i.e., weight multiplied by g-load). The weight of the spacer is applied to the appropriate region at the bottom of the canister.

Maximum stress values are obtained for the sections shown in Figure 2.6.7.2-1 by linearizing the stresses along the indicated sections. Components and nodes associated with these sections are shown in Table 2.6.7.1-1. A maximum stress intensity for the load case of "Bolt Preload + 50 psi Internal Pressure" obtained from Table 2.10.4-1 is added to the stress intensity for impact load to obtain a stress intensity associated with the combined loading of bolt preload, pressure, thermal expansion, impact and inertial loadings.

The summary of the maximum membrane stresses (P_m) and membrane plus bending ($P_m + P_b$) are presented in Tables 2.6.7.2-3 and 2.6.7.2-4. All margins of safety for the 1-foot side drop condition are positive. Therefore, the NAC-STC cask with the CY-MPC fuel configuration satisfies the requirements of 10 CFR 71.71 for the normal condition of transport 1-foot side drop condition.

Using the methodology to evaluate the range of primary plus secondary stress intensities described in 2.6.1.1, the allowable stress intensity of $1.5 S_m$ or 29.4 ksi should be compared to bounding primary plus secondary stress intensity. This value is obtained by adding the maximum thermal stress intensity of 8.1 ksi to 20.9 ksi (Table 2.6.7.2-4, Section 4, where the 20.9 ksi value includes the pressure + bolt preload) to obtain 29.0 ksi. Since $29.0 < 29.4$ ksi, it is concluded that the CY-MPC configuration meets the $3.0 S_m$ criteria for the primary plus secondary stress intensity range for the heat condition.

Figure 2.6.7.2-1 Section Locations for Stress Evaluation (Canister Configurations)

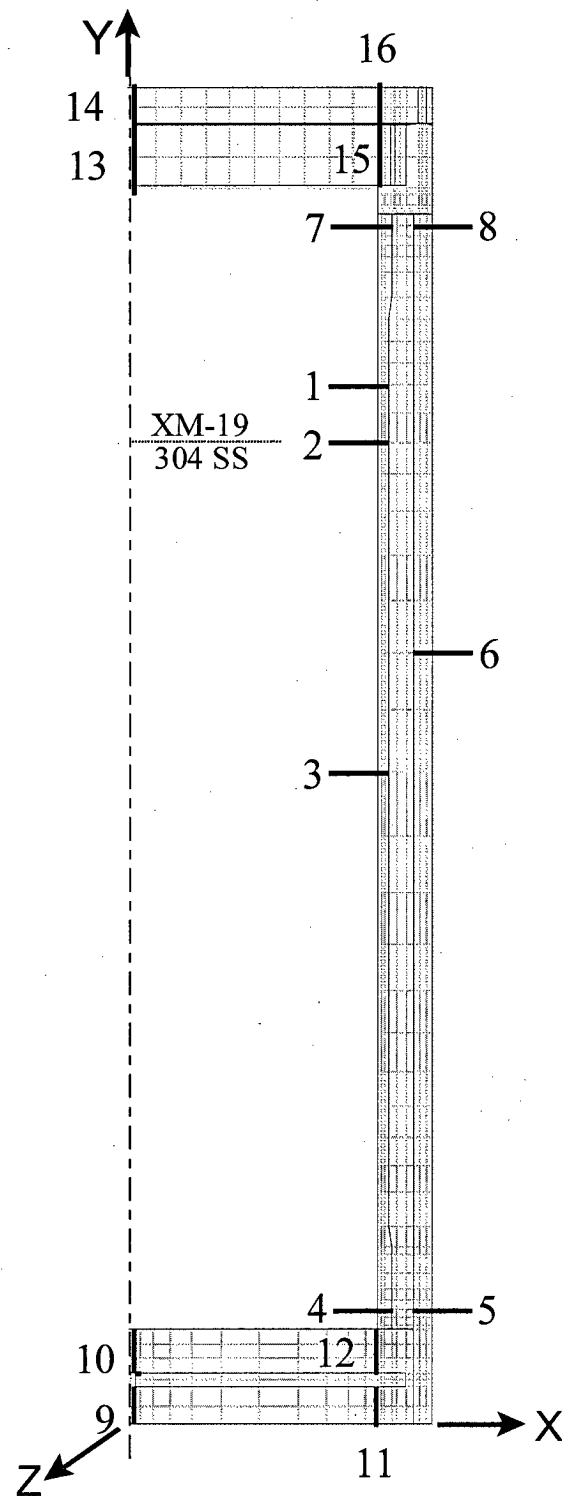


Figure 2.6.7.2-2 Yankee-MPC Model with Pressure Distribution Applied (Side Drop Case)

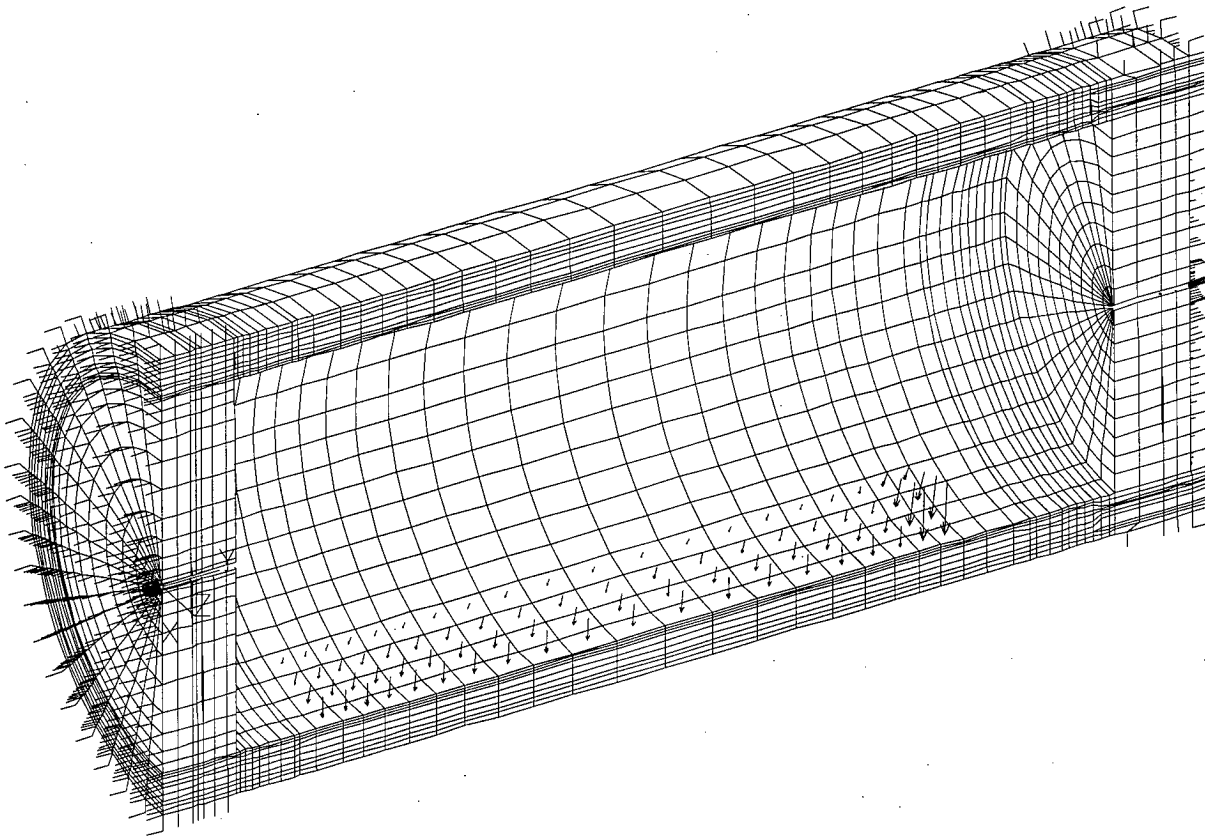


Figure 2.6.7.2-3 CY-MPC Model with Pressure Distribution Applied (Side Drop Case)

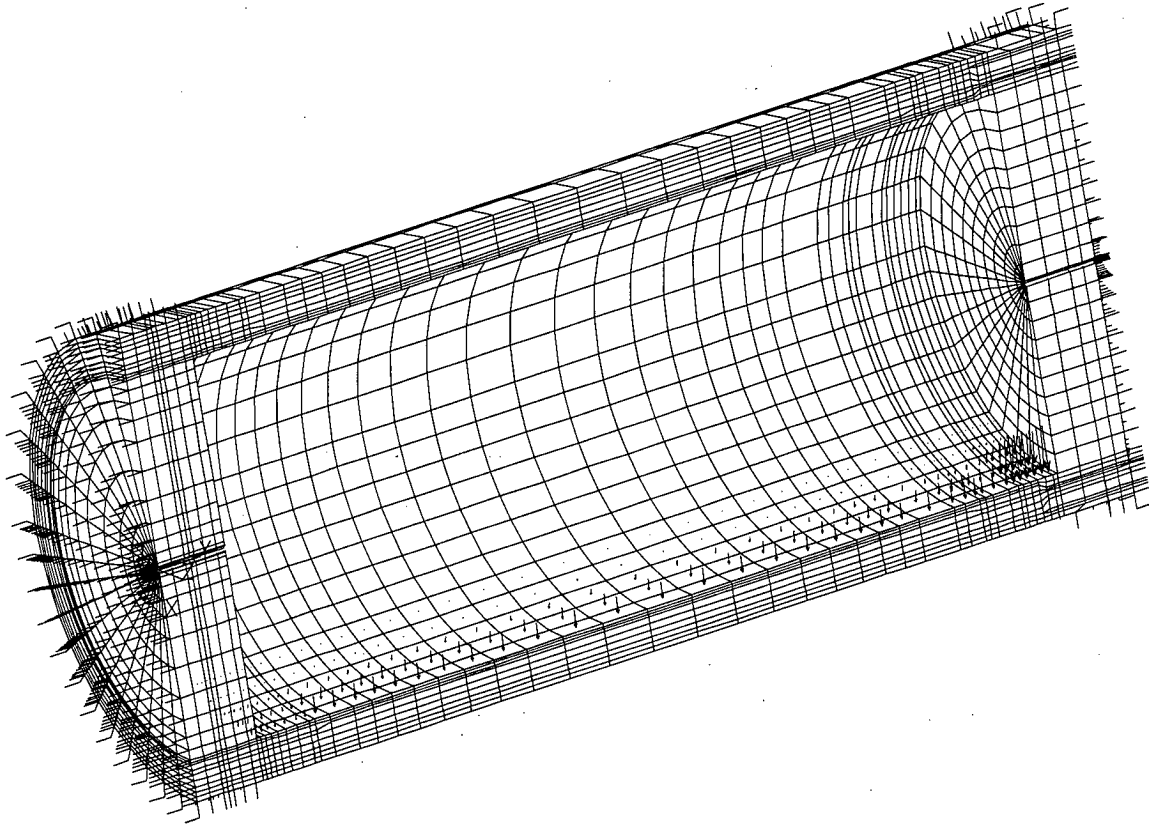


Table 2.6.7.2-1 Yankee-MPC Critical P_m Stress Summary; 1-ft. Side Drop; Drop Orientation = 90° (ksi)

Sec. No.	P_m Stresses						Principal Stresses			S.I.			Allow. Stress* S_m	Margin of Safety
	S_x	S_y	S_z	S_{xy}	S_{yz}	S_{xz}	S1	S2	S3	S.I. Impact	Bolt Preload + Pressure**	S.I. Total		
1	-1.2	3.7	5.8	-0.1	-0.7	0.6	6.1	3.5	-1.3	7.4	1.9	9.3	31.3	2.4
2	-0.8	4.8	5.3	0.2	-0.5	0.4	5.6	4.6	-0.9	6.5	1.9	8.4	19.9	1.4
3	-0.5	7.9	2.2	0.0	0.0	0.2	7.9	2.2	-0.5	8.5	1.9	10.4	19.9	0.9
4	-0.2	-5.2	-6.3	1.3	0.3	-0.4	0.1	-5.4	-6.4	6.6	1.9	8.5	19.9	1.3
5	-0.8	-1.1	-4.6	1.5	0.3	-0.4	1.6	-1.9	-4.7	6.3	1.9	8.2	19.9	1.4
6	-0.3	8.6	2.0	0.0	0.0	0.4	8.6	2.1	-0.4	9.0	1.9	10.9	19.9	0.8
7	0.0	-3.8	-4.3	-0.7	-0.2	-0.3	0.2	-3.8	-4.4	4.6	1.9	6.5	19.9	2.1
8	0.0	2.3	-0.8	-0.8	-0.3	-0.1	2.5	-0.2	-1.6	4.1	1.9	6.0	19.9	2.3

* Allowable at 311°F (maximum temperature for inner shell).

** Based on internal pressure of 50 psi.

Table 2.6.7.2-2 Yankee-MPC Critical $P_m + P_b$ Stress Summary; 1-ft. Side Drop; Drop Orientation = 90° (ksi)

Sec. No.	P_m Stresses						Principal Stresses			S.I.			Allow. Stress* S_m	Margin of Safety
	S_x	S_y	S_z	S_{xy}	S_{yz}	S_{xz}	S1	S2	S3	S.I. Impact	Bolt Preload + Pressure**	S.I. Total		
1	-1.5	12.7	16.9	-0.1	-0.3	1.3	17.0	12.7	-1.5	18.6	1.9	20.5	46.9	1.3
2	-0.9	11.7	16.6	0.1	-0.3	1.2	16.7	11.7	-0.9	17.6	1.9	19.5	29.8	0.5
3	-0.6	12.7	15.2	0.0	0.0	1.1	15.2	12.7	-0.6	15.9	1.9	17.8	29.8	0.7
4	-0.3	-20.3	-10.2	1.7	0.0	-0.7	0.5	-10.3	-20.4	21.0	1.9	22.9	29.8	0.3
5	1.2	-14.1	-7.8	0.4	0.0	-0.6	1.2	-7.9	-14.1	15.3	1.9	17.2	29.8	0.7
6	-0.3	13.9	15.8	0.0	0.0	1.3	15.9	13.9	-0.4	16.3	1.9	18.2	29.8	0.6
7	0.3	-9.6	-5.0	-1.0	0.1	-0.3	0.4	-5.0	-9.7	10.1	1.9	12.0	29.8	1.5
8	-0.5	7.4	-1.1	-1.0	-0.6	-0.0	7.6	-0.6	-1.2	8.8	1.9	10.7	29.8	1.8

* Allowable at 311°F (maximum temperature for inner shell).

** Based on internal pressure of 50 psi.

Table 2.6.7.2-3 CY-MPC Critical P_m Stress Summary; 1-ft Side Drop

Section No.	P_m Stresses (ksi)						Principal Stresses (ksi)			S.I. Impact	S.I. Bolt Preload + Pressure**	S.I. Total	Allowable Stress*	Margin of Safety
	S_x	S_y	S_z	S_{xy}	S_{yz}	S_{xz}	S1	S2	S3	(ksi)	(ksi)	(ksi)	(ksi) S_m	
1	-0.6	3.1	2.6	0.0	-0.5	0.1	3.4	2.3	-0.6	4.0	1.9	5.9	31.0	4.3
2	-0.5	4.0	2.2	0.0	-0.4	0.1	4.1	2.1	-0.5	4.6	1.9	6.5	19.6	2.0
3	-0.5	8.0	1.8	0.0	0.0	0.1	8.0	1.8	-0.6	8.6	1.9	10.5	19.6	0.87
4	-0.2	-3.7	-5.9	1.8	0.4	-0.5	0.6	-4.2	-6.1	6.7	1.9	8.6	19.6	1.28
5	1.0	1.8	-4.4	1.8	0.2	-0.5	3.2	-0.4	-4.5	7.7	1.9	9.6	19.6	1.0
6	-0.3	9.2	2.0	0.0	0.0	0.4	9.2	2.0	-0.4	9.6	1.9	11.5	19.6	0.70
7	-0.4	-4.8	-3.2	-1.8	-0.6	-0.2	0.2	-3.1	-5.5	5.7	1.9	7.6	19.6	1.6
8	0.0	3.8	0.0	-0.8	-0.3	0.1	4.0	0.0	-0.2	4.2	1.9	6.1	19.6	2.2

* Allowable at 331°F (maximum temperature for inner shell).

** Based on internal pressure of 50 psi.

Table 2.6.7.2-4 CY-MPC Critical $P_m + P_b$ Stress Summary; 1-ft Side Drop

Section No.	$P_m + P_b$ Stresses (ksi)						Principal Stresses (ksi)			S.I. Impact	S.I. Bolt Preload + Pressure**	S.I. Total	Allowable Stress*	Margin of Safety
	S_x	S_y	S_z	S_{xy}	S_{yz}	S_{xz}	S1	S2	S3	(ksi)	(ksi)	(ksi)	(ksi) $1.5S_m$	
1	-0.6	6.1	10.8	0.0	-0.3	0.7	10.9	6.1	-0.6	11.5	1.9	13.4	46.5	2.5
2	-0.5	6.8	10.9	0.0	-0.2	0.6	10.9	6.8	-0.5	11.4	1.9	13.3	29.4	1.2
3	-0.6	12.5	14.0	0.0	0.0	1.0	14.1	12.5	-0.6	14.7	1.9	16.6	29.4	0.77
4	0.7	-20.7	-10.4	2.1	0.0	-0.8	0.9	-10.5	-21.0	19.0	1.9	20.9	29.4	0.41
5	1.3	-11.5	-8.2	0.4	-0.3	-0.7	1.4	-8.2	-11.5	12.8	1.9	14.7	29.4	1.0
6	-0.2	14.2	15.0	0.0	0.0	1.3	15.1	14.2	-0.4	15.5	1.9	17.4	29.4	0.70
7	0.6	-10.5	-3.0	-2.3	0.1	-0.2	1.0	-3.0	-11.0	12.0	1.9	13.9	29.4	1.1
8	-0.5	7.0	-0.6	-1.1	-0.9	0.1	7.2	-0.6	-0.7	8.0	1.9	9.9	29.4	2.0

* Allowable at 331°F (maximum temperature for inner shell).

** Based on internal pressure of 50 psi.

2.6.7.3 One-Foot Corner Drop

This section presents the one-foot corner drop evaluation for the NAC-STC cask in the directly loaded, Yankee-MPC and CY-MPC configurations.

2.6.7.3.1 NAC-STC Cask One-Foot Corner Drop Evaluation for the Directly Loaded and Yankee-MPC Configurations

The NAC-STC in the directly loaded fuel configuration is structurally evaluated for the normal conditions of transport 1-foot corner drop in accordance with the requirements of 10 CFR 71.71. In this event, the NAC-STC (equipped with an impact limiter over each end) falls through a distance of 1 foot onto a flat, unyielding, horizontal surface. The cask strikes the surface on its top or bottom corner. The cask center of gravity is considered to be directly above the initial point of impact for the corner drop condition. For the NAC-STC, the orientation angle is 24 degrees for the corner drop.

Similar to the evaluation of the 1-foot end drop and side drop conditions, as presented in Sections 2.6.7.1 and 2.6.7.2, the 1-foot corner drop condition for the directly loaded fuel configuration is evaluated using finite element analysis (FEA), as shown in this Section. Based on the summary of finite element models and results (Sections 2.6.7.1 through 2.6.7.3) and the impact limiter analysis (Section 2.6.7.4), a comparison of the g-loads and finite element analysis stress results for the 1-foot end, side and corner drop conditions is shown below:

1-foot Drop Load Condition	Actual g-Load (Calculated)	g-load used in FEA	FEA Stress Results Minimum Margin of Safety
End	19.6	20	+ 0.4
Side	18.1	20	+ 0.6
Corner	5.3	20	+ 0.4

As shown, a very conservative g-load (20 g) is used in the analysis for the corner drop conditions, and the minimum margin of safety for the corner drop condition is similar to those of the end and side drop conditions. Therefore, it is concluded that the corner drop condition stresses for the directly loaded fuel configuration are bounded by the end drop and side drop condition stresses. The same conclusion can be reached for the 30-foot drop conditions using this comparison method. Since the calculated weight of the cavity contents for the directly loaded fuel configuration has been shown to be greater than that of the Yankee-MPC fuel or

GTCC waste configurations, and the center of gravity of the loaded cask is the same for both the directly loaded fuel configuration and canistered fuel configuration, it is also concluded that the corner drop condition stresses for the canistered fuel or GTCC waste configurations are bounded by the end drop and side drop condition stresses. Therefore, no additional evaluation of the 1-foot corner drop condition is required for the canistered fuel or GTCC waste configuration.

The types of loading involved in a corner drop accident are closure lid bolt preload, internal pressure, thermal, impact load, and inertial body load. There are six credible corner impact conditions to be considered, according to Regulatory Guide 7.8:

1. Top corner drop with 100°F ambient temperature, maximum decay heat load, and maximum solar insolation.
2. Top corner drop with -20°F ambient temperature, maximum decay heat load, and no solar insolation.
3. Top corner drop with -20°F ambient temperature, no decay heat load, and no solar insolation.
4. Bottom corner drop with 100°F ambient temperature, maximum decay heat load, and maximum solar insolation.
5. Bottom corner drop with -20°F ambient temperature, maximum decay heat load, and no solar insolation.
6. Bottom corner drop with -20°F ambient temperature, no decay heat load, and no solar insolation.

The finite element analysis method is utilized to perform the corner drop stress evaluations for the NAC-STC. The corner drop conditions are analyzed using a three-dimensional finite element model to accurately represent the non-axisymmetric loads involved in the corner drop case. One-half of the cask is modeled as a three-dimensional structure with one plane of symmetry. The ANSYS STIF45 3-D solid element is the primary element type used in the model. Two models have been constructed—a top fine mesh model and a bottom fine mesh model. Each model is a complete representation of the cask. There is a fine mesh region at the

impacting end of the cask with a relatively coarse mesh at the opposite end of the cask. The maximum stresses occur at the impacting end of the cask; therefore, the fine element mesh density is used in this region to provide accurate results. The stresses calculated using the coarse element mesh at the non-impacting end of the model are an accurate representation of the stresses present there; however, the maximum stresses occur in that end of the cask for the load condition, in which it is the impacting end of the cask. The detailed descriptions of the three-dimensional finite element models of the NAC-STC are described in Section 2.10.2.1.2.

During a corner impact event, the impact limiter will apply the load to the cask impacting corner to produce the deceleration. Since the deceleration represents an amplification factor for the inertial loading of the cask, the equivalent static method is adopted to perform the impact evaluations. Additionally, the fabrication stresses are considered to be negligible (Section 2.6.11).

Five categories of load—closure lid bolt preload, internal pressure, thermal, impact, and body inertia—are considered on the cask:

1. Closure lid bolt preload - The required total bolt preloads on the inner lid bolts and the outer lid bolts are 4.51×10^6 pounds and 6.02×10^5 pounds, respectively. Bolt preload is applied to the model by imposing initial strains to the bolt shafts, as explained in Section 2.10.2.2.3. The bolts are modeled as beam (ANSYS STIF4) elements.
2. Internal pressure - The cask internal pressure is temperature dependent and is evaluated in Section 3.4.4. Pressures of 50 psig and 12 psig are applied on the interior surfaces of the cask cavity for the hot ambient and cold ambient cases, respectively. These pressures envelope the calculated pressures for all cask configurations—directly loaded fuel (12 psig), canistered fuel (11.3 psig), and canistered GTCC waste (< 11.3 psig).
3. Thermal - The heat transfer analyses performed in Sections 3.4.2 and 3.4.3 determine the cask temperature distributions for the following three combinations of ambient temperature, heat load, and solar insolation for directly loaded fuel:

Condition 1: 100°F ambient temperature, with maximum decay heat load, and maximum solar insolation.

Condition 2: -20°F ambient temperature, with maximum decay heat load and no solar insolation.

Condition 3: -20°F ambient temperature, with no decay heat load, and no solar insolation.

The cask temperature distributions calculated for each of these three thermal conditions are used as inputs to the ANSYS structural analyses for the directly loaded fuel configuration. The ANSYS analysis determines the stresses induced by the thermal expansion of the cask from its initial 70°F condition. The cask temperature distributions are also used in the ANSYS structural analyses to determine the values of the temperature-dependent material properties, such as modulus of elasticity, density, and Poisson's ratio.

4. Impact loads - The impact loads are produced by the impact limiter acting on the cask end during a corner drop condition. The impact loads are determined from the energy absorbing characteristics of the impact limiters, as described in Section 2.6.7.4. The impact load is expressed in terms of the design cask weight (loaded or empty), multiplied by an appropriate deceleration factor (g). A design deceleration factor of 20 g is used for both top and bottom corner drops. This compares to the actual deceleration factor of 5.3 g, as documented in Section 2.6.7.4, Table 2.6.7.4.1-3.

The impact loads for the corner drop analyses have lateral and longitudinal components, which are calculated from the total impact load. The lateral load component is applied along the circumferential direction using a cosine-shaped distribution similar to that used in the side drop analysis (over a 0° to 79.4° arc on each side of the impact centerline). The longitudinal load component is applied using an uniform distribution on the end surface of the impacting end of the cask, over the same 0- to 79.4-degree arc on each side of the impact centerline.

Section 2.10.2.2.2 documents the calculation of the impact pressures for the NAC-STC design weight of 250,000 pounds and an impact limiter contact length of 24.06 inches (12.03 inches at each end). For the corner drop, the impact energy is absorbed by only one impact limiter; hence, the corner drop lateral impact pressures may be calculated by

multiplying the lateral impact pressures calculated for the side drop by 2 (the impact limiter contact length is only 12.03 inches) and by the sine of the drop angle (24° for the NAC-STC corner drop). For example, the corner drop lateral impact pressures for the elements located between the 0- and 8.29-degree circumferential planes is:

$$\begin{aligned}\text{Press}_1 &= (163.22)(2)(\sin 24^\circ) = 132.78 \text{ psi for 1 g} \\ \text{Press}_{20} &= (132.78)(20 \text{ g/1 g}) = 2655.6 \text{ psi for 20 g}\end{aligned}$$

The following is a summary of the lateral impact pressures for the directly loaded fuel configuration of the NAC-STC, for the elements at the different circumferential locations, for a 1-g deceleration:

ARC (deg)	LATERAL IMPACT PRESSURE FOR 1 g		DECELERATION (g)
	(psi)		
0 - 8.3	132.78		20
8.3 - 17.0	129.07		20
17.0 - 26.2	121.26		20
26.2 - 35.8	108.99		20
35.8 - 45.9	92.06		20
45.9 - 56.5	70.52		20
56.5 - 67.7	44.73		20
67.7 - 79.4	15.42		20

The longitudinal impact pressure may be calculated as the total impact load multiplied by the cosine of the drop angle and divided by twice the cask end area within the 0 to 79.4-degree arc. Therefore:

$$\begin{aligned}\text{Weight} &= 250,000 \text{ lbs} \\ \text{Area} &= (79.4/360)(2)(\pi)(43.35)^2 = 2,604 \text{ in}^2 \\ \text{Press}_1 &= (250,000)(\cos 24^\circ)/2604 = 87.70 \text{ psi for 1 g} \\ \text{Press}_{20} &= (87.70)(20 \text{ g/1 g}) = 1754.0 \text{ psi for 20 g}\end{aligned}$$

It should be noted that the design weight of the cask is 250,000 pounds, which includes the weight of the empty cask (194,000 lbs), plus the weight of the cavity contents (56,000 lbs).

5. Inertial body load - The inertial effects, which occur during the corner impact, are represented by equivalent static forces, in accordance with D'Alembert's principle. The inertial body load includes the weight of the empty cask (194,000 lbs) and the weight of the cavity contents (56,000 lbs).

Inertial loads resulting from the weight of the empty cask are imposed by applying an appropriate deceleration factor to the cask mass. The lateral and longitudinal components of inertial loading are determined in the same manner as they are for the impact loading.

The inertial load resulting from the 56,000-pound contents weight is represented as an equivalent static pressure load with the lateral and longitudinal components of the inertial load applied on the interior surface of the cask. The lateral load component is distributed to the cask model using the same circumferential cosine distribution as is used for the side drop load condition (over an arc from 0° to 79.4°). The longitudinal load component is distributed uniformly over the cask cavity end over the same 0-degree to 79.4-degree arc. The lateral load component may be determined by ratioing the side drop contents pressure values calculated in Section 2.10.2.2.1 by the deceleration (g) factor and multiplying by the sine of the drop orientation angle. The longitudinal load component is calculated by ratioing the end drop contents pressure by the deceleration (g) factor and multiplying by the cosine of the drop orientation angle. The design deceleration factor is 20 g for both the top and bottom 1-foot corner drops.

Section 2.10.2.2.1 contains the side drop contents pressures for a total contents weight of 56,000 pounds. The corner drop lateral contents pressure for the elements located between the 0- and 8.29-degree circumferential planes is, therefore:

$$\begin{aligned}\text{Press}_1 &= (6.51)(\sin 24^\circ) &= 2.65 \text{ psi for 1 g} \\ \text{Press}_{20} &= (2.65)(20 \text{ g/1 g}) &= 53.0 \text{ psi for 20 g}\end{aligned}$$

The following is a summary of the applied lateral contents pressures for the corner drop for the directly loaded fuel configuration of the NAC-STC, for the elements at the circumferential locations, for a 1-g deceleration.

ARC (deg)	LATERAL IMPACT PRESSURE FOR 1 g		DECELERATION (g)
	(psi)		
0 - 8.3	2.65		20
8.3 - 17.0	2.57		20
17.0 - 26.2	2.42		20
26.2 - 35.8	2.17		20
35.8 - 45.9	1.83		20
45.9 - 56.5	1.41		20
56.5 - 67.7	0.89		20
67.7 - 79.4	0.31		20

The longitudinal contents pressure is calculated from the longitudinal component of the total contents weight and the area over which it acts. Therefore:

$$\text{Weight} = 56,000 \text{ lbs}$$

$$\text{Area} = (\pi)(35.5)^2 = 3959 \text{ in}^2$$

$$\text{Press}_1 = (56,000)(\cos 24^\circ)/3959 = 12.92 \text{ psi for 1 g}$$

$$\text{Press}_{20} = (12.92)(20 \text{ g/1 g}) = 258.4 \text{ psi for 20 g}$$

In the ANSYS analyses, the inertial body loads are considered together with the impact loads. The results of the two simultaneous loadings are documented as "impact loads."

The stresses throughout the cask body are calculated for individual and combined loading conditions. The individual loading conditions are: (1) internal pressure (including bolt preload); (2) top corner impact (impact load only); and (3) bottom corner impact (impact load only). Stress results for the individual loading cases of internal pressure (including bolt preload) are documented in Tables 2.10.4-1 through 2.10.4-2. The combined loading conditions are: (1) the 1-foot top corner impact with bolt preload and 50 psig internal pressure and (2) 1-foot bottom corner impact with bolt preload and 50 psig internal pressure.

The finite element model has one plane of symmetry in the cask geometry and in the corner drop loading conditions. Symmetric boundary conditions are applied to the cask finite element model

by restraining the nodes on the symmetry plane to prevent translations in the direction normal to the symmetry plane. In addition, two nodes at the outer cask radius on the top and bottom ends of the cask, opposite the point of impact, are restrained laterally; a longitudinal restraint is applied at one of the above nodes opposite to the end of impact, i.e., a bottom corner drop is axially restrained at the top node. These lateral and axial restraints are only to prevent rigid body motion; there should be no significant reaction forces associated with these restraints. When the cask system is in equilibrium (i.e., the inertial body loads match the impact loads exactly), then the reaction forces at these restraints will be zero. However, it is difficult to balance the impact limiter pressure resultant with the contents pressure and inertial body load resultant. An eccentricity between the two resultants induces a moment on the cask model. Therefore, non-zero reactions are found at the restraints. The reaction forces cause very high localized stresses (or stress singularities) in the model at the restraints. These stresses are unrealistic and do not really exist in the cask. The stress singularity effect is minimized by distributing the reaction forces over the nodes in the top and bottom regions of the model. For the bottom corner drop, the reactions at the restraints are 222.6 pounds laterally and zero pounds longitudinally for the application of a 20 g deceleration. This means that the unbalanced force of the cask model system is only $222.6/20 = 11.1$ pounds. Compared to the half-cask design weight (125,000 lbs), the unbalanced force is negligible, amounting to only 0.009 percent of the design weight of the cask. For the top corner drop, the reactions at the restraints are 186.0 pounds laterally and zero longitudinally for the application of a 20 g deceleration. This means that the unbalanced force of the cask model system is only $186.0/20 = 9.3$ pounds. Compared to the half-cask design weight (125,000 lbs), the unbalanced force is negligible, amounting to only 0.007 percent of the design weight of the cask. The allowable stress limit criteria for containment and noncontainment structures are provided in Section 2.1.2. These criteria are used to determine the allowable stresses for each cask component, conservatively using the maximum transport temperature within a given component to determine the allowable stress throughout that component. Note that higher component temperatures result in lower allowable stresses. Table 2.10.2-5 documents the allowable stress values determined for each component, for condition 1 temperatures.

The stress results for the 1-foot corner drop load conditions for the directly loaded fuel configuration of the NAC-STC are described as follows. Stress results for the individual 1-foot top and bottom corner drop impact loading cases are documented in Tables 2.10.4-11 and 2.10.4-12. These are the nodal stress summaries obtained from the finite element analysis results. As described in Section 2.10.2.4.2 and Section 2.10.4, the nodal stresses are documented on the representative section cuts.

Stress results for the combined loading conditions discussed above are documented in Tables 2.10.4.8-84 through 2.10.4-111. All of the corner drop analyses are performed at temperature condition 1. Results from Sections 2.7.1.1 and 2.7.1.2 both indicate that the stresses associated with temperature condition 1 yield the smallest margins of safety due to the effect of higher temperatures upon the allowable stresses.

The stress result tables document the primary, primary plus secondary, primary membrane (P_m), primary membrane plus primary bending ($P_m + P_b$), primary plus secondary membrane plus bending (S_n), and critical P_m , $P_m + P_b$, and S_n stresses in accordance with the criteria presented in Regulatory Guide 7.6. As described in Sections 2.10.2.3 and 2.10.2.4, procedures have been implemented to document the nodal and sectional stresses, as well as to determine the critical stress summary for all cask components. The P_m and $P_m + P_b$ stresses documented in Tables 2.10.4-86 through 2.10.4-111 are stress results on the 0-, 45.9-, 91.7-, and 180-degree circumferential locations. They indicate that the stress variations in the circumferential direction are similar between the top and bottom corner drops. Furthermore, it is observed that the maximum calculated stresses are located on the circumferential locations in the 45.9- to 56.5-degree region. This is because the maximum shearing stresses are located near the 56.5-degree circumferential location. This shear stress is in the axial/circumferential location. It results from the cantilever support at the impact limiter pressure locations and is compounded by the uneven distribution of impact limiter and contents pressure loading.

For the individual impact loading cases, the maximum calculated membrane stress intensity for the top corner drop is 12.1 ksi. The maximum calculated membrane plus bending stress intensity is 24.4 ksi. By comparison, for the combined loading case, including impact, bolt preload, and internal pressure, the maximum calculated P_m stress intensity is 12.1 ksi and the maximum calculated $P_m + P_b$ stress intensity is 23.9 ksi. The maximum stress intensity for the impact loading condition and that for the primary loading condition are essentially identical, with a maximum difference of 2 percent. Therefore it is concluded that the impact stresses are the governing load condition for the 1-foot corner drop event.

The top corner drop cases result in higher maximum stress intensities than the bottom corner drop cases. As shown in Tables 2.10.4-89, 2.10.4-90, 2.10.4-103 and 2.10.4-104, the margins of

safety for the primary stress intensity category are positive for all of the 1-foot corner drop conditions. The most critically stressed component in the top corner drop is the top forging. In the bottom corner drop, the bottom forging is the most critically stressed component. The minimum margin of safety for the top corner drop condition is +0.4, as documented in Table 2.10.4-90. The minimum margin of safety for the bottom corner drop condition is +0.8, as documented in Table 2.10.4-104. The locations of the most critical sections for each cask component are provided in the critical stress summary tables.

Regulatory Guide 7.6 requires that the range of primary plus secondary stress intensities between any two normal conditions of transport be less than $3.0 S_m$. Therefore, it is necessary to evaluate the range of primary plus secondary stress intensities between all of the normal transport conditions (heat, cold, 1-foot end drop, 1-foot side drop, and 1-foot corner drop conditions). A simple, straightforward, and very conservative method of showing compliance with the $3.0 S_m$ criterion is to establish an allowable stress limit criterion of $1.5 S_m$ for the range of primary plus secondary stress intensities between each normal condition and the ambient condition. If each normal condition meets the $1.5 S_m$ allowable stress limit criterion at all locations within the cask, then all pairs of normal conditions meet the $3.0 S_m$ stress range criterion.

Table 2.10.4-105 presents the critical component primary plus secondary stress intensity calculations for the 1-foot bottom corner drop condition; the maximum calculated primary plus secondary stress intensity is 13.4 ksi, which is less than $1.5 S_m$.

Table 2.10.4-91 presents the critical component primary plus secondary stress intensity calculations for the 1-foot top corner drop. The maximum calculated primary plus secondary stress intensity for the 1-foot top corner drop for all cask components except the inner lid (component number 7) is 25.2 ksi, which is less than $1.5 S_m$. Therefore, all cask components, except the inner lid, meet the conservative $1.5 S_m$ criterion for the 1-foot top corner drop. The maximum primary plus secondary stress intensity for the inner lid, for the 1-foot top corner drop is $|-30.8|$ ksi, which is equal to $1.54 S_m$. Therefore, the inner lid must be evaluated in a more detailed manner to determine its compliance with the $3.0 S_m$ criterion for the extreme total stress intensity range. An examination of the maximum critical primary plus secondary (S_n) stress intensity on the inner lid, for each of the normal transport conditions (heat, cold, 1-foot end drop, 1-foot side drop, and 1-foot corner drop), indicates that the two maximum S_n stress intensities on the inner lid for the normal transport conditions are $|-30.8|$ ksi for the 1-foot top corner drop, as documented in Table 2.10.4-91, and $|24.8|$ ksi for the 1-foot side drop condition, as documented

in Table 2.10.4-72. Therefore, the primary plus secondary stress intensity range for the inner lid is $30.8 + 24.8 = 55.6$ ksi, which is less than $3.0 S_m$ (60 ksi). Thus, the inner lid also meets the $3.0 S_m$ criteria for extreme primary plus secondary stress intensity range limit.

It is important to note that this method of determining the maximum critical S_n stress intensity range on the inner lid is still very conservative, since the range calculation is being made between the maximum critical S_n stress intensities, which occur anywhere within the inner lid. A rigorous range calculation, using stress components on a section by section basis within the inner lid, would result in an even lower S_n stress intensity range (and hence a greater margin of safety) than that indicated by the above method.

For the fatigue evaluation of the NAC-STC, Section 2.1.3.2 documents that the requirements of Regulatory Guide 7.6 are satisfied by the $3.0 S_m$ criteria for the extreme total stress intensity range limit.

The documentation of the adequacy of the NAC-STC to satisfy the buckling criteria for the stresses of the 1-foot corner drop condition is presented in Section 2.10.5.

The NAC-STC satisfies all of the regulatory requirements for the normal conditions of transport 1-foot corner drop for the directly loaded fuel configuration.

2.6.7.3.2 NAC-STC Cask One-Foot Corner Drop Evaluation for the CY-MPC Configuration

The loaded canister weight for the CY-MPC configuration is 67,196 pounds as compared to the 56,000 pound content (fuel and basket) weight for the directly loaded fuel. This represents a 20% increase in contents weight. In comparing the total cask weight, the CY-MPC is only 4% heavier than the total cask weight for the directly loaded fuel. The comparison of the accelerations in 2.6.7.3.1 shows that the acceleration used in the corner evaluation was 3.8 (380%) times the actual acceleration imposed by the redwood impact limiters and 2.2 (220%) times that for the balsa impact limiters. The percentage increase of the accelerations used in the analysis above that of the impact limiter data is significantly larger than the percentage increase in the CY-MPC contents weight above that of the directly loaded fuel contents weight or the total cask weight. Additionally the heat loads responsible for the thermal stresses are larger for the directly loaded fuel than for the CY-MPC configuration. Therefore the corner drop evaluation performed for the directly loaded fuel bounds the corner drop condition for the CY-MPC configuration.

THIS PAGE INTENTIONALLY LEFT BLANK

2.6.7.4 Impact Limiters

Removable transport impact limiters are included in the NAC-STC design to ensure that the design impact loads on the cask are not exceeded for any of the defined impact load conditions. The defined loading conditions include the cask falling 1 foot or 30 feet and landing either on its side, impacting both impact limiters simultaneously, or vertically on one impact limiter at either end. As discussed in Section 2.10.7, the oblique impact events are bounded by the end and/or side drop events, as there is no "slap down" effect exhibited by the cask. Consequently, oblique drops and oblique drop angles are not evaluated.

Two impact limiter configurations are used. The first configuration, described in Section 2.6.7.4.1, is primarily redwood with a small amount of balsa wood (redwood impact limiter). The wood is encased in a stainless steel shell. The balsa wood is limited to the outer corner edges of the impact limiter for use in the corner drop orientations. These impact limiters may be used only with the directly loaded fuel and Yankee-MPC canistered fuel and GTCC waste cask contents. The second configuration, described in Section 2.6.7.4.2, is primarily balsa wood with a limited amount of redwood (balsa impact limiter). The wood is also encased in a stainless steel shell. This configuration may be used with the directly loaded fuel, Yankee-MPC fuel or GTCC waste or the CY-MPC fuel or GTCC waste cask contents.

2.6.7.4.1 Redwood Impact Limiter Evaluation

The package geometry, package weight, contents weight, and package center of gravity location are the parameters that control the impact limiter design. The impact limiter evaluation presented in this section is for the package (loaded NAC-STC cask with impact limiters, as described on the drawings in Section 1.3.2) with a total weight of 250,000 pounds, a center of gravity located 96.01 inches above the bottom outer surface of the cask body, and a cavity contents weight of 56,000 pounds. This evaluation envelops the NAC-STC cask directly loaded fuel and the Yankee-MPC canistered fuel and GTCC waste configurations. The package geometry is approximately identical for all of the configurations, as is the package center of gravity location. Axial spacers have been designed for the cask cavity to locate the Yankee-MPC canister loaded with fuel or GTCC waste such that the package center of gravity location is approximately identical to that of the directly loaded fuel configuration. The differences in the contents weight and the associated package weight for each of the contents configurations—56,000 pounds and 249,700 pounds for directly loaded fuel, 55,590 pounds and 249,290 pounds for the Yankee-MPC fuel, and 54,271 pounds and 247,971 pounds for the Yankee-MPC GTCC

waste—have no significant effect on the impact limiter design or performance. Therefore, the impact limiter analysis in this section, the cask drop analyses in Sections 2.6.7 and 2.7.1, and the scale model tests and results in Section 2.10.6 are applicable for the directly loaded and the Yankee-MPC canistered configurations of the NAC-STC.

Assumptions

The following assumptions form the basis for the transport impact limiter analysis:

1. The cask impacts on an unyielding surface.
2. The impact limiter remains in position on the cask during all impact events (The qualification of the impact limiter attachment is presented in Section 2.6.7.4.7.).

Load Conditions

The transport impact limiters described and analyzed in the following paragraphs decelerate the cask by applying a force in the direction opposite the motion of the cask. The deceleration force is generated by crushing the redwood and balsa wood materials of the impact limiter between the cask and the unyielding surface. The energy absorbed during crushing is the net force, the vector sum of the cask weight (downward) and the deceleration force (upward), multiplied by the distance crushed. The amount of energy an impact limiter can absorb is calculated for various cask impact orientations, from vertical (0°) to horizontal (90°).

The specific loading conditions for the transport impact limiters are defined by 10 CFR 71.71(c)(7), 10 CFR 71.73(c)(1) and Regulatory Guide 7.8, as follows:

1. A 1-foot drop of the cask impacting at any angle from vertical (flat end) to corner (cask center of gravity is directly above the point of impact).
2. A 1-foot drop of the cask in a horizontal orientation.
3. A 30-foot drop of the cask in an end, a side, or an oblique orientation.

Based on these loading conditions, the NAC-STC impact limiters are primarily designed for the 30-foot cask drops, but with consideration of the 1-foot flat end drop. The maximum impact forces and the maximum crush depth for the 1-foot and 30-foot cask drops are obtained from the

RBCUBED analyses of the impact limiters. RBCUBED is a proprietary NAC computer program that performs impact limiter analyses (Section 2.10.1.2).

2.6.7.4.1.1 Redwood Impact Limiter Description

Figures 2.6.7.4.1-1 and 2.6.7.4.1-2 show the locations on the cask and the primary dimensions of the transport impact limiters. Figure 2.6.7.4.1-2 shows the cross-section of an impact limiter. Except for the pockets for the lifting trunnions in the upper limiter, the upper and lower impact limiters are identical.

Each transport impact limiter consists of redwood and balsa wood, which are the energy-absorbing materials. The wood is enclosed in a thin stainless steel shell to maintain the wood orientation for a side impact.

To adequately specify the redwood crush strength, density, and their relationship to each other, NAC conducted compression tests of specimens taken from redwood purchased from a commercial supplier for the fabrication of scale model impact limiters. A total of 60 parallel-to-the-grain direction specimens from separate redwood boards and 59 perpendicular-to-the-grain direction specimens from those redwood boards (one specimen was accidentally destroyed) were tested. A density versus crush strength (at 0.4 in/in strain) plot of the test data results was constructed for each of the two crush directions. A strain value of 0.4 in/in was selected for use throughout this evaluation of redwood crush strength because it is a representative location of significant strain on the apparent plateau of the stress-strain curves for all of the redwood specimens. Based on the density versus crush strength parallel-to-the-grain direction plot, the 13 specimens with the highest densities and the two specimens with the lowest densities were discarded from the data base because they showed a significant scatter in crush strength values and inconsistent force-deflection plots, when compared with the specimens that were within the density criteria. Thus, an acceptable range of density for redwood was established, 23.5 ± 3.5 pounds per cubic foot, and only redwood with a density within this acceptable range will be used in the NAC-STC impact limiters. For the remaining 45 parallel-to-the-grain direction and 44 perpendicular-to-the-grain direction "statistical" specimens, the force and deflection test data was converted to stress-strain data by dividing the measured force by the cross-sectional area of the specimen and by dividing the deflection by the length of the specimen. A "least squares" straight line fit was calculated for each of the crush direction data sets to establish the design relationship between density and crush strength. An average crush stress-strain curve for the parallel-to-the-grain direction was calculated by summing and averaging the test data values for

the appropriate 45 statistical specimens. Similarly, an average crush stress-strain curve for the perpendicular-to-the-grain direction was calculated for the appropriate 44 statistical specimens. Figures 2.6.7.4.1-3 and 2.6.7.4.1-4 show the average, the design maximum, and the design minimum crush stress-strain curves for redwood in the parallel and perpendicular-to-the-grain directions, respectively.

The cold (-20°F) crush stress-strain curve for redwood in the parallel-to-the-grain direction was conservatively obtained from the nominal room-temperature crush stress-strain curve by ratioing based on the -40°F temperature effect shown in Figure 8 of NUREG/CR-0322. The design maximum crush stress-strain curve for redwood in the parallel-to-the-grain direction is determined by ratioing the cold crush stress-strain curve by 1.10 to account for the positive fabrication tolerance on the average crush strength of the redwood. Similarly, the design minimum crush stress-strain curve for redwood in the parallel-to-the-grain direction obtained by ratioing the nominal, room-temperature crush stress-strain curve based on the +230°F temperature effect shown in Figure 8 of NUREG/CR-0322 and on a factor of 0.90 to account for the negative fabrication tolerance. The design maximum and minimum crush stress-strain curves for redwood in the parallel-to-the-grain direction are used as the basis for the bounding impact limiter analyses in the RBCUBED program. Based on Figure 9 of NUREG/CR-0322, a dynamic crush load factor of 1.06 is appropriate for redwood. Since the design maximum and minimum crush stress-strain curves for redwood are based on quasi-static test results, but are then used directly in the RBCUBED program as dynamic crush stress-strain data, the 1.06 dynamic load factor is accounted for by reducing the specified static crush strength of the redwood to be used for the NAC-STC impact limiters. For each crush direction data set, the room-temperature average dynamic crush stress at 0.4 inch/inch strain is divided by 1.06 to obtain the average static crush stress at 0.4 inch/inch strain.

The average static crush stress ± 10 percent is used in conjunction with the "least squares" straight line for the data set to read off the equivalent density limits. The average of the density limits is the density value specified for each 30-degree pie-shaped section of redwood in the impact limiters.

The curve for the crush strength in the perpendicular-to-the-grain direction (Figure 2.6.7.4.1-4) was obtained from the compression tests of 44 specimens of redwood that were matched with the specimens used for the parallel-to-the-grain direction compression tests (one perpendicular-to-the-grain direction specimen was accidentally destroyed). The same procedure as outlined above was followed to establish the design maximum and minimum crush stress-strain curves for

redwood in the perpendicular-to-the-grain direction, which are also used as the basis for the bounding impact limiter analyses.

The redwood material to be used for the NAC-STC impact limiters must satisfy density, crush strength (converted from the force-deflection curve) and moisture content specifications. The density of any single redwood board shall be 23.5 ± 3.5 pounds per cubic foot. The density of any 15-degree or 30-degree pie-shaped section of redwood shall be 22.3 ± 1.2 pounds per cubic foot. Each 15-degree pie-shaped section of redwood in the side segment of the impact limiter shall have an average dynamic crush strength in the parallel-to-the-grain direction of $6,240 \pm 620$ psi at 0.4 inch/inch strain and 70°F. Each 30-degree pie-shaped section of redwood in the end segment of the impact limiter shall have an average dynamic crush strength in the perpendicular-to-the-grain direction of $1,260 \pm 130$ psi at 0.4 inch/inch strain and 70°F. The dynamic load factor of 1.06 for redwood, previously discussed, is included in the design specification of the redwood to be used in the NAC-STC impact limiters as a reduction in the density specified for any 15-degree or 30-degree pie-shaped section. The moisture content of any single board shall be greater than 5 percent, but less than 15 percent. The average moisture content for the lot of redwood shall be less than 12 percent.

The balsa wood to be used in the NAC-STC impact limiters shall meet the specifications of MIL-S-7998A: (1) density between 7 and 10 pounds per cubic foot and (2) moisture content between 5 and 15 percent for any one piece with an average of not more than 12 percent for any lot of balsa wood. The average crush strength of the balsa wood in the parallel-to-the-grain direction at room temperature is 1,550 psi based on Figure 16 of JPL Technical Report No. 32-944 for a density of 10 pounds per cubic foot. The room-temperature crush stress-strain curve for balsa wood (Figure 2.6.7.4.1-5) is determined based on Figure 6 of JPL Technical Report No. 32-1295. The -40°F cold and the +230°F hot crush stress-strain curves are obtained by ratioing based on Figure 15 of JPL Technical Report No. 32-944. To account for crush strength fabrication tolerances, the -40°F cold case comparison stresses are factored by 1.10 and the +230°F hot case compression stresses are factored by 0.90. The resulting design maximum and minimum crush stress-strain curves for balsa wood are also presented in Figure 2.6.7.4.1-5.

The variation of crush strength of redwood and balsa wood as a function of the angle between the impact direction and the grain direction of the wood is shown in Figure 2.6.7.4.1-6 (Ref. Baumeister, page 6-157).

The outside diameter of the NAC-STC transport impact limiters is 124.0 inches and the height is 44.0 inches. The overlap between the cask body and the impact limiters is 12.0 inches. Sixteen 1.0-inch diameter retaining rods attach each impact limiter to the end of the cask. The attachments are described in detail in Section 2.6.7.4.1.4.

The height of the redwood in the end section of the impact limiter is 30.0 inches. A ring of balsa wood forms a part of the end section of the impact limiter. The ring has an inside diameter of 99.2 inches, an outside diameter of 123.75 inches, and a height of 21.6 inches. The bottom region of the impact limiter is a 1.5-inch thick layer of balsa wood, which absorbs most of the kinetic energy in a 1-foot drop end impact, and limits the initial impact force to a value acceptable for normal transport conditions. The low crush strength is necessary because the impact area is considerably greater in a flat end impact than in any other drop orientation. The redwood and the balsa wood ring absorb the majority of the energy in a corner impact and all of the energy in a side impact.

The different segments and sections comprising the impact limiters are bonded to each other with DAP-Weldwood resorcinol adhesive.

For each of the impact load conditions in this analysis, the impact limiters remain in position on the cask and absorb the energy of the impact; thus, they limit the impact loads to the calculated values tabulated in Tables 2.6.7.4.1-1 and 2.6.7.4.1-2 and summarized in Table 2.6.7.4.1-3.

2.6.7.4.1.2 Method of Analysis – Redwood Impact Limiter

The primary areas of analytical evaluation that are required in an impact limiter analysis are: (1) crush depth; (2) maximum crush force; and (3) attachment to the cask. The crush depth and maximum crush force are dependent on the crush strength of the crushable material, the area engaged in crushing, the geometry of the impact limiter, and the energy to be dissipated.

Deceleration forces for the NAC-STC redwood and balsa wood impact limiters are directly related to the area crushing and the crush strength of the limiter materials. The area engaged in crushing can be best explained by examining an end drop impact. The cask and the unyielding surface are rigid and undeformable compared to the redwood and balsa wood materials. The redwood and balsa wood materials are trapped in place between the cask and the impacted surface over the end area of the cask.

The layer of balsa wood located in the end of the impact limiters is designed to absorb the potential energy of the cask for a 1-foot drop impact. The higher crush strength redwood structurally restrains or "backs" the lower crush strength balsa wood, even if just the cask backs the higher crush strength redwood. The redwood in the NAC-STC impact limiters absorbs the kinetic energy of the cask in a 30-foot drop impact.

During an end impact, a force imbalance is established in the impact limiter between the layer of balsa wood at the bottom end and the redwood during crushing. The lower crush strength balsa wood at the bottom will crush until lock-up occurs. When lock-up occurs, the crush strength of the balsa wood increases and exceeds that of the redwood and crushing now begins in the redwood beneath the cask.

The cask has kinetic energy gained while falling prior to the impact limiter contacting the unyielding surface (Section 2.10.7 gives a more complete description of the kinetic energy gain). Some kinetic energy was dissipated in crushing the balsa wood at the bottom of the impact limiter. The remaining energy will be absorbed by crushing the higher strength redwood between the cask and the impacted surface. The cask "backs" the higher crush strength redwood; therefore, the maximum force is easily compared with the average maximum force from the quasi-static test as adjusted to reflect the dynamic crush strength of the redwood (For an explanation of the term "dynamic" as applied to quasi-static tests, refer to Section 2.10.6.4.1).

From Figure 2.10.6-12, the measured quasi-static compression force in an end impact orientation is higher than the RBCUBED calculated values. This is a result of shearing across the grain of the redwood. Shearing acts in a plane surrounding the shear area. In an end impact crush, the plane is a thin ring with a diameter equal to the diameter of the cask. Since the crush force is proportional to the backed area, which depends on the square of the cask diameter, shearing becomes a much less significant part of the maximum force for the full-scale impact limiter.

The sequence of crushing and the backed area concept are initiated as the lower crush strength balsa wood is crushed to stack height completely to the outer edge of the impact limiter. Higher crush strength redwood beneath the cask in the "backed" region is then crushed, while the redwood on the "other side" of the shear plane in the "unbacked" region is essentially uncrushed.

The combination of the accurate prediction of measured impact limiter crush forces and the visual evidence in the sectioned eighth-scale impact limiter after the quasi-static test shows that only the backed-up area of the redwood is crushed.

The cask orientation for a corner impact is defined by the angle from vertical of the cask's longitudinal axis when the cask center of gravity is vertically aligned with the impact point on the limiter. This angle is approximately 24 degrees for the top and the bottom impact limiters for the NAC-STC.

The NAC proprietary computer program, RBCUBED, is used to analyze an impact limiter for an impact event to determine the dynamics of the event, the forces generated during that event, and the depth of crush (Section 2.10.1.2).

The RBCUBED computer program is run for various combinations of redwood and balsa wood in impact limiter designs until satisfactory results are obtained. Then, two runs are made for each impact orientation. One run is made using the cold maximum crush strength stress-strain values of redwood and balsa wood plus 10 percent fabrication tolerance to determine the maximum impact limiter crush force on the cask. A second run, using the hot minimum crush strength values of redwood and balsa wood minus 10 percent fabrication tolerance is also made to determine the maximum crush depth of the impact limiter.

2.6.7.4.1.3 Redwood Impact Limiter Evaluation Results

The data in Tables 2.6.7.4.1-1 and 2.6.7.4.1-2 give the results of the impact limiter design analyses for 1-foot drops and for 30-foot drops, respectively. The calculated g-loads in the tables are based on the cold crush strength of -40°F plus 10 percent fabrication tolerance and on the hot crush strength at 230°F minus the 10 percent fabrication tolerance of redwood and balsa wood. The design cask weight of 250,000 pounds is used.

The calculated (RBCUBED) and measured (quasi-static, adjusted for dynamic crush strength) force-deflection curves for the NAC-STC impact limiters for all drop orientations are presented in Section 2.10.7. To verify the results, the area under the curves is calculated by the trapezoidal method. This area represents the energy dissipated for each of the cases; i.e., $E_{\max} = 9.02 \times 10^7$ inch-pounds for the upper impact limiter at maximum strength and $E_{\min} = 8.997 \times 10^7$ inch-pounds for the upper impact limiter for the minimum crush strength condition. The potential energy to be dissipated is the cask weight (250,000 lbs) multiplied by the distance the cask drops (360 in); i.e., $E_p = (360)(250,000) = 9.0 \times 10^7$ inch-pounds. The calculated and actual values compare within 0.22 percent, which indicates that the proper amount of potential energy is dissipated in the RBCUBED analysis. Another check is made by multiplying the total crush area

(the maximum area backed by the cask) by the crush strength of the impact limiters to determine the reacting force. This hand-calculated value of the reaction force compares within 1.08 percent of the RBCUBED calculated value for the lower impact limiter and within 1.93 percent for the upper impact limiter. These results verify both the energy absorption and the reaction force calculations of RBCUBED for the impact limiters.

With both impact limiters at their minimum allowable crush strength (maximum crush depth case), clearance is maintained between the neutron shield and the unyielding surface for the 1-foot and 30-foot side impacts.

An evaluation of the displacements obtained from the RBCUBED runs is as follows:

1. The RBCUBED run for the 30-foot side drop assumes that the cask is a rigid element and does not include the trunnions; therefore, the displacement from the 30-foot drop must be analyzed by referring to Figure 2.6.7.4.1-2, as follows:

The depth of crushable redwood around the side of the cask is 18.28 inches. The height of the lifting trunnion is 3.38 inches, leaving a height of 14.9 inches of crushable redwood outside of the lifting trunnions. The RBCUBED run for a 30-foot side drop calculates a crush depth of 10 inches for the maximum crush strength condition and 14.7 inches for the minimum crush strength condition. For the maximum crush strength condition, the compression ratio of the redwood at the trunnion location is $10.0/14.9 = 0.67$, corresponding to a stress of 13,850 psi in the redwood. The compression ratio of the redwood away from the trunnion location is $10.0/18.28 = 0.55$, corresponding to a crush stress of 8,850 psi. The increase in crush stress due to the presence of the trunnion is, therefore, $13,850 - 8,850 = 5,000$ psi. The area of the trunnion covered by the impact limiter is 20.0 square inches. The increase in the deceleration force due to the presence of the trunnion is $(20.0)(5000) = 100,000$ pounds. The total deceleration force at the trunnion location increases from 1.35×10^7 pounds to 1.36×10^7 pounds, producing a deceleration increase of 0.3 g (0.5 percent) from 54.1 g to 54.4 g.

For the minimum crush strength condition, the compression ratio of the redwood at the trunnion location is $14.7/14.9 = 0.98$, corresponding to a stress of 18,900 psi in the redwood. The compression ratio of the redwood away from the trunnion location is $14.7/18.28 = 0.80$, corresponding to a stress of 11,400 psi in the redwood. The increase in deceleration force due to the presence of a trunnion is $(20.0)(18,900 - 11,400) =$

150,000 pounds. The total deceleration force increases from 1.24×10^7 pounds to 1.255×10^7 pounds, producing a deceleration increase of 0.5 g (1.0 percent) from 49.7 g to 50.2 g. Thus, it can be concluded that a side impact of the cask over a lifting trunnion has a minimal effect on the deceleration force and may be ignored.

2. The 30-foot flat top end drop of the NAC-STC produces a deformation of 17.7 inches in the redwood for the minimum crush strength condition with a compression ratio of $17.7/30 = 59$ percent. This corresponds to a stress of 2,440 psi in the redwood. Similarly, the deformation of the redwood for the maximum crush strength condition is 12.5 inches, with a compression ratio of $12.5/20 = 42$ percent. This corresponds to 1,810 psi. Both stress values are well below lock-up stresses, which start at a compression ratio of 69 percent.
3. For a 30-foot corner drop on the upper impact limiter, the maximum impact force occurs with the crushable material at hot condition. For this condition, the crush distance is 31.6 inches. The NAC-STC impact limiter depth in the 24-degree corner impact orientation is 35.1 inches. The maximum compression ratio of the impact limiter is $31.6/35.1 = 90$ percent for the upper impact limiter for the minimum crush strength condition. Thus, lock-up occurs, but only in a very local region. The calculated average compression stress is 1,783 psi. Similarly, the crush depth for the maximum crush strength condition is 26.6 inches (75.8 percent) with a calculated average compression stress of 1,937 psi.

The cask analysis for these impact conditions is based on the maximum deceleration (g) derived from the RBCUBED results. The critical condition for maximum deceleration from any 1-foot drop is for the maximum crush strength condition. This results from the higher crush strength of the redwood and balsa wood in the cold condition. No lock-up occurs in the redwood and balsa wood for the minimum crush strength condition for a 1-foot drop. The critical deceleration condition for a bottom end impact is the maximum crush strength (cold) condition; the critical deceleration condition for a top end impact is the minimum crush strength (hot) condition, where lock-up in the redwood occurs because of the high compression ratio. The critical deceleration condition for the bottom and top corner impacts is the minimum crush strength (hot) condition, where local lock-up in the redwood and balsa wood occurs. The critical deceleration condition for a side drop is the maximum crush strength (cold) condition.

The calculated g-load factors (deceleration values) for the NAC-STC, as determined by the RBCUBED analyses, are summarized in Table 2.6.7.4.1-3. Table 2.6.7.4.1-4 provides a

comparison of the deceleration g-loads for the 30-foot cask drop conditions, including the deceleration values determined by the RBCUBED analyses, those measured in the eighth-scale quasi-static tests, those measured in the 30-foot drop tests, and the values used in the stress qualifications of the cask and fuel basket design. The comparison demonstrates that the g-loads measured in the 30-foot drop tests are lower than the g-loads for which the cask and fuel basket were designed for all of the drop orientations. The table also indicates that the g-load values used for design are all greater than or equal to the g-load values predicted by RBCUBED for the corresponding drop orientations.

2.6.7.4.1.4 Redwood Impact Limiter Attachment Analysis

A three-part design criteria applies to the method of attachment of the impact limiters to the cask body. These three criteria are as follows:

1. The impact limiters must remain attached to the cask body during normal handling and transport. Satisfaction of this criterion ensures that the limiters will be in a proper position to perform their impact limiting function in the event of a free drop (normal or accident).
2. In a free drop (normal or accident), the limiter(s) making initial contact with the unyielding surface must remain in position on the end(s) of the cask for the full duration of the initial impact. Satisfaction of this criterion ensures that the limiter(s) will be able to properly perform their impact limiting function.
3. In a free drop (normal or accident) involving an initial impact on a single impact limiter, the limiter on the opposite end of the cask must remain attached to the cask during the initial impact. Satisfaction of this criterion ensures that the limiter will be in a proper position to perform its impact limiting function in a subsequent secondary impact following the initial impact.

These criteria are satisfied as described by the discussion presented below.

Redwood Impact Limiter Attachment During Normal Handling and Transport

Attachment of the redwood and balsa impact limiters to the cask body during normal handling and transport is ensured by demonstrating that the attachment hardware does not yield under normal handling and transport conditions. The worst case loading associated with normal

handling and transport is a 7.5-g load corresponding to the peak longitudinal shock loading expected as the result of rail transport (as specified by the Field Manual of the AAR). The design load, P, on the attachment is:

$$\begin{aligned} P &= (7.5)(8,865) \\ &= 66,490 \text{ lbs} \end{aligned}$$

where 8,865 pounds is the design weight of each impact limiter.

Analysis of Retaining Rods

There are 16 retaining rods, each 1-inch in diameter, equally spaced on a 76.0-inch diameter bolt circle. The attachment geometry is shown in Figure 2.6.7.4.1-7. The retaining rods are SA-276, Type 304 stainless steel, with a yield strength of 25.0 ksi at 200°F.

The load on each retaining rod due to a longitudinal shock load of 7.5 g is given as:

$$P = \frac{66,490}{16} = 4,156 \text{ lbs per retaining rod}$$

The tensile stress in the retaining rod, which has a tensile area of 0.606 in² in the threaded region, is calculated as:

$$S_t = \frac{P}{A} = 6,857 \text{ psi}$$

$$MS = \frac{25,000}{6,857} - 1 = +\text{Large}$$

Analysis of Retaining Rod Anchorage

The detail of the anchorage of the retaining rod to the impact limiter is shown in Figure 2.6.7.4.1-8. The nut of the retaining rod is bearing on a washer that has a diameter of 5.0 inches and a thickness of 0.50 inch. The washer is bearing on the bearing plate portion of the impact limiter shell, which bears on the redwood material.

The load on each of the 16 retaining rods due to the normal transportation acceleration is 4,156 pounds. The bearing area between the bearing plate and the redwood material is calculated as:

$$A = (\pi/4)(5.0^2 - 3.0^2) = 12.57 \text{ in}^2$$

The bearing pressure is:

$$p = 4156/12.57 = 331 \text{ psi}$$

The perpendicular-to-the-grain compressive stress in the redwood at 40 percent strain is 1,260 psi. The margin of safety for compression of the redwood is:

$$MS = 1260/331 - 1 = +\text{Large}$$

The washer is made of Type 304 stainless steel. It has a 1.09-inch diameter hole in the center. It is analyzed by assuming that it is simply supported along a circle having a diameter equal to the average of the diameters of the washer and the edge of the hole in the bearing plate $[(5.0 + 3.00)/2 = 4.0 \text{ inches}]$. The load of 4,156 pounds is distributed along the edge of the nut having an average diameter of 1.625 inches. From Roark, page 220, Case 15:

$$S_{\max} = \frac{3W}{2\pi m t^2} \left[\frac{2a^2(m+1)}{a^2 - b^2} \ln \frac{c}{d} + (m-1) \frac{c^2 - d^2}{a^2 - b^2} \right] = 22,368 \text{ psi}$$

where:

$$\begin{aligned} a &= 2.50 \text{ in} \\ b &= 0.545 \text{ in} \\ c &= 2.00 \text{ in} \\ d &= 0.8125 \text{ in} \\ t &= 0.50 \text{ in} \\ v &= 0.275 \\ m &= 3.636 \\ W &= 4,156 \text{ lbs} \end{aligned}$$

The yield strength of Type 304 stainless steel is 25.0 ksi at 200°F. The margin of safety is:

$$MS = 25.0/22.4 - 1 = +0.11$$

The positive margins of safety show that the attachment of the impact limiters is adequate during normal conditions of transport.

Evaluation of Redwood Impact Limiter Attachment for Vibration

During normal transport conditions, the impact limiter attachment may be subjected to vibration induced from the combination of component natural frequency and a dynamic load forcing function dependent on the transport media. Design of the impact limiter attachment eliminates the potential for the postulated vibration loading loosening the impact limiter attachment. Lock nuts are installed in back of each of the retaining rod attachment nuts to prevent them from becoming loose. Locking wires installed between sets of two retaining rods eliminate rotation of the impact limiter retaining rods relative to their anchorage. The combination of these two design features eliminates the potential for the impact limiter attachment from becoming loose as a result of postulated vibration loading during transport.

Response of the Impacted Limiter(s) During Initial Impact of Package with Ground

The second criterion applicable to the impact limiter attachments requires that the impact limiter(s) making initial contact with the unyielding surface must remain in position on the end(s) of the cask for the full duration of the initial impact. To satisfy this criterion, attachment hardware (mounting plate and bolts) may fail during an impact event, as long as the impact limiter(s) being crushed remains in position on the end of the cask and does not separate from the cask. The ability of the impact limiter to remain in position during an impact is demonstrated with reference to several static compression tests, during which the only attachment mechanism was a strip of duct tape. All of the compression tests were performed using eighth-scale models of the impact limiters. Analytic evaluations are also presented to further justify that the impact limiters will remain in position during the impact.

2.6.7.4.1.5 Dynamic Free Drop Test Results

As presented in Section 2.10.6 a series of 30-foot free drop tests were performed using a quarter-scale model of the NAC-STC. Drop orientations included an end drop, a center of gravity over struck corner drop, a side drop and an oblique drop with a subsequent secondary impact. Based on the results of the initial drop tests, the impact limiter attachment design was modified to ensure that the impact limiters remain attached to the cask throughout the impact event. Subsequent drop testing has verified the modified attachment design. Based on the above

considerations, it is concluded that the impact limiters will remain in position on the cask body for the full duration of the free drop impact event.

2.6.7.4.1.6 Redwood Impact Limiter Static Crush Test Results

A series of quasi-static crush tests have been performed on eighth-scale models of the impact limiters for the NAC-STC. The impact orientations tested were end (axial), side, and corner (center of gravity over corner). The purpose of the quasi-static crush tests was to document the force-deformation and energy absorption characteristics of the redwood and balsa wood used in the impact limiter. Additionally, the tests demonstrated that the impact limiters need not be mechanically attached to the cask body in order to remain in position to absorb the energy of crushing. No attachments (other than a strip of duct tape) between the model impact limiters and the test fixtures were used for the quasi-static crush tests. Once crushing of the impact limiter is initiated, its cup-shaped geometry causes it to maintain its position on the fixture, which is identical to an eighth-scale model cask body. The NAC-STC impact limiters are retained on the cask body by the attachment bolts and by the geometry of the impact limiter. As crushing occurs, the forces acting between the cask body and the unyielding surface act to keep the impact limiter in place.

Analytic Evaluations

Although the results from the above discussed test programs are considered to be the primary proof that the initially impacted impact limiter will remain in position during the impact event and properly perform its impact limiting function, analytic studies are used to confirm the test observations. Analytic assessments presented in this evaluation indicate that no failure of the attachment hardware can be expected to occur, but if an attachment failure does occur, separation of the cask and impact limiter does not occur. As shown, a significant resistance to the applied separation moment exists due to a combination of crushing of the limiter at the cask interface and due to frictional resistance that exists there. This total resistance is shown to be greater than the applied separation moment and is approximately 25 times greater than that provided by the attachment hardware alone.

Additionally, it is noted that the maximum applied separation moment occurs early in the impact when crush depths are small. As crush depths increase, the moment arm and the separation moment decrease to zero. The maximum separation moments occur early in the impact event when the package still possesses a significant downward velocity (87 percent of the initial

impact velocity). Thus, the cask “drives” into the limiter and physically “traps” the limiter between the cask body and the ground. Additionally, the duration of the impact is very short (approximately 0.04 to 0.06 seconds) and minimal rotation (approximately 1 degree) of the package occurs during the impact.

The remainder of this section presents a detailed analytic study of the center of gravity over top corner impact event. This near vertical orientation, coupled with the fact that little energy will be converted into rotational energy of the entire package (that is, the center of gravity is over the impacted corner), makes this particular orientation a representative worst case regarding the development of significant separation moments. The available impact limiter analysis program results associated with the corner drop are summarized in Figure 2.6.7.4.1-9. The crush depths, crush forces and package velocities presented in the summary figure are directly available from the impact limiter analysis program, RBCUBED, and the separation moment is calculated based on the geometry (that is, the crush footprint) existing at the particular position of interest. Of note, the velocity of the package is still 527 inches/second (just slightly less than the initial impact velocity) when the maximum separation moment of 3.59×10^5 inch-pounds is developed.

Capability of Redwood Impact Limiter Attachment Hardware

Figure 2.6.7.4.1-10 presents a free body diagram for the upper impact limiter during a top down center of gravity over corner impact. With point “A” being the pivot point of the impact limiter on the cask and conservatively assuming only 2 of the farthest attachment rods are actively resisting the separation moment, taking moments about point “A” yields the following:

$$2(F_i)(81.35) = \text{separation moment}$$

$$F_i = (3.59 \times 10^5 / 81.35) / 2$$

$$= 2,206 \text{ lbs}$$

where:

$$\text{Separation Moment} = 3.59 \times 10^5 \text{ in-lbs (Figure 2.6.7.4.1-10)}$$

The tensile stress in the retaining rod is:

$$S_t = 2,206 / 0.606 = 3641 \text{ psi}$$

The margin of safety is:

$$MS = 25.0/3.641 - 1 = +\text{Large}$$

The stress in the circular plate is calculated by ratioing the stress obtained in Section 2.6.7.4.1.4:
 $S_b = (2,206/4156)(22.4) = 11.9$ ksi. The margin of safety is:

$$MS = 25.0/11.9 - 1 = +1.1$$

The compressive stress in the redwood material is calculated as:

$$\begin{aligned} f &= 2,206/5.62 \\ &= 392 \text{ psi} \end{aligned}$$

The margin of safety against compression of the redwood is:

$$MS = 1,260/392 - 1 = +2.21$$

2.6.7.4.1.7 Resistance to Separation Following Attachment Hardware Failure

If the attachments do somehow fail, the cask tends to wedge itself into the impact limiter as shown in the free body diagram presented as Figure 2.6.7.4.1-11. From that figure:

$$\begin{aligned} f_{\max} &= \text{force required to crush redwood} \\ &= 86.7 S_c (\text{projected area} \times \text{crush strength}) = (86.7)(6240) \\ &= 541,000 \text{ lbs/in} \end{aligned}$$

where:

$$\begin{aligned} S_c &= \text{crush strength of redwood used in the impact limiter} \\ &= 6,240 \text{ psi (at 0.4 in/in strain - Section 2.6.7.4.1.1)} \end{aligned}$$

From moment equilibrium:

$$F_i x_i = (6)(6f_{\max}) = 36f_{\max}$$

$$= 1.95 \times 10^7 \text{ in-lbs}$$

A significant frictional resistance to separation of the impact limiter also exists. Selecting a coefficient of friction of approximately 0.5, the frictional resistance to the separation moment is:

$$\begin{aligned} M_f &= F_f d \\ &= 8.96 \times 10^7 \text{ in-lbs} \end{aligned}$$

where:

$$\begin{aligned} F_f &= \text{friction force} \\ &= (0.5)(6f_{\max}) = 3f_{\max} \\ &= 1,623,000 \text{ lbs} \end{aligned}$$

and with the centroid of a 180-degree arc (that is, the arc over which f_{\max} acts) being located at 63.7 percent of its radius:

$$\begin{aligned} d &= (0.637)(86.7) \\ &= 55.23 \text{ in} \end{aligned}$$

The total resistance to separation, therefore, becomes:

$$\begin{aligned} M_t &= 1.95 \times 10^7 + 8.96 \times 10^7 \\ &= 10.91 \times 10^7 \text{ in-lbs} \end{aligned}$$

This total resistance to separation exceeds the maximum applied separation moment of 3.59×10^5 inch-pounds (Figure 2.6.7.4.1-9). Separation of the limiter from the cask body will not occur. As discussed in Section 2.6.7.4.1.5, this particular center of gravity over corner case was tested. Test results are consistent with the preceding analysis in that the cask did tend to wedge itself into the impact limiter, and that physical separation did not occur.

2.6.7.4.1.8 Response of Secondary Impact Limiter During Initial Impact of Package

The final criterion to be satisfied is that for a free drop (normal or accident) involving an initial impact on a single impact limiter, the limiter on the opposite end of the cask (secondary limiter) must remain attached to the cask during the initial impact. This ensures that the secondary

limiter will be in position to absorb the secondary impact and it remains in position for the full duration of the secondary impact and performs its impact limiting function. Attachment is ensured by demonstrating that the attachment hardware (mounting plate and retaining rods) does not fail during the initial impact.

Drop Scenario

During a free drop of the cask (normal or accident) involving an initial impact on a single impact limiter, i.e., flat end, center of gravity over corner, or any oblique drop, the ground exerts an upward force on the impact limiter being impacted.

This force decelerates the impacted impact limiter. The impact limiter, in turn, exerts an upward force on the cask body, thus decelerating the cask body. The cask body, likewise, exerts an upward force on the secondary impact limiter, decelerating that impact limiter. This scenario is repeated during a rebound of the whole package; the ground exerts an upward force on the impacted impact limiter, the impacted impact limiter exerts an upward force on the cask body, which in turn exerts an upward force on the secondary impact limiter, accelerating the whole package upwards. When the entire package is in the air, its components (the initially impacted impact limiter, the cask body, and the secondary impact limiter) move with the same acceleration and velocity, involving no other force acting among them. Thus, it is evident that during a free drop impact on the first impact limiter, no separation force exists between the cask body and the second impact limiter. This ensures that the second impact limiter stays in position to absorb the second impact. For further evidence that the secondary impact limiter will stay attached to the cask body, the resistance to separation between the cask body and the second impact limiter is calculated in the sections below.

Analysis of the Mounting Plate

The stress in the mounting plate of the impact limiter due to a longitudinal loading of 7.5 g is calculated as 22.4 ksi in Section 2.6.7.4.1.4. The yield and ultimate strengths of Type 304 stainless steel at 200°F are 25.0 ksi and 71.0 ksi, respectively. The maximum g-load that the attachment plate can support without exceeding its yield strength is:

$$\begin{aligned} F_y &= (25.0/22.4)(7.5 \text{ g}) \\ &= 8.4 \text{ g} \end{aligned}$$

The g-load it can support without exceeding its ultimate strength is:

$$\begin{aligned}F_u &= (71.0/22.4)(7.5 \text{ g}) \\&= 23.8 \text{ g}\end{aligned}$$

Analysis of the Retaining Rods

The tensile stress in the retaining rod due to a 7.5 g longitudinal loading applied to the impact limiter is calculated in Section 2.6.7.4.1.4 as 6,857 psi. The yield and ultimate strengths of SA-276, Type 304 stainless steel at 200°F are 25.0 ksi and 71.0 ksi, respectively. The maximum g-load that the retaining rods can support without exceeding their yield strength is calculated as:

$$\begin{aligned}F_y &= (25.0/6.857)(7.5 \text{ g}) \\&= 27.3 \text{ g}\end{aligned}$$

The g-load that the retaining rods can support without exceeding their ultimate strength is calculated as:

$$\begin{aligned}F_u &= (71.0/6.857)(7.5 \text{ g}) \\&= 77.7 \text{ g}\end{aligned}$$

The maximum stress in the Type 304 stainless steel washer supporting the nut of the retaining rod is 22.4 ksi due to a normal transportation acceleration of 7.5 g. The yield stress of the plate material is 25.0 ksi at 200°F. The maximum g-load that the circular plate can support without exceeding its yield strength is calculated as:

$$\begin{aligned}a &= (25.0/22.4)(7.5 \text{ g}) \\&= 8.4 \text{ g}\end{aligned}$$

The compressive strength perpendicular to the grain of the redwood supporting the circular plate is 1,260 psi at 40 percent strain (Section 2.6.7.4.1). The maximum compressive stress in the redwood under the circular plate due to a normal transportation acceleration of 7.5 g is 740 psi.

The maximum g-load that the redwood material can support without exceeding its compressive stress is calculated as:

$$\begin{aligned} a &= (1260/740)(7.5 \text{ g}) \\ &= 12.8 \text{ g} \end{aligned}$$

Thus, the NAC-STC impact limiter attachments provide significant resistance to any unspecified separation force on the impact limiter.

Figure 2.6.7.4.1-1 NAC-STC with Redwood Impact Limiters

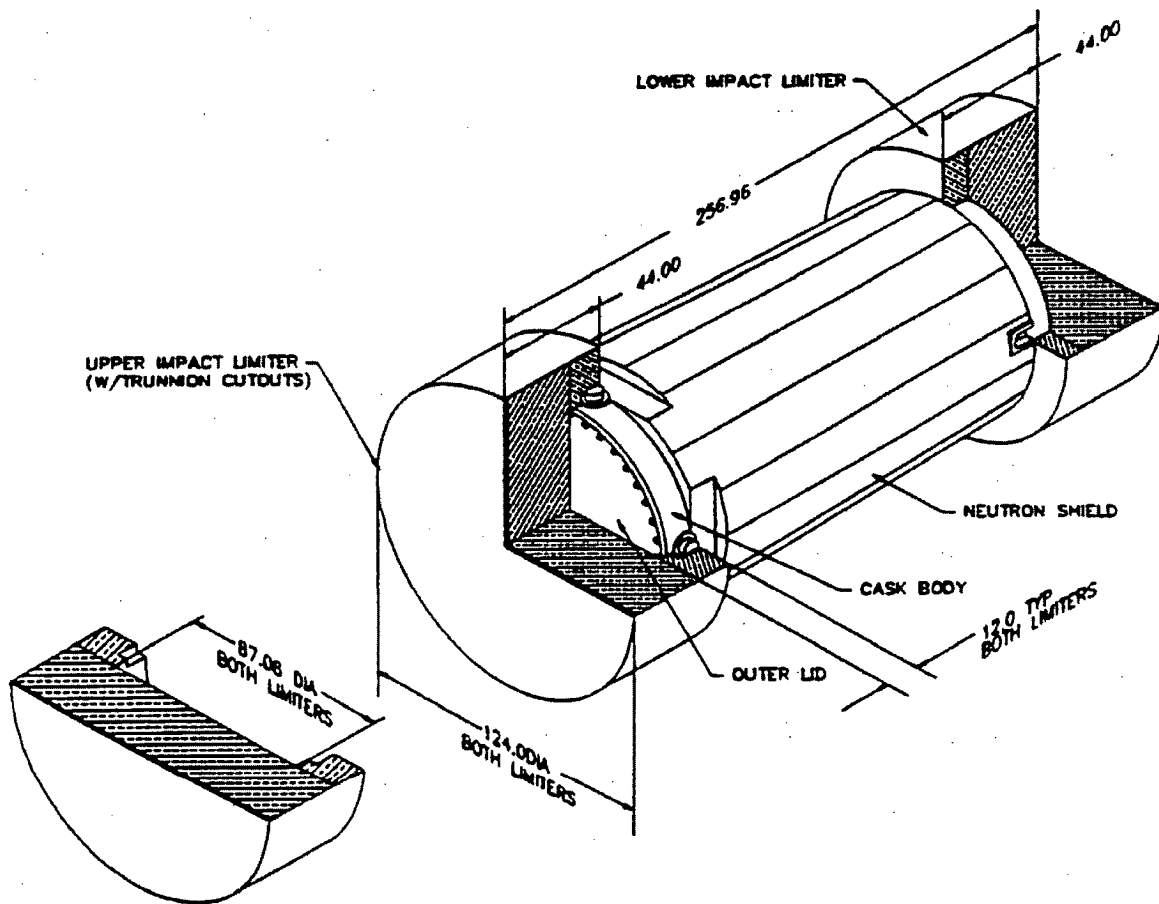


Figure 2.6.7.4.1-2 Cross-Section of Redwood Impact Limiter

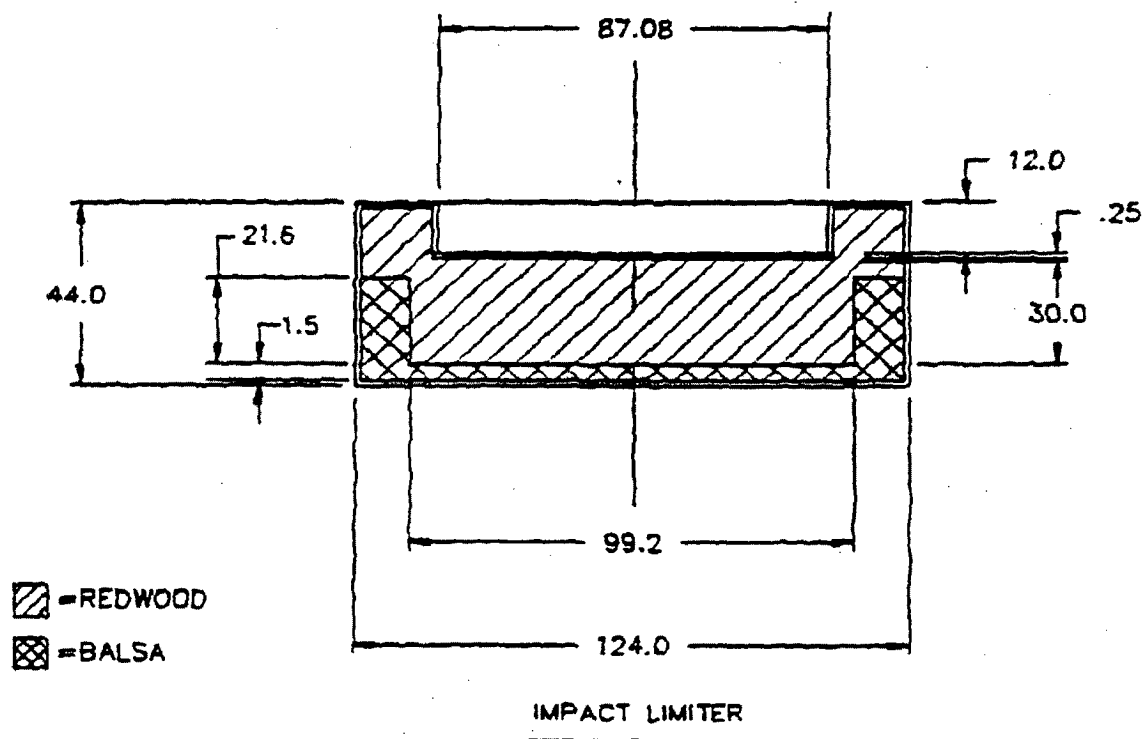


Figure 2.6.7.4.1-3 Crush Stress-Strain Curves for Redwood (Crush Strength Parallel to Grain)

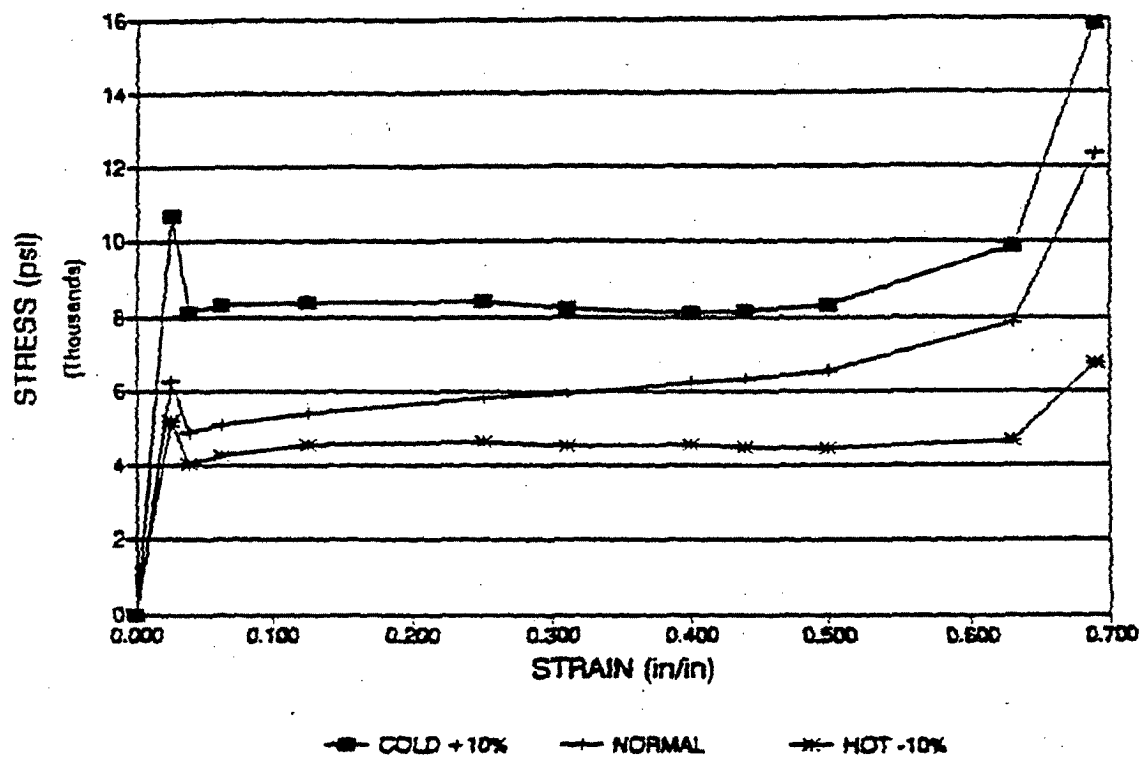


Figure 2.6.7.4.1-4 Crush Stress-Strain Curves for Redwood (Crush Strength Perpendicular to Grain)

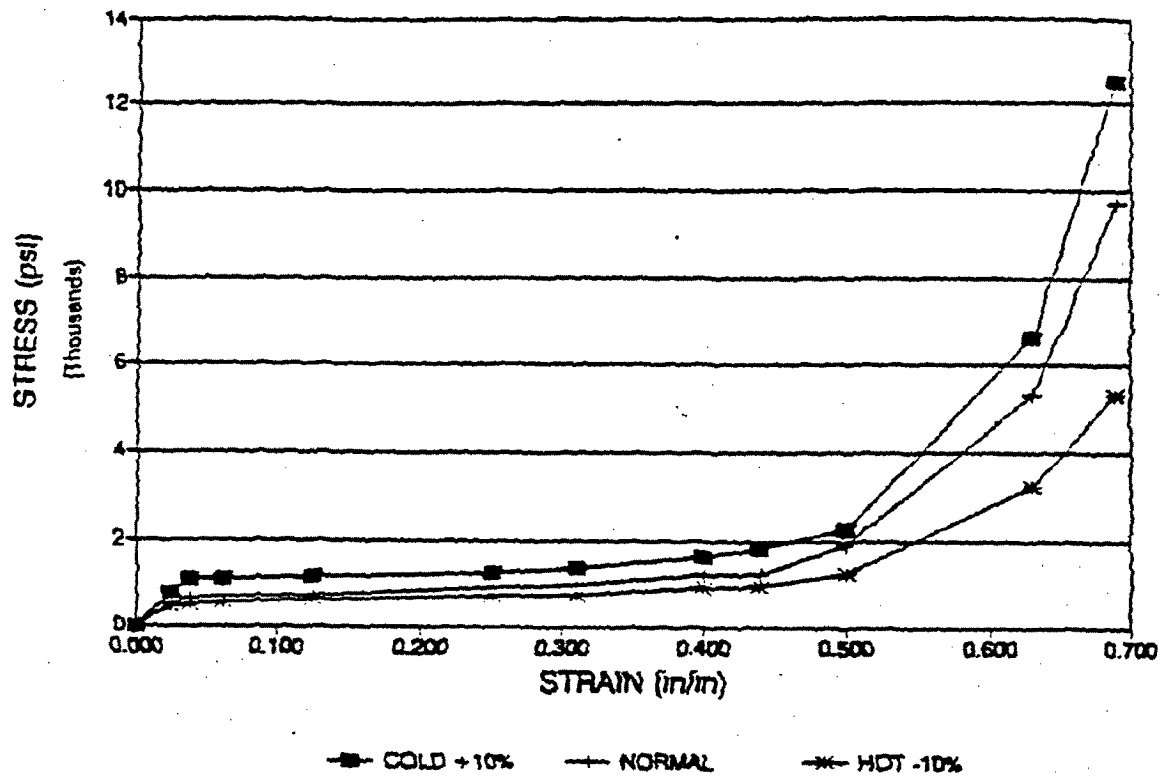


Figure 2.6.7.4.1-5 Crush Stress-Strain Curves for Balsa Wood (Crush Strength Parallel to Grain)

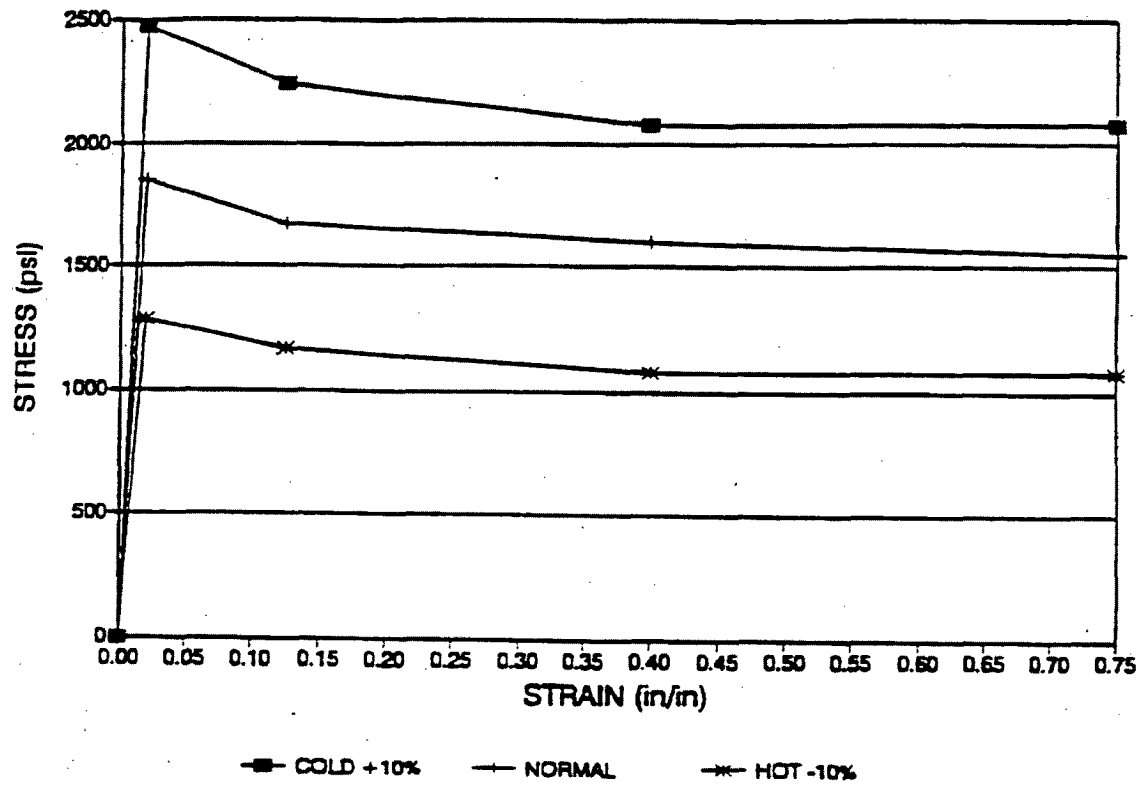


Figure 2.6.7.4.1-6 Variation of Crush Strength of Redwood and Balsa Wood with Impact Angle at 40 Percent Strain

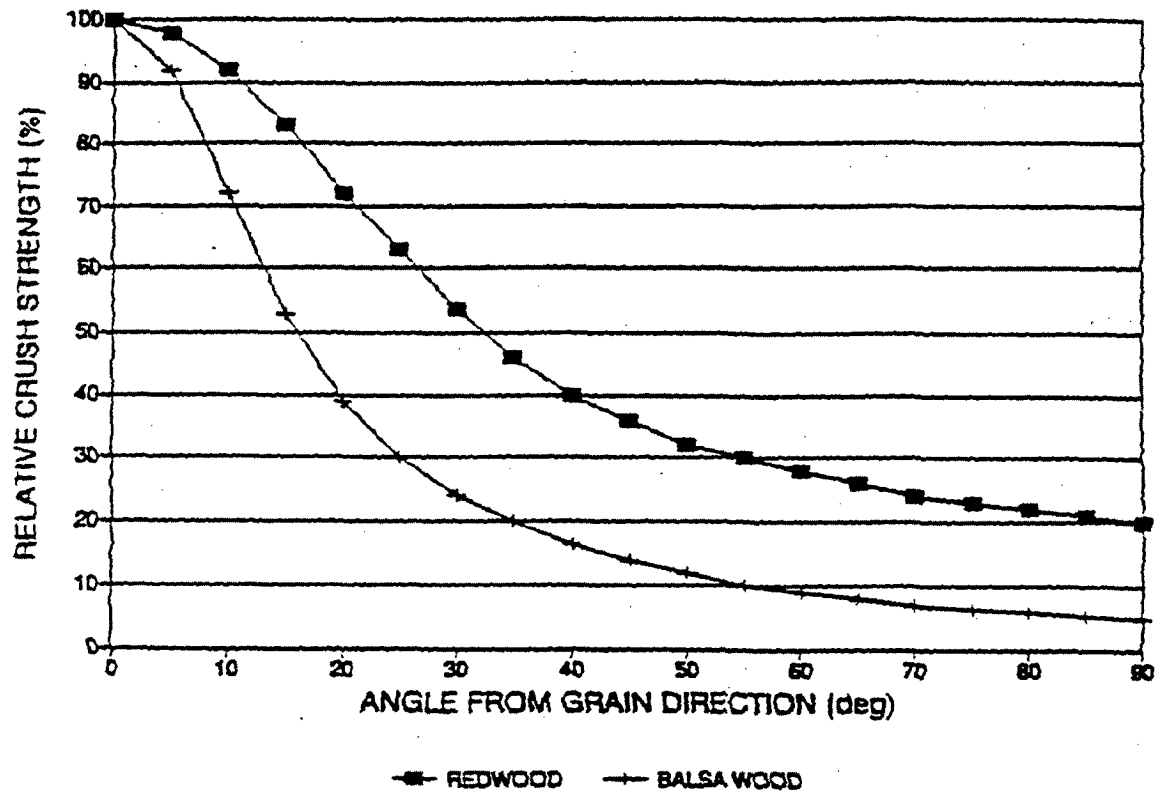


Figure 2.6.7.4.1-7 Redwood Impact Limiter Attachment Geometry

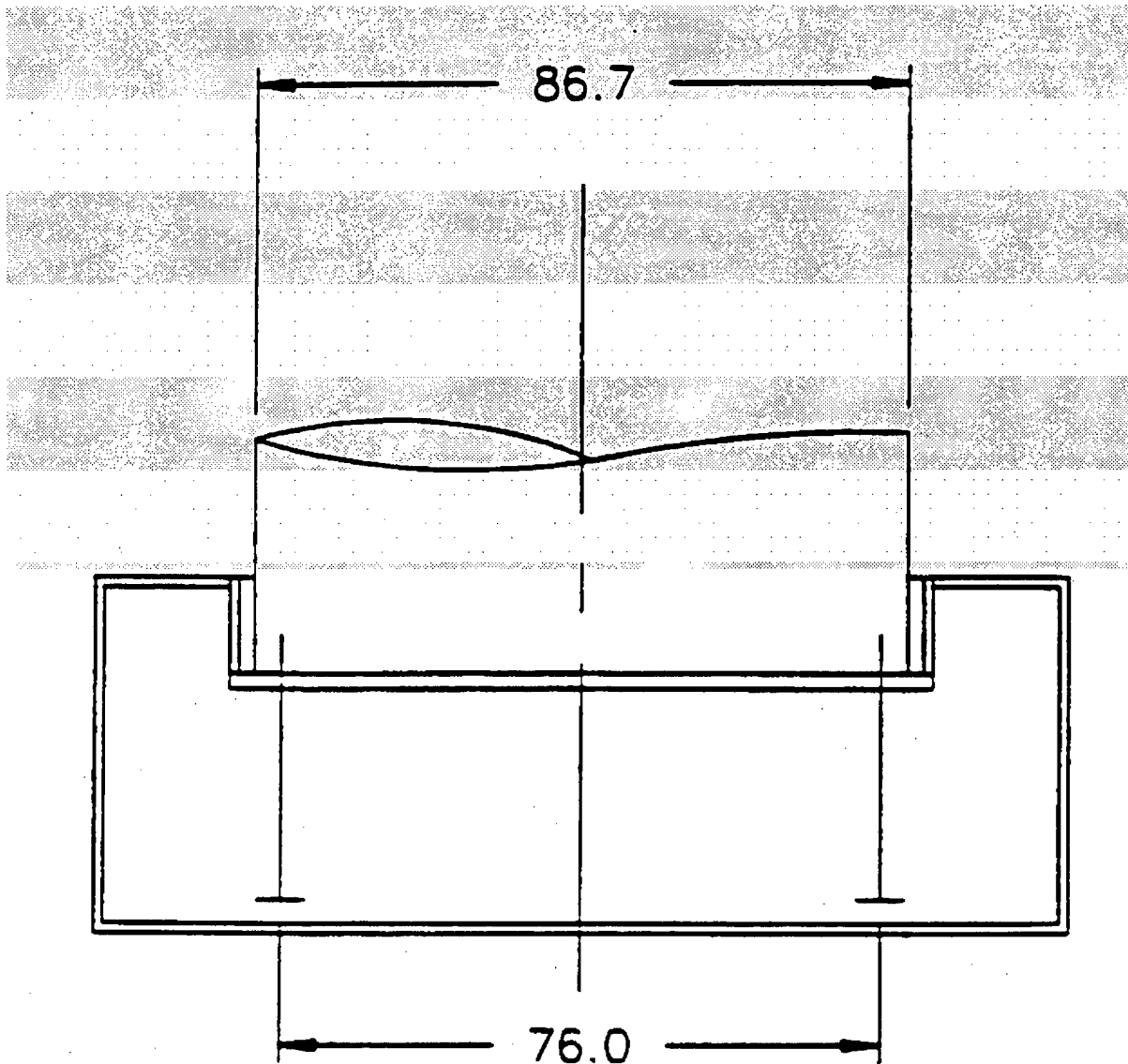


Figure 2.6.7.4.1-8 Anchorage Detail of the Retaining Rod at the End of the Impact Limiter

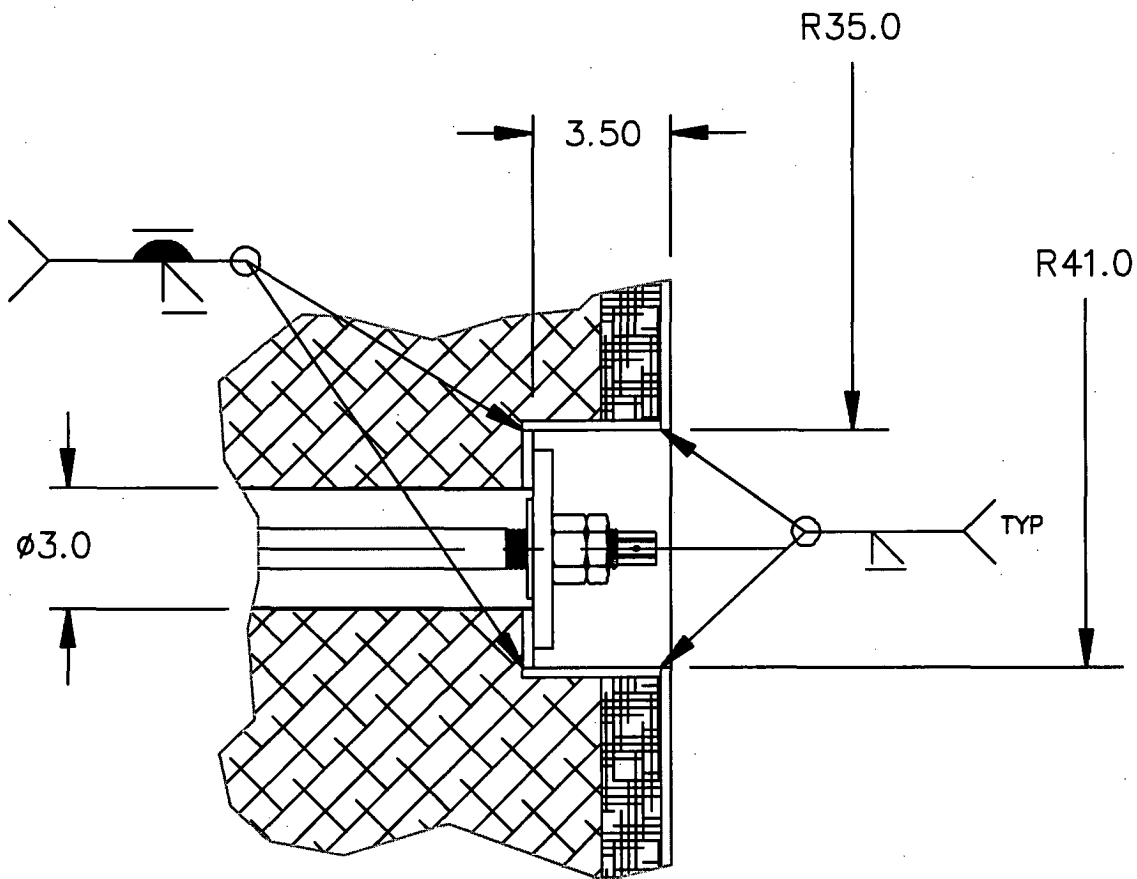


Figure 2.6.7.4.1-9 RBCUBED Output Summary - Center of Gravity Over Top Corner

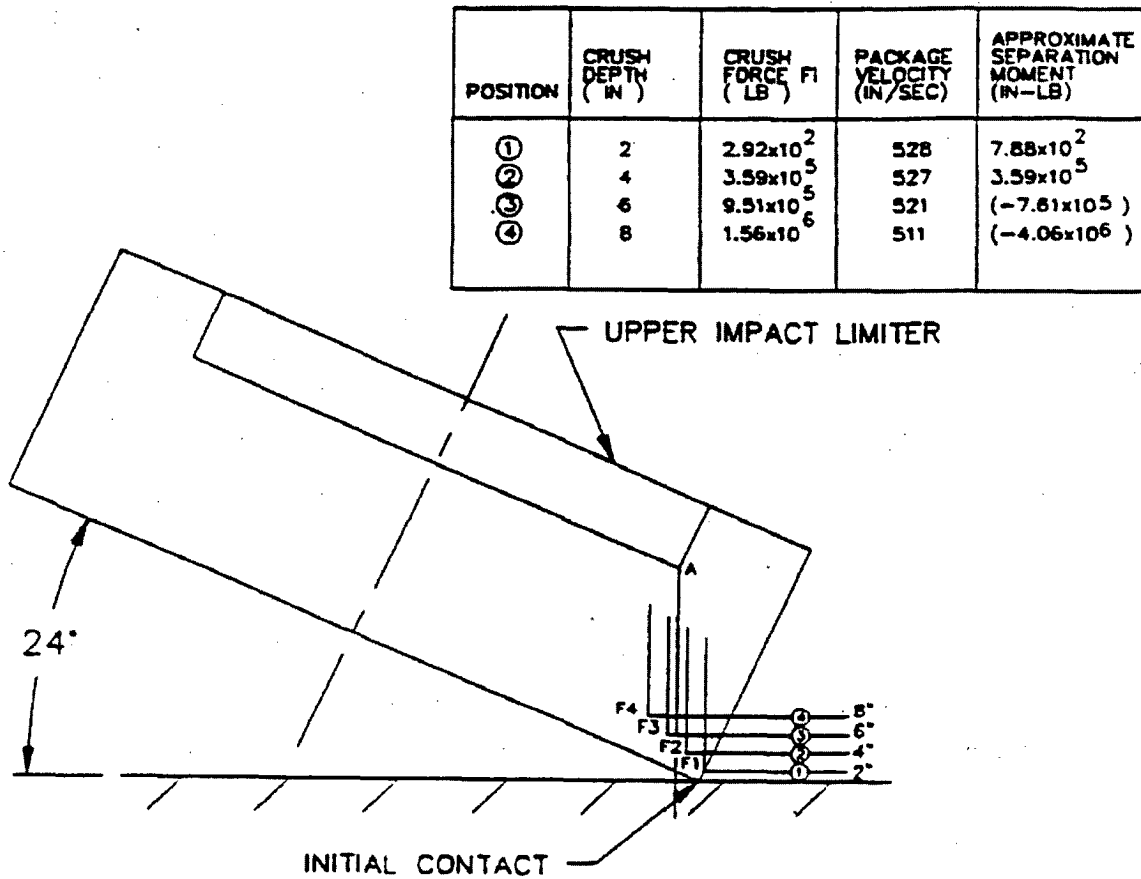


Figure 2.6.7.4.1-10 Free Body Diagram - Upper Impact Limiter - Center of Gravity Over Corner

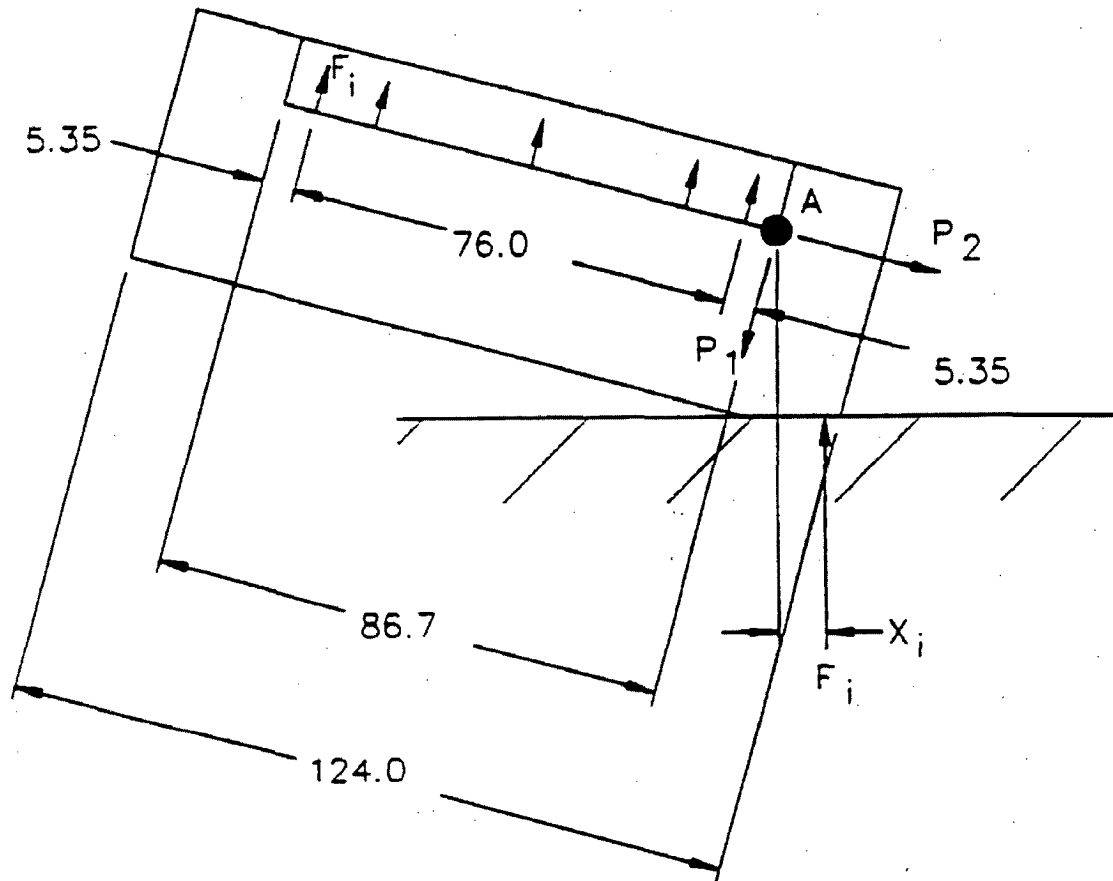


Figure 2.6.7.4.1-11 Free Body Diagram - Upper Impact Limiter - Cask Wedging Forces

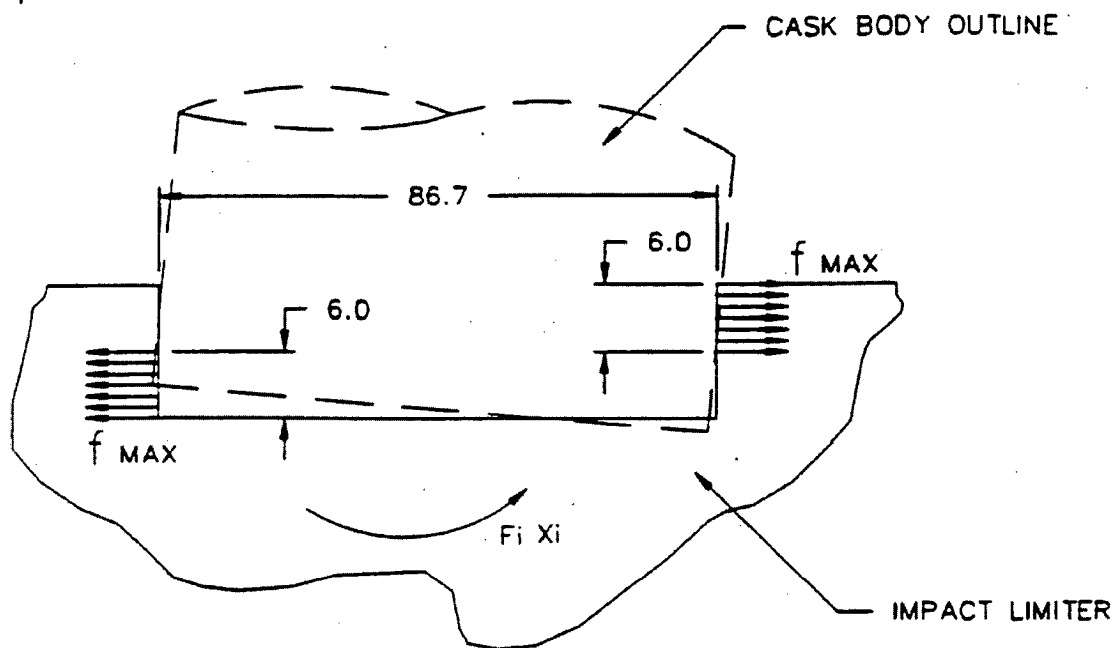


Table 2.6.7.4.1-1 Summary of Results - Impact Limiter Analysis for 1-Foot Free Drop

Analysis Description	Displacement (in)	Force (lb)	Equivalent* G-Load Factor
<u>End Impact</u>			
Lower Impact Limiter (Max. Crush Strength)	1.62	4.91×10^6	19.6
Lower Impact Limiter (Min. Crush Strength)	2.10	4.42×10^6	17.7
Upper Impact Limiter (Max. Crush Strength)	1.62	4.91×10^6	19.6
Upper Impact Limiter (Min. Crush Strength)	2.10	4.42×10^6	17.7
<u>Corner Impact</u>			
Lower Impact Limiter (Max. Crush Strength)	7.2	1.32×10^6	5.3
Lower Impact Limiter (Min. Crush Strength)	9.6	1.12×10^6	4.5
Upper Impact Limiter (Max. Crush Strength)	7.3	1.31×10^6	5.2
Upper Impact Limiter (Min. Crush Strength)	9.7	1.07×10^6	4.3

Table 2.6.7.4.1-1 Summary of Results - Impact Limiter Analysis for 1-Foot Free Drop
(continued)

Analysis Description	Displacement (in)	Force (lb)	Equivalent* G-Load Factor
<u>Side Impact</u>			
Lower Impact Limiter (Max. Crush Strength)	1.1	$4.53 \times 10^{6**}$	18.1
Lower Impact Limiter (Min. Crush Strength)	1.7	$2.78 \times 10^{6**}$	11.1
Upper Impact Limiter (Max. Crush Strength)	1.1	$4.53 \times 10^{6**}$	18.1
Upper Impact Limiter (Min. Crush Strength)	1.7	$2.78 \times 10^{6**}$	11.1

* Equivalent g-load factor = Force/250,000.

** Total force for both impact limiters.

Table 2.6.7.4.1-2 Summary of Results - Impact Limiter Analysis for 30-Foot Free Drop

Analysis Description	Displacement (in)	Force (lb)	Equivalent* G-Load Factor
<u>End Impact</u>			
Lower Impact Limiter (Max. Crush Strength)	10.4	1.12×10^7	44.6
Lower Impact Limiter (Min. Crush Strength)	16.1	1.07×10^7	42.8
Upper Impact Limiter (Max. Crush Strength)	12.5	1.02×10^7	40.6
Upper Impact Limiter (Min. Crush Strength)	17.7	1.40×10^7	56.1
<u>Corner Impact</u>			
Lower Impact Limiter (Max. Crush Strength)	24.2	9.35×10^6	37.4
Lower Impact Limiter (Min. Crush Strength)	30.0	1.09×10^7	43.6
Upper Impact Limiter (Max. Crush Strength)	26.6	1.10×10^7	44.0
Upper Impact Limiter (Min. Crush Strength)	31.6	1.23×10^7	49.3

Table 2.6.7.4.1-2 Summary of Results - Impact Limiter Analysis for 30-Foot Free Drop
(continued)

Analysis Description	Displacement (in)	Force (lb)	Equivalent* G-Load Factor
<u>Side Impact</u>			
Lower Impact Limiter (Max. Crush Strength)	10.3	$1.29 \times 10^{7**}$	51.7
Lower Impact Limiter (Min. Crush Strength)	15.1	$1.28 \times 10^{7**}$	51.3
Upper Impact Limiter (Max. Crush Strength)	10.3	$1.29 \times 10^{7**}$	51.7
Upper Impact Limiter (Min. Crush Strength)	15.1	$1.28 \times 10^{7**}$	51.3

* Equivalent g-load factor = Force/250,000.

** Total force for both impact limiters.

Table 2.6.7.4.1-3

Summary of Cask Drop Equivalent G-Load Factors

Direction	1-Foot Drop	Equivalent G-Load Factor*		
		30-Foot Drop		
		Total	Axial** Comp.	Lateral** Comp.
Lateral (Side)	18.1	51.7	0.0	51.7
Longitudinal (End)	19.6	56.1	56.1	0.0
Corner (24°)	5.3	49.3	45.0	20.1
Oblique (30°)	-	41.8	36.2	20.9
Oblique (45°)	-	34.5	24.4	24.4
Oblique (60°)	-	33.8	16.9	29.3

* Equivalent g-load factor = Force/250,000.

**

Axial Component	= total x cosθ	}	where: θ = 24°, 30°, 45° or 60°
Lateral Component	= total x sinθ		

Table 2.6.7.4.1-4 Summary of 30-Foot Cask Drop Deceleration G-Loads for the Redwood Impact Limiter Obtained from RBCUBED, Tests, and Design

	30-Foot Drop Decelerations (g)			
Drop Orientation	RBCUBED	Test	Quasi-Static Test	Design
End (0°)	56.1	55.6	54.8	56.1
Corner (24°)	44.2	29.2	32.6	55.0
Oblique (30°)	39.4	N/A	N/A	55.0
Oblique (45°)	36.4	N/A	N/A	55.0
Oblique (60°)	37.6	N/A	N/A	55.0
Oblique (75°)	34.0 ¹	53.8 ²	N/A	55.0
Side (90°)	54.1	51.3	45.6	55.0

RBCUBED: Impact limiter g-load calculations using RBCUBED program. Values taken from Table 2.6.7.4-3.

Drop Test: Quarter-scale cask model dynamic drop test results. Details provided in Section 2.10.6.5.

Quasi-Static Test: Extrapolated from eighth-scale model impact limiter quasi-static compression tests. Details are provided in Section 2.10.6.4.

Design: Design g-load values used in the cask and fuel basket analyses.

¹ Initial impact.

² Secondary impact.

2.6.7.4.2 Balsa Impact Limiters

The balsa impact limiter evaluation presented in this section is for all cask configurations, i.e., NAC-STC directly loaded fuel configuration, the Yankee-MPC and CY-MPC canistered fuel configurations, or the Yankee-MPC and CY-MPC canistered GTCC waste configurations, with a total package weight with impact limiters attached not exceeding 260,000 pounds.

The package geometry is similar for all of the configurations. Axial spacers are designed for the cask cavity to locate the canister loaded with fuel or GTCC waste such that the package center of gravity location is approximately the same as that of the directly loaded fuel configuration.

Differences in contents weight and the weights of the associated package configurations have no significant effect on the balsa impact limiter design or performance. Therefore, the balsa impact limiter analysis in this section and the cask drop analyses in Sections 2.6.7 and 2.7.1 are applicable for all contents configurations of the NAC-STC, Yankee-MPC, and CY-MPC.

2.6.7.4.2.1 Assumptions

The following assumptions form the basis for the balsa impact limiter analysis:

1. The cask impacts on an unyielding surface.
2. The balsa impact limiter remains in position on the cask during all impact events. (The qualification of the balsa impact limiter attachment is presented in Section 2.6.7.4.2.7.)

2.6.7.4.2.2 Load Conditions

The balsa impact limiters described and analyzed in the following paragraphs decelerate the cask by applying a force in the direction opposite the motion of the cask. Crushing the balsa wood and redwood materials, the stainless steel gussets, and stainless steel shells of the balsa impact limiter between the cask and the unyielding surface generates the deceleration force.

The specific loading conditions for the transport Balsa lightweight impact limiters are defined by 10 CFR 71.71(c)(7), 10 CFR 71.73(c)(1) and Regulatory Guide 7.8, as follows:

1. A 1-foot drop of the cask impacting at any angle from vertical (flat end) to corner (cask center of gravity is directly above the point of impact).
2. A 1-foot drop of the cask in a horizontal orientation position.
3. A 30-foot drop of the cask in an end, a side and an oblique orientation.

Based on these loading conditions, the NAC-STC balsa impact limiters are primarily designed for the 30-foot cask drops but with consideration of the 1-foot end, side and corner drops. The maximum impact forces and the maximum crush depth for the 1-foot and 30-foot cask drops are obtained from the LS-DYNA analyses of the balsa impact limiters. LS-DYNA is an explicit finite element program for the nonlinear dynamic analysis of three-dimensional structures (Section 2.10.1.3).

2.6.7.4.2.3 Description—Balsa Impact limiters

Figures 2.6.7.4.2-1 and 2.6.7.4.2-2 show the primary dimensions of the balsa impact limiters. Figure 2.6.7.4.2-2 shows the cross-section of a balsa impact limiter. Except for the pockets for the lifting trunnions in the upper limiter, the upper and lower balsa impact limiters are identical.

Each balsa impact limiter includes both balsa and redwood for energy absorption. The grain direction of the wood is oriented to achieve the desired crush strength. The balsa and redwood is enclosed in a stainless steel shell to protect and maintain its position and orientation. Stainless steel gussets are arranged in 15-degree increments to maintain the orientation of the wood during the side drop.

2.6.7.4.2.4 Properties of Balsa Wood and Redwood

The balsa wood to be used in the NAC-STC balsa impact limiter is specified to have a density between 7 and 10 pounds per cubic foot and to have a moisture content between 5 and 15 percent for any one piece with an average moisture content of not more than 12 percent for any lot. A density limit of 7 to 10 pounds/cubic foot is applied to be consistent with dynamic wood test density criteria.

To adequately specify the balsa crush strength, NAC conducted dynamic compression tests of specimens taken from balsa obtained from a commercial supplier. The average density of the balsa wood tested was 8.5 lbs/ft³ (8.5 ± 1.5 lbs/ft³). To ensure an adequate sampling, the following matrix was developed to test a series of specimens at various strain rates:

Grain Direction	Temp (°F)	Strain Rate (s ⁻¹)	Number of Tests
Perpendicular	70	25	8
Perpendicular	70	75	8
Perpendicular	70	175	8
Perpendicular	70	275	10
Perpendicular	70	375	9
Perpendicular	-40	25	3
		175	3
		375	3
Perpendicular	200	25	3
		175	3
		375	3
Perpendicular (Stack Configuration)	70	25	3
		175	4
		375	3
Parallel	70	25	8
Parallel	70	75	8
Parallel	70	175	8
Parallel	70	275	9
Parallel	70	375	10
Parallel	-40	25	3
		175	3
		375	3
Parallel	200	25	3
		175	3
		375	3
Parallel (Stack Configuration)	70	25	3
		175	3
		375	3

Static properties for balsa wood are discussed in Section 2.6.7.4.1 and presented in Figure 2.6.7.4.1-5

The redwood material to be used in the balsa impact limiters must satisfy density and moisture content specifications. The density of any single redwood board shall be 23.5 ± 3.5 pounds per cubic foot. The moisture content of any single board shall be greater than 5 percent, but less than 15 percent. The average moisture content for the lot of redwood shall be less than 12 percent.

To adequately specify the redwood crush strength, NAC conducted dynamic compression tests of specimens taken from redwood obtained from a commercial supplier. The average density of the redwood tested was 23.5 lbs/ft³ (23.5 ± 3.5 lbs/ft³). To ensure an adequate sampling, the following matrix was developed to test a series of specimens at various strain rates:

Grain Direction	Temp (°F)	Strain Rate (s ⁻¹)	Number of Tests
Perpendicular	70 ± 10	Static	10
Perpendicular	-40 ± 10	Static	10
Perpendicular	200 ± 10	Static	10
Parallel	70 ± 10	Static	10
Parallel	-40 ± 10	Static	10
Parallel	200 ± 10	Static	10
Perpendicular	70 ± 10	25	10
Perpendicular	-40 ± 10	25	10
Perpendicular	200 ± 10	25	10
Parallel	70 ± 10	25	10
Parallel	-40 ± 10	25	10
Parallel	200 ± 10	25	10
Perpendicular	70 ± 10	100	10
Parallel	70 ± 10	100	10
15° from Parallel	70 ± 10	Static	10
30° from Parallel	70 ± 10	Static	10

Note: Each specimen in a test series is to be taken out of a different board.

The tests included both parallel-to-the-grain (parallel) and perpendicular-to-the-grain (perpendicular) directions for hot, cold, and ambient temperature conditions. Compression testing of the wood specimen was performed using a servohydraulic test machine. The test machine consists primarily of a load frame, actuator for applying the dynamic load, a load cell, and associated voltage transducer. The maximum actuator speed is 200 inches/second with a load capacity of 20 kips. Fixturing is used to position the test specimen for the application of the load and to hold instrumentation used to record test results. Test specimens are sized to conform

to the geometry of the test machine and to allow the establishment of empirical relationships between actuator speed, actuator and specimen impact area, and total displacement, including crush. Test specimens are fabricated from larger wood boards having specified material properties for moisture content and density. Wood test specimen size was based on test machine requirements.

For each strain rate and temperature condition, a data set was created that consists of 10 to 15 individual test specimens. To reduce this data, individual files of a data set were averaged together. These average curves were then simplified using minimal (30) data points. To produce simplified curves, the peak acceleration was retained and the area under the curve that represents the energy absorption capacity was maintained. Stress-strain curves are developed in the parallel and perpendicular-to-the-grain directions for hot (200°F) and cold (-40°F) conditions. Table 2.6.7.4.2-1 and Table 2.6.7.4.2-2 provide a summary of the data used in the LS-DYNA analyses.

2.6.7.4.2.5 Balsa Impact Limiter Finite Element Model

The balsa impact limiter finite element model was built using the ANSYS pre-processor and LS-DYNA's Finite Element Model Builder. The impact analyses were performed using LS-DYNA. The model is constructed of 8-node brick and 4-node shell elements. A full half model of the impact limiters and cask was generated. The LS-DYNA model is shown in Figure 2.6.7.4.2-3.

Boundary Conditions and Initial Conditions

LS-DYNA "Surface_to_Surface" contact interface is employed between each part in the impact limiter and between the cask body and impact limiter shells. The model sits on a rigid plane ("Rigidwall_Geometric_Flat"). Symmetry boundary conditions are imposed on the nodes in the X-Z plane for all drop conditions. For the corner drop cases, the model is rotated so that the X-axis aligned in impact direction. The weight of the canister lids is included in the content weight and is distributed over the length of the cavity by varying the density of the elements in the different regions of the model. The weight and CG of the finite element model correspond to those of the NAC-STC cask. Therefore, the interaction between the cask body and impact limiters is correctly modeled.

To simulate a rigid cask body, all nodes of the cask shell elements were constrained. To achieve a total weight of 260,000 pounds, the density of the material representing the cask body was increased. The total weight was verified by checking the total kinetic energy of the quarter

model. An initial velocity of 96.3 in./sec and 527.4 in./sec was applied to the entire model to represent the 1-foot and 30-foot drops, respectively.

To bound the extreme temperature conditions and maximize accelerations and crush, cold (-40°F) and hot (200°F) analyses are performed for accident conditions. However, since the amount of crush is small during the 1-ft drop, cold balsa properties are used to maximize accelerations for normal conditions.

The drop orientations considered in the evaluation of the balsa impact limiter are shown in Figure 2.6.7.4.2-4. The top and bottom impact limiters are identical except for the trunnion pocket in the upper impact limiter. Since the trunnion provides additional backed area that may contribute to the total acceleration, the upper impact limiter is used to evaluate the end and corner impact conditions. For the side drop, the cask is dropped on the trunnion side of the impact limiter. This is conservative since less crush capacity is available during the hot conditions side drop.

Material Properties

To account for gross deformation and buckling, the Type 304 stainless steel shells and gussets were modeled with an elasto-plastic material. The LS-DYNA material Type 24 was used ("Piecewise_Linear_Plasticity"). The required input data is:

Steel Shell Property	Value
Mass Density, ρ	7.51E-04 lb-sec ² /in ⁴
Modulus of Elasticity, E	27.9E6 psi
Poisson's Ratio, ν	0.30

The stress-strain curve used for Type 304 stainless steel is:

STRESS (psi)	STRAIN (in/in)
23,809	0.000041
28,033	0.001180
29,500	0.003180
31,970	0.007180
36,900	0.015100
42,300	0.039200
85,080	0.230000

An elastic material model with the following properties was used to represent the NAC-STC cask body as shown in Figure 2.6.7.4.2-3.

NAC-STC Cask Body Properties	Value
Modulus of Elasticity, E	1.0E7 psi
Poisson's Ratio, ν	0.30

The NAC-STC cask body model consists of a single shell using an elastic material. The elastic modulus of the cask body was adjusted to allow the cross-sectional modulus of the finite element model to be equal to that of the full-scale cask. The mass density of the cask was also adjusted to ensure that the total kinetic energy is accounted for. Therefore, the mass density varies slightly depending on the drop orientation.

To account for the strain-rate sensitivity of the wood, the LS-DYNA analyses use material 163 (modified_crushable_foam). The modified_crushable_foam material model allows for the input of several stress-strain curves of various strain-rates. Up to three stress-strain curves are used ranging from 0 ϵ /sec to 175 ϵ /sec. For each time step during an analysis, LS-DYNA calculates the strain-rate of an individual element and uses the stress-strain data from the inputted stress-strain curves. For a strain rate between the inputted curves, LS-DYNA interpolated between the given curves. For low velocity impacts such as the 1-ft side drop, strain rates are essentially static. Therefore, LS-DYNA interpolates between the static stress-strain curve and the second stress-strain curve in the series. To account for crush strength fabrication tolerances, the -40°F cold case comparison stresses are factored by 1.10 and the +200°F hot case compression stresses are factored by 0.90.

The wood impact limiter surrounding the cask consists of 24 equally spaced angular wedges separated by radial gussets fabricated from steel plates. Since a half-symmetry finite element model is used to represent the impact limiters, only 12 of the wood wedges are modeled. Out of the 12 modeled wood wedges, only 3 wedges are loaded during a 30 foot side drop. The first wedge is loaded in the parallel to grain direction. The second and third wedges are loaded between the parallel and perpendicular to grain directions. For the wedges where the impact force is applied between the parallel and perpendicular to grain directions, Hankinson's formula (Baumeister, page 6-127) is used to vary the strength properties of wood with the orthotropic axes of the wood grain.

$$N = \frac{PQ}{P \sin^2 \theta + Q \cos^2 \theta}$$

where:

- N = stress induced by a load acting at an angle to the grain direction,
- P = stress parallel to the grain direction,
- Q = stress perpendicular to the grain direction,
- θ = angle between direction of load and grain direction.

Using Hankinson's formula, stress-strain curves are generated for the second and third wedges at 15 and 30 degrees, respectively. Therefore, in the LS-DYNA input files, unique stress-strain curves are applied to each wood wedge depending on the loading angle and strain rate.

2.6.7.4.2.6 Results

To obtain results from LS-DYNA, nodes of interest are used to record output data. The output is in the form of displacement and acceleration time histories. However, the acceleration time histories contain high frequency components that are induced by the model's interior geometry but do not represent a global response to the external impact. Therefore, the time histories have to be filtered to obtain true accelerations corresponding to the global response. For this evaluation, the Butterworth low-pass filter in LS-DYNA's post-processor is used with a filter at 100 Hz. Figures 2.6.7.4.2-5 through 2.6.7.4.2-10 provide the filtered acceleration time-history curves for the normal and accident conditions drop analyses.

Evaluation of the balsa impact limiter for the normal conditions of transport shows that a maximum acceleration of 16.5g occurs during the side drop. Table 2.6.7.4.2-3 summarizes the accelerations for the three normal condition cases considered. In each case, the calculated acceleration is less than the design acceleration of 20g.

For accident conditions, the maximum acceleration of 48.5g also occurs during the cold condition side drop aligned with the trunnion. During the end drop, the maximum acceleration of 40.8g occurs during hot conditions. The dynamic load factor (DLF) is calculated by performing a modal analysis on the basket support and applying the acceleration time histories from the side and end drops. The DLF calculated for the side and end drops is 1.02 and 1.00, respectively. Since the side and end drops bound the corner drop acceleration, the DLF is not reported for the corner drop acceleration.

Table 2.6.7.4.2-4 summarizes the accelerations for the three hot and cold accident cases considered. In each case, the calculated acceleration is less than the design acceleration of 55g for the side drop and 48g for the end and corner drops. As Table 2.6.7.4.2-2 shows, the

maximum strain of 72% occurs during the hot condition side drop at the trunnion. The high strain below the trunnion is considered a localized phenomenon. Strain outside of the trunnion region is less than 50%. Therefore, lock-up of the balsa wood does not occur.

2.6.7.4.2.7 Balsa Impact Limiter Attachment Analysis

Each balsa impact limiter is approximately 3,000 pounds lighter than the redwood impact limiter (refer to Tables 2.2-1 and 2.2-4). Due to the difference in contour of the outside surface, the balsa wood impact limiter uses shorter retaining rods than those used with the redwood impact limiter. Both designs use 16 stainless steel retaining rods, each 1-inch in diameter, equally spaced on a 76.0-inch diameter bolt circle and share the same interior dimensions and cask interface. The balsa impact limiter retaining rods are fabricated from high strength ASTM SA-193 grade B8S stainless steel, which has yield and ultimate strengths of 50 ksi and 95 ksi, respectively. This material is higher strength and more ductile than the retaining rods used with the redwood impact limiters. The retaining rods for the redwood impact limiters are SA-276, Type 304 stainless steel, having yield and ultimate strengths of 30 ksi and 75 ksi, respectively. Therefore, the redwood impact limiter attachment evaluation presented in Section 2.6.7.4.1.4, bounds the balsa impact limiter attachment design.

Figure 2.6.7.4.2-1 Three-Dimensional View of the Balsa Impact Limiter

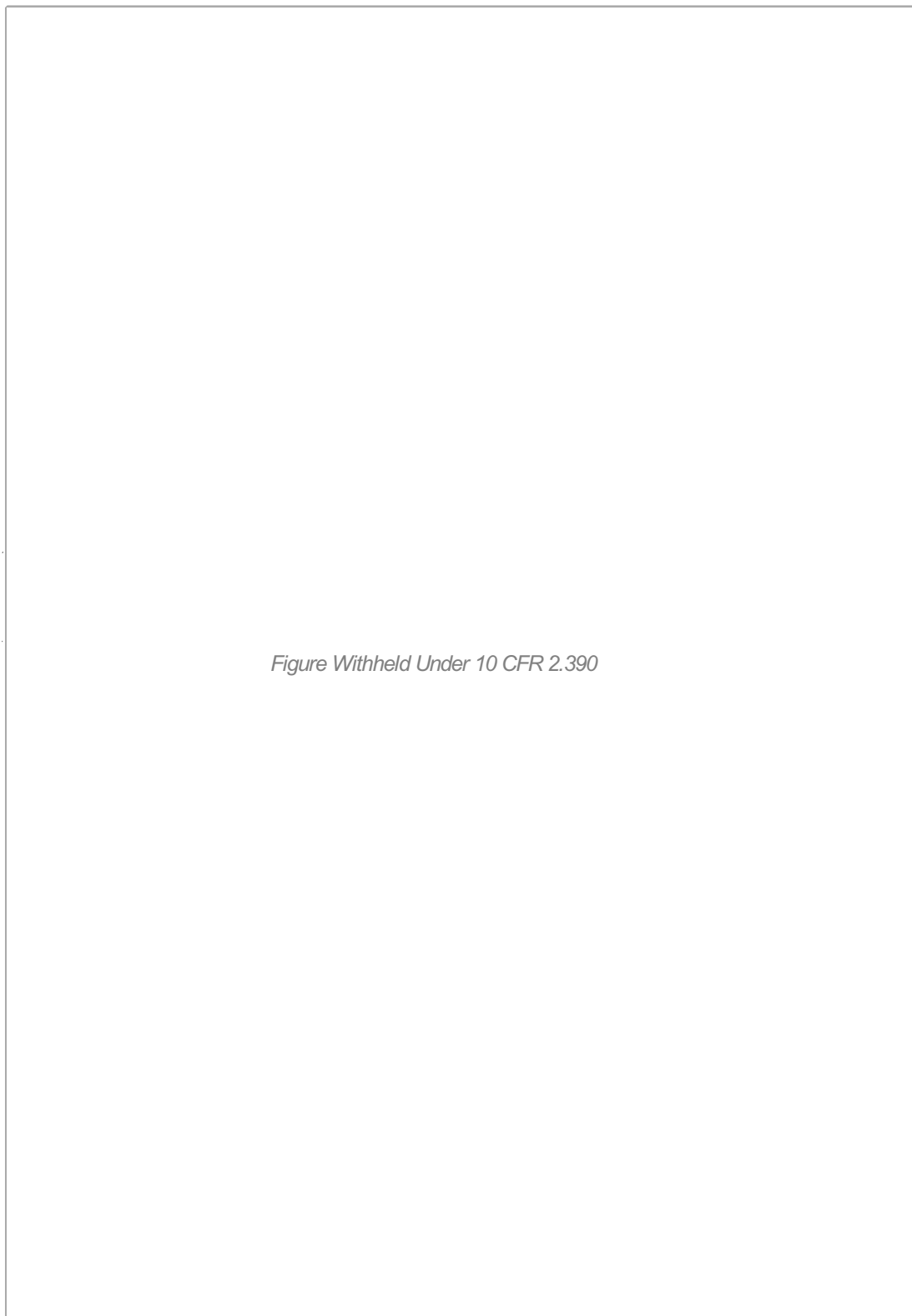


Figure 2.6.7.4.2-2 Cross-Sectional View of the Balsa Impact Limiter

Figure Withheld Under 10 CFR 2.390

Figure 2.6.7.4.2-3 LS-DYNA Model of the Balsa Impact Limiter

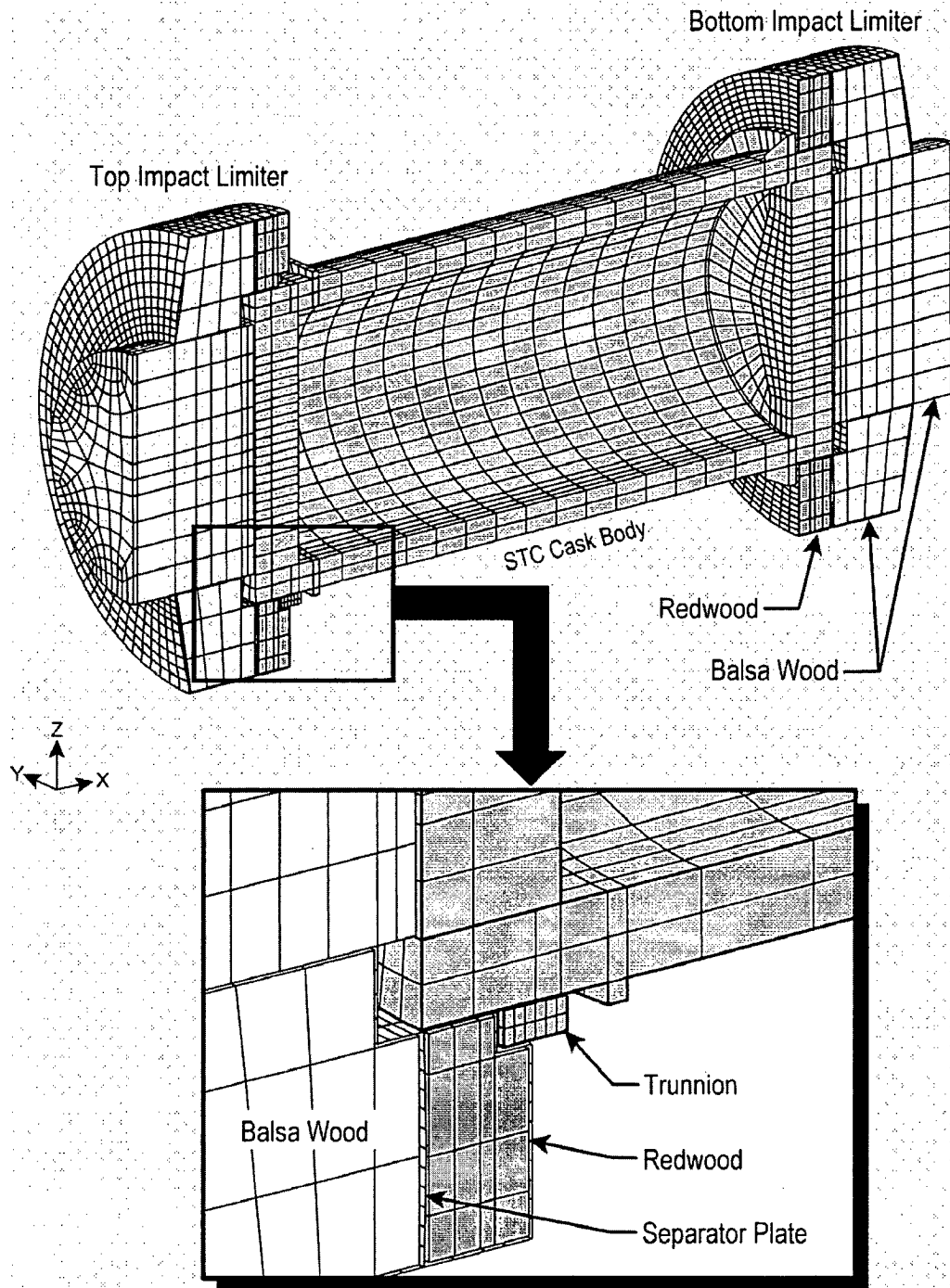


Figure 2.6.7.4.2-4 Balsa Impact Limiter Drop Orientations

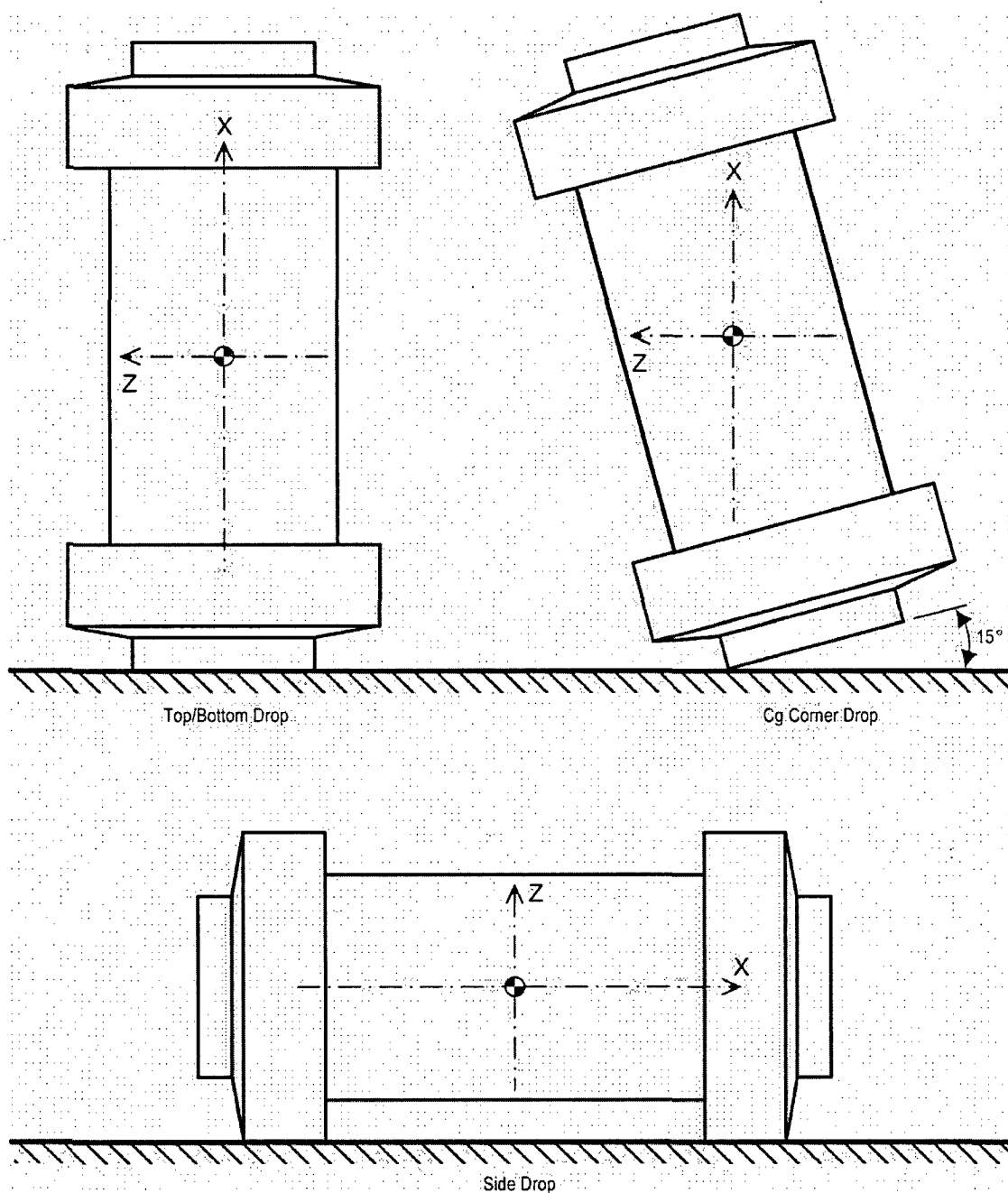


Figure 2.6.7.4.2-5 Acceleration Time-History for 1-ft Side Drop on the Trunnion (Cold Conditions)

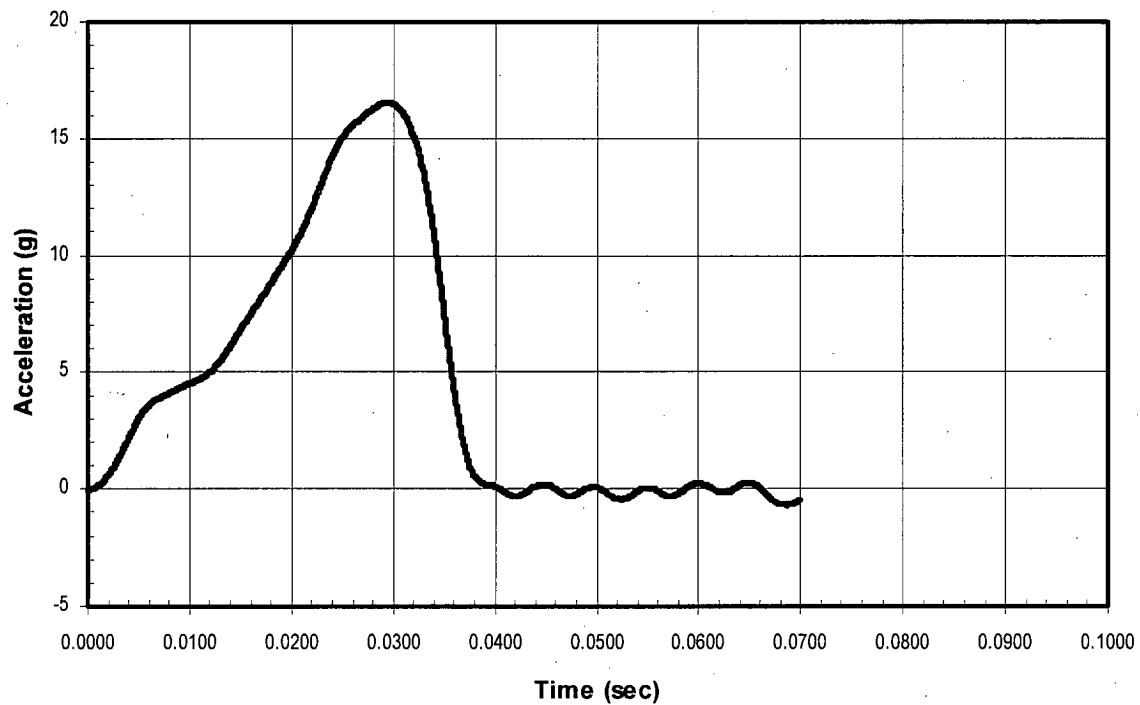


Figure 2.6.7.4.2-6 Acceleration Time-History for 1-ft End Drop (Cold Conditions)

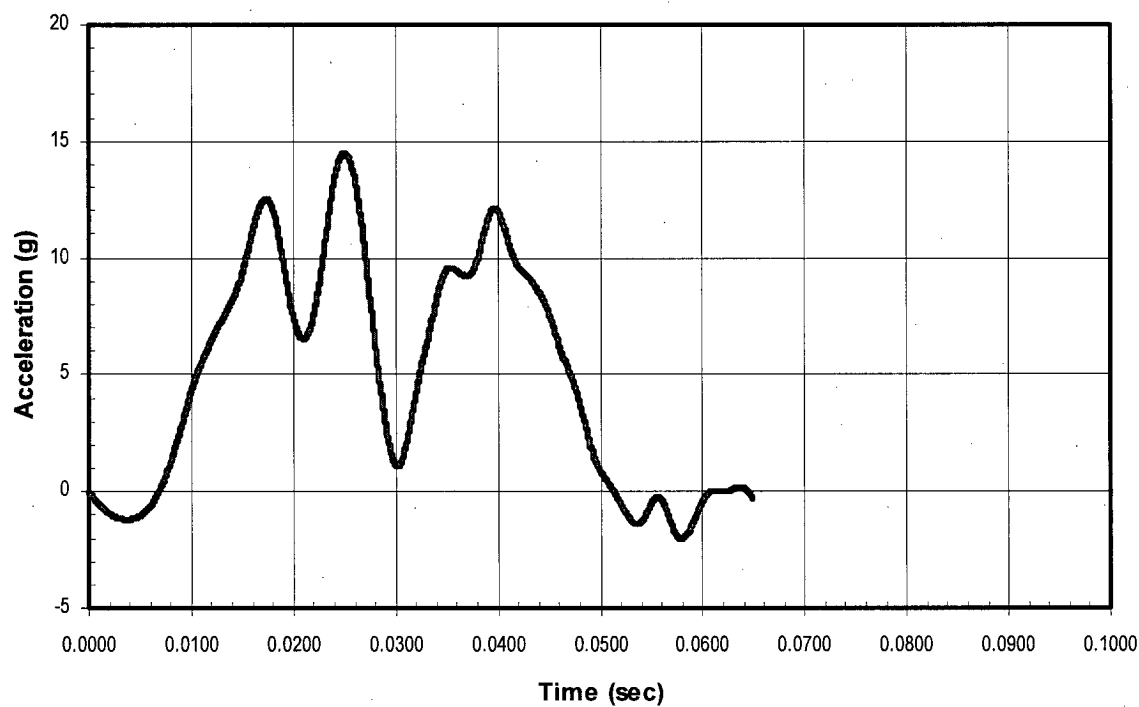


Figure 2.6.7.4.2-7 Acceleration Time-History for 1-ft Drop onto Corner (Cold Conditions)

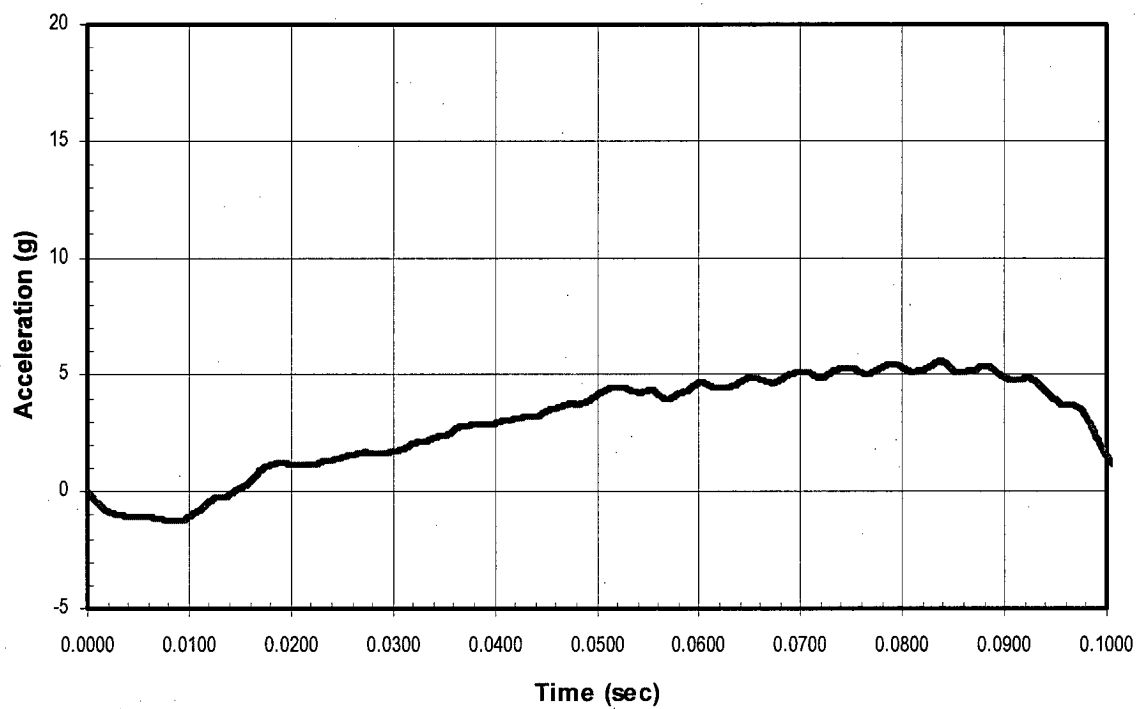


Figure 2.6.7.4.2-8 Acceleration Time-History for 30-ft Side Drop (Hot and Cold Conditions)

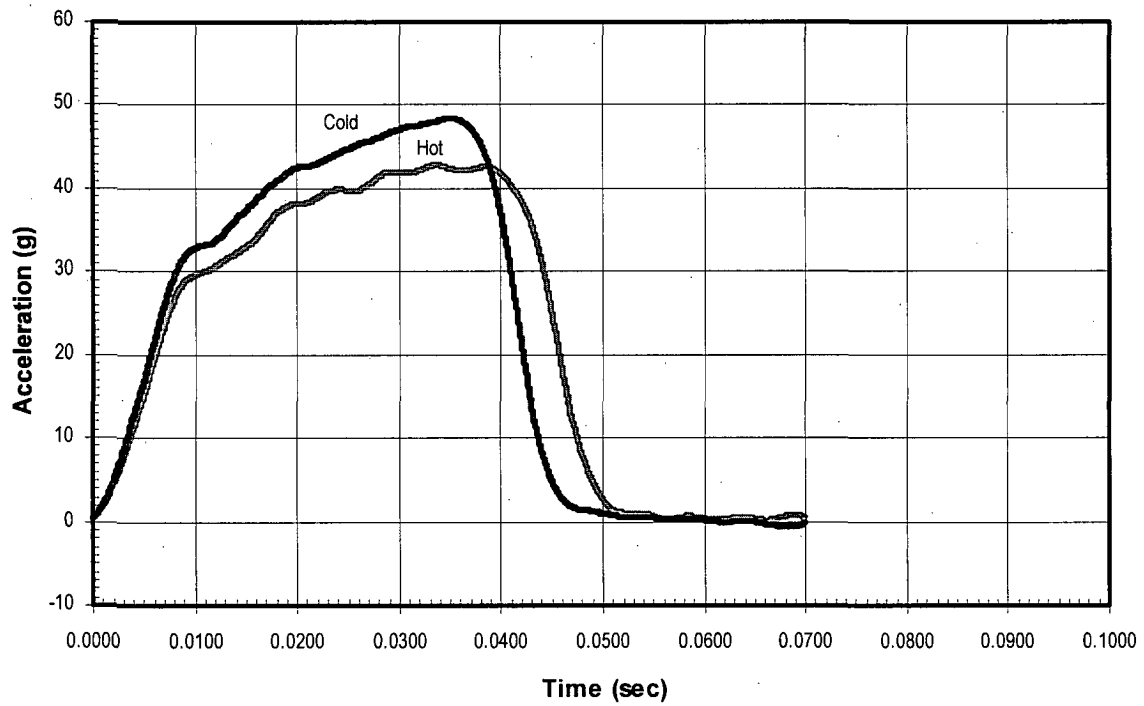


Figure 2.6.7.4.2-9 Acceleration Time-History for 30-ft End Drop (Hot and Cold Conditions)

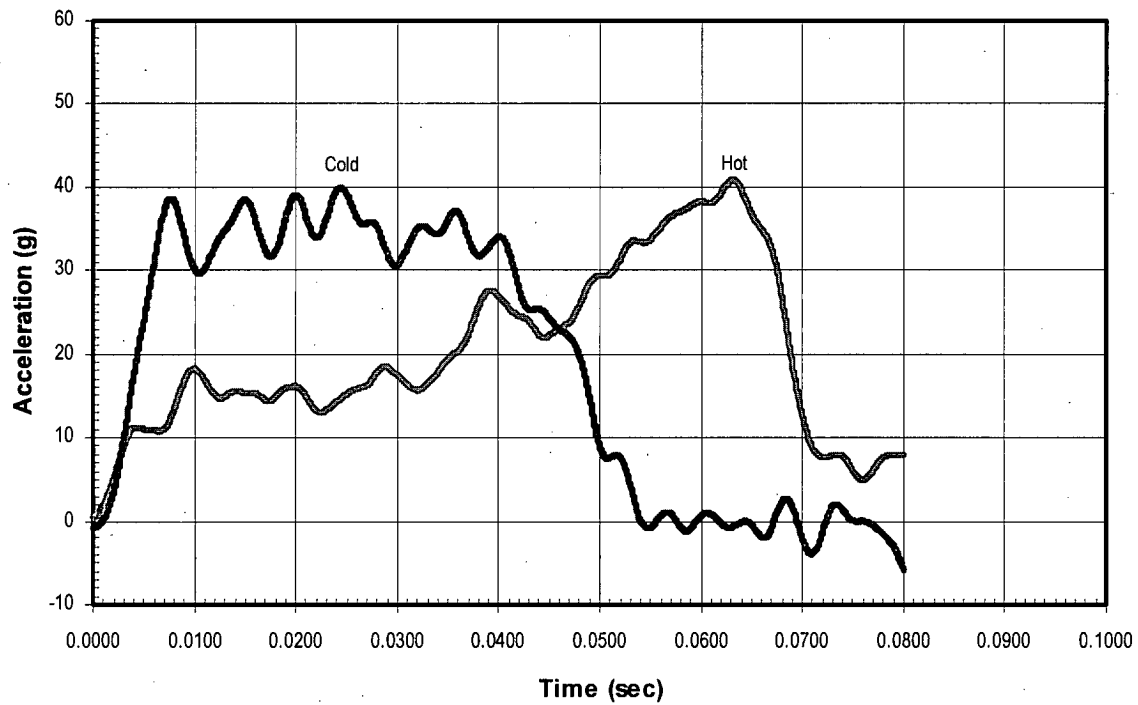


Figure 2.6.7.4.2-10 Acceleration Time-History for 30-ft Drop onto Corner (Hot and Cold Conditions)

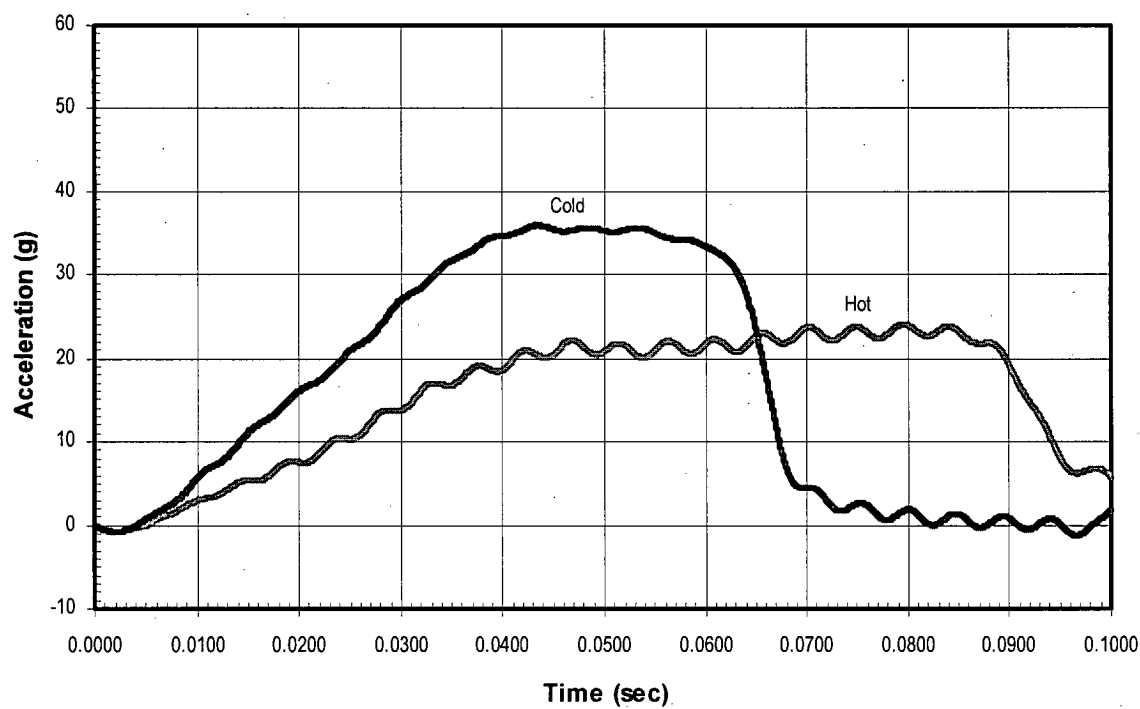


Table 2.6.7.4.2-1 Redwood Stress-Strain Properties

Strain (in/in)	Parallel to Grain—Stress (psi)			
	Hot Static	Hot 25 ϵ /sec	Cold Static	Cold 25 ϵ /sec
0.000	0	0	0	0
0.100	3736	5859	9294	8506
0.400	3685	4996	8531	10734
0.700	10004	15458	22085	19683

Strain (in/in)	Perpendicular to Grain—Stress (psi)			
	Hot Static	Hot 25 ϵ /sec	Cold Static	Cold 25 ϵ /sec
0.000	0	0	0	0
0.100	542	968	1396	1629
0.400	849	1363	2054	2608
0.700	7433	13553	17631	19017

Table 2.6.7.4.2-2 Balsa Wood Stress-Strain Properties

Strain (in/in)	Parallel to Grain—Stress (psi)			
	Hot Static	Hot 25 ϵ /sec	Cold Static	Cold 25 ϵ /sec
0.000	0	0	0	0
0.100	1724	1385	2306	2546
0.400	1550	1150	2073	2805
0.700	1550	1040	2073	2370

Strain (in/in)	Perpendicular to Grain—Stress (psi)			
	Hot Static	Hot 25 ϵ /sec	Cold Static	Cold 25 ϵ /sec
0.000	0	0	0	0
0.100	121	105	161	215
0.400	109	144	145	293
0.700	109	300	145	611

Table 2.6.7.4.2-3 Summary of Results for the Balsa Impact Limiter Normal Conditions of Transport Drop Analysis

Drop Orientation	Cold Condition (-40°F)	
	Normal Acceleration (g)	Design Acceleration (g)
Side	16.5	20.0
Top/Bottom End	14.5	20.0
c.g. over Corner	5.6	20.0

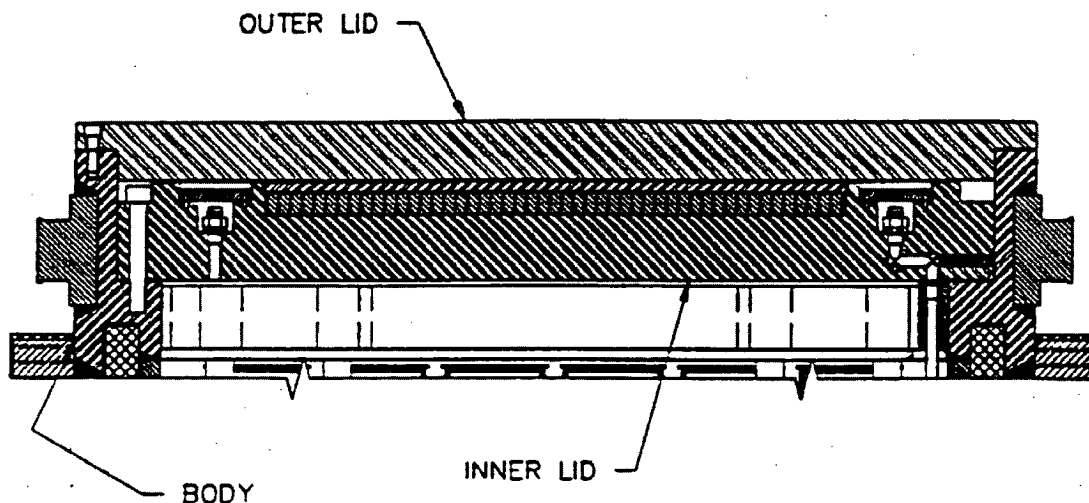
Table 2.6.7.4.2-4 Summary of Results for the Balsa Impact Limiter Hypothetical Accident Conditions Drop Analysis

Drop Orientation	Hot Condition (200°F)			Cold Condition (-40°F)			Maximum Acceleration × DLF	Design Acceleration (g)
	Accident Acceleration (g)	Crush Depth (in.)	Percent Strain	Accident Acceleration (g)	Crush Depth (in.)	Percent Strain		
Side	42.9	12.8	72%	48.5	11.9	70%	49.5	55.0
Top/Bottom End	40.8	21.0	55%	39.9	12.5	33%	40.8	48.0
c.g. over Corner	24.2	29.2	66%	36.0	21.1	48%	—	48.0

THIS PAGE INTENTIONALLY LEFT BLANK

2.6.7.5 Closure Analysis - Normal Conditions of Transport

The main closure of the NAC-STC is affected by an assembly of a bolted inner lid and a bolted outer lid. The Type 304 stainless steel inner lid is bolted to the top forging by forty-two 1 1/2 - 8 UN bolts fabricated from SB-637, Grade N07718 nickel alloy bolting material and is sealed by two O-rings. The SA-705, Type 630, 17-4 PH stainless steel outer lid is bolted to the end of the top forging by thirty-six 1 - 8 UNC bolts fabricated from SA-564, Type 630, 17-4 PH stainless steel, and is sealed to the top forging by one O-ring.



Closure Assembly of NAC-STC Body and Lids

2.6.7.5.1 Closure Geometry

The main body of the inner lid is 9.0 inches thick and 79.0 inches in diameter. A 3.0-inch thick, 2.75-inch wide integral outer rim on the top of the inner lid encloses a 2.0-inch thick layer of NS-4-FR neutron shielding material and a 1.0-inch thick, Type 304 stainless steel coverplate. The inner lid provides the primary containment for the NAC-STC main closure.

The outer lid is a plate consisting of a 5.25-inch thick central body having a 79.08-inch diameter and a 2.50-inch thick integral outer flange having an outside diameter of 86.70 inches. There is a 0.06-inch gap between the inner lid and the outer lid.

2.6.7.5.2 Closure Analysis Considerations

The closure assembly analysis must demonstrate that the lids and bolts satisfy two criteria: (1) calculated maximum stresses must be less than the allowable stress limit (the material yield strength is conservatively selected) and (2) lid deformation and/or rotation at the O-ring locations must be less than the elastic rebound of the O-rings.

Finite element evaluations of the closure are performed using the ANSYS computer program and a two-dimensional axisymmetric model. The critical design load conditions for the NAC-STC closure are three 10 CFR 71 accident loading conditions: (1) impact limiter crush pressure on the outer lid; (2) pin puncture on the outer lid; and (3) impact of the cavity contents on the inner lid. These accident condition analyses are presented in Section 2.7.1.6. The lids and bolts are evaluated at a temperature of 200°F and 270°F, respectively. The impact stresses in the closure components for the normal conditions of transport 1-foot drop are calculated by ratioing the impact stresses calculated in Section 2.7.1.6 according to the g-loads documented in Table 2.6.7.4-3.

The package geometry, package weight, and contents weight are the parameters that control the closure design. This fact is demonstrated to be true by the analysis results in Tables 2.6.7.5-1, -2, -3, and -4, as well as Tables 2.7.1.6-2, -3, -4, and -5. The tables show that the inner lid and bolts (the containment boundary) are critical for end or "near end" impact load conditions and the outer lid bolts are critical for side or "near side" impact load conditions. The closure evaluation presented in this section is for the package (loaded NAC-STC cask with impact limiters as described on the drawings in Section 1.3.2) with a total weight of 260,000 pounds and a cavity contents weight of 67,196 pounds. This evaluation envelopes all of the NAC-STC cask configurations, i.e., the directly loaded fuel configuration, the canistered fuel configuration, and the canistered GTCC waste configuration. The package geometry is identical for all of the configurations. Therefore, the closure analyses in this section and in Sections 2.7.1.6, 2.7.3.4, and 2.10.8 are applicable for the directly loaded and the canistered configurations of the NAC-STC.

2.6.7.5.3 Closure Analysis Results

2.6.7.5.3.1 Description

The critical normal conditions of transport loading for the inner lid is the 1-foot top end drop. Since the 45.1 psig maximum internal operating pressure (Section 4.2.2.1), produces a minimal portion of the inner lid stress, approximately 1,500 psi (Table 2.10.4-1, Sections U, V, W, and X), the maximum inner lid primary membrane plus bending stress for the 1-foot top end drop is calculated by ratioing from the 30-foot top end drop result shown in Table 2.7.1.6-1 (Load Condition 1):

$$S_{IL} = (18,088)(19.6/56.1) = 6,320 \text{ psi}$$

For the inner lid primary membrane plus primary bending stress ($P_m + P_b$) the allowable stress limit is $1.5 S_m$, which for Type 304 stainless steel is 30.0 ksi at 200°F.

Then,

$$MS = \frac{1.5S_m}{S_{IL}} - 1 = \underline{+Large}$$

The critical normal conditions of transport loading for the outer lid is also the 1-foot top end drop. The outer lid is loaded on its outer surface by the crush pressure of the upper impact limiter. The maximum outer lid primary membrane plus bending stress for the 1-foot top end drop is calculated by ratioing from the 30-foot top end drop result shown in Table 2.7.1.6-1 (Load Condition 1):

$$S_{OL} = (19,647)(19.6/56.1) = 6,864 \text{ psi}$$

For the outer lid primary membrane plus bending stress ($P_m + P_b$), the allowable stress limit is $1.5 S_m$, which for Type 17-4 PH, H1150 stainless steel is 67.5 ksi at 200°F.

Then,

$$MS = \frac{1.5S_m}{S_{OL}} - 1 = \underline{+Large}$$

2.6.7.5.4 Lid Bolt Analysis - Normal Conditions of Transport

The NAC-STC inner and outer lid bolts are preloaded at installation to ensure that the sealing function of the O-rings located in the inner and in the outer lids is maintained. The lid bolts are installed with a torque that is calculated to produce a total tensile load that is not less than the total load on the lid bolts; that is, the sum of: (1) internal pressure force on the lid; (2) O-ring compression force; (3) inertial weight of the lid (calculated weight multiplied by the impact load factor); and (4) inertial weight of any other components that can contact the lid (calculated weight multiplied by the impact load factor). Since the total bolt preload exceeds the total load on the lid, there is no movement of the lid relative to its mating component and the status of the seal at the O-ring(s) is maintained.

2.6.7.5.4.1 Inner Lid Bolts

The inner lid of the NAC-STC is bolted to the top forging of the cask body by forty-two 1 1/2 - 8 UN bolts that are fabricated from SB-637, Grade N07718 nickel alloy bolting material. An installation torque of $2,540 \pm 200$ foot-pounds is selected for the inner lid bolts.

Minimum Preload Evaluation

The required minimum preload on the inner lid bolts considers the following factors: (1) an internal pressure force on the inner lid of 45.3 psig (60 psia); (2) the O-ring compression force due to the two metallic O-rings for the inner lid (which bounds the compression force for the non-metallic [EPDM and Viton] O-rings); and (3) the inertial load of the inner lid and cask contents due to the 30-foot accident drop event.

The inertial load used to determine the required bolt preload is determined by the weight of the cask contents multiplied by the design g-load for the applicable 30-foot drop. The cask contents weight is 66,690 pounds and 77,885 pounds for the Yankee-MPC and CY-MPC configurations, respectively. The design g-load for the 30-foot end drop is 56.1g for the Yankee-MPC (redwood impact limiters, see Table 2.6.7.4.1-4), and is 48g for the CY-MPC (balsa impact limiters, Table 2.6.7.4.2-2). Since $66,690 \times 56.1$ is greater than $77,885 \times 48$, the cask content weight and g-load corresponding to the Yankee-MPC are used to determine the bolt preload. The required preload torque is calculated to be less than the minimum design torque (2,540 – 200 ft-lbs). Detailed analysis is provided in Section 2.10.8.2.1.

Bolt Stress Evaluation

The maximum preload on the inner lid bolts in combination with the internal pressure force on the lid, the O-ring compression force on the lid, thermally induced loads and the inertial load of the inner lid and cask contents due to the normal conditions of transport 1-foot drop must not exceed the allowable strength of the inner lid bolts.

A complete range of impact orientations is evaluated, from an end impact at 0° to a side impact at 90°, using 5° increments. A design acceleration of 20g is considered for all impact orientations in the bolt evaluation for normal conditions for both impact limiter designs (redwood and balsa). The cask contents weight for the CY-MPC is used since it bounds the cask content weight of the Yankee-MPC configuration. The details of this evaluation are described and an example calculation is provided in Section 2.10.8.2 for the hypothetical accident condition. Normal conditions of transport results are summarized in Tables 2.6.7.5-1 and 2.6.7.5-2, corresponding to a "hot" condition and a "cold" condition, respectively. The hot condition bolt temperatures are assumed to be 200°F, as summarized in Table 3.4-5. The cold condition bolt temperature is assumed to be -20°F, in accordance with regulatory requirements. Physical properties for the SB-637 Grade N07718 nickel alloy bolts are conservatively taken at 270°F for both hot and cold conditions. As defined in Table 2.1.2-1, the allowable maximum bolt stress for normal conditions for primary membrane stress is two times the design stress intensity, $2S_m$, resulting in an allowable direct tension stress of 94.5 ksi at 270°F. As shown in Tables 2.6.7.5-1 and 2.6.7.5-2, the total bolt stress is calculated to be less than the allowable stress for normal conditions of transport. The minimum margin of safety is +0.06.

Bolt Thread Engagement Evaluation

The ultimate load capacity of the inner lid bolt/top forging threaded connection relative to the ultimate tensile load capacity of the inner lid bolt is evaluated to ensure that the length of engagement is sufficient to develop the full strength of the bolt. The inner lid bolt holes have threaded inserts to protect the threads during the installation and removal of the bolts.

Component Description

- | | |
|----------------|---|
| Inner lid Bolt | <ul style="list-style-type: none">- 1 1/2 - 8 UN- SB-637, Grade N07718 Nickel Alloy Steel Bolting Material- Length in cask body = 2.63 inches- $S_u = 174.7$ ksi at 270°F |
|----------------|---|

- Threaded Insert
- Helicoil #4190-24 CN x 2.50
 - (AMS 7245) 18-8 Stainless Steel
 - Length of insert = 2.50 inches
 - O.D. = 1 5/8 - 8 UN Thread
 - $S_u = 200.0$ ksi
- Top Forging (Cask Body)
- Type 304 Stainless Steel
 - Thread depth = $3.0 - 0.125 = 2.875$ in
 - $S_u = 62.9$ ksi at 270°F

Bolt Strength

$$\begin{aligned}\text{Tensile Area, } A_t &= 1.492 \text{ in}^2 \text{ (1 1/2 - 8 UN Thread)} \\ \text{Tensile Strength, } S_u &= 174.8 \text{ ksi} \\ \text{Bolt-Tensile Load Capacity, } P_{BLC} &= (1.492)(174,700) \\ &= 260,652 \text{ lbs}\end{aligned}$$

Threaded Insert/Bolt Interface

$$\begin{aligned}\text{Thread Size} &= 1 \frac{1}{2} - 8 \text{ UN} \\ \text{Engaged Length} &= 2.50 - 0.12 = 2.38 \text{ in} \\ \text{Bolt: } S_u &= 174.7 \text{ ksi} \\ \text{Insert: } S_u &= 200.0 \text{ ksi}\end{aligned}$$

External (Bolt) Thread Shear Area

$$\begin{aligned}AS_s &= (\pi)(n)(L_e)(K_{nmax})[(1/2n) + (0.57735)(E_{Smin} - K_{nmax})]^* \\ &= 6.123 \text{ in}^2\end{aligned}$$

where:

$$\begin{aligned}n &= 8 \text{ threads/in} \\ L_e &= 2.38 \text{ in} \\ E_{smin} &= 1.4093 \text{ in Min. Pitch Diameter of External Threads} \\ K_{nmax} &= 1.390 \text{ in Max. Minor Diameter of Internal Threads}\end{aligned}$$

* FED-STD-H28 (1963), Page 103.

$$\begin{aligned}\text{Bolt Thread-Tensile Load Capacity, } P_{BT} &= (6.123)(0.5^* \times 174,700) \\ &= 534,844 \text{ lbs}\end{aligned}$$

Internal (Insert) Thread Shear Area

$$\begin{aligned}AS_n &= (\pi)(n)(L_e)(D_{Smin})[(1/2n) + (0.57735)(D_{Smin} - E_{nmax})]** \\ &= 8.334 \text{ in}^2\end{aligned}$$

where:

$$\begin{aligned}D_{smin} &= 1.4828 \text{ in Min. Major Diameter of External Thread} \\ E_{nmax} &= 1.4283 \text{ in Max. Pitch Diameter of Internal Thread}\end{aligned}$$

$$\begin{aligned}\text{Insert Thread-Tensile Load Capacity, } P_{ITI} &= (8.334) (0.5^* \times 200,000) \\ &= 833,430 \text{ lbs}\end{aligned}$$

Threaded Insert/Top Forging Interface

$$\begin{aligned}\text{Thread Size} &= 1 \frac{5}{8} - 8 \text{ UN} \\ \text{Engaged Length} &= 2.50 - 0.12 = 2.38 \text{ in} \\ \text{Insert: } S_u &= 200 \text{ ksi} \\ \text{Top Forging: } S_u &= 62.9 \text{ ksi}\end{aligned}$$

External (Insert) Thread Shear Area

$$\begin{aligned}AS_s &= (\pi)(n)(L_e)(K_{nmax})[(1/2n) + (0.57735)(E_{Smin} - K_{nmax})]** \\ &= 6.668 \text{ in}^2\end{aligned}$$

* Shear Strength Conservatively Assumed = (0.5)(Tensile Strength).

** FED-STD-H28 (1963), page 103.

where:

$$\begin{aligned}n &= 8 \text{ threads/inch} \\L_e &= 2.38 \text{ in} \\E_{smin} &= 1.5342 \text{ in Min. Pitch Diameter of External Threads} \\K_{nmax} &= 1.515 \text{ in Max. Minor Diameter of Internal Threads}\end{aligned}$$

$$\begin{aligned}\text{Insert Thread-Tensile Load Capacity, } P_{ITO} &= (6.668)(0.5^* \times 200,000) \\&= 666,800 \text{ lbs}\end{aligned}$$

Internal (Top Forging) Thread Shear Area

$$\begin{aligned}AS_n &= (\pi)(n)(L_e)(D_{Smin})[(1/2n) + (0.57735)(D_{Smin} - E_{nmax})]** \\&= 9.026 \text{ in}^2\end{aligned}$$

where:

$$\begin{aligned}D_{smin} &= 1.6078 \text{ in Min. Major Diameter of External Thread} \\E_{nmax} &= 1.5535 \text{ in Max. Pitch Diameter of Internal Thread}\end{aligned}$$

$$\begin{aligned}\text{Top Forging Thread - Tensile Load Capacity, } P_{TFT} &= (9.026)(0.5^* \times 62,900) \\&= 283,868 \text{ lbs}\end{aligned}$$

<u>Component</u>	Ultimate Load Capacity
	<u>(lbs)</u>
Inner Lid Bolt	260,652
Bolt Thread	534,844
Insert I.D. Thread	833,430
Insert O.D. Thread	666,800
Top Forging Thread	283,868

$$MS = (283,868/260,652) - 1 = +0.09$$

Since the minimum Tensile Load Capacity of the threaded joint exceeds the maximum Tensile Load Capacity of the inner lid bolt, the design requirements are satisfied. The inner lid bolt threaded-joint design is satisfactory.

* Shear Strength Conservatively Assumed = (0.5)(Tensile Strength).

** FED-STD-H28 (1963), page 103.

Using consistently conservative assumptions, the NAC-STC inner lid is shown to satisfy the performance and structural integrity requirements of 10 CFR 71.71(c)(7) for normal conditions of transport.

2.6.7.5.4.2 Outer Lid Bolts

The outer lid of the NAC-STC is bolted to the end of the top forging by thirty-six 1 - 8 UNC bolts that are fabricated from SA-564, Type 630, H1150, 17-4 PH stainless steel, which has mechanical properties that are identical to those of the material of the outer lid (SA-705, Type 630, H1150, 17-4 PH stainless steel). Thus, there is negligible differential thermal expansion between the outer lid bolts and the outer lid, since they are at essentially the same temperature and have the same mechanical properties.

The required preload on the outer lid bolts considers the following factors: (1) a conservative interlid pressure force on the outer lid of 7.35 psig (1.5 atm absolute) to provide operational flexibility; (2) the O-ring compression force due to the metallic O-ring located between the cask forging and the outer lid (which bounds the compression force for the non-metallic [EPDM and Viton] O-rings); and (3) the inertial weight of the outer lid and impact limiter, due to the 30-foot accident drop conditions, considering the impact limiter together with the outer lid for the 30-foot accident drop condition envelopes the transport conditions when the influence of the impact limiter is actually transmitted to the outer lid bolts. Based on these loading conditions for the outer lid bolts, an installation torque of 550 ± 50 foot-pounds is conservatively selected for the outer lid bolts. The required preload torque is calculated to be less than the required minimum torque. The detailed analysis is presented in Section 2.10.8.3.1.

The outer lid bolts are evaluated under normal transport conditions in the same manner as the inner lid bolts were evaluated in Section 2.6.7.5.4.1. The method of analysis used is described and an example calculation is performed in Section 2.10.8.3. The lid impact loads are assumed to impose unequal forces in the closure bolts. A complete range of impact orientations is evaluated, from an end impact at 0 degrees to a side impact at 90 degrees, at 5-degree increments. A design acceleration of 20g is considered for all impact orientations in the bolt evaluation for normal conditions for both impact limiter designs (redwood and balsa).

Table 2.6.7.5-3 summarizes the results of the evaluation of the outer lid bolt stresses under the normal conditions of transport corresponding to a "hot" condition and a "cold" condition,

respectively. The hot condition bolt temperature is taken at 200°F, as summarized in Table 3.4-5. The cold condition bolt temperature is assumed to be -20°F, per regulatory requirements. Physical properties for the SA-564, Type 630, H1150, 17-4 PH stainless steel bolt material are conservatively taken at 270°F for both the hot and cold condition. As defined in Table 2.1.2-1, the allowable primary membrane stress is taken as $2S_m$, resulting in allowable direct tension stresses of 90,000 psi. As shown in Table 2.6.7.5-3, the total bolt stress is calculated to be less than the allowable stress for normal conditions of transport. The minimum margin of safety is + 0.42.

Bolt engagement may be evaluated by computing shear stresses within the SA-336, Type 304, inner lid. At 270°F, the allowable shear stress is $0.6S_m$, or 12.0 ksi, according to Table 2.3.2-2. The maximum tensile bolt load is found as the product of the maximum bolt stress intensity, noted above, and the bolt stress area ($63,343 \times 0.606 = 38,386$ lbs). The shear area per inch of engagement for a 1 - 8 UNC internal thread is 2.325 square inches (Screw-Thread Standards for Federal Services). The resultant shear stress and margin of safety within the inner lid forging is:

$$\begin{aligned}\tau &= 38,386 / (2.325)(2.0) \\ &= 8,255 \text{ psi}\end{aligned}$$

$$MS = (12,000 / 8,255) - 1 = + 0.45$$

2.6.7.5.5 Conclusion

Using consistently conservative assumptions, the NAC-STC closure assembly has been shown to satisfy the performance and structural integrity requirements of 10 CFR 71.71(c)(7) for normal conditions of transport.

Table 2.6.7.5-1 NAC-STC "Hot" Inner Lid Bolt Analysis (Normal Conditions of Transport)

Nominal Bolt Diameter (in):	1.5	Longitudinal Weight (lb):	77,885
Number of Bolts:	42	Lateral Weight (lb):	10,690
Service Stress, 2Sm (ksi):	94,400		
Bolt Expansion (in/in):	7.30E-06 at a 270°F		
Bolt Modulus of Elasticity (ksi):	28,000 Service Temp.		
Lid Expansion (in/in):	8.94E-06	Calculated Loads and Stiffness	
Lid Modulus of Elasticity (ksi):	27,180	Bolt Thermal Load (lb):	13,703
Bolt Stress Area (in ²):	1.492	Bolt Preload (lb):	115,066
		Bolt Static Load (lb):	8,308
Maximum Pressure (psig):	38.1	Bolt Stiffness (lb/in):	4.57E+06
Seal Diameter (in):	73.247	Lid Stiffness (lb/in):	5.40E+07
Preload Torque (ft-lb):	2540+200 room temperature		
Nominal Room Temp. °F:	70		
Bolt Circle Diameter (in):	75.31		
Lid Diameter (in):	79.00		

Angle wrt. Vert. (deg)	Impact Accel. (g)	LOAD (lbs)			STRESS (psi)					Margin of Safety
		Impact		Bolt Tension	Direct	Shear	Principal		Stress	
		Tension	Shear		Tension		S2	S1	Intens.	
0 End	20.0	45396	0	132311	88680	0	0	88680	88680	0.06
5	20.0	49619	444	133289	89336	298	-1	89337	89338	0.06
10	20.0	49052	884	133245	89306	592	-4	89310	89314	0.06
15	20.0	48111	1318	133171	89257	883	-9	89266	89275	0.06
20	20.0	46805	1741	133069	89188	1167	-15	89203	89218	0.06
25	20.0	45142	2151	132940	89102	1442	-23	89125	89148	0.06
30	20.0	43135	2545	132783	88997	1706	-33	89030	89063	0.06
35	20.0	40801	2920	132601	88875	1957	-43	88918	88961	0.06
40	20.0	38155	3272	132394	88736	2193	-54	88790	88844	0.06
45	20.0	35220	3600	132165	88582	2413	-66	88648	88714	0.06
50	20.0	32016	3900	131915	88415	2614	-77	88492	88569	0.07
55	20.0	28569	4170	131646	88235	2795	-88	88323	88411	0.07
60	20.0	24904	4408	131360	88043	2954	-99	88142	88241	0.07
65	20.0	21050	4614	131060	87842	3092	-109	87951	88060	0.07
70	20.0	17035	4783	130746	87631	3206	-117	87748	87865	0.07
75	20.0	12891	4917	130423	87415	3296	-124	87539	87663	0.08
80	20.0	8649	5013	130092	87193	3360	-129	87322	87451	0.08
85	20.0	4341	5071	129756	86968	3399	-133	87101	87234	0.08
90 Side	20.0	0	5090	129417	86741	3412	-134	86875	87009	0.08

Table 2.6.7.5-2 NAC-STC "Cold" Inner Lid Bolt Analysis (Normal Conditions of Transport)

Nominal Bolt Diameter (in):	1.5	Longitudinal Weight (lb):	77,885
Number of Bolts:	42	Lateral Weight (lb):	10,690
Service Stress, 2Sm (ksi):	94,400		
Bolt Expansion (in/in):	7.30E-06 at 270°F		
Bolt Modulus of Elasticity (ksi):	28,000 Service Temp.		
Lid Expansion (in/in):	8.94E-06	Calculated Loads and Stiffness	
Lid Modulus of Elasticity (ksi):	27,180	Bolt Thermal Load (lb):	0
Bolt Stress Area (in ²):	1.492	Bolt Preload (lb):	115,066
		Bolt Static Load (lb):	8,308
Maximum Pressure (psig):	38.1	Bolt Stiffness (lb/in):	4.57E+06
Seal Diameter (in):	73.247	Lid Stiffness (lb/in):	5.40E+07
Preload Torque (ft-lb):	2540+200 room temperature		
Nominal Room Temp. °F:	70		
Bolt Circle Diameter (in):	75.31		
Lid Diameter (in):	79.00		

Angle wrt. Vert. (deg)	Impact Accel. (g)	LOAD (lbs)				STRESS (psi)					Margin of Safety
		Impact		Bolt Tension	Direct Tension	Shear	Principal		Stress Intens.		
		Tension	Shear				S2	S1			
0	End	20.0	45396	0	118608	79496	0	0	79496	79496	0.19
5		20.0	49619	444	119586	80151	298	-1	80152	80153	0.18
10		20.0	49052	884	119542	80122	592	-4	80126	80130	0.18
15		20.0	48111	1318	119468	80072	883	-10	80082	80092	0.18
20		20.0	46805	1741	119366	80004	1167	-17	80021	80038	0.18
25		20.0	45142	2151	119237	79918	1442	-26	79944	79970	0.18
30		20.0	43135	2545	119080	79812	1706	-36	79848	79884	0.18
35		20.0	40801	2920	118898	79690	1957	-48	79738	79786	0.18
40		20.0	38155	3272	118691	79552	2193	-60	79612	79672	0.18
45		20.0	35220	3600	118462	79398	2413	-73	79471	79544	0.19
50		20.0	32016	3900	118212	79231	2614	-86	79317	79403	0.19
55		20.0	28569	4170	117943	79050	2795	-99	79149	79248	0.19
60		20.0	24904	4408	117657	78859	2954	-110	78969	79079	0.19
65		20.0	21050	4614	117357	78658	3092	-121	78779	78900	0.20
70		20.0	17035	4783	117043	78447	3206	-131	78578	78709	0.20
75		20.0	12891	4917	116720	78231	3296	-139	78370	78509	0.20
80		20.0	8649	5013	116389	78009	3360	-144	78153	78297	0.21
85		20.0	4341	5071	116053	77784	3399	-148	77932	78080	0.21
90	Side	20.0	0	5090	115714	77556	3412	-150	77706	77856	0.21

Table 2.6.7.5-3 NAC-STC "Hot and Cold" Outer Lid Bolt Analysis (Normal Conditions of Transport)

Nominal Bolt Diameter (in):	1	Longitudinal Weight (lb):	16,985
Number of Bolts:	36	Lateral Weight (lb):	8,120
Service Stress, 2Sm (psi):	90,000		
Bolt Expansion (in/in):	5.90E-06 at a 270°F		
Bolt Modulus of Elasticity (ksi):	27,300 Service Temp.		
Lid Expansion (in/in):	5.90E-06	Calculated Loads and Stiffness	
Lid Modulus of Elasticity (ksi):	27,300	Bolt Thermal Load (lb):	0
Bolt Stress Area (in ²):	0.606	Bolt Preload (lb):	36,810
		Bolt Static Load (lb):	4,000
		Bolt Stiffness (lb/in):	5.49E+06
Maximum Pressure (psig):	7.35	Lid Stiffness (lb/in):	6.83E+07
Seal Diameter (in):	81.81		
Preload Torque (ft-lb):	550+50		
Nominal Room Temp. °F:	70		
Bolt Circle Diameter (in):	83.7		
Lid Diameter (in):	86.7		

Angle wrt. Vert. (deg)	Impact Accel. (g)	LOAD (lbs)			STRESS (psi)					Margin of Safety
		Impact		Bolt Tension	Direct	Shear	Principal		Stress	
		Tension	Shear		Tension		S2	S1	Intens.	
0	End	13436	0	37810	62393	0	0	62393	62393	0.44
5		12601	393	38045	62781	649	-7	62788	62795	0.43
10		12457	783	38034	62762	1292	-27	62789	62816	0.43
15		12218	1168	38017	62734	1927	-59	62793	62852	0.43
20		11886	1543	37992	62693	2546	-103	62796	62899	0.43
25		11464	1906	37961	62642	3145	-158	62800	62958	0.43
30		10954	2256	37923	62579	3723	-221	62800	63021	0.43
35		10361	2587	37878	62505	4269	-290	62795	63085	0.43
40		9690	2900	37829	62424	4785	-365	62789	63154	0.43
45		8944	3190	37773	62332	5264	-441	62773	63214	0.42
50		8131	3456	37713	62233	5703	-518	62751	63269	0.42
55		7255	3695	37647	62124	6097	-593	62717	63310	0.42
60		6325	3907	37578	62010	6447	-663	62673	63336	0.42
65		5346	4088	37505	61889	6746	-727	62616	63343	0.42
70		4326	4239	37429	61764	6995	-782	62546	63328	0.42
75		3274	4357	37351	61635	7190	-828	62463	63291	0.42
80		2196	4443	37271	61503	7332	-862	62365	63227	0.42
85		1102	4494	37190	61370	7416	-883	62253	63136	0.43
90	Side	0	4511	37108	61234	7444	-892	62126	63018	0.43

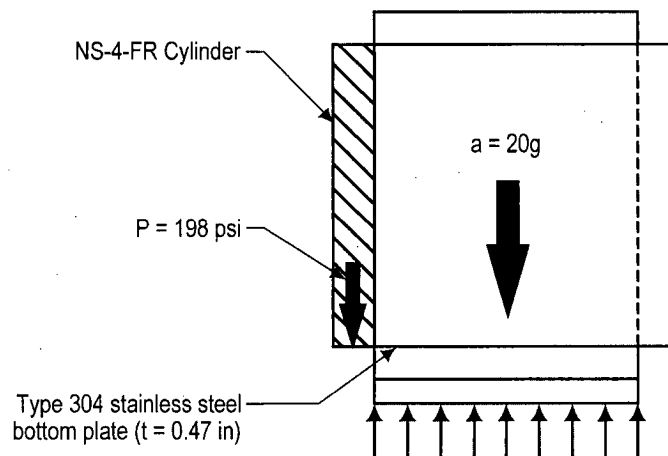
THIS PAGE INTENTIONALLY LEFT BLANK

2.6.7.6 Neutron Shield Analysis

The NAC-STC neutron shield is evaluated for two distributed-load conditions: a 1-foot end drop event and a 1-foot side drop event. For each of these conditions, the solid neutron shielding material applies a load on the neutron shield shell. The weights of the neutron shield shell and fins are included in the analysis. The neutron shield geometry is shown in Figure 2.6.7.6-1.

2.6.7.6.1 End Plate One-Foot End Drop Analysis

The primary loading on the neutron shield shell and end plates is the weight of the NS-4-FR neutron shielding material. The neutron shield is evaluated for the impact loading of the NS-4-FR during a 1-foot bottom end drop event.



The load on the bottom plate, including the weight of the plate itself, is calculated as:

$$\begin{aligned} p &= d_B L + d_p t \\ &= 9.89 \text{ psi} \end{aligned}$$

where:

$$d_B = (1.68) \frac{62.4}{1,728}$$

$$= 0.0607 \text{ lbs/in}^3, \text{ density of NS-4-FR}$$

$$\text{NS-4-FR specific gravity} = 1.68$$

$$L = 160.7 \text{ in, height of NS-4-FR material}$$

$$d_p = 0.288 \text{ lbs/in}^3, \text{ density of Type 304 stainless steel}$$

$$t = 0.472 \text{ in, plate thickness}$$

The deceleration of the package during a 1-foot end drop event is 20 g (Table 2.6.7.4.1-1). The impact load on the plate is calculated as:

$$P_I = p(20)$$

$$= 194 \text{ psi}$$

The material properties (conservatively taken at 300°F) for the Type 304 stainless steel shell, fins, and bottom plate are:

$$S_u = 66.0 \text{ ksi}$$

$$S_y = 22.5 \text{ ksi}$$

$$S_m = 20.0 \text{ ksi}$$

$$S_s = (0.60)S_m$$

$$= 12.0 \text{ ksi}$$

(Allowable Stresses)

The allowable stress intensity for the normal condition loading, according to Regulatory Guide 7.6, is:

$$\text{Axial + Bending } (S_{\text{allow}})_n = 1.5 S_m = 30.0 \text{ ksi}$$

where

$$S_m = 20.0 \text{ ksi for Type 304 stainless steel}$$

Stress Analysis

From Table 26, Case 1a, of Formulas for Stress and Strain, the stress in the end plate is:

$$\sigma_{\max} = \frac{\beta P b^2}{t^2}$$

$$= 18,248 \text{ psi.}$$

where

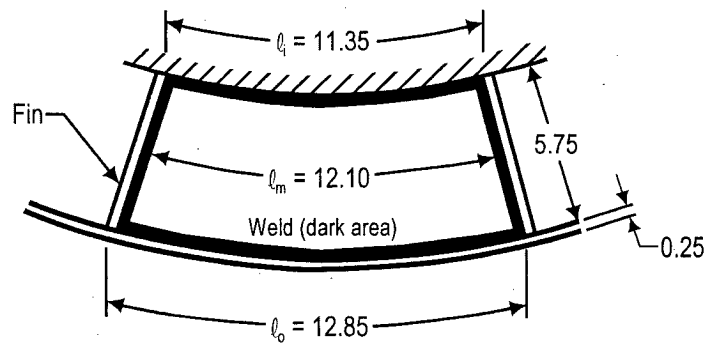
$$\begin{aligned} P &= P_1 = 198 \text{ psi} \\ a &= 12.1 \text{ in} \\ b &= 5.75 \text{ in} \\ t &= 0.472 \text{ in (12 mm)} \\ a/b &= 2.10 \\ \beta &= 0.621 \end{aligned}$$

The margin of safety is:

$$MS = \frac{(\sigma_{\text{allow}})_n}{\sigma_{\max}} - 1 = +0.64$$

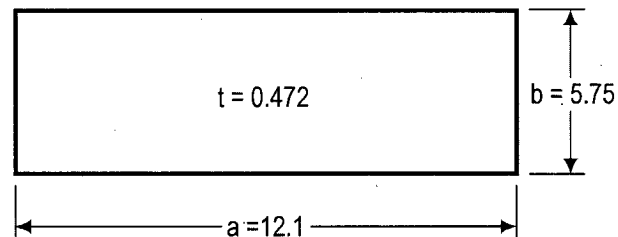
where

$$(\sigma_{\text{allow}})_n = 1.5 S_m = 30,000 \text{ psi}$$



(Dimensions in inches)

Neutron Shield Bottom Plate



(Dimensions in inches)

Equivalent Flat Plate Simply

For the reaction in the welds, assume all welds are quarter-inch fillets, which is conservative.

$$q_w = \frac{(198)(5.75)(12.1)}{(2)(5.75 + 12.1)}$$

$$= 386 \text{ lb/in}$$

$$\begin{aligned} q_i &= \text{allowable shear/inch} \\ &= (S_s)(0.707)(0.25) \\ &= 2,121 \text{ lb/in} \end{aligned}$$

The margin of safety is:

$$MS = \frac{q_i}{q_w} - 1 = +4.49$$

2.6.7.6.2 Side Drop Analysis

This analysis assumes that the cask is subjected to a 1-foot side drop event. The side drop impact force is limited by the upper and lower impact limiters. For this analysis, an impact force that is equivalent to a 20 g side impact is used. The impact limiter stops the cask before the neutron shield contacts the impacted surface. Therefore, the impact force is distributed through the cask body from the impact limiters. The impact deceleration force of the weight of the neutron shielding material is reacted by the neutron shield shell and fins, which transfer the load to the cask body. The NS-4-FR neutron shielding material is assumed to act as an internal pressure on the shell.

Since the structural function of the neutron shield shell and radial heat transfer fin provides support for the NS-4-FR radial neutron shield, ASME Code Section III, Subsection NF, Component Supports, is used as governing structural criteria for the evaluation of the welds connecting the radial heat transfer fins to the neutron shield shell and cask outer shell.

In addition to assuming the conservative load combination resulting from cold impact loads and discontinuity thermal expansion between the NS-4-FR and radial fin from hot steady state conditions, an additional 3 psi pressure is assumed to have been created from potential gas loss from the NS4FR subjected to extended service in a high end temperature environment.

Load on the weld joints has been categorized into the following service level conditions following the methodology of ASME Section III criteria and cask design practice.

Service Level B

- 1) Pressure developed on the neutron shield shell from differential radial thermal expansion of the NS-4-FR neutron shield relative to the Type 304 stainless steel radial heat transfer fin. Considering differential thermal expansion and three percent initial compression of the HT800 expansion foam on the inside surface of the neutron shield shell, compression of the foam develops a service load of:

$$\begin{aligned}\text{Compression} &= 3\% (0.125) + 0.05143 \\ &= 0.05519\end{aligned}$$

$$\begin{aligned}\% \text{ Compression} &= \frac{0.05519}{0.125} \times 100 \\ &= 44.15\%\end{aligned}$$

From the manufacturer design information presented in Table 2.6.7.6-1, the equivalent pressure load developed on the neutron shield shell is 16.8 psi.

- 2) Potential pressure developed from extended service of the NS-4-FR neutron shield at highend temperature defined as 3 psi for this evaluation.

Service Level C

- 1) Service Level B loads plus dynamic induced load from a postulated one foot side impact (20g):

Considering the mass of the neutron shield shell and NS-4-FR, the effective pressure load becomes:

$$\begin{aligned}M &= \left[(0.2885)(0.25) + (0.0607) \left[\frac{\frac{(99+98.2)}{2} - 86.7}{2} - 0.25 - 0.125 \right] \frac{12.1}{12.85} \right] \\ &= 0.392 \text{ pound} \\ P &= MA = (0.392)(20) \\ &= 7.8 \text{ psi}\end{aligned}$$

Service Level D

- 1) Service Level B loads plus dynamic induced load from a postulated 30-foot side impact (55g).

Considering the mass of the neutron shield shell and the NS-4-FR, the affective pressure load becomes:

$$P = (0.392)(55) \\ = 21.56 \text{ psi}$$

The following evaluation is presented for two different load orientations of the heat transfer fin welds. Case 1 represents the loads induced as a result of loading applied to the neutron shield shell and Case 2 represents loading applied to the radial heat transfer fin.

Case 1 - Neutron Shield Shell Loading

Implementing the design criteria for noncontainment support structures presented in NF-3250, normal operation load service level stress in the weld region connecting the neutron shield shell to the radial heat transfer fin is evaluated using a conservative simplification of the plate and shell structure to that of a uniformly loaded beam having unit depth.

The maximum tension stress from Service Level B is:

$$S = \frac{6q}{t^2} = 26,112 \text{ psi}$$

where:

$$q = \frac{wl^2}{12} = 272 \text{ lb}$$

$$w = 19.1 + 3 = 22.1 \text{ psi}$$

$$l = 12.85 \text{ inch}$$

$$t = 0.25 \text{ inch}$$

Allowable stress limits defined in NF-3256.2 for full penetration groove welds defines acceptable stress for this condition of load as:

$$S_{\text{allowable}} = 1.33 \times 1.5 \times 17,300 \\ = 34,514 \text{ psi}$$

$$\text{Margin of Safety} = \frac{34,514}{26,112} - 1 = +0.18$$

The maximum tension stress for Service Level C load is:

$$S = \frac{6q}{t^2} = 36,461 \text{ psi}$$

where:

$$q = \frac{wl^2}{12} = 379.8 \text{ lb}$$

$$w = 19.8 + 7.8 = 27.6 \text{ psi}$$

$$l = 12.85 \text{ inch}$$

$$t = 0.25$$

Allowable membrane plus bending stress limits defined in NF-3256.2 for Service Level C limits is:

$$\begin{aligned} S_{\text{allowable}} &= 1.5 \times 1.5 \times 17,300 \\ &= 38,925 \text{ psi} \end{aligned}$$

The Margin of Safety is:

$$MS = \frac{38,925}{36,461} - 1 = +0.07$$

The maximum tension stress for Service Level D load is:

$$S = \frac{6q}{t^2} = 40,973 \text{ psi}$$

As directed by NE-3256.2 for Level D, qualification of the structure is based on ASME Code Section III, Appendix F, Paragraph F-1340, "Acceptance Criteria Using Plastic System Analysis".

Considering plastic failure of fixed-ended beams with uniformly distributed load, the plastic moment is (M.R. Horne, "Plastic Theory of Structures", 2nd Edition, Pergamon Press.):

$$M = \frac{wl^2}{16} = 426.8 \text{ lb}$$

where

$$w = 19.8 + 21.56 = 41.4 \text{ psi}$$

$$l = 12.85 \text{ inch}$$

$$t = 0.25 \text{ inch}$$

Paragraph F-1340 defines the allowable primary membrane plus primary bending stress intensity as the lesser of $1.5 (2.4S_m)$ and $1.5 (0.7S_u)$. Implementation of this criteria limits Service Level D stress to 69,300 psi. The resulting Margin of Safety is:

$$MS = \frac{69,300}{40,973} - 1 = +0.69$$

In addition to the evaluation of the maximum local bending stress in the weld region, shear stress is evaluated as:

$$S_s = \frac{wl}{2t}$$

where

$$l = 12.85$$

$$t = 0.25$$

Service Level	w (psi)	S_s (psi)	$S_{\text{Allowable}}$ (psi)	Margin of Safety
B	19.8	509	$1.33 (.4S_y) = 11,790$	Large
C	27.6	709	$1.5 (.4S_y) = 13,500$	Large
D	41.4	1,064	$0.42S_u = 27,720$	Large

Case 2 - Heat Transfer Fin Loading

Following a similar method as used in the evaluation of the neutron shield shell, the heat transfer fin is evaluated using a uniformly loaded beam with a fixed end at the cask outer shell surface and a simple support at the neutron shield shell. Since Level B load is developed from radial thermal growth of the NS-4-FR and postulated off gas pressure, service level B does not load the fin in the lateral direction. Tension stress developed in the fin from these radial loads is 70 psi and insignificant.

Lateral load from service level C produces the following stress:

$$S = \frac{6q}{t^2} = 4,481 \text{ psi}$$

where

$$q_{\text{Max}} = \frac{wl^2}{6} = 74.1 \text{ lb}$$

$$w = (0.0607)(12.1)(20) = 14.7 \text{ psi}$$

$$l = \frac{98.2 - 86.7}{2} - 0.25 = 5.5 \text{ inch}$$

$$t = 0.315 \text{ inch}$$

From the evaluation of the neutron shield shell above, the service level C allowable is 38.7 ksi, therefore, the Margin of Safety is:

$$MS = \frac{38,925}{4,481} - 1 = +7.7$$

Lateral load for Service Level D produces the following stress:

$$S = \frac{6q}{t^2} = 12,317 \text{ psi}$$

where

$$q_{\text{Max}} = \frac{wl^2}{6} = 203.7 \text{ inch lb}$$

$$w = (0.0607)(12.1)(55) = 40.4 \text{ psi}$$

$$l = 5.5 \text{ inch}$$

$$t = 0.315 \text{ inch}$$

Using the Acceptance Criteria for an elastic system analysis provided in ASME Section III, Appendix F, Paragraph F-1332.2, $(1.5 \times 1.2S_y \text{ or } 1.5 \times 1.55 S_m < 1.5 \times .7S_u)$.

$$S_{\text{Allowable}} = 46,500 \text{ psi}$$

$$MS = \frac{46,500}{12,317} - 1 = +2.8$$

In addition to the evaluation of the maximum local bending stress in the weld region, shear stress is evaluated as:

$$S_s = \frac{wl}{2t}$$

where

$$l = 5.5 \text{ inch}$$

$$t = 0.31 \text{ inch}$$

Service Level	w (psi)	S _s (psi)	S _{Allowable} (psi)	Margin of Safety
C	14.7	130	1.5(0.4Sy) = 13,500	Large
D	40.4	358	0.42(Su) = 27,720	Large

Therefore, the heat transfer load path through the welds connecting the neutron shield skin to the radial heat transfer fins is maintained for all transport package normal and accident condition loads.

2.6.7.6.3 Tiedown Bearing Analysis

The maximum vertical tiedown load applied to the cask during transport in a railcar is 4g (Section 2.5.2.2.1). Considering half of this tiedown load to be restrained by the tiedown strap (the other half of the load is carried by the rear support, through the rotation trunnion), the load on the tiedown strap is:

$$P = 1/2 (4)(260,000)$$

$$= 520,000 \text{ lb}$$

The tiedown strap bears on the cask top forging between the lifting trunnion and the neutron shield endplates.

Bearing stress, S , of 5,091 psi is calculated by conservatively assuming 90° contact between the tiedown bar and the cask top forging.

Bearing stress:

$$\text{Bearing stress, } S_s = \frac{2P}{\pi R t} = 5,091 \text{ psi}$$

where:

$t = 1.5$ inches, Thickness of tiedown bar

$R = 43.35$ inches, Cask surface radius

The temperature of the neutron shield shell during normal operation is 241°F with material yield stress, S_y , of 23,980 psi.

$$MS = \frac{S_y}{S_s} - 1 = +3.71$$

Figure 2.6.7.6-1 Neutron Shield Shell Geometry

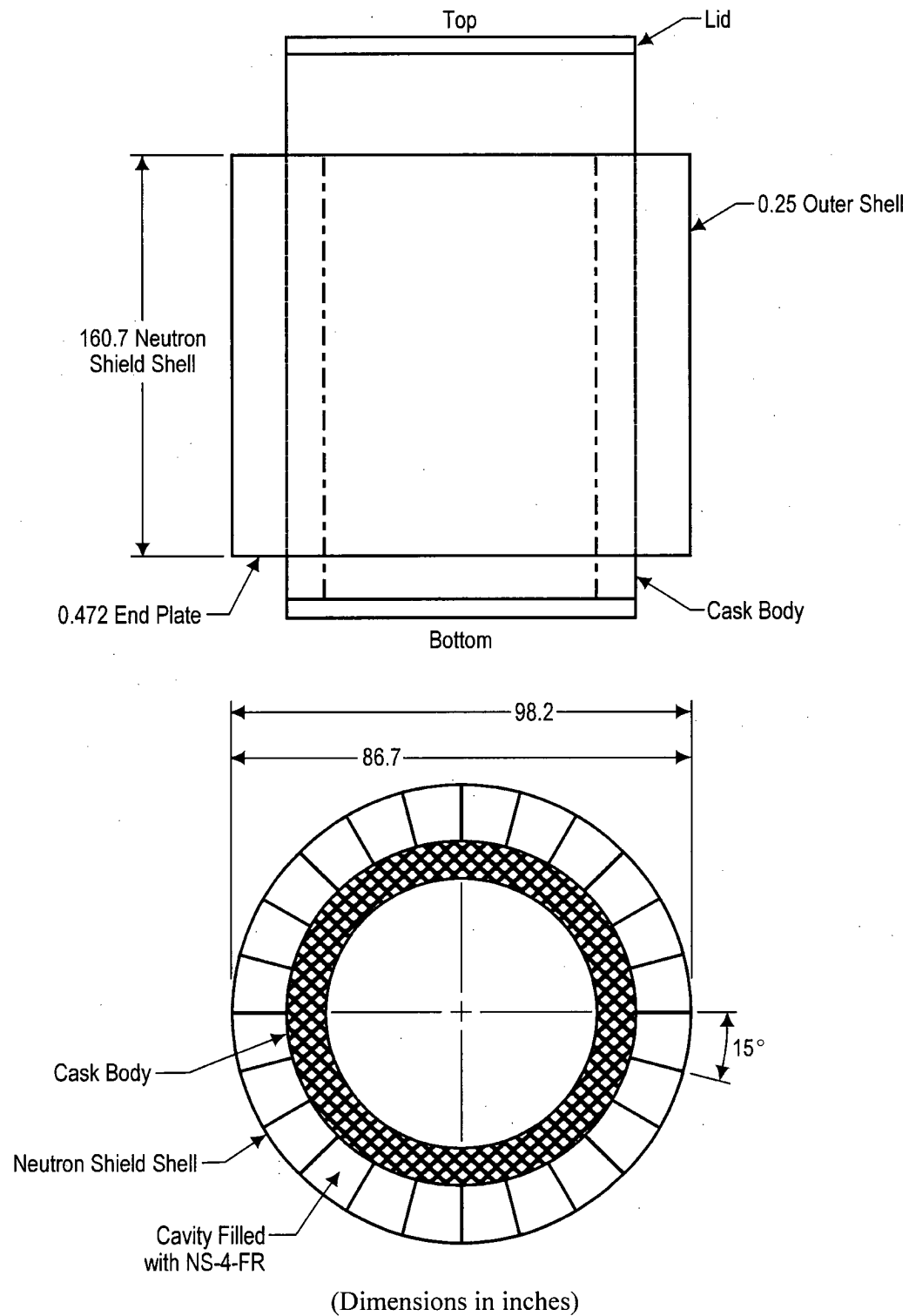


Table 2.6.7.6-1 Neutron Shield Expansion Foam - Manufacturer's Force-Deflection Data

% COMPRESSED	HT800¹ DEFLECTION FORCE (psi)
10 %	3.6
25 %	8.3
40 %	13.7
55 %	24.9
70 %	60.9

1. Data provided by BISCO Products, Inc.

THIS PAGE INTENTIONALLY LEFT BLANK

2.6.7.7 Upper Ring/Outer Shell Intersection Analysis

A bounding analysis of the directly loaded fuel configuration and the canistered Yankee-MPC and CY-MPC configurations of the NAC-STC is presented in this section. A weight of 260,000 pounds (CY-MPC design weight) is used, which bounds the 250,000-pound design weight of the Yankee-MPC and directly loaded fuel configurations. Bending stresses are induced in the upper ring and outer shell intersection region of the cask body when the cask is lifted at the lifting trunnions. These stresses are evaluated via a closed form ring solution based on a method described in the paper, "How to Find Deflection and Moment of Rings and Arcuate Beams," (Blake). For the purpose of the calculation, this region is taken to be a ring (shown below). The support provided by the bolted inner and outer lids is conservatively neglected in this analysis.

Figure Withheld Under 10 CFR 2.390

(Dimensions in inches)

Forces Applied to Trunnion For Cask Lifting Analysis

The geometry and loading of the equivalent ring are defined as follows:

$$F = \text{lifting force} = \frac{260,000}{2}$$

$$= 130,000 \text{ lb}$$

q = dead weight load per unit length

w = width of equivalent ring = 3.79 in

$$r = \text{mean radius of the equivalent ring} = \frac{43.35 + 39.56}{2}$$
$$= 41.455 \text{ in}$$

$$a = \text{moment arm for the equivalent ring} = 45.1 - 41.455$$
$$= 3.645 \text{ in}$$

Based on a total weight of 260,000 pounds, q is calculated as:

$$q (\pi)(41.455)(2) = 260,000$$

$$q = 998.2 \text{ lb/in}$$

The moment and torque on the equivalent ring are given by:

$$M = \frac{T_o \sin \theta}{2} - qr^2 \left(1 - \frac{\pi}{2} \sin \theta \right)$$

$$T = \frac{T_o \cos \theta}{2} + qr^2 \left(\theta + \frac{\pi}{2} \cos \theta - \frac{\pi}{2} \right)$$

where

θ is measured from the trunnion ($\theta = 0$) in plane perpendicular to the centerline of the cask ($0 \leq \theta \leq 180$)

$$T_o = (F)(a) = (130,000)(3.645) = 473,850 \text{ in-lb}$$

Substituting for T_o , q , r (Table 2.6.7.7-1)

$$M = 2.369 \times 10^5 \sin \theta - 1.715 \times 10^6 \left(1 - \frac{\pi}{2} \sin \theta\right)$$

$$T = 2.369 \times 10^5 \cos \theta + 1.715 \times 10^6 \left(\theta + \frac{\pi}{2} \cos \theta - \frac{\pi}{2}\right)$$

The normal stress is treated as bending, due to the moment acting over a cross section.

$$\sigma = \frac{M(h/2)}{I}$$

where

$$h = 15.81 \text{ in}$$

$$I = \frac{wh^3}{12}$$

$$= 1248.1 \text{ in}^4$$

so

$$\sigma = \frac{(15.81/2)}{1,248.1} (M)$$

$$= 0.00633 (M)$$

The shear stress is obtained from Roark and Young, 5th Edition, Table 20, Case 4:

$$\tau = \frac{T \left[3 \left(\frac{h}{2} \right) + 1.8 \left(\frac{w}{2} \right) \right]}{8 \times \frac{h^2}{4} \times \frac{w^2}{4}}$$
$$= \frac{2T[(1.5)(h) + (0.9)(w)]}{(h)^2 (w)^2}$$

$$= \frac{2T[(1.5)(15.85) + (0.9)(3.79)]}{(15.85)^2 (3.79)^2}$$

$$= 0.151T$$

The maximum stress intensity, where the moment and torque are functions of σ , is calculated as:

$$\begin{aligned} \text{S.I.} &= 2\sqrt{\sigma^2/4 + \tau^2} \\ &= 2\sqrt{(10.017 \times 10^{-6})M^2 + (2.28 \times 10^{-4})T^2} \end{aligned}$$

Resultant values of the stress intensity are evaluated in Table 2.6.7.7-1.

The margin of safety is:

$$\text{MS} = \frac{30,000}{22,790} - 1 = \underline{+.32}$$

where

$$S_m = 20,000 \text{ psi}$$

$$S_{\text{allow}} = 1.5 S_m = 30,000 \text{ psi}$$

Table 2.6.7.7-1 Resultant Stress Intensity Values in the Equivalent Ring

Angle (degrees)	Moment (E+6) (in-lbs)	Torque (E+5) (in-lbs)	S.I. (psi)
0.0	-1.715	2.369	13,000
5.0	-1.460	3.754	14,620
10.0	-1.206	4.917	16,700
15.0	-.956	5.860	18,700
20.0	-.713	6.588	20,400
25.0	-.476	7.106	21,670
30.0	-.249	7.422	22,470
35.0	-.034	7.545	22,790
40.0	.169	7.485	22,630
45.0	.357	7.254	22,020
50.0	.530	6.866	21,000
55.0	.686	6.334	19,620
60.0	.823	5.674	17,910
65.0	.941	4.903	15,960
70.0	1.039	4.038	13,850
75.0	1.116	3.096	11,720
80.0	1.171	2.096	9,749
85.0	1.205	1.058	8,268
90.0	1.216	0.000	7,696

THIS PAGE INTENTIONALLY LEFT BLANK

2.6.8 Corner Drop (1 Foot)

According to 10 CFR 71.71(c)(8), this test is not applicable to the NAC-STC because the cask is composed of materials other than fiberboard or wood and the cask weight exceeds 220 pounds (100 kg).

THIS PAGE INTENTIONALLY LEFT BLANK

2.6.9 Compression

According to 10 CFR 71.71(c)(9), this test is not applicable to the NAC-STC because the package weight is greater than 5,000 kilograms (11,023 lb).

THIS PAGE INTENTIONALLY LEFT BLANK

2.6.10 Penetration

This condition is defined in 10 CFR 71 as a 40-inch drop of a 13-pound, 1.25-inch diameter penetration cylinder with a hemispherical end onto any exposed surface of the cask. The acceptance criteria is that the drop will not adversely affect the ability of the cask to maintain containment of the contents or to survive a hypothetical accident. The impact limiters, the neutron shield, and the port covers could potentially be damaged by this penetration impact. An evaluation of a penetration impact on each of these components follows.

THIS PAGE INTENTIONALLY LEFT BLANK

2.6.10.1 Impact Limiter - Penetration

There are two NAC-STC cask impact limiter configurations. The first is constructed of redwood and balsa and may be used in the transport of directly loaded fuel or the Yankee-MPC canistered fuel or GTCC waste. This impact limiter configuration is referred to as the redwood impact limiter. The second is constructed of all balsa and must be used with the CY-MPC canistered fuel or GTCC waste configurations, but may be used with the directly loaded and Yankee-MPC configurations. Both impact limiter configurations have the impact absorbing wood enclosed in a stainless steel shell.

2.6.10.1.1 Redwood Impact Limiter Penetration

The 0.25-inch thick stainless steel outer shell of the impact limiter, backed by redwood and balsa wood, resists puncture by the penetration cylinder. However, the puncture resistance of the shell is conservatively not considered in this analysis. The 13-pound penetration cylinder drops 40 inches, producing $(13)(40) = 520$ inch-pounds of energy, which is assumed to be absorbed only by the redwood and balsa wood materials. The minimum crush strength of the redwood material in the perpendicular to the grain direction is about 500 psi for initial strain conditions. The perpendicular to the grain direction corresponds to the penetration cylinder impacting the end of the impact limiter and bounds an impact on the side of the limiter where the redwood is oriented in the stronger parallel to the grain direction. The area of the penetration cylinder is 1.227 square inches. Therefore, using the redwood crush strength and the average impact area in the conservation of energy equation, the penetration cylinder might penetrate bare redwood material to a depth of $520/[(500)(1.227)/2] = 1.7$ inches. This depth of penetration would not significantly affect the performance of the impact limiter.

2.6.10.1.2 Balsa Impact Limiter Penetration

Similar to the redwood impact limiter evaluation, the 0.25-inch thick stainless steel outer shell of the balsa impact limiter, backed by balsa wood, resists puncture by the penetration cylinder. The dropped cylinder produces 520 inch-pounds of energy, which is absorbed by the balsa wood. The minimum crush strength of the balsa wood in the parallel to the grain direction, is about 1,500 psi for initial strain conditions. The parallel to grain direction of the balsa wood corresponds to the penetration cylinder impacting the end of the impact limiter and bounds an impact on the side of the limiter where the redwood is oriented in the parallel to the grain

direction. The area of the penetration cylinder is 1.227 square inches. Therefore, using the balsa wood crush strength and the average impact area in the conservation of energy equation, the penetration cylinder might penetrate bare balsa wood material to a depth of $520/[(1,500)(1.227)/2] = 0.57$ inches. This depth of penetration would not significantly affect the performance of the impact limiter.

2.6.10.2 Neutron Shield Shell - Penetration

The neutron shield shell, with NS-4-FR material backing it up, can be simulated as an infinitely large plate sitting on an elastic foundation. This simulation is conservative since the arch effect of the curved neutron shield shell and the fin stiffness are not included. The following formulas are from Theory of Plates and Shells, pages 267 through 269 (Timoshenko):

$$W = \frac{Pl^2}{8D}$$

$$M = \frac{(1+\nu)P}{4\pi} \left[\ln\left(\frac{l}{c}\right) + 0.616 \right]$$

$$\sigma = \frac{6M}{t^2}$$

$$D = \frac{E_{sec} t^3}{12(1-\nu^2)}$$

$$l^2 = \sqrt{\frac{D}{K}}$$

where:

P = center concentrated load

C = radius of applied load, 0.625 in

ν = Poisson ratio, 0.275

t = neutron shield shell thickness, 0.236 in (6 mm)

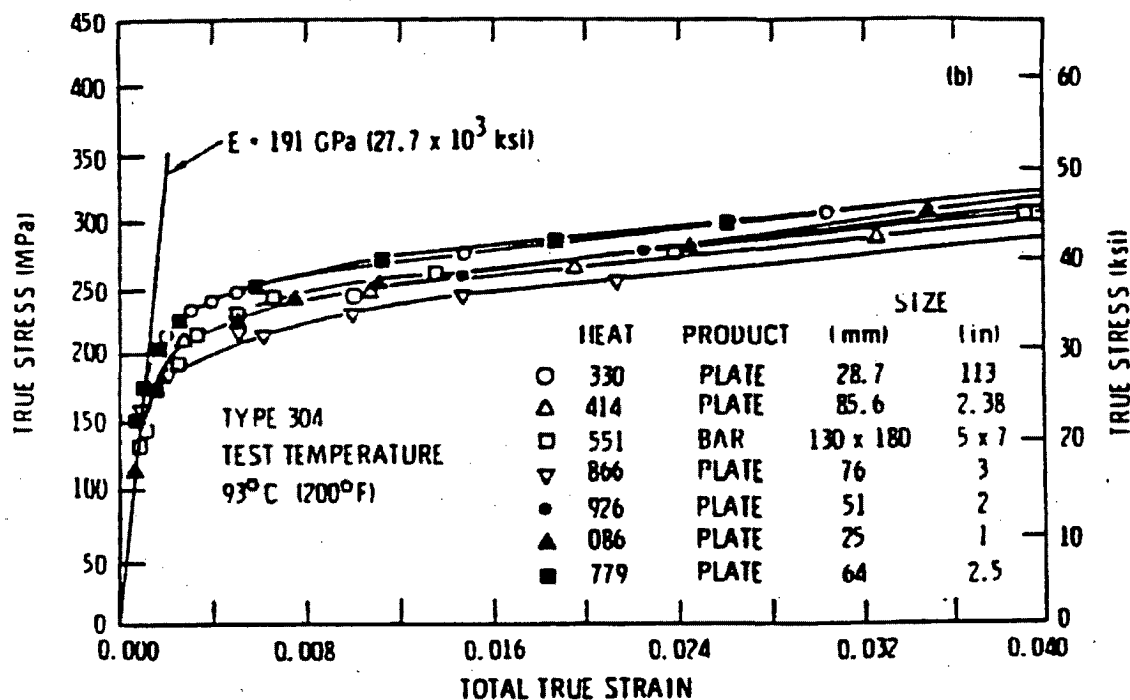
E = compressive modulus of elasticity for NS-4-FR

E_{sec} = the secant modulus (used in evaluating the plastic response of the neutron shield shell)

K = elastic foundation modulus for NS-4-FR, $\frac{561,000}{5.2}$ lb/in²/in

The material properties of the Type 304 stainless steel shell and fins and of NS-4-FR are presented in Section 2.3.

A conservative stress-strain diagram for Type 304 stainless steel is shown below. The stress-strain diagram is used to determine the secant modulus for use in the plastic analysis of the penetration event.



Stress-Strain Diagrams for Type 304 Stainless Steel

The plastic analysis is based on an iterative process. Figure 2.6.10.2-1 is a flow diagram of the plastic analysis. The calculation is shown in Table 2.6.10.2-1. The result shows that the true stress is approximately 41 ksi. Since the ultimate tensile strength of SA 240, Type 304 stainless steel is 71 ksi, the margin of safety is:

$$\text{M.S.} = \frac{71}{41} - 1 = +0.73$$

Thus, the neutron shield shell will not be penetrated.

Figure 2.6.10.2-1 Flow Diagram of the Plastic Analysis of Neutron Shield Shell

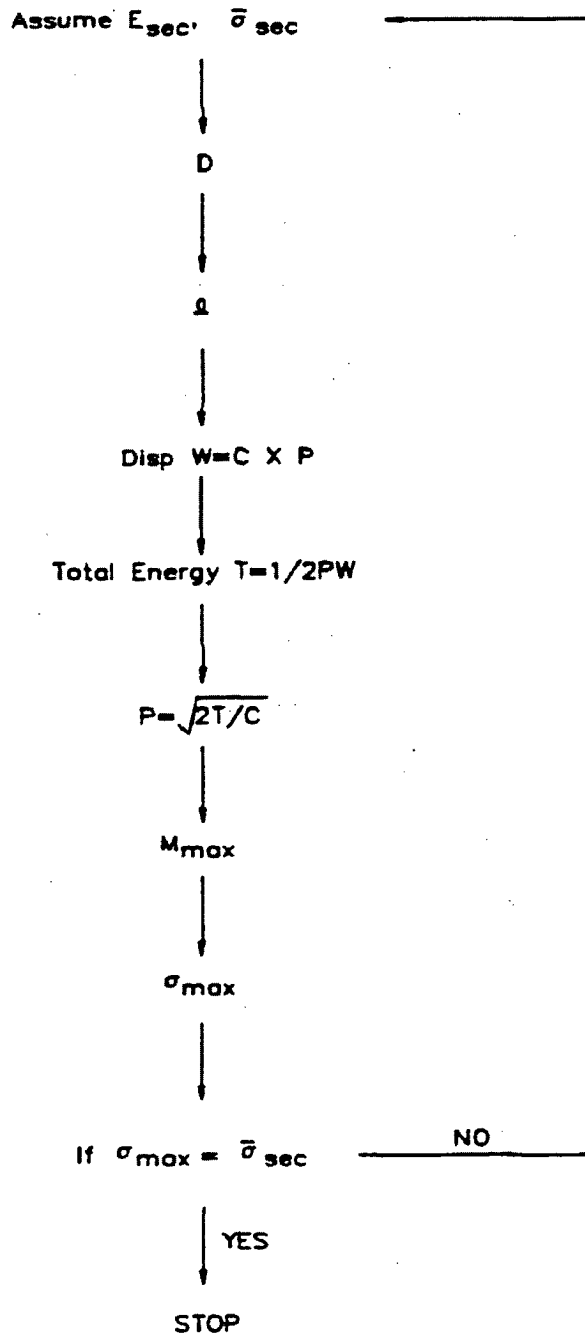


Table 2.6.10.2-1 Stress Iteration Table for the Penetration Analysis of the Neutron Shield Shell
(13-Pound Cylinder Drop From a 40-Inch Height)

Strain (in/in)	S_1 (psi)	Secant Modulus (psi)	D	ℓ^2	$\ell^2/8D$ (E-05)	P (lb)	Moment (in-lb)	S_2 (psi)	S_1-S_2
.0009	25000	.2770E+08	.3282E+05	.5516E+00	.2101E-05	.2225E+05	.1780E+04	.1918E+06	> 0
.004	29500	.7375E+07	.8739E+04	.2846E+00	.4071E-05	.1598E+05	.7422E+03	.7996E+05	> 0
.008	33000	.4125E+07	.4888E+04	.2129E+00	.5443E-05	.1382E+05	.4382E+03	.4720E+05	> 0
.012	35100	.2925E+07	.3466E+04	.1792E+00	.6464E-05	.1268E+05	.2915E+03	.3140E+05	< 0
.016	36600	.2288E+07	.2711E+04	.1585E+00	.7309E-05	.1193E+05	.1998E+03	.2152E+05	< 0
.020	37500	.1875E+07	.2222E+04	.1435E+00	.8074E-05	.1135E+05	.1328E+03	.1431E+05	< 0
.024	38600	.1608E+07	.1905E+04	.1329E+00	.8718E-05	.1092E+05	.8523E+02	.9182E+04	< 0
.028	39600	.1414E+07	.1676E+04	.1246E+00	.9297E-05	.1058E+05	.4805E+02	.5176E+04	< 0
.032	40600	.1262E+07	.1495E+04	.1177E+00	.9841E-05	.1028E+05	.1704E+02	.1836E+04	< 0
.036	41500	.1153E+07	.1366E+04	.1125E+00	.1030E-04	.1005E+05	-.6364E+01	-.6856E+03	< 0
.040	42400	.1060E+07	.1256E+04	.1079E+00	.1074E-04	.9841E+04	-.2723E+02	-.2933E+04	< 0

2.6.10.3 Port Cover - Penetration

Two analyses are performed to demonstrate that the 10 CFR 71 penetration event will not cause loss of the cask containment capability by damaging a port cover. The first analysis uses classical methods; the second uses the ANSYS finite element structural analysis code. The port cover geometry and loading are shown in Figure 2.6.10.3-1.

$$\begin{aligned}\text{P.E.} &= \text{Projectile Potential Energy} \\ &= (W)(h) \\ &= 520 \text{ in-lb}\end{aligned}$$

where

$$\begin{aligned}W &= 13 \text{ lb} \\ h &= 40 \text{ in}\end{aligned}$$

The geometric properties of the port cover lid are:

$$\begin{aligned}t &= 1.01 \text{ in} \\ D &= 3.75 \text{ in (bolt circle)} \\ v &= 0.275 \\ m &= 1/v = 3.6364 \\ a &= 1.875 \text{ in} \\ r_o &= 0.625 \text{ in} \\ a/r_o &= 3.0 \\ \ln(a/r_o) &= 1.0986\end{aligned}$$

The material properties for SA-705, Type 630, H1150, 17-4 PH stainless steel at normal transport temperatures (200°F) are as follows:

$$\begin{aligned}S_y &= 97,100 \text{ psi} \\ S_u &= 135,000 \text{ psi} \\ E &= 27.6 \times 10^6 \text{ psi}\end{aligned}$$

2.6.10.3.1 Classical Analysis

For the deflection equations in the classical analysis (Roark, Case 2, pages 370 and 216), a thin plate formula is used as an approximation to obtain a conservative result, since no shear stiffness is considered.

$$\frac{d_i}{d} = 1 + \left(1 + \frac{2h}{d}\right)^{0.5}$$

where

d_i = vertical deformation due to an impact load from a moving body

d = vertical deformation due to the weight of the moving body
applied as a static load

h = height from which the body falls
= 40 in

For the static loading, the maximum displacement of the port cover is:

$$\begin{aligned} d_{\text{Maxy}} &= \frac{3W(m-1)(3m+1)a^2}{4\pi E m^2 t^3} \\ &= 9.11 \times 10^{-7} \text{ in} \end{aligned}$$

where

W = 13 lb

a = 1.875 in (radius of bolt circle)

ν = 0.275

m = $1/\nu$ = 3.636

t = 1.01 in

E = 27.6×10^6 psi

then

$$d_i = d \left[1 + \left(1 + 2 \left[\frac{40}{d} \right] \right)^{0.5} \right]$$
$$= 0.00854 \text{ in}$$

For such a small displacement, the port cover is adequate to protect the port against the penetration event.

This analytical method is deemed reasonable for a “relatively heavy body moving at low velocity.” The initial assumption of perfect elasticity of the plate and rigidity of the projectile leads to a conservative analysis. The following ANSYS analysis removes part of the conservatism by allowing plastic deformation of the plate.

2.6.10.3.2 ANSYS Finite Element Analysis

The penetration loading condition was evaluated using an ANSYS program solution for a finite element model of a similar port cover system. Figure 2.6.10.3-2 depicts the finite element model of the port cover. The impact of the 13-pound, 1.25-inch diameter projectile dropped from a height of 40 inches is assumed to occur at the center of the port cover. The bolt preload is 2557 pounds.

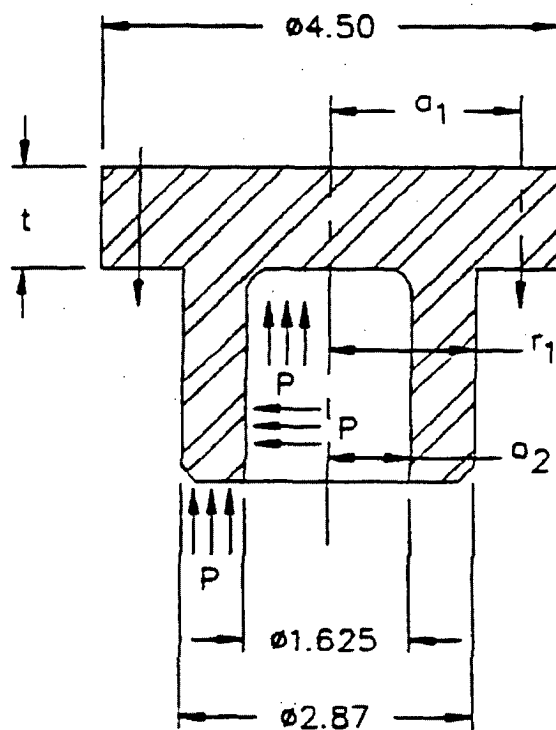
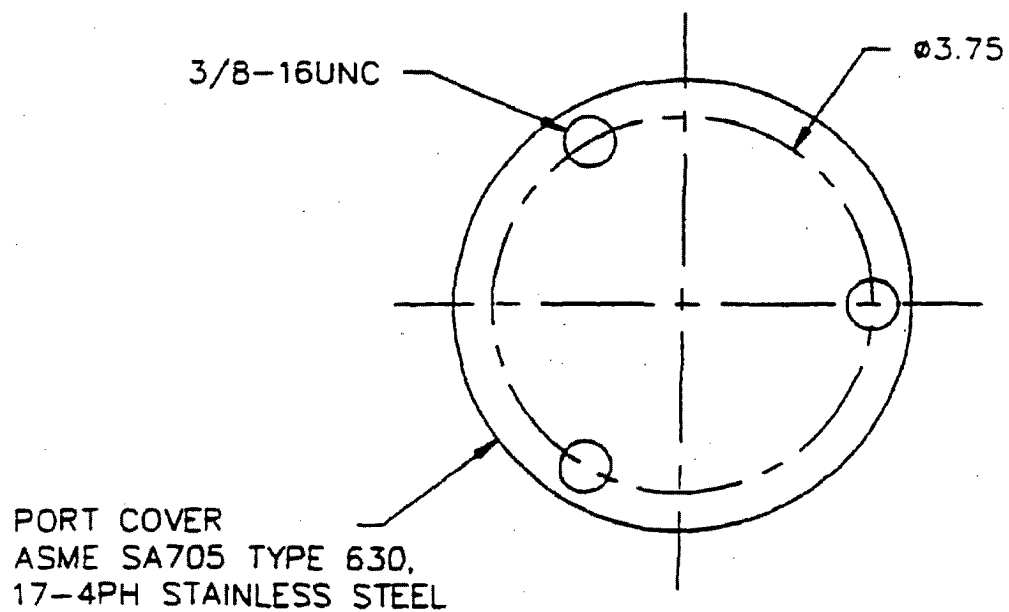
The dynamic impact load is applied as a center concentrated load, and elastic/plastic material property stress-strain curves are used. The analysis is based on the following two assumptions:

1. 100 percent of the projectile's momentum is absorbed by the cover.
2. The time of impact is 0.001 second. The load peaks at 0.0005 second, increasing and decreasing linearly.

Momentum calculations yield an average load of 5915 pounds over the 0.001-second impact time interval. Therefore, the peak loading is 11,830 pounds at 0.0005 second. This peak load is distributed over the impact area.

The ANSYS analysis results calculate a maximum port cover displacement of 0.00541 inch at 0.0005 second, which is less than the conservative 0.00854-inch displacement calculated by classical methods. Plasticity effects occur only very locally in the vicinity of the load application region. The plastic ratio of the cross-section at the port cover center is only 9.64×10^{-4} . The cover bolts are also shown to be preloaded sufficiently to maintain the gap elements closed between the port cover and the cask body during the impact. Figure 2.6.10.3-3 presents a plot of the cover displacement at the top of the plate versus time. The port cover is shown to be adequate to protect the valve against the 10 CFR 71 penetration event.

Figure 2.6.10.3-1 Port Cover Geometry and Loading



(DIMENSIONS IN INCHES)

Figure 2.6.10.3-2 Finite Element Model of Port Cover

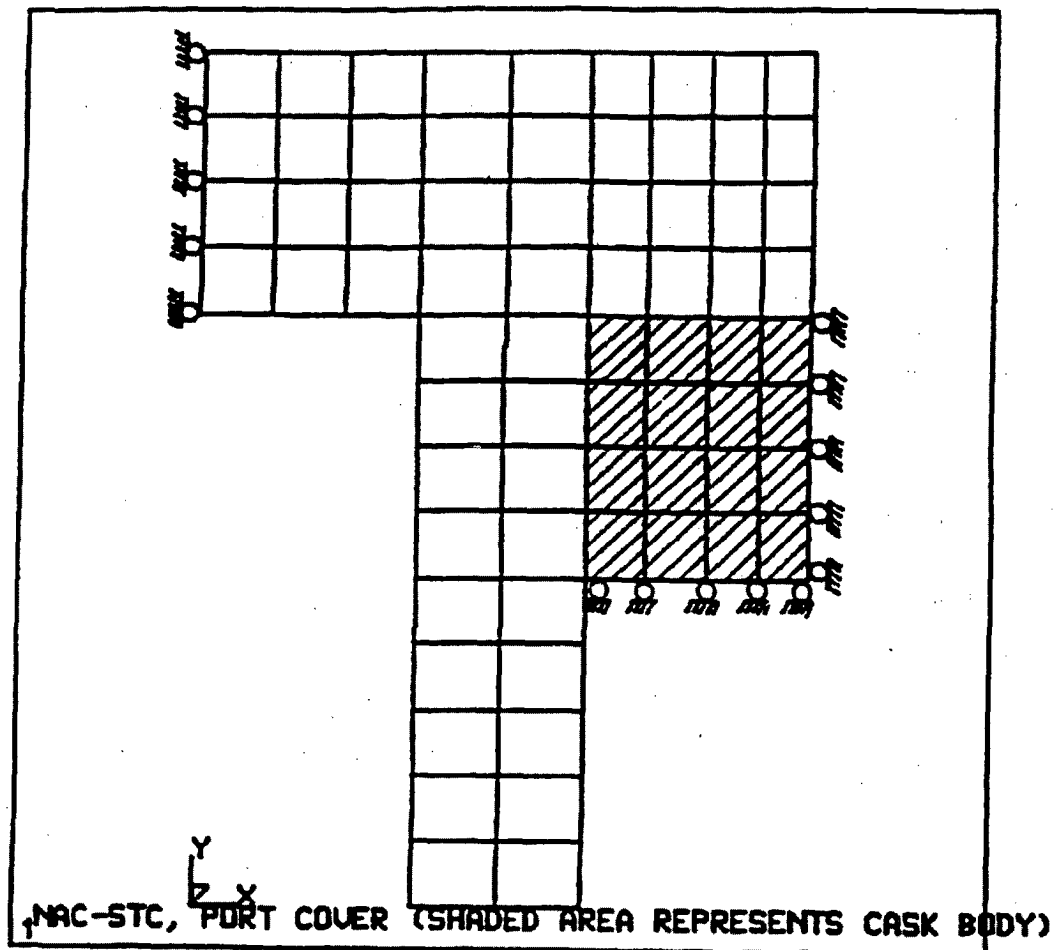
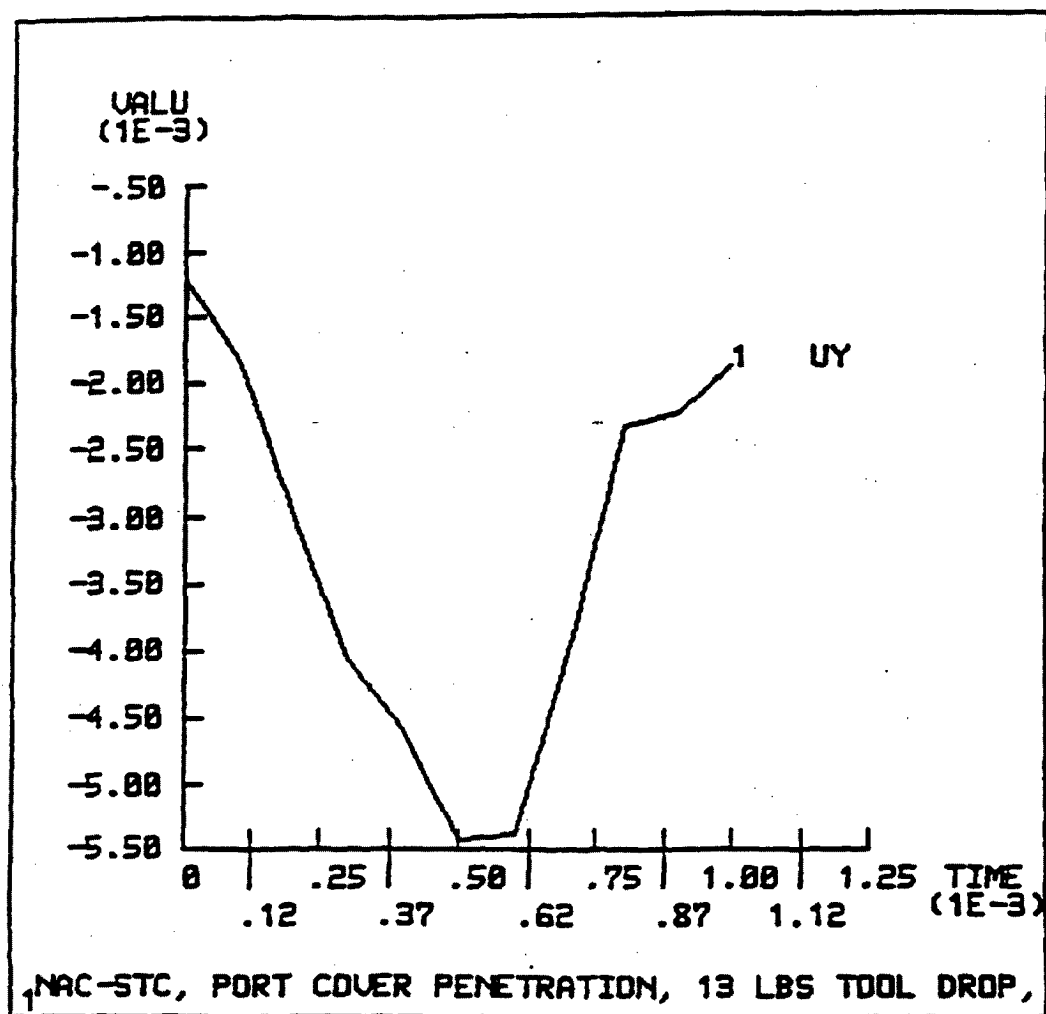


Figure 2.6.10.3-3 Port Cover Response to Penetration Event



THIS PAGE INTENTIONALLY LEFT BLANK

2.6.11 Fabrication Conditions

The process of manufacturing the NAC-STC can introduce thermal stresses in the inner and outer shells as a result of pouring molten lead between them. These thermal stresses are evaluated in this section to provide assurance that the manufacturing process does not adversely affect the normal operation of the cask or its ability to survive an accident. Any residual stresses in the containment vessel shell due to inelastic strain associated with the secondary local bending stresses, which result from the lead pour thermal gradient, must be considered in the total stress range for normal and accident load conditions according to Regulatory Position 7 of Regulatory Guide 7.6. Residual stresses in the containment vessel and the outer shell induced by shrinkage of the lead shielding after the lead pouring operation are relieved early in the life of the cask because of the low creep strength of lead.

For the lead pouring process, the temperatures of the cask shells are controlled between 640°F (338°C) and 740°F (393°C), and the lead temperature before pouring is between 650°F (343°C) and 750°F (399°C). Heating of the cask is performed using heaters inside the inner shell and heating rings around the outside of the outer shell. Heat up is time controlled, consistent with maintaining shell temperatures uniformly. The heating procedures ensure that the surface temperature of the cask does not exceed 800°F (427°C). The shell temperatures are measured by thermocouples attached to the shell surfaces. A portable thermometer is also used to measure temperature at any location. Cask heating is carried out after all of the preparations have been completed (including melting of the lead) in order to minimize the time that the cask is at elevated temperatures.

The lead is poured after the cask reaches the specified temperatures. Prior to lead pouring, the cask flange area is heated with hand-held burners to between 640°F (338°C) and 740°F (393°C). Pouring is carried out continuously using a filling tube with its open end maintained under the lead surface. The pouring time is kept as short as possible. During pouring, the interior heaters and exterior heating rings are continuously energized.

The cooling process consists of sequentially turning the exterior heating rings and interior heaters off, starting from the lowest point, and of spraying the cask with water from the outside. A layer of molten lead is maintained until the upper surface starts to solidify. This process allows the molten lead to fill the open space below it created by the lead shrinkage as it cools.

The basic requirements and procedures for the NAC-STC lead pour operations are described in Section 8.4.2.

2.6.11.1 Lead Pour

2.6.11.1.1 Cask Shell Geometry

At 70°F, the Type 304 stainless steel shell geometry is as follows:

Inner Shell

Inside Diameter (d_i)	= 71.0 in
Outside Diameter (d_o)	= 74.0 in
Shell Thickness (t_i)	= 1.5 in

Outer Shell

Inside Diameter (D_i)	= 81.4 in
Outside Diameter (D_o)	= 86.7 in
Shell Thickness (T_o)	= 2.65 in

2.6.11.1.2 Stresses Due to Lead Pour

As stated in Section 8.4.2, Description of Lead Pour Procedures, the maximum lead temperature during the pouring operations is 750°F. Assuming that the lead and the inner and outer shells are uniformly at 750°F, the hydrostatic pressure produced by the column of lead is:

$$p = \rho h$$

$$= 66 \text{ psi}$$

where

$$\rho = 0.41 \text{ lb/in}^3 \text{ (lead density)}$$

$$h = 161 \text{ in (maximum height of lead column)}$$

At 750°F, the shell geometric dimensions are:

$$d_o' = d_o (1 + \alpha \Delta T)$$

$$D_i' = D_i (1 + \alpha \Delta T)$$

$$d_m' = \left[\frac{d_i + d_o}{2} \right] (1 + \alpha \Delta T)$$

$$D_m' = \left[\frac{D_i + D_o}{2} \right] (1 + \alpha \Delta T)$$

$$t' = t (1 + \alpha \Delta T)$$

where

$$\alpha = 9.76 \times 10^{-6} \text{ in/in/}^\circ\text{F at } 750^\circ\text{F (stainless steel)}$$

$$\Delta T = 750 - 70 = 680^\circ\text{F}$$

$$\begin{aligned} d_o' &= (74.0) [1 + (9.76 \times 10^{-6})(680)] \\ &= 74.49 \text{ in} \end{aligned}$$

$$\begin{aligned} d_m' &= \left[\frac{71.0 + 74.0}{2} \right] [1 + (9.76 \times 10^{-6})(680)] \\ &= 72.98 \text{ in} \end{aligned}$$

$$\begin{aligned} d_i' &= (81.4) [1 + (9.76 \times 10^{-6})(680)] \\ &= 81.94 \text{ in} \end{aligned}$$

$$\begin{aligned} D_m' &= \left[\frac{81.4 + 86.7}{2} \right] [(1 + (9.76 \times 10^{-6})(680))] \\ &= 84.61 \text{ in} \end{aligned}$$

$$\begin{aligned}t_i' &= (1.50) [1 + (9.76 \times 10^{-6})(680)] \\ &= 1.51 \text{ in}\end{aligned}$$

$$\begin{aligned}t_o' &= (2.65) [1 + (9.76 \times 10^{-6})(680)] \\ &= 2.668 \text{ in}\end{aligned}$$

The inner shell is subjected to an external hydrostatic pressure, and the outer shell to an internal hydrostatic pressure, of 66 psi. This causes the inner shell to decrease in diameter and the outer shell to increase in diameter.

The inner shell decreases in size radially (Roark and Young, 5th ed., Case 1b, page 448):

$$\Delta r_o = \frac{q(d_o'/2)^2}{Et_i'} = \frac{(-66)(74.9/2)^2}{(24.4 \times 10^6)(1.51)} = -0.00248 \text{ in}$$

$$\Delta r_m = \frac{q(d_m'/2)^2}{Et_i'} = \frac{(-66)(72.98/2)^2}{(24.4 \times 10^6)(1.51)} = -0.00239 \text{ in}$$

where

$$E = 24.4 \times 10^6 \text{ psi at } 750^\circ\text{F.}$$

The outer shell increases in size radially:

$$\Delta R_i = \frac{q(d_i'/2)^2}{Et_o'} = \frac{(66)(81.94/2)^2}{(24.4 \times 10^6)(2.668)} = 0.00170 \text{ in}$$

$$\Delta R_m = \frac{q(D_m'/2)^2}{Et_o'} = \frac{(66)(84.61/2)^2}{(24.4 \times 10^6)(2.668)} = 0.00181 \text{ in}$$

The shell geometries at 750°F and 66 psi hydrostatic pressure are:

$$d''_o = 74.49 - (2)(0.00248) = 74.485 \text{ in}$$

$$D''_o = 81.94 + (2)(0.00170) = 81.943 \text{ in}$$

$$d''_m = 72.98 - (2)(0.00239) = 72.975 \text{ in}$$

$$D''_m = 84.61 + (2)(0.00181) = 84.614 \text{ in}$$

The hoop stresses are evaluated at the mean diameter of the inner and outer shells at 750°F:

$$\begin{aligned} S_{hi} &= \frac{Pd''_m}{2t_i} \\ &= \frac{(-66)(72.975)}{(2)(1.51)} = -1595 \text{ psi (inner shell)} \end{aligned}$$

$$\begin{aligned} S_{ho} &= \frac{PD''_m}{2t_o} \\ &= \frac{(66)(84.614)}{(2)(2.668)} = 1047 \text{ psi (outer shell)} \end{aligned}$$

These stresses are negligible.

2.6.11.2 Cooldown

2.6.11.2.1 Hoop Stresses

Lead decreases in volume during solidification. As the lower lead region solidifies, the molten lead above fills the shrinkage void between the solidifying lead and the inner and outer shells, thus, maintaining the 66 psi pressure on the shells.

The stress-free inner and outer radii of the solidified lead can be calculated (Roark and Young, 5th ed., Cases 1a and 1c, page 504) as:

$$\begin{aligned}\Delta a &= \frac{q}{E} \left[\frac{2ab^2}{a^2 - b^2} \right] - \frac{qa}{E} \left[\frac{a^2 - b^2}{a^2 - b^2} - \nu \right] = \frac{q}{E} a(\nu - 1) \\ &= -0.001104 \text{ in}\end{aligned}$$

$$\begin{aligned}\Delta b &= \frac{qb}{E} \left[\frac{a^2 + b^2}{a^2 - b^2} + \nu \right] - \frac{q}{E} \left[\frac{2a^2b}{a^2 - b^2} \right] = \frac{q}{E} b(\nu - 1) \\ &= -0.001003 \text{ in}\end{aligned}$$

where

$$q = 66 \text{ psi (pressure)}$$

$$E = 1.47 \times 10^6 \text{ psi at } 620^\circ\text{F (modulus of elasticity)}$$

$$\nu = 0.4 \text{ (Poisson's ratio)}$$

$$a = D''_i/2 = 81.943/2 = 40.9715$$

$$b = d''_o/2 = 74.485/2 = 37.2425$$

then

$$R_{ol} = 40.9715 - 0.001104 = 40.9704$$

$$R_{il} = 37.2425 - 0.001003 = 37.2415$$

When cooled to 70°F, the inside radius of the lead is such that:

$$\frac{R_{il}}{1 + \alpha\Delta T} = R'_{il}$$

where

R'_{il} = inside radius of the stress-free lead at 70°F

$$\alpha = 20.4 \times 10^{-6} \text{ in/in/}^{\circ}\text{F}$$

$$\Delta T = 550^{\circ}\text{F} \quad (620-70)$$

then

$$R'_{il} = 36.828 \text{ in}$$

likewise

$$\frac{R_{ol}}{1 + \alpha\Delta T} = R'_{ol}$$

$$R'_{ol} = 40.516 \text{ in}$$

The outside radius of the stress-free inner shell is $74.0/2 = 37.0$ inches, which is larger than the stress-free inner radius of the lead shell. Therefore, there exists an interface pressure between the lead and the inner shell after cooling to 70°F. The interface pressure, when acting on the lead cylinder and inner shell, is such that the inner radius of the lead cylinder is the same as the outer radius of the inner shell (Roark and Young, 5th ed., Case 1a, page 504).

$$R'_{il} = b + \Delta b$$

$$= b + \frac{qb}{E} \left[\frac{a^2 + b^2}{a^2 - b^2} + \nu \right]$$

where

R'_{il} = inside radius of lead cylinder at 70°F

$$\nu = 0.4$$

$$E = 2.28 \times 10^6 \text{ psi at } 70^\circ\text{F}$$

$$a = 40.516 \text{ in}$$

$$b = 36.828 \text{ in}$$

then

$$\begin{aligned} R'_{il} &= 36.828 + \left(\frac{36.828q}{2.28 \times 10^6} \right) \left(\frac{(40.516)^2 + (36.828)^2}{(40.516)^2 - (36.828)^2} + 0.4 \right) \\ &= 36.828 + 1.762 \times 10^{-4} q \end{aligned}$$

The outside radius of the inner shell at 70°F under the interface pressure, q , (Roark and Young, 5th ed., Case 1c, page 504) is:

$$\begin{aligned} r_o &= a_s - \Delta a_s \\ &= a_s - \frac{qa_s}{E} \left(\frac{a_s^2 + b_s^2}{a_s^2 - b_s^2} - \nu \right) \end{aligned}$$

where

r_o = outside radius of inner shell at 70°F

$$a_s = 74.0/2 = 37.0 \text{ in}$$

$$b_s = 71.0/2 = 35.5 \text{ in}$$

$$E = 28.3 \times 10^6 \text{ psi at } 70^\circ\text{F}$$

$$\nu = 0.275$$

then

$$\begin{aligned} r_o &= 37.0 - \left(\frac{37.0q}{28.3 \times 10^6} \right) \left(\frac{(37.0)^2 + (35.5)^2}{(37.0)^2 - (35.5)^2} - 0.275 \right) \\ &= 37.0 - 3.125 \times 10^{-5} q \end{aligned}$$

Equating R'_{il} and r_o and solving for q :

$$q = 1187 \text{ psi interface pressure}$$

The lead shell geometry is:

$$\begin{aligned} R'_{il} &= 36.828 + \left(\frac{(36.828)(1187)}{2.28 \times 10^6} \right) \left(\frac{(40.516)^2 + (36.828)^2}{(40.516)^2 - (36.828)^2} - 0.4 \right) \\ &= 37.037 \text{ in} \end{aligned}$$

$$\begin{aligned} R'_{ol} &= R'_{ol} + \frac{q}{E} \left(\frac{2R'_{ol}R'^2_{il}}{R'^2_{ol} - R'^2_{il}} \right) \\ &= 40.516 + \left(\frac{1187}{2.28 \times 10^6} \right) \left(\frac{(2)(40.516)(36.828)^2}{(40.516)^2 - (36.828)^2} \right) \\ &= 40.521 \text{ in} \end{aligned}$$

The interference between the lead shell and the inner shell is 0.172 inches (37.0 - 36.828). To fully accommodate this interference, the lead must undergo a strain of $0.172/36.828 = 0.0047$ or 0.47 percent. From Figure 24 of NUREG/CR-0481, the lead stress for the above strain is 800 psi. The corresponding interface pressure for this stress in the lead shell is:

$$\begin{aligned} q &= (S) \left(\frac{R_{ol}'^2 - R_{il}'^2}{R_{ol}'^2 + R_{il}'^2} \right) \\ &= (800) \left(\frac{(40.521)^2 - (37.037)^2}{(40.521)^2 + (37.037)^2} \right) \\ &= 72 \text{ psi interface pressure} \end{aligned}$$

The change in geometry of the inner shell for this interface pressure is:

$$\begin{aligned} \Delta a &= \left[\frac{-72}{28.3 \times 10^6} \right] \left[\frac{(2)(37.0)(35.5)^2}{(37.0)^2 - (35.5)^2} \right] \\ &= 0.0022 \text{ in} \end{aligned}$$

This can conservatively be neglected in the analysis. The inner shell hoop stress is:

$$\begin{aligned} S_{his} &= (-72) \left[\frac{(37.0)^2 + (35.5)^2}{(37.0)^2 - (35.5)^2} \right] \\ &= -1740 \text{ psi} \end{aligned}$$

This stress is negligible.

2.6.11.2.2 Axial Stresses

Axial stresses also develop in the lead shell and inner shell during fabrication as a result of the unequal shrinkage of the lead and steel shells. Assume bonding of the lead shell to the inner shell during the cooldown process after completion of lead pouring. The strain in the lead, when cooled to 70°F, is:

$$\begin{aligned} \epsilon_\ell &= (\alpha_l - \alpha_s) \Delta T \\ &= 0.0060 \text{ in/in or 0.60 percent} \end{aligned}$$

where

$$a_\ell = 20.4 \times 10^{-6} \text{ in/in/}^\circ\text{F}$$

$$a_s = 9.56 \times 10^{-6} \text{ in/in/}^\circ\text{F}$$

$$\Delta T = 620 - 70 = 550^\circ\text{F}$$

Extrapolating from Figure 24 of NUREG/CR-0481 for this strain, an axial stress of approximately 825 psi exists in the lead shell. The total force in the lead caused by assuming no deformation of the inner shell is:

$$\begin{aligned} P_{sPb} &= p_\ell A_\ell \\ &= 825\pi[(40.7)^2 - (37.0)^2] \\ &= 745,120 \text{ lb tensile force} \end{aligned}$$

The corresponding compression stress in the inner shell to maintain equilibrium is:

$$\begin{aligned} p_{sSI} &= \frac{P_s}{A_s} \\ &= \frac{-745,120}{\pi[(37.0)^2 - (35.5)^2]} \\ &= -2180 \text{ psi} \end{aligned}$$

This stress is negligible.

This is a highly conservative estimate of the compressive stress that can develop in the inner shell for the following reasons:

1. It assumes no axial deformation of the inner shell and no load development in the outer shell.
2. Creep in the lead is neglected. This also reduces the stress and force in the lead (Section 2.6.11.3).

3. It assumes the strain is uniform through the thickness of the lead shell, i.e., no shear strain exists in the plane formed by the radial axis and the longitudinal axis. A particle away from the inner shell should develop less strain, consequently lower stress, than a particle adjacent to the inner shell; this also reduces the total force in the lead shell.

2.6.11.2.3 Effects of Temperature Differential During Cooldown

The preceding analyses assume that the inner and outer shells and the lead are always at the same temperature at any time during the cooldown process. This assumption may not be true under actual conditions. However, because of the high thermal conductivity of the stainless steel and the lead and because of the time-controlled cooldown process, the temperature differential between any two of the above shells is kept to a minimum. To determine the effect of temperature differential on the stresses in the shells, a temperature differential of 100°F is used (Ref. Section 8.4.2).

If the inner shell is cooler than the lead, the interference between them as well as the corresponding interface pressure and hoop stresses are less than for the case of equal temperatures. Hence, the preceding analysis is conservative.

If the inner shell is hotter than the lead shell, an analysis is required. Assume the temperature of the inner shell to be 170°F and that of the lead to be 70°F. The inner radius of the stress-free lead shell at 70°F is 36.828 inches (R_{il}); the outer radius of the inner shell at 170°F is:

$$\begin{aligned} R &= 37.0 [1 + (8.71 \times 10^{-6})(100)] \\ &= 37.032 \text{ in} \end{aligned}$$

The interference between the inner shell and the lead is $37.032 - 36.828 = 0.204$ inch. To fully accommodate this interference, the lead has to undergo a strain of $0.204/36.828 = 0.0055$ inch/inch or 0.55 percent. From Figure 24 of NUREG/CR-0481, the hoop stress in the lead is approximately 810 psi for a 0.0055 inch/inch strain. The interface pressure is:

$$q = (810) \left[\frac{(40.516)^2 - (36.828)^2}{(40.516)^2 + (36.828)^2} \right]$$

$$= 77 \text{ psi}$$

The hoop stress in the inner shell becomes:

$$S_{his} = (-77) \left[\frac{(37)^2 + (35.5)^2}{(37)^2 - (35.5)^2} \right]$$
$$= -1862 \text{ psi}$$

Note that the thermal expansion or contraction of a shell subjected to a constant pressure does not affect the hoop stress; i.e.,

$$S_h = q \left[\frac{(ka)^2 + (kb)^2}{(ka)^2 - (kb)^2} \right] = q \left[\frac{a^2 + b^2}{a^2 - b^2} \right]$$

where

$$k = 1 + \alpha \Delta T$$

This -1862 psi hoop stress (the inner shell is assumed to be 100°F hotter than the lead shell) reduces to the previously calculated hoop stress of -1837 psi as both the inner shell and lead reach an ambient temperature of 70°F. This does not take into account the beneficial effect of the creep properties of the lead.

The axial stress in the inner shell also increases when the inner shell is 100°F hotter than the lead shell. The axial stress of -2180 psi calculated when both the inner shell and lead shell are at 70°F is recalculated for the inner shell temperature of 170°F, $\alpha = 8.71 \times 10^{-6}$ inch/inch/°F (Type 304 stainless steel):

$$\epsilon_t = (20.38 - 9.56)(10^{-6})(620 - 70) + (8.71 \times 10^{-6})(170 - 70)$$
$$= 0.00595 \text{ in/in or } 0.595 \text{ percent}$$

Referring to Figure 24 of NUREG/CR-0481, the axial stress in the lead is approximately 820 psi. The corresponding axial stress in the inner shell is -2167 psi. As before, cooling of the inner

shell reduces this stress. The previous assumptions apply in arriving at this inner shell compressive stress.

Temperature differentials between the inner and outer shells are of no consequence, since the axial restraint between them is welded in place after cooldown, when the cask is at a uniform ambient temperature. Welding of the outer shell and the bottom inner forging to the bottom outer forging after cooldown is, therefore, a necessary fabrication step.

The question of buckling of the inner shell due to the combined effect of external pressure and fabrication inaccuracies must also be addressed. According to the "ASME Boiler and Pressure Vessel Code," Article NE-4221.1, the difference between the maximum and minimum inside diameters at any cross section shall not exceed 1 percent of the nominal diameter at the cross section under consideration. This amounts to $(0.01)(71.0) = 0.71$ inch. The relation between the initial radial deviation, ω_1 , and the maximum and minimum diameter (Timoshenko and Gere, Figure 7-10) is:

$$D_{\max} = D_{\text{nom}} + 2\omega_1$$

$$D_{\min} = D_{\text{nom}} - 2\omega_1$$

thus

$$D_{\max} - D_{\min} = 4\omega_1$$

or

$$\Delta D = 4\omega_1$$

Hence, the maximum initial radial deviation allowed is:

$$\omega_{\max} = \Delta D/4 = 0.71/4 = 0.1775 \text{ in}$$

From Timoshenko and Gere, equation (7-15), page 293:

$$\begin{aligned} S_{\text{cr}} &= \left[\frac{E}{1 - \nu^2} \right] \left[\frac{h}{2R} \right]^2 \\ &= 12,856 \text{ psi} \end{aligned}$$

where

$$E = 27.76 \times 10^6 \text{ psi at } 170^\circ\text{F}$$

$$\nu = 0.275$$

$$h = \text{shell thickness} = 1.50 \text{ in}$$

$$R = \text{shell radius} = 36.25 \text{ in}$$

Then from Timoshenko and Gere, equation (7-12), page 289:

$$\begin{aligned} q_{cr} &= \left[\frac{E}{4(1-\nu^2)} \right] \left[\frac{h}{R} \right]^3 \\ &= S_{cr} \left[\frac{h}{r} \right] \\ &= 532 \text{ psi} \end{aligned}$$

When the cylinder has fabrication inaccuracies, the external pressure, q_{YP} , required to produce yielding in the extreme fibers can be solved in the following equation (Timoshenko and Gere, equation (e), page 296):

$$q_{YP}^2 - \left[\frac{S_{YP}}{m} + (1 + 6mn)q_{cr} \right] q_{YP} + \frac{S_{YP}}{m} q_{cr} = 0$$

where

$$S_{YP} = 26,150 \text{ psi at } 170^\circ\text{F for Type 304 stainless steel}$$

$$m = R/h = 36.25/1.50 = 24.1667$$

$$n = \omega_1/R = \omega_1/36.25$$

then

$$q_{YP}^2 - [1082 + (1 + 4\omega_1)(532)] q_{YP} + 575,660 = 0$$

The value of ω_1 can vary from 0.0 inches (perfect cylinder) up to 0.1775 inch (maximum allowed according to the "ASME Boiler and Pressure Vessel Code"). Solving q_{YP} for varying values of ω_1 gives the following:

Initial Radial Deviation <u>ω^1 (in)</u>	Yield Pressure <u>q_{YP} (psi)</u>
0.001	530
0.06	443
0.12	389
0.1775	351

Thus, the margin of safety against yielding for the inner shell with maximum allowed radial deviation subjected to 77 psi lead pressure (inner shell temperature is assumed to be 100°F higher than lead temperature) is:

$$MS = \frac{351}{77} - 1 = +3.55$$

Since the margin of safety for this conservative load case is positive, the inner shell does not buckle when subjected to the lead pressure produced during the cooling of the cask.

THIS PAGE INTENTIONALLY LEFT BLANK

2.6.11.3 Lead Creep

As shown in Sections 2.6.11.2.1 and 2.6.11.2.2, cooling of the lead shell and inner shell introduces a hoop stress of -1837 psi and an axial stress of -2180 psi in the inner shell. However, the significant creep rate of lead at room, or elevated, temperatures causes the stresses to be relieved early in the life of the cask. From Figure 21 of Tietz, it can be seen that maintaining a constant strain of 0.59 percent at 250°F for only five hours reduces the lead stress to approximately 200 psi. For this stress in the lead, the corresponding hoop and axial stresses in the inner shell are:

$$\sigma_h = \frac{200}{800} (-1837) = -459 \text{ psi}$$

$$\sigma_a = \frac{200}{825} (-2180) = -528 \text{ psi}$$

During fabrication following the lead pour, the lead creep relieves the stresses in the lead shell, and the stresses in the inner shell, to a point that they become negligible.

THIS PAGE INTENTIONALLY LEFT BLANK

2.6.12 Fuel Basket Analysis (For Directly Loaded Fuel) - Normal Transport Conditions

The NAC-STC fuel basket for directly loaded fuel is designed to accommodate 26 fuel assemblies. The basket is a right circular cylinder structure, and is fabricated with the following components: 26 square fuel tubes, 31 circular support disks equally spaced between top and bottom plates, 20 aluminum heat transfer disks, and 6 threaded rods with spacer nuts. The basket components and their geometry are illustrated in Figure 2.6.12-1 and 2.6.12-2. Each fuel tube has an 8.78-inch square inside dimension, a 0.142-inch thick composite wall (includes encased BORAL), and holds one design basis PWR fuel assembly. Figure 2.6.12-3 shows details of the stainless steel tube with the encased BORAL. The fuel tubes are open at each end; therefore, longitudinal fuel assembly loads are imparted to the cask body and not the fuel basket structure. The fuel assemblies, together with the tubes, are laterally supported in the holes in the stainless steel support disks. Each support disk is 0.5 inches thick, 70.86 inches in diameter, and has 26 holes that are each 9.234 inches square. There are two different web widths in the support disk. One web width is 1.47 inches between the holes and the other web width is 3.27 inches between the holes. The top and bottom plates are both 1.0 inch thick and have the same diameter as the support disks. The support disks are spaced at 4.87-inch center-to-center intervals and structurally connected by threaded spacer nuts located at six positions near the periphery of each disk. Aluminum heat transfer disks are located at the mid section of the cask cavity to fully optimize heat rejection from the package. Each heat transfer disk is 0.625 inch thick, 70.65 inches in diameter, and has 26 holes that are each 9.20 inches square. There are two different web widths, 1.50 inches and 3.3 inches. The dimensional difference between the heat transfer disk and the support disk accommodates the different rate of thermal growth between different materials preventing interference between the tube, support disk, and heat transfer disk. The heat transfer disks are supported by the six threaded rods and serve no structural function. The fuel basket contains the fuel and is laterally supported by the inner shell of the cask.

The 31 support disks and 2 end plates are fabricated from 17-4 PH and Type 304 stainless steel. The 20 heat transfer disks are fabricated from Type 6061-T651 aluminum alloy. The 26 fuel tubes are fabricated from Type 304 stainless steel. The threaded rods and spacer nuts are fabricated from 17-4 PH stainless steel. The stainless steel tubes are not structural components; therefore, they are not considered in the evaluation of the basket structural strength. The primary function of the threaded spacer nuts is to locate and structurally assemble the support disks, heat transfer disks and top and bottom weldment plates into an integral assembly. The threaded rod

carries the inertial weight of the spacer nuts, support disks, heat transfer disks, one end plate, and their own inertial weight for a normal transport conditions 1-foot end drop. The end drop loading of the spacer nuts and threaded rods represents a classical closed form structural analysis. Therefore, the only basket component that requires a detailed finite element structural evaluation is the support disk.

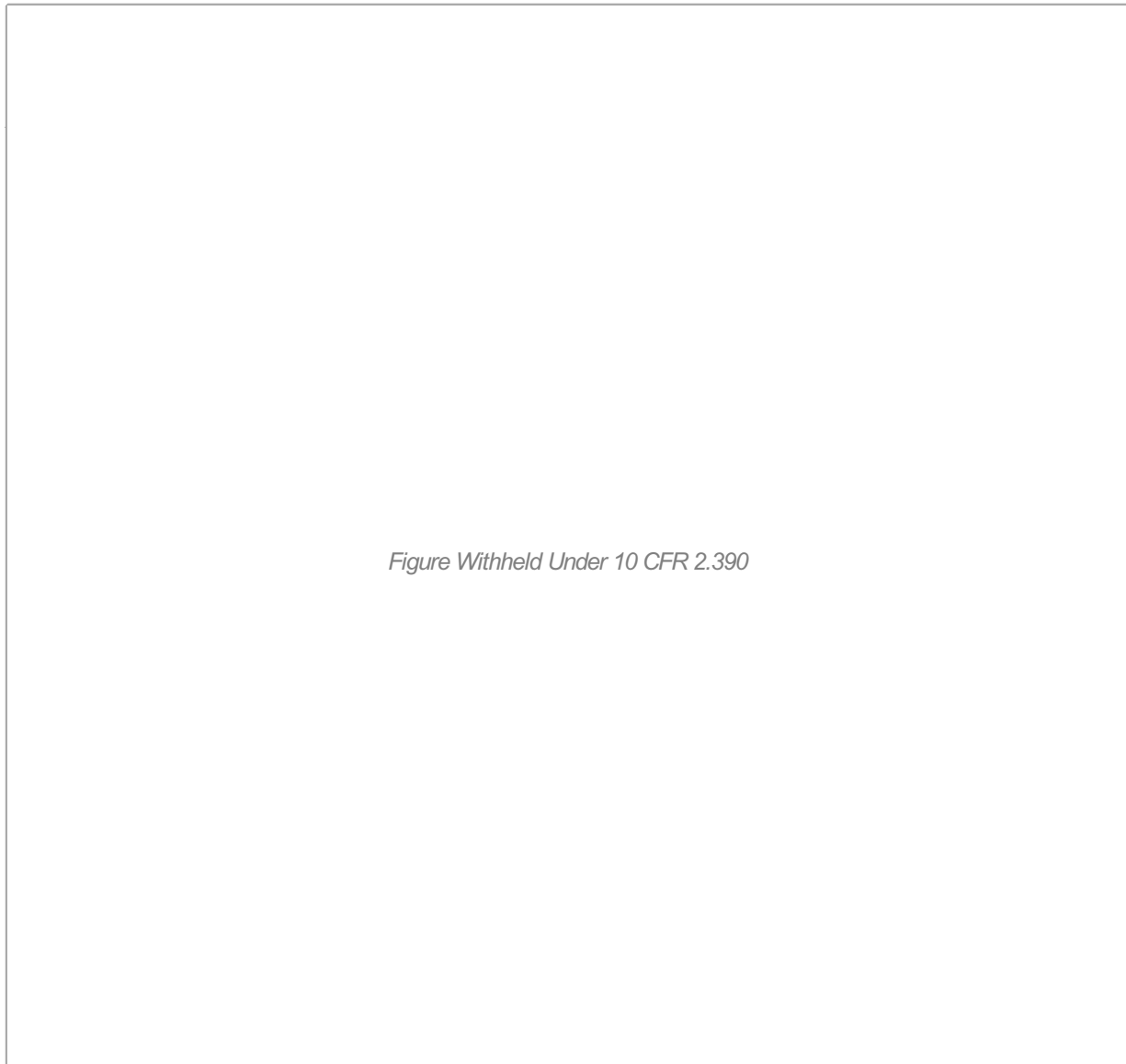
The fuel basket is evaluated for the normal transport condition loads in this section and is evaluated for the hypothetical accident condition loads in Section 2.7.8.

Figure 2.6.12-1 NAC-STC PWR Fuel Assembly Basket for Directly Loaded Fuel

Figure Withheld Under 10 CFR 2.390

(Dimension in inches)

Figure 2.6.12-2 Support Disk Cross-Section Configuration for Directly Loaded Fuel



(Dimensions in inches)

Figure 2.6.12-3 Fuel Tube Configuration for Directly Loaded Fuel



Figure Withheld Under 10 CFR 2.390

THIS PAGE INTENTIONALLY LEFT BLANK

2.6.12.1 Detailed Analysis - PWR Basket For Directly Loaded Fuel

Based on criticality control requirements, the directly loaded fuel configuration fuel basket design criteria requires the maintenance of fuel support and control of spacing of the fuel assemblies for all load conditions. The structural design criteria for the structural components in the fuel basket is the ASME Boiler and Pressure Vessel Code, Section III, Division 1, Subsection NG, "Core Support Structures." Consistent with this criteria, the main structural component in the fuel basket, the stainless steel support disk, is shown to have a maximum stress intensity in any disk for any normal condition load and position orientation to be less than the design stress intensity value, S_m . The material design stress intensity used in this evaluation is based on the maximum material temperature of 650°F for all locations in the basket unless otherwise indicated. Using a stress allowable at 650°F is conservative since the material design stress intensity reduces with temperature and the hottest location in the basket structure during normal conditions is 498°F (Table 3.4-1). In the vertical orientation, the fuel basket components are loaded by their own inertial weight and do not experience load from the guided, but free standing fuel assemblies. Structural loads are experienced in the basket components from the fuel assemblies when the cask is in any orientation other than vertical. All possible orientations are evaluated. In addition to the load from inertial weight, the differential thermal expansion on the support disk is also evaluated.

THIS PAGE INTENTIONALLY LEFT BLANK

2.6.12.2 Finite Element Model Description - Directly Loaded PWR Fuel Basket

Three separate finite element analyses are performed for the directly loaded fuel configuration PWR basket support disk evaluations: One for the structural (stress) analysis of the normal transport conditions free thermal expansion, a second for the side drop impact condition, and a third for the evaluation of the end drop impact condition. These evaluations are performed using ANSYS, Revision 4.4.

The temperature distribution on the support disk is determined in a separate thermal analysis, which uses a three-dimensional finite element model representing one-quarter of the cask. The thermal analysis model, documented in Section 3.4, considers the fuel, fuel tubes, cavity gas, support disks, heat transfer disks, and basket end plates, lids, cask shells, neutron shield, and impact limiters.

The support disk and heat transfer disk nodes and elements at the axial location of maximum temperature in the thermal analysis model, Section 3.4, are extracted and converted into structural models. The temperature distribution determined from the thermal analysis is then respectively mapped to the thermal stress analysis models. An overall view of the finite element model for thermal stress analysis is shown in Figure 2.6.12.2-1. In the thermal stress analysis model, the support disk is modeled with ANSYS three-dimensional isoparametric solid elements (STIF45). The radius at the corners of the support disk holes is not modeled; thus, the corners of the holes in the support disk will behave as a notch in a uniaxial stress field. This finite element model is conservative for this analysis.

No displacement restraints are applied on the thermal expansion stress model. Thermal expansion stress is developed from the temperature gradient from the hot center of the disk to the cooler free edge. Since the center of the disk wants to expand faster than the edge, a tension stress is developed in the disk.

The finite element model for the side drop impact analysis uses (STIF42) ANSYS quadrilateral elements as shown in Figure 2.6.12.2-2, with ANSYS two-dimensional gap elements (STIF12) at all nodes on the periphery of the support disks. The gap elements are used to simulate the interface between the support disk and the inner shell of the cask. Each gap element contains two nodes; one, specified at the inner shell, is restrained. The gap size at each gap element is determined by the difference between the support disk diameter and the inside diameter of the cask inner shell at the calculated normal transport conditions temperature. The stiffness of the gap elements is dependent upon the contact area between the disk and the inner shell.

A typical triangular element at the periphery of the support disk is shown in Figure A below in the cylindrical coordinate system R, θ , with respect to the support disk global cylindrical coordinate with its origin at the center of disk. The stiffness K of the gap element between the cask cavity and basket support disk is based on the stiffness of the adjacent isoparametric elements, in this case, ANSYS STIF42 triangular elements, as shown in Figure 2.6.12.2-2. Figures A through E depict the methodology used to calculate the stiffness for a typical element at the periphery of the support disk.

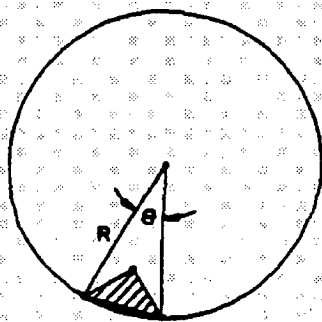


FIGURE A:
TYPICAL BOUNDARY ELEMENTS

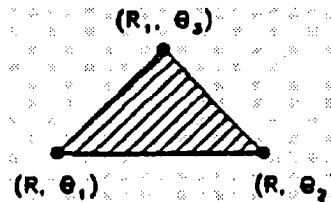


FIGURE B:
SPATIAL LOCATION OF NODE

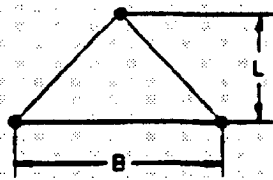


FIGURE C:

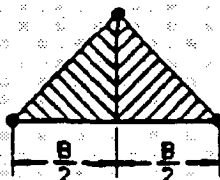


FIGURE D:

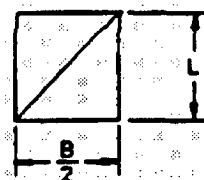


FIGURE E:

Basket/Cavity Gap Element Stiffness

Implementing this methodology, the gap element stiffness is calculated as follows:

$$K = \left(\frac{AE}{L} \right) = \left(\frac{BtE}{2L} \right) = 7.9E + 6 \text{ pounds/in.}$$

where:

- t = Thickness of support, disk = 0.5 inch
- E = Elastic modulus = 28.3E+6 psi at 70°F

L and B as shown in Figures C through E are calculated as follows:

$$\begin{aligned} R &= 35.41 \\ R_1 &= 34.594 \\ \theta_1 &= 56.744^\circ \\ \theta_2 &= 55.273^\circ \\ \theta_3 &= 56.016^\circ \\ B &= 2R \sin (\theta/2) \\ \theta &= 56.744 - 55.273 = 1.469^\circ \quad (\text{From coordinates shown in Figure B}) \\ R &= 35.41 \text{ in} \\ L &= R \cos (\theta/2) - R_1 = 0.8131 \\ R_1 &= 34.594 \text{ From coordinates shown in Figure B)} \\ \frac{\theta}{2} &= \frac{1.469^\circ}{2} = 0.7345^\circ \end{aligned}$$

The stiffness value used in all analyses is 1.0E+6 pounds per inch.

The analysis results are then examined to ensure that any overlapping between the loaded support disk and the cask inner shell in the ANSYS model is less than 1 percent of the thickness of the inner shell; the actual overlap is only 0.5 percent; therefore, the gap element stiffness of 1.0E+6 psi is appropriate for use in the basket support disk side drop evaluations.

The finite element model for the thermal stress conditions, ANSYS STIF45 (Figure 2.6.12.2-1), is used to evaluate the heat transfer disk and the support disk for the end impact condition. The gravity loading is applied in the cask longitudinal direction (lateral to the plane of the heat transfer disk and support disk). The support disks and the heat transfer disks are separated by spacer nuts on threaded rods at six locations near the periphery of the disks; therefore, displacement restraints are applied at the nodes on the disk models where the six threaded rods are located.

Figure 2.6.12.2-1 Finite Element Model - Thermal Stress Analysis (NAC-STC PWR Basket Support Disk for Directly Loaded Fuel)

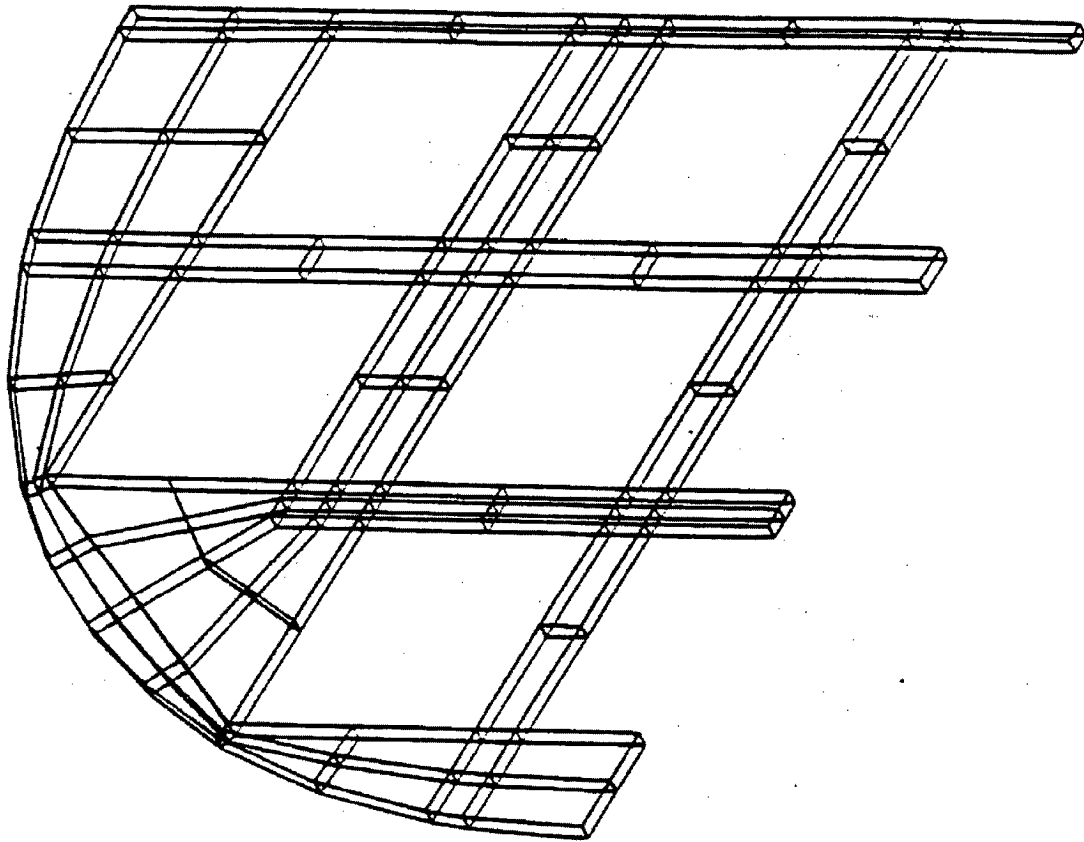
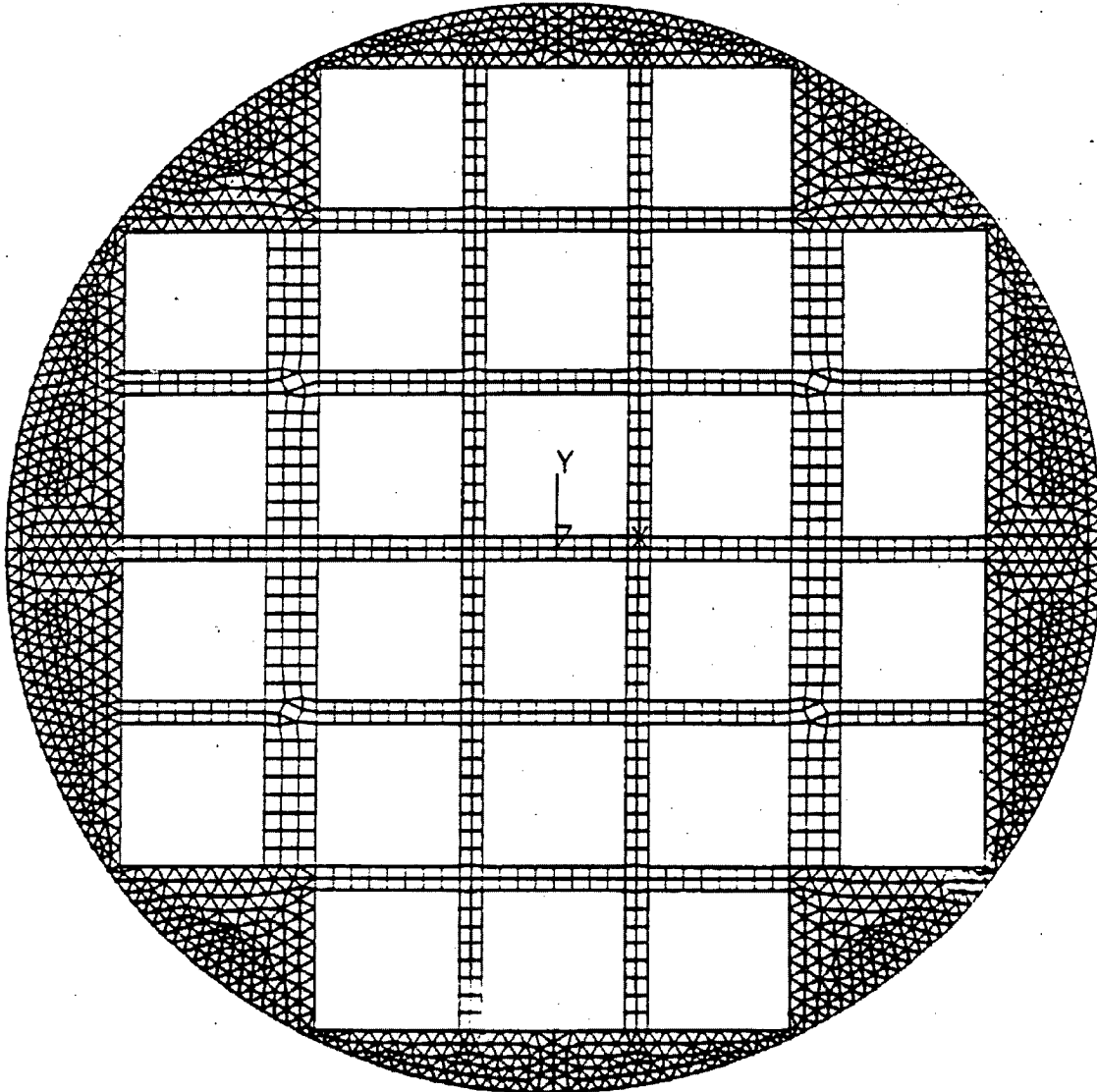


Figure 2.6.12.2-2 Finite Element Model - Side Impact Analysis (NAC-STC PWR Basket Support Disk for Directly Loaded Fuel)



THIS PAGE INTENTIONALLY LEFT BLANK

2.6.12.3 Thermal Expansion Evaluation of Support Disk - Directly Loaded PWR Fuel Basket

A thermal stress analysis is performed, using ANSYS, to determine the differential thermal expansion and the associated thermal stresses in a support disk for the directly loaded fuel configuration that result from the heat load generated by the 26 fuel assemblies. The thermal stresses in the support disk are developed by differential thermal expansion resulting from a nonuniform temperature distribution, which is calculated using the ANSYS program for a heat load of 0.85 kilowatts per assembly in the thermal analysis (Section 3.4). The temperatures obtained from the thermal analysis are also used to determine the temperature-dependent material properties of the support disk and to evaluate the thermal strains in the support disk. No displacement restraints are imposed on the support disk for the free thermal stress analysis.

The stress summary for the 20 nodes with the maximum thermal stress intensity is shown in Table 2.6.12.3-1. The location of these nodes on the support disk is shown in Figure 2.6.12.3-1.

Evaluation of thermal expansion of the fuel basket relative to the inside surface of the inner shell of the cask has been performed for compatible sets of thermal data and transport package configurations.

The transport configuration with the cask in the horizontal position with impact limiters installed represents the normal transport configuration. Although the cask is backfilled with an inert atmosphere of helium at the time of fuel loading, in order to eliminate the need to disturb the containment boundary to perform tests to validate that helium remained in the cask cavity throughout an extended period of storage prior to package transport, heat transfer analysis has been performed considering the cask in a horizontal orientation, cavity filled with air, and fresh fuel decay heat of 0.85 kilowatts per assembly. Temperature data from this analysis is used to calculate the diametral thermal expansion of the inside diameter of the inner shell (0.134 inches), outer diameter of the steel support disk (0.148 inches) and the outer diameter of the aluminum heat transfer disk (0.336 inches). Considering maximum material conditions and the horizontal orientation as shown in Figure 2.6.12.3-2, the minimum gap between the basket steel support disk and the cask wall is 0.086 inches. For the heat transfer disk, the minimum gap is 0.108 inches.

Cask Horizontal With Air in Cavity (Directly Loaded Fuel Configuration)

	Hot Diameter (inches)	Tolerance (inches)	Gap (inches)
Inner Shell Surface	71.134	+0.06/-0.04	----
Steel Support Disk	71.008	+0.0/-0.02	0.086
Aluminum Heat Transfer Disk	70.986	+0.0/-0.02	0.108

Similar to the analysis performed for the cask in the horizontal configuration, temperatures throughout the cask and basket for the freshly loaded fuel backfilled with helium without impact limiters in the vertical configuration were calculated. This set of temperatures were then used to calculate the thermal expansion of the cask inside surface and the basket support disk and heat transfer disk. Considering maximum material conditions and manufacturing tolerances for the package in the vertical configuration, as shown in Figure 2.6.12.3-3, the minimum diametral gap between the steel support disk and cask wall is 0.084 inches, or 0.042 inches on the radius. The minimum diametral gap between the aluminum heat transfer disk and the cask wall is 0.062 inches, or 0.031 inches on the radius.

Cask Vertical With Helium In Cavity (Directly Loaded Fuel Configuration)

	Hot Diameter (inches)	Tolerance (inches)	Gap (inches)
Inner Shell Surface	71.1583	+0.06/-0.04	----
Steel Support Disk	71.0348	+0.0/-0.02	0.084
Aluminum Heat Transfer Disk	71.056	+0.0/-0.02	0.062

In addition to these steady state conditions, it has been postulated that the greatest difference in temperature of the basket relative to that of the cask body/inner shell is during the thermal transient created during the loading, and vacuum drying and heat-up process. This potential worst case condition is evaluated using component temperatures calculated as a function of time beginning from a 70°F material temperature condition through a steady state temperature profile for the design bases heat load. Considering maximum material conditions and manufacturing tolerances for the package in the vertical configuration as shown in Figure 2.6.12.3-3, the minimum gap between the basket and cask wall is 0.0778 inches over the diameter and 0.0389

inches on the radius for the steel support disk, and 0.0774 inches over the diameter and 0.0387 inches on the radius for the aluminum heat transfer disk. The results are summarized as:

Heat up Transient (Directly Loaded PWR Fuel Configuration)

	Hot Diameter (inches)	Tolerance (inches)	Gap (inches)
Inner Shell Surface	71.1378	+0.06/-0.04	-----
Steel Support Disk	71.0200	+0.0/-0.02	0.0778
Aluminum Heat Transfer Disk	70.0204	+0.0/-0.02	0.0774

Based on these analyses for normal transport, vertical steady-state, and heat-up transient, the basket assembly does not contact the cask inner shell wall and does not produce restrained thermal expansion loads on the steel support disks or aluminum heat transfer disks considering maximum design bases heat load, maximum material conditions, and worst case tolerance stack-up.

Figure 2.6.12.3-1 Location of the 20 Maximum SI Nodal Stresses in the NAC-STC Fuel Basket Support Disk for Directly Loaded Fuel - Thermal Condition

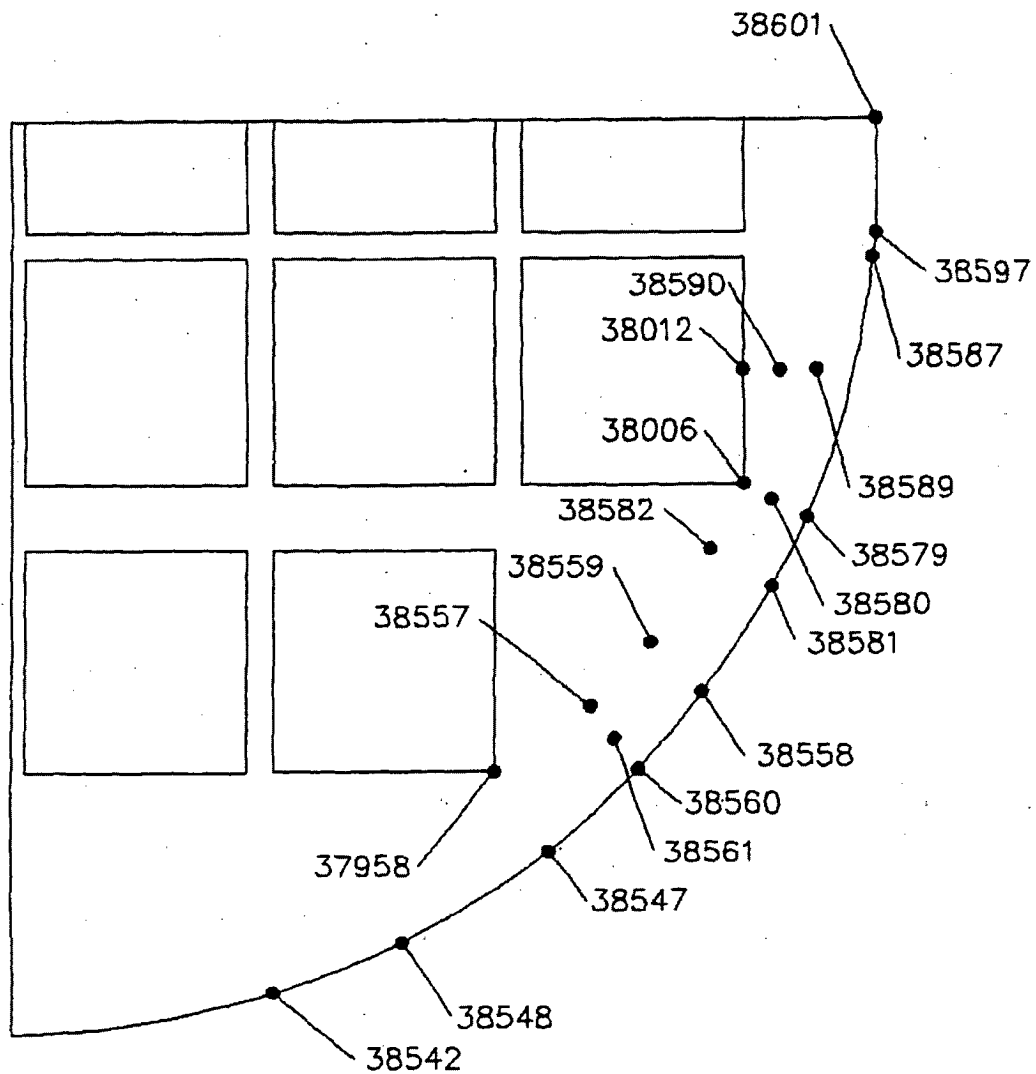


Figure 2.6.12.3-2 Basket Maximum Material Condition for the Directly Loaded Fuel Configuration in the Horizontal Orientation (inches)

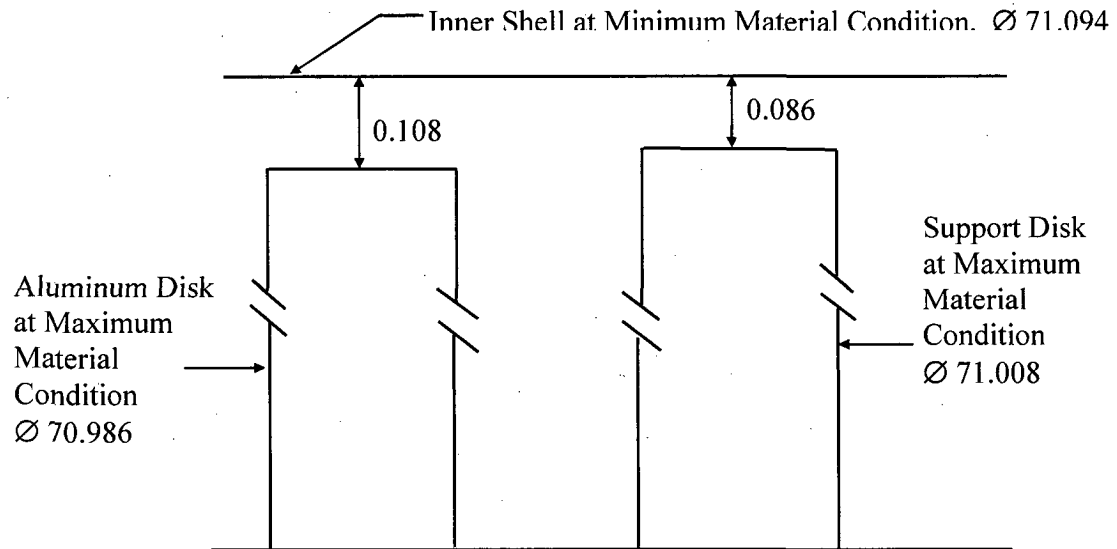
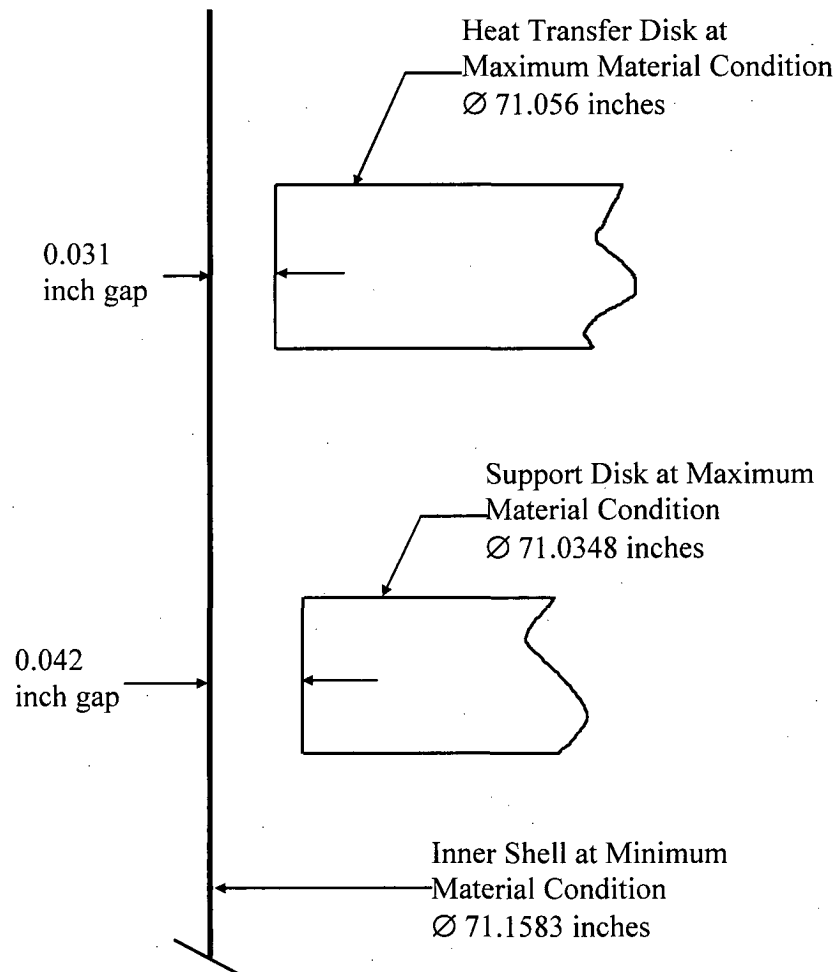


Figure 2.6.12.3-3 Basket Maximum Material Condition for Directly Loaded Fuel Configuration - Cask Vertical



The basket is assumed to be located at the center of the cask cavity.

Table 2.6.12.3-1 Thermal Stresses (NAC-STC PWR Basket - Directly Loaded Fuel Configuration)

Node No. ¹	S _x (ksi)	S _y (ksi)	S _z (ksi)	S _{xy} (ksi)	S _{yz} (ksi)	S _{xz} (ksi)	SI (ksi)
38006	2.3	23.6	0.8	10.1	0.0	-0.1	32.0
37958	19.6	8.2	-1.3	11.8	0.0	0.0	30.6
38558	12.2	17.8	-0.6	14.5	0.0	0.0	30.4
38580	4.7	18.7	-2.6	10.0	0.0	-0.1	29.4
38560	12.7	10.3	-0.7	12.6	-0.2	0.2	27.6
38581	8.2	18.3	0.3	11.4	0.0	0.2	26.4
38587	0.0	23.7	-0.3	3.9	0.0	0.0	25.4
38547	12.9	8.2	-2.3	9.5	0.2	-0.1	25.2
38589	0.6	20.3	0.1	6.7	0.0	0.0	24.0
38590	-1.1	19.8	0.0	5.3	0.0	-0.1	23.8
38561	12.3	8.6	0.9	10.9	-0.2	0.1	23.8
38579	4.7	15.6	-0.4	8.4	0.0	0.0	23.3
38559	8.9	13.6	-0.5	10.9	0.0	0.0	22.9
38597	0.1	22.8	0.4	1.2	0.0	0.0	22.8
38557	9.9	6.6	1.1	10.4	0.0	0.0	21.8
38582	7.6	16.3	1.4	9.2	0.0	0.0	21.5
38012	-3.3	15.6	-2.1	4.0	0.0	-0.1	20.7
38542	17.6	0.8	-0.5	5.6	0.0	0.0	20.5
38601	0.0	20.1	0.2	0.6	0.0	0.0	20.1
38548	13.3	2.5	-0.3	7.8	-0.1	0.0	19.4

¹ Stress components are listed for the nodes with the 20 highest thermal stresses (see Figure 2.6.12.3-1 for locations of these nodes). Note that S_x is the stress in the radial direction, S_y is the stress in the circumferential direction and S_{xy} is the shear stress.

THIS PAGE INTENTIONALLY LEFT BLANK

2.6.12.4 Stress Evaluation of Support Disk for a 1-Foot End Drop Load Condition
(Directly Loaded Fuel Configuration)

The support disks of the directly loaded fuel configuration of the NAC-STC fuel basket are located by threaded rods and spacer nuts positioned at six points on the circumference near the periphery of each disk. A structural analysis is performed, using ANSYS, to evaluate the effect of a 1-foot end drop impact (out-of-plane loading) on the support disks in the NAC-STC with the cask in the vertical position. The ANSYS STIF45 brick element as described in Section 2.6.12.2 is used in the model as shown in Figure 2.6.12-2. The end drop impact loading is applied in the cask longitudinal direction (perpendicular to the plane of the support disk). A load factor of 19.6 g is applied to the mass of the support disk. The value of 19.6 g is the maximum deceleration of the NAC-STC for the 1-foot end drop impact (Table 2.6.7.4.1-3). Displacement restraints are applied in the ANSYS model at the nodes where the six threaded rods with spacer nuts are located.

The stress summary for the locations of the 20 nodes with the highest stress intensity, SI, 1-foot end drop impact stresses shown in Figure 2.6.12.4-1 is provided in Table 2.6.12.4-1. The maximum SI nodal stress is 12.65 ksi. The minimum margin of safety calculated relative to the design stress intensity, S_m is +2.56. The margin of safety of +2.56 is conservative since further stress classification in accordance with ASME Code, Section III, Subsection NG criteria permits the membrane stress, P_m , which is lower than the total node point stress, SI, to reach S_m , or the primary membrane plus primary bending stress, $P_m + P_b$, to reach the value of $1.5S_m$.

Figure 2.6.12.4-1 Support Disk For the Directly Loaded Fuel Configuration - 19.6-g
End Drop

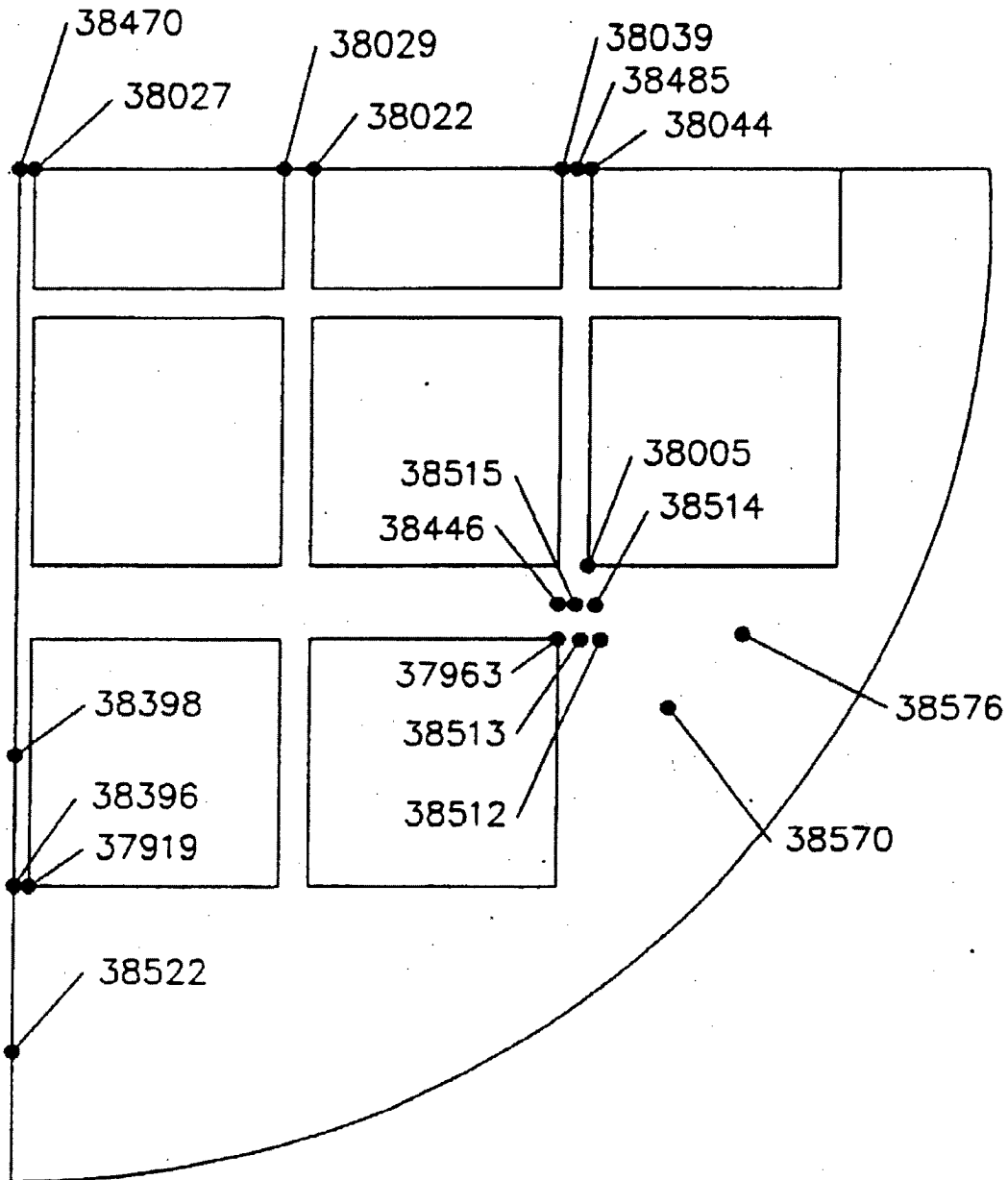


Table 2.6.12.4-1 Stresses for 1-Foot End Drop Impact with a 19.6-g Deceleration
(NAC-STC PWR Basket - Directly Loaded Fuel Configuration)

Node No. ¹	S _x (ksi)	S _y (ksi)	S _z (ksi)	S _{xy} (ksi)	S _{yz} (ksi)	S _{xz} (ksi)	SI (ksi)	MS ²
38512	-7.6	-8.3	1.8	0.7	1.7	0.0	12.7	2.6
38522	-3.2	-2.4	-0.4	-2.4	-4.6	-0.7	11.4	3.0
38513	-4.0	-4.9	1.2	1.4	-0.9	-0.7	10.9	3.1
38570	-3.6	-3.8	-0.5	0.5	0.0	1.2	10.4	3.3
38396	-3.3	-8.2	-0.2	2.0	2.4	-0.2	10.1	3.5
38514	-6.1	-5.5	0.5	0.6	0.9	0.8	10.0	3.5
37963	-2.8	-4.5	0.5	2.8	0.8	-1.0	9.7	3.6
37919	-2.7	-5.9	0.0	1.5	-1.6	-0.2	9.1	3.9
38515	-7.9	-7.0	-0.9	0.4	-0.8	1.4	8.4	4.3
38027	-0.7	6.5	-0.6	-0.2	-0.1	0.7	7.9	4.7
38576	-3.7	-5.7	-0.9	1.0	1.1	-0.5	7.9	4.7
38470	-0.8	6.3	-0.7	0.0	0.1	-0.8	7.8	4.7
38005	-5.0	-4.6	-0.4	1.5	0.7	-0.6	7.8	4.7
38029	0.1	7.1	-0.2	0.0	0.0	-0.5	7.6	4.9
38032	0.1	7.0	-0.2	0.0	0.0	0.0	7.6	4.9
38039	0.0	7.6	0.0	0.0	0.0	0.0	7.6	4.9
38044	0.0	7.4	0.0	0.0	0.0	0.0	7.4	5.0
38485	0.0	7.3	0.0	0.0	0.0	0.0	7.4	5.1
38446	-6.5	-5.0	-0.6	1.4	0.0	0.0	7.4	5.1
38398	0.8	-4.5	0.7	-0.6	-1.1	0.7	7.1	5.3

¹ Stress components are listed for the nodes with the 20 highest thermal stresses (see Figure 2.6.12.4-1 for locations of these nodes). Note that S_x is the stress in the radial direction, S_y is the stress in the circumferential direction and S_{xy} is the shear stress.

² The allowable stress is conservatively defined as S_m at the node point temperature defined by the quarter symmetry heat transfer analysis.

THIS PAGE INTENTIONALLY LEFT BLANK

2.6.12.5 Stress Evaluation of Support Disk (Directly Loaded Fuel Configuration) for Thermal Plus a 1-Foot End Drop Combined Load Condition

The thermal expansion loads in Section 2.6.12.3 are applied to the finite element model simultaneously with the 19.6 g end drop loads in Section 2.6.12.4 to produce a combined thermal expansion plus end impact loading. The stress evaluation is performed according to the ASME Code Section III, Division 1, Subsection NG. Table 2.6.12.5-1 documents the 20 highest total stresses (thermal expansion stresses plus 1-foot end drop impact stresses) at normal transport condition temperatures and the associated margins of safety. Figure 2.6.12.5-1 shows the locations for each of the 20 maximum stress intensity. Comparing these maximum nodal point primary plus secondary stress intensities to the material $3 S_m$ value validates the ASME Code elastic analysis methodology.

Figure 2.6.12.5-1 Location of the 20 Maximum SI Nodal Stresses in the NAC-STC Fuel Basket Support Disk (Directly Loaded Fuel Configuration) - Thermal + 19.6-g End Drop

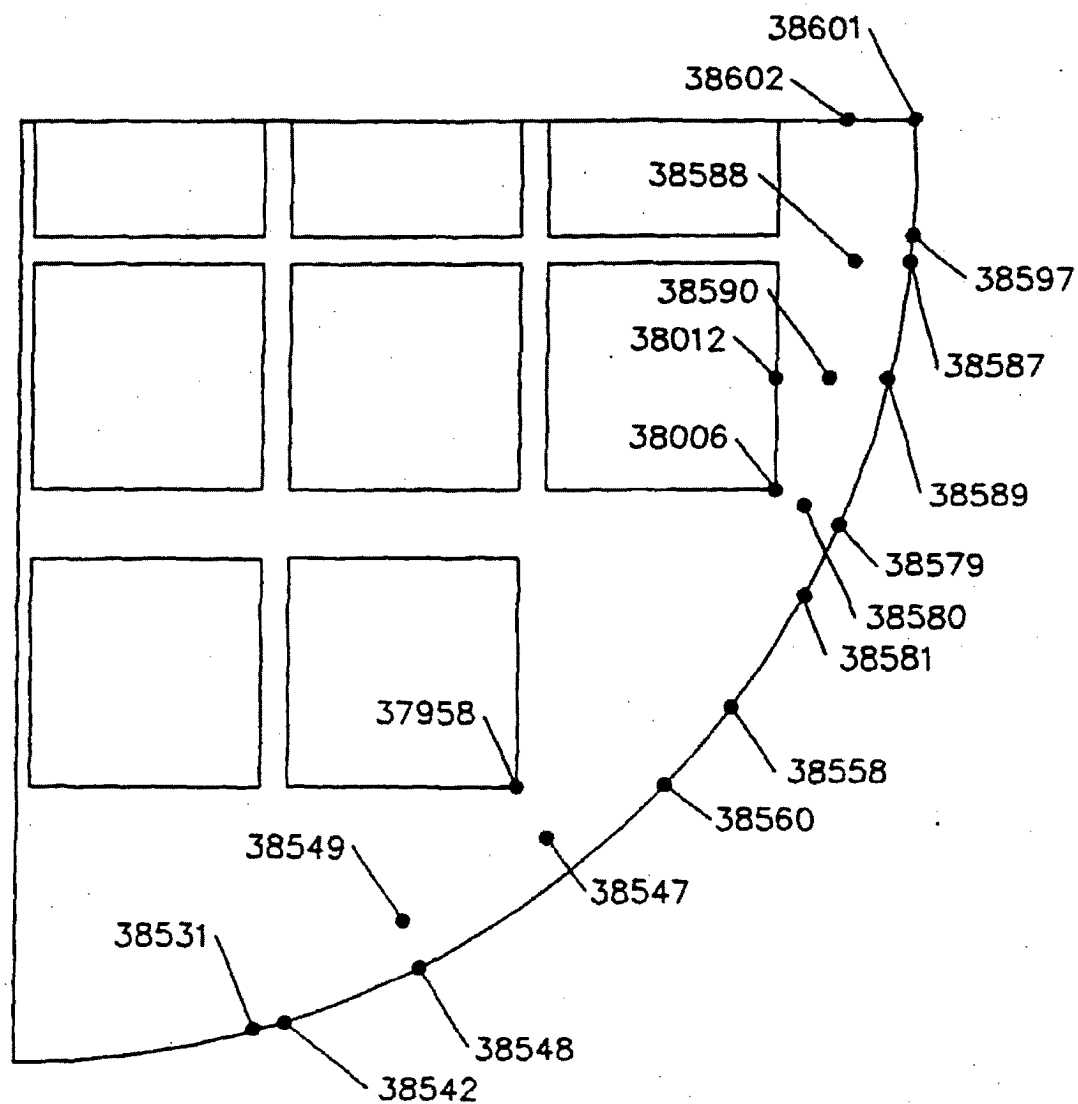


Table 2.6.12.5-1 Combined Stresses for Thermal + 19.6-g End Drop Impact (Directly Loaded Fuel Configuration - Support Disk)

Node No.	S _x (ksi)	S _y (ksi)	S _z (ksi)	S _{xy} (ksi)	S _{yz} (ksi)	S _{xz} (ksi)	SI (ksi)	3S _m ¹ (ksi)
38006	0.4	26.8	0.0	11.3	0.3	1.3	39.4	125.7
38587	0.4	35.9	0.3	4.2	-0.4	-0.2	38.2	125.7
38580	2.0	22.8	-5.4	11.1	0.2	-0.1	37.8	125.7
38590	-0.6	32.1	0.9	6.0	0.2	-0.6	36.5	125.7
38589	0.8	32.3	0.7	7.6	-0.9	0.2	35.9	125.7
38597	0.0	34.9	0.4	1.9	-0.9	0.3	35.6	125.7
37958	21.3	7.5	-1.8	12.7	0.8	0.0	35.3	125.7
38012	-2.9	28.4	-1.2	4.6	0.0	-1.4	35.0	125.7
38601	0.3	33.6	0.2	0.9	1.1	0.4	33.8	125.7
38542	26.6	1.8	0.0	6.4	0.4	0.5	30.4	125.7
38579	2.4	20.3	-0.9	9.5	0.0	-2.0	30.1	125.7
38547	15.3	7.1	-3.3	10.5	0.3	-0.5	29.9	125.7
38558	11.5	17.0	-0.6	13.7	0.0	0.0	28.7	125.7
38531	25.9	1.0	0.2	4.6	-0.1	1.0	27.4	125.7
38560	12.7	9.9	-0.7	12.1	-0.5	0.8	27.3	125.7
38549	19.4	0.5	0.4	7.7	0.6	-0.2	26.5	125.7
38548	19.5	2.6	-0.2	9.2	0.2	0.4	26.3	125.7
38581	8.0	18.4	0.5	10.8	-0.5	0.4	26.1	125.7
38588	-0.3	23.4	0.8	2.0	0.7	-0.3	25.3	125.7
38602	0.0	24.1	0.0	0.3	0.0	0.0	24.8	125.7

¹ S_m is conservatively defined for a temperature of 650°F.

THIS PAGE INTENTIONALLY LEFT BLANK

2.6.12.6 Stress Evaluation of Threaded Rods and Spacer Nuts for a 1-Foot End Drop Load Condition (Directly Loaded Fuel Configuration)

The deceleration for the NAC-STC for the normal conditions of transport 1-foot end drop is 19.6 g. During the 1-foot end drop, the threaded rods and spacer nuts in the directly loaded fuel configuration fuel basket are loaded with the weight of the 31 support disks, 20 aluminum heat transfer disks, one end plate and the weights of the threaded rods and spacer nuts. A conservative basket weight of 17,000 pounds is used. The loads are calculated as follows:

Total weight of basket	= 17,000 lbs
Less weight of bottom weldment	= -671 lbs
Less weight of fuel tubes	= <u>-3,666</u> lbs
1-g load on the tie rods and spacer nuts	= 12,663 lbs
Normal conditions of transport load on tie rods and spacer nuts	= (12,663)(19.6) = 248,195 lbs

The effective area of one threaded rod and spacer nut at each of the six locations supporting the weight of the support disks is equivalent to the gross area of the square spacer nut and is calculated as:

$$\begin{aligned} A &= (2.5)(2.5) \\ &= 6.25 \text{ in}^2 \end{aligned}$$

The average compressive stress in the threaded rods and spacer nuts is:

$$\begin{aligned} S_c &= \frac{248,195}{(6)(6.25)} \\ &= 6,619 \text{ psi} \end{aligned}$$

The allowable stress of the 17-4 PH stainless steel under normal conditions of transport is S_m .

Then, the margin of safety is:

$$MS = \frac{(S_m)}{S_c} - 1 = \underline{+Large}$$

where:

$$S_m = 43.8 \text{ ksi (17-4 PH stainless steel at 405°F)}$$

Therefore, the threaded rods and spacer nuts in the directly loaded fuel configuration of the fuel basket are structurally adequate for a 19.6-g end impact under normal conditions of transport.

2.6.12.7 Stress Evaluation of Support Disk (Directly Loaded Fuel Configuration) for a 1-Foot Side Drop Impact Load Condition

To determine the structural adequacy of the support disks in the 26 PWR fuel assembly basket (directly loaded fuel configuration) for the 1-foot side drop impact load condition, a quasi-static impact load equal to the weight of the fuel and tubes multiplied by an 18.1 g amplification factor is applied to the support disk structure. The 18.1 g inertial loading of the support disk is also included. Each support disk also carries the weight of a single aluminum heat transfer disk, which is applied through the six threaded rods. This additional load is applied to the support disk at the six threaded rod locations in the form of lumped masses. The value of 18.1 g is the NAC-STC impact limiter's design deceleration for a 1-foot side drop condition (Table 2.6.7.4.1-1). The fuel assembly loads are transmitted in direct compression through the tube wall to the web structure of each support disk. These loads are transmitted to the inner shell of the cask by the series of 31 support disks and the top and bottom plates.

The maximum loading occurs on a support disk during a side drop event. Thus, a detailed structural evaluation is required. Figure 2.6.12-2 shows a support disk cross-sectional configuration. A finite element analysis is performed, using the ANSYS computer code, to calculate the stresses in a support disk. The finite element model of the support disk for the side drop analysis is described in Section 2.6.12.2; the model is shown in Figure 2.6.12.2-2.

2.6.12.7.1 Drop Orientations

To bound all possible impact orientations, the support disk configuration (Figure 2.6.12-2) is analyzed for nine drop orientations: 0, 15, 30, 37, 45, 60, 64, 75, and 90 degrees. The drop orientations are identified in Figure 2.6.12.7-1. As shown in Figure 2.6.12.7-1, drop orientations 37 degrees and 64 degrees respectively put each of the support disk minimum ligaments in the direct load line. As discussed in Section 2.6.12.7, the maximum side impact force on the NAC-STC for normal conditions of transport is 18.1 g for a 1-foot side drop.

2.6.12.7.2 Analysis Results (1-Foot Side Drop)

Finite element stress analyses are performed for the 1-foot side impact load cases for the nine different impact orientations listed previously.

The allowable stress limit for the support disk primary membrane stress (P_m) is S_m , and primary membrane plus primary bending stress ($P_m + P_b$) is $1.5S_m$. The stress evaluation is performed in accordance with the ASME Code, Section III, Division 1, Subsection NG adopting the conservative methodology of evaluating nodal stress, $P_m + P_b$, at a maximum temperature of 650°F relative to the smaller P_m allowable of S_m . Implementing this method of structural evaluation is very conservative and demonstrates significant margins of safety.

The locations of the 20 highest nodal SI stresses in the support disk for each of the nine 1-foot side impact orientations evaluated are shown in Figures 2.6.12.7-2 through 2.6.12.7-10. Tables 2.6.12.7-1 through 2.6.12.7-9, respectively, provide tabulations of the nodal SI stresses at those 20 maximum stress locations in the support disk for each of the nine impact orientation. The tables also show the margin of safety for each analysis location for the 18.1 g side impact load condition. Table 2.6.12.7-10 presents a summary of the minimum margins of safety for the 18.1 g side impact analysis for the nine impact orientations.

The minimum conservatively calculated margin of safety for the support disk of the NAC-STC directly loaded fuel configuration basket for a 1-foot side drop is +1.52 which occurs at the 30 degree drop orientation. The margin of safety of +1.52 is conservative since further stress classification shows that the membrane stress, P_m and the membrane plus bending stress, $P_m + P_b$ is lower than the nodal stress intensity SI. The margin of safety of +1.52 is obtained by evaluating an allowable design stress, S_m relative to the total stress intensity, $P_m + P_b$ at a single node point. The ASME Code, Section III, Subsection NG, criteria permits this stress intensity to reach a level of $1.5 S_m$. Therefore, the support disks in the NAC-STC PWR fuel basket are structurally adequate for a 1-foot side drop load condition.

Figure 2.6.12.7-1 Support Disk Side Drop Orientations (Directly Loaded Fuel Configuration)

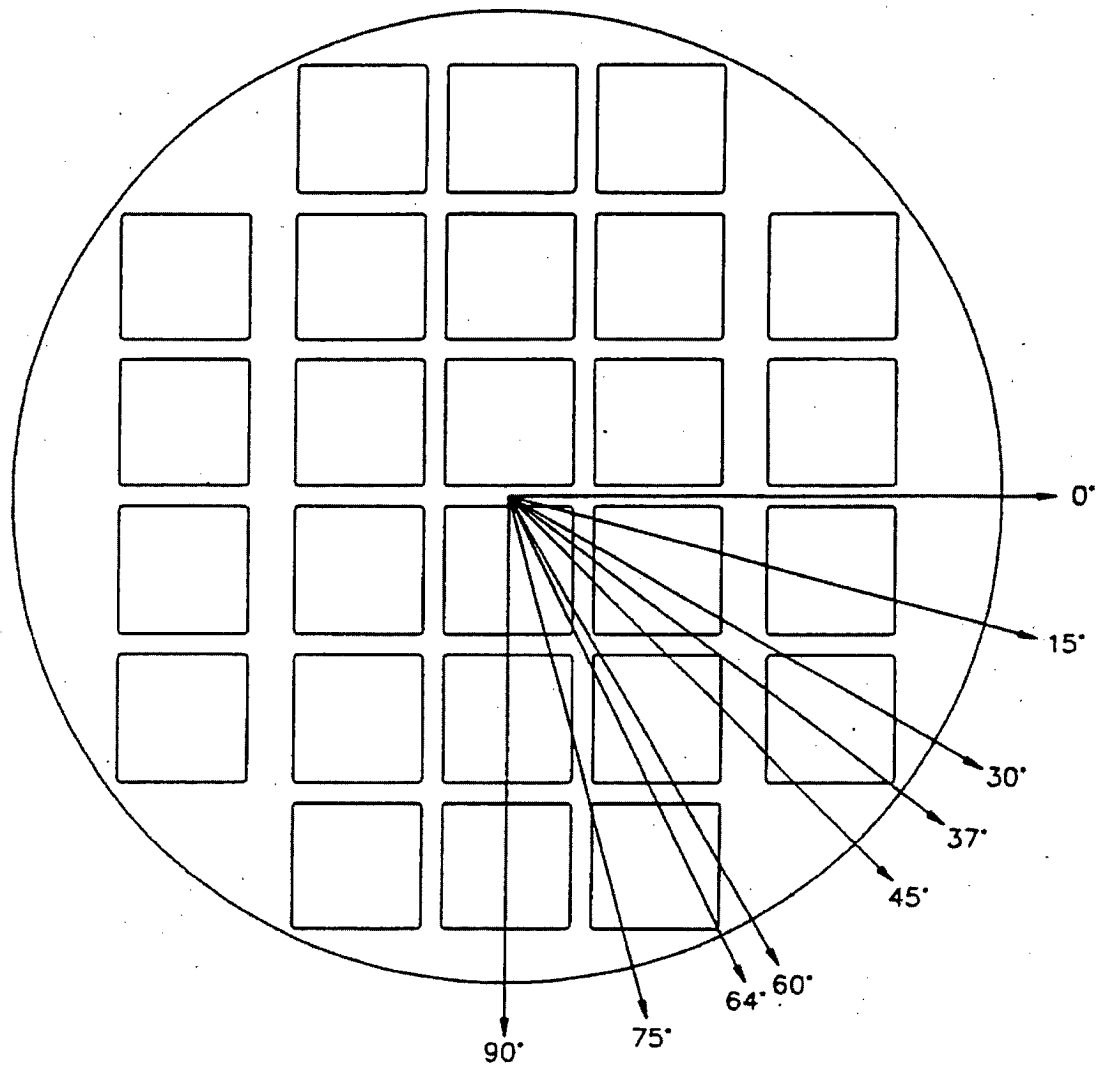


Figure 2.6.12.7-2 Locations of Maximum Nodal SI Stresses (Directly Loaded Fuel Configuration - Support Disk) - 18.1-g Side Impact Condition (0° Drop Orientation)

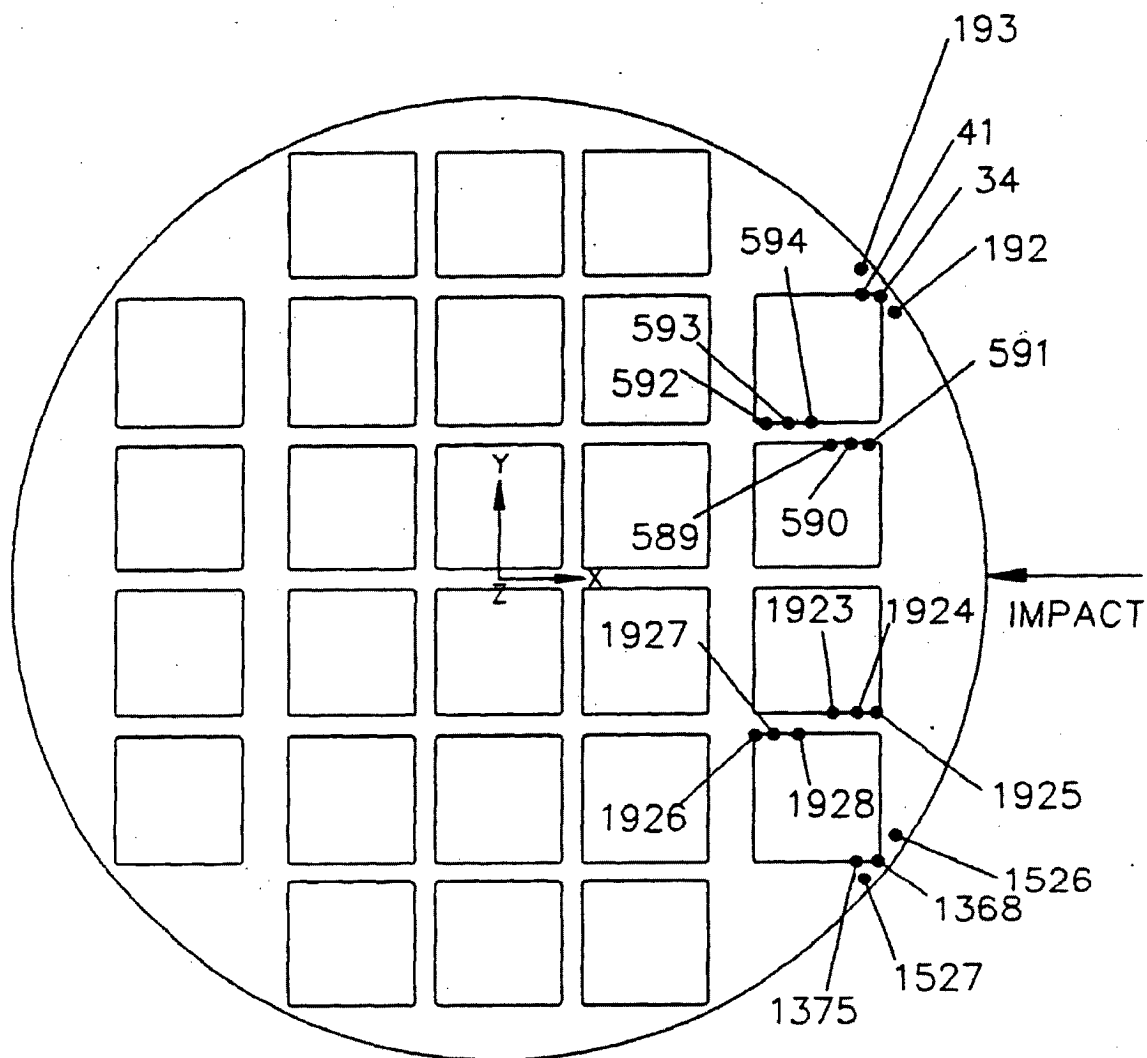


Figure 2.6.12.7-3 Location of Maximum Nodal SI Stresses (Directly Loaded Fuel Configuration - Support Disk) - 18.1-g Side Impact Condition (15° Drop Orientation)

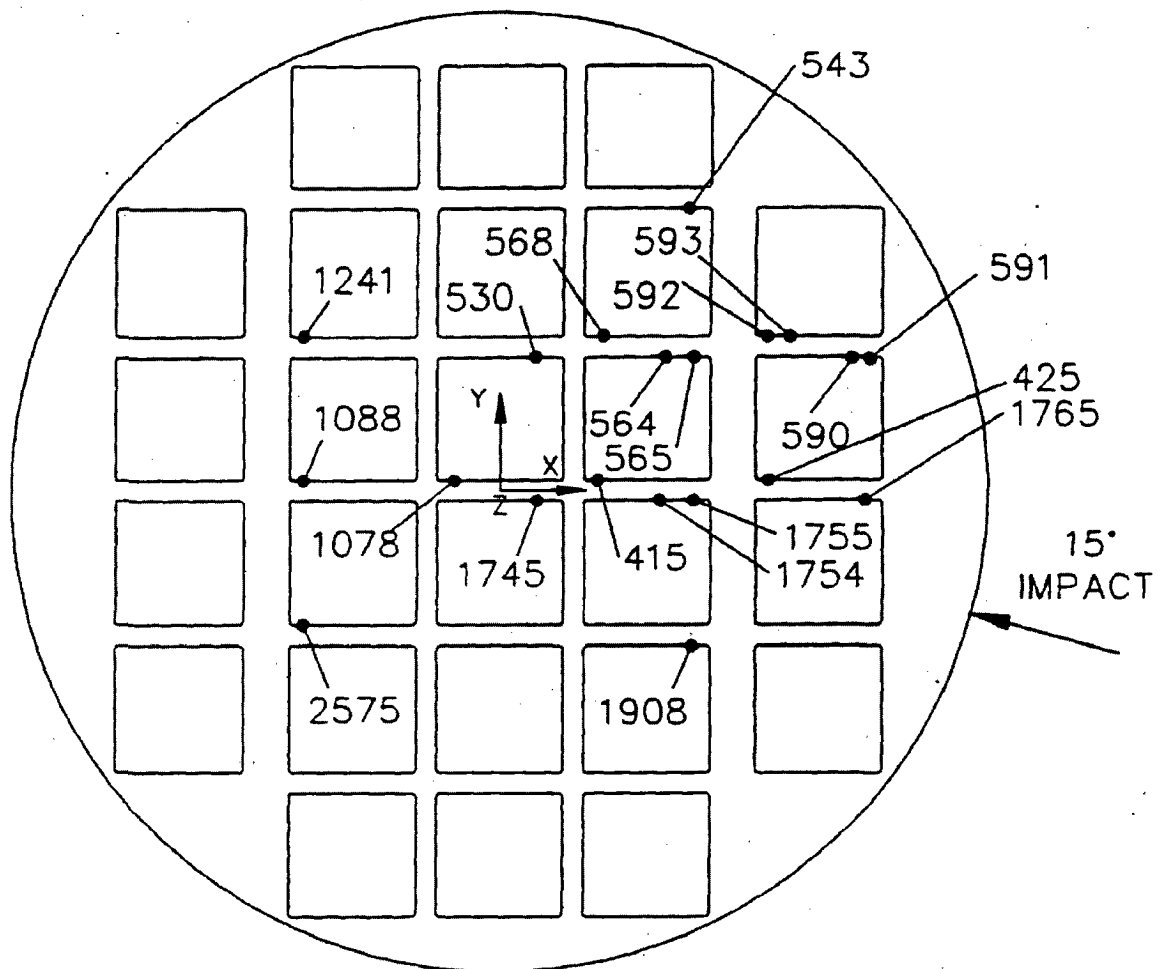


Figure 2.6.12.7-4 Location of Maximum Nodal SI Stresses (Directly Loaded Fuel Configuration - Support Disk) - 18.1-g Side Impact Condition (30° Drop Orientation)

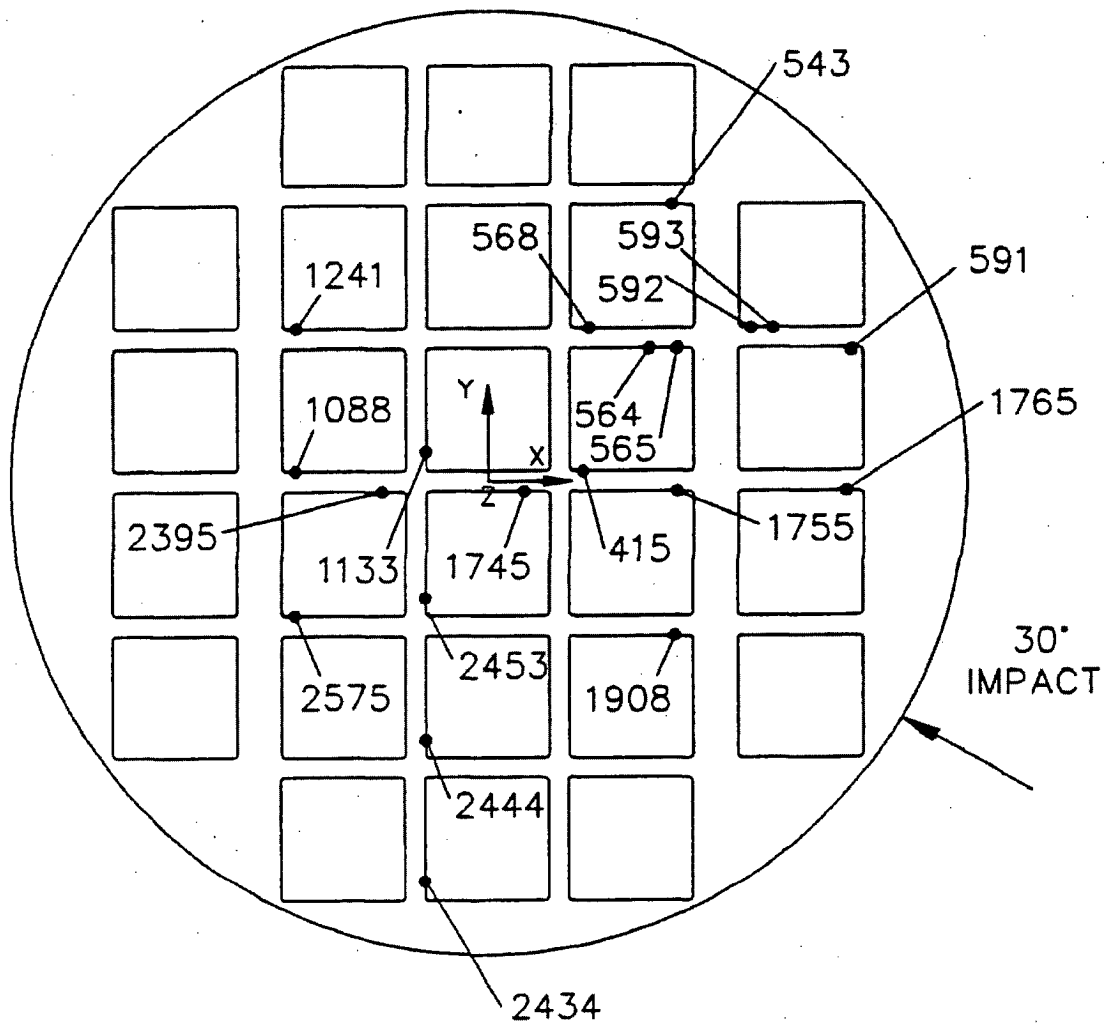


Figure 2.6.12.7-5 Location of Maximum Nodal SI Stresses (Directly Loaded Fuel Configuration - Support Disk) - 18.1-g Side Impact Condition (37° Drop Orientation)

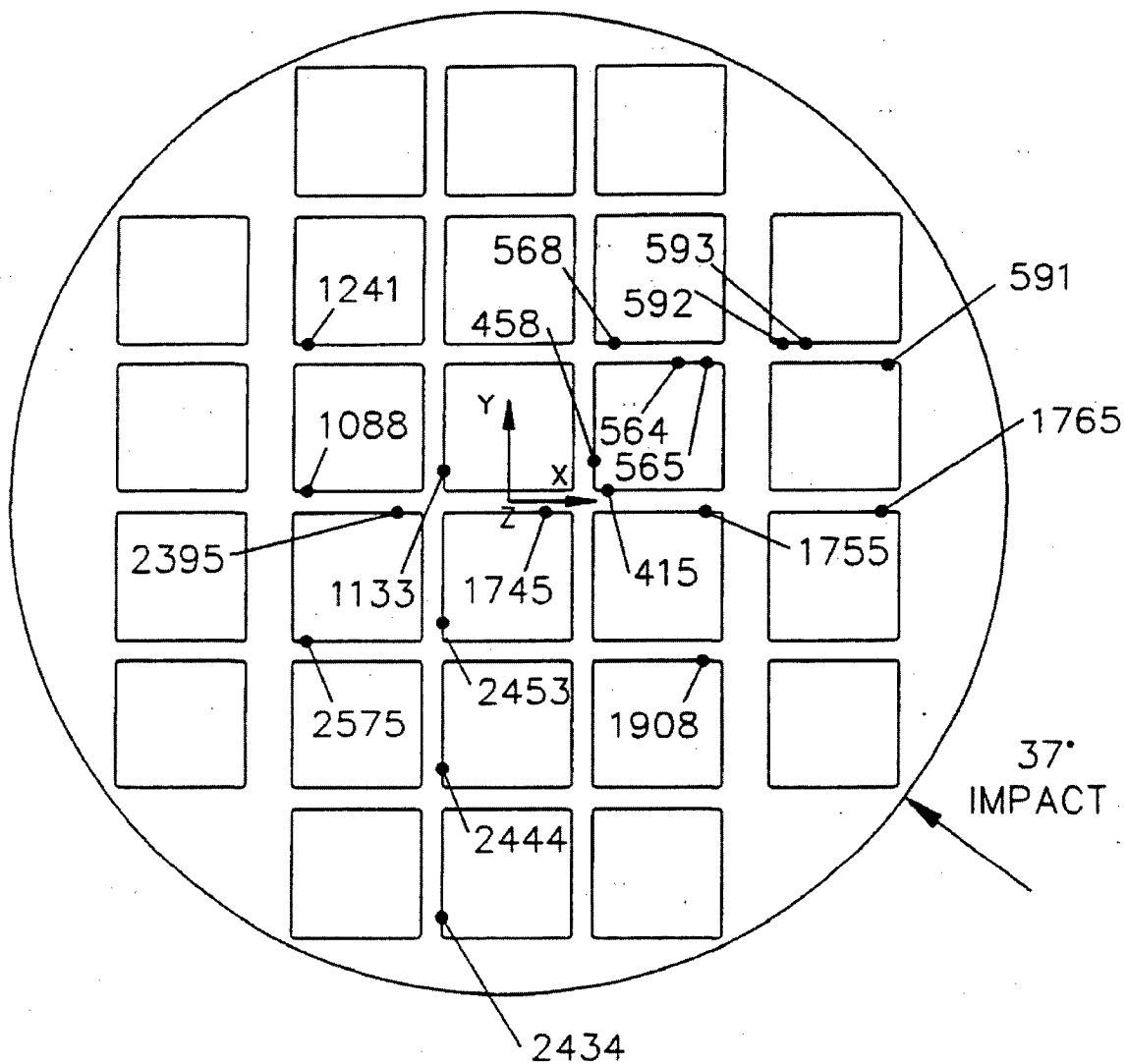


Figure 2.6.12.7-6 Location of Maximum Nodal SI Stresses (Directly Loaded Fuel Configuration - Support Disk) - 18.1-g Side Impact Condition (45° Drop Orientation)

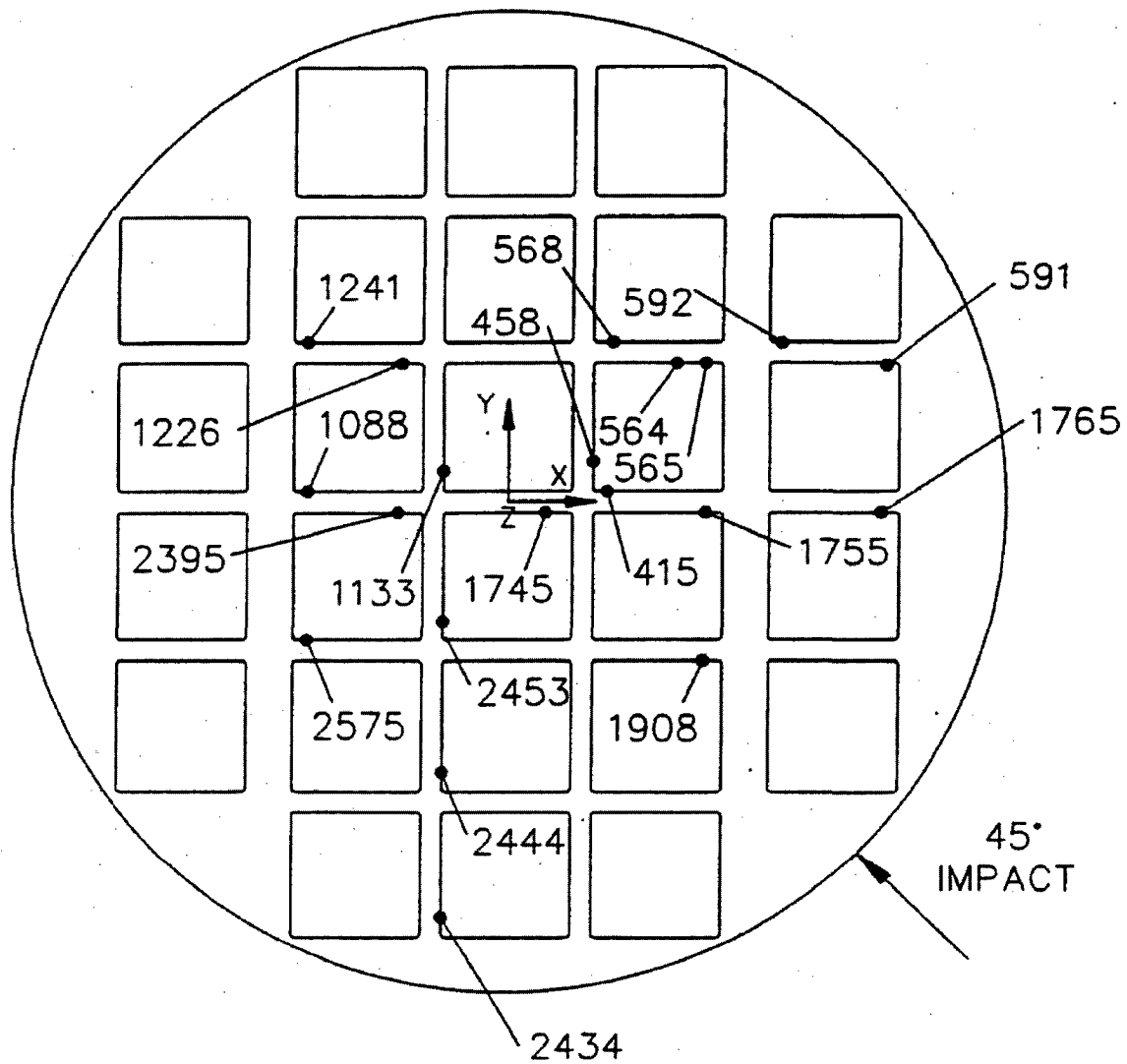


Figure 2.6.12.7-7 Location of Maximum Nodal SI Stresses (Directly Loaded Fuel Configuration - Support Disk) - 18.1-g Side Impact Condition (60° Drop Orientation)

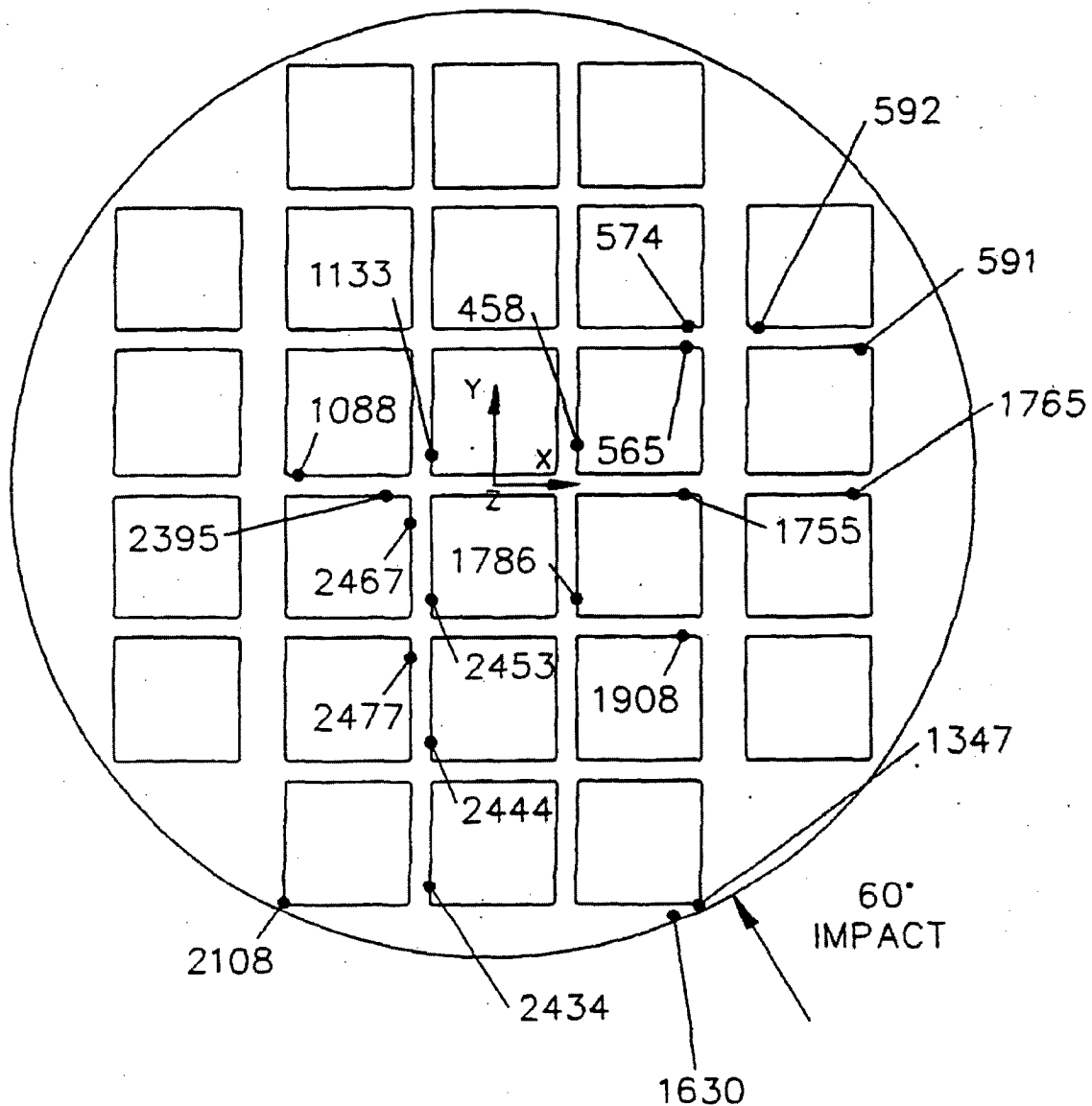


Figure 2.6.12.7-8 Location of Maximum Nodal SI Stresses (Directly Loaded Fuel Configuration - Support Disk) - 18.1g Side Impact Condition (64° Drop Orientation)

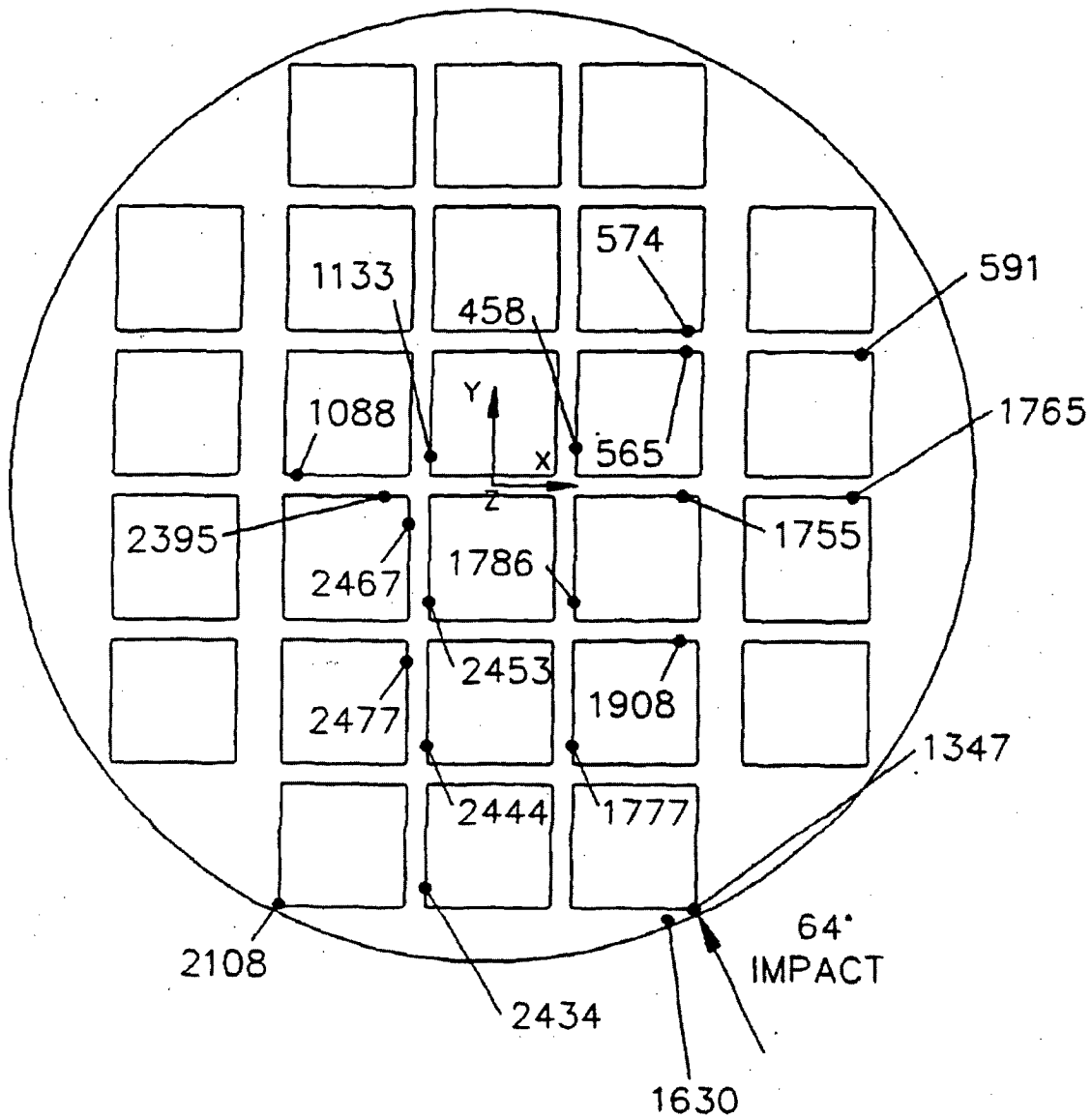


Figure 2.6.12.7-9 Location of Maximum Nodal SI Stresses (Directly Loaded Fuel Configuration - Support Disk) - 18.1-g Side Impact Condition (75° Drop Orientation)

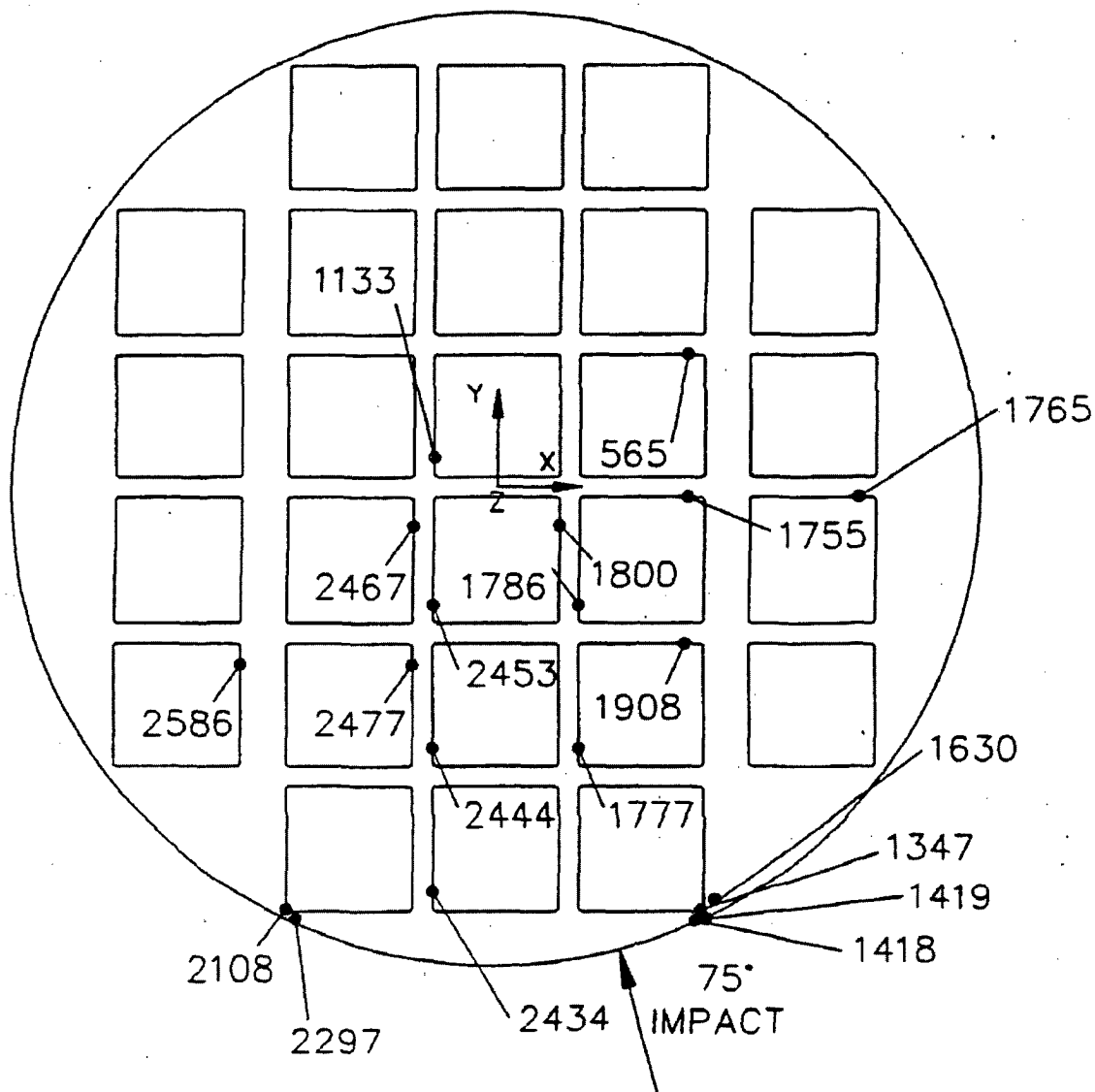


Figure 2.6.12.7-10 Location of Maximum Nodal SI Stresses (Directly Loaded Fuel Configuration - Support Disk) - 18.1-g Side Impact Condition (90° Drop Orientation)

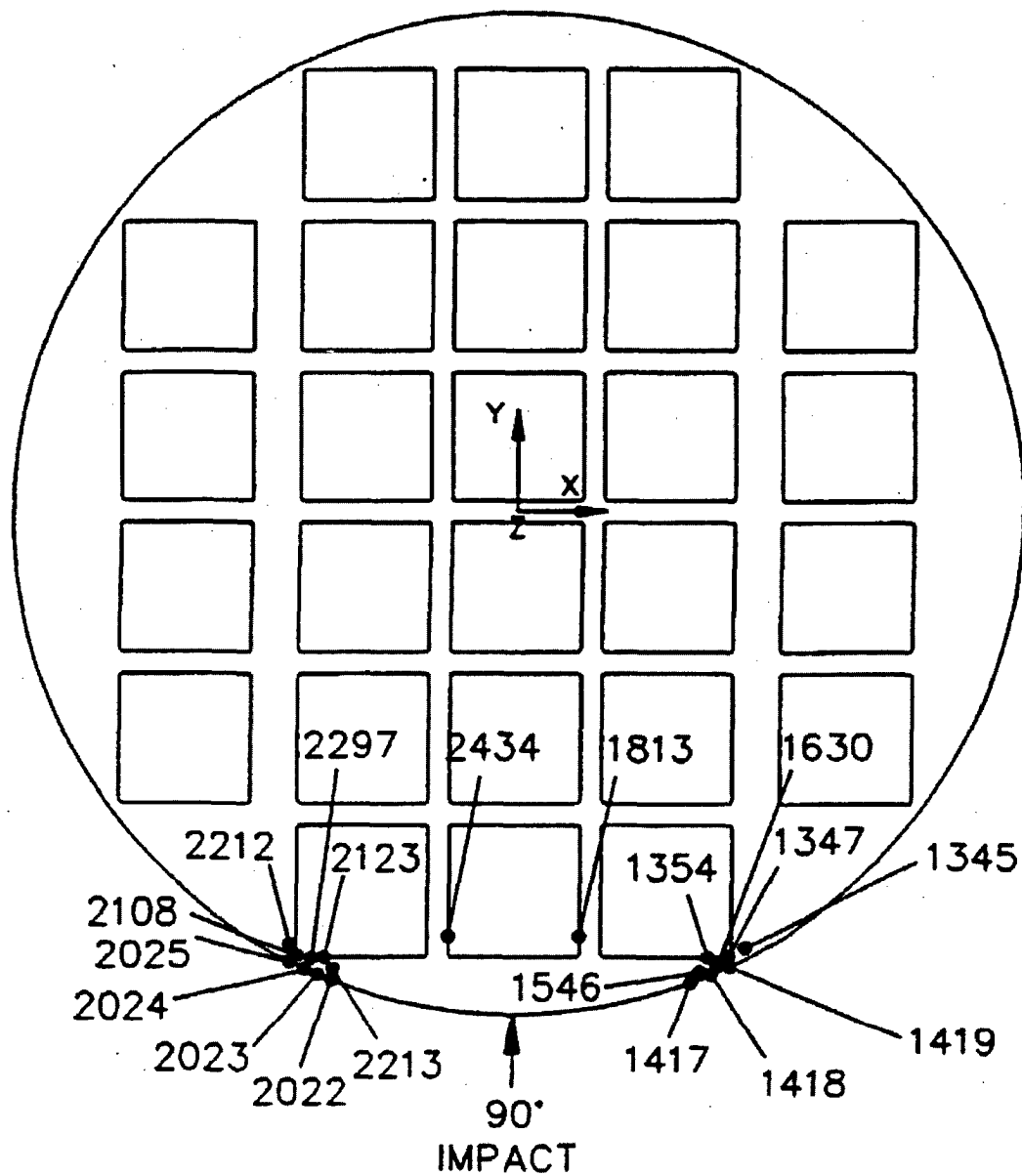


Table 2.6.12.7-1 18.1-g Side Impact Stresses for 0-Degree Drop Orientation (NAC-STC PWR Basket - Directly Loaded Fuel Configuration)

Node No. ¹	S _x (ksi)	S _y (ksi)	S _z (ksi)	S _{xy} (ksi)	SI (ksi)	MS ²
1368	-6.2	-6.0	0.0	-3.7	10.4	3.0
34	-6.2	-6.0	0.0	3.7	10.4	3.0
591	-9.6	0.3	0.0	0.3	10.0	3.2
1925	-9.6	0.3	0.0	-0.3	10.0	3.2
592	-9.7	0.2	0.0	0.4	10.0	3.2
1926	-9.7	0.2	0.0	-0.4	10.0	3.2
593	-8.4	0.0	0.0	0.0	8.4	4.0
1927	-8.4	0.0	0.0	0.0	8.4	4.0
590	-8.3	0.0	0.0	0.0	8.4	4.0
1924	-8.3	0.0	0.0	0.0	8.4	4.0
1527	-6.0	-4.2	0.0	-2.4	8.3	4.1
193	-6.0	-4.2	0.0	2.4	8.3	4.1
594	-8.0	0.0	0.0	0.2	8.0	4.3
1928	-8.0	0.0	0.0	-0.2	8.0	4.3
589	-7.9	0.0	0.0	0.2	8.0	4.3
1923	-7.9	0.0	0.0	-0.2	7.9	4.3
1526	-3.2	-5.3	0.0	-3.0	7.9	4.3
192	-3.2	-5.3	0.0	3.0	7.9	4.3
1375	-6.9	-1.6	0.0	-2.3	7.9	4.3
41	-6.9	-1.6	0.0	2.3	7.9	4.3

¹ Stress components are listed for the nodes with the 20 highest SI stresses (see Figure 2.6.12.7-2 for locations of these nodes). Note that S_x is the stress in the radial direction, S_y is the stress in the circumferential direction and S_{xy} is the shearing stress.

² The allowable stress is conservatively defined as S_m. S_m for 17-4 PH stainless steel at the conservative temperature of 650°F is 41.9 ksi.

Table 2.6.12.7-2 18.1-g Side Impact Stresses for 15-Degree Drop Orientation (NAC-STC PWR Basket - Directly Loaded Fuel Configuration)

Node No. ¹	S _x (ksi)	S _y (ksi)	S _z (ksi)	S _{xy} (ksi)	SI (ksi)	MS ²
565	-15.9	0.3	0.0	0.8	16.3	1.6
1755	-14.5	0.2	0.0	0.8	14.8	1.8
591	-14.0	0.5	0.0	0.8	14.6	1.9
592	-13.2	0.4	0.0	0.5	13.6	2.1
568	-11.9	0.8	0.0	0.7	12.8	2.3
1908	-12.4	0.2	0.0	0.7	12.7	2.3
1088	-11.9	0.5	0.0	0.5	12.4	2.4
415	-11.5	0.8	0.0	0.6	12.3	2.4
1241	-11.8	0.5	0.0	0.6	12.3	2.4
564	-12.1	0.1	0.0	0.7	12.3	2.4
1765	-11.5	0.4	0.0	0.6	12.0	2.5
2575	-10.7	0.5	0.0	0.5	11.3	2.7
1754	-11.1	0.0	0.0	0.6	11.2	2.7
543	-10.4	0.6	0.0	0.7	11.1	2.8
593	-11.0	0.0	0.0	0.3	11.1	2.8
1745	-10.7	0.3	0.0	0.6	11.1	2.8
590	-10.9	0.0	0.0	0.4	11.0	2.8
425	-10.6	0.2	0.0	0.4	10.9	2.9
1078	-9.8	0.8	0.0	0.5	10.7	2.9
530	-10.3	0.3	0.0	0.6	10.7	2.9

¹ Stress components are listed for the nodes with the 20 highest SI stresses (see Figure 2.6.12.7-3 for locations of these nodes). Note that S_x is the stress in the radial direction, S_y is the stress in the circumferential direction and S_{xy} is the shearing stress.

² The allowable stress is conservatively defined as S_m. S_m for 17-4 PH stainless steel at the conservative temperature of 650°F is 41.9 ksi.

Table 2.6.12.7-3 18.1-g Side Impact Stresses for 30-Degree Drop Orientation (NAC-STC PWR Basket - Directly Loaded Fuel Configuration)

Node No. ¹	S _x (ksi)	S _y (ksi)	S _z (ksi)	S _{xy} (ksi)	SI (ksi)	MS ²
565	-16.1	0.4	0.0	1.0	16.7	1.5
1755	-14.7	0.3	0.0	0.9	15.1	1.8
591	-14.5	0.5	0.0	0.9	15.1	1.8
592	-13.0	0.3	0.0	0.4	13.4	2.1
1908	-12.5	0.3	0.0	0.8	12.9	2.3
1765	-11.9	0.4	0.0	0.7	12.3	2.4
568	-11.4	0.8	0.0	0.6	12.3	2.4
1088	-11.7	0.5	0.0	0.5	12.2	2.4
1241	-11.5	0.5	0.0	0.5	12.0	2.5
564	-11.8	0.2	0.0	0.8	11.9	2.5
415	-11.0	0.8	0.0	0.5	11.9	2.5
1745	-10.7	0.5	0.0	0.7	11.3	2.7
2395	-10.4	0.7	0.0	0.9	10.2	2.7
1133	0.9	-10.2	0.0	0.9	11.2	2.7
2575	-10.6	0.5	0.0	0.4	11.2	2.8
593	-11.1	0.0	0.0	0.3	11.1	2.8
2453	0.4	-10.6	0.0	0.9	11.1	2.8
2444	0.2	-10.7	0.0	0.8	11.0	2.8
2434	0.5	-10.4	0.0	0.8	10.7	2.9
530	-10.3	0.3	0.0	0.6	11.0	2.8
543	-10.1	0.7	0.0	0.8	11.0	2.8

¹ Stress components are listed for the nodes with the 20 highest SI stresses (see Figure 2.6.12.7-4 for locations of these nodes). Note that S_x is the stress in the radial direction, S_y is the stress in the circumferential direction and S_{xy} is the shearing stress.

² The allowable stress is conservatively defined as S_m. S_m for 17-4 PH stainless steel at the conservative temperature of 650°F is 41.9 ksi.

Table 2.6.12.7-4 18.1-g Side Impact Stresses for 37-Degree Drop Orientation (NAC-STC PWR Basket - Directly Loaded Fuel Configuration)

Node No. ¹	S _x (ksi)	S _y (ksi)	S _z (ksi)	S _{xy} (ksi)	SI (ksi)	MS ²
565	-16.0	0.4	0.0	1.0	16.6	1.5
591	-14.5	0.5	0.0	1.0	15.2	1.8
1755	-14.7	0.4	0.0	1.0	15.2	1.8
592	-12.8	0.3	0.0	0.4	13.1	2.2
1908	-13.3	0.4	0.0	0.9	12.8	2.3
1765	-11.9	0.4	0.0	0.8	12.4	2.4
1088	-11.6	0.5	0.0	0.4	12.1	2.5
568	-11.1	0.8	0.0	0.5	11.9	2.5
1241	-11.3	0.5	0.0	0.4	11.8	2.7
2444	-0.2	-11.4	0.0	0.8	11.7	2.6
564	-11.5	0.2	0.0	0.9	11.6	2.6
2453	0.3	-11.1	0.0	0.9	11.6	2.6
415	-10.7	0.8	0.0	0.4	11.5	2.6
2395	-10.5	0.8	0.0	0.9	11.5	2.7
1133	0.8	-10.5	0.0	0.9	11.5	2.7
2434	0.5	-10.7	0.0	0.8	11.3	2.7
1745	-10.6	0.6	0.0	0.8	11.3	2.7
2575	-10.5	0.6	0.0	0.4	11.1	2.8
458	1.0	-9.8	0.0	1.0	11.0	2.8
593	-11.0	0.0	0.0	0.3	11.0	2.8

¹ Stress components are listed for the nodes with the 20 highest SI stresses (see Figure 2.6.12.7-5 for locations of these nodes). Note that S_x is the stress in the radial direction, S_y is the stress in the circumferential direction and S_{xy} is the shearing stress.

² The allowable stress is conservatively defined as S_m. S_m for 17-4 PH stainless steel at the conservative temperature of 650°F is 41.9 ksi.

Table 2.6.12.7-5 18.1-g Side Impact Stresses for 45-Degree Drop Orientation (NAC-STC PWR Basket - Directly Loaded Fuel Configuration)

Node No. ¹	S _x (ksi)	S _y (ksi)	S _z (ksi)	S _{xy} (ksi)	SI (ksi)	MS ²
565	-15.7	0.5	0.0	1.1	16.3	1.6
591	-14.5	0.5	0.0	1.0	15.1	1.8
1755	-14.4	0.4	0.0	1.0	15.0	1.8
1908	-12.1	0.5	0.0	0.9	12.7	2.3
592	-12.3	0.3	0.0	0.4	12.7	2.3
1765	-11.8	0.4	0.0	0.8	12.4	2.4
2444	0.1	-12.0	0.0	0.8	12.2	2.4
2453	0.3	-11.6	0.0	0.8	12.0	2.5
1088	-11.3	0.5	0.0	0.4	11.9	2.5
1133	0.7	-10.7	0.0	0.9	11.3	2.6
2395	-10.6	0.8	0.0	1.0	11.6	2.6
2434	0.6	-10.9	0.0	0.7	11.6	2.6
1241	-10.9	0.4	0.0	0.4	11.4	2.7
458	1.0	-10.1	0.0	0.9	11.2	2.7
568	-10.5	0.7	0.0	0.5	10.2	2.7
564	-11.0	-0.2	0.0	0.9	11.1	2.8
1745	-10.4	0.6	0.0	0.8	11.1	2.8
415	-10.2	0.8	0.0	0.4	11.0	2.8
1226	-9.9	0.8	0.0	1.0	10.9	2.9
593	-11.0	0.0	0.0	0.3	11.0	2.8
2575	-10.3	0.6	0.0	0.3	10.9	2.9

¹ Stress components are listed for the nodes with the 20 highest SI stresses (see Figure 2.6.12.7-6 for locations of these nodes). Note that S_x is the stress in the radial direction, S_y is the stress in the circumferential direction and S_{xy} is the shearing stress.

² The allowable stress is conservatively defined as S_m. S_m for 17-4 PH stainless steel at the conservative temperature of 650°F is 41.9 ksi.

Table 2.6.12.7-6 18.1-g Side Impact Stresses for 60-Degree Drop Orientation (NAC-STC PWR Basket - Directly Loaded Fuel Configuration)

Node No. ¹	S _x (ksi)	S _y (ksi)	S _z (ksi)	S _{xy} (ksi)	SI (ksi)	MS ²
565	-14.0	0.6	0.0	1.1	14.9	1.8
1755	-13.5	0.5	0.0	1.1	14.2	1.9
591	-13.3	0.5	0.0	1.1	14.0	2.0
2444	0.0	-12.7	0.0	0.7	12.8	2.3
2453	0.2	-12.1	0.0	0.8	12.3	2.4
2108	-7.1	-6.6	0.0	4.0	12.2	2.5
1908	-11.3	0.6	0.0	1.8	12.0	2.5
1765	-11.5	0.4	0.0	0.9	12.0	2.5
2434	0.6	-11.0	0.0	0.6	11.7	2.6
1133	0.6	-10.8	0.0	0.7	11.4	2.7
1347	-8.9	-3.6	0.0	-3.9	11.4	2.7
2395	-10.1	1.0	0.0	1.1	11.3	2.7
458	0.8	-10.3	0.0	0.8	11.2	2.7
2467	0.9	-10.3	0.0	0.4	11.2	2.7
1630	-9.3	-2.5	0.0	-3.5	11.0	2.8
2477	0.6	-10.5	0.0	0.3	11.0	2.8
1088	-10.4	0.5	0.0	0.3	10.9	2.8
1786	0.3	-10.5	0.0	0.7	10.9	2.8
574	9.7	-0.9	0.0	1.0	10.8	2.9
592	-10.5	0.2	0.0	0.3	10.8	2.9

¹ Stress components are listed for the nodes with the 20 highest SI stresses (see Figure 2.6.12.7-7 for locations of these nodes). Note that S_x is the stress in the radial direction, S_y is the stress in the circumferential direction and S_{xy} is the shearing stress.

² The allowable stress is conservatively defined as S_m. S_m for 17-4 PH stainless steel at the conservative temperature of 650°F is 41.9 ksi.

Table 2.6.12.7-7 18.1-g Side Impact Stresses for 64-Degree Drop Orientation (NAC-STC PWR Basket - Directly Loaded Fuel Configuration)

Node No. ¹	S _x (ksi)	S _y (ksi)	S _z (ksi)	S _{xy} (ksi)	SI (ksi)	MS ²
565	-13.3	0.7	0.0	1.1	14.1	2.0
1755	-13.1	0.6	0.0	1.1	13.9	2.0
591	-12.5	0.5	0.0	1.1	13.2	2.2
2444	0.0	-12.7	0.0	0.7	12.8	2.3
2108	-7.4	-6.7	0.0	4.1	12.5	2.4
2453	0.1	-12.1	0.0	0.7	12.3	2.4
1765	-11.3	0.4	0.0	1.0	11.8	2.5
1908	-11.0	0.6	0.0	1.0	11.8	2.6
1347	-9.1	-3.8	0.0	-4.0	11.7	2.6
2434	0.6	-10.9	0.0	0.6	11.6	2.6
2467	0.9	-10.4	0.0	0.5	11.4	2.7
1630	-9.5	-2.6	0.0	-3.6	11.3	2.7
1133	0.5	-10.6	0.0	0.7	11.3	2.7
2477	0.6	-10.7	0.0	0.3	11.3	2.7
2395	-9.9	1.0	0.0	1.1	11.1	2.8
458	0.7	-10.2	0.0	0.8	11.1	2.8
1786	0.3	10.6	0.0	0.7	10.9	2.8
574	9.8	-0.8	0.0	1.1	10.8	2.9
1777	0.0	-10.4	0.0	0.6	10.6	3.0
1088	-10.1	0.5	0.0	0.2	10.5	3.0

¹ Stress components are listed for the nodes with the 20 highest SI stresses (see Figure 2.6.12.7-8 for locations of these nodes). Note that S_x is the stress in the radial direction, S_y is the stress in the circumferential direction and S_{xy} is the shearing stress.

² The allowable stress is conservatively defined as S_m. S_m for 17-4 PH stainless steel at the conservative temperature of 650°F is 41.9 ksi.

Table 2.6.12.7-8 18.1-g Side Impact Stresses for 75-Degree Drop Orientation (NAC-STC PWR Basket - Directly Loaded Fuel Configuration)

Node No. ¹	S _x (ksi)	S _y (ksi)	S _z (ksi)	S _{xy} (ksi)	SI (ksi)	MS ²
2108	-8.4	-6.9	0.0	4.4	13.3	2.1
2444	0.0	-12.7	0.0	0.6	12.7	2.3
1347	-9.6	-4.2	0.0	-4.3	12.4	2.4
1755	-11.1	0.7	0.0	1.0	12.0	2.5
1630	-10.0	-2.8	0.0	-3.8	11.9	2.5
2453	0.0	-11.8	0.0	0.6	11.9	2.5
2477	0.5	-11.1	0.0	0.4	11.7	2.6
2467	0.8	-10.7	0.0	0.5	11.6	2.6
565	-10.4	0.8	0.0	1.0	11.4	2.7
2434	0.6	-10.6	0.0	0.5	11.3	2.7
2297	-8.3	-3.6	0.0	4.0	11.2	2.7
1908	-9.9	0.7	0.0	1.0	10.8	2.9
1786	0.2	-10.5	0.0	0.6	10.7	2.9
1777	0.0	-10.5	0.0	0.5	10.6	3.0
1800	0.7	-9.7	0.0	0.4	10.4	3.0
1419	-8.3	-3.7	0.0	-3.5	10.4	3.0
2586	-9.4	0.8	0.0	1.0	10.3	3.1
1765	-9.5	0.5	0.0	1.0	10.2	3.1
1418	-8.5	-2.7	0.0	-3.6	10.2	3.1
1133	0.3	-9.7	0.0	0.6	10.2	3.1

¹ Stress components are listed for the nodes with the 20 highest SI stresses (see Figure 2.6.12.7-9 for locations of these nodes). Note that S_x is the stress in the radial direction, S_y is the stress in the circumferential direction and S_{xy} is the shearing stress.

² The allowable stress is conservatively defined as S_m. S_m for 17-4 PH stainless steel at the conservative temperature of 650°F is 41.9 ksi.

Table 2.6.12.7-9 18.1-g Side Impact Stresses for 90-Degree Drop Orientation (NAC-STC PWR Basket - Directly Loaded Fuel Configuration)

Node No. ¹	S _x (ksi)	S _y (ksi)	S _z (ksi)	S _{xy} (ksi)	SI (ksi)	MS ²
2108	-10.7	5.9	0.0	5.0	14.7	1.9
1347	-10.7	-5.9	0.0	-5.0	14.7	1.9
2297	-11.1	-3.6	0.0	4.5	13.7	2.1
1630	-11.1	-3.6	0.0	-4.5	13.7	2.1
2024	-9.7	-3.3	0.0	4.2	11.8	2.5
1418	-9.7	-3.3	0.0	-4.2	11.8	2.5
2025	-9.1	-4.9	0.0	3.9	11.6	2.6
1419	-9.1	-4.9	0.0	-3.9	11.6	2.6
2123	-10.2	-1.2	0.0	2.6	11.2	2.8
1354	-10.2	-1.2	0.0	-2.6	11.2	2.8
2023	-9.3	-1.8	0.0	3.2	10.5	3.0
1417	-9.3	-1.8	0.0	-3.2	11.5	3.0
2212	-6.9	-5.7	0.0	3.4	10.3	3.1
1545	-6.9	-5.7	0.0	3.4	10.3	3.1
2213	-8.5	-1.7	0.0	2.7	9.7	3.3
1546	-8.5	-1.7	0.0	-2.7	9.7	3.3
2022	-8.2	-1.2	0.0	2.3	9.0	3.7
1416	-8.2	-1.2	0.0	-2.3	9.0	3.7
1813	0.5	-8.3	0.0	-0.3	8.9	3.7
1088	-10.1	0.5	0.0	0.2	10.5	3.0
2434	0.5	-8.3	0.0	0.3	8.9	3.7

¹ Stress components are listed for the nodes with the 20 highest SI stresses (see Figure 2.6.12.7-10 for locations of these nodes). Note that S_x is the stress in the radial direction, S_y is the stress in the circumferential direction and S_{xy} is the shearing stress.

² The allowable stress is conservatively defined as S_m. S_m for 17-4 PH stainless steel at the conservative temperature of 650°F is 41.9 ksi.

Table 2.6.12.7-10 18.1-g Side Impact Analysis Results (NAC-STC PWR Basket - Directly Loaded Fuel Configuration)

Drop Orientation (deg)	Maximum Nodal SI Stress (ksi)	Operating Temperature (°F)	Allow. Stress (ksi)	Margin of Safety
0	10.4	650	41.9	+3.03
15	16.3	650	41.9	+1.57
30	16.65	650	41.9	+1.52
37	16.61	650	41.9	+1.52
45	16.33	650	41.9	+1.57
60	14.86	650	41.9	+1.82
64	14.14	650	41.9	+1.96
75	13.33	650	41.9	+2.14
90	11.67	650	41.9	+1.86

2.6.12.8 Stress Evaluation of Support Disk (Directly Loaded Fuel Configuration) for Thermal Plus a 1-Foot Side Drop Combined Load Condition

The highest nodal stresses in the support disk from the thermal expansion analysis (Table 2.6.12.3-1) and the 1-foot side drop at the 30 degree drop orientation (Table 2.6.12.7-3) (since the minimum safety margin occurs at this drop orientation) are conservatively used as a basis to determine the maximum primary plus secondary stress for normal operations. The maximum stress intensity, SI, for thermal expansion and 1-foot side drop for the 30 degree drop orientation are respectively 32.2 ksi and 16.65 ksi. Using the conservative absolute summation method, the maximum bounding combined stress is 48.85 ksi.

The combined thermal plus impact stress of 48.85 ksi is very conservative since the dominant principal stresses for thermal expansion and the side impact analyses are respectively tensile and compressive in nature. Therefore, the stresses from the combination of thermal expansion and impact loads will tend to negate one another with the maximum combined stress located opposite to the region of impact and exactly at the same point of maximum thermal expansion stress. The magnitude of the maximum combined stress must therefore be equal to or slightly less than the maximum thermal expansion stress because the contribution of stress from inertial loads in this region is negligible.

Evaluation of peak stress and the fatigue mode of failure for normal operation events is conservatively performed by using the highest primary plus secondary stress calculated for the steel support disk in combination with a stress concentration factor of 3.0 to establish a stress range. Since the side drop analysis produced a conservative primary plus secondary stress of 48.9 ksi, which is higher than 39.4 ksi, that produced from the end drop (Section 2.6.12.5), the maximum peak stress intensity range is conservatively defined as twice the defined primary plus secondary stress times the stress concentration factor of 3.0. The maximum alternating stress intensity then becomes

$$S_{alt} = \frac{3(2)(48.9)}{2} = 146.7 \text{ ksi}$$

The allowable number of cycles for an alternating stress intensity range of 146.7 ksi at the conservative temperature of 500°F is approximately 1000 cycles. This number of allowable cycles considerably exceeds the number of normal operating cycles that the NAC-STC will meet during its lifetime.

2.6.12.9 Support Disk Web Stresses for a 1-Foot Side Drop Condition (Directly Loaded Fuel Configuration)

The support disk is analyzed for nine drop orientations in Section 2.6.12.7. The 20 maximum stress intensities for each drop orientation are listed in Tables 2.6.12.7-1 through 2.6.12.7-9. In this section, a supplementary stress summary of the support disk webs are presented for the same drop orientations.

The locations of the nodes in the ANSYS model of the support disk webs for each of the nine 1-foot side impact orientations evaluated are shown in Figure 2.6.12.9-1. Tables 2.6.12.9-1 through 2.6.12.9-9 summarize the nodal stress intensities at the defined locations on the web for each of the nine impact orientation. The tables also show the margin of safety for each node location for the 18.1 g side impact load condition using the conservative design stress intensity, S_m , at a maximum enveloping temperature of 650°F.

The conservative minimum margin of safety relative to the design strength, S_m at 650°F, for the support disk web of the NAC-STC PWR basket (directly loaded fuel configuration) for a 1-foot side drop is +4.52 for the 90 degree drop orientation.

Figure 2.6.12.9-1 Node Point Locations for Basket Web Stress Summaries (Directly Loaded Fuel Configuration)

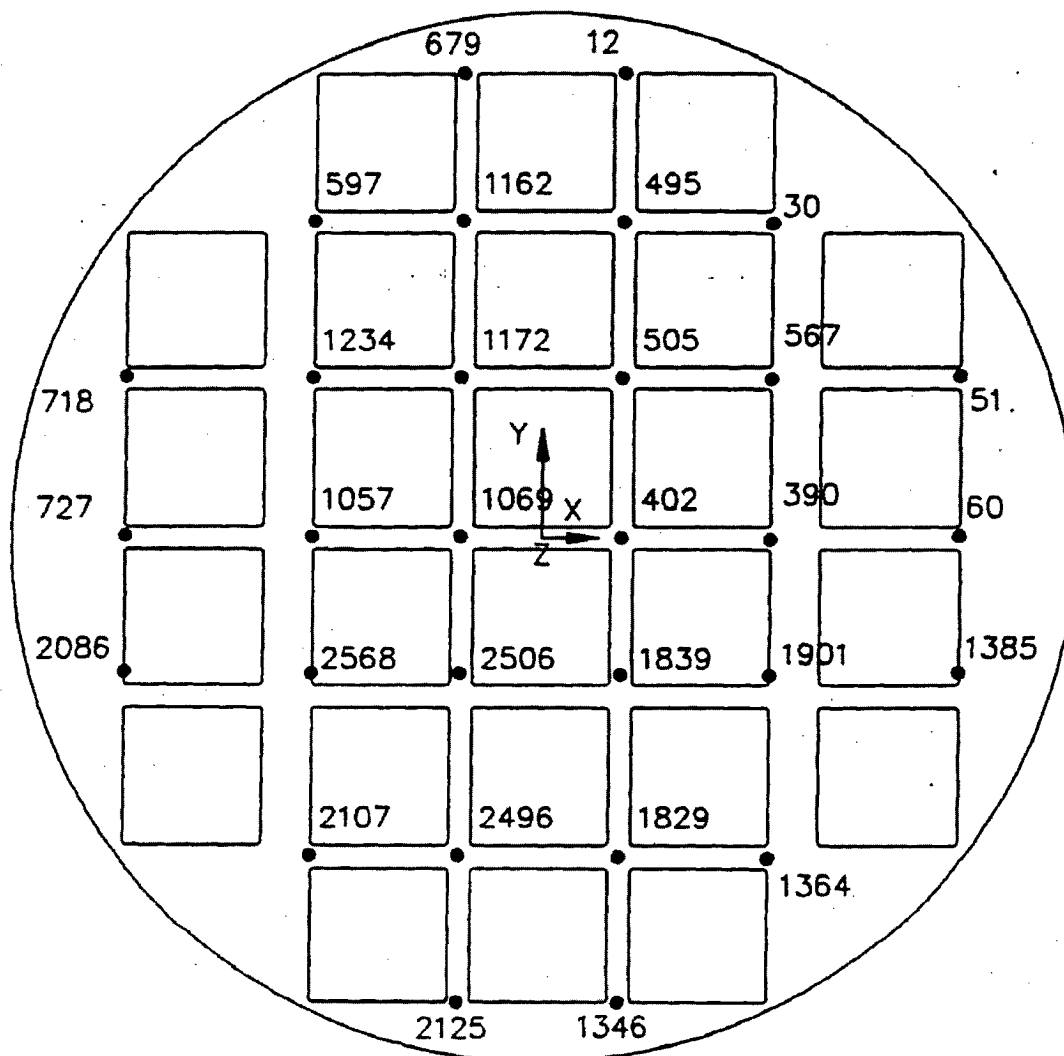


Table 2.6.12.9-1 18.1-g Side Impact Web Stresses for 0-Degree Drop Orientation (NAC-STC PWR Basket - Directly Loaded Fuel Configuration)

Node No. ¹	S _x (ksi)	S _y (ksi)	S _z (ksi)	S _{xy} (ksi)	SI (ksi)	MS ²
402	-4.7	1.3	0.0	0.0	6.0	6.0
390	-4.7	0.8	0.0	0.0	5.6	6.5
1901	-4.5	1.0	0.0	0.0	5.6	6.5
567	-4.5	1.0	0.0	0.0	5.6	6.5
60	-5.3	-1.5	0.0	0.0	5.4	6.7
1839	-4.1	1.2	0.0	0.4	5.4	6.8
505	-4.1	1.2	0.0	-0.4	5.4	6.8
51	-4.9	-1.9	0.0	0.0	5.1	7.2
1385	-4.9	-1.9	0.0	0.0	5.2	7.2
1829	-2.7	-0.9	0.0	0.4	3.7	10.2
495	-2.7	0.9	0.0	-0.5	3.7	10.2
1069	-3.3	0.4	0.0	-0.4	3.7	10.4
2506	-2.7	0.2	0.0	0.3	3.0	12.9
1172	-2.7	0.2	0.0	-0.3	3.0	12.9
1364	-2.4	-0.1	0.0	0.3	2.8	14.2
30	-2.4	-0.1	0.0	-0.3	2.8	14.2
1057	-2.0	-1.2	0.0	0.0	2.1	19.1
2568	-1.6	-1.2	0.0	0.0	1.7	23.0
1234	-1.6	-1.2	0.0	0.0	1.7	23.1
2496	-1.4	0.0	0.0	0.3	1.5	26.3
1162	-1.4	0.0	0.0	-0.3	1.5	26.3
727	-0.9	-0.6	0.0	0.0	1.0	41.8
697	-0.6	0.2	0.0	-0.1	0.8	53.5
2107	-0.6	0.2	0.0	0.1	0.8	53.5
1346	0.0	0.3	0.0	0.2	0.7	58.4
12	0.0	0.3	0.0	-0.2	0.7	58.4
2125	-0.1	-0.1	0.0	0.1	0.7	62.5
679	-0.1	0.1	0.0	-0.1	0.7	62.5
718	-0.3	-0.4	0.0	0.0	0.5	88.6
2086	-0.3	-0.4	0.0	0.0	0.5	88.6

¹ Stress components are listed for the nodes noted on Figure 2.6.12.9-1. Note that S_x is the stress in the radial direction, S_y is the stress in the circumferential direction and S_{xy} is the shearing stress.

² The allowable stress is conservatively defined as S_m. S_m for 17-4 PH stainless steel at the conservative temperature of 650°F is 41.9 ksi.

Table 2.6.12.9-2 18.1-g Side Impact Web Stresses for 15-Degree Drop Orientation (NAC-STC PWR Basket - Directly Loaded Fuel Configuration)

Node No. ¹	S _x (ksi)	S _y (ksi)	S _z (ksi)	S _{xy} (ksi)	SI (ksi)	MS ²
402	-4.3	0.2	0.0	-2.4	6.5	5.4
505	-3.6	0.3	0.0	-2.6	6.5	5.4
567	-4.2	0.8	0.0	0.3	5.7	6.3
1069	-2.9	-0.5	0.0	-2.5	5.5	6.6
390	-4.5	0.4	0.0	-0.3	5.5	6.6
1172	-2.3	-0.3	0.0	-2.6	5.5	6.6
1839	-3.8	-0.1	0.0	-1.9	5.3	6.9
60	-5.0	-1.4	0.0	-0.1	5.3	6.9
51	-4.9	-1.6	0.0	-0.2	52.2	7.0
1901	-4.1	0.1	0.0	-0.2	4.9	7.5
495	-1.7	0.2	0.0	-2.2	4.8	7.8
2506	-2.4	-1.2	0.0	-2.1	4.5	8.3
1385	-4.3	-1.6	0.0	-0.1	4.5	8.4
1162	-0.6	-0.1	0.0	-2.1	4.3	8.8
1364	-2.9	0.8	0.0	-0.1	3.9	9.8
2496	-1.5	-1.8	0.0	-1.8	3.8	9.9
1829	-3.0	-0.5	0.0	-1.3	3.8	10.0
30	-1.6	-1.7	0.0	-0.7	3.2	12.0
2125	-0.1	-1.7	0.0	-0.3	2.9	13.3
1057	-1.8	-1.1	0.0	-0.4	2.7	14.5
1234	-1.2	-0.8	0.0	0.4	2.6	15.4
2568	-1.6	-1.2	0.0	-0.4	2.4	16.2
697	-0.1	1.2	0.0	-0.6	2.3	17.5
2107	-0.8	-0.9	0.0	-0.5	2.1	19.1
1346	-0.3	-1.0	0.0	-0.1	1.9	20.9
12	-0.3	0.1	0.0	-0.4	1.1	37.1
727	-0.8	-0.5	0.0	-0.2	1.1	38.2
679	0.0	0.0	0.0	-0.4	1.0	39.8
718	0.0	0.0	0.0	-0.2	0.8	51.5
2086	-0.4	-0.6	0.0	-0.1	0.8	52.3

¹ Stress components are listed for the nodes noted on Figure 2.6.12.9-1. Note that S_x is the stress in the radial direction, S_y is the stress in the circumferential direction and S_{xy} is the shearing stress.

² The allowable stress is conservatively defined as S_m. S_m for 17-4 PH stainless steel at the conservative temperature of 650°F is 41.9 ksi.

Table 2.6.12.9-3 18.1-g Side Impact Web Stresses for 30-Degree Drop Orientation (NAC-STC PWR Basket - Directly Loaded Fuel Configuration)

Node No. ¹	S _x (ksi)	S _y (ksi)	S _z (ksi)	S _{xy} (ksi)	SI (ksi)	MS ²
505	-3.1	-0.2	0.0	-2.7	6.1	5.9
402	-3.7	-0.7	0.0	-2.5	5.8	6.2
1172	-2.0	-0.8	0.0	-2.6	5.4	6.8
1069	-2.5	-1.4	0.0	-2.6	5.3	6.9
567	-3.8	0.6	0.0	-0.2	5.3	6.9
390	-4.0	0.1	0.0	-0.2	5.1	7.3
51	-4.5	-1.3	0.0	-0.2	5.0	7.4
60	-4.6	-1.1	0.0	-0.1	4.9	7.6
2506	-1.8	-2.4	0.0	-2.2	4.8	7.8
1839	-3.1	-1.2	0.0	-2.0	4.6	8.0
495	-1.3	-0.1	0.0	-2.1	4.5	8.4
2496	-0.6	-3.3	0.0	-1.7	4.5	8.4
1901	-3.6	-0.2	0.0	-0.2	4.4	8.5
1162	-0.4	-0.3	0.0	-2.0	4.1	9.2
1385	-3.7	-1.4	0.0	-0.1	4.0	9.6
2125	-1.5	-2.8	0.0	-0.1	3.4	11.3
1829	-2.3	-1.9	0.0	-1.2	3.4	11.4
30	-1.2	-2.0	0.0	-0.7	3.4	11.4
1364	-2.5	0.3	0.0	-0.1	3.3	11.8
2107	-0.4	-2.3	0.0	-0.5	2.8	14.0
1057	-1.6	-1.3	0.0	-0.5	2.6	15.0
1346	-1.3	-2.0	0.0	-0.1	2.5	15.6
1234	-1.1	-0.9	0.0	-0.5	2.5	16.1
2568	-1.4	-1.5	0.0	-0.4	2.4	16.6
697	-0.1	1.4	0.0	-0.6	2.3	17.5
727	-0.7	-0.4	0.0	-0.3	1.2	33.9
12	-0.2	0.0	0.0	-0.4	1.0	40.4
2086	-0.4	-0.7	0.0	-0.3	1.0	41.2
718	0.0	0.1	0.0	-0.3	1.0	42.6
679	0.1	0.0	0.0	-0.4	1.0	43.5

¹ Stress components are listed for the nodes noted on Figure 2.6.12.9-1. Note that S_x is the stress in the radial direction, S_y is the stress in the circumferential direction and S_{xy} is the shearing stress.

² The allowable stress is conservatively defined as S_m. S_m is for 17-4 PH stainless steel at the conservative temperature of 650°F is 41.9 ksi.

Table 2.6.12.9-4 18.1-g Side Impact Web Stresses for 37-Degree Drop Orientation (NAC-STC PWR Basket - Directly Loaded Fuel Configuration)

Node No. ¹	S _x (ksi)	S _y (ksi)	S _z (ksi)	S _{xy} (ksi)	SI (ksi)	MS ²
505	-2.8	-0.5	0.0	-2.7	5.9	6.1
402	-3.4	-1.1	0.0	-2.5	5.5	6.6
1069	-2.2	-1.8	0.0	-2.6	5.3	6.9
1172	-1.7	-1.0	0.0	-2.6	5.3	6.9
567	-3.5	0.5	0.0	-0.2	5.1	7.3
2506	-1.5	-2.9	0.0	-2.3	5.0	7.4
2496	-0.6	-4.0	0.0	-1.7	5.0	7.5
391	-3.7	-0.0	0.0	-0.2	4.8	7.7
51	-4.2	-1.1	0.0	-0.2	4.8	7.7
60	-4.3	-0.9	0.0	0.1	4.7	8.0
1839	-2.7	-1.7	0.0	-2.0	4.5	8.3
495	-1.1	-0.2	0.0	-2.1	4.3	8.7
1901	-3.2	-0.3	0.0	-0.2	4.1	9.1
1162	-0.3	-0.4	0.0	-2.0	4.0	9.4
2125	-1.9	-3.3	0.0	-0.1	3.8	10.1
1385	-3.4	-1.2	0.0	-0.1	3.7	10.3
1829	-2.0	-2.5	0.0	-1.2	3.5	10.9
30	-1.0	-2.2	0.0	-0.7	3.5	11.1
2107	-0.3	-2.8	0.0	-0.5	3.3	11.9
1364	-2.3	0.2	0.0	-0.1	3.0	13.2
1346	-1.7	-2.5	0.0	-0.1	2.9	13.5
1057	-1.5	-1.4	0.0	-0.5	2.6	15.1
1234	-1.0	-0.9	0.0	-0.5	2.4	16.5
2568	-1.2	-1.7	0.0	-0.5	2.4	16.5
697	-0.1	1.5	0.0	-0.6	2.3	17.4
727	-0.7	-0.4	0.0	-0.3	1.3	31.7
2086	-0.4	-0.7	0.0	-0.3	1.1	37.7
718	0.0	0.1	0.0	-0.3	1.0	39.5
12	-0.2	0.0	0.0	-0.4	1.0	42.3
679	0.1	0.0	0.0	-0.4	0.9	45.4

¹ Stress components are listed for the nodes noted on Figure 2.6.12.9-1. Note that S_x is the stress in the radial direction, S_y is the stress in the circumferential direction and S_{xy} is the shearing stress.

² The allowable stress is conservatively defined as S_m. S_m for 17-4 PH stainless steel at the conservative temperature of 650°F is 41.9 ksi.

Table 2.6.12.9-5 18.1-g Side Impact Web Stresses for 45-Degree Drop Orientation (NAC-STC PWR Basket - Directly Loaded Fuel Configuration)

Node No. ¹	S _x (ksi)	S _y (ksi)	S _z (ksi)	S _{xy} (ksi)	SI (ksi)	MS ²
505	-2.4	-0.8	0.0	-2.7	5.7	6.5
2496	-0.3	-4.7	0.0	-1.6	5.5	6.6
1069	-1.9	-2.2	0.0	-2.7	5.4	6.8
402	-2.9	-1.5	0.0	-2.5	5.3	6.9
2506	-1.2	-3.4	0.0	-2.3	5.3	6.9
1172	-1.5	-1.3	0.0	-2.6	5.2	7.0
567	-3.1	0.3	0.0	-0.2	4.7	8.0
51	-3.8	-0.9	0.0	-0.3	4.5	8.2
390	-3.3	-0.1	0.0	-0.2	4.5	8.3
1839	-2.3	-2.3	0.0	-2.0	4.5	8.4
60	-3.8	-0.7	0.0	-0.1	4.4	8.4
2125	-2.4	-3.8	0.0	-0.1	4.2	8.9
495	-0.8	-0.4	0.0	-2.0	4.1	9.2
1162	-0.1	-0.5	0.0	-1.9	3.9	9.8
1829	-1.6	-3.2	0.0	-1.2	3.8	10.0
1901	-2.8	-0.5	0.0	-0.1	3.8	10.0
2107	-0.1	-3.4	0.0	-0.5	3.8	10.0
30	-0.7	-2.4	0.0	-0.7	3.5	10.9
1385	-3.0	-1.0	0.0	-0.1	3.4	11.4
1346	-2.1	-3.0	0.0	-0.1	3.3	11.6
1364	-2.1	0.0	0.0	-0.2	2.7	14.8
1057	-1.3	-1.5	0.0	-0.6	2.6	15.4
2568	-1.0	-1.8	0.0	-0.5	2.4	16.4
1234	-0.9	-0.9	0.0	-0.6	2.3	17.0
697	0.0	1.5	0.0	-0.6	2.3	17.5
727	-0.6	-0.4	0.0	-0.4	1.4	30.0
2086	-0.4	-0.7	0.0	-0.3	1.2	34.6
718	0.1	0.2	0.0	-0.4	1.1	36.8
12	-0.1	0.0	0.0	-0.4	0.9	44.6
679	0.1	0.0	0.0	-0.4	0.9	47.9

¹ Stress components are listed for the nodes noted on Figure 2.6.12.9-1. Note that S_x is the stress in the radial direction, S_y is the stress in the circumferential direction and S_{xy} is the shearing stress.

² The allowable stress is conservatively defined as S_m. S_m for 17-4 PH stainless steel at the conservative temperature of 650°F is 41.9 ksi.

Table 2.6.12.9-6 18.1-g Side Impact Web Stresses for 60-Degree Drop Orientation (NAC-STC PWR Basket - Directly Loaded Fuel Configuration)

Node No. ¹	S _x (ksi)	S _y (ksi)	S _z (ksi)	S _{xy} (ksi)	SI (ksi)	MS ²
2496	0.1	-5.6	0.0	-1.5	6.5	5.4
2506	-0.5	-4.2	0.0	-2.3	5.9	6.1
1069	-1.2	-2.8	0.0	-2.6	5.5	6.6
505	-1.4	-1.4	0.0	-2.6	5.1	7.2
402	-1.9	-2.2	0.0	-2.5	5.1	7.2
1172	-0.8	-1.7	0.0	-2.5	5.0	7.3
2125	-3.0	-4.5	0.0	-0.1	4.9	7.5
1839	-1.4	-3.2	0.0	-2.0	4.7	7.9
2107	0.1	-4.3	0.0	-0.5	4.7	8.0
1829	-0.9	-4.2	0.0	-1.1	4.6	8.2
1346	-2.6	-3.7	0.0	-0.1	4.1	9.3
60	-2.9	-0.2	0.0	-0.1	3.9	9.7
390	-2.4	-0.4	0.0	-0.2	3.8	10.0
51	-2.5	-0.5	0.0	-0.2	3.7	10.3
567	-2.0	-0.3	0.0	-0.2	3.7	10.4
495	-0.2	-0.7	0.0	-1.8	3.7	10.4
1162	0.2	-0.6	0.0	-1.7	3.5	10.8
30	-0.2	-2.4	0.0	-0.6	3.5	11.0
1901	-2.0	-0.7	0.0	-0.1	3.2	12.1
1385	2.1	-0.4	0.0	-0.1	2.8	14.2
2568	-0.7	-2.0	0.0	-0.6	2.4	16.2
1057	-0.9	-1.5	0.0	-0.6	2.4	16.6
1364	-1.6	-0.4	0.0	-0.2	2.2	17.8
697	0.0	1.6	0.0	-0.6	2.1	18.7
1234	-0.5	-0.8	0.0	-0.6	2.1	19.0
727	-0.5	-0.3	0.0	-0.4	1.5	27.5
2086	-0.4	-0.7	0.0	-0.4	1.3	30.7
718	0.2	0.4	0.0	-0.4	1.2	33.8
12	0.1	0.1	0.0	-0.3	0.8	49.3
679	0.2	0.0	0.0	-0.3	0.8	53.0

¹ Stress components are listed for the nodes noted on Figure 2.6.12.9-1. Note that S_x is the stress in the radial direction, S_y is the stress in the circumferential direction and S_{xy} is the shearing stress.

² The allowable stress is conservatively defined as S_m. S_m for 17-4 PH stainless steel at the conservative temperature of 650°F is 41.9 ksi.

Table 2.6.12.9-7 18.1-g Side Impact Web Stresses for 64-Degree Drop Orientation (NAC-STC PWR Basket - Directly Loaded Fuel Configuration)

Node No. ¹	S _x (ksi)	S _y (ksi)	S _z (ksi)	S _{xy} (ksi)	SI (ksi)	MS ²
2496	0.2	-5.8	0.0	-1.4	6.7	5.2
2506	-0.3	-4.4	0.0	-2.3	6.1	5.9
1069	-0.9	-3.0	0.0	-2.6	5.6	6.5
2125	-3.1	-4.7	0.0	-0.1	5.1	7.2
402	-1.6	-2.4	0.0	-2.5	5.1	7.3
505	-1.1	-1.5	0.0	-2.5	5.0	7.4
1172	-0.5	-1.8	0.0	-2.4	5.0	7.4
2107	0.2	-4.4	0.0	-0.5	4.9	7.6
1839	-1.1	-3.4	0.0	-2.0	4.8	7.7
1829	-0.7	-4.5	0.0	-1.0	4.8	7.8
1346	-2.8	-3.9	0.0	-0.1	4.2	8.9
60	-2.5	-0.1	0.0	-0.1	3.7	10.3
390	-2.1	-0.4	0.0	-0.2	3.6	10.8
495	-0.1	-0.7	0.0	-1.7	3.5	10.9
1162	0.2	-0.6	0.0	-1.7	3.4	11.4
567	-1.6	-0.5	0.0	-0.1	3.4	11.4
30	-0.1	-2.3	0.0	-0.5	3.4	11.4
51	-2.1	-0.7	0.0	-0.2	3.3	11.6
1901	-1.7	-0.8	0.0	-0.1	3.0	12.7
1385	-1.8	-0.3	0.0	-0.1	2.6	15.1
2568	-0.6	-2.0	0.0	-0.6	2.5	16.0
1157	-0.8	-1.5	0.0	-0.6	2.3	17.0
1364	-1.4	-0.5	0.0	-0.2	2.1	18.5
697	0.0	1.5	0.0	-0.6	2.0	19.5
1234	-0.3	-0.7	0.0	-0.6	2.0	20.0
727	-0.4	-0.3	0.0	-0.4	1.5	27.4
2086	-0.4	-0.7	0.0	-0.4	1.3	30.1
718	0.2	0.4	0.0	-0.4	1.2	33.6
12	0.0	-0.1	0.0	-0.3	0.8	50.5
679	0.2	0.1	0.0	-0.3	0.8	54.7

¹ Stress components are listed for the nodes noted on Figure 2.6.12.9-1. Note that S_x is the stress in the radial direction, S_y is the stress in the circumferential direction and S_{xy} is the shearing stress.

² The allowable stress is conservatively defined as S_m. S_m for 17-4 PH stainless steel at the conservative temperature of 650°F is 41.9 ksi.

Table 2.6.12.9-8 18.1-g Side Impact Web Stresses for 75-Degree Drop Orientation (NAC-STC PWR Basket - Directly Loaded Fuel Configuration)

Node No. ¹	S _x (ksi)	S _y (ksi)	S _z (ksi)	S _{xy} (ksi)	SI (ksi)	MS ²
2496	0.5	-6.2	0.0	-1.3	7.2	4.8
2506	0.2	-4.7	0.0	-2.2	6.6	5.4
1069	0.1	-3.3	0.0	-2.4	5.8	6.3
2125	-3.4	-4.9	0.0	0.0	5.4	6.8
1829	-0.2	-5.0	0.0	-0.9	5.4	6.8
1839	-0.3	-3.9	0.0	-1.9	5.3	6.9
2107	0.3	-4.8	0.0	-0.5	5.3	3.9
402	-0.5	-2.9	0.0	-2.3	5.2	7.0
1346	-3.1	-4.3	0.0	-0.1	4.6	8.1
1172	0.1	-2.0	0.0	-2.1	4.6	8.1
505	-0.2	-1.9	0.0	-2.1	4.5	8.3
495	0.0	-0.8	0.0	-1.4	3.0	13.1
390	-1.0	-1.0	0.0	-0.1	2.9	13.6
1162	0.2	-0.7	0.0	-1.4	2.8	13.7
30	0.0	-1.7	0.0	-0.4	2.8	13.8
567	-0.6	-1.1	0.0	-0.1	2.8	14.2
60	-1.3	-0.3	0.0	0.0	2.7	14.5
1901	-0.9	-1.0	0.0	-0.1	2.7	14.7
2568	-0.2	-1.9	0.0	-0.6	2.4	16.2
51	-0.8	-1.0	0.0	-0.2	2.4	16.5
1385	-1.0	0.1	0.0	-0.1	2.2	18.2
1057	-0.3	-1.2	0.0	-0.6	2.0	19.6
1364	-1.0	-0.8	0.0	-0.2	2.0	20.1
697	0.0	1.2	0.0	-0.5	1.7	23.7
1234	0.0	-0.4	0.0	-0.6	1.6	29.1
2086	-0.3	-0.6	0.0	-0.5	1.4	29.1
727	0.0	0.0	0.0	-0.4	1.4	19.1
718	0.2	0.6	0.0	-0.4	1.2	35.4
12	0.0	0.1	0.0	-0.2	0.8	53.4
679	0.2	0.0	0.0	-0.2	0.7	59.9

¹ Stress components are listed for the nodes noted on Figure 2.6.12.9-1. Note that S_x is the stress in the radial direction, S_y is the stress in the circumferential direction and S_{xy} is the shearing stress.

² The allowable stress is conservatively defined as S_m. S_m for 17-4 PH stainless steel at the conservative temperature of 650°F is 41.9 ksi.

Table 2.6.12.9-9 18.1-g Side Impact Web Stresses for 90-Degree Drop Orientation (NAC-STC PWR Basket - Directly Loaded Fuel Configuration)

Node No. ¹	S _x (ksi)	S _y (ksi)	S _z (ksi)	S _{xy} (ksi)	SI (ksi)	MS ²
1829	1.4	-6.2	0.0	0.2	7.6	4.5
2496	1.4	-6.2	0.0	-0.2	7.6	4.5
1839	1.6	-4.9	0.0	0.2	6.5	5.4
2506	1.6	-4.9	0.0	-0.2	6.5	5.4
1346	-3.7	-4.9	0.0	0.0	5.3	6.9
2125	-3.7	-4.9	0.0	0.0	5.3	6.9
402	0.7	-3.6	0.0	0.1	4.3	8.8
1069	0.7	-3.5	0.0	-0.1	4.3	8.8
1364	0.6	-3.6	0.0	0.1	4.2	8.9
2107	0.6	-3.6	0.0	-0.1	4.2	8.9
2568	0.8	-1.6	0.0	-0.3	2.5	15.6
1901	0.8	-1.6	0.0	0.3	2.5	15.6
1172	0.0	-2.1	0.0	0.0	2.2	18.0
505	0.0	-2.1	0.0	0.0	2.2	18.0
1057	0.2	-1.2	0.0	-0.3	1.6	24.8
390	0.2	-1.2	0.0	0.3	1.6	24.8
1234	-0.3	-0.9	0.0	-0.3	-1.1	36.8
567	-0.3	-0.9	0.0	0.3	1.1	36.8
697	-0.4	-0.1	0.0	0.0	0.9	45.0
30	-0.4	-0.1	0.0	0.0	0.9	45.0
1162	-0.3	-0.9	0.0	0.0	0.9	47.0
495	-0.3	-0.9	0.0	0.0	0.9	47.0
2086	0.4	-0.1	0.0	-0.3	0.8	50.7
1385	0.4	-0.1	0.0	0.3	0.8	50.7
727	0.0	0.0	0.0	-0.3	0.6	72.3
60	0.0	0.0	0.0	0.3	0.6	72.3
51	-0.3	0.0	0.0	0.2	0.6	72.9
718	-0.3	0.0	0.0	-0.2	0.6	72.9
679	0.0	-0.2	0.0	0.0	0.3	138.9
12	0.0	-0.2	0.0	0.0	0.3	139.0

¹ Stress components are listed for the nodes noted on Figure 2.6.12.9-1. Note that S_x is the stress in the radial direction, S_y is the stress in the circumferential direction and S_{xy} is the shearing stress.

² The allowable stress is conservatively defined as S_m. S_m for 17-4 PH stainless steel at the conservative temperature of 650°F is 41.9 ksi.

THIS PAGE INTENTIONALLY LEFT BLANK

2.6.12.10 Support Disk Shear Stresses for a 1-Foot Side Drop and a 1-Foot End Drop Conditions (Directly Loaded Fuel Configuration)

The maximum stress intensity for the 1-foot side drop is reported in Table 2.6.12.7-3 as 16.65 ksi, (30 degree drop orientation). Similarly, the maximum stress intensity for the 1-foot end drop is reported in Table 2.6.12.4-1 as 12.65 ksi. Therefore, the maximum enveloping shear stress anywhere for either of the two loading conditions mentioned above is 16.65/2 or 8.325 ksi.

ASME Code, Section III, Division 1, Subdivision NG, criteria defines the allowable for shear stress to be 0.6 S_m . The design stress intensity, S_m , for 17-4 PH at a bounding temperature of 650°F is 41.9 ksi.

Minimum Margin of Safety for Shear

$$\begin{aligned} MS &= \frac{(2)(0.6)S_m}{SI} - 1 \\ &= \frac{(2)(0.6)(41.9)}{16.65} - 1 = +2.02 \end{aligned}$$

Therefore, structural adequacy of the NAC-STC fuel basket support disk directly loaded fuel configuration design for the normal conditions of transport, 1-foot side drop and 1-foot end drop, is demonstrated for shear stress criteria.

THIS PAGE INTENTIONALLY LEFT BLANK

2.6.12.11 Bearing Stress - Basket Contact with Inner Shell (Directly Loaded Fuel Configuration)

During the 1-foot side drop the bearing load on the outer edge of the support disk is a maximum for the normal condition loads. Considering the total cavity design weight of 56,000 pounds being supported by the 31 stainless steel support disks and the contact area being limited to a 90 degree arch length the bearing stress is:

$$S_{br-1g} = 56,000 / (0.5 \times 31 \times 3.14 \times 71.0 \times 0.25) \\ = 64.8 \text{ psi}$$

For the 18.1 g 1-foot drop the maximum bearing stress in the support disk is:

$$S_{br-18.1g} = 18.1 \times 64.8 = 1170 \text{ psi}$$

Using a material allowable stress based on the conservative support disk temperature on the outer bearing surface, 1.0 $S_y = 89.5$ ksi at 400°F (Table 3.4-1), the margin of safety is:

$$MS = 89.5 / 1.17 - 1 = \underline{+Large}$$

Therefore, the NAC-STC basket directly loaded fuel configuration design is acceptable relative to bearing stress limits for the basket cavity wall interface.

THIS PAGE INTENTIONALLY LEFT BLANK

2.6.12.12 Evaluation of Triaxial Stress for the Fuel Basket Support Disk (Directly Loaded Fuel Configuration)

The ASME Code Section III, Division 1, Subsection NG criteria requires that the combination of all stress components be limited to a value of $4S_m$. Since the structural analysis of the fuel basket is conservatively performed by calculating the stress intensity values at specific node point for all membrane and bending stress components acting at the node and the value compared to S_m to evaluate acceptance, previously summarized stress results will have a minimum margin of safety of four times the reported value for this specific evaluation criteria.

Therefore, the NAC-STC stainless steel fuel basket (directly loaded fuel configuration) satisfies ASME Code structural criteria for Core Support Structures and basket design normal condition loading.

THIS PAGE INTENTIONALLY LEFT BLANK

2.6.12.13 Fuel Basket (Directly Loaded Fuel Configuration) Weldment Analysis for 1-Foot
End Drop

The responses of the top and the bottom weldment plates of the fuel basket assembly to a 19.6g normal operation deceleration load are examined. The top and the bottom weldment plates are both 1-inch thick and fabricated from SA 240, Type 304 stainless steel. The top weldment supports its own weight and 26 fuel tubes (without the fuel assemblies) during a 1-foot top end drop. Similarly the bottom weldment supports its own weight and 26 fuel tubes (without the fuel assemblies) during a 1-foot bottom end drop. The responses of the end plates to the 1-foot end drop are analyzed using ANSYS STIF63 three-dimensional, six degrees-of-freedom, elastic quadrilateral shell elements. The finite element model for both plates is shown in Figure 2.6.12.13-1. Figure 2.6.12.13-2 and 2.6.12.13-3 display the boundary conditions for the top weldment plate and the bottom weldment plate respectively. The evaluation is based on material properties of SA 240, Type 304 at a conservative temperature of 500°F. The hottest steel support disk during normal transport conditions is 498°F, see Table 3.4-1.

The primary membrane plus primary bending stress in the top weldment plate for the 1-foot top end drop is 21.5 ksi. The primary membrane plus primary bending stress in the bottom weldment plate for the 1-foot bottom end drop is 17.9 ksi. At 500°F, the normal condition stress allowable, $1.5 S_m$, is 26.25 ksi. The minimum margin of safety for the top weldment plate and the bottom weldment plate are +0.22 and +0.47 respectively. Therefore, the structural adequacy of the NAC-STC fuel basket weldment end plates (directly loaded fuel configuration) for the normal condition of transport is demonstrated.

Figure 2.6.12.13-1 Fuel Basket Weldment Model (Directly Loaded Fuel Configuration)

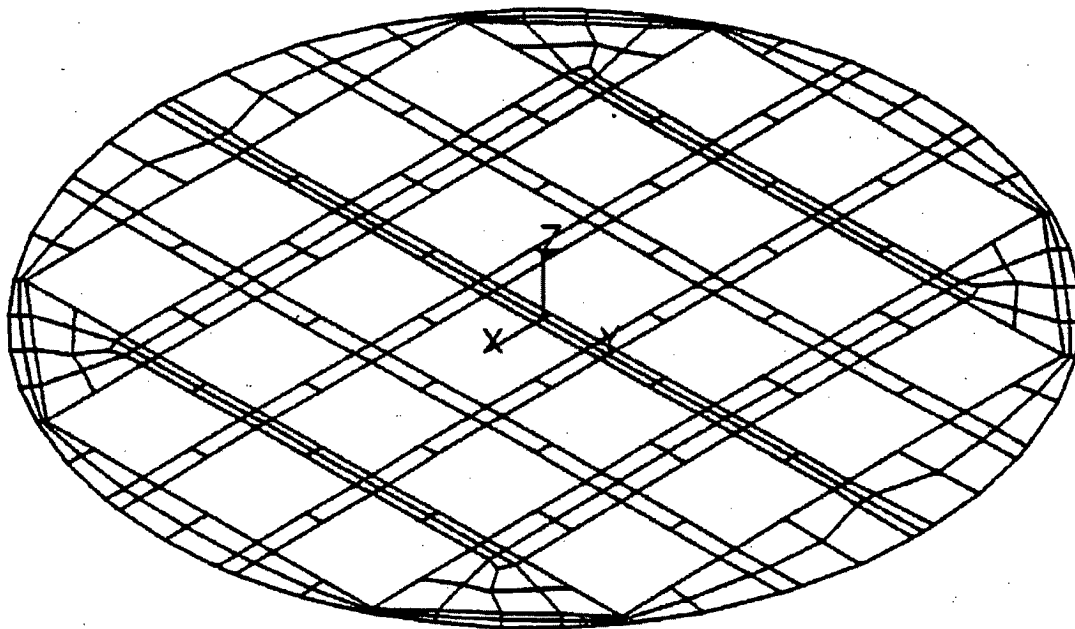


Figure 2.6.12.13-2 Fuel Basket Top Weldment Boundary Conditions (Directly Loaded Fuel Configuration)

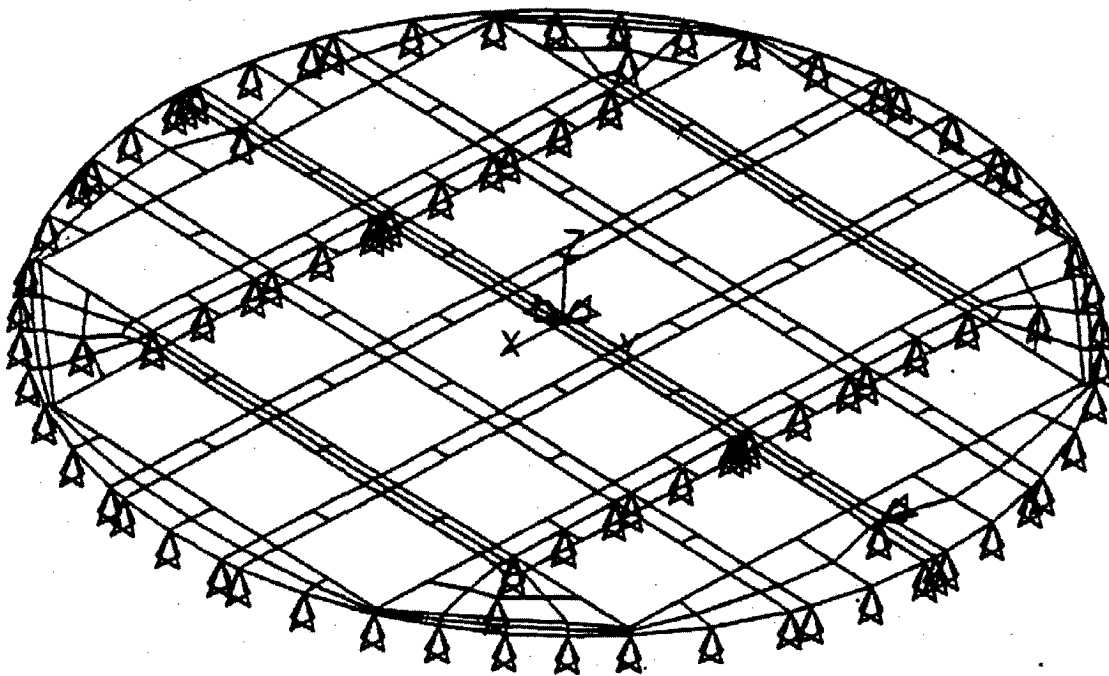
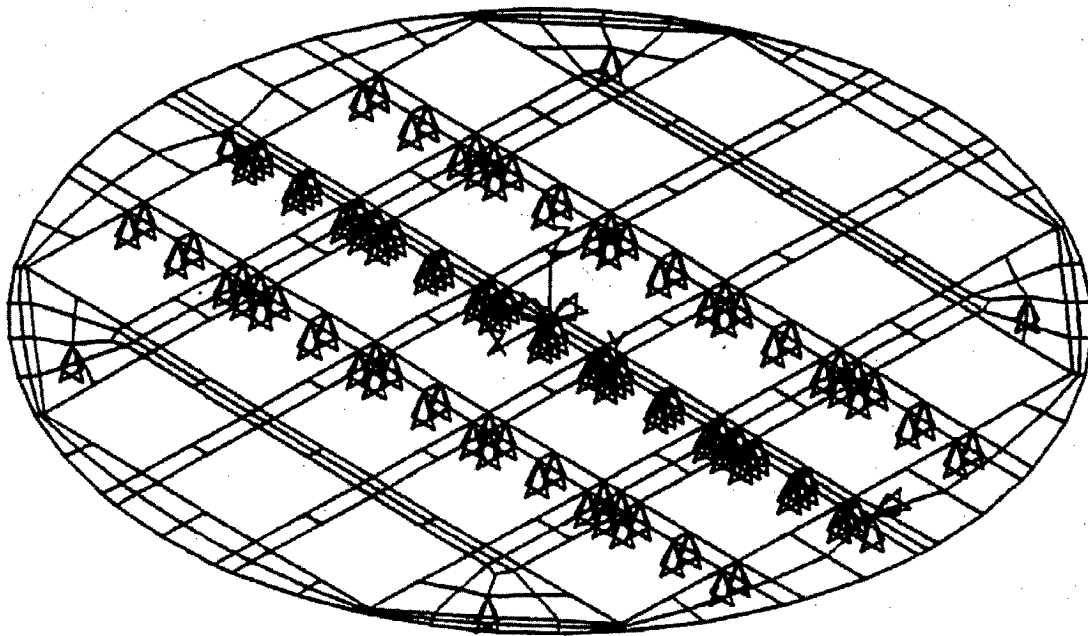


Figure 2.6.12.13-3 Fuel Basket Bottom Weldment Boundary Conditions (Directly Loaded Fuel Configuration)



2.6.13 Yankee-MPC Transportable Storage Canister Analysis - Normal Transport Condition

The NAC-STC has three contents configurations - uncanistered (directly loaded fuel); canistered Yankee Class spent fuel or Greater Than Class C (GTCC) waste; and, canistered Connecticut Yankee spent fuel or GTCC. The canistered Yankee Class spent fuel or GTCC waste is referred to as the Yankee-MPC configuration. The Yankee-MPC canister is evaluated for the Normal Conditions of Transport in this section and for the Hypothetical Accident Conditions in Section 2.7.11. The Normal Conditions of Transport analysis of the Yankee-MPC canistered fuel basket is presented in Section 2.6.14, and that of the canistered Yankee-MPC GTCC basket is presented in Section 2.6.19.1.

The canistered fuel configuration consists of a transportable storage canister with top and bottom spacers to properly locate the canister in the NAC-STC cask cavity. The analysis of the top and bottom spacers is presented in Section 2.6.15. The principal components of the transportable storage canister are the canister, the canister fuel basket, the shield lid, and the structural lid. In an alternate configuration, the transportable storage canister may include the Yankee-MPC GTCC basket instead of the canister fuel basket. Detailed descriptions of the geometries and materials of construction of the canister, baskets, and spacers are provided in Sections 1.2.1.2.8, 1.2.1.2.8.1, 1.2.1.2.8.2, and 1.2.1.2.8.3, respectively.

The Yankee-MPC transportable storage canister and the canister shell, bottom, and lids are shown in Figures 2.6.13-1 and 2.6.13-2, respectively.

Figure 2.6.13-1 Yankee-MPC Transportable Storage Canister

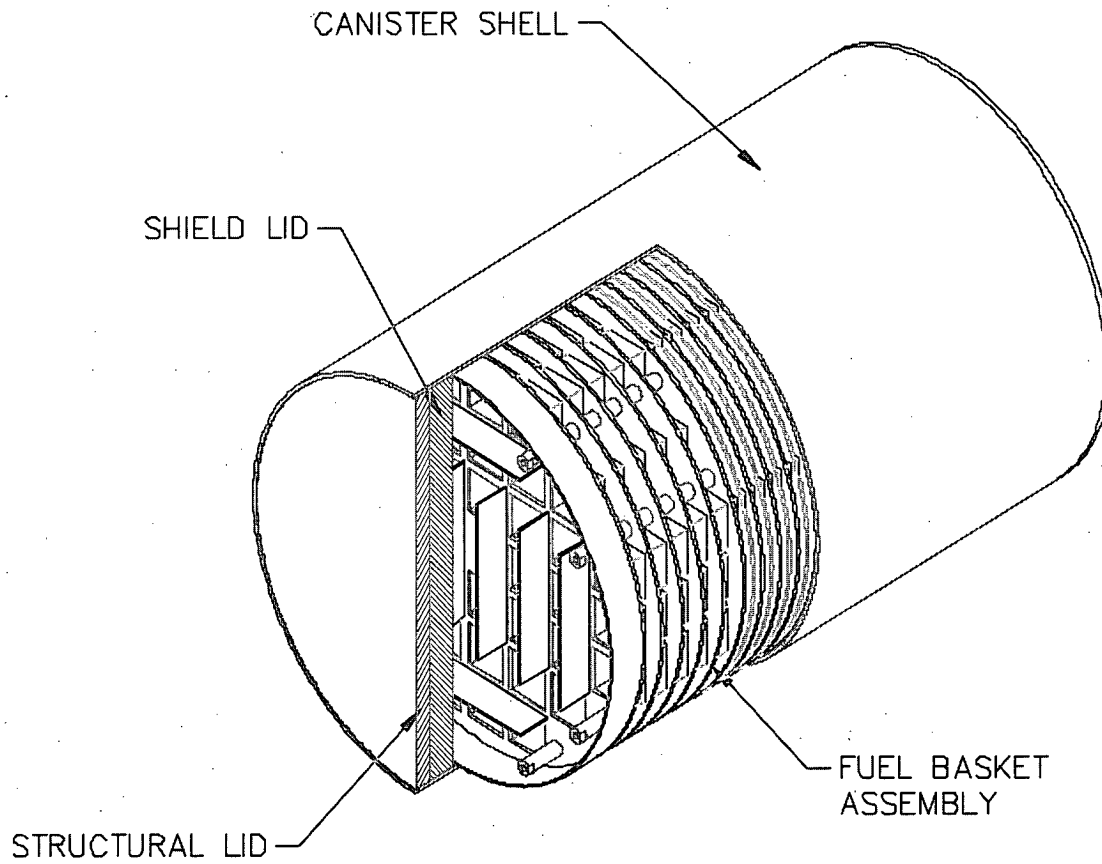
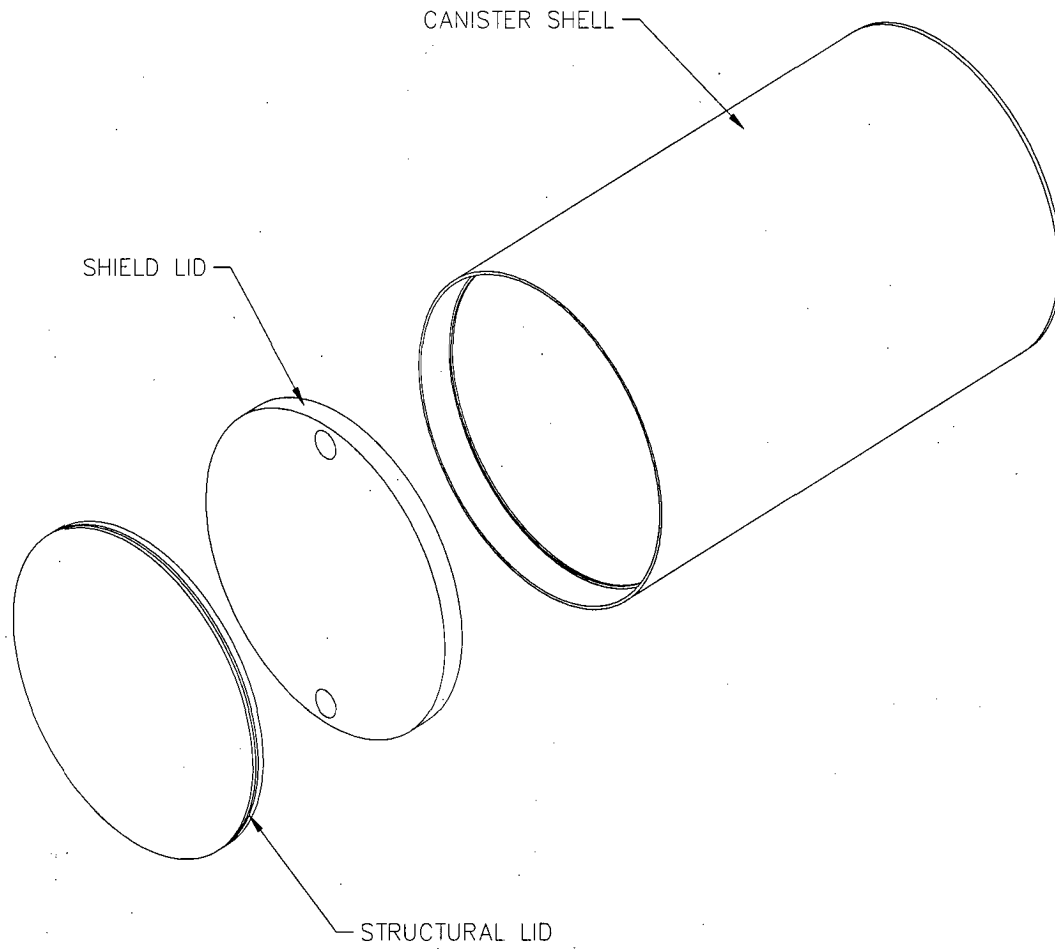


Figure 2.6.13-2 Yankee-MPC Canister for Fuel Basket or GTCC Basket



THIS PAGE INTENTIONALLY LEFT BLANK

2.6.13.1 Yankee-MPC Canister Description and Analysis

The transportable storage canister contains/confines the spent fuel in the canister fuel basket or the waste in the canister GTCC basket. The canister is the defined confinement boundary for its contents during storage operation, but the canister is not considered for containment during transport operation; the NAC-STC provides the containment boundary for transport. The canister in the transfer cask serves as the handling component for its basket and contents during loading, closure, and transfer from the pool to storage and/or transport.

The canister is a right-circular shell fabricated from rolled 5/8-inch thick, Type 304L stainless steel plate and closed by a circular 1-inch thick, Type 304L stainless steel plate that is welded to one end of the shell. The canister is closed at the top end by the installation and welding of the 5-inch thick, Type 304 stainless steel shield lid and the 3-inch thick, Type 304L stainless steel structural lid. For the configuration containing the damaged fuel cans, the damaged fuel can extends through the bottom and top weldments of the basket, and is captured between the shield lid configured for damaged fuel cans and the canister bottom plate. To accommodate the damaged fuel can, the shield lid is machined on the underside in four places to mate with the damaged fuel can lid. These machined areas occur in regions of low stress and, therefore, additional evaluation is not required.

The canister may enclose either the canister fuel basket and contents or the canister GTCC basket and contents. The empty canister with basket is handled using lifting rings located on the top end of the basket. The loaded canister is lifted using 6 hoist rings threaded into the top of the structural lid. Type 304L stainless steel was selected for the canister's exterior components based on its enhanced corrosion resistance, especially in the weld regions (refer to Section 2.5.1.3).

The structural design criteria for the canister is the ASME Code Section III, Subsection NB, "Class 1 Components." Consistent with this criteria, the structural components of the canister are shown to satisfy the allowable stress limits presented in Tables 2.1.2-1 and 2.1.2-2 as applicable. The allowable stresses used in this analysis are based on a maximum material temperature of 350°F for all locations in the canister, unless otherwise indicated. These allowables are conservative because the maximum calculated canister material temperature is 338°F.

The canister is analyzed using the ANSYS finite element computer program for the 1-foot drop condition in the end and side impact orientations.

The canister structural lid closure weld is specifically evaluated for the normal conditions of transport. The lid weld is identified as Section 8 in Figure 2.6.13.3-1. Either a progressive liquid penetrant examination is performed on the root, each successive 3/8-inch layer, and the final surface of the weld in accordance with the ASME Code, Section V, Article 6, or an ultrasonic examination of the weld is performed in accordance with Section V, Article 5. In accordance with NRC guidance, if a multi-pass liquid penetrant examination is performed on the structural lid closure weld, two separate weld stress reduction factors are applied to the structural lid canister shell weld – a 0.8 factor to conservatively consider the weld configuration and a 0.8 factor per NRC ISG-4, Item 5. Thus, a total weld stress reduction factor of 0.64 (0.8×0.8) is applied to the stress allowable for the structural lid weld. The canister closure weld evaluation for normal conditions is presented in Section 2.6.13.12. The evaluation, which is based on the finite element analysis stress result as shown in Sections 2.6.13.4 through 2.6.13.7, shows a minimum margin of safety of +0.17 for the weld.

2.6.13.2 Yankee-MPC Canister Finite Element Model

A finite element model of the Yankee-MPC canister was constructed using ANSYS solid (SOLID45) elements. The model represents a one-half (180°) section of the canister and basket. The basket support discs were modeled with three-dimensional shell (SHELL63) elements. The model uses gap-spring elements to simulate contact between adjacent components. Interaction between the basket and canister were accomplished using three-dimensional gap elements (CONTAC52) along the periphery of the support disks. Contact between the canister and the cask inner shell is also modeled using CONTAC52 gap elements. Contact between the canister structural lid and shield lid is modeled using COMBIN40 combination elements in the axial degree of freedom. Simulation of the backing ring is accomplished using a ring of COMBIN40 spring gap elements connecting the shield lid and the canister in the axial direction at the lid lower outside radius. In addition, CONTAC52 elements are used to model interaction between the structural lid and canister shell and the shield lid and canister shell just below the respective lid weld joints. The size of the CONTAC52 gaps were determined from the nominal dimensions of contacting components. The COMBIN40 elements used between the structural and shield lids and for the backing ring are assigned gap sizes of 1E-8 inches. The maximum gap size is 0.08 inches. However, use of the small gap size results in the highest stresses at critical sections, resulting in the lowest margin of safety. All gap-spring elements are assigned a stiffness of 1E8 lb/in.

A central hole was modeled in the bottom, shield and structural lids. These holes were then filled with solid elements. This technique was used to avoid a small hole (which can cause a stress concentration) or a series of degenerate solid elements (which can produce a region of excessive stiffness).

Spring elements were inserted over the gap elements located on the model symmetry plane to help stabilize the model during solutions phases. The springs were given a low stiffness of 10 lb/in so their presence would not adversely affect the accuracy of the solutions.

Boundary conditions were applied to enforce symmetry at the cut boundary of the model. All nodes on the cask shell side of the canister to cask spring gap elements were fixed in all degrees of freedom. In addition, the axial and inplane rotational degrees of freedom of the basket nodes were fixed.

Additionally, the structural analyses of the canister were performed with temperature distributions corresponding to the hot (100°F ambient with solar heat load) and cold (-40°F ambient) external conditions.

Table 2.6.13.2-1 lists the real constants assigned to specific components of the model. Table 2.6.13.2-2 lists the material properties used for the model.

Figure 2.6.13.2-1 is a plot of the entire canister finite element model. An isolated view of the canister shield and structural lids portion of the model is presented in Figure 2.6.13.2-2 and an enlarged view of the model in the structural lid and shield lid weld regions is shown in Figure 2.6.13.2-3. The canister bottom plate portion of the model is shown in Figure 2.6.13.2-4.

The loading for the normal operating condition is based on 1-foot drops in conjunction with the internal pressure loading (to the canister). Drop orientations considered are the end and side drops. In the end drop orientation, the fuel contents load is transferred to the canister end and directly to the transport cask end through the cavity spacer. This corresponds to a compressive stress in the canister ends which is present in the finite element model. For the side drop condition, the loads from the canister contents weight is transferred through the support disks into the canister wall, which is backed by the NAC-STC inner shell. Since the canister wall and the inner shell have different radii, a gap exists between the two surfaces. This results in the load passing only through regions in which the canister shell deflects to contact the inner shell. This load pattern is reflected in the side drop analysis. The operational conditions also contain loads developed from the temperature distribution in the canister. These are included in the canister model analyses.

Figure 2.6.13.2-1 Yankee-MPC Canister Finite Element Model

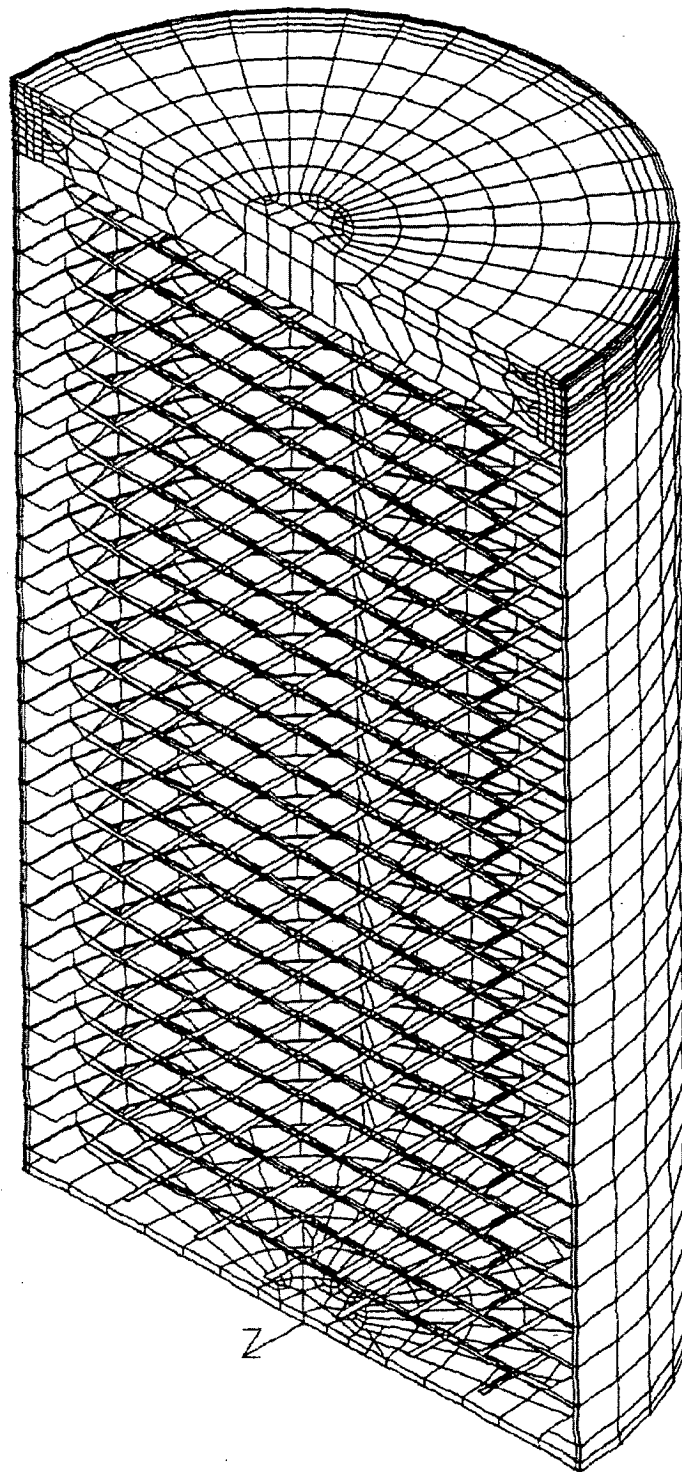


Figure 2.6.13.2-2 Yankee-MPC Canister Structural and Shield Lid Finite Element Mesh

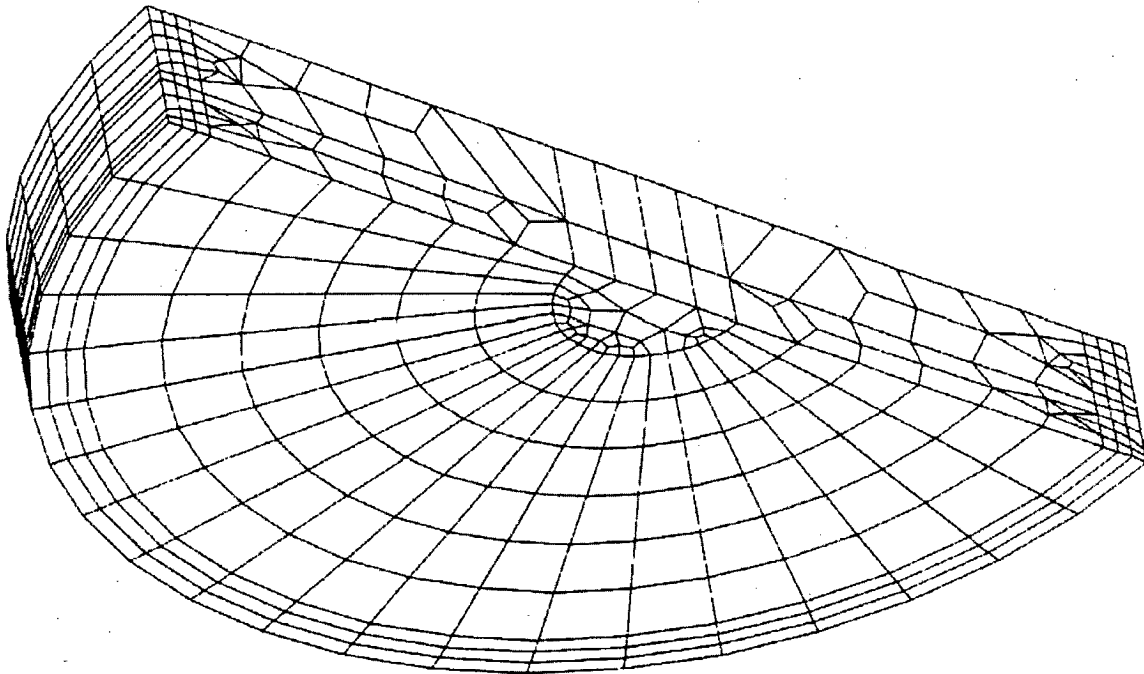


Figure 2.6.13.2-3 Yankee-MPC Structural and Shield Lid Weld Regions Finite Element Mesh

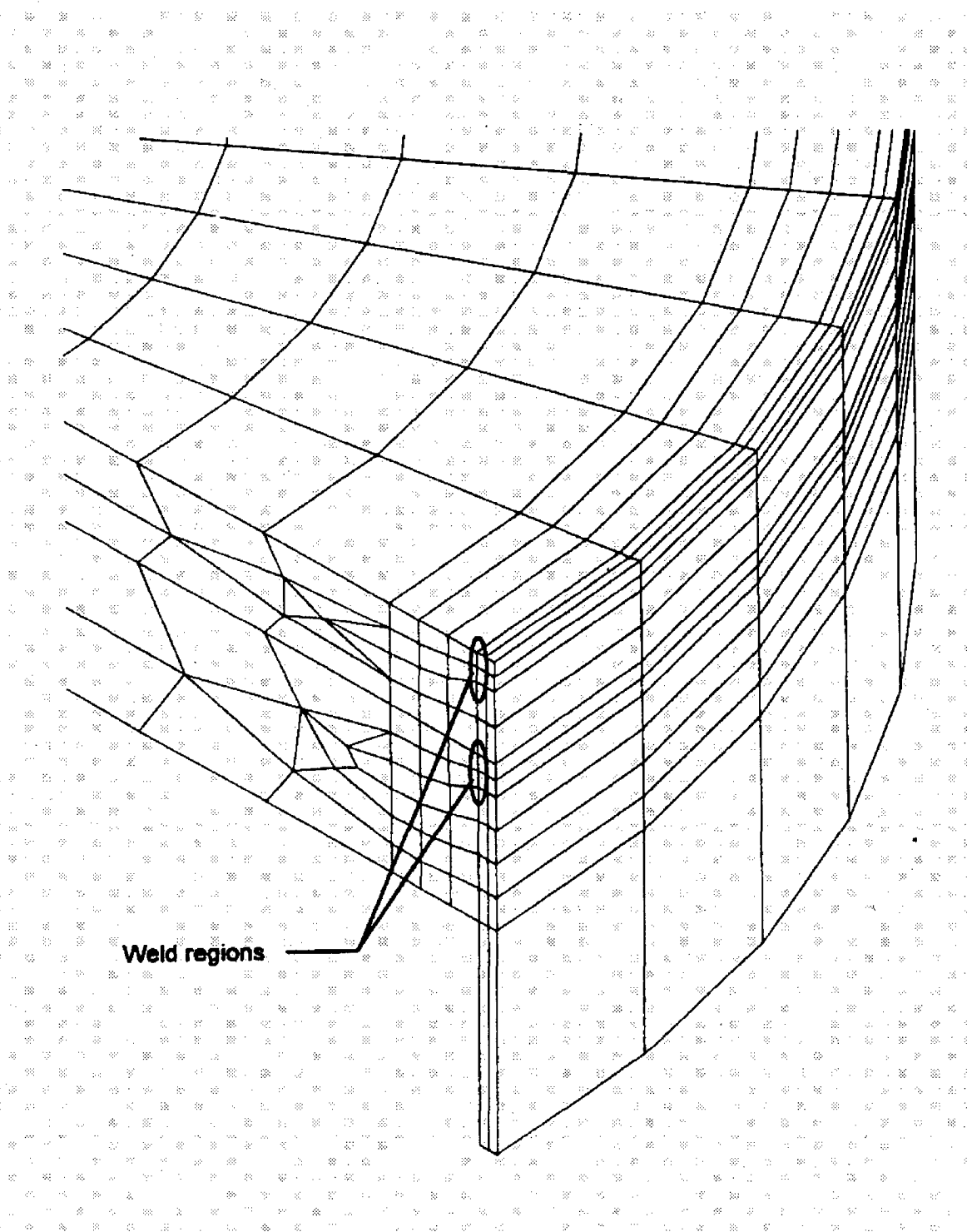


Figure 2.6.13.2-4 Yankee-MPC Canister Bottom Plate Finite Element Mesh

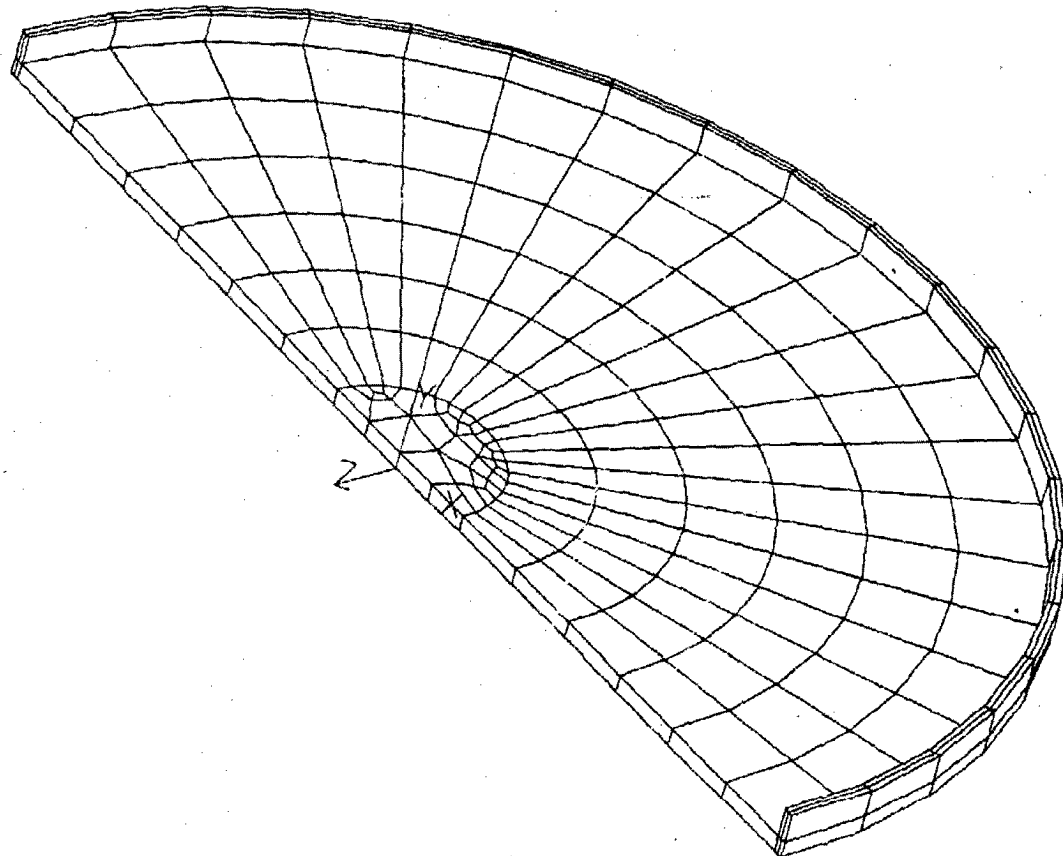


Table 2.6.13.2-1 Real Constant Sets Defined in Yankee-MPC Canister Model

Real Constant Set	Component
1	Canister Bottom Plate (SOLID45)
2-9	Canister Shell (SOLID45)
10-11	Shield Lid (SOLID45)
12-13	Structural Lid (SOLID45)
100	Axial Gaps from Canister Bottom Plate to Cask Shell (CONTAC52)
200	Radial Gaps from Canister Side to Cask Shell (CONTAC52)
300	Axial Gaps from Structural Lid Top to Cask Shell (CONTAC52)
400	Axial Gaps Between Structural and Shield Lid (COMBIN40)
500	Radial Gaps Between Shield Lid and Canister Inner Surface (CONTAC40)
600	Radial Gaps Between Shield Lid and Canister Inner Radius (CONTAC52)
700	Axial Gaps Between Shield Lid and Canister Wall to Simulate Backing Ring (COMBIN40)
800	Radial Gaps Between Basket and Canister Inner Surface (CONTAC52)
1000	Intermediate Basket Thickness Real Constant
1100	End Basket Thickness Real Constant
1200	Weak Spring Real Constant

Table 2.6.13.2-2 Material Sets Defined in Yankee-MPC Canister Model

Material Property Set	Component	Material
1	Canister Shell and Structural Lid	304L Stainless Steel; ASME SA240
2	Top and Bottom End Basket Disk	304 Stainless Steel; ASME SA240
3	Shield Lid	304 Stainless Steel; ASME SA240
4	Intermediate Basket Disk (support disk)	ASME SA693 Type 630

THIS PAGE INTENTIONALLY LEFT BLANK

2.6.13.3 Thermal Expansion Evaluation of Yankee-MPC Canister with Spent Fuel

A thermal stress evaluation is performed using ANSYS to determine the differential thermal expansion and the associated thermal stresses that result from a heat load of 12.5 kW. In assessing the thermal stresses, three extreme conditions are considered:

Condition	Ambient Temperature	Solar Insolance Applied to Cask Surface	12.5 kW Fuel Load
1	100°F	Yes	Yes
2	-40°F	No	Yes
3	-40°F	No	No

The following temperatures are obtained from the Yankee-MPC thermal analysis:

Location	Temperature (°F)		
	Condition 1	Condition 2	Condition 3
Structural Lid (center, top)	206	67	-40
Structural Lid (outer, top)	192	55	-40
Shield Lid (center, bottom)	209	71	-40
Bottom Plate (center, bottom)	255	121	-40
Bottom Plate (outer radius, bottom)	225	92	-40
Lateral Shell (mid-height)	338	215	-40

While most of the temperature gradients between the different locations are very close for condition 3, no thermal gradient exists, so there are no thermal stresses. The most significant gradient is between the lateral shell mid-height and the outer surface of the structural lid. The ΔT values are 132°F and 148°F for conditions 1 and 2, respectively (the change in temperature for condition 2 is 12% larger than that of condition 1). Thermal stresses are also increased because the modulus of elasticity and the coefficient of thermal expansion increase with temperature. The values of the coefficient of thermal expansion and the modulus of elasticity are obtained from Table 2.3.2-4. For condition 1, the product of the coefficient of thermal expansion and the modulus of elasticity at an average temperature of 272°F $((338+206)/2)$ is 242.9 psi/°F; whereas for condition 2, the corresponding value is 241.2 psi/°F. The effect of the temperature is,

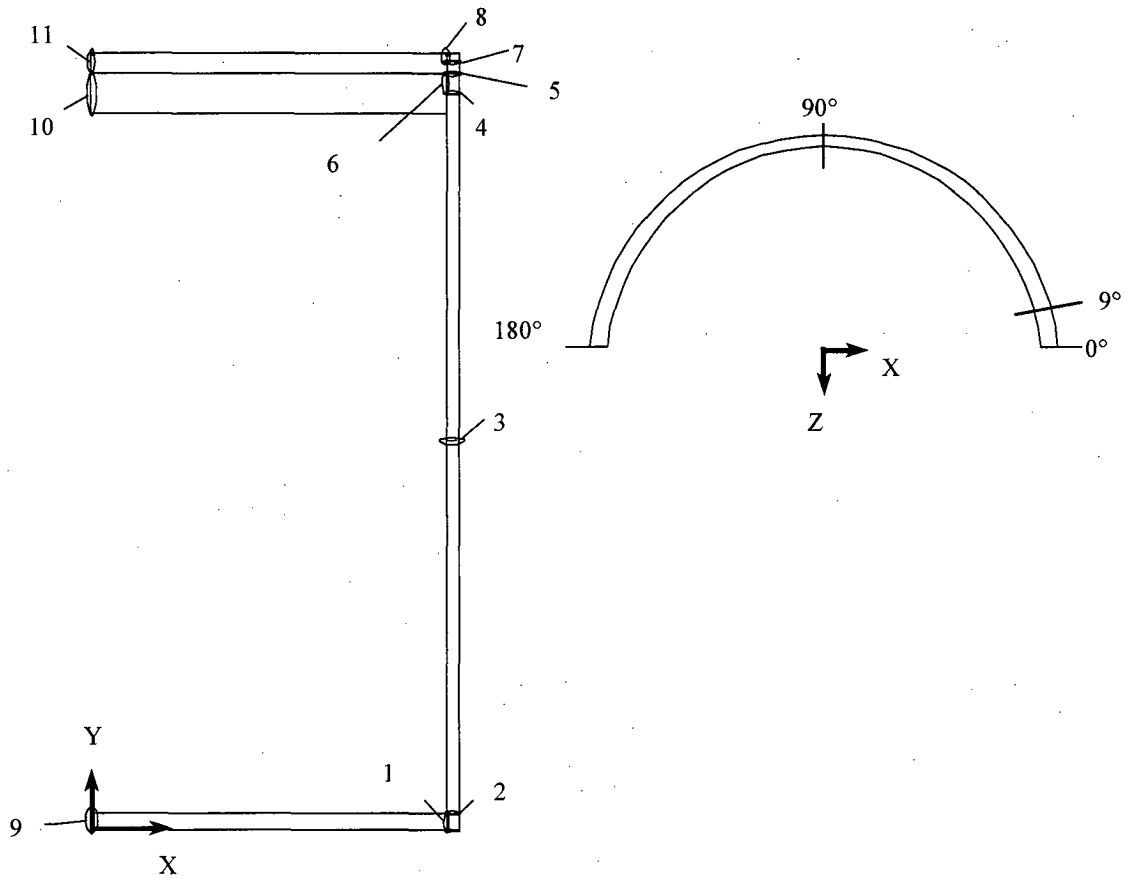
therefore, considered to be negligible. For normal condition thermal stresses, $3 S_m$ is the allowable stress criteria. Below 300°F, the value of S_m (16.7 ksi) does not change for SA-240, Type 304L stainless steel. For heat condition 1, the maximum temperature is 338°F and $S_m = 16.35$ ksi. This results in a 2% decrease in the allowable stress for condition 1, which is offset by the 12% increase in the temperature gradient for condition 2. For this reason, only condition 2 thermal stresses are included in the canister evaluations. In the three conditions considered above, the cask is assumed to be in the horizontal position and both the canister cavity and the cask cavity are assumed to be backfilled with helium.

The temperatures employed in the thermal stress analysis were obtained by applying the above temperatures as thermal boundary conditions to the thermal equivalent model of the structural canister model. The structural finite element model is described in Section 2.6.13.2. The equivalent thermal model is obtained by changing the structural element (SOLID45, which has three global displacements for degrees of freedom) to a SOLID70, which has temperature degrees of freedom at the individual nodes. The temperature dependent thermal conductivity for the canister material was employed in the thermal conduction analysis. The temperatures generated in this analysis were used in the thermal stress analysis to evaluate the properties at temperature, as well as the stresses due to thermal expansion.

According to ASME Code, Section III, Subsection NB, the allowable stress criteria is based on the evaluation of linearized stresses across critical cross sections through the canister wall. For the evaluation of the thermal stresses, the criteria for the stresses is based on peak stresses. The stress values taken from the analyses are the nodal stresses at the surface. The sections used in this evaluation are shown in Figure 2.6.13.3-1. For the sections identified, the thermal stresses are reported in Table 2.6.13.3-1. The thermal stresses reported in Table 2.6.13.3-1 correspond to the maximum stresses for any circumferential section, for the location shown in Figure 2.6.13.3-1.

For condition 1 or 2, the canister is hotter than the cask body and will undergo more thermal expansion than the cask body. To conservatively determine the minimum gap between the canister and the cask body due to thermal expansion, only expansion of the canister will be considered. The canister is considered to be at 338°F (shell temperature for condition 1) and the cask inner shell temperature is assumed to be 70°F. Using the outer radius of the canister of 35.32 inches and the coefficient of expansion for Type 304L stainless steel of $9.0722E-6$, the canister inner shell gap is reduced by $(9.0722E-6)(35.32)(268) = 0.086$ inches. Since the nominal radial canister-inner shell gap is 0.18 inches, the canister shell does not bind with the inner shell due to thermal expansion.

Figure 2.6.13.3-1 Identification of the Sections for Evaluating the Linearized Stresses in the Yankee-MPC Canister



Section	Node 1		Node 2	
	X	Y	X	Y
1	34.695	0.000	34.695	1.000
2	34.695	1.000	35.320	1.000
3	34.695	57.269	35.320	57.269
4	34.695	118.000	35.320	118.000
5	34.695	119.000	35.320	119.000
6	34.695	118.000	34.695	119.000
7	34.695	121.120	35.320	121.120
8	34.695	121.120	34.695	122.000
9	0.000	0.000	0.000	1.000
10	0.000	114.000	0.000	119.000
11	0.000	119.000	0.000	122.000

Table 2.6.13.3-1 Linearized Stresses in the Yankee-MPC Canister - Thermal Only
(Condition 2)

Section No.	Q Stresses (psi)						Principal Stresses (psi)			S.I. (psi)
	SX	SY	SZ	SXY	SYZ	SXZ	S1	S2	S3	
1	89.9	278.7	782.4	22.8	13.7	-52.3	786.6	281.3	83.1	703.5
2	-76.6	-485.6	376.6	35.1	2.8	-35.5	379.4	-76.4	-488.6	868.0
3	-76.6	1374.0	-532.6	0.1	-0.3	13.7	1374.0	-76.2	-533.0	1907.0
4	254.4	-1722.0	-1224.0	-174.8	-19.8	111.8	278.3	-1232.0	-1738.0	2016.0
5	-339.4	102.5	-818.1	-27.0	11.5	-34.3	104.4	-338.7	-820.7	925.0
6	386.1	1361.0	-178.7	-81.8	1.7	38.1	1368.0	381.8	-181.3	1549.0
7	-652.7	1073.0	-18.4	0.0	62.9	0.0	1077.0	-22.0	-652.7	1730.0
8	-568.3	156.3	84.5	89.8	-6.6	47.3	167.3	87.9	-582.7	750.0
9	-5120.0	-2081.0	-5059.0	6.5	-210.8	62.4	-2066.0	-5030.0	-5164.0	3097.0
10	-9.6	1020.0	-211.7	-3.9	30.1	21.0	1021.0	-7.4	-214.6	1235.0
11	435.2	1412.0	226.1	23.1	-65.6	26.7	1416.0	438.3	218.8	1197.0

2.6.13.4 Stress Evaluation of the Yankee-MPC Canister for 1-Foot End Drop Load Condition

A structural analysis is performed using ANSYS to evaluate the effect of a 1-foot end drop impact for both the bottom and top end orientations of the Yankee-MPC canister. The ASME Code, Section III, NB requires the stresses arising from operational loads be assessed based on the primary loads. The primary loads for the 1-foot drop are due to the deceleration of the canister and its contents (56,000 pounds) and the conservatively assumed 20 psig pressure load internal to the canister. The applied deceleration is 20g for both orientations. The inertial load of the canister is addressed by the deceleration factor applied to the canister density. The fuel weight (30,600 pounds) is represented by a pressure load on the inner end surface of the canister. Displacement constraints are applied to the plane of symmetry and the gap elements attached at the canister end to represent the top or bottom of the transport cask.

To determine the effect of the 20 psig pressure load, the top end and bottom end orientations with and without the pressure load were analyzed. The maximum stresses are summarized below:

Drop Orientation	Internal Pressure (psi)	Maximum Stress Intensity (ksi)
Bottom End Drop	0	4.6
Bottom End Drop	20	3.0
Top End Drop	0	7.6
Top End Drop	20	12.5

It is concluded that the bottom end drop without pressure is limiting for the bottom end drop orientation. For the top end drop, the addition of pressure is limiting.

The location of the linearized stresses is shown in Figure 2.6.13.3-1. The maximum stresses for P_m and $P_m + P_b$ are tabulated in Tables 2.6.13.4-2 through 2.6.13.4-7. The critical sections for the pressure and the pressure plus the deceleration load, with reference to the section and the appropriate tables, are shown in Table 2.6.13.4-1.

Additional analysis is performed for the bottom end drop conditions assuming a maximum gap size of 0.08 inch between the structural lid and shield lid (see Section 2.6.13.2). The minimum margins of safety for P_m and $P_m + P_b$ (see Table 2.6.13.4-1) are +4.93 (at Section No. 8) and +3.84 (at Section No. 7), respectively. The margins of safety in these tables are calculated as: $M.S. = (\text{allowable stress}/S.I.) - 1$.

Table 2.6.13.4-1 Summary of Critical Sections of the Yankee-MPC Canister for the 1-Foot End Drop Condition

Condition	Stress	Critical Section	Table	Minimum Margin of Safety
Pressure (only)	P_m	1	2.6.13.4-2	+ 1.43
Pressure (only)	$P_m + P_b$	2	2.6.13.4-3	+ 0.39
Top End Drop Pressure + Inertia	P_m	1	2.6.13.4-4	+ 2.95
Top End Drop Pressure + Inertia	$P_m + P_b$	2	2.6.13.4-5	+ 1.25
Bottom End Drop Inertia	P_m	8	See Note 1	+ 4.53
Bottom End Drop + Inertia	$P_m + P_b$	7	See Note 1	+ 3.84

Note:

1. The minimum margin of safety for the bottom end drop condition is based on the analysis considering the maximum gap of 0.08 inch between the structural lid and shield lid.

Table 2.6.13.4-2 Internal Pressure Only (20 psi) – Yankee-MPC Canister Primary Membrane Stresses (psi)

Section No.	P _m Stresses						Principal Stresses			S.I.	S _m Allow. Stress	Margin of Safety
	SX	SY	SZ	SXY	SYZ	SXZ	S1	S2	S3			
1	-1104.0	5051.0	1657.0	1170.0	533.2	-168.1	5333.0	1613.0	-1342.0	6675.0	16250.0	1.43
2	2664.0	-2093.0	-1670.0	-1001.0	165.0	-258.0	2884.0	-1668.0	-2314.0	5198.0	16250.0	2.13
3	4.9	550.0	1106.0	0.0	0.0	87.4	1113.0	550.0	-2.0	1115.0	16250.0	13.57
4	209.6	379.2	383.3	-142.6	-12.2	-17.0	460.4	385.0	126.8	333.6	16250.0	47.71
5	-437.2	327.2	269.9	-19.3	-2.5	48.4	327.9	272.9	-441.0	768.9	16250.0	20.13
6	-84.6	-378.3	118.7	-11.7	-14.6	18.0	120.7	-85.8	-379.1	499.9	16250.0	31.51
7	426.5	-125.8	146.4	-22.9	-2.9	13.1	428.1	145.8	-126.8	554.9	16250.0	28.28
8	-68.5	420.6	135.7	62.7	-7.7	16.8	428.6	137.1	-77.8	506.4	10400.0*	19.54
9	677.2	-15.6	676.7	189.9	-981.0	-0.2	1388.0	677.1	-726.9	2115.0	16250.0	6.68
10	-26.2	8.7	-22.9	-8.4	13.8	-1.2	15.5	-26.1	-29.8	45.3	19350.0	426.25
11	73.0	0.6	72.9	0.2	-0.3	0.0	73.0	72.9	0.6	72.3	16250.0	223.63

* Includes two stress reduction factors for weld: $0.8 \times 0.8 = 0.64$ (See Section 2.6.13.12).

Table 2.6.13.4-3 Internal Pressure Only (20 psi) – Yankee-MPC Canister Primary Membrane Plus Primary Bending Stresses (psi)

Section No.	P _m + P _b Stresses						Principal Stresses			S.I.	1.5 S _m Allow. Stress	Margin of Safety
	SX	SY	SZ	SXY	SYZ	SXZ	S1	S2	S3			
1	-7041.0	331.6	676.6	1704.0	661.0	-357.5	1274.0	138.7	-7446.0	8720.0	24375.0	1.80
2	1390.0	-15890.0	-6275.0	1254.0	7.0	559.8	1521.0	-6315.0	-15980.0	17500.0	24375.0	0.39
3	0.0	551.5	1118.0	-2.6	-0.2	-88.7	1125.0	551.5	-7.0	1132.0	24375.0	20.53
4	154.5	213.3	312.5	-193.2	-14.1	-15.4	379.3	313.8	-12.9	392.2	24375.0	61.15
5	-251.0	2063.0	855.3	-105.9	-4.7	-78.9	2068.0	860.9	-261.5	2330.0	24375.0	9.46
6	-569.9	-1205.0	-233.8	-131.7	-10.5	23.1	-231.8	-545.6	-1231.0	999.0	24375.0	23.40
7	650.3	1548.0	-52.3	0.1	-34.6	0.0	1549.0	650.3	-53.0	1602.0	24375.0	14.22
8	-587.5	235.5	-104.6	80.7	-9.9	32.8	243.5	-102.4	-597.6	841.1	15600.0*	17.55
9	16730.0	1006.0	16720.0	189.9	-980.7	222.1	16970.0	16540.0	942.3	16030.0	24375.0	0.52
10	-1202.0	-48.9	-1194.0	-5.3	14.4	-5.7	-48.7	-1191.0	-1205.0	1156.0	29025.0	24.11
11	130.7	3.9	130.6	-0.2	0.1	0.2	130.8	130.4	3.9	126.9	24375.0	191.08

* Includes two stress reduction factors for weld: $0.8 \times 0.8 = 0.64$ (See Section 2.6.13.12).

Table 2.6.13.4-4 Top End Drop: 1-ft. Drop + Internal Pressure (20 psi) - Yankee-MPC Canister Primary Membrane Stresses (psi)

Section No.	P _m Stresses						Principal Stresses			S.I.	S _m Allow. Stress	Margin of Safety
	SX	SY	SZ	SXY	SYZ	SXZ	S1	S2	S3			
1	-683.1	3107.0	1031.0	723.2	334.6	-105.1	3283.0	1003.0	-831.1	4114.0	16250.0	2.95
2	1662.0	-1303.0	-973.3	615.2	102.9	155.2	1795.0	-973.1	-1436.0	3231.0	16250.0	4.03
3	1.9	7.3	1105.0	0.0	0.0	-87.5	1112.0	7.3	-5.0	1117.0	16250.0	13.55
4	98.4	-443.9	-17.7	46.0	-9.1	-6.0	102.7	-17.9	-448.0	550.7	16250.0	28.51
5	-44.0	-400.2	-36.0	0.0	-23.4	0.0	-34.5	-44.0	-401.7	367.2	16250.0	43.25
6	23.0	-201.0	-14.8	0.0	-15.7	0.0	23.0	-13.5	-202.3	225.3	16250.0	71.13
7	10.2	-357.3	-25.4	11.0	-7.1	1.5	10.5	-25.3	-357.8	368.3	16250.0	43.12
8	5.0	-257.4	-7.8	0.0	-11.0	0.0	5.0	-7.3	-257.9	262.9	10400.0*	38.56
9	431.4	-17.3	432.2	199.8	-597.3	-0.2	876.2	431.3	-461.3	1337.0	16250.0	11.15
10	0.7	-233.0	3.2	-1.0	2.1	-0.2	3.3	0.7	-233.0	236.3	19350.0	80.89
11	-9.8	-263.2	0.8	-0.8	-2.0	-0.7	0.9	-9.8	-263.2	264.1	16250.0	60.53

* Includes two stress reduction factors for weld: $0.8 \times 0.8 = 0.64$ (See Section 2.6.13.12).

Table 2.6.13.4-5 Top End Drop: 1-ft. Drop + Internal Pressure (20 psi) - Yankee-MPC Canister Primary Membrane Plus Primary Bending Stresses (psi)

Section No.	P _m + P _b Stresses						Principal Stresses			S.I.	1.5 S _m Allow. Stress	Margin of Safety
	SX	SY	SZ	SXY	SYZ	SXZ	S1	S2	S3			
1	-4384.0	198.5	371.7	1057.0	415.0	-220.7	768.3	52.5	-4635.0	5403.0	24375.0	3.51
2	861.9	-9812.0	-3818.0	770.9	3.2	340.4	941.6	-3842.0	-9867.0	10810.0	24375.0	1.25
3	-3.0	8.7	1117.0	-1.6	-0.2	-88.8	1124.0	8.8	-10.1	1134.0	24375.0	20.49
4	72.0	-940.5	-176.8	57.7	-9.0	-17.0	76.5	-177.9	-943.8	1020.0	24375.0	22.90
5	-11.9	-443.8	-59.4	33.0	-10.1	-5.0	-8.7	-59.9	-446.5	437.8	24375.0	54.68
6	-56.8	-370.6	-104.1	0.0	-12.3	0.0	-56.8	-103.6	-371.2	314.3	24375.0	76.55
7	-1.2	-394.9	-43.9	-4.6	-6.9	-0.5	-1.2	-43.8	-395.1	394.0	24375.0	60.87
8	-5.3	-295.0	-1.0	0.0	-17.5	0.0	0.0	-5.3	-296.0	296.0	15600.0*	51.70
9	10210.0	608.9	0.1	200.1	-597.1	100.1	10300.0	10130.0	567.4	9736.0	24375.0	1.50
10	35.9	-233.3	39.3	-0.3	4.3	0.2	39.3	35.9	-233.4	272.7	29025.0	105.44
11	-4.3	-263.5	3.6	1.3	3.7	0.0	3.7	-4.3	-263.5	267.2	24375.0	90.22

* Includes two stress reduction factors for weld: $0.8 \times 0.8 = 0.64$ (See Section 2.6.13.12).

Table 2.6.13.4-6 Bottom End Drop: 1-ft. Drop + Internal Pressure (0 psi) - Yankee-MPC Canister Primary Membrane Stresses (psi)

Section No.	P _m Stresses						Principal Stresses			S.I.	S _m Allow. Stress	Margin of Safety
	SX	SY	SZ	SXY	SYZ	SXZ	S1	S2	S3			
1	-25.3	-704.5	-129.2	63.1	25.1	8.0	-18.5	-129.1	-711.3	692.8	16250.0	22.46
2	103.7	-1854.0	-422.7	32.7	19.4	33.8	106.4	-424.7	-1855.0	1961.0	16250.0	7.29
3	0.8	-1740.0	0.3	0.0	0.1	0.0	0.8	0.3	-1740.0	1741.0	16250.0	8.33
4	-760.4	-800.7	-389.0	0.0	263.2	0.0	-260.7	-760.4	-929.1	668.4	16250.0	23.31
5	905.9	-756.4	-546.9	-107.1	0.2	99.9	919.5	-553.5	-763.5	1683.0	16250.0	8.66
6	196.5	704.2	-233.2	5.1	30.5	-37.5	705.2	199.7	-237.4	942.6	16250.0	16.24
7	-1072.0	339.2	-546.8	-127.7	13.9	19.5	350.9	-546.2	-1084.0	1435.0	16250.0	10.32
8	207.7	-1240.0	-718.6	162.8	42.2	74.7	232.4	-723.0	-1260.0	1493.0	10400.0*	5.97
9	29.5	-243.2	33.7	2.3	20.8	-0.2	35.3	29.5	-244.7	280.0	16250.0	57.04
10	70.7	23.7	69.5	16.0	-20.2	0.7	80.9	71.0	12.1	68.8	19350.0	280.17
11	-161.1	50.4	-157.0	16.1	-39.4	-1.4	58.9	-161.5	-165.1	223.9	16250.0	71.58

* Includes two stress reduction factors for weld: $0.8 \times 0.8 = 0.64$ (See Section 2.6.13.12).

Table 2.6.13.4-7 Bottom End Drop: 1-ft. Drop + Internal Pressure (0 psi) - Yankee-MPC Canister Primary Membrane Plus Primary Bending Stresses (psi)

Section No.	P _m + P _b Stresses						Principal Stresses			S.I.	1.5 S _m Allow. Stress	Margin of Safety
	SX	SY	SZ	SXY	SYZ	SXZ	S1	S2	S3			
1	142.5	-957.2	-136.2	45.1	24.2	13.3	145.1	-136.2	-959.7	1105.0	24375.0	21.06
2	-711.1	-2701.0	30.4	0.0	-11.5	0.0	30.5	-711.1	-2701.0	2731.0	24375.0	7.93
3	0.8	-1741.0	1.0	0.4	0.1	0.0	1.053	0.8	-1741.0	1742.0	24375.0	12.99
4	-808.8	-1111.0	-254.6	0.0	290.6	0.0	-165.3	-808.8	-1200.0	1035.0	24375.0	22.55
5	522.1	-3735.0	-1569.0	111.2	1.6	147.5	535.4	-1580.0	-3738.0	4273.0	24375.0	4.70
6	1194.0	1910.0	344.1	288.9	19.6	-60.7	2012.0	1097.0	338.7	1674.0	24375.0	13.56
7	-838.6	2970.0	331.1	-166.6	14.8	69.5	2977.0	335.2	-850.0	3827.0	24375.0	5.37
8	1555.0	-560.8	-178.8	213.3	56.8	122.6	1586.0	-183.1	-587.0	2173.0	15600.0*	6.18
9	37.6	-244.7	35.9	2.9	21.5	-0.6	38.0	37.2	-246.4	284.4	24375.0	84.71
10	2529.0	140.9	2515.0	13.6	-17.2	12.0	2536.0	2508.0	140.7	2395.0	29025.0	11.12
11	-1383.0	-19.4	-1389.0	14.6	-41.9	-6.1	-17.9	-1380.0	-1393.0	1375.0	24375.0	16.73

* Includes two stress reduction factors for weld: $0.8 \times 0.8 = 0.64$ (See Section 2.6.13.12).

THIS PAGE INTENTIONALLY LEFT BLANK

2.6.13.5 Stress Evaluation of the Yankee-MPC Canister for Thermal Plus a 1-Foot End
Drop Load Condition

The thermal expansion loads described in Section 2.6.13.3 are applied in conjunction with the primary loads in Section 2.6.13.4 to produce a combined thermal expansion plus end impact loading. The stress evaluation is performed according to the ASME Code, Section III, Subsection NB. Based on the results in Section 2.6.13.4, the pressure is included with the inertia loading for the top end drop. For the bottom end drop, the pressure is not considered in order to produce the smallest margins. The most critical sections are listed in Table 2.6.13.5-1 and 2.6.13.5-2. The stresses reported in this table correspond to the nodal stress at the surface. The minimum margin of safety is +3.33 when $3 S_m$ is used as the stress criteria. It is clear from the table that all of the stress intensities are less than $1.5 S_m$, so the stress intensity range criterion of $3.0 S_m$ is satisfied. The margins of safety are calculated as: $M.S. = (\text{allowable stress}/S.I.) - 1$.

Table 2.6.13.5-1 Yankee-MPC Canister Bottom End Drop: 1-ft. Drop + Internal Pressure (0 psi) + Thermal (cold) (psi)

Section No.	$P_m + P_b + Q$ Stresses						Principal Stresses			S.I.	$3 S_m$ Allow. Stress	Margin of Safety
	SX	SY	SZ	SXY	SYZ	SXZ	S1	S2	S3			
1	-362.7	-390.4	485.1	-110.5	35.3	57.0	489.9	-265.7	-492.1	982.0	48750.0	48.64
2	93.2	-4076.0	-653.9	85.0	22.6	49.6	98.2	-657.1	-4078.0	4176.0	48750.0	10.67
3	112.2	-3128.0	-1243.0	0.1	0.3	-81.8	117.2	-1248.0	-3128.0	3245.0	48750.0	14.02
4	118.2	-3626.0	-2174.0	-66.7	-5.4	-177.6	133.1	-2188.0	-3628.0	3761.0	48750.0	11.96
5	468.8	-3854.0	-2210.0	41.3	-18.6	-194.2	483.2	-2224.0	-3855.0	4338.0	48750.0	10.24
6	344.6	1651.0	-694.2	-282.5	27.6	84.3	1709.0	293.9	-702.1	2411.0	48750.0	19.22
7	-665.0	2034.0	25.0	96.2	3.6	-33.3	2038.0	26.6	-670.0	2708.0	48750.0	17.00
8	1029.0	-397.2	-362.8	-120.6	66.4	-97.5	1046.0	-328.1	-449.6	1496.0	31200.0*	19.86
9	-5218.0	-2696.0	-5209.0	-3.2	51.1	68.6	-2695.0	-5145.0	-5283.0	2588.0	48750.0	17.84
10	-2483.0	718.4	-2668.0	20.5	-52.6	10.8	719.3	-2482.0	-2670.0	3389.0	58050.0	16.13
11	-3704.0	-1983.0	-3642.0	22.9	96.4	19.7	-1977.0	-3643.0	-3710.0	1733.0	48750.0	27.13

* Includes two stress reduction factors for weld: $0.8 \times 0.8 = 0.64$ (See Section 2.6.13.12).

Table 2.6.13.5-2 Yankee-MPC Canister Top End Drop: 1-ft. Drop + Internal Pressure (20 psi) + Thermal (cold) (psi)

Section No.	$P_m + P_b + Q$ Stresses						Principal Stresses			S.I.	$3 S_m$ Allow. Stress	Margin of Safety
	SX	SY	SZ	SXY	SYZ	SXZ	S1	S2	S3			
1	-4572.0	171.1	793.8	1088.0	436.4	-269.6	1033.0	191.8	-4832.0	5865.0	48750.0	7.31
2	783.6	-10270.0	-3431.0	804.1	6.1	304.0	863.2	-3452.0	-0.1	11190.0	48750.0	3.36
3	112.9	-1374.0	-146.4	-1.7	0.1	-6.8	113.1	-146.5	-1374.0	1488.0	48750.0	31.76
4	485.2	-2765.0	-1075.0	474.6	-48.6	-114.3	561.8	-1083.0	-2834.0	3395.0	48750.0	13.36
5	-1740.0	-3805.0	-1358.0	0.0	382.8	0.0	-1299.0	-1740.0	-3864.0	2565.0	48750.0	18.01
6	-1420.0	-3327.0	-1626.0	407.6	0.9	28.4	-1334.0	-1628.0	-3411.0	2077.0	48750.0	22.47
7	775.6	-5663.0	-1230.0	31.3	-27.1	-138.2	785.3	-1240.0	-5663.0	6449.0	48750.0	6.56
8	51.3	-132.1	-1047.0	0.0	-148.5	0.0	51.3	-108.6	-1071.0	1122.0	31200.0*	26.81
9	-10390.0	832.9	-10350.0	182.6	-460.5	-32.7	854.9	-10350.0	-10410.0	11260.0	48750.0	3.33
10	305.0	478.7	120.0	-8.3	-55.5	20.9	487.8	306.2	109.7	378.2	58050.0	152.49
11	-2044.0	-2872.0	-1970.0	0.3	-13.0	28.9	-1960.0	-2054.0	-2872.0	912.2	48750.0	52.44

* Includes two stress reduction factors for weld: $0.8 \times 0.8 = 0.64$ (See Section 2.6.13.12).

2.6.13.6 Stress Evaluation of the Yankee-MPC Canister for a 1-Foot Side Drop Load Condition

The determination of the stresses in the canister due to a 1-foot side drop is accomplished using ANSYS. In the local regions of the lids and bottom plate, the loads are transmitted through the canister shell into the cask body inner shell. Outside of the lid and bottom plate regions, stress develops in the canister shell as a result of the basket loading the canister wall. The basket, canister and cask body have different radii which implies that the contact angle between the components is dependent on the loading. For this reason, the finite element model described in Section 2.6.13.2 contains a half model of the basket. Gap elements between the basket and the canister allow the interface to be dependent on the loading. The interface between the canister and the cask body inner shell is also represented by gap elements.

The load due to the contents is applied to the basket via pressure acting in the plane of the disks. The weight is assumed to act over the effective width of 8.254 inches in which the disk is .5 inches thick. The content weight includes the 900 pounds per fuel assembly (for 36 fuel assemblies) plus the fuel tube weight (58.6 pounds). This weight is distributed over the 22 support disks plus two end weldments. A deceleration factor of 20g is applied to the load and the pressure per slot is computed as:

$$(900+58.6)(20) / [(8.254)(.5)(24)] \text{ psi} = 193.6 \text{ psi}$$

The 45° circumferential orientation of the basket is the configuration that results in the greatest distortion of the canister. This requires that both sides of the slots be loaded and factored by .707. This loading differs from the loading used in the basket analysis since the purpose of this loading in the canister model is to obtain the overall deflection of the basket. In addition to the contents load, a 20 psig pressure is conservatively applied to the inner surface of the canister.

The methodology used to evaluate the stresses for this condition is taken from Section 2.6.13.4 and the location of the sections are identified in Figure 2.6.13.3-1. The critical section stresses are reported in Table 2.6.13.6-1 and Table 2.6.13.6-2 for P_m and $P_m + P_b$ stresses, respectively. The minimum margin of safety for the canister in the side drop, assuming the minimum gap size, (Section 2.6.13.2) is +0.04, which occurs at Section 1 in Figure 2.6.13.3-1.

The minimum margin of safety for P_m assuming a maximum gap of 0.08 inches, is +0.16, at Section 6, and for $P_m + P_b$ it is +0.12 at Section 1. The margins of safety are calculated as: $M.S. = (\text{allowable stress}/S.I.) - 1$.

Table 2.6.13.6-1 Yankee-MPC Canister Side Drop: 1-ft. Drop + Internal Pressure (20 psi) - Primary Membrane Stresses (psi)

Section No.	P _m Stresses						Principal Stresses			S.I.	S _m	
	SX	SY	SZ	SXY	SYZ	SXZ	S1	S2	S3		Allow. Stress	Margin of Safety
1(0°)	-10227.0	856.0	-4685.1	375.9	199.7	-908.3	873.9	-4543.6	-10386.4	11262.0	16250	0.44
2(0°)	5431.7	1884.3	-732.0	-276.8	-292.7	-442.5	5481.0	1902.2	-800.0	6281.1	16250	1.59
3(0°)	-692.7	765.9	1360.0	4.7	-5.3	114.9	1367.4	765.9	-699.1	2065.7	16250	6.87
4(9°)*	-292.6	2090.9	659.1	159.2	1019.3	427.2	2660.3	279.9	-482.3	3142.7	16250	4.17
5(0°)	-9019.0	-32.9	-3701.6	-1049.6	954.2	-599.5	345.1	-3914.4	-9184.7	9529.7	16250	0.71
6(0°)	-15561.2	-2614.2	-4803.6	-1996.5	811.3	-748.8	-2010.2	-5071.0	-15896.8	13883.5	16250	0.17
7(9°)*	1925.2	1097.9	814.8	69.9	485.8	-45.5	1931.5	1460.7	446.1	1484.8	16250	9.94
8(0°-4.5°)	-10240.0	-2130.0	-3090.0	-490.0	750.0	-1260.0	-1574.5	-3351.3	-10544.7	8880.0	10400**	0.17
9	-478.9	-198.6	806.7	71.4	22.0	-22.2	807.5	-181.7	-496.6	1304.5	16250	11.46
10	-425.3	-1.7	78.9	-25.7	6.7	-10.9	79.7	-0.7	-427.1	506.8	19350	37.18
11	-382.5	-2.7	174.5	-16.4	2.8	-13.3	174.9	-2.1	-383.6	558.5	16250	28.10

* See bearing stress calculation for section stress at 0°.

** Includes two stress reduction factors for weld: $0.8 \times 0.8 = 0.64$ (See Section 2.6.13.12).

Table 2.6.13.6-2 Yankee-MPC Canister Side Drop: 1-ft. Drop + Internal Pressure (20 psi) - Primary Membrane Plus Primary Bending Stresses (psi)

Section No.	P _m + P _b Stresses						Principal Stresses			S.I.	1.5 S _m	
	SX	SY	SZ	SXY	SYZ	SXZ	S1	S2	S3		Allow. Stress	Margin of Safety
1(0°)	-26047.2	-2107.7	-10104.3	413.8	217.7	-1116.8	-2095.1	-10030.9	-26131.1	24044.4	25000**	0.04
2(90°)	-4429.3	-11241.0	1092.6	364.4	886.8	-75.4	1156.6	-4409.4	-11324.9	12478.3	24375	0.95
3(0°)	-759.6	1198.5	2829.1	7.8	-5.9	227.3	2842.8	1198.5	-774.0	3617.7	24375	5.74
4(9°)*	599.0	4274.1	2236.7	208.0	755.2	1088.4	4603.4	2456.9	50.1	4553.0	24375	4.35
5(0°)	-11146.6	26.7	-3044.1	-1644.2	728.4	-827.9	466.5	-3185.6	-11450.7	11912.1	24375	1.05
6(0°)	-19996.8	-4548.8	-6797.0	-2643.5	1026.7	-594.2	-3707.8	-7185.0	-20447.7	16735.7	24375	0.46
7(9°)*	2385.6	321.5	419.3	86.5	664.6	-648.9	1677.8	651.1	-962.1	2639.3	24375	8.24
8(0°-4.5°)	-13310.0	-3190.0	-4740.0	-1000.0	1090.0	980.0	-2460.0	-5252.4	-13526.9	10930.0	15600***	0.43
9	-956.6	-172.7	869.4	75.4	9.5	10.3	869.6	-165.6	-963.9	1833.0	24375	12.30
10	-1095.8	-29.5	-493.6	-25.3	7.2	-18.4	-28.7	-493.2	-1096.8	1068.5	29025	26.16
11	-814.4	-19.7	-190.1	-16.0	3.0	-15.9	-19.4	-189.8	-815.2	795.8	24375	29.63

* See bearing stress calculation for section stress at 0°.

** Allowable stress taken at 225°. Refer to page 2.6.13.3-1

*** Includes two stress reduction factors for weld: $0.8 \times 0.8 = 0.64$ (See Section 2.6.13.12).

2.6.13.7 Stress Evaluation of the Yankee-MPC Canister for Thermal Plus a 1-Foot Side Drop Load Condition

The thermal expansion loads described in Section 2.6.13.3 are applied in conjunction with the primary loads in Section 2.6.13.6 to produce a combined thermal expansion plus 1-foot side drop loading. The stress evaluation is performed according to the ASME Code, Section III, Subsection NB. The most critical sections are listed in Table 2.6.13.7-1. The stresses reported in this table correspond to the nodal stress at the surface. The minimum margin is +0.75 at location 4 (see Figure 2.6.13.3-1) when $3 S_m$ is used as the stress criteria. The calculated stress intensity for each section location except No. 4 is less than $1.5 S_m$, so the P+Q stress limit is satisfied as discussed in Section 2.6.7.1. For section no. 4, the P+Q stress intensity is calculated conservatively by combining the bottom end drop condition stress intensity with that of the side drop as: $|3761.0 + 27892.8| = 31,653.8$ psi, which is less than $3 S_m = 48750$ psi, so the criteria is satisfied. The margins of safety are calculated as: $M.S. = (\text{allowable stress}/S.I.) - 1$.

Table 2.6.13.7-1 Yankee-MPC Canister Side Drop: 1-ft. Drop + Internal Pressure (20 psi) + Thermal (cold) (psi)

Section No.	P _m + P _b + Q Stresses						Principal Stresses			S.I.	3 S _m Allow. Stress	Margin of Safety
	SX	SY	SZ	SXY	SYZ	SXZ	S1	S2	S3			
1(0°)	-23971.0	-2690.7	-6679.6	65.7	335.6	-1001.4	-2663.4	-6650.2	-24033.9	21370.5	48750	1.28
2(90°)	-4942.1	-12352.5	1044.5	-93.3	972.2	-35.4	1114.7	-4941.0	-12415.4	13537.4	48750	2.60
3(0°)	-621.9	-4204.9	-6819.0	-1.4	-7.2	-449.7	-589.4	-4204.9	-6851.6	6262.2	48750	6.78
4(0°)	-21999.6	5747.4	-7234.3	-184.1	1304.5	322.8	5877.4	-7357.0	-22010.1	27892.8	48750	0.75
5(0°)	-11241.0	-904.7	-3601.9	-1774.2	672.4	-1122.0	-379.1	-3707.8	-11660.4	11282.9	48750	3.32
6(0°)	-20269.4	-4268.9	-6936.5	-2993.8	1044.4	-800.3	-3344.0	-7294.1	-20846.2	17501.1	48750	1.79
7(0°)	-15403.9	619.3	-5682.4	82.0	1114.7	47.0	811.0	-5873.2	-15403.9	16211.4	48750	2.01
8(0°)	-14690.9	-3475.1	-4428.2	-1008.3	1114.7	-834.8	-2599.5	-5162.3	-14837.7	12237.2	31200*	1.55
9	-5518.8	-2656.1	-4895.9	-42.9	60.8	77.8	-2653.0	-4888.6	-5529.3	2876.3	48750	15.95
10	-2743.1	-1511.0	-1608.6	-20.3	-62.2	-6.1	-1480.6	-1639.0	-2743.1	1262.5	58050	44.98
11	153.9	1367.4	576.6	10.5	-29.2	15.3	1368.4	576.1	153.3	1215.3	48750	39.11

* Includes two stress reduction factors for weld: $0.8 \times 0.8 = 0.64$ (See Section 2.6.13.12).

2.6.13.8 Yankee-MPC Canister Shear Stresses for a 1-Foot Side Drop and a 1-Foot End Drop Condition

The evaluation of the maximum shear stress utilizes the membrane values of the stress intensity due to primary loading which were evaluated for the pressure, end drops and side drop loading. The maximum membrane stress intensity is 13.88 ksi for location 6 (Table 2.6.13.6-1). Using a bounding temperature of 338°F, the S_m for Type 304L stainless steel is 16.36 ksi, the margin of safety is determined by:

$$M.S. = (0.6)(16.36)/(13.88/2) - 1$$

$$M.S. = +.41$$

THIS PAGE INTENTIONALLY LEFT BLANK

2.6.13.9 Yankee-MPC Canister Bearing Stresses for a 1-Foot Side Drop

The bearing stress of the canister on the cask inner shell is evaluated in the region of the canister lids and over the length of the canister shell. The bearing stress associated with the lids is calculated using the membrane S_x stress at Section 7 (see Figure 2.6.13.3-1). The S_x stress component, associated with the radial direction at the plane of symmetry of the canister, is 20.3 ksi based on the finite element evaluation (Section 2.6.13.6). The bearing stress allowable is S_y for the operational condition. Using a bounding temperature of 206°F, $S_y=21.5$ ksi. The margin of safety is:

$$M.S. = (21.5/20.3)-1$$

$$M.S. = +0.06$$

For the bearing stress acting along the inner shell, an angular contact of 18 degrees is assumed (at a radius of 35.5 inches). In this bearing stress, the lids are not considered to be a contributor. This reduces the contents weight to $56,000-10,000 = 46,000$ pounds = 46 kips. For a basket length of 98 inches (removing the lengths of both weldments and the first spacer), the margin for the bearing stress is computed as:

$$S_{br} = (46.0)(20)/[(98)(35.5)(18/57.2958)]$$
$$= 1.09 \text{ ksi}$$

$$M.S. = (18.55/S_{br}) - 1 = +21$$

$$M.S. = + \text{Large}$$

THIS PAGE INTENTIONALLY LEFT BLANK

2.6.13.10 Yankee-MPC Canister Buckling Evaluation for 1-Foot End Drop

The Yankee-MPC canister shell is axially loaded by the weights of the structural lid, the shield lid, and the inertial weight of the shell during a 1-foot end drop impact. The impact load amplification factor is 20g. The shell is evaluated as an unsupported, right circular cylinder using a critical buckling load per Blake, 2nd Edition, "Practical Stress Analysis in Engineering Design":

$$S_{cr} = \frac{E(0.605 - 10^{-7} M^2)}{M(1 + 0.004\phi)}$$

$$= 40.3 \text{ ksi}$$

Where the canister material is Type 304L stainless steel, conservatively assumed to be at 400°F for normal operation, and:

$$E = 26.5 \text{ E03 ksi} \quad R = (69.39 + 0.625)/z = 35.01 \text{ in.}$$

$$S_y = 17.5 \text{ ksi} \quad t = 0.625 \text{ in.}$$

$$\phi = \frac{E}{S_y} = 1514.3 \quad M = \frac{R}{t} = 56.0$$

The axial compression load in the canister shell is:

$$P_A = \left[\left(\frac{\pi}{4} \right) (69.03)^2 (0.291)(8) + \left(\frac{\pi}{4} \right) (70.64^2 - 69.39^2) (1215)(0.291) \right] (20)$$

$$= 271,464 \text{ pounds}$$

and the axial compression stress is:

$$S_A = \frac{P_A}{\left(\frac{\pi}{4} \right) (70.64^2 - 69.39^2)} = 1,975 \text{ psi}$$

Then, the margin of safety for canister shell buckling is:

$$M.S. = \frac{S_{cr}}{S_A} - 1 = +19.4$$

THIS PAGE INTENTIONALLY LEFT BLANK

2.6.13.11 Yankee-MPC Canister Lifting Evaluation

The lifting of the Yankee-MPC canister is accomplished by attaching vendor qualified eyehooks to six locations in the structural lid. During the lifting of the canister, the contents weight of 40,130 pounds is transmitted to the canister bottom and up through the canister 0.625-inch thick shell. A pressure load of 11.3 psig is also applied to the canister during normal operations. The evaluation of this load configuration of the canister is accomplished by a three-dimensional finite element model, as shown in Figure 2.6.13.11-1. This model is essentially the same model presented in Section 2.6.13.2, with the elements for the basket removed. The model is used to evaluate the lower portion of the canister, especially the bottom plate and the junction of the bottom plate and the canister shell. Since the canister is in a vertical position under a lift condition, the model is only restrained at the lift locations at the structural lid. The loads considered in the analysis are internal pressure, dead load with a dynamic load factor of 1.1, and the thermal load. A pressure of 11.5 psig is conservatively applied to represent the operating pressure (the calculated internal pressure is 11.3 psig). The weight of the contents is applied to the bottom plate as a uniform pressure. The 1.1 dynamic load factor is also applied to the contents weight. The thermal stress analysis is performed using the methodology described in Section 2.6.13.3. The temperatures of the key locations considered in the analysis are:

Top center of the structural lid	=	140°F
Top outer diameter of the structural lid	=	100°F
Bottom center of the bottom plate	=	250°F
Bottom outer diameter of the bottom plate	=	130°F
Mid-elevation of the canister shell	=	500°F

The table below shows the temperature differences (ΔT) in the radial and axial directions applied in the model and those calculated by thermal analysis for normal conditions of transport.

	Applied in Model ($\Delta^\circ\text{F}$)	Thermal Analysis Calculation	
		Heat Condition ($\Delta^\circ\text{F}$)	Cold Condition ($\Delta^\circ\text{F}$)
Lid (Radial)	40	14	12
Bottom Plate (Radial)	120	30	29
Shell (Axial)	400	146	160

As shown in the table, the temperature differences in the model envelope the calculated values. Therefore, the thermal stress analysis is conservative.

Allowable stresses at a temperature of 250°F for the lid region, 550°F for the canister shell and 250°F for the bottom plate region, are applied. These temperatures envelope the calculated maximum temperatures of the canister components (see Tables 3.4-1 and 3.4-2) except for the bottom plate, which has a calculated maximum temperature of 255°F for the heat condition of transport. Since the value of design stress intensity (S_m) for SA 240 Type 304L does not change for temperatures below 300°F, the allowable stresses used in this evaluation remain bounding.

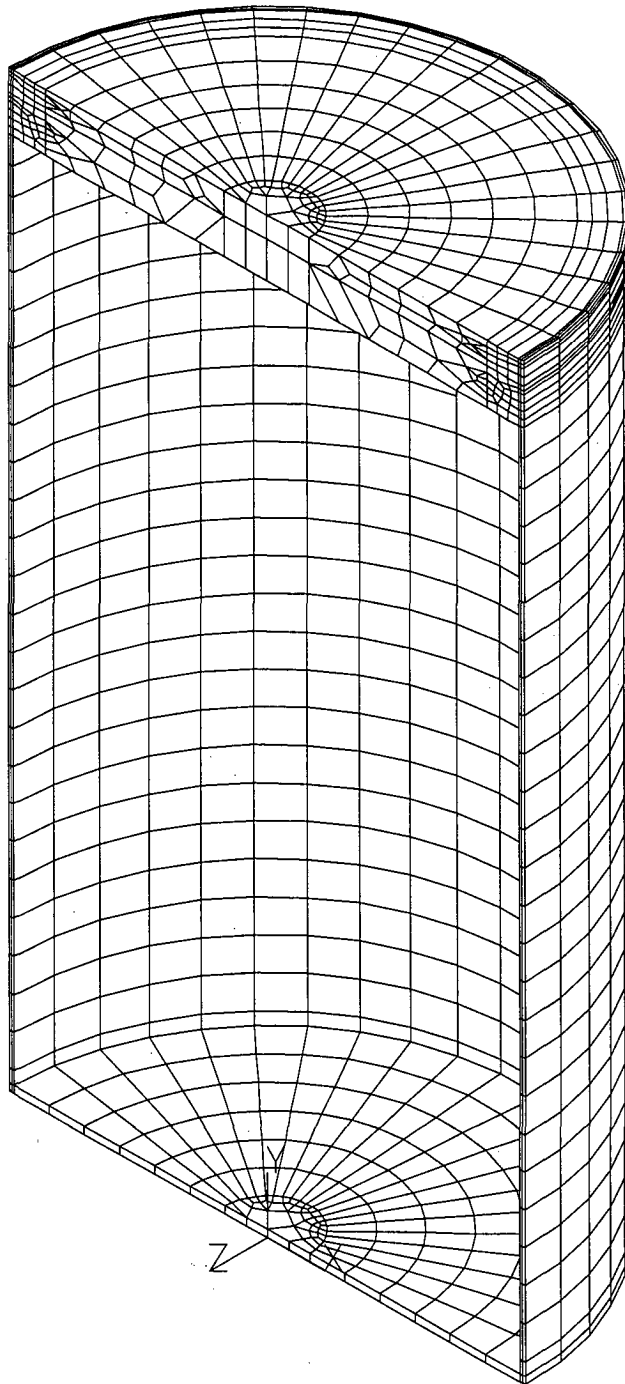
Based on the stress allowables required by the ASME Code, Section III, Subsection NB, the minimum margins of safety are:

Stress Category	Max. Stress (ksi)	Allowable Stress (ksi)	Margin of Safety
P_m	9.47 ¹	16.7	0.76
$P_m + P_b$	20.5 ²	25.05	0.22
$P + Q$	27.74 ¹	50.1	0.81

¹ Maximum stress occurs at the center of bottom plate.

² Maximum stress occurs at junction of the bottom plate and the canister shell.

Figure 2.6.13.11-1 Finite Element Model for Yankee-MPC Canister Lift Evaluation



THIS PAGE INTENTIONALLY LEFT BLANK